

**Chemical Studies on Pyrrolidine Derivatives:  
Synthesis of Bulgecinine and Aminomethyl  
Prolyl Peptide Nucleic Acids**

**THESIS SUBMITTED TO  
THE UNIVERSITY OF PUNE  
FOR THE DEGREE OF  
DOCTOR OF PHILOSOPHY**

**IN  
CHEMISTRY**

**BY  
G. SUNIL KUMAR**

**DIVISION OF ORGANIC CHEMISTRY (SYNTHESIS)  
NATIONAL CHEMICAL LABORATORY  
PUNE 411008**

**CERTIFICATE**

This is to certify that the work presented in the thesis entitled “**Chemical Studies on Pyrrolidine Derivatives: Synthesis of Bulgecinine and Aminomethyl Prolyl Peptide Nucleic Acids**” submitted by **G. SUNIL KUMAR** by the candidate at the National Chemical Laboratory, Pune, under our supervision. Such materials as obtained from other sources have been duly acknowledged in the thesis.

**Dr. K. N. GANESH**  
**(Research Guide)**

**Dr. N. P. ARGADE**  
**(Research Co-Guide)**

**October, 2006**

## **CANDIDATE'S DECLARATION**

I here by declare that the thesis entitled **Chemical Studies on Pyrrolidine Derivatives: Synthesis of Bulgecinine and Aminomethyl Prolyl Peptide Nucleic Acids** submitted for the degree of Doctor of Philosophy in Chemistry to the University of Pune has not been submitted by me to any other university or institution. This work was carried out at the National Chemical Laboratory, Pune, India.

National Chemical Laboratory

**G. SUNIL KUMAR**

Pune 411 008.

**OCTOBER 2006**

## ACKNOWLEDGEMENT

It gives me an immense pleasure to express my deep sense of gratitude towards my research guide Prof. K. N. Ganesh for all the advice, guidance, support and encouragement during every stage of this work. He made me realize the importance of doing quality research, in a better way at crucial stage of my career, of course is a turning point. Although this eulogy is insufficient, I preserve an everlasting gratitude for him.

It gives me great pleasure to express my heartfelt gratitude to my research co-guide

Dr. N. P. Argade for his astute guidance, invaluable suggestions while carrying out the present work. His enduring passion, moral support and help out of the way led me to overcome all the difficulties I encountered during this endeavor. I am certain that the guidance and training provided by him has laid a foundation for future success.

I have no words to express my gratitude to my parents, without knowing where and what I am doing, just wishing me all the time with no expectations. My wife Vani and my son Jishnu Anirudh have taken great pains so that my work does not suffer for which I owe to them. I also thank my Sister and brother in law for their support.

My special thanks to my in-laws- Brhmanandarao, Annapurnadevi, Sambashivarao, Lakshmi, Subramanyeswarrao, and mallashwari, and their family members. I also thank to Chinatalapudi family members for their encouragement.

My special thanks to Dr. V. A. Kumar and Mrs. Anita Gunjal for their help and encouragement during the course of this work. I am also thankful to Mrs. M. V. Mane and Mrs. S. S. Kunte for HPLC analysis, Mrs. Shantakumari and Dr. Mahesh kulkarni for mass analysis. The kind support from NMR group is greatly acknowledged and thanks to Dr. Rajmohan and Dr. usha palgune.

My special thanks to Dr. D. Subramanyam, Dr. N. Selvakumar and Prof. Javed Iqbal for their training and inspiration for to do the Doctorate degree of Philosophy in chemistry.

My special thanks to lab-friends Mangaleswaran, Santhosh, Anirban, Easwar, Mukulesh, Mehrajuddin, Sanjib, Manoj, Kishan, Ramesh, Umesh and Prasad for their cheerful co-operation and help in every aspect throughout this work.

I thank Moneesha, Nagamani, Dinesh, Pallavi, Nagendra, Govind Praveen, Umashankara, Gourishankar, Khirud,, Madhuri, Smita, Patwa, Ashwini, geetali, Mrs.Manish, Nasreen, Satish, roopa, Mansvini, pradnya sachin and Mahesh sonar. I also thank chavan, Pawar, and Bhumkar, for their assistance.

My special thanks to D. Srinivas and his family, Raman, Swaroop, Sridhar, and Gnaneshwar, Srikanth, Rajender for their encouragement and constant support for during the course of this work.

I take this opportunity to thank, Dr. Vijayamohan, Deepali, Mahima, Jadav, Venkatesh, Sattireddy, Abhijit, Bala, Vasu, Praveen, jayanthi, Hareesh, Bhargav, Srinivas naidu, shiva, Praksh, Ragupathi.

I thank director NCL, for allowing me to work in this premier institute, providing the infrastructure. It is my sincere thanks to CSIR, New Delhi, for the financial support

G. Sunil kumar.

## ABBREVIATIONS

$\beta$ -ala	$\beta$ -alanine
A	Adenine
aeg	Aminoethylglycine
aep	Aminoethylpropyl
ala	Alanine
amp	Aminomethyl prolyl
ap	Antiparallel
Boc Tert.	butyloxycarbonyl
BF <sub>3</sub> .OEt <sub>2</sub>	Boranetriflouride diethyl etherate
C	Cytosine
Cbz	benzyloxy carbonyl
CD	Circular Dichroism
dA	Deoxy adenine
DCC	Dicyclohexylcarbodiimide
DCM	Dichloromethane
DEAD	Diethyl azadicarboxylate
dG	2'-deoxyguanine
DIAD	Diisopropylazodicarboxylate
DIPEA	Diisopropylethylamine
DMF	N,N-Dimethylformamide
DMS	Dimethylsulphite
DNA	2'-deoxyribonucleic acid
DP	D-Proline
ds	Double stranded
Fmoc	9-Fluorenylmethoxycarbonyl
FPLC	Fast Protein Liquid Chromatography
g	Gram
G	Guanine
gly	Glycine
h	Hours
HBTU	<i>O</i> -(1H-Benzotriazol-1-yl) <i>N,N,N',N'</i> -tetramethyluronium hexafluorophosphate
HOBt	1-Hydroxybenztriazole
HPLC	High Performance Liquid Chromatography
Hz	Hertz
IR	Infra red
ITC	Isothermal Titration Calorimetry
LP	L-Proline
MALDI-TOF	Matrix Assisted Laser Desorption Ionisation-Time Of Flight
MF	Merrifield Resin
MBHA	4-Methyl benzhydryl amine
mg	Milligram
MHz	Megahertz
M	Molar

M	Micromolar
ml	Milliliter
mmol	Millimoles
N	Normal
nm	Nanometer
NMP	N-methyl pyrrolidine
NMR	Nuclear Magnetic Resonance
ONs	Oligonucleotides
p	Parallel
PCR	Polymerase Chain Reaction
PPh <sub>3</sub>	Triphenyl phosphine
PNA	Peptide Nucleic Acid
Pro	Proline
Pyr	pyrrolidinone
RNA	Ribonucleic acid
r.t.	Room temperature
ss	Single strand/ Single stranded
s	Seconds
T	Thymine
TBATFB	Tetra butyl ammonium tetra flo borate
TBTU	<i>O</i> -(1H-Benzotriazol-1-yl) <i>N,N,N',N'</i> -tetramethyl uronium tetrafluoroborate
TEA	Triethylamine
TFA	Trifluoroacetic acid
TFMSA	Trifluoromethanesulphonic acid
THF	Tetrahydrofuran
TMSi-Cl	Trimethyl silyl chloride
TMSoTF	Trimethyl silyl tirflate
UV-Vis	Ultraviolet- Visible

## CONTENTS

<b>PUBLICATIONS</b>		I
<b>ABSTRACT</b>		III
<b>CHAPTER 1</b>	<b>INTRODUCTION</b>	
1.1	Nucleic Acids: Chemical Structure	1
1.2	Oligonucleotide as therapeutic agents	4
1.3	Chemical Modifications of DNA	6
1.3.1	Phosphate modified linkages	6
1.3.2	Oligonucleotides with backbones not containing phosphorous	7
1.3.3	Boranophosphate DNA	9
1.4	Sugar modifications	10
1.4.1	Sugar skeleton modifications	10
1.5	Locked nucleic acids (LNA)	11
1.6	Carbocyclic nucleic acid	12
1.7	Morpholino nucleosides	13
1.8	Base modifications	14
1.9	Spectroscopic methods for studying the DNA duplexes, triplexes and DNA-PNA complexes	15
1.9.1	UV Spectroscopy	15
1.9.2	Circular dichroism	17
1.10	Peptide Nucleic Acids	18
1.10.1	Triplex formation with complementary DNA and RNA	20
1.10.2	Duplex formation with complementary DNA and RNA	20
1.11	Structure of PNA complexes	21
1.11.1	Structure of PNA-DNA duplexes	22
1.11.2	Structure of PNA-RNA duplexes	23
1.12	Chemical modifications of PNA	24
1.13	Construction of bridged structures	28
1.14	Thiazane and thiazolidine PNA	35
1.15	PNA with six membered ring structures	36
1.16	Modified nucleobases	41
1.17	PNA-Conjugates	42
1.17.1	PNA-DNA Chimera	42
1.17.2	PNA-Oligopeptide chimera	43
1.17.3	PNA-Liposome chimera	44
1.18	PNA-Applications	45
1.18.1	Diagnostic applications	45
1.19	Biological applications	49
1.19.2	PNA as anticancer agent 1a PNA as anticancer agent	49
1.19.3	PNA as delivery agent	50

	1.20	Antisense and antigene applications	51
	1.20.1	PNA as artificial transcription promoters	52
	1.20.2	PNA conjugates as artificial restriction enzymes	53
	1.21	Present work	54
	1.22	Reference	57
<b>CHAPTER 2</b>		<b>Synthesis and assignment of configuration of <i>amp</i>-PNA monomers and its incorporation in to <i>aeg</i>-PNA oligomers</b>	71
	2.1	Introduction	72
	2.2	Rational behind the design	74
	2.3	Objectives of the present chapter	76
	2.4	Synthesis of <i>amp</i> -PNA monomers	77
	2.5	Assignment of absolute stereochemistry at C <sub>5</sub> position of <i>amp</i> PNA monomers (9 and 10)	83
	2.6	Synthesis of (2 <i>R</i> ,5 <i>S</i> ) and (2 <i>R</i> ,5 <i>R</i> )-N1-( <i>tert</i> -Butoxycarbonyl)-5-[(N-Fluorenyl methoxycarbonyl) aminomethyle]-proline (22 and 23).	84
	2.7	Assignment of absolute stereochemistry at C5 position of compound 18 and 19 ( <i>amp</i> monomers).	86
	2.8	4-Hydroxy <i>amp</i> monomer: Rational behind the design	88
	2.9	Synthesis of 4-hydroxy aminomethyl prolyl ( <i>amp</i> ) monomer	91
	2.10	Synthesis of Aminoethylglycyl ( <i>aeg</i> ) PNA monomers	93
	2.11	Alkylation of Nucleobases	95
	2.12	Solid Phase peptide Synthesis	97
	2.13	Synthesis of <i>amp</i> PNA oligomers	101
	2.14	Cleavage of the PNA Oligomers from the Solid Support	103
	2.15	Purification and characterization of PNA oligomers	103
	2.16	Synthesis of Complementary Oligonucleotides	105
	2.17	CONCLUSIONS	105
	2.18	Experimental	106
	2.19	Functionalization of MBHA resin	127
	2.19.1	Picric acid assay for the estimation of the amino acid loading	127
	2.20	Reference	129
	2.21	Appendix	134
<b>CHAPTER 3</b>		<b>BIOPHYSICAL STUDIES</b>	173
	3	Introduction	174
	3.1	Biophysical techniques	174
	3.2	CD spectroscopy of PNA	177

3.3	UV-Spectroscopy	179
3.4	Gel electrophoresis	181
3.5	CD Studies: Effect of Chiral PNAs	181
3.5.1	CD studies of <i>amp</i> monomers	182
3.5.2	CD studies of single strand <i>amp</i> PNA oligomers	183
3.5.3	CD studies of <i>amp</i> -PNA <sub>2</sub> :DNA/RNA triplexes	184
3.5.4	CD studies of Homooligomers	187
3.6	Binding Stoichiometry: CD and UV-mixing Curves	189
3.7	CD Spectra of duplexes	192
3.8	UV-Melting studies of (2 <i>S</i> ,5 <i>R</i> ) and (2 <i>S</i> , 5 <i>S</i> ) <i>amp</i> PNA <sub>2</sub> -DNA triplexes	194
3.8.1	UV- <i>T</i> <sub>m</sub> Studies of Duplexes	198
3.8.2	Mismatch studies of (2 <i>S</i> ,5 <i>R</i> ) and (2 <i>S</i> ,5 <i>S</i> )- <i>amp</i> -PNA triplexes.	201
3.9	UV- <i>T</i> <sub>m</sub> studies of (2 <i>R</i> ,5 <i>S</i> ) and (2 <i>R</i> ,5 <i>R</i> ) <i>amp</i> PNA <sub>2</sub> :DNA triplexes	203
3.9.1	UV- <i>T</i> <sub>m</sub> studies of (2 <i>R</i> ,5 <i>S</i> ) and (2 <i>R</i> ,5 <i>R</i> )- <i>amp</i> -PNA:DNA duplex	206
3.9.2	Mismatch studies of (2 <i>R</i> ,5 <i>S</i> ) and (2 <i>R</i> ,5 <i>R</i> ) <i>amp</i> -PNA triplex with DNA	208
3.10	UV- <i>T</i> <sub>m</sub> Studies of 4-hydroxy- <i>amp</i> -PNA	210
3.10.1	UV- <i>T</i> <sub>m</sub> studies of 4-hydroxy- <i>amp</i> -PNA duplexes	211
3.10.2	Mismatch studies of (2 <i>S</i> ,4 <i>S</i> ,5 <i>R</i> )- <i>amp</i> -PNA	213
3.11	UV- <i>T</i> <sub>m</sub> studies of (2 <i>S</i> ,5 <i>R</i> ) and (2 <i>S</i> ,5 <i>S</i> ) <i>amp</i> -PNA/RNA triplexes	214
3.11.1	UV- <i>T</i> <sub>m</sub> studies of (2 <i>S</i> ,5 <i>R</i> ) and (2 <i>S</i> ,5 <i>S</i> ) <i>amp</i> -PNA:RNA duplexes	216
3.12	UV- <i>T</i> <sub>m</sub> studies of (2 <i>R</i> ,5 <i>S</i> ) and (2 <i>R</i> ,5 <i>R</i> ) <i>amp</i> PNA <sub>2</sub> :RNA triplexes	217
3.12.1	UV- <i>T</i> <sub>m</sub> studies of (2 <i>R</i> ,5 <i>S</i> ) and (2 <i>R</i> ,5 <i>R</i> )- <i>amp</i> -PNA:RNA duplexes	220
3.13	UV- <i>T</i> <sub>m</sub> studies of (2 <i>S</i> ,4 <i>S</i> ,5 <i>R</i> )- <i>amp</i> -PNA <sub>2</sub> :RNA Triplexes	221
3.13.1	UV- <i>T</i> <sub>m</sub> studies of (2 <i>S</i> ,4 <i>S</i> ,5 <i>R</i> )- <i>amp</i> -PNA:RNA duplexes	222
3.14	Comparison studies of <i>amp</i> PNA hybrids with complementary DNA	224
3.15	Comparison studies of <i>amp</i> -PNA hybrids with the complementary RNA	225
3.16	Comparison studies of <i>amp</i> -PNA:DNA and <i>amp</i> -PNA:RNA hybrids	226
3.16.1	Studies of triplex hybrids of <i>amp</i> -PNAs	226
3.16.2	Comparison studies of duplex hybrids of <i>amp</i> -PNAs	228

	3.16.3	Studies of triplex and duplex hybrids of <i>amp</i> -PNAs: DNA Vs RNA	229
	3.16.4	Studies of (2 <i>S</i> ,4 <i>S</i> ,5 <i>R</i> )- <i>amp</i> -PNA:DNA and (2 <i>S</i> ,4 <i>S</i> ,5 <i>R</i> )- <i>amp</i> -PNA:RNA hybrids Studies of triplex hybrids of (2 <i>S</i> ,4 <i>S</i> ,5 <i>R</i> )- <i>amp</i> -PNAs	229
	3.16.5	Studies of duplex hybrids of (2 <i>S</i> ,4 <i>S</i> ,5 <i>R</i> )- <i>amp</i> -PNAs	230
	3.17	Aminomethy thiazolidine ( <i>amt</i> ) PNA	231
	3.18	Conclusion	231
	3.19	Reference	234
<b>CHAPTER 4</b>		<b>2,5-disubstituted pyrrolidines</b>	236
		<b>SECTION I</b>	
	4.1	<b>Introduction of 2,5-disubstituted pyrrolidines</b>	237
	4.1.1	Synthesis with formation of the pyrrolidine ring	238
	4.2	Synthesis from aza-heterocycles	250
	4.3.	Syntheses from commercially available pyrrolidines and pyrrolines	256
	4.4	Conclusion	261
	4.5	Reference	263
		<b>SECTION II</b>	267
	4.6	(2 <i>S</i> ,5 <i>S</i> )-Pyrrolidine-2,5-dicarboxylic acid	268
	4.6.1	Earlier Synthesis of (2 <i>S</i> ,5 <i>S</i> )-pyrrolidine-dicarboxylicacid	268
	4.6.2	Present work	269
	4.7	Experimental Procedure	271
	4.8	Chemical studies towards the synthesis of Bulgecinine	274
	4.8.1	Earlier synthesis	274
	4.9	Present work	276
	4.10	Attempts to increase the diastereoselectivity of the reaction	277
	4.11	Diazotisation approach	281
	4.12	Experimental	282
	4.13	Reference	289
	4.14	Appendix	291

## LIST OF PUBLICATIONS

1. Synthesis of novel tricyclic oxazolidinones by a tandem SN<sub>2</sub> and SNAr reaction: SAR Studies on conformationally constrained analogues of Linezolid.  
Selvakumar, N.; Yadi Reddy, B.; **Sunil Kumar, G.**; Khera, M.; et al.  
*Bioorganic. Med Chem. Lett.* **2006**, *16*, 4416-4419
2. Synthesis of Marine Natural Product (2*S*, 5*S*)-Pyrrolidine-2,5-dicarboxylic acid  
**Sunilkumar, G.**; Nagamani, D.; Argade, N. P.; Ganesh, K. N.  
*Synthesis* 2003, *15*, 2304
3. Novel Indole[2,1-*b*]quinazoline Analogues as Cytostatic Agents: Synthesis, Biological Evaluation and Structure-Activity Relationship  
Sharma, V. M.; Prasanna, P.; **Sunil kumar, G.** et al  
*Bioorganic. Med Chem. Lett.* **2002**, *12*, 2303
4. Dimethyl malonate as a one-carbon source: a novel method of introducing carbon substituents onto aromatic nitro compounds.  
Selvakumar, N.; Yadi Reddy, B.; **Sunil Kumar, G.**; Javed Iqbal.  
*Tetrahedron Lett.* **2001**, *42*, 8395
5. 9-Deoxypodophyllotoxin Derivatives as Anti-Cancer Agents.  
Duvvuri Subramanyam, B.Renuka, **G.Sunil Kumar**, V.Vandana and D. S. Deevi  
*Bioorganic. Med Chem. Lett.* **1999**, *9*, 2131.
6. Synthesis, SAR and antibacterial studies on novel chalcone oxazolidinone hybrids  
Selvakumar, N.; **Sunil Kumar, G.**; Malar Azhagan, A.; Govinda Rajulu, G.; Shikha Sharma, Sitaram Kumar, M.; Jagattaran Das, Javed Iqbal, Sanjay Trehan.  
(Manuscript submitted for **Bioorganic medicinal chemistry**).
7. Synthesis, Characterization and cDNA/RNA hybridization Studies of Amino Methyl Prolyl Peptide Nucleic Acids. (Manuscript under preparation).
8. Synthesis of 4hydroxy- *amp* PNA oligomers and it' hybridization properties with complementary DNA. (Manuscript under preparation).

**Presentations:**

1. Synthesis and Biophysical Studies of AminoMethylProlyl Peptide Nucleic Acids.  
**Oral and poster Presentation** in Royal Society of Chemistry students Symposium  
Presentation #OP-1 & Poster # P9, National Chemical Laboratory, PuneSynthesis,  
**Sunil Kumar, G.**; Argade, N. P.; Ganesh, K. N
2. Characterization and cDNA Hybridization studies of AminoMethyl Prolyl  
Peptide Nucleic Acids. Poster #156, ACS-CSIR-OCCB Symposium, January 7-9,  
Pune-INDIA. **Sunil Kumar, G.**; Argade, N. P.; Ganesh, K. N
3. Synthesis and Antibacterial Activity of Novel Chalcone Oxazolidinone Hybrids.  
42<sup>nd</sup> Interscience Conference on Antimicrobial Agents and Chemotherapy,  
Abstract # F-1323. September 27-30, 2002, CANADA. Selva Kumar, N.; **Sunil  
Kumar, G.**; Malar Azagan, A.; Sanjay trehan, Jagattaran das, and Javed Iqbal.
4. SAR Studies on Certain Conformationally Constrained Oxazolidinones.  
42<sup>nd</sup> Interscience Conference on Antimicrobial Agents and Chemotherapy,  
Abstract # F-1324. September 27-30, 2002, CANADA. Selva Kumar, N.; Yadi  
Reddy, B.; **Sunil Kumar, G.**; Sanjay trehan, Jagattaran das, and Javed Iqbal.

## **ABSTRACT**

The thesis entitled “**Chemical Studies on Pyrrolidine Derivatives: Synthesis of Bulgecinine and Aminomethyl Prolyl Peptide Nucleic Acids**” is divided in to four chapters as follows.

The thesis comprises the studies towards design, synthesis and DNA/RNA hybridization properties of nucleic acid analogs having chiral polyamide backbone (Peptide Nucleic Acids, PNA) with five-membered nitrogen heterocycles.

**Chapter 1** introduces the background literature for undertaking the research work.

**Chapter 2** describes the synthesis, characterization of five *amp*-monomers, and incorporation of these monomers into *aeg*-PNA backbone for hybridizational studies with complementary DNA and RNA. These *amp*-PNA oligomers were characterized by HPLC and MALDI-TOF mass spectroscopy.

**Chapter 3** illustrates the hybridizational studies with complementary DNA/RNA sequences.

**Chapter 4** portrait the chemical studies towards the synthesis of (2*S*,5*S*)-Pyrrolidine di-carboxylic acid and (2*S*,4*S*,5*R*)-Bulgecinine.

### **Chapter 1 Introduction to peptide Nucleic Acids (PNAs)**

The origin of the concept of antisense and antigene therapy made nucleic acids a target for potential therapeutic interventions. A variety of micro and macro molecules, both natural and synthetic, are capable of interacting with DNA or RNA. These interactions can lead to the inactivation of gene expression. Selective inhibition of disease causing genes is theoretically possible by taking advantage of the known specific hydrogen bonding interactions between complementary base pairs of nucleic acids. Based on these interactions, tailored short nucleic acid sequences or oligonucleotides, could selectively bind to the target DNA/RNA. Oligonucleotides that interact with single stranded RNA are termed as ‘antisense’ whereas those interacting with double stranded DNA are called ‘antigene’ oligonucleotides. However, intracellular enzymes such as nucleases and proteases, rapidly cleave the unmodified oligodeoxy nucleotides ODNs

with sugar-phosphate backbone. The development of new classes of modified oligonucleotides has been triggered to allow the industrious application of antisense/antigen principle.

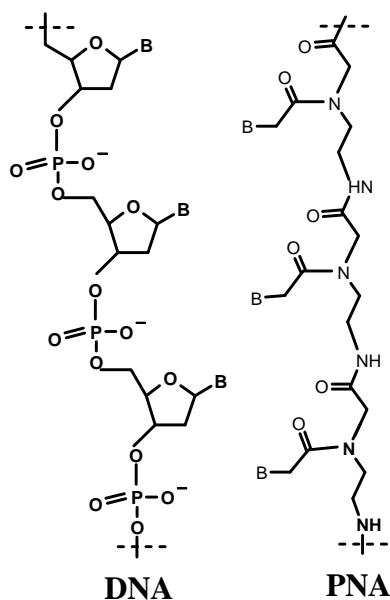


**Figure 1** Chemical structure of DNA and PNA

Among all the DNA mimics, PNA introduced by Nielsen et. al in 1991 has been found to mimic many properties of DNA. The structure of PNA is remarkably simple, the repeating unit of PNA consisting of N-(1-aminoethyl)-glycine units linked by amide bonds and the nucleobases (A,G,C and T) attached to the backbone through methylene carbonyl linkages (Figure 1). Thus PNA lacks sugar and phosphate groups, making it acyclic, neutral, achiral and homomorphous. PNA is resistant to cellular enzymes and has strong affinity towards complementary DNA/RNA. Homopyrimidine PNA oligomers bind strongly to complementary DNA by Watson-Crick and Hoogsteen bonding to form [(PNA)<sub>2</sub>:DNA] triple helices that are much more stable than the corresponding DNA-DNA hybrids. The unique character of PNA is binding to duplex DNA by strand invasion forming both *parallel* (N-terminus of PNA to 5' end of the DNA) and *antiparallel* (C-terminus to 5' end respectively) complexes. In contrast to homopyrimidine sequences, mix sequences of PNA bind to complementary DNA/RNA with 1:1 stoichiometry to form duplexes. Here binding can be in either parallel or antiparallel mode, the latter mode

having higher stability than parallel hybrids with high sequence specificity and affinity. These favorable hybridization properties with high chemical and bio-stability make PNA a promising lead for developing as efficient antisense agent and medicinal drugs.

Though PNAs encompass some disadvantages like poor water solubility, less orientational selectivity between parallel and antiparallel binding modes, lack of selective in binding affinity between DNA and RNA, low membrane penetration and inefficient cellular uptake. Various attempts have been made to address these shortcomings of PNA. Introduction of various modifications/substitutions in the PNA backbone that resulted in preorganized and chiral PNA, are aimed to achieve directional selective binding to target DNA/RNA. PNAs suffixed with negatively charged DNA or modified PNAs with positively charged polypeptide sequence at either 'C' or 'N' terminus, resulted in PNA-DNA/PNApeptide chimera with favorable aqueous solubility, cellular uptake and DNA binding/recognition properties.

This chapter gives an outline of the oligonucleotide analogues and various modifications of PNAs carried out to improve their applications as therapeutic agents with special emphasis on PNAs containing 5- and 6- membered rings. Rationale for the design of chiral, pyrrolidine based new PNAs are presented that forms the basis for the present work.

The five membered aminomethyl prolyl (*amp*)-PNAs were designed to induce controlled rigidity in to the *aeg*-backbone, and to introduce chirality for better discrimination between DNA and RNA.

## **Chapter 2 Synthesis, characterization of *amp*-monomers and *amp*-PNAs**

The constant efforts from our lab towards generating constrained and chiral PNA analogues resulted in the synthesis of various *amp* monomers Figure 3. This modification was designed by bridging the  $\alpha$  and  $\alpha'$  carbons of the *aeg*-backbone. Such modifications locks the fluctuation segments of *aeg*-PNA (glycyl/ethlendiamine) by restraining the torsional angles ( $\gamma$  and  $\delta$ ) and introduce rigidity along with the chirality in to the *aeg*-PNA backbone in the form of pyrrolidinyl ring, while simultaneously keeping a certain degree of flexibility in the linker to the nucleobases (Figure 2).

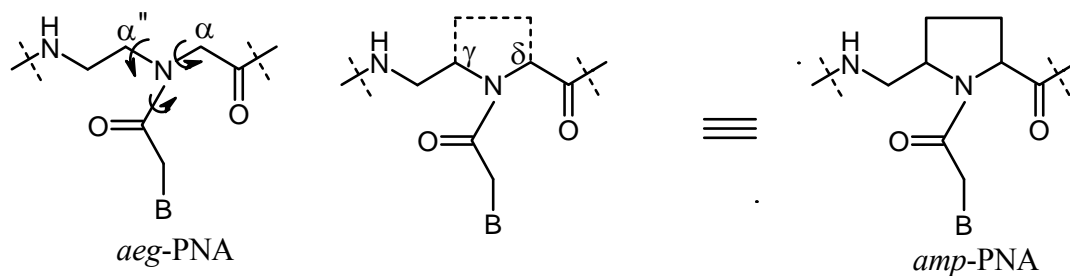


**Figure 2** Structural preorganisation of *amp*-PNA

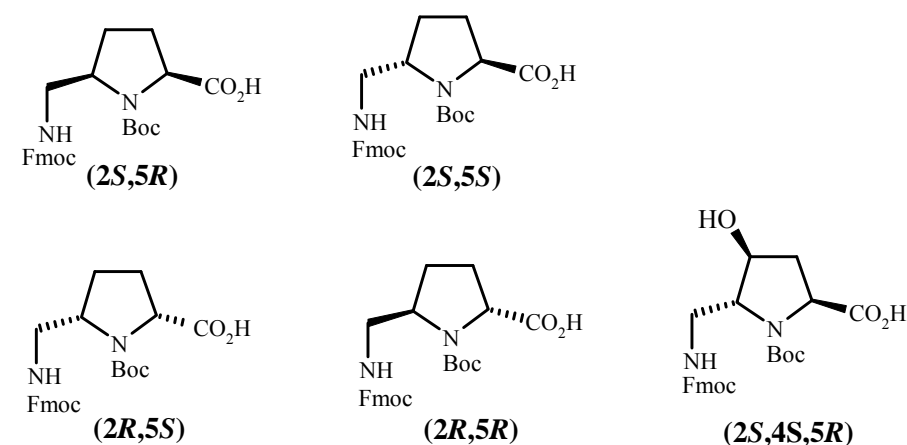


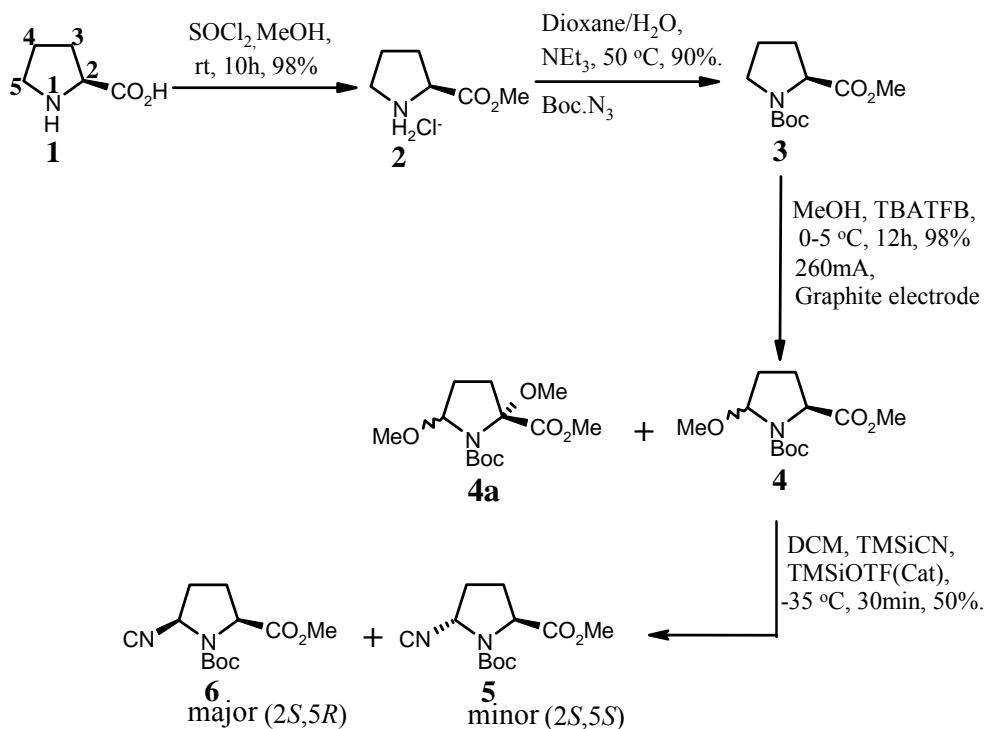
**Figure 3** *amp* (aminomethylprolyl) monomers

## 2.1 Synthesis and characterization of *amp*-PNA monomers

### 2.1a Synthesis of (2*S*,5*S*) and (2*S*,5*R*)-N1-(*tert*-Butoxycarbonyl)-5-[(NFluorenylmethoxycarbonyl) aminomethyl]-Proline (**9** and **10**)

The synthesis of target *amp* PNA monomers **9** and **10** (Figure 3) was achieved starting from L-proline **1** (Scheme 1), which on treatment with thionyl chloride in methanol afforded the 2-carboxymethyl ester **2** as its hydrochloride salt. The ring nitrogen (N1) of the ester **2** was protected as *tert*-butoxycarbonyl by treatment with *tert*-butylcarbazine and triethylamine in dioxane/water to provide the N-(*tert*-butoxycarbonyl) proline carboxymethyl ester **3**. This was then subjected to electro-chemical oxidation employing Ross-Eberson- Nyberg reaction.

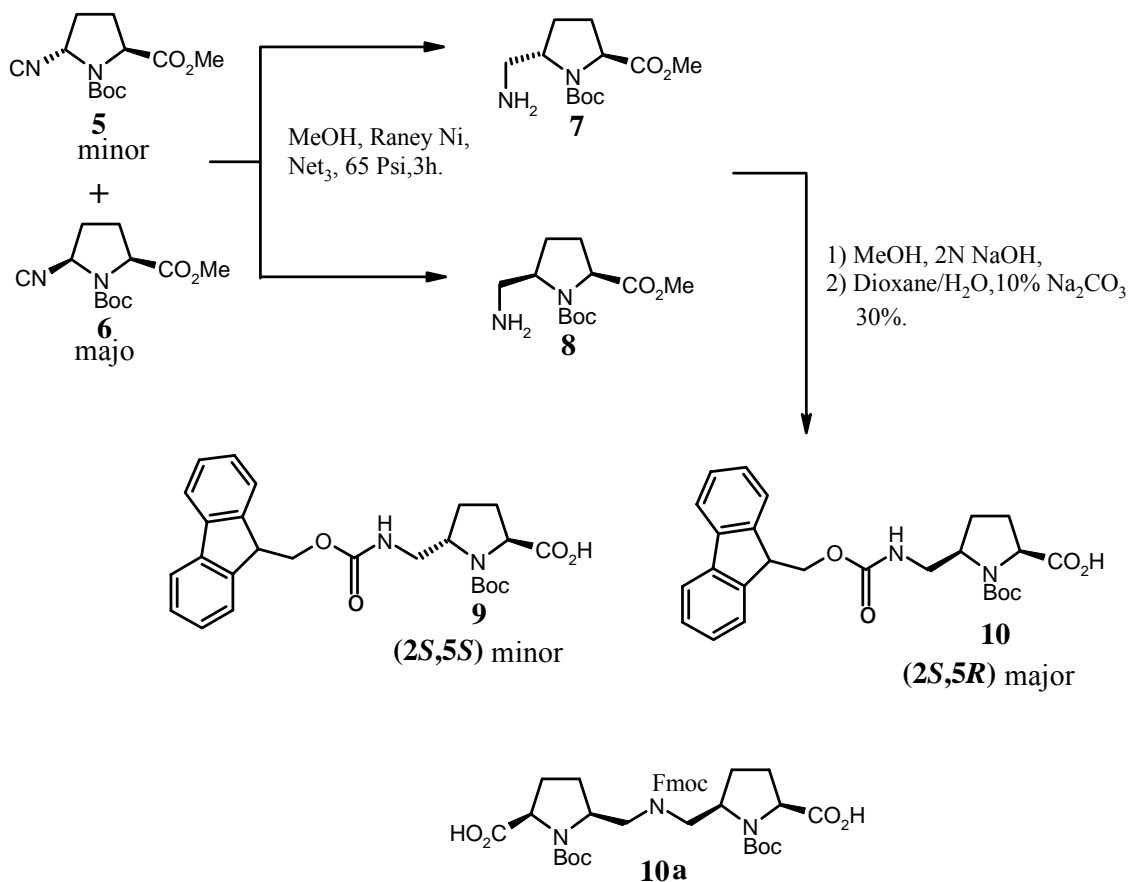
The anodic oxidation involved the treatment of ester **3** with methanol as a solvent-reagent and tetrabutylammonium-tetrafluoroborate as a supporting electrolyte and passing a constant current of 0.06F/cm<sup>2</sup> (260 mA) using graphite electrodes.



**Scheme 1** Synthesis of (2*S*,5*R*) and (2*S*,5*S*) nitriles

The reaction mixture was cooled to ice temperature before passing the current and the temperature of the reaction was maintained between 0-10 °C for about 12 h. The efficiency of the reaction depends on controlling the temperature and current optimally to avoid the formation of C-2 and C-5 dimethoxylated products. Compound **4** formed in 95% yield, as a non-separable diastereomeric mixture.

The diastereomeric mixture of compound **4** was treated with TMSiCN in DCM employing catalytic amount of TMSTF at -35 °C for about 30 min, the reaction was quenched at -35 °C using dry methanol resulting the formation of C5-nitriles **5** and **6** in 50% yield. The product obtained as diastereomeric mixture was separable by chromatography on neutral alumina.

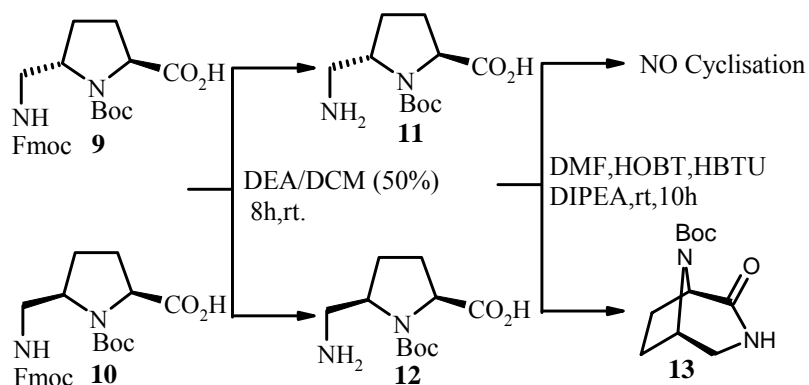


**Scheme 2** Synthesis of (2*S*,5*S*) and (2*S*,5*R*) *amp*-PNA monomers

The diastereomers **5** and **6** were individually subjected to hydrogenation at 65 psi, in MeOH employing Raney Ni as catalyst to afford the 5-methylaminopropine methyl esters **7** and **8**. These amino compounds upon hydrolysis in 2N NaOH in MeOH yielded the sodium salt of the acid, which on treatment with fluorenyl chloroformate afforded the required *amp* monomers **9** and **10** in 30% yield, along with the by-product **10a** (Scheme2).

## 2.2 Assignment of absolute stereochemistry at C<sub>5</sub> position of *amp* PNA monomers (9,10)

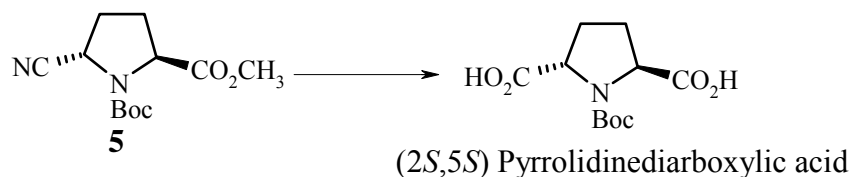
An important aspect remaining in the characterization of (2*S*,5*S*) and (2*S*,5*R*) *amp* PNA is the assignment of the configuration at C<sub>5</sub> position where a new chiral center was generated upon anodic oxidation. This was achieved as described in Scheme 3.



**Scheme 3** Configuration assignment of compound **9** and **10** *amp* monomers

Compounds **9** and **10** were individually treated with 50% DCM/DEA at rt for about 8 h to furnish the amino acids **11** and **12**. Compound **12** when treated with HOBT/HBTU, in DMF, amino acid **12** furnished the compound **13**. In case of amino acid **11**, no cyclisation product was observed. In compound **12** and hence in **10** the C5 and C2 substituents must be *cis* to each other to obtain the cyclized product. Since the configuration at C2 is known in acid **10**, which is same as in starting material L-proline the absolute configuration at C5 in the compound **10** that is *cis* to C2, would be *R* (*2S,5R*). The absolute configuration of acid **9** is therefore (*2S,5S*).

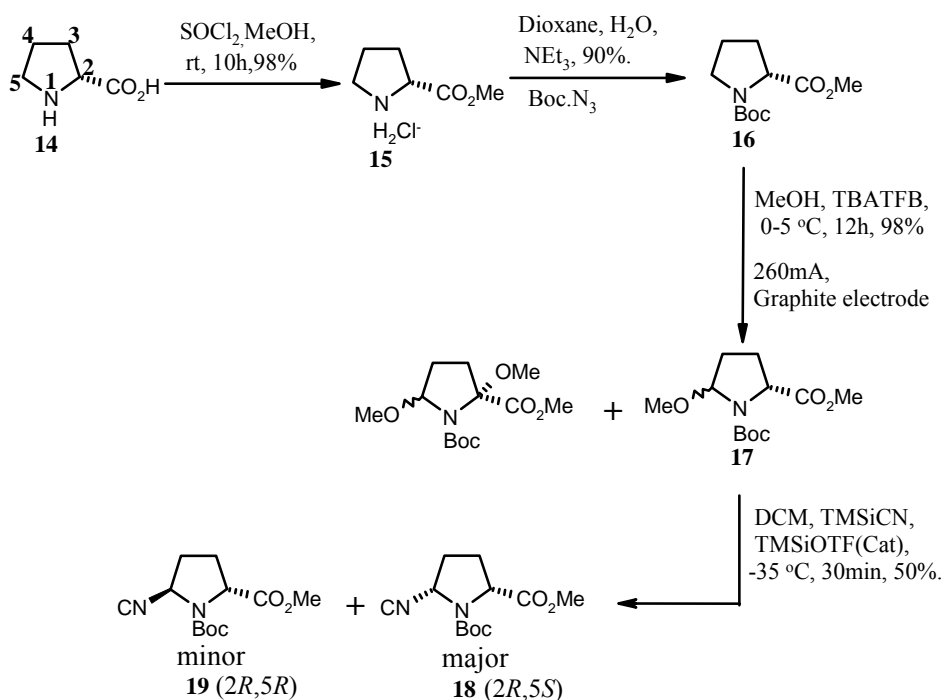
In another approach the configuration at C5 was assigned by preparing (*2S,5S*) pyrrolidine dicarboxylic acid a marine natural product from the nitrile ester **5**, which is discussed in chapter 4.



**Scheme 3a**

### 2.3 Synthesis of (2*R*,5*S*) and (2*R*,5*R*)-N1-(*tert*-Butoxycarbonyl)-5-[(*N*-Fluorenylmethoxycarbonyl) aminomethyl]-proline (**22** and **23**).

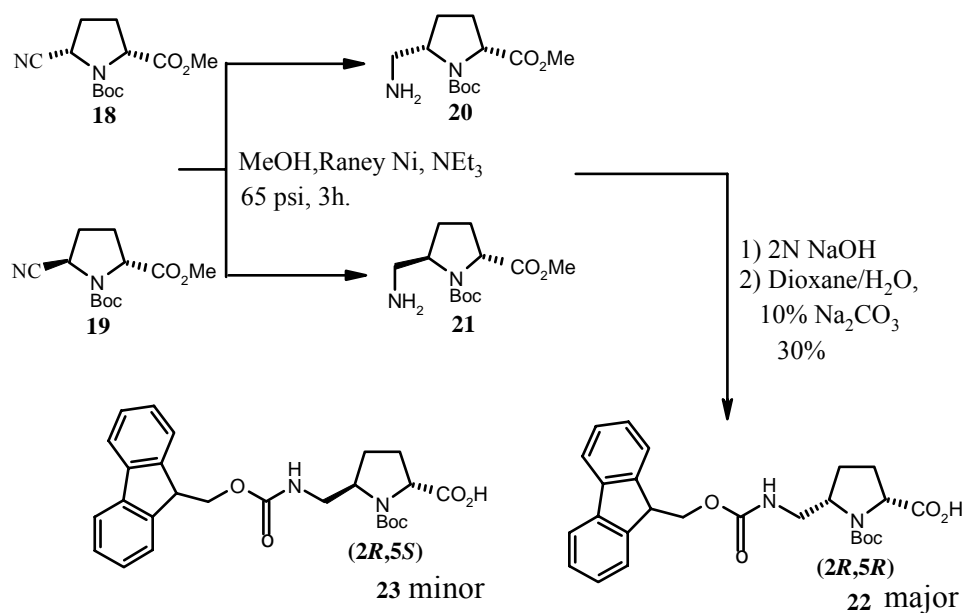
The synthesis of (2*R*)-5-[(*N*-fluorenylmethoxycarbonyl) aminomethyl]-N1-(*tert*butoxycarbonyl) proline **22** and **23** were similarly achieved starting from D-proline **14** (Scheme 4).



**Scheme 4** Synthesis of (2*R*,5*R*) and (2*R*,5*S*) nitriles

The steps involved esterification of D-proline, protection of the ring nitrogen, C5-functionalization by anodic oxidation and conversion of the 5-methoxy-N1-(*tert*butoxycarbonyl) proline methyl ester **17** to the separable C5-nitrile diastereomers **18** and **19**.

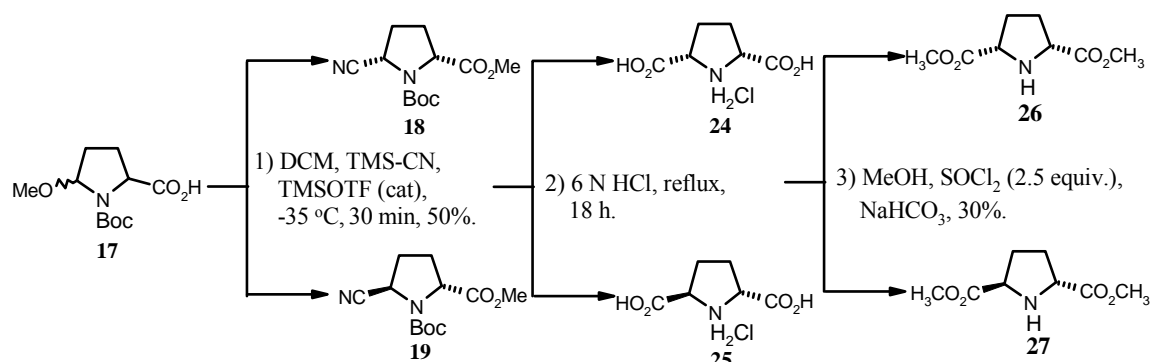
The two nitrile compounds were subjected to reduction to get the amino-methyl ester **20** and **21**, which were hydrolysed using 2N NaOH, followed by protection of amino group employing Fmoc-Cl to furnish the required *amp* PNA monomers **22** and **23**.



**Scheme 5** Synthesis of (2*R*,5*R*) and (2*R*,5*S*)-amp monomers.

#### 2.4 Assignment of absolute stereochemistry at C5 position of compound **18** and **19** (amp monomers)

The absolute stereochemistry at C5 of the compounds **18** and **19** was assigned as described in Scheme 6. The two 5-cyano proline esters **18** and **19** were individually subjected to hydrolysis in 6 N HCl for about 14 h to afford the hydrochloride salt of pyrrolidine 2,5-dicarboxylic acids **24** and **25**.



**Scheme 6** Configuration assignment of esters **18** and **19**.

These diacids were subjected esterification employing  $\text{SOCl}_2$  in MeOH followed by neutralization to furnish the diester **26** and **27** in 30% yield. The magnitude of the optical rotation of compound **26** is  $[\alpha]_D = 0$  since the configuration at C2 in ester **18** is known as R, the stereochemistry at C5 of diester **26** is *cis* to C2 (meso) with R configuration, and hence the configuration of ester **18** is (2*R*,5*S*). The stereochemistry of compounds *amp* **22** and **23** are therefore (2*R*,5*S*) and (2*R*,5*R*) respectively.

## 2.5 4-Hydroxy *amp* monomer

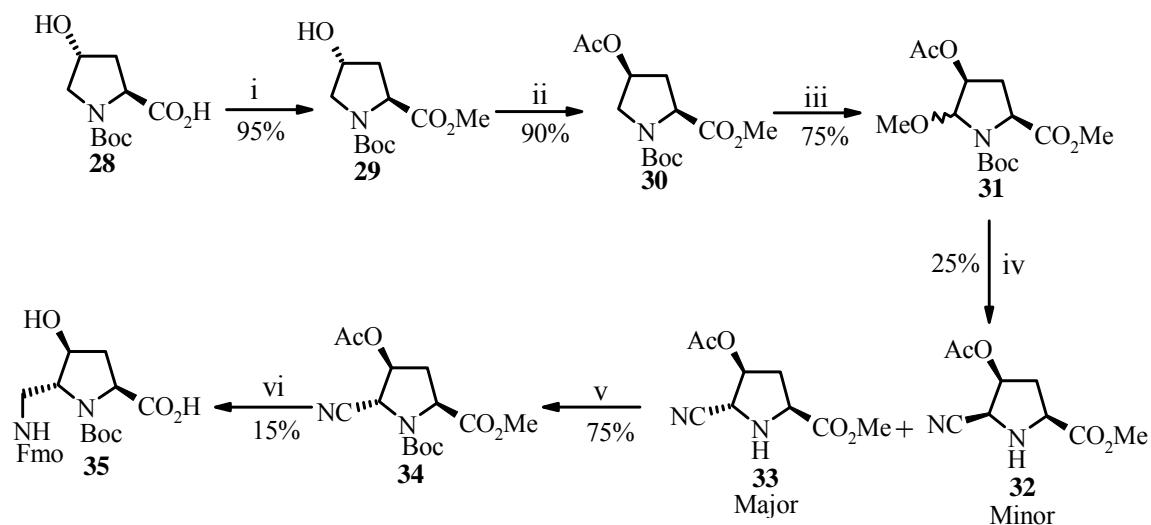
### Rational behind the design

The *amp* monomers (**9**, **10**) and (**22**, **23**) enable the study of the constrain and steric effects on the hybridization properties of incorporated PNA oligomers with complementary DNA. It will not provide any information about conformational effect of the proline ring.

## 2.6 Synthesis of 4-hydroxy aminomethyl prolyl (*amp*) monomer (**35**)

The synthesis of 4-hydroxy *amp*PNA monomer was achieved (Scheme 8a) starting from N-Boc hydroxyproline **28**, which on treatment with DMS/ $\text{K}_2\text{CO}_3$  in acetone afforded the methyl ester of hydroxyproline **29**. This under Mitsunobu conditions using acetic acid yielded the acetate **30**, which on electrochemical anodic oxidation afforded the methoxy compound **31** as a nonseparable diastereomeric mixture. Treatment of **31** with TMSCN in presence of  $\text{BF}_3 \cdot \text{Et}_2\text{O}$  in DCM, furnished the cyano derivatives **32** (minor) and **33** (major).

The ring nitrogen in cyano derivative **33** was protected as Boc by treating with Boc anhydride in DCM employing catalytic amount of DMAP to provide nitrile compound **34**. The configuration at C-5 was assigned from the small coupling constant of H-4 and H-5 as reported in literature. This was subjected to hydrogenation at 60 psi in the presence of Raney/Ni, followed by hydrolysis using 2N NaOH in MeOH to afford the sodium salt of 4-hydroxy aminomethyl proline (not isolated). This on treatment with Fmoc-Cl in presence of 10%  $\text{Na}_2\text{CO}_3$  in dioxane furnished the 4-hydroxy *amp* monomer **35**. Employing  $\text{BF}_3 \cdot \text{Et}_2\text{O}$  during the cyanation reaction afforded the ester compound **33**, as the major isomer, with the diastereomeric ratio being 80:20.



**Reagents and conditions:** (i) Acetone,  $K_2CO_3$  (3 equiv.), DMS (2 equiv.), Reflux 5 h; (ii) THF, DEAD (1.2 equiv.),  $(Ph)_3P$  (1.1 equiv.),  $CH_3CO_2H$  (1.1 equiv.), rt, 8 h; (iii) MeOH, TBATFB, 260 mA, 0-5 °C, 6 h; (iv) DCM,  $BF_3 \cdot Et_2O$  (2.2 equiv.),  $TMSiCN$  (3.5 equiv.), 0 °C-rt, 3 h; (v) DCM,  $(Boc)_2O$ , DMAP (Catalytic), rt, 12 h; (vi) (a) MeOH, RaneyNi,  $NEt_3$  (3 equiv.), 60 Psi, rt, 4 h, (b) MeOH, 2 N NaOH, (c) Dioxane/ $H_2O$ ,  $Na_2CO_3$  (2 equiv.), Fmoc-Cl (1.2 equiv.).

## 2.7 Synthesis of *amp* PNA oligomers

The readily available MBHA resin was chosen as the polymer matrix on which the *aeg* PNA oligomers as well as the *amp* PNA oligomers were assembled. In the present work the orthogonal strategy was employed to construct the *amp* PNA oligomers followed by subsequent attachment of the nucleobases (sub monomer) strategy to monomers at specific positions in the *aeg*-PNA oligomeric sequences. The oligomers were cleaved from the resin, purified by HPLC and characterized by MALDI-TOF.

**Table 1** PNA Oligomers synthesized for the present study

Entry	Sequence code	PNA Sequence
1	<i>aeg</i> PNA <b>57</b>	H-T-T-T-T-T-T-T-(CH <sub>2</sub> ) <sub>2</sub> -CO <sub>2</sub> NH <sub>2</sub>
2	<i>aeg</i> PNA <b>58</b>	H-G-T-A-G-A-T-C-A-C-T-(CH <sub>2</sub> ) <sub>2</sub> -CO <sub>2</sub> NH <sub>2</sub>
3	<i>amp</i> PNA <b>59</b>	H-(t <sub>SR</sub> )-T-T-T-T-T-T-(CH <sub>2</sub> ) <sub>2</sub> -CO <sub>2</sub> NH <sub>2</sub>
4	<i>amp</i> PNA <b>60</b>	H-T-T-T-(t <sub>SR</sub> )-T-T-T-T-(CH <sub>2</sub> ) <sub>2</sub> -CO <sub>2</sub> NH <sub>2</sub>
5	<i>amp</i> PNA <b>61</b>	H-T-T-T-T-T-T-(t <sub>SR</sub> )-(CH <sub>2</sub> ) <sub>2</sub> -CO <sub>2</sub> NH <sub>2</sub>
6	<i>amp</i> PNA <b>62</b>	H-T-T-T-(t <sub>SR</sub> )-T-T-T-(t <sub>SR</sub> )-(CH <sub>2</sub> ) <sub>2</sub> -CO <sub>2</sub> NH <sub>2</sub>
7	<i>amp</i> PNA <b>63</b>	H-T-T-T-(t <sub>SR</sub> )-T-T-T-(t <sub>SS</sub> )-(CH <sub>2</sub> ) <sub>2</sub> -CO <sub>2</sub> NH <sub>2</sub>
8	<i>amp</i> PNA <b>64</b>	H-G-(t <sub>SR</sub> )-A-G-A-(t <sub>SR</sub> )-C-A-C-(t <sub>SR</sub> )-(CH <sub>2</sub> ) <sub>2</sub> -CO <sub>2</sub> NH <sub>2</sub>
9	<i>amp</i> PNA <b>65</b>	H-(t <sub>SR</sub> ) <sub>8</sub> -(CH <sub>2</sub> ) <sub>2</sub> -CO <sub>2</sub> NH <sub>2</sub>
10	<i>amp</i> PNA <b>66</b>	H-(t <sub>SS</sub> )-T-T-T-T-T-T-(CH <sub>2</sub> ) <sub>2</sub> -CO <sub>2</sub> NH <sub>2</sub>
11	<i>amp</i> PNA <b>67</b>	H-T-T-T-(t <sub>SS</sub> )-T-T-T-T-(CH <sub>2</sub> ) <sub>2</sub> -CO <sub>2</sub> NH <sub>2</sub>
12	<i>amp</i> PNA <b>68</b>	H-T-T-T-T-T-T-(t <sub>SS</sub> )-(CH <sub>2</sub> ) <sub>2</sub> -CO <sub>2</sub> NH <sub>2</sub>
13	<i>amp</i> PNA <b>69</b>	H-T-T-T-(t <sub>SS</sub> )-T-T-T-(t <sub>SS</sub> )-(CH <sub>2</sub> ) <sub>2</sub> -CO <sub>2</sub> NH <sub>2</sub>
14	<i>amp</i> PNA <b>70</b>	H-G-(t <sub>SS</sub> )-A-G-A-(t <sub>SS</sub> )-C-A-C-(t <sub>SS</sub> )-(CH <sub>2</sub> ) <sub>2</sub> -CO <sub>2</sub> NH <sub>2</sub>
15	<i>amp</i> PNA <b>71</b>	H-(t <sub>SS</sub> ) <sub>8</sub> -(CH <sub>2</sub> ) <sub>2</sub> -CO <sub>2</sub> NH <sub>2</sub>
16	<i>amp</i> PNA <b>72</b>	H-(t <sub>RS</sub> )-T-T-T-T-T-T-(CH <sub>2</sub> ) <sub>2</sub> -CO <sub>2</sub> NH <sub>2</sub>
17	<i>amp</i> PNA <b>73</b>	H-T-T-T-(t <sub>RS</sub> )-T-T-T-T-(CH <sub>2</sub> ) <sub>2</sub> -CO <sub>2</sub> NH <sub>2</sub>
18	<i>amp</i> PNA <b>74</b>	H-T-T-T-T-T-T-(t <sub>RS</sub> )-(CH <sub>2</sub> ) <sub>2</sub> -CO <sub>2</sub> NH <sub>2</sub>
19	<i>amp</i> PNA <b>75</b>	H-T-T-T-(t <sub>RS</sub> )-T-T-T-(t <sub>RS</sub> )-(CH <sub>2</sub> ) <sub>2</sub> -CO <sub>2</sub> NH <sub>2</sub>
20	<i>amp</i> PNA <b>76</b>	H-G-(t <sub>RS</sub> )-A-G-A-(t <sub>RS</sub> )-C-A-C-(t <sub>RS</sub> )-(CH <sub>2</sub> ) <sub>2</sub> -CO <sub>2</sub> NH <sub>2</sub>
21	<i>amp</i> PNA <b>77</b>	H-(t <sub>RS</sub> ) <sub>8</sub> -(CH <sub>2</sub> ) <sub>2</sub> -CO <sub>2</sub> NH <sub>2</sub>
22	<i>amp</i> PNA <b>78</b>	H-(t <sub>RR</sub> )-T-T-T-T-T-T-(CH <sub>2</sub> ) <sub>2</sub> -CO <sub>2</sub> NH <sub>2</sub>
23	<i>amp</i> PNA <b>79</b>	H-T-T-T-(t <sub>RR</sub> )-T-T-T-T-(CH <sub>2</sub> ) <sub>2</sub> -CO <sub>2</sub> NH <sub>2</sub>
24	<i>amp</i> PNA <b>80</b>	H-T-T-T-T-T-T-(t <sub>RR</sub> )-(CH <sub>2</sub> ) <sub>2</sub> -CO <sub>2</sub> NH <sub>2</sub>
25	<i>amp</i> PNA <b>81</b>	H-T-T-T-(t <sub>RR</sub> )-T-T-T-(t <sub>RR</sub> )-(CH <sub>2</sub> ) <sub>2</sub> -CO <sub>2</sub> NH <sub>2</sub>
26	<i>amp</i> PNA <b>82</b>	H-G-(t <sub>RR</sub> )-A-G-A-(t <sub>RR</sub> )-C-A-C-(t <sub>RR</sub> )-(CH <sub>2</sub> ) <sub>2</sub> -CO <sub>2</sub> NH <sub>2</sub>
27	<i>amp</i> PNA <b>83</b>	H-(t <sub>RR</sub> ) <sub>8</sub> -(CH <sub>2</sub> ) <sub>2</sub> -CO <sub>2</sub> NH <sub>2</sub>
28	<i>amp</i> PNA <b>84</b>	H-(t <sub>SSR</sub> )-T-T-T-T-T-T-(CH <sub>2</sub> ) <sub>2</sub> -CO <sub>2</sub> NH <sub>2</sub>
29	<i>amp</i> PNA <b>85</b>	H-T-T-T-(t <sub>SSR</sub> )-T-T-T-T-(CH <sub>2</sub> ) <sub>2</sub> -CO <sub>2</sub> NH <sub>2</sub>
30	<i>amp</i> PNA <b>86</b>	H-T-T-T-T-T-T-(t <sub>SSR</sub> )-(CH <sub>2</sub> ) <sub>2</sub> -CO <sub>2</sub> NH <sub>2</sub>
31	<i>amp</i> PNA <b>87</b>	H-G-T-A-G-A-(t <sub>SSR</sub> )-C-A-C-T-(CH <sub>2</sub> ) <sub>2</sub> -CO <sub>2</sub> NH <sub>2</sub>

A/G/C/T = *aeg* PNA Adenine/Guanine/Cytosine/Thymine monomers, t<sub>SR</sub> = (2*S*,5*R*)-*amp*-PNA Thymine monomer, t<sub>SS</sub> = (2*S*,5*S*)-*amp* PNA Thymine monomer, t<sub>RS</sub> = (2*R*,5*S*)-*amp*-PNA Thymine monomer, t<sub>RR</sub> = (2*R*,5*R*)-*amp* PNA Thymine monomer, t<sub>SSR</sub> = (2*S*,4*S*,5*R*)-*amp* PNA Thymine monomer

Next chapter describes the hybridization studies of above synthesized *amp/aeg*-PNA oligomers towards DNA and RNA.

## Chapter 3: Hybridizational studies of *amp*-PNA oligomers with complementary DNA /RNA.

### 3.1 Comparison studies of *amp*PNA hybrids with complementary DNA

Various *amp*-PNA derived homopyrimidine (octamers) and mixed purine-pyrimidine oligomers (decamers) were synthesized with different degree of modification (Table 1) to examine the binding efficiency and selectivity towards DNA and RNA. The mixed purine-pyrimidine oligomers (decamers) were synthesized to study the orientational selectivity in binding to DNA and RNA.

The UV- $T_m$  studies with DNA (Table 2) and RNA (Table 3) were carried out with all synthesized oligomers and the  $T_m$  data was compared with the control *aeg*-PNA. The CD spectra of *amp* PNA single strands and corresponding complexes with complementary DNA and RNA were recorded.

**Table 2** UV- $T_m$  ( $^{\circ}$ C) of *amp*-PNA<sub>2</sub>:DNA and *amp*-PNA:DNA complexes

Entry	PNA	$T_m$							
1	H-T-T-T-T-T-T-T-(CH <sub>2</sub> ) <sub>2</sub> -CONH <sub>2</sub>	43							
2	H-GTAGATCACT-(CH <sub>2</sub> ) <sub>2</sub> CONH <sub>2</sub> ( <i>ap</i> )	50							
	H-GTAGATCACT-(CH <sub>2</sub> ) <sub>2</sub> CONH <sub>2</sub> ( <i>p</i> )	48							
		<i>S/R</i>	$\Delta T_m$	<i>S/S</i>	$\Delta T_m$	<i>R/S</i>	$\Delta T_m$	<i>R/R</i>	$\Delta T_m$
3	H-t-T-T-T-T-T-T-T-CH <sub>2</sub> ) <sub>2</sub> -CONH <sub>2</sub>	53	10	47	4	62	18	44	1
4	H-T-T-T-t-T-T-T-T-(CH <sub>2</sub> ) <sub>2</sub> -CONH <sub>2</sub>	35	-8	43	-2	39	-4	36	-5
5	H-T-T-T-T-T-T-T-t-(CH <sub>2</sub> ) <sub>2</sub> -CONH <sub>2</sub>	46	3	50	7	52	9	46	3
6	H-t-T-T-T-t-T-T-T (CH <sub>2</sub> ) <sub>2</sub> -CONH <sub>2</sub>	39	-4	40	-3	44	1	43	-0
7	H-(t t t t t t t t)-(CH <sub>2</sub> ) <sub>2</sub> -CONH <sub>2</sub>	77	34	43	0	46	3	44	1
8	H-G-t-AGA-t-CAC-t-(CH <sub>2</sub> ) <sub>2</sub> CONH <sub>2</sub> ( <i>ap</i> )	43	-7	50	0	52	2	46	-4
	H-G-t-AGA-t-CAC-t-(CH <sub>2</sub> ) <sub>2</sub> CONH <sub>2</sub> ( <i>p</i> )	39	-9	37	-11	48	0	-	-

A/G/C/T = *aeg*-PNA Adenine /Guanine /Cytosine /Thymine monomers,  $t_{SR} = (2S,5R)$ -  $t_{SS} = (2S,5S)$ ,  $t_{RS} = (2R,5S)$ ,  $t_{SS} = (2S,5S)$ -*amp*-PNA Thymine monomer.  $T_m$  values are accurate to ( $\pm$ ) 0.5 $^{\circ}$ C. Experiments were repeated at least thrice and the  $T_m$  values were obtained from the peaks in the first derivative plots.  $\Delta T_m$  indicates the difference in  $T_m$  with the control experiment *aeg*-PNA **57** and PNA **58** (mixed sequence). T and t indicating *aeg* and *amp*-PNA respectively. (measured in the buffer 10 mM sodium phosphate, 10mM NaCl, pH = 7.3), PNA<sub>2</sub>-DNA complexes. DNA **88** = 5'(CGC-AAAAAAAAA-CGC)3' DNA **90** = 5'AGTGATCTAC 3' (*antiparallel*); DNA **91** = 5' CATCTAGTGA 3'(*parallel*).

A single modification of the *amp* monomer unit at center of the sequence destabilized the corresponding DNA triplex except in the case of (2S,5S) *amp* monomer

(Table 2, entry 4). In case of doubly modified *amp*-PNAs (*2S,5S*) and (*2S,5R*) derived *amp* units exhibited destabilization whereas (*2R,5S*) derived *amp* units marginally stabilized the corresponding DNA hybrids (Table 2, entry 6). The triplexes of the *amp*-PNA homooligomers stabilized the corresponding DNA hybrids in comparison to *aeg*-PNA **57**. Homooligomer derived of (*2S,5R*) *amp* monomer unit showed strong stabilization (+34 °C) and a minimal destabilization was observed in case of (*2S,5S*) *amp* monomer (Table 2, entry 7).

The (*2S,5S*) and (*2S,5R*) derived *amp*-PNA:DNA duplex complexes exhibited large destabilization, whereas (*2R,5S*) derived *amp*-PNA:DNA exhibited marginal stabilization in comparison to *aeg*-PNA **58**. The above results are presented in Table 2.

### 3.2 Comparison studies of *amp*-PNA hybrids with the complementary RNA

Unmodified *aeg*-PNA binds to DNA and RNA equally well without appreciable selectivity among these nucleic acids. To see if there is any binding selectivity for *amp*-PNA between DNA and RNA, *amp*PNA<sub>2</sub>:RNA **92** complexes were constituted from *aeg*-PNA-T<sub>8</sub> **57**, and homooligomers. *T<sub>m</sub>* values derived from various *aeg*-PNA and *amp*-PNA sequences with different degrees of modifications are in listed in Table 3.

The *T<sub>m</sub>* values indicate that, a single modification of *amp* (*2S,5S* and *2R,5R*) unit at N-terminus caused destabilization in *amp*-PNA:RNA **92** triplexes, where as corresponding *cis-amp* units stabilized the triplexes (Table 3 entry 1).

A single modification at C-terminus caused stabilization or minimal destabilization (S/R and R/R, Table 3 entry 5) in *amp*-PNA:RNA hybrids. A single modification at center of the sequence exhibited destabilization of the triplexes irrespective of the stereochemistry of the *amp* unit incorporated (Table 3, entry 4).

Homooligomeric (*2S,5S* and *2S,5R*) *amp* PNAs exhibited stabilization, where as (*2S,5R*)-*amp*-PNA caused destabilization of corresponding RNA triplexes. In case of purine, pyrimidine mix sequence, (*2R,5S*)-*amp*PNA oligomers exhibited good stabilization as well as orientational selectivity, where as (*2S,5S*) *amp*-PNA oligomers showed stabilization in antiparallel orientation and destabilized parallel PNA:RNA triplexes (Table 3, entry 8).

**Table 3** UV- $T_m$  ( $^{\circ}\text{C}$ ) of *amp*-PNA<sub>2</sub>:RNA and *amp*-PNA:RNA complexes

Entry	PNA	$T_m$								
1	H-T-T-T-T-T-T-T-(CH <sub>2</sub> ) <sub>2</sub> -CONH <sub>2</sub>	50								
2	H-GTAGATCACT-(CH <sub>2</sub> ) <sub>2</sub> CONH <sub>2</sub> ( <i>ap</i> )	53								
	H-GTAGATCACT-(CH <sub>2</sub> ) <sub>2</sub> CONH <sub>2</sub> ( <i>p</i> )	49								
		<i>S/</i>	$\Delta$	<i>S/S</i>	$\Delta$	<i>R/</i>	$\Delta$	<i>R/</i>	$\Delta$	
		<i>R</i>	<i>Tm</i>		<i>Tm</i>	<i>S</i>	<i>Tm</i>	<i>R</i>	<i>Tm</i>	
3	H- <b>t</b> -T-T-T-T-T-T-T-CH <sub>2</sub> ) <sub>2</sub> -CONH <sub>2</sub>	52	2	38	-12	56	6	49	-4	
4	H-T-T-T-T- <b>t</b> -T-T-T-T-(CH <sub>2</sub> ) <sub>2</sub> -CONH <sub>2</sub>	33	-18	48	-2	46	-4	43	-7	
5	H-T-T-T-T-T-T-T- <b>t</b> -(CH <sub>2</sub> ) <sub>2</sub> -CONH <sub>2</sub>	49	-1	51	1	52	2	45	-5	
6	H- <b>t</b> .T-T-T- <b>t</b> -T-T-T (CH <sub>2</sub> ) <sub>2</sub> -CONH <sub>2</sub>	ND		ND	-	50		44	-6	
7	H-( <b>tttttttt</b> ) -(CH <sub>2</sub> ) <sub>2</sub> -CONH <sub>2</sub>	40	-10	52	2	49	-1	ND		
8	H-G- <b>t</b> -AGA- <b>t</b> -CAC- <b>t</b> -(CH <sub>2</sub> ) <sub>2</sub> CONH <sub>2</sub> ( <i>ap</i> )	44	-9	50	-3	59	6	ND		
9	H-G- <b>t</b> -AGA- <b>t</b> -CAC- <b>t</b> -(CH <sub>2</sub> ) <sub>2</sub> CONH <sub>2</sub> ( <i>p</i> )	40	-9	42	-7	51	2			

$\Delta T_m$  Indicate the difference in  $T_m$  with the control experiment *aeg*-PNA **57** and PNA **58** (mixed sequence). (measured in the buffer 10 mM sodium phosphate, 10 mM NaCl, pH = 7.3), PNA<sub>2</sub>-DNA complexes. A/G/C/T = *aeg*PNA Adenine /Guanine /Cytosine /Thymine monomers,  $t_{SR} = (2S,5R)$ -  $t_{SS} = (2S,5S)$ ,  $t_{RS} = (2R,5S)$ ,  $t_{SS} = (2S,5S)$ -*amp*PNA Thymine monomer The values reported here are the average of 3 independent experiments and are accurate to  $\pm 0.5^{\circ}\text{C}$ . T and **t** indicating *aeg* and *amp*-PNA respectively. RNA **92** = 5'CGCA<sub>8</sub>CGC3'; RNA **93** = 5'AGUGAUCUAC 3'; RNA **94** = 5'CAUCUAGUGA3'.

### 3.3 Studies of (2*S*,4*S*,5*R*)-*amp*-PNA:DNA and (2*S*,4*S*,5*R*)-*amp*-PNA:RNA hybrids

UV melting temperatures (Ttable 4) of these *amp*-PNAs with complementary DNA and RNA indicated that N-terminal modification stabilized both (2*S*,4*S*,5*R*)-*amp*-PNA:DNA and (2*S*,4*S*,5*R*)-*amp*-PNA:RNA triplexes by 6  $^{\circ}\text{C}$  and 2  $^{\circ}\text{C}$  respectively in comparison to *aeg*-PNA **57**.

Middle modification of (2*S*,4*S*,5*R*)-*amp*-PNA exhibited the 2  $^{\circ}\text{C}$  of stabilization with DNA but a large destabilization was observed in case of RNA. C-terminal modification of (2*S*,4*S*,5*R*)-*amp*-PNA stabilized the (2*S*,4*S*,5*R*)-*amp*-PNA<sub>2</sub>:DNA **88** complex by 7  $^{\circ}\text{C}$  whereas same modification exhibited large destabilization with RNA triplexes.

Thus (2*S*,4*S*,5*R*)-*amp*-PNA:DNA triplexes demonstrated more stability for DNA than RNA triplexes. These results are summarized in Table 4.

Table 4 UV- $T_m$  ( $^{\circ}\text{C}$ ) of *amp*-PNA:DNA and *amp*-PNA:RNA hybrids

Entry	PNA	DNA $T_m$ (control)	RNA $T_m$ (control)		
1	H-T-T-T-T-T-T-T-(CH <sub>2</sub> ) <sub>2</sub> -CONH <sub>2</sub>	43	50		
2	H-GTAGATCACT-(CH <sub>2</sub> ) <sub>2</sub> CONH <sub>2</sub> ( <i>ap</i> )	50 ( <i>ap</i> )	53 ( <i>ap</i> )		
	H-GTAGATCACT-(CH <sub>2</sub> ) <sub>2</sub> CONH <sub>2</sub> ( <i>p</i> )	48 ( <i>p</i> )	49 ( <i>p</i> )		
				$\Delta T_m$	$\Delta T_m$
3	H-t-T-T-T-T-T-T-CH <sub>2</sub> ) <sub>2</sub> -CONH <sub>2</sub>	48.50	52	6	2
4	H-T-T-T-t-T-T-T-(CH <sub>2</sub> ) <sub>2</sub> -CONH <sub>2</sub>	45	40	2	-10
5	H-T-T-T-T-T-T-t-(CH <sub>2</sub> ) <sub>2</sub> -CONH <sub>2</sub>	49.50	49	7	-1
6	H-G-T-AGA-t-CAC-T-(CH <sub>2</sub> ) <sub>2</sub> CONH <sub>2</sub> ( <i>ap</i> )	55 ( <i>ap</i> )	50( <i>ap</i> )	5	-3
7	H-G-T-AGA-t-CAC-T-(CH <sub>2</sub> ) <sub>2</sub> CONH <sub>2</sub> ( <i>p</i> )	53 ( <i>p</i> )	47 ( <i>p</i> )	5	-2

$\Delta T_m$  Indicate the difference in  $T_m$  with the control experiment *aeg*-PNA **57** and PNA **58** (mixed sequence). (measured in the buffer 10 mM sodium phosphate, 10 mM NaCl, pH = 7.3), PNA<sub>2</sub>-DNA complexes. A/G/C/T = *aeg*PNA Adenine /Guanine /Cytosine /Thymine monomers,  $t_{SR} = (2S,5R)$ -  $t_{SS} = (2S,5S)$ ,  $t_{RS} = (2R,5S)$ ,  $t_{SS} = (2S,5S)$ -*amp*PNA Thymine monomer. The values reported here are the average of 3 independent experiments and are accurate to  $\pm 0.5^{\circ}\text{C}$ . T and t indicating *aeg* and *amp*-PNA respectively. RNA **92** = 5'CGCA<sub>8</sub>CGC3'; RNA **93** = 5'AGUGAUCUAC3'; RNA **94** = 5' CAUCUAGUGA3'.

### 3.4 Studies of duplex hybrids of (2S,4S,5R)-*amp*-PNAs

To see the *parallel* and *antiparallel* orientational preferences of PNA:DNA and PNA:RNA binding, mixed purine pyrimidine sequence (2S,4S,5R)-*amp*-PNA **87** was synthesized. The duplex complexes of (2S,4S,5R)-*amp*-PNA **87** with DNA **90** and **91** stabilized by 5  $^{\circ}\text{C}$  in comparison to un modified *aeg*-PNA **58**. No selectivity was observed between *antiparallel* and *parallel* mode of binding orientation.

In case of RNA, destabilization was observed in both orientations by -3  $^{\circ}\text{C}$  (*ap*) and -1  $^{\circ}\text{C}$  (*p*) in comparison to *aeg*-PNA **58**. These results suggest that (2S,4S,5R)-*amp*-PNAs having more affinity towards DNA than the RNA. The above results are presented in Table 4.

## Chapter 4

### 4.1 Section 1: Introduction to (2,5)-disubstituted pyrrolidines

2,5-Dialkylated pyrrolidines extracted from venomous ants and frogs have shown insecticide hemolytic and antiendinergetic activities. Polyhydroxy pyrrolidines isolated from several plants of the *companulaceae* and *fabaceae* families have shown very potent activity as enzyme inhibitors (e.g. codonosine).

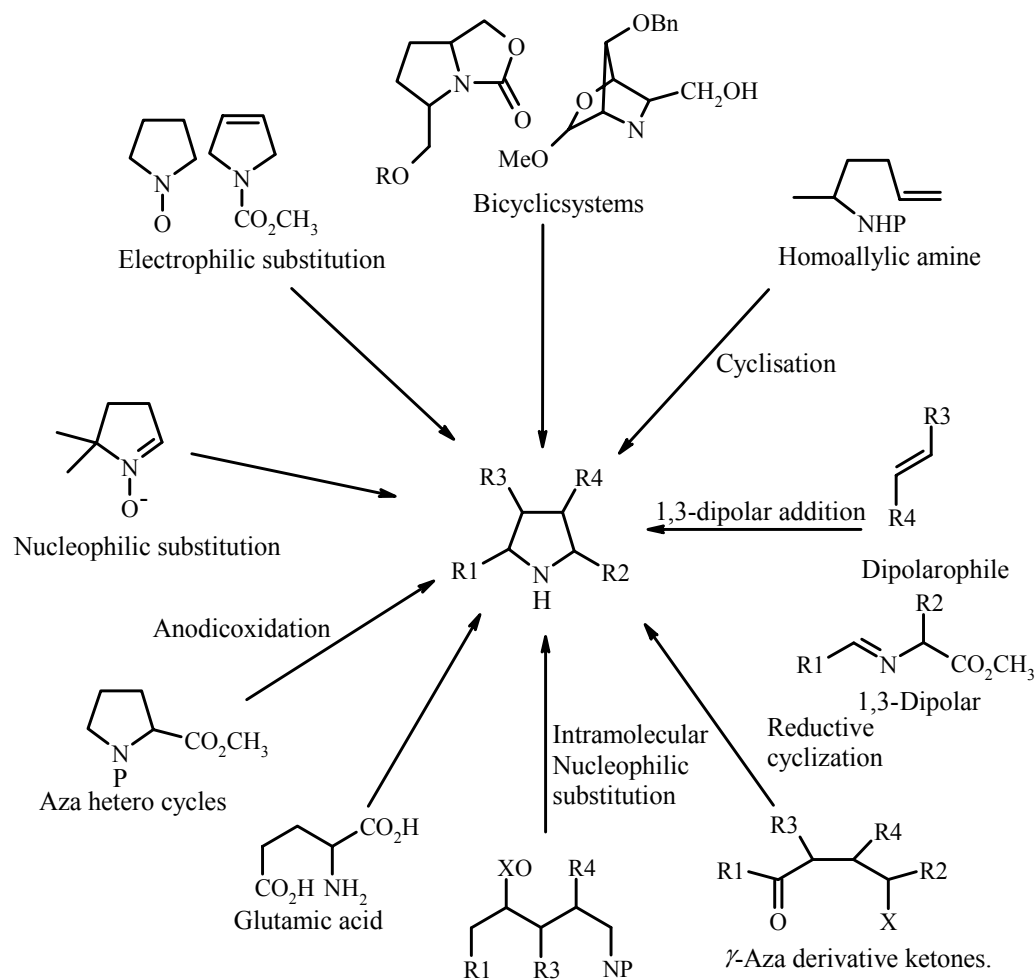


**Figure 5** Various pathways for the synthesis of substituted pyrrolidines

Apart from the medicinal uses, these compounds possessing a  $C_2$  symmetry axis, may be used as very powerful catalyst in numerous asymmetric reactions. All these reasons make these compounds interesting targets for synthetic chemist.

This section briefly presents the stereoselective synthesis of 2,5-disubstituted pyrrolidines and will be subdivided in two main sections : (1) where the 5-membered ring is formed by stereospecific methods and (2) where the already formed ring is functionalized at the 2<sup>nd</sup> and 5<sup>th</sup> positions.

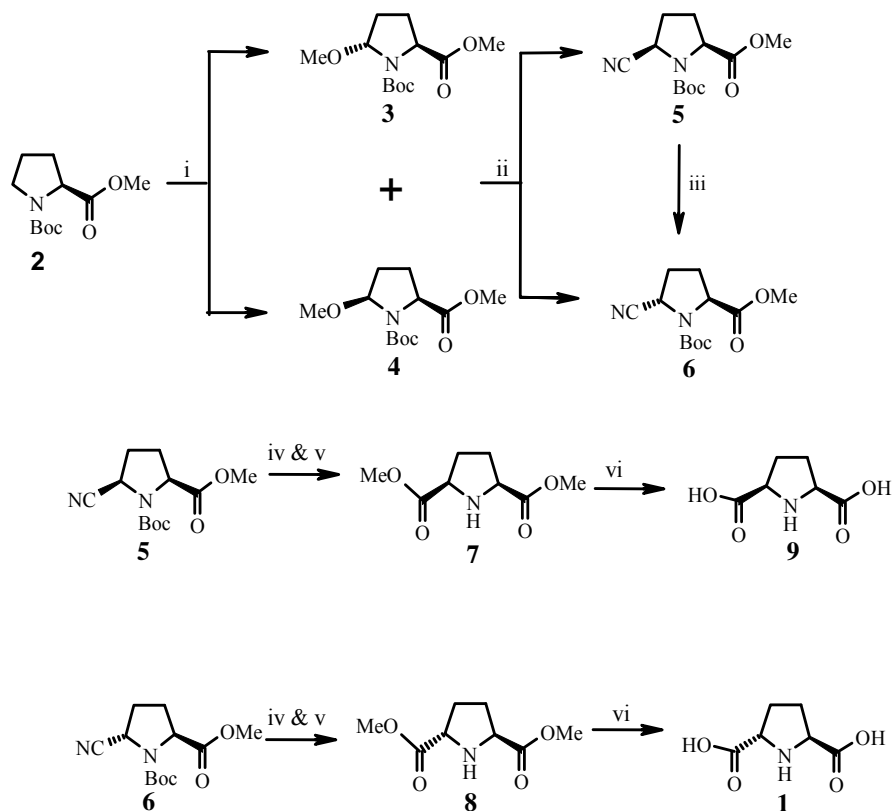
## 4.2 Section II

This section describes the chemical studies towards the synthesis of (2*S*,5*S*)-Pyrrolidine dicarboxylic acid and (2*S*,4*S*,5*R*)-Bulgecinine.

### 4.2.1 Synthesis of (2*S*,5*S*)-Pyrrolidine dicarboxylic acid

The methyl ester of BOC-protected (*S*)-proline **2** on stereoselective electrochemical oxidation at 230 mA current in methanol using tetrabutylammonium tetrafluoroborate (TBATFB) as an electrolyte furnished mixture of 5-methoxylated proline derivatives **3** and **4** in 7:3 ratio (by <sup>1</sup>H NMR) with 95% yield. The mixture of diastereomers **3** and **4** was not separable using column chromatography.

The mixture of compounds **3** plus **4** on treatment with trimethylsilyl cyanide (1.1 equiv) in CH<sub>2</sub>Cl<sub>2</sub> at -30 °C gave the mixture of cyano compounds **5** and **6**. The *trans*-cyanoester **6** in refluxing 6 N hydrochloric acid yielded the hydrochloride salt of the natural product **1** in 92% yield. The hydrochloride of **1** on reaction with methanol-thionyl chloride followed by base induced neutralization of formed hydrochloride yielded the *trans* dimethyl ester **8** in 75% yield, which on refluxing in water for 24 hours furnished the natural product (2*S*,5*S*)-pyrrolidine-2,5-dicarboxylic acid (**1**) in 92% yield



*Reagents and conditions* (i) Electrochemical oxidation (Carbon electrode, 230 mA/28 cm<sup>2</sup>), MeOH, TBATFB (0.5 M solution), 0-15 °C, 10 h (95% , **3**:**4** = 7:3); (ii) TMSOTf (0.1 equiv), TMSiCN (1.1 equiv), DCM, - 35 °C, 30 min (70%, **5**:**6** = 3:7); (iii) *t*-BuOK (1 equiv), THF, rt, 6 h (80%, racemic mixture); (iv) 6 N HCl, reflux, 24 h (92%); (v) SOCl<sub>2</sub>, MeOH, rt, 12 h (75%); (vi) H<sub>2</sub>O, reflux, 24 h (92%).

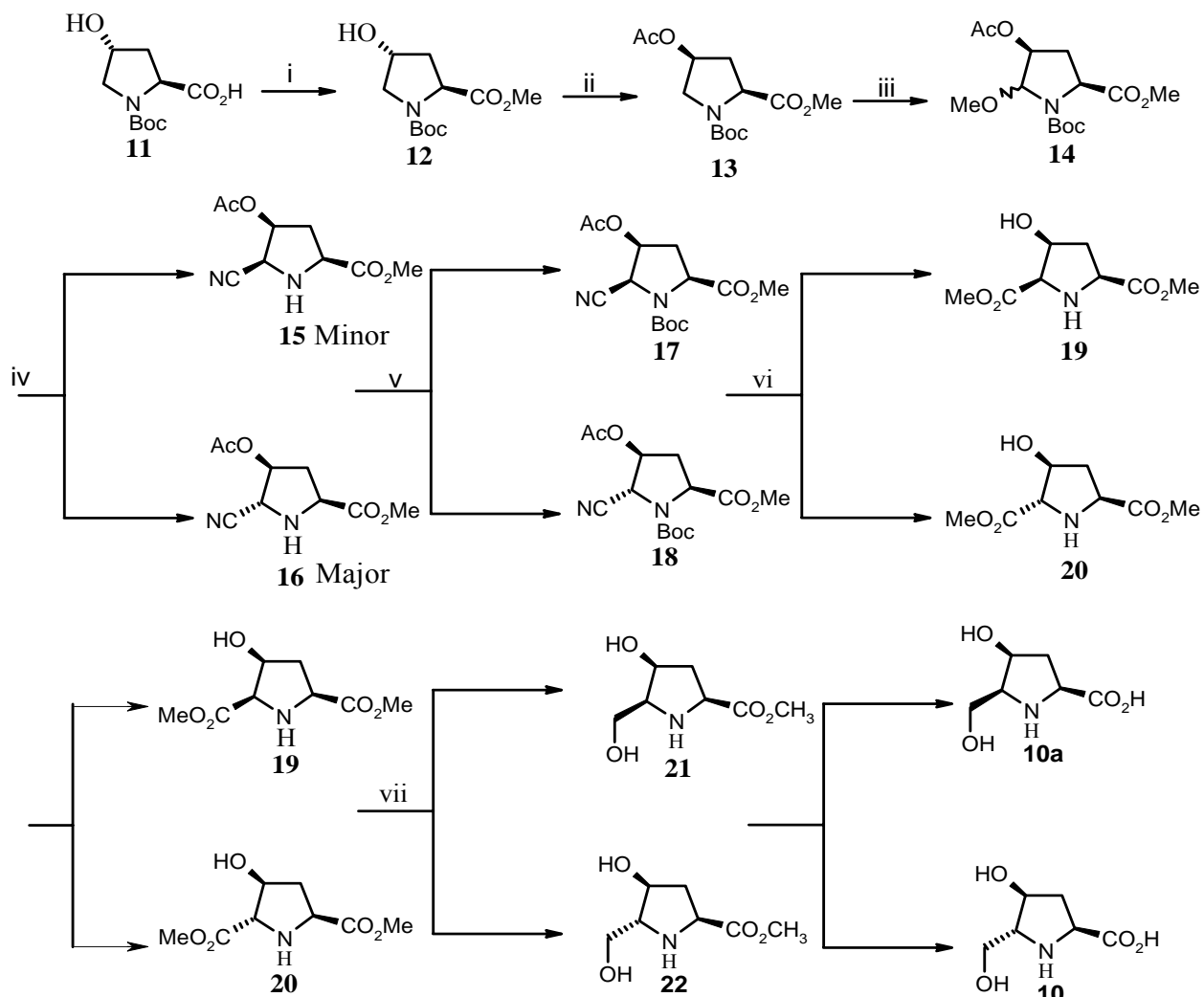
### Scheme 8 Synthesis of (2*S*,5*S*)-Pyrrolidine dicarboxylic acid

## 4.3 Synthesis of Bulgecinine

Synthesis of (2*S*,4*S*,5*R*) Bulgecinine was carried out as in Scheme 8 by employing 4-hydroxy proline as a starting material. On treatment with DMS (dimethylsulphate), K<sub>2</sub>CO<sub>3</sub> in acetone furnished proline ester **12**, which under Mitsunobu conditions using acetic acid furnished proline ester **13**. Subjecting ester **13** to electrochemical oxidation 5-methoxyproline ester **14** was obtained as non-separable diastereomeric mixture. This on treatment with TMSiCN/TMSOTf in DCM gave 5-nitrile proline ester as separable mixture.

Nitrile **15** and **16** (major) were converted to diester compounds **19** and **20** by refluxing in 6 N HCl followed by esterification using SOCl<sub>2</sub> in MeOH. The configuration at C-5 was assigned from the small coupling constant of H-4 and H-5 of compounds **17**

and **18** as reported in literature. Diester **20** on treatment with with  $\text{BH}_3\text{-DMS}$  and  $\text{NaBH}_4$  in THF gave 5-methyl hydroxyl ester **22**. Conversion of **22** and **21** to desired **10** and **10a** are in progress.



*Reagents and conditions:* (i) Acetone,  $\text{K}_2\text{CO}_3$  (3 equiv.), DMS (2 equiv.), Reflux 5 h; (ii) THF, DEAD (1.2 equiv),  $(\text{Ph})_3\text{P}$  (1.1 equiv.),  $\text{CH}_3\text{CO}_2\text{H}$  (1.1 equiv), rt, 8 h; (iii) MeOH, TBATFB, 260mA, 0-5 °C, 6 h; (iv) DCM, TMSO-tf (3 equiv.), HMDS (2.5 equiv.), TMSiCN (3.5 equiv.); (v) DCM,  $(\text{Boc})_2\text{O}$ , DMAP (cat), rt, 6h; (vi) (a) 6 N HCl, reflux, 12 h, (b)  $\text{SOCl}_2$ , MeOH, rt, 16 h; (vii) THF,  $\text{BH}_3\text{-DMS}$ ,  $\text{NaBH}_4$  (cat), rt 50h.

**Scheme 9** Synthesis of Bulgecinine

---

## **CHAPTER 1**

### **INTRODUCTION**

---

## 1.1 Nucleic Acids: Chemical Structure

Nucleic acids are long, thread like biopolymers, dominating the modern molecular science after the Watson-Crick discovery of the double helical structure of DNA.<sup>1</sup> Their vital roles are fundamental for the storage and transmission of genetic information within cells and contain all information required for transmission and execution of steps necessary to make proteins which are another important class of biopolymers, important for cellular function. Nucleic acids are made up of a linear array of monomers called nucleotides.

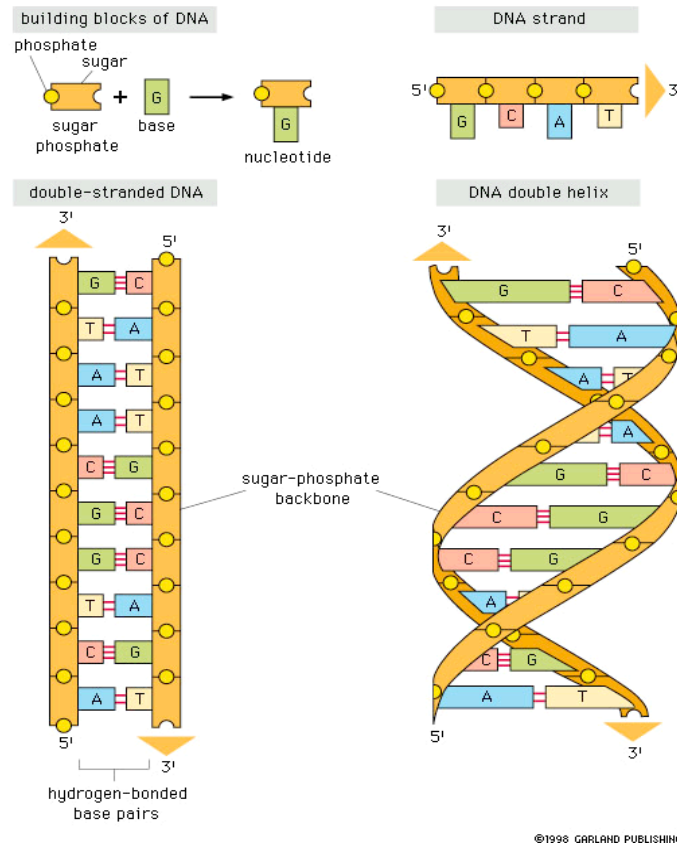


**Figure 1:** Model of DNA

Self-recognition by nucleic acids through complementary base pairing is one of the fundamental processes in biological systems.<sup>2</sup> DNA is the basic genetic material, consisting of two complementary strands held together by Watson-Crick hydrogen bonds through the donor-acceptor sites of the four nucleobases A, T, G and C (Figure 2). All biological functions of DNA take place via molecular recognition. The structure of the double-stranded DNA allows it to have a number of molecular interactions through electrostatic, intercalation<sup>3,4</sup> and groove binding mechanisms<sup>5-7</sup> (Figure 3) with other molecules such as proteins, drugs, metal ions etc. Such molecular recognitions mediated by weak non-covalent interactions are important in regulating the biological functions.

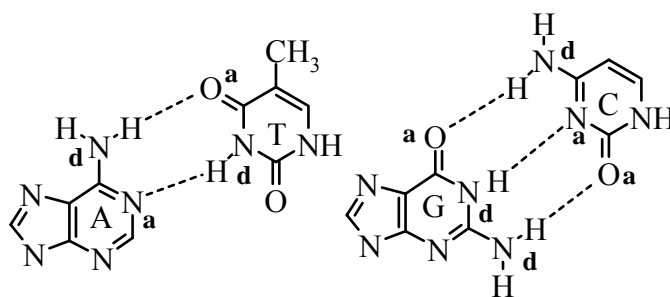


**Figure 2:** Base pair recognition by Watson-Crick Hydrogen bonding

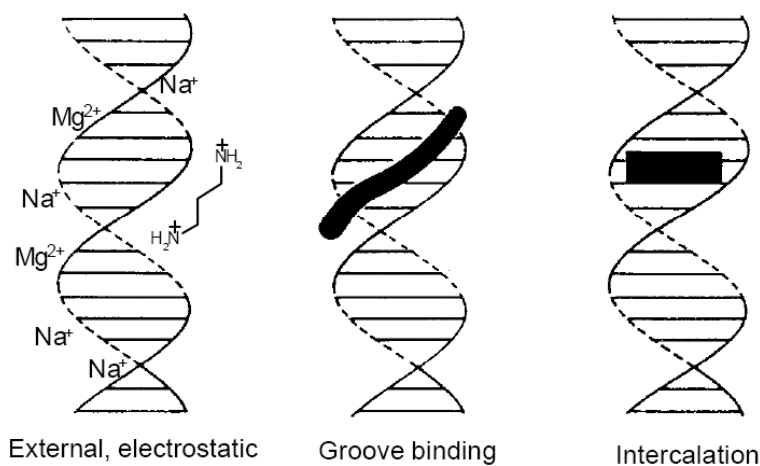


**Figure 3** The three primary binding modes seen in DNA

## 1.2 Oligonucleotide as therapeutic agents

The concept of 'antisense oligonucleotides' as potential therapeutic agents<sup>8</sup> introduced by Zamecnik and Stephenson<sup>9</sup> has aroused much interest in search of potent DNA mimics. Antisense oligonucleotides (Figure 4) recognize a complementary sequence on target m-RNA through Watson-Crick base pairing and form a duplex (RNA-DNA hybrid) that is not processed by the protein synthesis machinery and hence would retard the expression of the corresponding protein. When target proteins are disease related, this will have a therapeutic value.

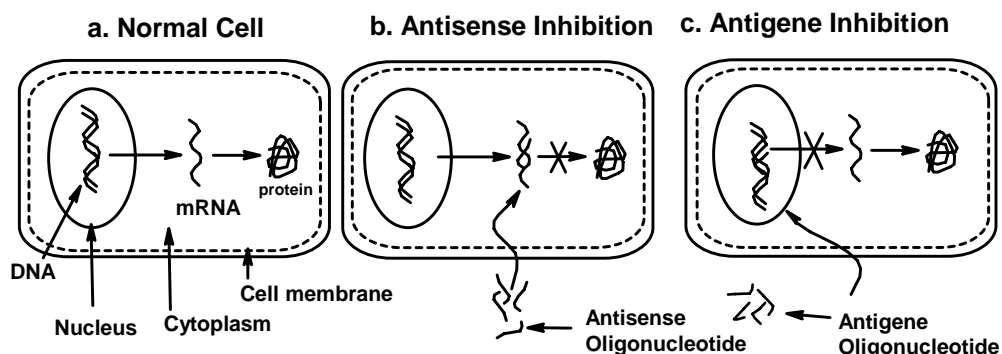


**Figure 4:** Mechanism of action of antisense and antigene oligonucleotides

In another approach, the 'antigene strategy', (Figure 4) obstruction of gene expression can be achieved by binding of oligonucleotides to duplex DNA through Hoogsteen hydrogen bonds (Figure 5) leading to the formation of a triple helix.<sup>10</sup> Thus the double stranded DNA itself can act as a target for the third strand oligonucleotides or

analogues and the limitation for triplex formation is that it is possible only at homopurine stretches of DNA.<sup>10, 11</sup>

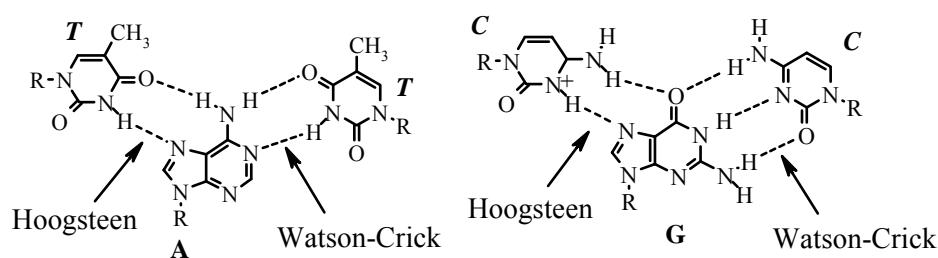


**Figure 5** Triplexes involving Hoogsteen and Watson-Crick base pairing

In order for the triplex strategy to be effective, it requires oligonucleotides that effectively compete with ligands bound to DNA. Hence one of the major research goals is to achieve better triplex forming abilities with modified oligonucleotides. Triplex-forming oligonucleotides (TFOs) that bind DNA in a sequence-specific manner may provide an effective way to modulate selectively gene expression via transcriptional repression, mutagenesis and recombination.<sup>12-14</sup> Binding of a TFO requires the presence of a relatively long and uninterrupted homopurine:homopyrimidine tract in DNA to ensure optimal stability and specificity of the triple helical complex.<sup>12-14</sup>

The prime requisites for oligonucleotides to be effective as antisense oligonucleotides are (a) they should have high specificity to the RNA template, the sense strand, (b) improved cellular uptake and (c) resistance to cellular enzymes eg. Nucleases and proteases. The latter attribute (b and c) are also necessary for the access of antigene drugs.

Natural oligonucleotides have been shown to exhibit both antisense and antigene properties *in vitro*.<sup>15</sup> However, a serious drawback that limits the use of oligonucleotides as therapeutic agents is that they are rapidly degraded by nucleases *in vivo*.<sup>15a</sup>

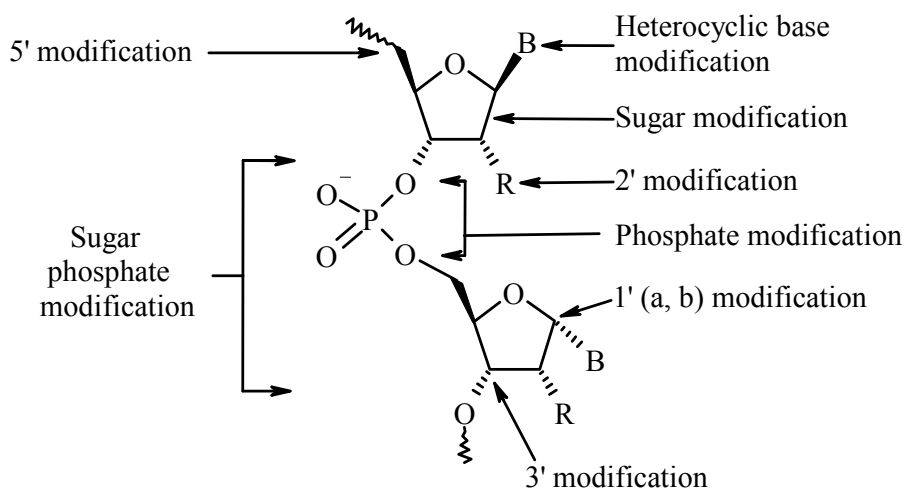


**Figure 6** Structurally possible various DNA modifications

This has led to several chemical modifications<sup>15</sup> of the oligonucleotide structure to impart them the resistance towards cellular enzymes.<sup>16</sup> The various possible sites of modifications in a nucleotide are shown in Figure 6.

### 1.3 Chemical Modifications of DNA

#### 1.3.1 Phosphate modified linkages

The first generation backbone modifications and the most widely studied and effective analogue is the phosphorothioate. Although first introduced into DNA enzymatically by Eckstein and co-workers the phosphoramidite method followed by thiolation has greatly facilitated the synthesis of these ODNs.

In the first generation ‘antisense oligonucleotides’ (Figure 7) the phosphodiester backbone has been replaced by phosphorothioates **1a**, phosphorodithioates **1b**, methyl phosphonates **1c**, hydroxymethyl phosphonates **2**, phosphotriesters **3**, and phosphoramidates **4** as shown in Figure 7. The backbone modifications displayed a greatly improved resistance towards nucleases<sup>17</sup> and a therapeutic agent based on phosphorothioates already has been approved as a drug by US FDA.<sup>18</sup> The chemical modifications also modulate the binding ability of analogs to complementary sequences.

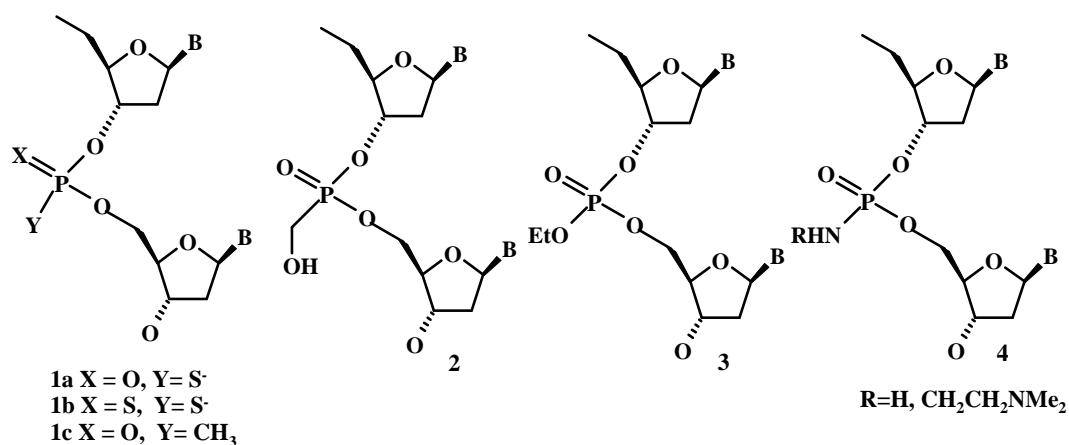


**Figure 7** Phosphate modifications

### 1.3.2 Oligonucleotides with backbones not containing phosphorous

To increase the nuclease resistance and binding affinity, several modifications have been introduced. In which the four atom chain W, X, Y and Z in DNA phosphodiester backbone of **5** has been replaced by other combination of atoms (Figure

8). Only a few of these phosphodiester mimics have shown good binding but none showed the potential to be a good drug.

The second generation modifications comprises of backbone replacements involving elimination of phosphorous atom from the phosphodiester backbone (Figure 8). A common problem for all anionic analogs is the ineffective permeation of cellular membranes. Anionic ODNs are taken up by endosomes, but are unable to cross the endosomal membrane in the absence of cationic lipids.<sup>19</sup> Based on this observation, neutral isosters of the phosphodiester linkage (Figure 8) have been designed.<sup>20</sup> An increasing number of neutral ODN analogs have been developed that do not contain stereogenic phosphorous centers.<sup>21</sup> Substitution of the PO linkage with neutral SO<sub>2</sub> group resulted in a series of sulfonyl containing linkages. Sulfones **1**<sup>22a</sup>, sulfonamides **2**<sup>22b</sup> and sulfamates **3**<sup>22c</sup> (Figure 8) have been prepared as ODN analogs, but very little in vitro and cellular data are available.

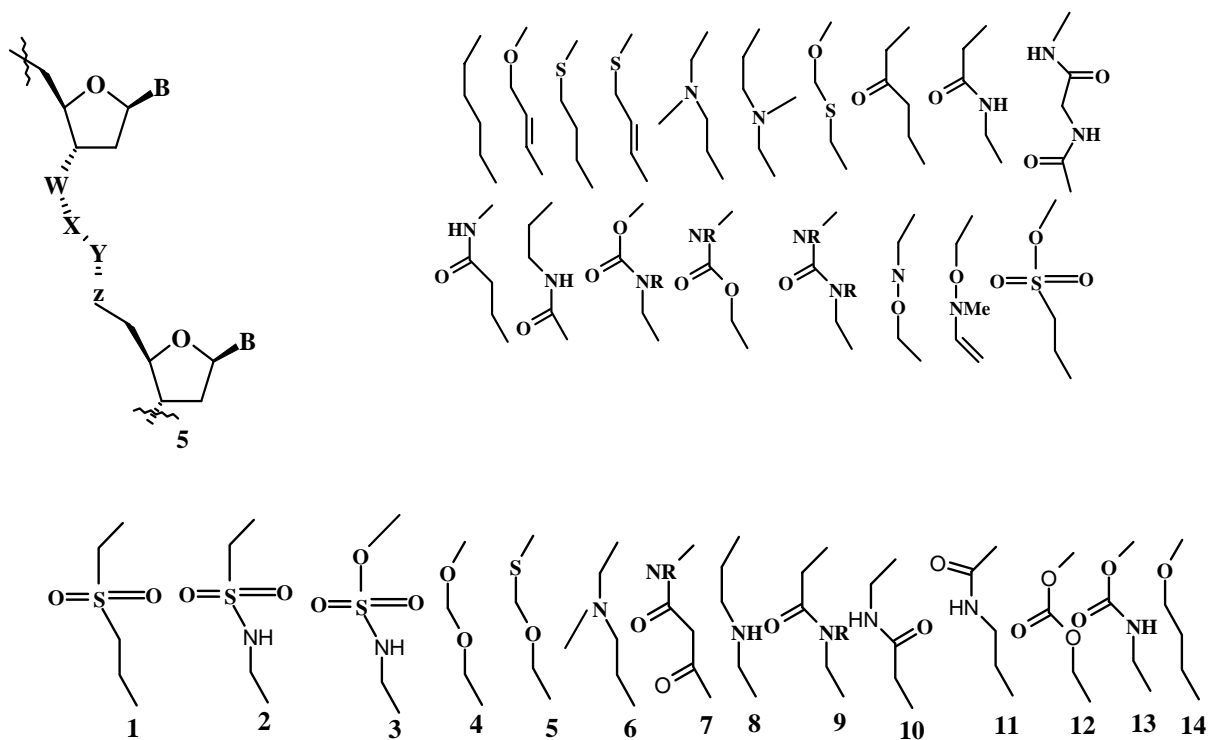


**Figure 8:** Phosphodiester linkage modifications

The formacetal linkage **4** exhibits somewhat inferior sequence specific binding affinities.<sup>23</sup> Slightly increased RNA binding properties were observed with the 3'-thio formacetal **5**<sup>24</sup> and N-methylhydroxylamine **6**<sup>25</sup> linkages. 5'- thioformacetal containing ODNs do not hybridize as well as the unmodified ODNs to either RNA or DNA. Replacement of the PO backbone by amide groups **7-11** resulted in neutral and achiral linkages that were tested for RNA binding and nuclease stability. Analogs **9** and **11** were identified as having good binding affinity to the RNA targets and high stability towards cellular nucleases.<sup>26</sup> Modifications of the 2'-position with a methoxy provided ODNs with even greater binding affinity and nuclease stability.<sup>27</sup> Carbonate **12** and carbamate **13** linkages have also been reported as replacements for the PO backbone. The carbonate linkage has been prepared as dimer, but no biochemical data is available. The 5'-N-

carbamate linkage **13** is chemically stable, and cytidine hexamers were found to bind complementary DNA and RNA with high affinity,<sup>28a</sup> However the thymidine hexamer carbamate ODN bound nucleic acid targets with relatively low affinity.<sup>28b</sup> Replacement of the PO linkage with an acetylenic bond **14** resulted in decreased RNA affinity.<sup>29</sup>

### 1.3.3 Boranophosphate DNA

These are designed by replacing one of the non-bridging oxygen atoms in the phosphodiester group of DNA with borane (BH<sub>3</sub>) (Sood et al., 1990; Spielvogel et al., 1991; Sergueev et al., 1998) (Figure 9). The boranophosphate diester is isoelectronic with phosphodiester, isosteric with the methylphosphonate group and is chiral. These negatively charged oligos are highly water soluble, but more lipophilic than DNA.

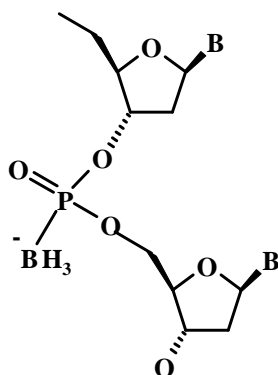


**Figure 9:** Structure of boranophosphate DNA

### 1.4 Sugar modifications

Sugar modifications have also been used to enhance stability and affinity. The  $\alpha$ -anomer of a 2'-deoxyribose sugar has the base inverted with respect to the natural anomer

(Figure 10). ODNs containing ((-anomer sugars are resistant to nuclease degradation and bind in a parallel mode to the RNA target.<sup>30</sup>

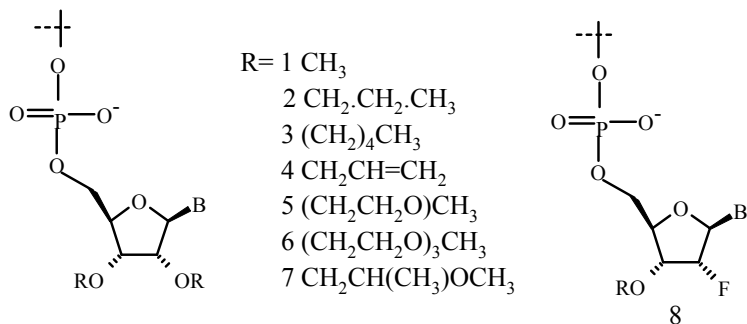


**Figure 10** 2' modified oligonucleotides

### 1.4.1 Sugar skeleton modifications

Apart from the 2' modifications of sugar moiety the other modifications related to sugar skeleton are hexitol nucleic acids (HNA), D-AltrioI nucleic acids (ANA), pentapyranosyl, and threofuranosyl (TNA).

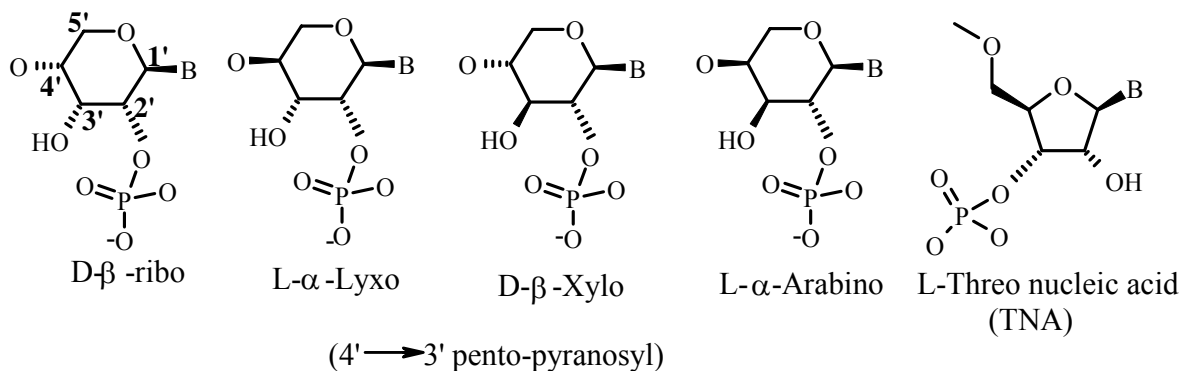


**Figure 12** The family of four (4' → 3') penta-pyranosyl and threofuranosyl oligonucleotides

The first two modifications were discovered by Herdewijn et al,<sup>31a</sup> and the later two modifications were introduced by Eschenmoser group. The (l)-α-lyxopyranosyl-(4' to 3')-oligonucleotide system a member of a pentopyranosyl oligonucleotide family

containing a shortened backbone is capable of cooperative base-pairing and of cross-pairing with DNA and RNA. In contrast, the corresponding (d)-D-ribofuranosyl-(4'(3')-oligonucleotides do not show base-pairing under similar conditions.<sup>31b</sup>

### 1.5 Locked nucleic acids (LNA)

LNA is a bicyclic nucleic acid where a ribonucleoside is linked between the 2'-oxygen and the 4'-carbon atoms with a methylene unit (Figure 13). Locked Nucleic Acid (LNA) was first described by Wengel<sup>32</sup> and Imanishi<sup>33a</sup> et al in as a novel class of conformationally restricted oligonucleotide analogues.

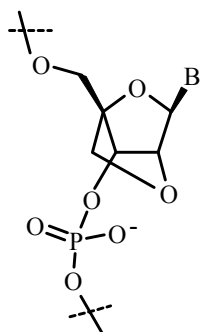


**Figure 13** Locked nucleic acid (LNA)

The design and ability of oligos containing locked nucleic acids (LNAs) to bind super coiled, double-stranded plasmid DNA in a sequence-specific manner has been described by Hertoghs et al<sup>33b</sup> for the first time. The main mechanism for LNA oligos binding to plasmid DNA is demonstrated to be by strand displacement. LNA oligos are more stably bound to plasmid DNA than similar peptide nucleic acid (PNA) 'clamps' for procedures such as particle mediated DNA delivery (gene gun).

### 1.6 Carbocyclic nucleic acid

In carbocyclic nucleic acids, the furanose ring is completely replaced by saturated cycloalkane or cycloalkene rings. The replacement of the furanose moiety of DNA by a cyclohexene ring gives cyclohexene nucleic acids (CeNA).<sup>34</sup>

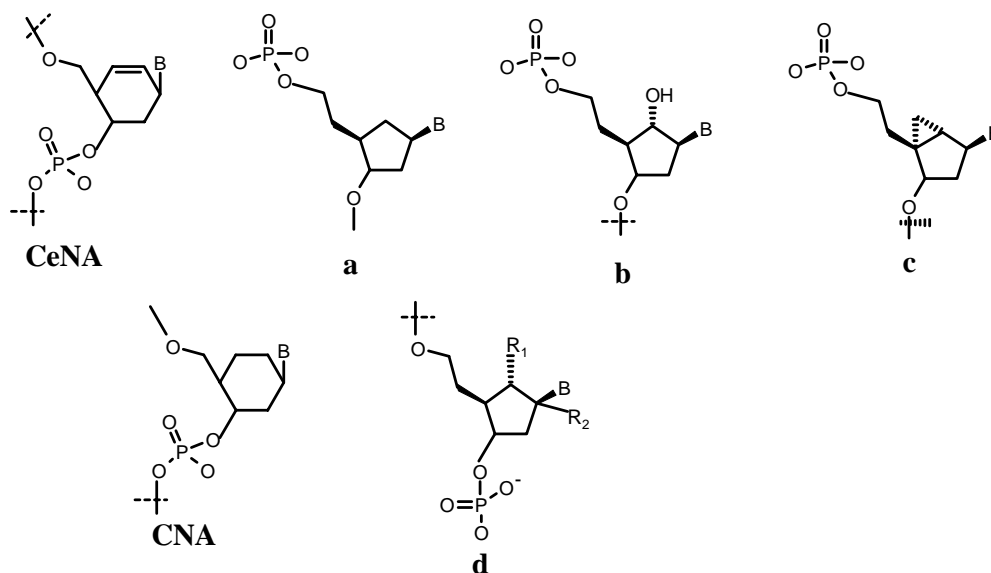


**Figure 14** Carbocyclic analogues

Incorporation of cyclohexenyl nucleosides in a DNA chain increases the stability of a DNA/RNA hybrid. CeNA is stable against degradation in serum and a CeNA/RNA hybrid is able to activate *E. Coli* RNase H, resulting in cleavage of the RNA strand. In case of carbocyclic pyranosyl analogues, cyclohexanyl-nucleic acid (CNA, Figure 14) was prepared in both enantiomeric (D/L) forms and D-CNA hybridizes to complementary RNA as compared to DNA with reduced affinity.

### 1.7 Morpholino nucleosides

So far, only a few attempts to replace the entire (deoxy) ribose phosphate backbone have been successful. One of these is the morpholino oligomer (Figure 15) wherein the monomers are linked through a carbamate linkage.<sup>35a</sup> The second generation



Backbone analogues	Activation of Rnase H	Resistant to Nuclease	Chiral center
<b>Phosphorous Analogues</b>			
Phosphodiester	Yes	-	NO
Phosphorothioate	Yes	+	Yes
Phosphorodithioate	Yes	++	NO
Methylphosphonoate	NO	++	Yes
Phosphoramidate	NO	+	Yes
Alkylphosphoro triester	NO	+	Yes
<b>Non- Phosphorous Analogues</b>			
Sulfamate	NO	++	NO
3'-Thio formacetal	NO	++	NO
Methylene methylimino	NO	++	NO
3'-N-carbamate	NO	++	NO
Morpholino carbamate	NO	++	NO
Peptide Nucleic acids	NO	++	NO

-Rapidly degraded by Nuclease, + Resistant to Nuclease, ++ NO nuclease degradation

## 1.8 Base modifications

Modification of the heterocyclic bases may enhance binding affinity with the complementary RNA fragment via WC bonding or with the duplex DNA via Hoogsteen bonding and may impart nuclease resistance. These modifications may have an impact on stacking interaction, hydrogen-bonding, donor/acceptor properties, pKa, steric or electrostatic effects. Selected modified bases are shown in the Figure 16.

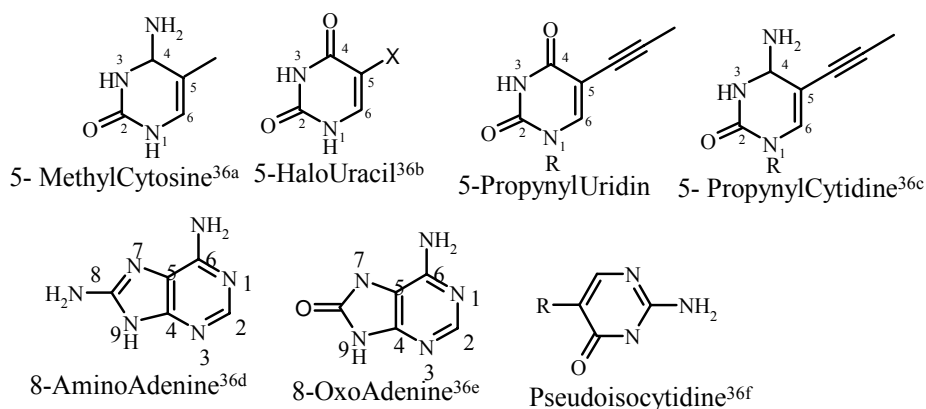


**Figure 16** Modified Nucleobases

## **1.9 Spectroscopic methods for studying the DNA duplexes, triplexes and DNA-PNA complexes.**

A number of physicochemical techniques have been used to study the properties of duplexes and triplexes of nucleic acids. In the spectroscopic methods, UV absorbance and circular dichroism are very sensitive to the interactions of nearby bases which are stacked in the helical complexes. The principles are outlined in the following sections.

### **1.9.1 UV Spectroscopy**

The two strands of a DNA helix readily come apart when hydrogen bonds between its paired bases are disrupted. This can be accomplished by heating a solution of DNA (called DNA-melting) or by adding acid or alkali to ionize its bases. The melting temperature ( $T_m$ ) is defined as the temperature at which the duplex and the single strands exist in equal proportion (50% each). DNA double helix, in which the two strands are held together by several reinforcing bonds, is a highly cooperative structure. The double helix is stabilized by the stacking of bases as well as by base pairing. Hydrogen bonding contributes in the order of 5-15 kcal/mol/base pair to the stability of the nucleic acid helix (electronic or intrinsic energy). This contribution is selective, i.e., there is a preferential stability of the Watson-Crick guanosine-cytosine (G-C) pair relative to all other pairs. Stacking interactions contribute approximately the same amount as H bonding. The DNA melting is readily monitored by measuring its absorbance at a wavelength of 260 nm. A plot of absorbance against the temperature of measurement gives a sigmoidal curve in the case of duplexes and the midpoint of the transition gives the  $T_m$ . In case of triplexes, the first dissociation leads to the duplex (Watson-Crick duplex) and the third strand (Hoogsteen strand), followed by the duplex dissociation at higher temperature into two

single strands. The DNA triplex melting shows a characteristic double sigmoid transition with separate melting temperature ( $T_m$ ) for each transition. The lower melting temperature corresponds to the triplex(duplex transition while the second transition gives the  $T_m$  of the duplex single strand (Figure 17).

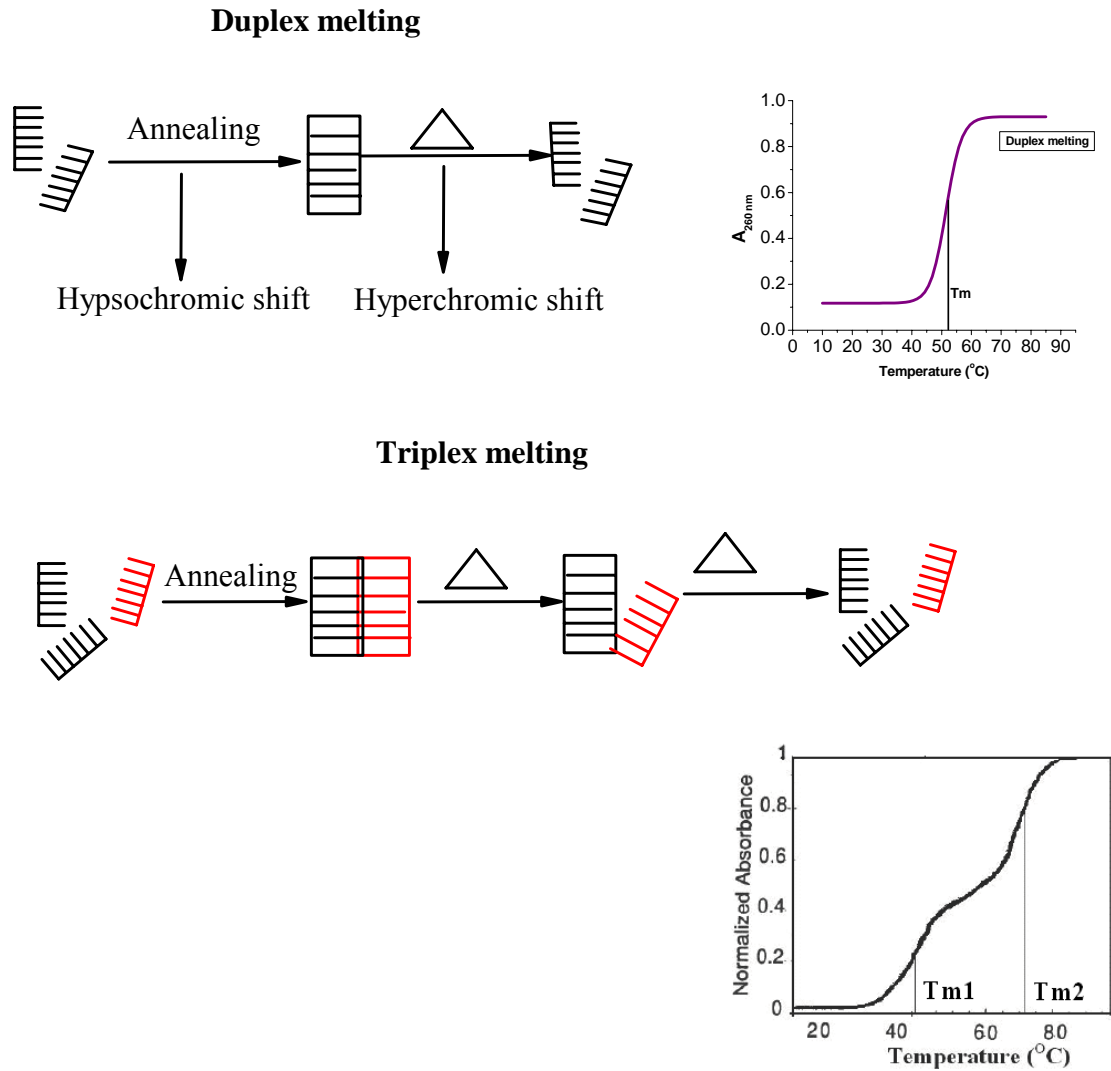


**Figure 17** Schematic representation of thermal dissociation of DNA double and triple helices. Mid point of the transition corresponds to the melting temperature.

### 1.9.2 Circular dichroism

Circular dichroism<sup>37-38</sup> is a technique to study the chiral molecules that have chromophores. In case of nucleic acids, the sugar units of the backbone provide chirality and the bases attached to the sugars are the chromophores. In the CD spectrum of a polynucleotide with stacked bases, the magnitude of CD signals is larger in the 260-280 nm region and significantly higher at 200 nm than that of individual bases. The base stacking in a chiral fashion induces the coupling of CD transitions leading to characteristic patterns. Single stranded ODNs are structurally less well defined than duplex ODNs and their CD signal is smaller. The CD pattern of the nucleic acid reflects the polymorphic forms of DNA such as A-, B-, and Z- forms. The CD signature of B-form DNA as seen from longer to shorter wavelength is a positive band centered at 275 nm, a negative band at 240 nm, with a crossover at 258 nm (Figure 18). A-DNA is characterized by a positive CD band at 260 nm that is larger than the corresponding B-DNA band and a fairly intense negative band at 210 nm. Naturally occurring RNAs and RNA-DNA hybrids adopt this polymorphic form. The left handed Z-form DNA shows a negative CD band at 290 nm and a positive band at 260 nm.

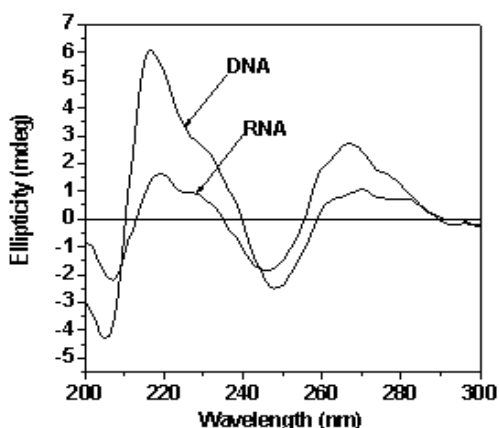


**Figure 18** CD profiles of ssDNA and RNA

### 1.10 Peptide Nucleic Acids:

PNA is peptide nucleic acid and was invented by Nielsen et. al 1991<sup>39</sup> with physical properties similar to DNA or RNA but differing in the composition of its "backbone." PNA does not occur naturally and is synthesized for use in biological research and diagnostics.

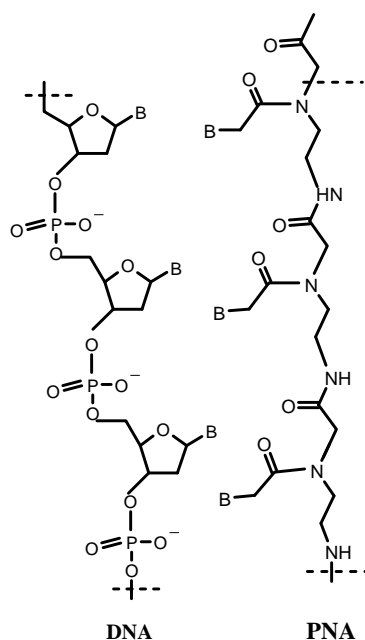


**Figure 19** Chemical structure of DNA and PNA

DNA and RNA have backbone containing deoxyribose and ribose sugars respectively, whereas the backbone of PNAs is composed of repeating N-(2-aminoethyl)-glycine units linked by peptide bonds (Figure 19). The various purine and pyrimidine bases are linked to the backbone by methylene carbonyl bonds. PNAs are depicted like peptides, with the N-terminus at the first (left) position and the C-terminus at the right. Since the backbone of PNA contains no charged phosphate groups, the binding between

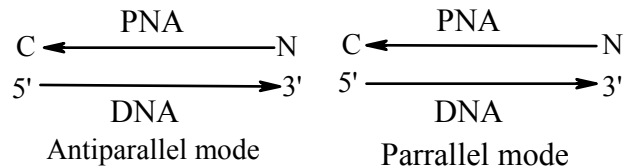


**Figure 19a**

PNA/DNA strands is stronger than between DNA/DNA strands due to the lack of electrostatic repulsion. Early experiments with homopyrimidine strands (strands consisting of only one repeated pyrimidine base) have shown that the  $T_m$  ("melting" temperature) of a 6-base thymine PNA/adenine DNA double helix was  $31^\circ\text{C}$  in comparison to an equivalent 6-base DNA/DNA duplex that denatures at a temperature less than  $10^\circ\text{C}$ .<sup>39,40</sup> Mixed base PNA molecules are true mimics of DNA molecules in terms of base-pair recognition. PNA/PNA binding is stronger than PNA/DNA binding.

Synthetic peptide nucleic acid oligomers have been used in recent years in molecular biology procedures, diagnostic assays and for potential therapeutics. Due to their higher binding strength it is not necessary to design long PNA oligomers for use in these roles, which usually require oligonucleotide probes of 20-25 bases. The main concern of the length of the PNA-oligomers is to guarantee the specificity. PNA oligomers also show greater specificity in binding to complementary DNAs, with a PNA/DNA base mismatch being more destabilizing than a similar mismatch in a DNA/DNA duplex. This binding strength and specificity also applies to PNA/RNA duplexes. PNAs are not easily recognized by either nucleases or proteases,<sup>41</sup> making them resistant to enzyme degradation. PNAs are also stable over a wide pH range. Finally,

their uncharged nature should make crossing through cell membranes easier, which may improve their therapeutic value.

### **1.10.1 Triplex formation with complementary DNA and RNA**

Homopyrimidine peptide nucleic acids are known to form highly stable and sequence specific triplexes upon binding to complementary homopurine sites of ss and dsDNA.<sup>42</sup> Displacement of the second, homopyrimidine strand takes place upon binding of PNA to dsDNA, forming a so-called P-loop. The extremely high stability of PNA<sub>2</sub>/DNA triplexes<sup>43,44</sup> is at least partly due to the charge neutrality of the PNA backbone, that excludes electrostatic repulsion from the DNA molecule, and the presence of additional hydrogen bonds between the Hoogsteen strand of the PNA and the oxygen atoms of the DNA backbone. A unique property of PNAs is their ability to displace one strand of a DNA double helix to form strand invasion complexes, which is an additional attribute for their application as antisense/antigene agents. Such strand invasion process is inefficient or absent in DNA or any other DNA analogues studied so far. The strand invasion by PNA (Figure 20) is dictated by the formation of triple helical structures via Watson-Crick and Hoogsteen binding modes and is by far confined to the polypyrimidine PNA oligomers, which form PNA<sub>2</sub>:DNA triplexes.

### **1.10.2 Duplex formation with complementary DNA and RNA**

PNAs obey Watson- Crick rules of hybridization with complementary DNA (Figure 20) and RNA. Antiparallel PNA-DNA hybrids are considerably more stable than the corresponding DNA-DNA complexes.<sup>40</sup> The increased stability results in an increase in T<sub>m</sub> of approximately 1 °C/base. Antiparallel PNA-RNA duplexes are even more stable

compared to DNA-RNA hybrids, and PNA-DNA duplexes.<sup>41</sup> The stability of parallel PNA-DNA and PNA-RNA duplexes is almost exactly the same as that of (antiparallel) DNA-DNA and DNA-RNA duplexes respectively. An interesting aspect of PNA-DNA duplex formation is, that the  $T_m$  decreases with increase in salt concentration (ionic strength) which is contrast to that of DNA-DNA duplex, for which increase in  $T_m$  with salt concentration is observed.<sup>40</sup> Base pair mismatches result in reduction of the  $T_m$  value by 8-20 °C.<sup>41</sup> This discrimination is, in some cases, approximately double that observed for DNA-DNA duplexes.

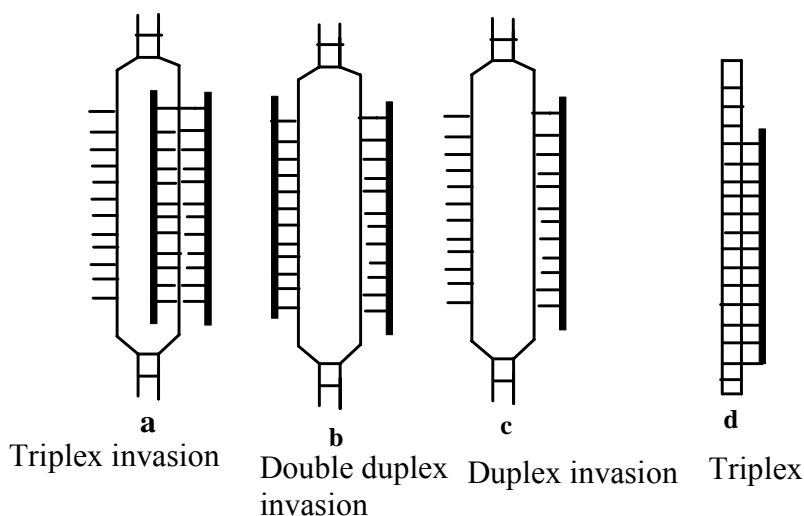


**Figure 20** Schematic representation of PNA binding for targeting *ds* DNA, PNA (Thick line)

### 1.11 Structure of PNA complexes

Till date the three-dimensional structures of four PNA complexes have been established. The PNA-RNA<sup>45</sup> and PNA-DNA<sup>46</sup> duplex structures were determined by NMR methods, while the structures of a PNA<sub>2</sub>:DNA triplex<sup>47</sup>, PNA-PNA duplex<sup>48</sup> and PNA-RNA duplexes were solved by X-ray crystallography (Figure 21).

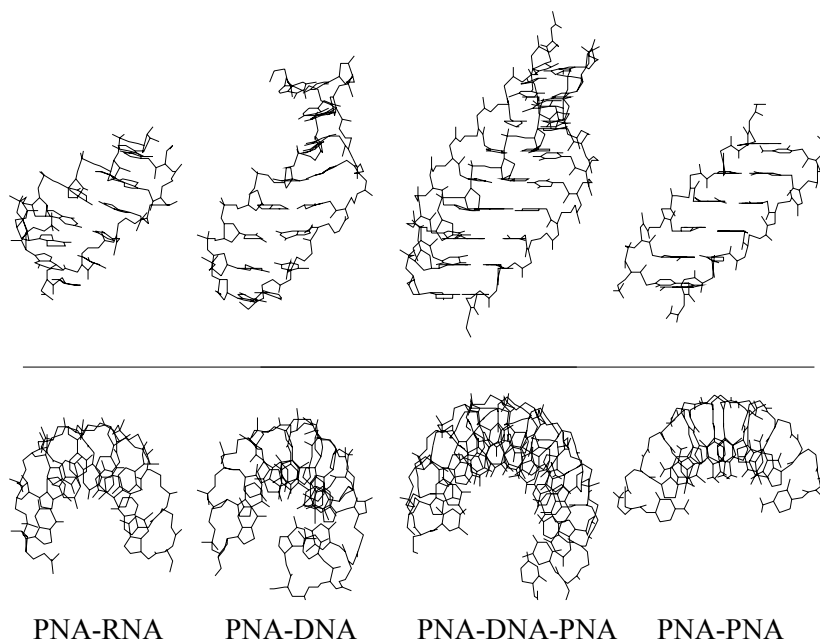


**Figure 21** Structures of PNA complexes shown in (a) side view (b) top view. The complexes from left to right PNA-RNA, PNA-DNA duplex, PNA-DNA-PNA and PNA-PNA (ref Erickson, M. Nielsen, P. E. *Quart. Rev. Biophysics* **1996**, *29*, 369.)

### 1.11.1 Structure of PNA-DNA duplexes

Almost complete structural information has been deduced from the NMR spectroscopic study of two antiparallel PNA-DNA duplexes (Figure 21).<sup>49</sup> The DNA strand is in a conformation similar to the B-form, with a glycosidic *anti*-conformation, and the deoxyribose in *C2'-endo* form. A more recent NMR study<sup>45</sup> showed that an octameric antiparallel PNA-DNA duplex contained elements of both A-form and B-form. The primary amide bonds of the backbone are in *trans* conformation and the carbonyl oxygen atoms of the backbone-nucleobase linker point towards the carboxy-terminus of the PNA strand. The CD spectra of antiparallel PNA-DNA complexes are similar to DNA-DNA spectra and indicate the formation of right handed helix.<sup>40,49</sup>

### 1.11.2 Structure of PNA-RNA duplexes

The first report elucidating the structure of a nucleic acid-PNA hydrogen-bonded complex was reported by Brown et al<sup>45</sup> from solvent NMR solution structure study of hexameric PNA, GAACTC, with complementary RNA. The study revealed that in PNA all bases form Watson-Crick base pairs, the glycosidic torsion angle in the RNA strand indicates an *anti*-conformation, and the ribose sugars are in the 3'-*endo* form. The RNA strand thus resembles an A-form structure. The tertiary amide bonds all are in the *cis*-conformation. The carbonyl group of the tertiary amide in PNA backbone is isosteric to the C2'-hydroxyl group, which increases the solvent contact of the carbonyl oxygen atom. The CD spectra of antiparallel PNA-RNA duplexes also indicate the formation of a right-handed helix with geometry similar to the A- or B-form.

### 1.11.3 Structure of PNA<sub>2</sub>-DNA triplexes

The structure of PNA<sub>2</sub>-DNA triple-helix was resolved by the X-ray crystal structure analysis of the complex formed by bis-(PNA) and its complementary antiparallel DNA (Figure 21).<sup>47</sup> The nucleobases of the PNA strand bind to the DNA by Watson-Crick pairing and Hoogsteen hydrogen bonding. The structure exhibited, both A-form and B-form DNA, and forms a "P-helix" with 16 bases per turn. The DNA phosphate groups are hydrogen bonded to the PNA backbone amide protons of the Hoogsteen strand. These hydrogen bonds, together with additional Vander-waal's contact and the lack of electrostatic repulsion are the main factors responsible for the enormous stability of the triplex. The deoxyribose sugar adopted C3'-*endo* conformation like A-form and bases lie almost perpendicular to the helix axis, which is characteristic of B-form DNA. The crystal structure is in agreement with the CD spectra of PNA<sub>2</sub>-DNA

triple-helices measured in solution.<sup>50</sup> The X-ray structure of self-complementary PNA-PNA duplex bears a strong similarity to the P-form of PNA<sub>2</sub>-DNA triplex (Figure 21).<sup>48</sup>

Several general conclusions can be drawn from these structural studies, because of its flexible backbone, PNA to a great extent is able to adapt its partner's conformation in the complexes. In the PNA-RNA and PNA-DNA duplexes the oligonucleotide adopts close to its natural A and B-conformations respectively in terms of sugar puckering, while the helix parameters have both A and B-form characteristics. The PNA however, prefers a unique, different helix form, the P-form, which is adapted to some extent in the PNA<sub>2</sub>:DNA triplex and completely in the PNA-PNA duplex. This P-helix is very wide (28 Å diameter) and has a very large pitch (18 base pairs). In terms of base pair conformations it is a very regular helix, and the base pairs are virtually perpendicular to the helix axis.

### **1.12 Chemical modifications of PNA**

The limitations of PNA include low aqueous solubility, ambiguity in DNA binding orientation and poor membrane permeability. Structurally, the analogues can be derived from modifications of ethylenediamine or glycine sector of the monomer, linker to the nucleobase, the nucleobase itself or a combination of the above. The strategic rationale behind the modifications (Dueholm et al., 1997) are (i) introduction of chirality into the achiral PNA backbone to influence the orientation selectivity in complementary DNA binding, (ii) rigidification of PNA backbone via conformational constraint to preorganize the PNA structure and to entropically drive the duplex formation, (iii) introduction of cationic functional groups directly in the PNA backbone, in a side chain substitution or at the N or C terminus of PNA, (iv) to modulate nucleobase pairing either

by modification of the linker or the nucleobase itself and (v) conjugation with ‘transfer’ molecules for effective penetration into cells. In addition to improving the PNA structure for therapeutics, several modifications are directed towards their applications in diagnostics.

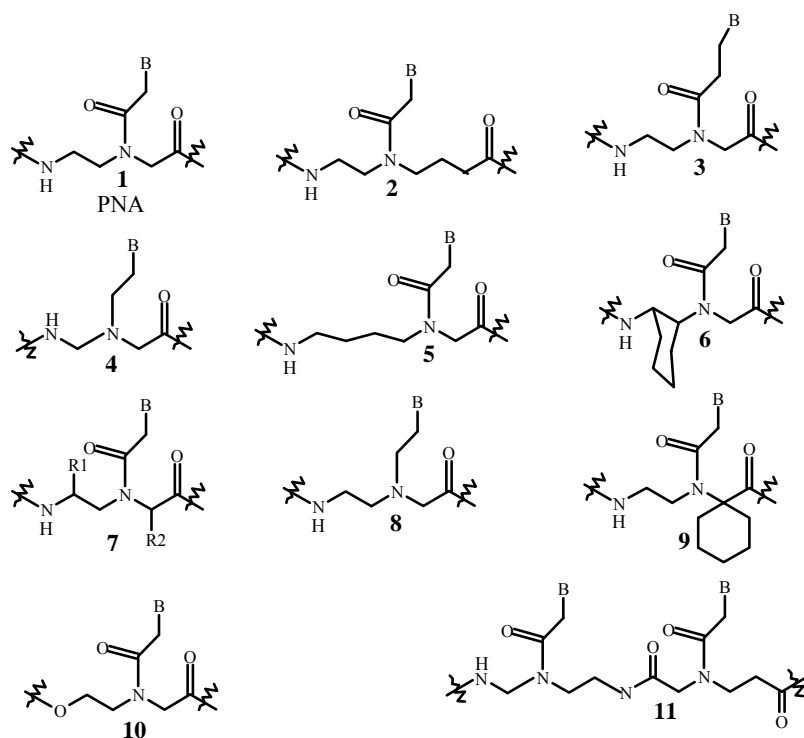


**Figure 22** Chemical modifications of PNA

Solubility was improved by introducing positive charges in the PNA monomers or by introducing ether linkages in the backbone. Charges were integrated into the PNA by replacing the acetamide linker with a flexible ethylene linker<sup>53</sup> (Figure 23a) or by the attachment of terminal lysine residues<sup>54</sup> (Figure 23c).

Recently, a novel class of cationic PNA (Figure 23b) (DNG/PNA) analogs has been reported.<sup>55</sup> In these alternating PNA /DNG chimeras, the O-(PO<sub>2</sub>)-O- linkage of nucleotide was replaced by strongly cationic guanidino [N-C(=N+H)-N] function. These

analogs with neutral and positive linker showed high binding affinity with DNA/RNA targets.

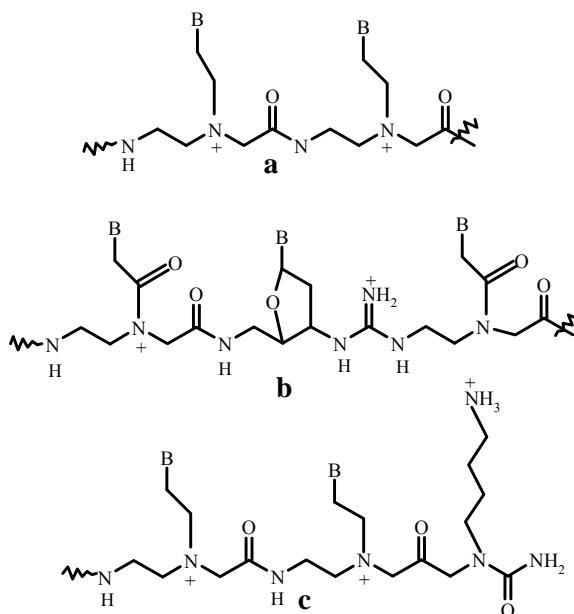


**Figure 23** Positively charged PNAs a) Flexible ethylene linker, b) Gaunidium linkages, C) Lysine residues

Introduction of negative charges in the PNA backbone (Figure 24) improved aqueous solubility and showed good binding with both DNA and RNA.

However, these modified complexes were found to be less stable compared to the unmodified PNA sequences.<sup>56</sup> In a similar approach pPNA-Hyp chimeras were also synthesized.<sup>57</sup> Ether linked PNAs (Figure 24) showed co-operative binding with complementary antiparallel RNA in a sequence specific manner.<sup>58</sup> Oligomers with **29b** showed significantly lower affinity than **24a** due to the increased flexibility of the side chain homologation. The replacement of these monomers with  $\alpha$ -methylated derivatives led to significant enhancement in RNA binding affinity in case of *2R* stereoisomer.

Whereas, presence of 2*S* isomer resulted in substantial decrease in *T<sub>m</sub>* indicating that the substitution in case of *S* configuration may sterically interfere with RNA binding.

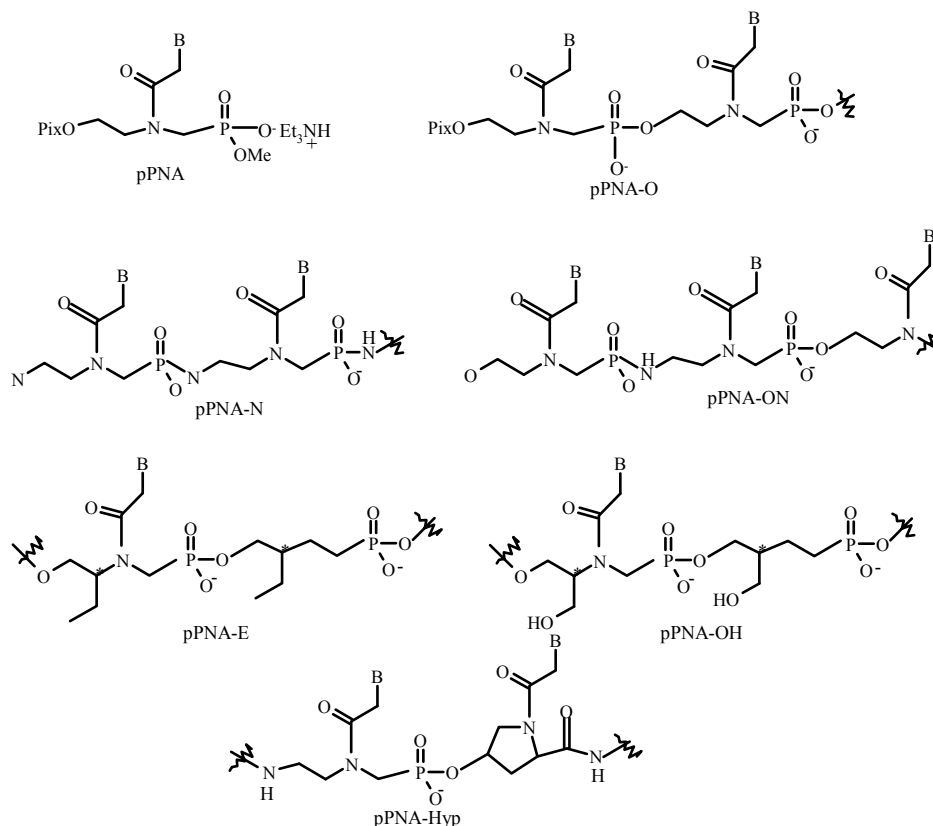


**Figure 24** Anionic PNAs

To ensure sufficient water solubility for RNA binding experiments, lysine was attached to the N/C terminus of these oligomers (Figure 25).<sup>59</sup> This was followed by another similar report using oxy-PNA oligomers bearing adenine as nucleobase. Binding studies of these oligomers with complementary DNA showed all-or-none type hybridization and with high sequence specificity useful for the detection of single base mismatch DNAs.<sup>60</sup>

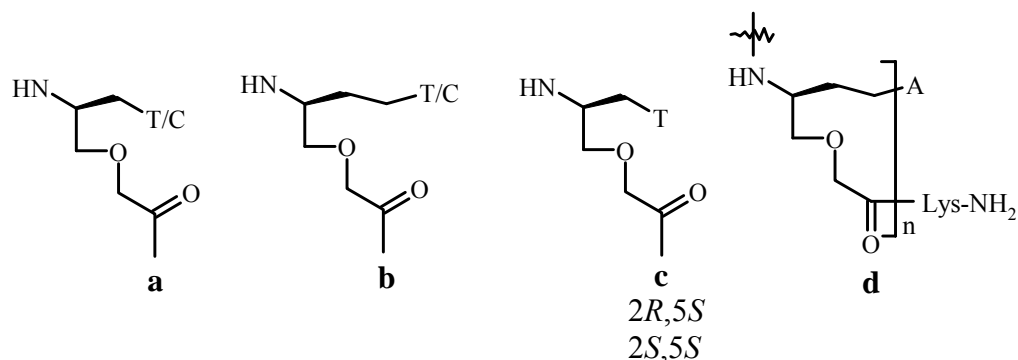


**Figure 25** Ether linked oxy PNAs

### 1.13 Construction of bridged structures

Conformationally preorganized DNA analogues such as locked nucleic acids<sup>32,33</sup> (LNA) in which the prelocked 3'-*endo* sugar conformation, like in DNA:RNA hybrids, favors its binding with complementary DNA/RNA sequences.<sup>32</sup> Other examples include conformationally frozen six-membered cyclohexenyl, hexitol,<sup>31</sup> and altrito<sup>31</sup> nucleic acids.

The *cis* and *trans* rotamers arising from the tertiary amide linkage in each PNA monomer leads to different PNA:DNA/RNA hybridization kinetics in parallel and antiparallel hybrids due to the high rotational energy barrier between *cis* and *trans* rotameric populations. Any favorable structural preorganization of PNA may activate a shift in equilibrium towards the preferred complex formation because of the reduced entropy loss upon complex formation, provided that the enthalpic contributions suitably compensate. This may be achieved if the conformational freedom in *aeg*-PNA is reduced by bridging the aminoethyl/glycyl acetyl linker arms to give rise to cyclic analogs with preorganized structure. Such modifications also restrain the fluctuation domains of the

*aeg*-PNA (glycyl and ethylene diamine) along with introducing the chirality into PNA monomeric units with the possibility of further fine-tuning the structural features of PNA to mimic DNA.

### 1.13.1 PNA with 5-membered nitrogen heterocycles

The naturally occurring amino acid *trans*-4-hydroxy-proline, a five-membered nitrogen heterocycle with useful substitutions and well known and easily manipulated stereochemistry,<sup>51, 52</sup> is a versatile, commercially available starting material amenable for creating structural diversity to mimic the DNA/PNA structures. Many researchers have exploited *trans*-4-hydroxy-L-proline for the synthesis of a wide range of chiral, constrained and structurally preorganized PNAs.

#### 1.13.1a Aminopropyl PNA

The introduction of a methylene bridge between  $\beta$ -carbon atom of the aminoethyl segment and the  $\alpha''$  carbon atom of the glycine segment of the *aeg*-PNA resulted in 4-aminopropyl PNA, accompanied by creation of two chiral centers (Figure 26).<sup>61</sup>

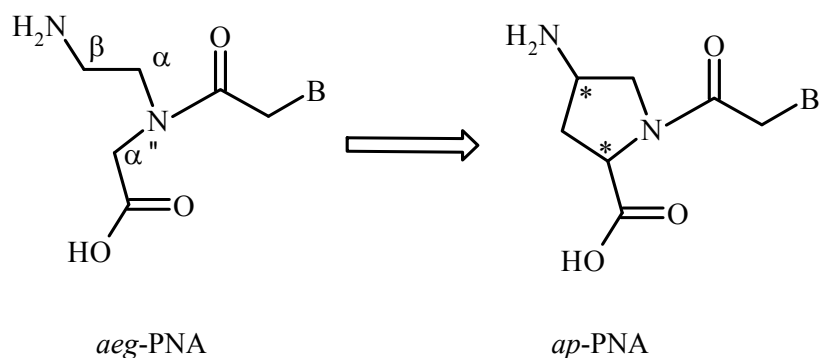
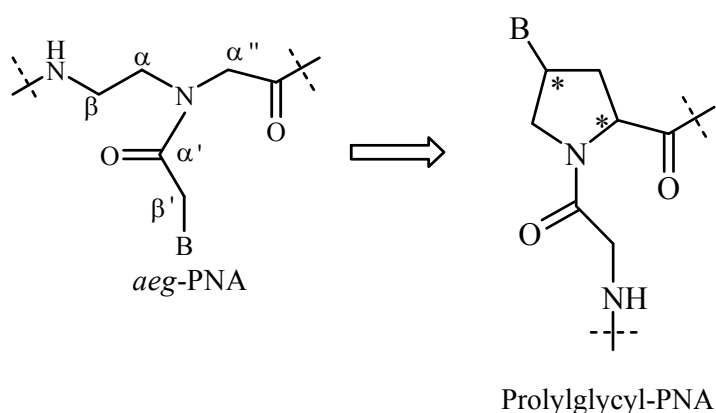


Figure 26

Incorporation of these monomers at N terminus of *aeg*-PNA enhanced the inherent binding and also showed significant discrimination in the orientation of binding. The stability of such complexes decreases with increasing number of chiral prolyl units and homooligomers derived from each of the diastereomers (L and D-hydroxy proline) completely failed to form duplexes. Incorporation of alternating 4-aminoprolyl and glycine units<sup>62</sup> stabilize the complex suggesting that in the homo-oligomer, inter-nucleoside distances are too low.

### 1.13.1b Gly-Pro-Peptide PNA

Lowe *et al.*<sup>63</sup> used 4-Hydroxyproline for the synthesis of a novel chiral prolyl-glycyl PNA. The methylene bridge was inserted between the  $\alpha''$ -carbon atom of the glycine unit and the  $\beta'$ -carbon atom of the nucleobase linker of *aeg*-PNA (Figure 27).<sup>64,65</sup> Oligomers derived of Prolyl-glycyl derived PNAs did not bind to the target complementary sequences due to the high rigidity in the structure, which has the tertiary amide nitrogen as part of a cyclic ring system on the backbone.



**Figure 27**

### 1.13.1c Aminoethylprolyl PNA (*aep*-PNA)

Bridging of the  $\alpha''$ -carbon atom of the glycol segment with the  $\beta'$ -carbon atom of the nucleobase linker by a methylene group, accompanied by replacement of the side chain carbonyl with a methylene group, leads to *aep*-PNA (Figure 28). The flexibility in the aminoethyl segment of *aeg*-PNA was retained, unlike that in the proline-glycine PNA. The oligomers comprising 4-(*S*)-2-(*S/R*) *aep*PNA thymine units showed very favorable binding properties towards the target sequences without compromising the specificity. The stereochemistry at the C-2 centre did not bring any significant effect on the binding ability of the homooligomeric sequences. The mixed pyrimidine hairpin sequences with cytosine and N-7 guanine *aep*PNA<sup>66</sup> units exhibited directional discrimination in binding to parallel/antiparallel DNA sequences.

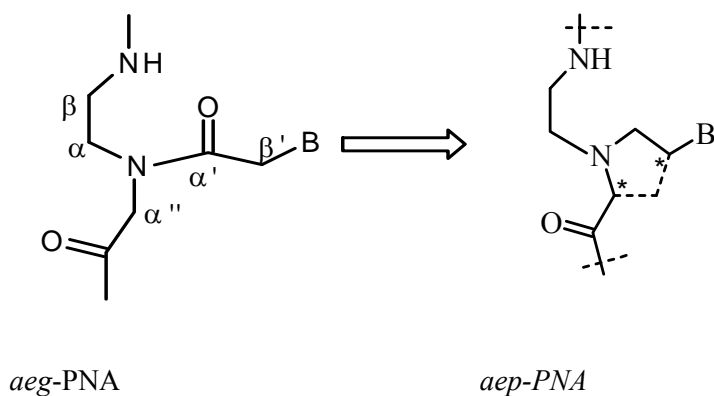


**Figure 28**

### 1.13.1d Pyrrolidinone PNA:

A methylene bridge was inserted between the  $\alpha$  carbon atom of the aminoethyl segment and the  $\beta'$ -carbon atom of the acetyl linker to the nucleobase of *aeg*PNA (Figure 29).<sup>67</sup> The hybridization properties of PNA decamers containing this analogue with

complementary DNA, RNA and PNA strands were investigated. The oligomers incorporating the (3*S*,5*R*) isomer were shown to have the highest affinity towards RNA in comparison with DNA.<sup>68</sup> The fully modified decamer bound to rU<sub>10</sub> with a small decrease in binding efficiency with compared to *aeg*-PNA.

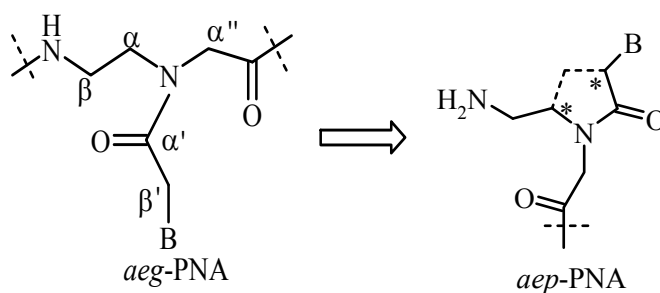


**Figure 29**

In order to get the best characteristics from both the *aeg*PNA and the *aep*-PNA, monomer was synthesized restoring the amide character to the pyrrolidine ring nitrogen *via* selective C5 oxidation of *aep*-proline derivatized intermediate<sup>69</sup> (Figure 20). *aepone*-PNA oligomer stabilizes the derived triplexes with DNA but destabilizes the complexes formed with poly (rA).

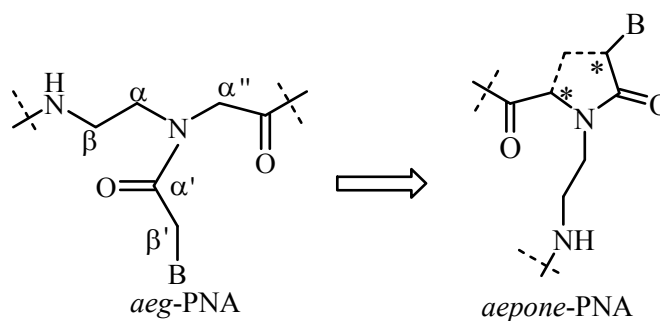


**Figure 29a**

### 1.13.1e Prolyl-( $\beta$ -amino acid) peptide PNA

The conformational strain in the alternating proline-glycine backbone was released by replacement of the  $\alpha$ - amino acid residue by different  $\beta$  amino acid spacers with appropriate rigidity.<sup>70</sup> Novel pyrrolidinyl PNAs comprising alternate units of nucleobases modified with D-proline, either D/L aminopyrrolidine 2 carboxylic acid, (1*R*,2*S*)-2-aminocyclopentanecarboxylic acid or  $\beta$  alanine were synthesized (Figure 30).<sup>71</sup>

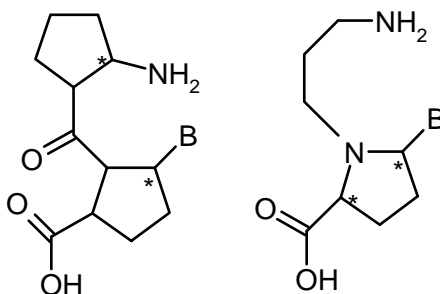
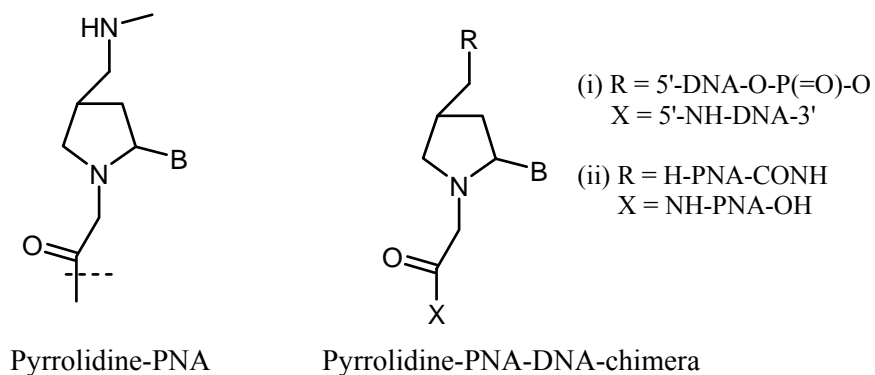


Figure 30

### 1.13.1f Pyrrolidine PNA and pyrrolidine PNA-DNA chimera

Insertion of a methylene bridge in *aeg*PNA, linking the  $\alpha$ -carbon atom of the aminoethyl segment and the  $\beta'$ -carbon atom of the tertiary amide linker, afforded the pyrrolidine PNA Figure 31.<sup>72a</sup> A fully modified (2*R*,4*S*) pyrrolidine PNA decamer formed very stable complexes with both DNA and RNA targets. The incorporation of the (2*S*,4*S*) thymine monomer into oligomers and mixed pyrimidine oligomers resulted in a decreased binding efficiency with the target DNA/RNA sequences.<sup>72b</sup> The (2*R*,4*R*) isomer was incorporated into a PNA:DNA dimer amenable to the synthesis of PNA:DNA chimeras.<sup>72c</sup> The chimeric PNA:DNA bound to the target DNA with decreased efficiency relative to the native DNA.



**Figure 31**

Introduction of the  $\alpha'$ - $\beta$  methylene bridge led to another pyrrolidine-PNA in which, unlike the previous analogues, the base is away from the pyrrolidine ring by one carbon (Figure 31a).<sup>72d,e</sup> The enantiomeric pairs (2*S*,4*S*) and (2*R*,4*R*) formed antiparallel complexes with RNA much stronger than that of *aeg*-PNA or other diastereomers. The (2*R*,4*S*) pyrrolidinyl PNA analogues of all four bases lacked the discrimination effects with respect to either parallel/antiparallel or DNA/RNA binding

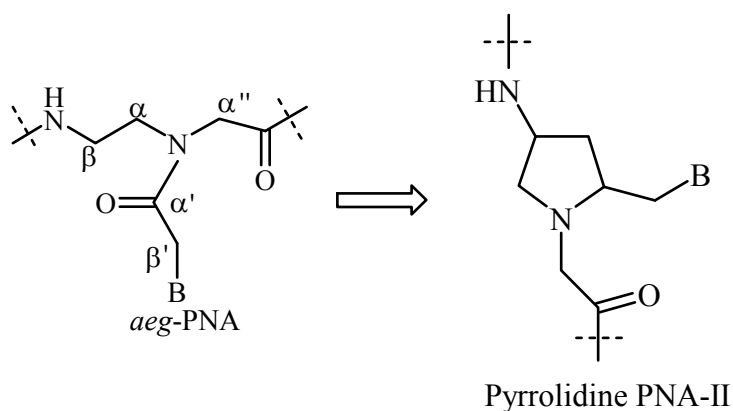


**Figure 31a**

### 1.13.1g A cyclopentane conformational restraint for a peptide nucleic

Based on molecular modeling studies (*S,S*) cyclopentadiamine ring was used for conformational restraint of the C2-C3 dihedral angle of the PNA backbone. The *trans* cyclopentane modification improves the stability of PNA-DNA triplexes and PNA-RNA duplexes for a poly-T PNA.<sup>73</sup> Recently cyclopentyl PNAs<sup>74,75</sup> having *cis* and *trans* isomers have been reported (Figure 32). The results suggest that these have a stereochemistry dependent stabilization effect on binding both DNA and RNA. The *cp*PNAs have better selectivity for mismatch DNA sequence and a higher binding to complementary DNA sequence than the unmodified PNA.

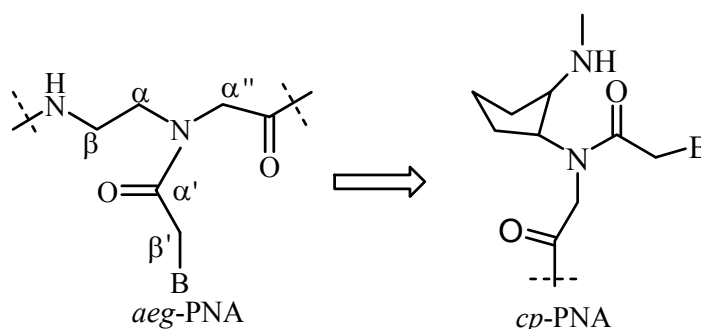
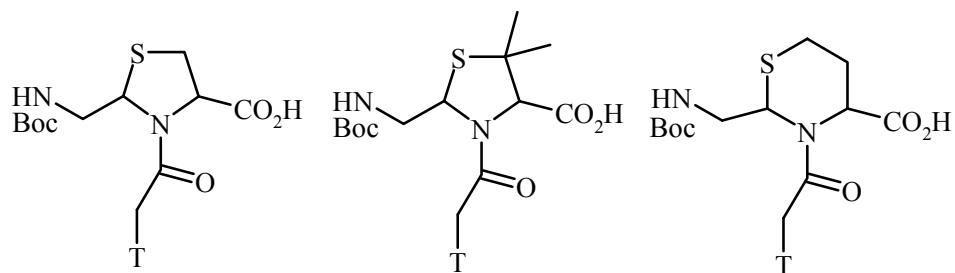


Figure 32

### 1.14 Thiazane and thiazolidine PNA

Bregant, et al.<sup>76</sup> introduced rigidity by induction of ring containing thiazane and thiazolidine in the backbone of PNA (Figure 33). With the presence of sulfur in ring, both PNAs showed improved solubility, but, the derived PNA/DNA and PNA/RNA triplexes were destabilized by larg extent.



**Figure 33**

### 1.15 PNA with six membered ring structures

The six-membered ring systems are conformationally more rigid when compared to their five-membered counterparts due to high-energy barriers between chair-boat conformations and preferred low-energy equatorial dispositions of substituents. The binding abilities of hexose sugar phosphate containing oligonucleotide have been extensively studied by Eschenmoser et al.<sup>77</sup> The ability of morpholino, hexitol, and cyclohexene oligonucleotides to bind to DNA/RNA is well established and is dictated by the conformational preferences of the six membered ring structures. The ability of six-membered ring to impart more rigidification into PNA backbone significantly effects the hybridization properties of PNAs.

#### 1.15a Glucose amine nucleic acids (GNA)

Novel glucosamine based oligonucleotide analogs (GNA) derived from conformationally constrained sugar scaffold have been synthesized (Figure 34).<sup>78</sup> GNA derived oligomers are highly water-soluble.

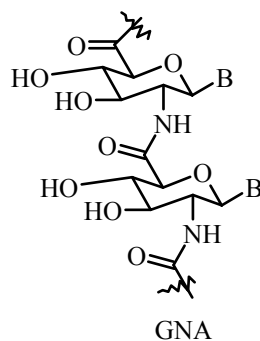


**Figure 34**

In contrast to the homo DNA and hexose oligonucleotides, these bind to RNA to form stable complexes with an overall affinity comparable to that of DNA to RNA and are sequence selective. Thermodynamic parameters suggested an entropy gain in GNA due to the pre-organized scaffold.

### 1.15b Aminopipecolyl PNA, *pip*-PNA

Insertion of an ethylene bridge between the  $\alpha''$ -carbon atom of the glycol segment and the  $\beta$  carbon of the aminoethyl segment afforded the isomeric analogue 5-aminopipecolyl PNA (Figure 35).<sup>79</sup> The preliminary studies indicated that the homothyminyl mixed-*aeg*PNA sequences consisting the 5-aminopipecolyl unit form stable complexes with target DNA oligomers.

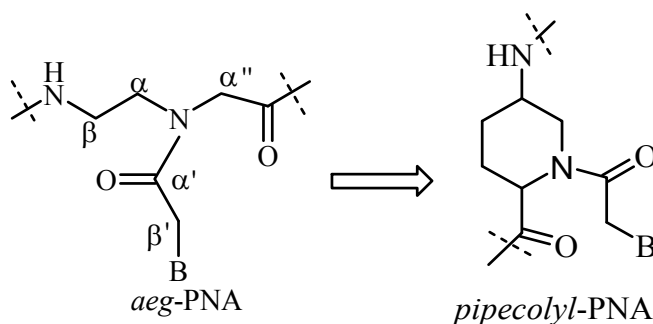


**Figure 35**

### 1.15c Aminoethyl pipercolyl PNA (*aepip*-PNA)

Bridging the  $\alpha$ -carbon of the glycol unit with the  $\beta'$ -carbon of the nucleobase linker by a two-carbon ethylene bridge leads to the homologous analogue of *aep*-PNA,<sup>80b</sup> namely, *aepip*-PNA (Figure 36).<sup>80</sup>

This chiral six-membered analogue with (2*S*,5*R*) stereochemistry upon incorporation into *aeg*-PNA-T8 homooligomer or into a mixed T/C PNA oligomer at different positions stabilized the corresponding PNA<sub>2</sub>:DNA triplexes. This is interesting since it was suggested earlier<sup>80c</sup> that six-membered piperidines are unlikely to stabilize the PNA:DNA complexes.

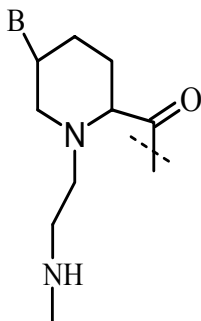
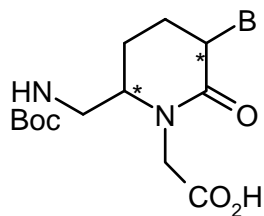


Figure 36 *aepip*-PNA

### 1.15d Piperidinone PNA

Introduction of an ethylene bridge between the  $\alpha$  carbon atom and  $\beta'$  carbon atom in the aminoethyl and acetyl linker resulted in a six-membered ring piperidinone PNA (Figure 37).<sup>80c</sup> (3*R*,6*R*) and (3*S*,6*R*) Adenine monomers were synthesized and incorporated into *aeg*PNA which resulted in a large decrease in the duplex stability.



**Figure 37** Piperidinone PNA

### 1.15e Cyclohexyl PNA (*ch*-PNA)

One of the earliest PNA modifications was to constrain the flexibility in the aminoethyl segment by introducing a cyclohexyl ring (Figure 38).<sup>81</sup> PNA oligomers that contain cyclohexyl rings in the aminoethyl part showed similar hybridization properties as unmodified *aeg*-PNA with complementary DNA whereas the (*R,R*) cyclohexyl moiety lacked such a property. The complexes formed by the two isomers were of the opposite handedness, as evident from CD spectroscopy. The synthesis of ethyl *cis*-(1*S*,4*R*/1*R*,2*S*)-2-aminocyclohex-1-yl-*N*-(thymine-1-yl-acetyl) glycinate was reported *via* enzymatic resolution of the *trans*-2-azido cyclohexanols. The crystal structure of the intermediate showed an equatorial disposition of the tertiary amide group, with the torsion angle  $\beta$  in the range 60°-70°. UV-Tm experiments showed that (1*S*,2*R*) isomer preferred to bind RNA and (1*R*,2*S*) isomer showed higher affinity towards DNA in homothymine sequences leading to stereo discrimination in recognition of DNA and RNA.<sup>82</sup>

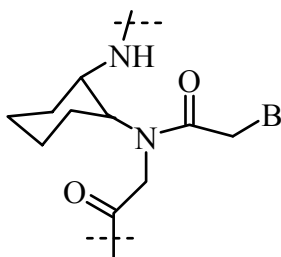


**Figure 38** *ch*-PNA

### 1.15f Aminoethyl-amino-cyclohexanoic acid:

Rigidity was introduced into the *aeg*-PNA by replacing the glycyl segment in the backbone by  $\alpha$ -amino cyclohexanoic acid (Figure 39).<sup>83</sup> Incorporation of these monomers into oligomers and their DNA/RNA binding properties has not yet been reported.

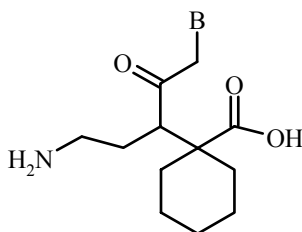


**Figure 39** Aminoethyl-aminocyclohexanoic acid

### 1.15g Morpholino PNA

The set of morpholino analogues with phosphonate esters, amide or ester linkages between the morpholino nucleoside residues was synthesized (Figure 40).<sup>84</sup> Preliminary results indicated that amide-linked morpholino PNAs were better accommodated in the complexes than the ester or the phosphonate linked oligomers.

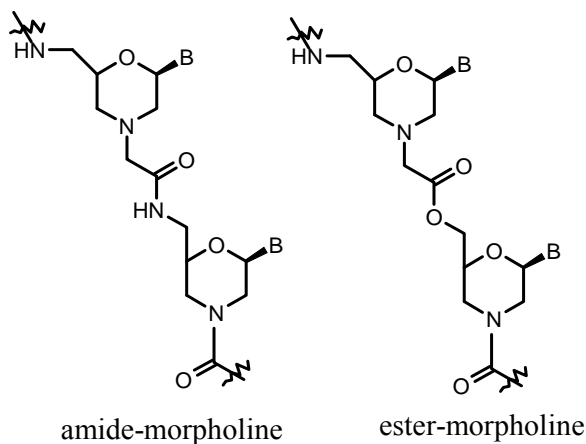


**Figure 40**

## 1.16 Modified nucleobases

Incorporation of modified nucleobases (Figure 41) would facilitate in understanding the recognition process between natural nucleobases in terms of various factors such as hydrogen bonding and inter-nucleobase stacking. Further, new recognition motifs may also have potential applications in diagnostics. 2-aminopurine<sup>85</sup> hydrogen bonds with U and T in reverse Watson-Crick mode and being inherently fluorescent, it permits the study of the kinetics of PNA-DNA hybridization process. 2,6-Diaminopurine has increased affinity and selectivity for thymine.<sup>86</sup>

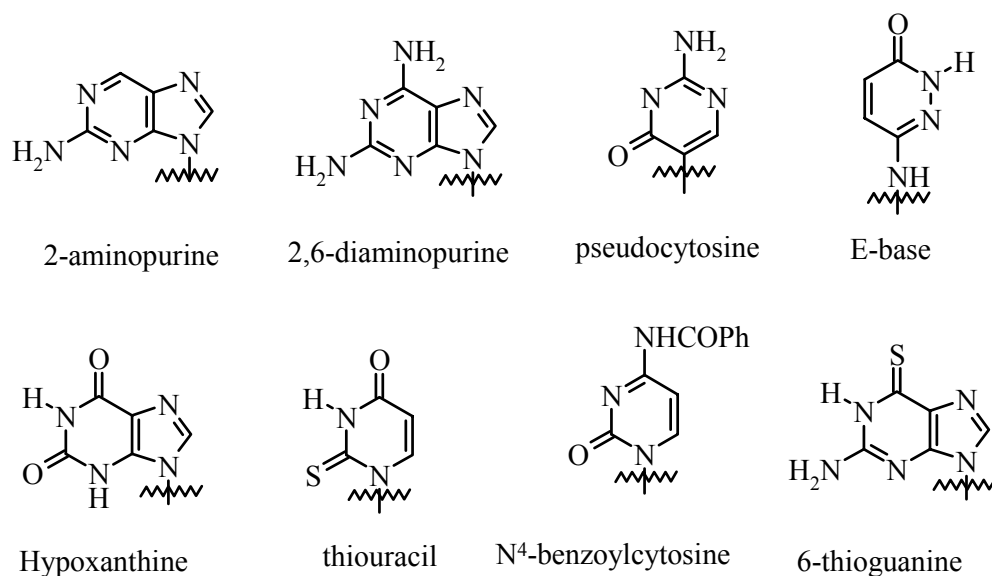


**Figure 41** Modified Nucleobases

Pseudo-isocytosine<sup>87</sup> is an efficient mimic of protonated cytosine for triplex formation. E-base<sup>88</sup> was designed for the recognition of T:A base pair in major groove and forms a stable triad with T in central position.

Other modifications like hypoxanthine<sup>89</sup> N<sup>4</sup>-benzoylcytosine and thiouracil<sup>90</sup> have also been incorporated as modified nucleobases. Combination of thiouracil in PNA chain

and 2,6-diaminopurine in DNA has been used in the “double duplex invasion” for the first time. 6-Thioguanine<sup>91</sup> was found to decrease PNA-DNA hybrid stability

### 1.17 PNA-Conjugates

The covalent linking of PNA hybrids to various other molecules like peptides, DNA, RNA etc. has been exploited to overcome the limitations of PNA such as aggregation, solubility, cellular uptake and resistance to cellular enzymes and to impart better therapeutic applications.

#### 1.17.1 PNA-DNA Chimera

The successful applications of the remarkable DNA binding properties of PNAs are sometimes (sequence/length dependent) hampered by their tendency to self-aggregate and poor aqueous solubility. Overcoming these limitations and imparting other abilities

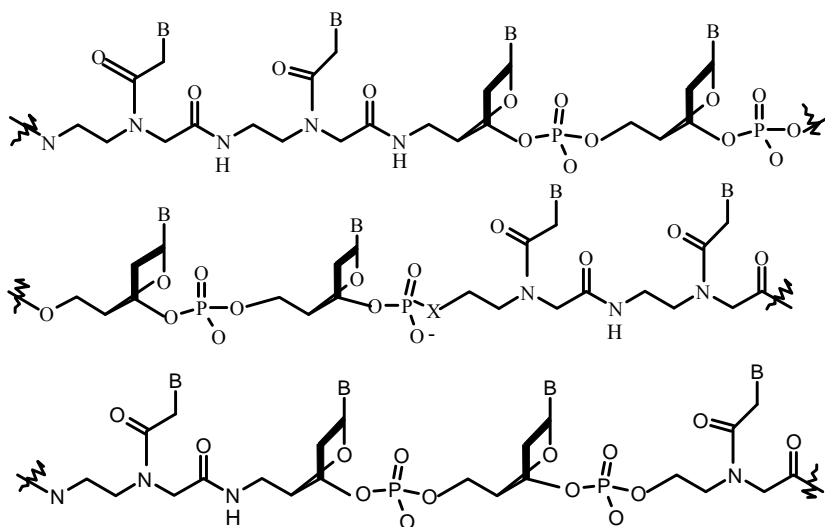


**Figure 42** PNA-DNA Chimera

for therapeutic applications such as cellular uptake, RNase H activation properties, have been addressed by designing covalent hybrids or chimaeras of PNA with DNA,

functional peptides and other effect or molecules. Three types of PNA-DNA chimeras (Figure 42) are in place (i) 5'-DNA-linker X- PNA -pseudo-3'<sup>92</sup> (ii) pseudo-5'-DNA-linker X- DNA-3' and (iii) pseudo -5'-PNA-linker X- DNA-3'. Synthetic protocols have been developed with protecting groups compatible for carrying out online synthesis of both PNA and DNA to generate the chimeras. Several interesting properties were noticed in such covalent hybrids such as co-operative stabilizing effects against proteases and nucleases, enhanced water solubility and duplex/triplex stabilities dependent on the structure of chimerae and the linker. The linker can also be a fragment of DNA to generate PNA-(5')-DNA-(3')- PNA chimera which formed stable duplexes with both DNA and RNA with a lower stability than corresponding DNA:DNA and DNA:RNA duplexes.

### 1.17.2 PNA-Oligopeptide chimera

The conjugation of PNA with peptides containing basic amino acids like lysine (Figure 43) or arginine resulted in an increase in solubility as well as formation of stable complexes with DNA<sup>93</sup> due to the interaction of the positively charged amino acids of the peptide with the negative anionic phosphate groups of DNA. A PNA-peptide chimera involving linking a 10-mer oligopeptide containing serine, which is a substrate for protein kinase A was used to assay phosphorylation of serine by kinase.<sup>94</sup> The 5-mer PNA

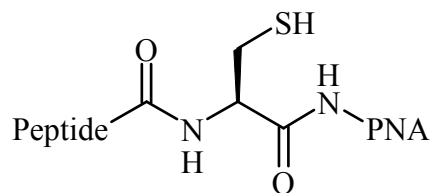


**Figure 43** PNA-Peptide conjugation

sequence H<sub>2</sub>N-TAGGGCOOH linked to the N-terminus of various homooligomeric peptides of cationic amino acids lysine, ornithine and arginine are shown to inhibit human telomerase.

### 1.17.3 PNA-Liposome chimera:

A liposome is a spherical vesicle with a membrane composed of a phospholipid bilayer used to deliver drugs or genetic material into a cell. Liposomes can be composed of naturally-derived phospholipids with mixed lipid chains.

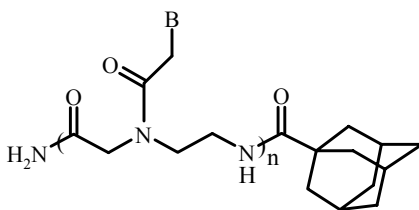


**Figure 44** PNA-adamantyl conjugation

The use of liposomes for transformation or transfection of DNA into a host cell is known as lipofection. In an effort to equip PNAs with a lipophilic tail that would confer liposome affinity,<sup>95</sup> PNA lipid (adamantyl) conjugates (Figure 44) have been prepared and studied their liposome mediated cellular uptake.<sup>96</sup> Liposomal delivery that is often used for transfection with oligonucleotides has, not been successfully used for PNA transport.

In recent years, some peptides that translocate over the plasma membrane in an energy and endocytotic independent manner, have been designed and synthesized. An extensively studied sequence, derived from the third helix of the Antennapedia homeodomain,<sup>97</sup> is called penetratin. Penetratin or penetratin analogs have been used to

transport, moreover penetratin is not the only transport peptide that can mediate PNA transport.<sup>98</sup> Antisense PNAs targeted to Escherichia coli genes can specifically inhibit gene expression, and attachment of PNA to the cell-permeabilizing peptide KFFKFFKFFK dramatically improves antisense potency. The improved potency observed earlier was suggested to be due to better cell uptake.

### 1.18 PNA-Applications

PNA has attracted major attention at the interface of chemistry and biology because of its interesting chemical, physical, and biological properties and potential to act as an active component for diagnostic, molecular biological and pharmaceutical applications. According increase application fields of PNA, the development of cost-effective method of PNA synthesis becomes more important.

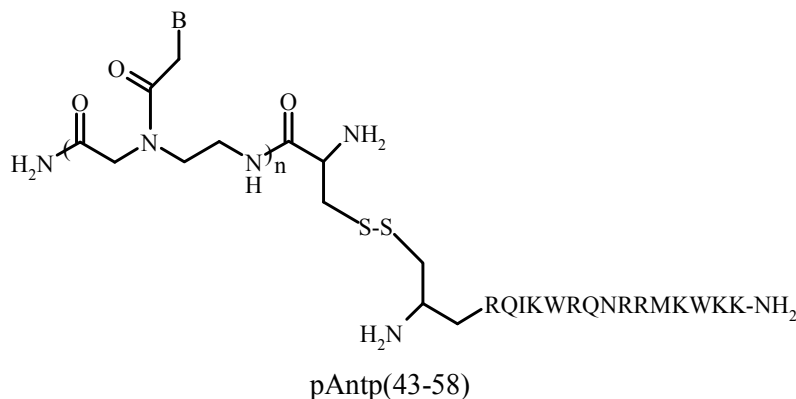


**Figure 45** PNA-Lipid conjugate

#### 1.18.1 Diagnostic applications

PNA has received great attention due to its several favorable properties including chemical and thermal stability, resistance to the nuclease and protease, stronger and faster binding affinity to the complementary nucleic acid, hybridization under low salt

concentration, and higher specificity and sensitivity to the single mismatch. These properties make PNA a powerful tool for diagnostic applications.

### **1.18.1a PCR clamping**

Inhibition of PCR amplification of a specific target by ‘PCR clamping’<sup>99</sup> by which a PNA oligomer is used to inhibit the amplification of a specific target, e.g., by direct competition with a PCR primer has been used very successfully to detect and screen for single base-pair gene variants.<sup>100,101</sup> PNAs were shown to serve as primers<sup>102</sup> for certain DNA polymerases eg. Klenow fragment of DNA polymerase I (E coli) and reverse transcriptases, even though they have no phosphate residues to interact with polymerase, which were presumed to be necessary for binding via highly conserved amino acid residues. When PNA carrying a 5'-amino- 5'-deoxythymidine at the carboxyl terminal end was used as the primer, there was no elongation of PNA primer to yield a PNA-DNA chimera, in cases of phage T4, phage T7 exo (Sequenase 2.0), *Thermus aquaticus* and Deep Vent exo DNA polymerases, as well as HIV-1 reverse transcriptase. It was also found that the elongation of PNA primer was less efficient for the Polymerase (*Thermus thermophilus*) and the reverse transcriptases from avian myeloblastosis virus (AMV) and moloney murine leukemia virus (M-MuLV).<sup>103</sup>

### **1.18.1b Lightup probes**

The method involves the detection of specific nucleic acid sequences in homogeneous solution using a probe with such a dye covalently attached to PNA (peptide nucleic acid) via an aliphatic linker (Figure 46). This so called LightUp probe<sup>104</sup> upon hybridisation with complementary DNA, results in affording a strong enhancement of the

fluorescence. Up to a fifty-fold increase in fluorescence intensity has been achieved with a Lightup probes. The common binding mode of asymmetric cyanine dyes is intercalation between the bases of DNA.

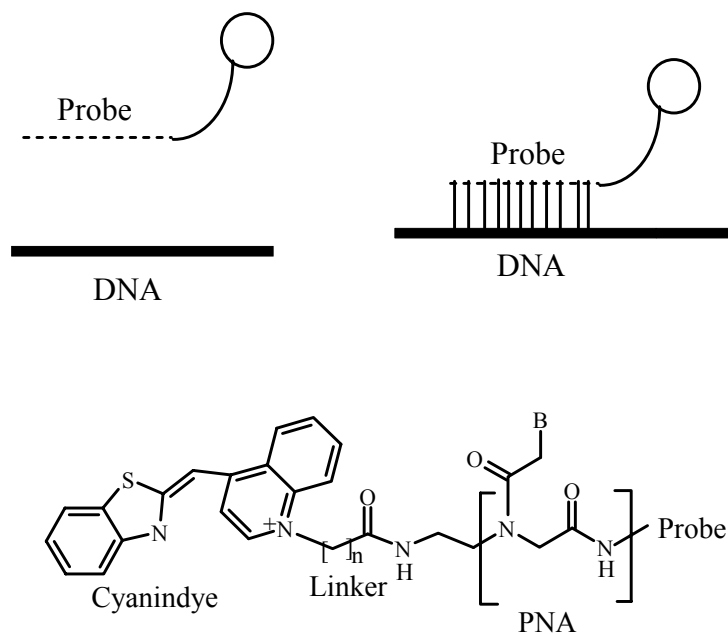


**Figure 46** Schematic representation of lightup probes

### 1.18.1c Molecular beacons (MB)

These represent probes carrying a fluorophore and a quencher at their termini.<sup>104</sup> These probes are ingeniously designed to exhibit a fluorescence signal on binding to complementary targets, thus allowing the real-time quantitative monitoring of hybridization (Figure 47).

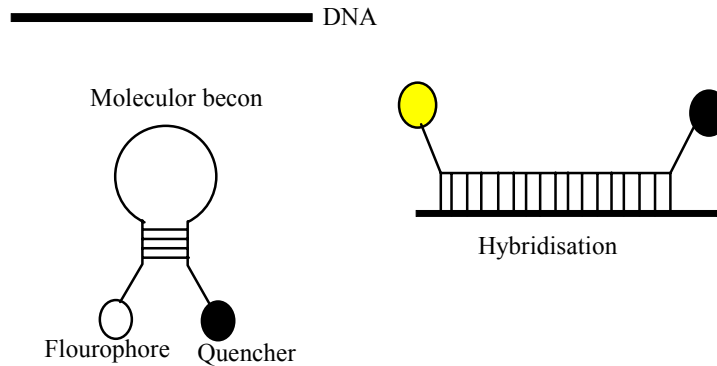


**Figure 47** Molecular beacon

MB and other fluorescent probes have become very useful tools for DNA diagnostics. To use them, however, DNA must be in a denatured single-stranded (ss) form to allow Watson-Crick pairing of the MB to the target site. This requirement limits applications of MB. To overcome this Heiko Khun et al reported PNA beacons for duplex DNA.<sup>105</sup>

#### **1.18.1d Q-PNA:**

It is a new fluorogenic method for sealed-tube PCR analysis using a quencher-labeled peptide nucleic acid (Q-PNA) probe. The Q-PNA hybridizes to a complementary tag sequence located at the 5' end of a 5' fluorophore-labeled oligonucleotide primer, quenching the primer's fluorescence. Incorporation of the primer into a doublestranded amplicon causes displacement of the Q-PNA such that the fluorescence of the sample is a direct indication of the amplicon concentration. The Q-PNA is able to quench multiple primers bearing distinct 5' fluorophores in a single reaction.<sup>106</sup>

#### **1.18.1e Micro Array:**

An array is an orderly arrangement of samples. It provides a medium for matching known and unknown DNA samples based on base-pairing rules and automating the

process of identifying the unknowns.<sup>107</sup> In PNA micro array technology PNA probe is synthesized either *in-situ* or by conventional synthesis followed by immobilization on-chip. The array is exposed to the labeled DNA, and the identity and the abundance of the complementary sequence are determined. This technology is use full in gene discovery, disease diagnosis, pharmacogenomics and toxicogenomics.

## 1.19 Biological applications

### 1.19.1a PNA as anticancer agent (Inhibition of human telomerase)

PNA-peptide duplexes, which can penetrate into cells, have been used in anti-cancer applications. In this manner, telomerase activity in human melanoma cells and tumour specimens was inhibited by PNA conjugated with Antennapedia derived peptide (Antp) at nm concentrations.<sup>108a</sup>

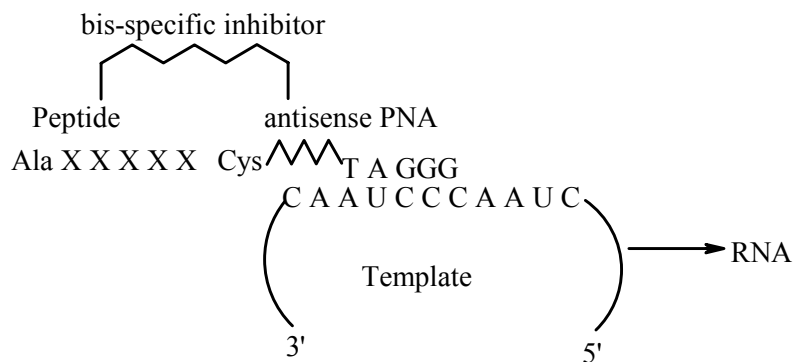


**Figure 48** Design of PNA-peptide conjugates for inhibition of human telomerase

Telomerase is almost ubiquitously expressed in human tumors. Human telomerase is a ribonucleoprotein that adds repeated units of TTAGGG to the ends of chromosomes known as telomeres.<sup>108b</sup> Human telomerase consists of a catalytic protein subunit the telomerase- reverse transcriptase component (hTERT), one or more additional proteins and an integral RNA component (hTR) that serves as a template for the synthesis of

telomeric repeats.<sup>109</sup> The high telomerase activity found in tumor cells has aroused interest in its use as a potential target for anticancer chemotherapy.<sup>110</sup> Inhibition of telomerase activity by conventional DNA oligomers and phosphorothioates showed poor sequence selectivity of these compounds.<sup>111</sup> *In-vitro* studies by Corey et al<sup>112</sup> using Telomere Repeat Amplification Protocol (TRAP) showed that PNA can inhibit the telomerase activity by binding to RNA component of enzyme in picomolar to nanomolar range and the inhibition is due to sequence-selective PNA-mediated inhibition of telomerase activity.

In another approach PNAs were introduced into the cells by transfection using cationic lipids<sup>113</sup> (lipofection). These PNAs were directed to non-template regions of the telomerase RNA that can overcome RNA secondary structure and inhibit telomerase by intercepting the RNA component prior to the holoenzyme assembly. The presence of cationic peptides at the N-terminus of the PNA resulted in enhanced inhibition of telomerase activity when targeted to the RNA template.<sup>114</sup> In addition to these applications, PNAs have been exploited for plasmid labeling<sup>115</sup> and duplex DNA capture,<sup>116</sup> PNAs composed of trans-4-hydroxy-L-proline based monomers and phosphono derivatives were used to isolate mRNA free of genomic DNA.

#### **1.19.1b PNA as delivery agent.**

A major limitation of non-viral gene therapy is the low efficiency of gene transfer into target cells. PNAs can be used as adapters to link peptides, drugs or molecular tracers to plasmid vectors. According to the binding site, the coupling of PNAs to plasmids has no effect either on the transcription of genes included in the plasmid or on the plasmid's physiological activities. Thus, this approach allows circumventing such barriers to gene

transfer and fixing drugs to plasmids in order to enhance the gene delivery or tissue specific targeting. Using a triplex forming PNA as linker, Braden et al <sup>117</sup> observed an 8 times higher nuclear localization of a coupled nuclear localization signal (NLS) than did the free oligonucleotide (Figure 49).

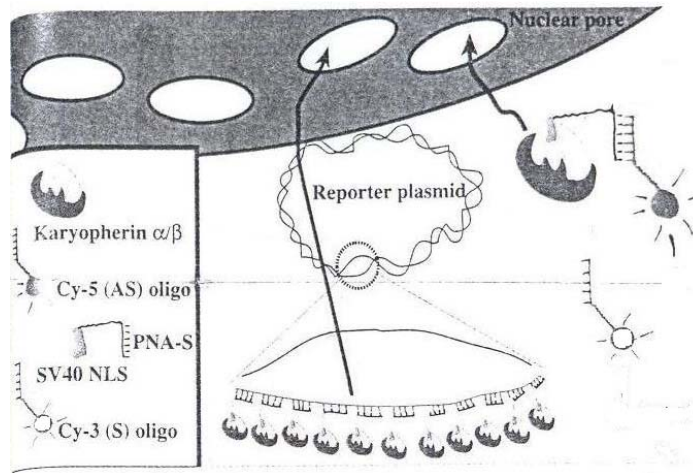


**Figure 49** Schematic representation of the target site in the antisense Cy-5 oligonucleotide hybridizing to the sense PNA-NLS peptide. The PNA-NLS/oligonucleotide complex binds to the karyopherin- $\alpha/\beta$  proteins. The complex is then transported in to the nucleus.

## 1.20 Antisense and antigene applications

Originally conceived as agents for double stranded DNA binding, the unique properties of PNAs as DNA mimics were first exploited for gene therapy drug design. PNAs can inhibit transcription (antigene) and translation (antisense) of genes by tight binding to DNA or mRNA. PNA-mediated inhibition of gene transcription is mainly due to the formation of strand invaded complexes or strand displacement in DNA target. Several in vitro studies have shown that the binding of PNA or bis-PNA to dsDNA can efficiently block transcriptional elongation and inhibit the binding of transcriptional factors and helicases. Thus, Boffa et al<sup>118</sup> reported that PNA invasion of the tandem CAG repeat of the human androgen receptor and the TATA binding protein, inhibits the

transcription of these genes. Application of PNAs as antisense reagents was first demonstrated in 1992. The nuclear microinjection of a 15-mer PNA targeting the translation start region of SV40 large T antigen mRNA inhibited transcription in cell extracts.<sup>119</sup> This inhibition was both

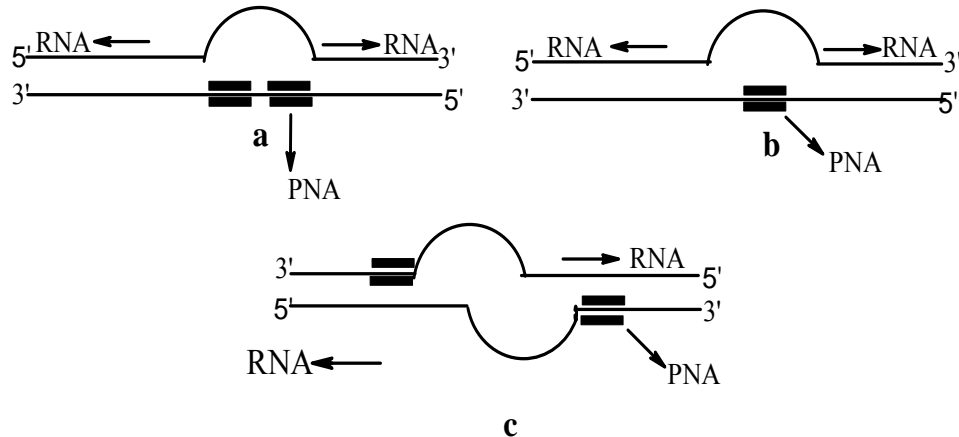


**Figure 50** Transcription initiation from PNA:DNA strand displacement loops

Schematic representation of in vitro transcription from purified DNA fragments containing a single (a) or a double [two sites in cis] (b) or two sites in trans (c) PNA target showing the displacement loops and the start and possible directions of RNA synthesis indicated by arrows (full line:observed).

sequence-specific and dose-dependent. More recently, Mologni et al<sup>120</sup> reported the effect of 3 different types of antisense PNAs on the in vitro expression of PML/RAR gene. The PNAs used targeted various sites involving AUG sites, coding sequences and the 5'-untranslated region (UTR).

### 1.20.1 PNA as artificial transcription promoters

In genetics, a promoter is a DNA sequence that enables a gene to be transcribed. The promoter is recognized by RNA polymerase, which then initiates transcription. In RNA synthesis, promoters are a means to demarcate which genes should be used for messenger RNA creation and, by extension, control which proteins the cell manufactures.

Homopyrimidine peptide nucleic acids (PNAs) form loop structures when binding to complementary double-stranded DNA by strand displacement. RNA polymerase recognizes these and initiates RNA transcription from PNA/double-stranded DNA strand displacement complexes at an efficiency comparable to that of the strong *Escherichia coli* lac UV5 promoter.

### **1.20.2 PNA conjugates as artificial restriction enzymes**

A restriction enzyme (or restriction endonuclease) is an enzyme that cuts double-stranded DNA. This method involves peptide nucleic acid (PNA)-directed design of a DNA-nicking system that enables selective and quantitative cleavage of one strand of duplex DNA at a designated site, thus mimicking natural nickases and significantly extending their potential (Figure 51). This system exploits the ability of pyrimidine PNAs to serve as openers for specific DNA sites by invading the DNA duplex and exposing one DNA strand for oligonucleotide hybridization. The resultant secondary duplex can act as a substrate for a restriction enzyme, which ultimately creates a nick in the parent DNA.<sup>121</sup>

The efficiency of this cleavage is more than 10 fold enhanced when a tandem PNA site is targeted and the site is trans oriented. Thus, PNA targeting makes the single strand specific nuclease S1 behave like a pseudorestriction end nuclease. Tethering a metal binding ligand such as Gly-Gly-His tripeptide to bis-PNA has been used to probe the structure of the DNA. Gly-Gly-His tripeptide placed on either the Watson- Crick or Hoogsteen bis-PNA strand forms a nickel complex that mediates cleavage at specific sites on the proximal displaced and hybridized DNA strands.<sup>122</sup>

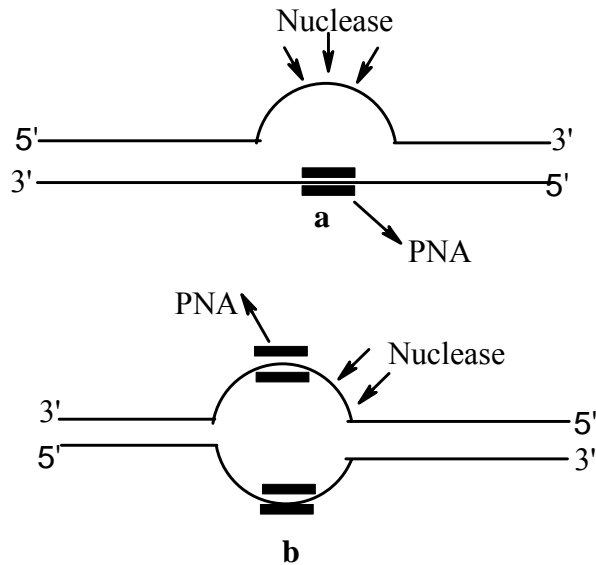


**Figure 51.** Artificial restriction enzymes: a) single cleavage by PNA  
b) double strand cleavage by double PNA clamping.

### 1.21 Present work

The above sections describe the current literature on Peptide Nucleic Acids with reference to structural variations and biological applications. The strand invasion property along with its high affinity and specificity to complementary DNA/RNA has prompted it as a useful tool in therapeutics and biology. However, due to limitations like poor aqueous solubility, self-aggregation, poor cellular uptake and ambiguity in binding orientation has limited further exploitation of PNA in practical applications. In order to circumvent these problems further modifications and the synthesis of newer PNAs to improve their properties, continue to elicit interest. To overcome the problems associated with PNA, there is considerable interest in chemical modifications of PNA backbone to enhance the selectivity as well as the discrimination towards the DNA/RNA and cellular uptake. To induct these properties into PNA, certain degree of chirality and rigidity is needed in PNA backbone.

In this connection Chapter 2 deals with the synthesis and characterization of novel *amp* monomers (Figure 52) and their site specific incorporation in to *aeg* PNA oligomers. The rationale behind the synthesis of *amp* monomers was to induce rigidity and chirality in to the *aeg* backbone. The synthesis of these *amp*-monomers can be achieved by bridging the backbone atoms with the side chain as shown in (Figure 53) to bridge the  $\alpha$ -carbon of the ethylenediamine with  $\alpha'$ -carbon of the glycine unit.

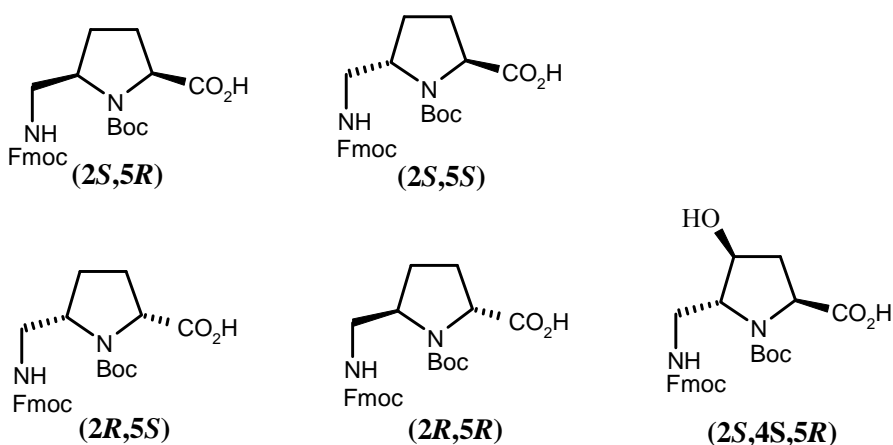


**Figure 52** *amp* (aminomethylprolyl) monomers

This modification restricts movement in both the aminoethyl and the glycol segments of the *aeg*-PNA and restrain the fluctuation region of  $\gamma$  and  $\delta$  torsion angles.

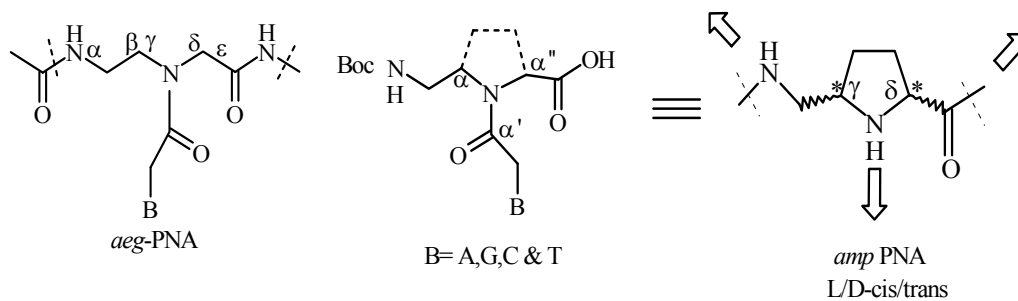


**Figure 53**

**Chapter 3** describes the biophysical studies various *amp* PNA oligomers (octamers) were synthesized, by incorporation of (2*S*,5*R*), (2*S*,5*S*), (2*R*,5*S*), (2*R*,5*R*) and (2*S*,4*S*,5*R*) *amp* PNA monomers at specific sites to investigate the binding efficiency and selectivity towards DNA/RNA. The UV-melting studies were carried out with all synthesized oligomers (Table-1) and the  $T_m$  data was compared with the control *aeg*-PNA- $T_8$ . The CD spectra of *amp* PNA single strands and corresponding complexes with complementary DNA were recorded.

**Chapter 4** is divided in to two sections, section I presents a brief account of various synthetic methodologies to achieve the synthesis of 2,5-disubstituted pyrrolidines.

Section II describes the chemical studies towards synthesis of (2*S*,5*S*) Pyrrolidine dicarboxylic acid and (2*S*,4*S*,5*R*) Bulgecinine (Figure 54) by employing electrochemical oxidation to functionalize the C5 carbon of the proline and 4-hydroxyl proline respectively. These disubstituted pyrrolidine based natural products with structure close to *amp* PNA monomers (Figure 52).

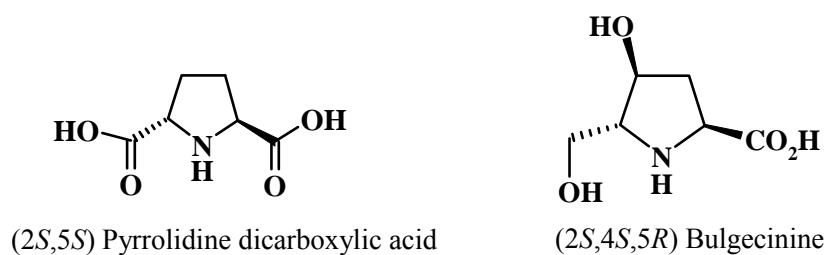


**Figure 54**

## 1.22 Reference

1. Watson, J. D.; Crick, F. H. C. Molecular structure of nucleic acid. A structure for deoxyribose nucleic acid: *Nature* **1953**, *171*, 737.
2. Sanger, W. *Principles of Nucleic Acid Structure* Springer Verlag, New York **1984**.
3. Assa-Munt, N.; Denny, W. A.; Leupin, W.; Kearns, D. R. *Biochemistry* **1985**, *24*, 1441.
4. Hogan, M.; Dattagupta, N.; Crothers, D. M. *Biochemistry* **1979**, *18*, 280.
5. Kopka, M. L.; Yoon, C.; Goodsell, D.; Pjura, P.; Dickerson, R. E. *J. Mol. Biol.* **1985**, *183*, 553.
6. Kopka, M. L.; Yoon, C.; Pjura, P.; Goodsell, D.; Dickerson, R. E. *Proc. Natl. Acad. Sci.* **1985**, *82*, 1376. Reddy, B. S. P.; Sondhi, M.; Lown, J. W. *Pharmacology & Therapeutics* **1999**, *84*, 1.
7. Sanghvi, Y. S. *Antisense Research and application*. Eds. Crooke, S. T.; Lebleu, B. **1993**, CRC Boca Raton. (b) Philips, I. (Ed.) *Methods in Enzymology* 313. (c) Philips, I. (Ed.) *Methods in Enzymology* 314. (d) Antisense Oligonucleotides- Chemical modifications. Uhlmann, E.; Peyman, A. in *Encyclopaedia of Molecular Biology and Biotechnology* (Ed. Meyer, E.) VCH, New York, **1995**.
8. Zamechnik, P.C.; Stephenson, M. L. *Proc. Natl. Acad. Sci.* **1978**, *75*, 280.
9. (a) Felsenfeld, G.; Davies, D. R.; Rich, A. *J. Am. Chem. Soc.* **1957**, *79*, 2023. (b) Moser, H. E.; Dervan, P. B. *Science* **1987**, *238*, 645. (c) Beal, P.A.; Dervan, P. B. *Science* **1991**, *251*, 1360.
10. Soyfer, V. N.; Potamann, V. N. *Triple Helical Nucleic Acids* **1996**, Springer-Verlag, NY.
11. Chan P. P. and Glazer, P. M. Triplex DNA: fundamentals, advances and potential applications for gene therapy. *Mol. Med.* **1997**, *75*, 267.
12. Praseuth D.; Guieysse, A. L.; Helene, C. Triple helix formation and the antigene strategy for sequence-specific control of gene expression. *Biochim. Biophys. Acta.* **1999**, *489*, 181.
13. Casey, B. P.; Glazer, P. M. Gene targeting via triple-helix formation. *Prog. Nucleic Acid Res. Mol. Biol.* **2001**, *67*, 163.

14. (a) Uhlmann, E.; Peyman, A. *Chem. Rev.* **1990**, *90*, 544. (b) Milligan, J. F.; Matteucci, M. D.; Martin, J. C. *J. Med. Chem.* **1993**, *36*, 1923.
15. (a) Strivchak, E. P.; Summerton, J. E.; Weller, D. D. *Nucleic Acids Res.* **1989**, *17*, 6129. (b) Nielsen, P. E. *Annu. Rev. Biophys. Biomol. Struct.* **1995**, *24*, 167.
16. Varma, R. S. *Syn Lett.* **1993**, *9*, 621.
17. Toulme, J. J. *Nature Biotech.* **2001**, *19*, 17.
18. (a) Chin, D. J.; Green, G. A.; Zon, G.; Szoka, Jr. F. C.; Straubinger, R. M. Rapid nuclear accumulation of injected oligodeoxyribonucleotides. *New Biologist*, **1990**, *2*, 1091. (b) Leonetti, J. P.; Mechti, N.; Degols, G.; Gagnor, C.; Lebleu, B. Intracellular distribution of microinjected antisense oligonucleotides. *Proc. Natl. acad. Sci. USA.* **1991**, *88*, 2702.
19. Halford, M. H.; Jones, M. S. Synthetic analogues of polynucleotides. *Nature* **1968**, *217*, 638.
20. (a) Sanghvi, Y. S.; Cook, P. D. in *Carbohydrate Modifications in Antisense Research*. Washington, DC: *American Chemical Society* **1994**, *1*, 297.
21. (a) Roughton, A. L.; Portmann, S.; Benner, S. A.; Egli, M. Crystal structure of a dimethylene sulfone-linked ribonucleoside analog. *J. Am. Chem. Soc.* **1995**, *117*, 7249. (b) McElroy, E. B.; Bandarn, R.; Huand, J.; Widlanski, T. S. Synthesis and physical properties of sulfonamide-containing oligonucleotides. *Bioorg. Med. Chem. Lett.* **1994**, *4*, 1071. (c) Huie, E. M.; Kirshenbaum, M. R.; Trainos, G. L. Oligonucleotides with a nuclease resistant sulfurbased linkage. *J. Org. Chem.* **1992**, *57*, 4569.
22. Veal, J. M.; Gao, X.; Brown, F. K. A comparison of DNA-oligomer duplexes containing formacetal and phosphodiester linkers using molecular dynamics and quantum mechanics. *J. Am. Chem. Soc.* **1993**, *115*, 7139.
23. Jones, R. J.; Lin, K. Y.; Milligan, J. F.; Wadwani, S.; Matteucci, M. D. Synthesis and binding properties of pyrimidines oligodeoxy nucleoside analogs containing neutral phosphodiester replacements. The formacetal and 3'-thioformacetal Internucleoside linkages. *J. Org. Chem.* **1993**, *58*, 2983.

24. Vasseur, J. J.; Debart, F.; Sanghvi, Y. S.; Cook, P. D. Oligonucleosides: Synthesis of a novel methylhydroxylamine-linked nucleoside dimer and its incorporation into antisense sequences. *J. Am. Chem. Soc.* **1992**, *114*, 4006.
25. De Mesmaeker, A.; Lebreton, J.; Waldner, A.; Fritsch, V.; Wolf, R. M. Replacement of the phosphodiester linkage in oligonucleotides: comparison of two structural amide isomers. *Bioorg. Med. Chem. Lett.* **1994**, *4*, 873. De Mesmaeker, A.; Lesueur, C.; Bevierre, M. O.; Waldner, A.; Fritsch, V.; Wolf, R. M. Increased affinity of modified oligonucleotides with conformationally constrained furanose rings to complementary RNA strands. *Angew. Chem.* **1996**, *108*, 2960.
26. (a) Stirchak, E. P.; Summerton, J. E.; Weller, D. D. Uncharged stereoregular nucleic acids analogs. Synthesis of a cytosine-containing oligomer with carbamate internucleoside linkages. *J. Org. Chem.* **1987**, *52*, 4202. (b) Coull, J. M.; Carlson, D. G.; Weith, H. L. Synthesis and characterization of a carbamate linked oligonucleotide. *Tetrahedron Lett.* **1987**, *28*, 745
27. Wendeborn, S.; Jounno, C.; Wolf, R. M.; De Mesmaeker, A. Replacement of the phosphodiester linkage in oligonucleotides by an acetylenic bond. Comparison between carbon-, sulfur, and oxygen containing analogs. *Tetrahedron Lett.* **1996**, *37*, 5511.
28. Imbach, J. L.; Rayner, B.; Morvan, F. Sugar-Modified Oligonucleotides: Synthesis, Physicochemical and Biological Properties. *Nucleosides Nucleotides* **1989**, *8*, 627.
29. (a) Allart, B.; Khan, K.; Rosemeyer, A. H.; Schepers, G.; Hendrix, C.; Rothenbacher, K.; Seela, F.; Aerschot, V.; Herdewijn, P. *d*-Altritol Nucleic Acids (ANA): Hybridisation Properties, Stability, and Initial Structural Analysis *Tetrahedron* **1999**, *55*, 6527. (b) Harald, W.; Folkert, R. Rene.; Mahesh, R.; Griet, A.; Martin, B.; Ramanarayanan K.; Albert E. Pentopyranosyl Oligonucleotide Systems. Part 11: Systems with Shortened Backbones. (D)- $\beta$ -Ribopyranosyl- (4'→3')-and(L)- $\alpha$ -Lyxopyranosyl- (4'→3')- oligonucleotides. *Bioorganic & Medicinal Chemistry* **2001**, *9*, 2411.
30. (a) Petersen, M.; Wengel, J. LNA. A versatile tool for therapeutic and genomics. *Trends Biotechnol.* **2003**, *21*, 74. (b) Koshkin, A.; Singh, S. K.; Nielsen, P.; Rajwanshi, V. K.; Kumar, R.; Meldgaard, M.; Olsen, C. E.; Wengel, J. LNA (locked

- nucleic acid): synthesis of the adenine, cytosine, guanine, 5-methylcytosine, thymine and uracil bicyclonucleotide monomers, oligomerization and unprecedented nucleic acid recognition. *Tetrahedron* **1998**, *54*, 3607. (c) Singh, S. K.; Nielsen, P.; Koshkin, A. A.; Wengel, J. LNA (locked nucleic acid): Synthesis and high affinity nucleic acid recognition. *Chem. Commun.* **1998**, 455.
31. (a) Obika, S.; Nanbu, D.; Hari, Y.; Andoh, J. I.; Mori, K. I.; Doi, T.; Imanshi, T. Stability and structural features of the duplexes containing nucleoside analogues with fixed type conformation, 2'-O, 4'-C-methyleneribonucleosides. *Tetrahedron Lett.* **1998**, *39*, 5401. (b) Hertoghs, K. M.; Ellis, J. H.; Catchpole, I. R. Use of locked nucleic acid oligonucleotides to add functionality to plasmid DNA. *Nucleic Acid Res.* **2003**, *20*, 5817.
32. Jing, W.; Birgit, V.; Ingrid, L.; Eveline, L.; Matthias, F.; Chris, H.; Helmut, R.; Frank, Seela.; Arthur, Van Aerschot.; Herdewijn. Cyclohexene Nucleic Acids (CeNA). Serum Stable Oligonucleotides that Activate RNase H and Increase Duplex Stability with Complementary RNA. *J. Am.Chem. Soc.* **2000**, *122*, 8595.
33. (a) Strivchak, E. P.; Summerton, J. E.; Weller, D. D. *Nucleic Acids Res.* **1989**, *17*, 129. (b) Summerton, J.; Weller, D. Morpholino antisense oligomers: Design, preparation, and properties. *Antisense Nucleic Acid Drug Dev.* **1997**, *7*, 187.
34. (a)W. Saenger. (Ed.) *Principles of Nucleic Acids Structure*, Springer-Verlag, New York, **1984**. (b) Povsic, T. J.; Dervan, P. B. Triple helix formation by liganucleotides on DNA extended to the physiological pH range *J. Am. Chem. Soc.* **1989**, *111*, 3059. (c) Durland, R. H.; Rao, T. S.; Revankar, G. R.; Myrick, M. A.; Seth, D. M.; Rayford, J.; Singh, P.; Jayaraman, K. *Nucleic. Acids Res.* **1994**, *22*, 3233. (d) Soliva, R.; Garcia, R. G.; Blas, J. R.; Eritja, R.; Asensio, J. L.; Gonzalez, C.; Luque, F. J. Orozco, M. *Nucleic Acids Res.* **2000**, *28*, 4531. (e) Avino, A.; Morales, J. C.; Frieden, M.; de la Torre, B. G.; Garcia, R. G.; Cubero, E.; Luque, F. J.; Orozco, M.; Ferran, A.; Eritja, R. Parallel-stranded hairpins containing 8-aminopurines. Novel efficient probes for triple-helix formation *Bioorg. Med. Chem. Lett.* **2001**, *11*, 1761. (f) Shimizu, M.Koizumi, T.; Inoue, H.; Ohtsuka, E. Effects of 5-methyl substitution in 2'-O-methyloligo-(pyrimidine) nucleotides on triple-helix formation *Bioorg. Med. Chem.Lett.* **1994**, *4*, 1029. (g) Miller, P. S.; Bhan, P.; Cushman, C. D.; Trapane, T. L.

- Biochemistry*, **1992**, *31*, 6788. Davison, E. C., Johnsson, K. *Nucleosides Nucleotides* **1993**, *12*, 237-243. (h). Ono, A.; Ts'o, P. O. P.; Kan, L-S. *J. Org. Chem.* **1992**, *57*, 3225.
35. (a) Pooga, M.; Soomets, U.; Hällbrink, M.; Valkna, A.; Saar, K.; Rezaei, K.; Kahl, U.; Hao, J. X.; Xu, X. J. Iesenfeld-Hallin, Z.; Hökfelt, T.; Bartfai, T.; Langel, Ü. Cell penetrating PNA constructs regulate galanin receptor levels and modify pain transmission in vivo. *Nat Biotechnol.* **1998**, *16*, 857. (b) Behn, M.; Schuermann, M. Sensitive detection of p53 gene mutations by a 'mutant enriched' PCR-SSCP technique. *Nucleic Acids Res.* **1998**, *26*, 1356.
36. Murdock, D. G.; Christacos, N. C.; Wallace, D. C. The age-related accumulation of a mitochondrial DNA control region mutation in muscle, but not brain, detected by a sensitive PNA-directed PCR clamping based method. *Nucleic Acids Res* **2000**, *28*, 4350.
37. Nielsen, P. E.; Egholm, M.; Berg, R. H.; Buchardt, O. Sequence-selective recognition of DNA by strand displacement with a thymine-substituted polyamide. *Science* **1991**, *254*, 1497.
38. Egholm, M.; Buchardt, O.; Christensen, L.; Behrens, C.; Freier, S. M.; Driver, D. A.; Berg, R.H.; Kim, S. K.; Nordon, B.; Nielsen, P. E. PNA hybridizes to complementary oligonucleotides obeying the Watson-Crick hydrogen-bonding rules. *Nature* **1993**, *365*, 566.
39. Jensen, K. K.; Qrum, H.; Nielsen, P. E.; Norden, B. Hybridization kinetics of peptide nucleic acids (PNA) with DNA and RNA studied with BIAcore Technique. *Biochemistry* **1997**, *36*, 5072.
40. Kuhn, H.; Demidov, V. V.; Nielsen, P. E.; Frank-Kamenetskii, M. D. *J. Mol. Biol.* **1999**, *286*, 1337.
41. Demidov, V.V.; Cherny, D. I.; Kurakin, A. V.; Yavnilovich, M. V.; Malkov, V. A. Frank-Kamenetskii, M. D.; Sönnichsen, S. H.; Nielsen, P. E. *Nucl. Acids.Res.* **1994**, *22*, 5218.
42. Møllegaard, N. E.; Buchardt, O.; Egholm, M.; Nielsen, P. E. *Proc. Natl. Acad. Sci.* **1994**, USA *91*, 3892.

43. Brown, S. C.; Thomson, S. A.; Veal, J. M.; Davis, D. G. NMR Solution structure of a peptide nucleic acid complexed with RNA. *Science* **1994**, *265*, 777.
44. Eriksson, M.; Nielsen, P. E. Solution structure of a peptide Nucleic Acid-DNA duplex. *Nature Struct. Biol.* **1996**, *3*, 410.
45. Betts, L.; Josey, J. A.; Veal, J. M.; Jordan, S. R. A nucleic acid triple helix formed by a Peptide Nucleic Acid-DNA complex. *Science* **1995**, *270*, 1838.
46. Rasmussen, H.; Kastrup, J. S.; Nielsen, J. N.; Nielsen, J. M.; Nielsen, P.E. Crystal structure of a Peptide Nucleic acid (PNA) duplex at 1.7 Å Resolution. *Nature Struct. Biol.* **1997**, *4*, 98.
47. (a) Leijo, M. *et al*: Structural characterization of PNA-DNA duplexes by NMR. Evidence for DNA in a B-like conformation. *Biochemistry* **1994**, *22*, 9820.
48. Kim, S. K.; Nielsen, P.E.; Egholm, M.; Buchardt, O.; Berg, R. H.; Norden, B: Right handed triple helix formed between peptide nucleic acid PNA-T8 and poly dA shown by linear and circular dichroism spectroscopy. *J. Am. Chem. Soc.* **1993**, *115*, 6477.
49. Hyrup, B.; Egholm, M.; Rolland, M.; Nielsen, P. E.; Berg, R. H.; Buchardt, O. *J. Chem. Soc. Chem. Commun.* **1993**, 518.
50. Hyrup, B.; Egholm, M.; Nielsen, P. E.; Wittung, P.; Nordén, B.; Buchardt, O. *J. Am. Chem. Soc.* **1994**, *116*, 7964.
51. Hyrup, B.; Egholm, M.; Buchardt, O.; Nielsen, P.E. *Bioorg. Med. Chem. Lett.* **1996**, *6*, 1083.
52. (a) Haiima, G.; Lohse, A.; Buchardt, O.; Nielsen, P. E. *Angew. Chem. Int. Ed. Engl.* **1996**, *35*, 1939. (b) Sforza, S.; Haiima, G.; Marchelli, R.; Nielsen, P. E.; *Eur. J. Org. Chem.* **1999**, 197. (c) Zhang, L.; Min, J.; Zhang, L. *Bioorg. Med. Chem. Lett.* **1999**, *9*, 2903.
53. Barawkar, D. A.; Bruice, T. C. *J. Am. Chem. Soc.* **1999**, *121*, 10418.
54. Efimov, V. A.; Choob, M. V.; Buryakova, A. A.; Chakhmakhcheva, O. G. *Nucleosides & Nucleotides* **1998**, *17*, 1671.
55. Efimov, V. A.; Buryakova, A. A.; Choob, M. V.; Chakhmakhcheva, O. G. *Nucleosides & Nucleotides* **1999**, *18*, 1393.

56. Altmann, K. H.; Chiesi, C. S.; Gracia-Echeverria, C. Polyamide Based Nucleic Acid Analogs -Synthesis of 8-Amino Acids with Nucleic Acid Bases Bearing Side Chains *Bioorg. Med. Chem. Lett.* **1997**, *7*, 1119.
57. Garcia-Echeverria, C.; Husken, D.; Chiesi, C. S.; Altmann, K-H. Novel Polyamide Based Nucleic Acid Analogs - Synthesis of Oligomers and RNA-Binding Properties *Bioorg. Med. Chem. Lett.* **1997**, *7*, 1123.
58. Kuwahara, M.; Arimitsu, M.; Sisido, M. *J. Am. Chem. Soc.* **1999**, *121*, 256.
59. Krotz, A. H.; Buchardt, O.; Nielsen P. E. Synthesis of retro-inverso peptide nucleic acids: 1characterisation of the monomer. *Tetrahedron Lett.* **1995**, *36*, 6937. (b) Jordan, S.; Schwemler, C.; Kosch, W.; Kretschmer, A.; Schwenner, E.; Stropp, U.; Mielke, B. New hetero-oligomeric peptide nucleic acids with improved binding properties to complementary DNA, *Bioorg. Med. Chem. Lett.* **1997**, *7*, 687.
60. (a) Kumar, V. A.; Ganesh, K. N. Conformationally constrained PNA analogues: structural evolution toward DNA/RNA binding selectivity. *Acc. Chem. Res.* **2005**, *38*, 404. (b) Kumar, V. A. Structural preorganization of peptide nucleic acids: chiral cationic analogues with five- or sixmembered ring structures. *Eur. J. Org.Chem.* **2002**, 2021.
- 63 Meena; Kumar, V. A.; Ganesh, K. N. Synthesis and evaluation of prolyl carbamate nucleic acids (PrCNA). *Nucleosides, Nucleotides, Nucleic Acids.* **2001**, *20*, 1193.
- 64 Lowe, G.; Vilaivan, T. Amino acids bearing nucleobases for the synthesis of novel peptide nucleic acids. *J. Chem. Soc. Perkin Trans 1*, **1997**, 539.
- 65 Lowe, G.; Vilaivan, T. Solid phase synthesis of novel peptide nucleic acids. *J.Chem. Soc. Perkin Trans I* **1997**, 555.
- 66 D'Costa, M.; Kumar, V. A.; Ganesh, K. N. N7-Guanine as a C+ Mimic in Hairpin *aeg/aep*PNA-DNA Triplex: Probing Binding Selectivity by UV-T<sub>m</sub> and Kinetics by Fluorescence-Based Strand-Invasion Assay. *J. Org. Chem.* **2003**, *68*, 4439.
- 67 Puschl, A.; Boesn, G.; Zuccarello, G.; Dahl, O.; Pitsch, S.; Nielsen, P. E. Synthesis of pyrrolidinone PNA: A novel conformationally restricted peptide nucleic acid analogues *J. Org. Chem.* **2001**, *66*, 707.

- 68 Samuel, T. H.; David, T.; Hickman, T.; Morral, J.; Beadham, I. G.; Micklefield, J. Nucleic acid binding properties of thyminy and adeniny pyrrolidine-amide oligonucleotide mimics (POM). *Chem. Comm.* **2004**, 516.
- 69 Sharma, N. K.; Ganesh, K. N. Expanding the repertoire of pyrrolidyl PNA analogues for DNA/RNA hybridization selectivity: aminoethylpyrrolidinone PNA (*aepone*-PNA) *Chem. Commun.* **2003**, 2484.
- 70 Vilaivan, T.; Khongdeesameor, C.; Harnyuttanokam, P.; Lowe, G. Synthesis and properties of novel pyrrolidinyl PNA carrying b amino acid spacers. *Tetrahedron Lett.* **2001**, 42, 5533.
- 71 Vilaivan, T.; Khongdeesameor, C.; Harnyuttanokam, P.; Lowe, G. J. A novel pyrrolidinyl PNA showing high sequence specificity and preferential binding to DNA over RNA. *J. Am. Chem. Soc.* **2002**, 124, 9326.
- 72 (a) Puschl, A.; Tedeschi, T.; Nielsen, P. E. Pyrrolidine PNA: A novel conformationally restricted PNA analogues. *Org. Lett.* **2000**, 2, 4161. (b) Kumar, V. A.; Pallan, P. S.; Meena,; Ganesh, K. N. Pyrrolidine nucleic acids: DNA/PNA oligomers with 2- hydroxy/aminomethyl-4-(thymine-1-yl)pyrrolidine-N- acetic acid. *Org. Lett.* **2001**, 3, 1269. (c) Kumar, V. A.; Pallan, P. S.; Meena,; Ganesh, K. N. Pyrrolidine nucleic acids: DNA/PNA oligomers with 2-hydroxyl aminomethyl-4-(thymine-1-yl)pyrrolidine-N-acetic acid. *Org. Lett.* **2001**, 3, 1269. (d) D'Costa, M.; Kumar, V. A.; Ganesh, K. N. Synthesis of 4(S)-(NBoc-amino)-2(S/R)-(thymine-1-yl)-pyrrolidine-N-1-acetic acid: a novel cyclic PNA with constrained flexibility. *Tetrahedron. Lett.* **2002**, 43, 883. (e) Lonkar, P.; Ganesh, K. N.; Kumar, V. A. Chimeric (aeg-pyrrolidine) PNA: Synthesis and stereo- discriminative duplex binding with DNA/RNA. *Org. Biomol. Chem.* **2004**, 2, 2604.
- 73 Michael, C. Mark, M.; Witschi, A.; Larionova, N.; John, M.; Russell; Haynes, D.; Toshiaki, H.; Grajkowski, A.; Appella, D. H. A cyclopentane conformational restraint for a Peptide Nucleic Acid: Design, asymmetric synthesis and improved binding affinity o DNA & RNA. *Org. Lett.* **2003**, 5, 2695.
- 74 Govindaraju, T.; Kumar, V. A.; Ganesh, K. N. *cis*-Cyclopentyl PNA (*cpPNA*) as constrained chiral PNA analogues: stereochemical dependence of DNA/RNA hybridization. *Chem. Commun.* **2004**, 7, 860.

- 75 Pokorski, J. K.; Witschi, M. A.; Purnell, B. L.; Appella, D. H. (*S,S*)-*trans*-cyclopentane constrained peptide nucleic acids. A general backbone.
- 76 Bregant, S.; Burlina, F.; Vaissermann, J.; Chassaing, G.; *Eur. J. Org. Chem.* **2001**, 3285-3294. (b) Bregant, S.; Burlina, F.; Chassaing, G. New thiazane and thiazolidine PNA monomers: synthesis, incorporation into PNAs and hybridization studies. *Bioorg. Med. Chem. Lett.* **2002**, *12*, 1047.
- 77 (a) Schoning, K.; Scholz, P.; Guntha, S.; Wu, X.; Krishnamurthy, R.; Eschenmoser, Chemical etiology of nucleic acid structure: The-threofuranosyl (3'-2) oligonucleotide system. *Science* **2000**, *290*, 1347. (b) Miculka, C.; Windhab, N.; Eschenmoser, A.; Sherer, S.; Quinkert, G. PCT Int. Appl. WO 9915509 A2 **1999**, 43. (c) Kozlov, A.; Politis, K.; Van, A.; Busson, R.; Herdewijn, P.; Orgel, E. Nonenzymatic synthesis of RNA and DNA oligomers on hexitol nucleic acids templates: The importance of the A-structure. *J. Am. Chem. Soc.* **1999**, *121*, 2653.
- 78 Goodnow Jr., R. A.; Richou, A. R.; Tam, S. *Tetrahedron Lett.* **1997**, *38*, 3195  
Goodnow Jr., R. A.; Tam, S.; Preuss, D. L.; McComas, W. W. Oligomer synthesis and DNA/RNA recognition properties of a novel oligonucleotide backbone analog: Glucopyranosyl nucleic amide (GNA). *Tetrahedron Lett.* **1997**, *38*, 3199.
- 79 Lonkar, P. S.; Kumar, V. A. *trans*-5-Aminopipercolyl-*aep*PNA chimera: design, synthesis, and study of binding preferences with DNA/RNA in duplex/triplex mode. *J. Org. Chem.* **2005**, *70*, 6956.
- 80 (a) Shirude, P.; Kumar, V. A.; Ganesh, K. N. Chimeric peptide nucleic acids incorporating (2*S*,5*R*)-aminoethyl pipercolyl units : synthesis and DNA binding studies. *Tetrahedron Lett.* **2004**, *45*, 3085. (b) D'Costa, M.; Kumar, V. A.; Ganesh, K. N. Aminoethylprolyl peptide nucleic acids (*aep*PNA): chiral PNA analogues that form highly stable DNA:*aep*PNA<sub>2</sub> triplexes. *Org. Lett.* **1999**, *1*, 1513. (c) Puschl, A.; Boesen, T.; Tedeschr, T.; Dahl, O.; Nielsen, P. E. Synthesis of (3*R*,6*R*) and (3*S*,6*R*)-piperidinone PNA. *J. Chem. Soc., Perkin 1* **2001**, 2757.
- 81 Lagriffoule, P.; Wittung, P.; Eriksson, M.; Jensen, K. K.; Norden, B.; Buchardt, O.; Nielsen, P. E. Peptide nucleic acids (PNAs) with conformationally constrained, chiral cyclohexyl derived backbone. *Chem. Eur. J.* **1997**, *3*, 912.

- 82 (a) Govindaraju, T.; Gonnade, R.; Badbhade, M.; Kumar V. A.; Ganesh, K. N. (1*S*, 2*R*/1*R*,2*S*)-Aminocyclohexyl glycylyl thymine PNA: Synthesis, monomer crystal structures and DNA/RNA hybridization studies. *Org. Lett.* **2003**, *5*, 3013. (b) Govindaraju, T.; Kumar, V. A.; Ganesh, K. N. Synthesis and evaluation of (1*S*,2*R*/1*R*,2*S*) aminocyclohexylglycylyl PNAs as conformationally preorganized PNA analogues for DNA/RNA recognition. *J. Org. Chem.* **2004**, *69*, 1858. (c) Govindaraju, T.; Kumar, V. A.; Ganesh, K. N. *cis*-Cyclopentyl PNA (cp-PNA) as constrained chiral PNA analogues: stereochemical dependence of DNA/RNA hybridization. *Chem. Commun.* **2004**, 860.
- 83 Maison, W.; Schlemminger, I.; Westerhoff, O.; Martens, J. Modified PNAs: a simple method for the synthesis of monomeric building blocks. *Bioorg. Med. Chem. Lett.* **1999**, *9*, 581.
- 84 Sazani, P.; Kang, S. H.; Maier, M. A.; Wei, C.; Dillman, J.; Summerton, J.; Manoharan, M.; Kole, R. Nuclear antisense effects of neutral, anionic and cationic oligonucleotide analogs. *Nucleic Acids Res.* **2001**, *29*, 3965.
- 85 Maison, W.; Schlemminger, I.; Westterhoff, O.; Martens, J. Modified PNAs: A simple method for the synthesis of monomeric building blocks. *Bioorg. Med. Chem. Lett.* **1999**, *9*, 581.
- 86 Haaïma, G.; Hansen, H. F.; Christensen, L.; Dahl, O.; Nielsen, P. E. Increased DNA binding and sequence discrimination of PNA oligomers containing 2,6-diaminopurine. *Nucleic Acids Res.* **1997**, *25*, 4639.
- 87 Egholm, M.; Christensen, L.; Dueholm, K.; Buchardt, O.; Coull, J.; Nielsen, P. E. Efficient pH-independent sequence-specific DNA binding by pseudoisocytosine containing bis-PNA. *Nucleic Acids Res.* **1995**, *23*, 217.
- 88 Eldrup, A. B.; Dahl, O.; Nielsen, P. E. A novel Peptide Nucleic Acid monomer for recognition of thymine in triple helix structure. *J. Am. Chem. Soc.* **1997**, *119*, 11116.
- 89 Timar, Z.; Bottka, S.; Kovacs, L.; Penke, B. Synthesis and preliminary thermodynamic investigation of hypoxanthine-containing peptide nucleic acids. *Nucleosides Nucleotides* **1999**, *18*, 1131.

- 90 Gangamani, B. P.; Kumar, V. A.; Ganesh, K. N. 2-Aminopurine peptide nucleic acids (2-*ap*PNA): intrinsic fluorescent PNA analogues for probing PNA-DNA interaction dynamics. *Chem. Commun.* **1997**, 1913.
- 91 Finn, P. J.; Gibson, N. J.; Fallon, R.; Hamilton, A.; Brown, T. Synthesis and properties of DNA-PNA chimeric oligomers. *Nucleic Acids Res.* **1996**, *24*, 3357.
- 92 Petersen, K. H.; Buchardt, O.; Nielsen, P. E. Synthesis and oligomerization of Nδ-Boc-N α-) thymine-1-yl-acetyl)-ornithine. *Bioorg. Med. Chem. Lett.* **1996**, *6*, 793.
- 93 Van der Laan, A. C.; Brill, R.; Kulimelis, R. G.; Kuyl-Yeheskiety, E.; van Boom, J. H.; Andrus, A.; Vinayak, R. *Tetrahedron Lett.* **1997**, *38*, 2249.
- 94 Koch, T.; Naesby, M.; Wittung, P.; Jørgensen, M.; Larsson, C.; Buchardt, O.; Stanley, C. J.; Nordén, B.; Nielsen, P.E.; Grum H. *Tetrahedron Lett.* **1995**, *36*, 6933.
- 95 Luca Mologni, Edoardo Marchesi, Peter E. Nielsen and Carlo Gambacorti-Passerini Inhibition of Promyelocytic Leukemia (PML)/Retinoic Acid Receptor- and PML Expression in Acute Promyelocytic Leukemia Cells by Anti-PML Peptide Nucleic Acid. *Cancer Research.* **2001**, *61*, 5468.
- 96 Knudsen, H. PhD. Thesis university of Copenhagen, 1997: T. Ljungstrom, H.; Knudsen, H.; Nielsen, P. E.
- 97 (a) Derossi, D.; Calvet, S.; Trembleau, A.; Brunissen, A.; Chassaing, G.; Prochiantz, Cell internalization of the third helix of the Antennapedia homeodomain is receptorindependent. *J. Biol. Chem.* **1996**, *128*, 18188-18193. (b) Derossi, D.; Chassaing, G.; Prochiantz, A. Trojan peptides: the penetratin system for intracellular delivery. *Trends Cell.* **1998**, *8*, 84.
- 98 Pooga, M.; Soomets, U.; Hällbrink, M.; Valkna, A.; Saar, K.; Rezaei, K.; Kahl, U.; Hao, J. X.; Xu, X. J.; Iesenfeld-Hallin, Z.; Hökfelt, T.; Bartfai, T.; Langel, Ü. Cell penetrating PNA constructs regulate galanin receptor levels and modify pain transmission in vivo. *Nat Biotechnol.* **1998**, *16*, 857.
- 99 Behn, M.; Schuermann, M. Sensitive detection of p53 gene mutations by a 'mutant enriched' PCR-SSCP technique. *Nucleic Acids Res.* **1998**, *26*, 1356.
- 100 Murdock, D.G.; Christacos, N. C.; Wallace, D. C. The age-related accumulation of a mitochondrial DNA control region mutation in muscle, but not brain, detected by a

- sensitive PNA-directed PCR clamping based method. *Nucleic Acids Res.* **2000**, *28*, 4350.
- 101 Behn, M.; Thiede, C.; Neubauer, A.; Pankow, W.; Schuermann, M. Facilitated detection of oncogene mutations from exfoliated tissue material by a PNA-mediated 'enriched PCR' protocol. *J. Pathol.* **2000**, *190*, 69.
- 102 Lutz, M. J.; Benner, S. A.; Hein, S.; Breipohl, G.; Uhlmann, E. *J. Am. Chem. Soc.* **1997**, *119*, 3177.
- 103 Will, D. W.; Breipohl, G.; Benner, S. A.; Uhlmann, E. *Nucleosides & Nucleotides* **1999**, *18*, 393.
- 104 (a) Svanvik, N.; Westman, G.; Wang, D.; Kubista, M. *Anal. Biochem.*, **2000**, *281*, 26. (b) Platek, A.S.; Tyagi, S.; Pol, A.C.; Telenti, A.; Miller, L. P.; Kramer, F.R.; and Alland, D. Molecular beacon sequence analysis for detecting drug resistance in *Mycobacterium tuberculosis*. *Nature Biotech.* **1998**, *16*, 359. (c) Tyagi, S.; Bratu, D.P.; Kramer, F.R. Multicolor molecular beacons for allele discrimination. *Nature Biotech.* **1998**, *16*, 49. (d) Tyagi, S.; Kramer, F.R. Molecular beacons: Probes that fluoresce upon hybridization. *Nature Biotech.* **1996** *14*, 303. (e) Tyagi, S.; Marras, S.A.E.; Kramer, F.R. Wavelength-shifting molecular beacons. *Nature Biotech.* **2000** *18*, 1191.
- 105 Kuhn, H.; Demidov, V. V.; Brian D.; Gildea.; Mark J. F.; Coull, J. M.; Frank-amenetskiti M. D. *Antisense & Nucleic Acid drug development*, **2001**, *11*, 265.
- 106 Mark J. F.; Hyldig, J. J.; Nielsen, P. E.; Gildea, B. D.; Coull, J. M. Self-Reporting PNA/DNA Primers for PCR Analysis. *Genome research.* **2001**, *11*, 609.
- 107 (a) Winssinger, N. et al From split-pool libraries to spatially addressable microarrays and its application to functional proteomic profiling. *Angew. Chem. Int. Ed. Engl.* **2001**, *40*, 3152–3155 (b) Winssinger, N. et al. (Profiling proteinfunction with small molecule microarrays. *Proc. Natl. Acad. Sci. U. S. A.* **2002**, *99*, 1139.
- 108 (a) Norton, J. C.; Piatyszek, M.A.; Wright, W. E.; Shay, J. W.; Corey. D. R.: Inhibition of human telomerase activity by peptide nucleic acids. *Nat Biotechnol.* **1996**, *14*, 615. (b) Morin, G. B. *Cell.* **1989**, *59*, 521.
- 109 Nugent, C. I.; Lundblad, V. *Genes Dev.* **1998**, *1073*.

- 110 Kim, N. W.; Piatyszek, M. A.; Prowse, K. R.; Harley, C. B.; West, M. D.; Ho, P. L. C.; Coviello, G. M.; Wright, W. E.; Weinrich, S. L.; Shay, J. W. *Science* **1994**, *266*, 2011.
- 111 Norton, J. C.; Piatyszek, M. A.; Wright, W. E.; Shay, J. W.; Corey, D. R. *Nature Biotech.* **1996**, *14*, 615.
- 112 Hamilton, S. E.; Pitts, A. E.; Katipally, R. R.; Jia, X.; Rutter, J. P.; Davies, B. A.; Shay, J. W.; Wright, W. E. Corey, D. R. *Biochemistry* **1997**, *36*, 11873.
- 113 Hamilton, S. E.; Simmons, C. G.; Kathiriya, I. F.; Corey, D. R. *Chemistry & Biology* **1999**, *6*, 343.
- 114 Harrison, J. G.; Frier, C.; Laurant, R.; Dennis, R.; Raney, K. D.; Balasubramanian, S. *Bioorg. Med. Chem. Lett.* **1999**, *9*, 1273.
- 115 (a) Zelphati, O.; Liang, X.; Hobart, P.; Felgner, P. L. *Human Gene Therapy* **1999**, *10*, 15. (b) Zelphati O.; Liang X.; Nguyen C.; Barlow S.; Sheng S.; Shao Z.; Felgner P.L. *Biotechniques* **2000**, *28*, 304.
- 116 (a) Bukanov, N. O.; Demidov, W.; Nielsen, P. E.; Frank-Kamenetskii, M. D. *Proc. Natl. Acad. Sci.* **1998**, *95*, 5516. (b) Boffa, L. C.; Carpaneto, E. M.; Allfrey, V. G. *Proc. Natl. Acad. Sci.* **1995**, *92*, 1901.
- 117 Braden, L. J.; Mohamed, A. I.; Smith, C. I. E. A peptide nucleic acid nuclear localization signal fusion that mediates nuclear transport of DNA. *Nat Biotechnol.* **1999**, *17*, 784.
- 118 Boffa, L. C.; Morris, P. L.; Carpaneto, E. M.; Louissaint, M.; Allfrey, V. G. Invasion of the CAG triplet repeats by a complementary peptide nucleic acid inhibits transcription of the androgen receptor and TATA binding protein genes and correlates with refolding of an active nucleosome containing a unique AR gene sequence. *J. Biol. Chem.* **1996**, *271*, 13228.
- 119 Hanvey, J. C.; Peffer, N. J.; Bisi, J. E. Antisense and antigene properties of peptide nucleic acids. *Science* **1992**, *258*, 1481.
- 120 Mologni, L. L.; Nielsen, P. E.; Passerini, C. Additive antisense effects of different PNAs on the in vitro translation of the PML/RAR alpha gene. *Nucleic Acids Res.* **1998**, *26*, 1934.

- 121 Kuhn, H.; Hu, Y.; Frank-Kamenetskii, M. D.; Demidov, V. V. Artificial site-specific DNA-nicking system based on common restriction enzyme assisted by PNA openers *Biochemistry* **2003**, *42*, 4985.
- 122 Footer, M.; Egholm, M.; Kron, S.; Coull, J. M.; Matsudaira, P. Biochemical Evidence That a D-Loop Is Part of a Four-Stranded PNA-DNA Bundle. Nickel-Mediated Cleavage of Duplex DNA by a Gly-Gly-His Bis-PNA *Biochemistry* **1996**, *35*, 10673.

---

## **CHAPTER 2**

Synthesis and assignment of configuration of *amp*-monomers and  
it's incorporation into *aeg*-PNA oligomers.

---

### **2.1 Introduction**

Among all the DNA mimics, PNA introduced by Nielsen et. al<sup>1</sup> in 1991 has been found to mimic many properties of DNA. The structure of PNA is remarkably simple, the repeating unit of PNA consisting of N-(1-aminoethyl)-glycine units linked by amide bonds and the nucleobases (A, G, C and T) attached to the backbone through methylene carbonyl linkages. Thus PNA lacks sugar and phosphate groups, making it acyclic, neutral, achiral and homomorphous. PNA is resistant to cellular enzymes and has strong affinity towards complementary DNA/RNA. Homopyrimidine PNA oligomers bind strongly to complementary DNA by Watson-Crick and Hoogsteen bonding to form [(PNA)<sub>2</sub>:DNA] triple helices that are much more stable than the corresponding DNA-DNA hybrids. The unique character of PNA is binding to duplex DNA by strand invasion forming both *parallel* (N-terminus of PNA to 5' end of the DNA) and *antiparallel* (C-terminus to 5' end respectively) complexes.

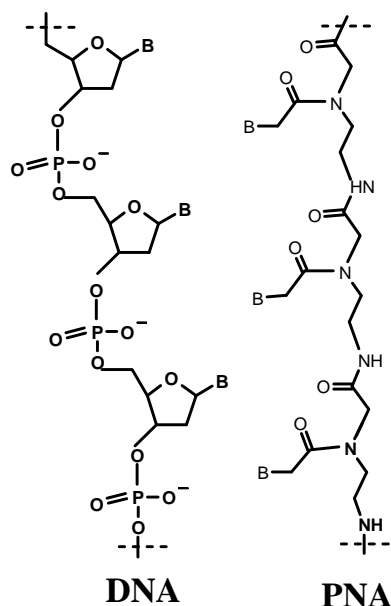


**Figure 1** Chemical structure of DNA and RNA

In contrast to homopyrimidine sequences, mix sequences of PNA bind to complementary DNA/RNA with 1:1 stoichiometry to form duplexes. Here binding can be

in either parallel or antiparallel mode, the latter mode having higher stability than parallel hybrids with high sequence specificity and affinity.<sup>2</sup> These favorable hybridization properties<sup>2,3</sup> with high chemical and bio-stability<sup>4</sup> make PNA a promising lead for development as efficient antisense agents and medicinal drugs.<sup>5</sup> However in spite of these advantages, PNA suffers from poor membrane permeability, inadequate solubility problems, ambiguity in binding orientation and lack of selectivity towards DNA/RNA. These characters limit PNAs potential as an antisense agent.

To address the limitations of PNA for biological applications several modifications have been introduced into the classical PNA monomer<sup>6</sup> and many of these modifications have resulted in only marginal effects in terms of hybridization properties. However, these studies have pointed out the importance of rigidity and preorganization of PNA for effective complexation with complementary DNA. From this laboratory there have been several reports on the introduction of novel five membered pyrrolidine rings into PNA backbone to impart chirality as well as conformational constrain in the PNA backbone<sup>7</sup> resulting in both neutral and positively charged PNA oligomers (Figure 2).

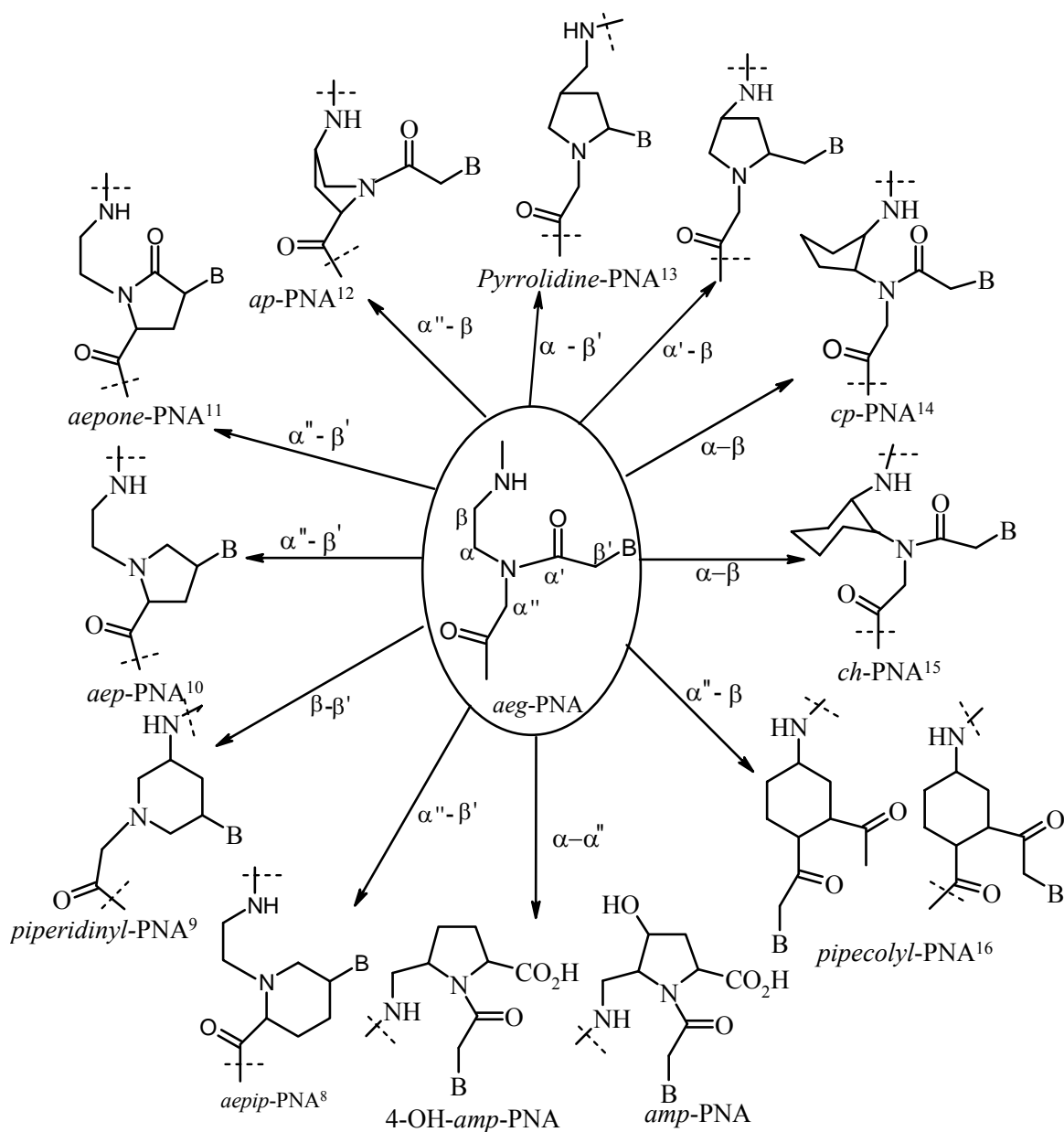


**Figure 2** Conformationally constrained PNA analogues<sup>7</sup>

## 2.2 Rationale behind the design:

The work presented in this thesis is directed towards the introduction of chirality and conformational constrain in the classical PNA backbone to control the orientation selectivity and specificity in binding by preorganization. This can be achieved in several

ways as shown in Figure 2 to obtain neutral and positively charged monomers. Bridging the  $\beta$ -carbon of ethylene diamine unit and  $\alpha''$ -C of glycine unit with a methylene afforded the neutral *ap*-PNA analogues. Bridging the  $\alpha$ - $\alpha''$  carbons of the classical PNA results the another class of neutral monomers (*amp*-PNA). Bridging the  $\alpha$ - $\beta'$ ,  $\beta$ - $\alpha'$  and  $\alpha''$ - $\beta'$  gave the positively charged preorganized PNA monomers. These kind of modifications involve the introduction of rigidity to the flexible aminoethyl glycylic backbone and or nucleobase side chain, simultaneously introducing chirality in the molecule with the generation of one or two asymmetric centers.

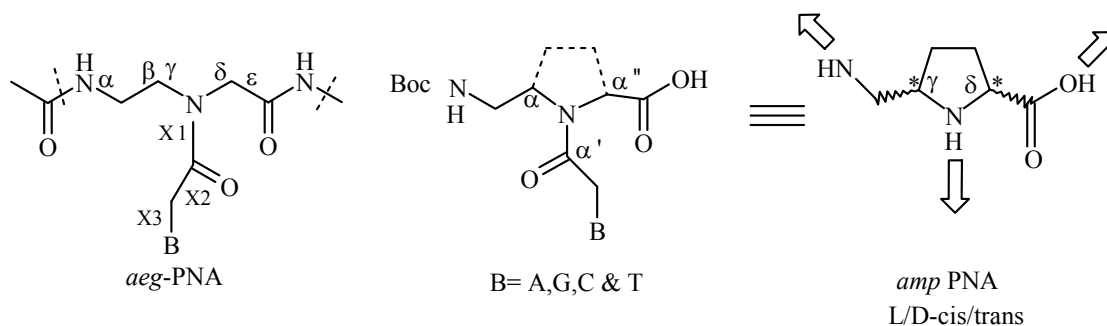


**Figure 3** Rational behind the design

The present work is directed towards the synthesis of aminomethyl prolyl *amp*-PNA which were designed by bridging the  $\alpha$ - $\alpha''$  carbons of the classical *aeg*-PNA with ethylene bond (Figure 3). This novel approach creates two chiral centers and less rigidity in *aeg* backbone compared to other cyclic modifications. This modification restricts movement in both the aminoethyl and the glycylic segments of the *aeg*PNA and restrain the fluctuation region of  $\gamma$  and  $\delta$  torsion angles.

A similar kind of modification but containing a sulphur atom in the ring was reported by Chassaing et. al in 2001(Figure 3a).<sup>6a</sup>

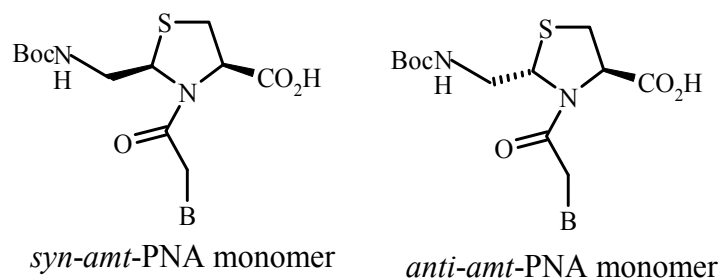
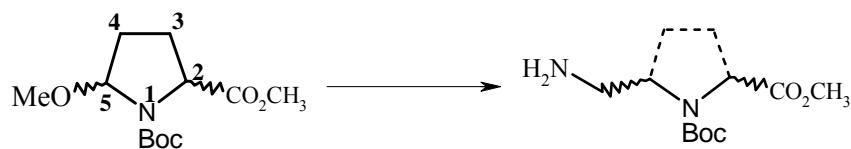


**Figure 3a** *amt*-PNA monomers

### 2.3 The Objectives of the present chapter are:

1. Functionalization of *C5* of the proline ring to introduce a methoxy function that can be subsequently used for the conversion to the *amino-methyl* group, which is a part of the aminoethyl segment of the *aeg* PNA backbone.



2. Synthesis of *N*-(*tert*-butoxycarbonyl)-fluorenylmethoxycarbonyl-aminomethyl- L/D proline isomers (Figure 4) for the synthesis of the PNA oligomers starting from L/D-proline.

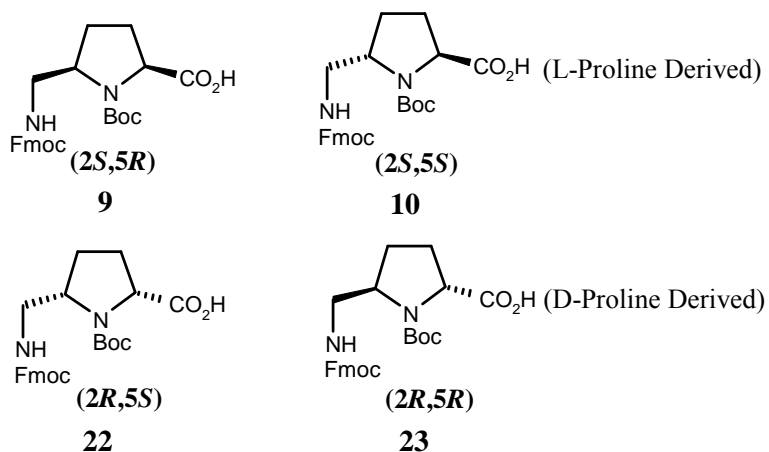


**Figure 4** *amp* (aminomethylprolyl) monomers

3. Synthesis and characterization of *amp*-PNA oligomers (Figure 5) employing both orthogonal and submonomer strategy.
4. Biophysical studies of the characterized *amp*-PNA oligomers using thermal UV- and CD-spectroscopy.

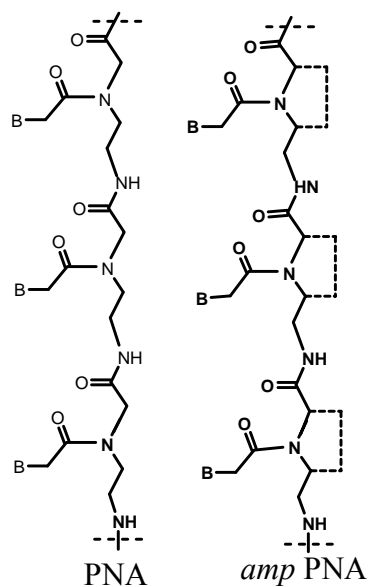
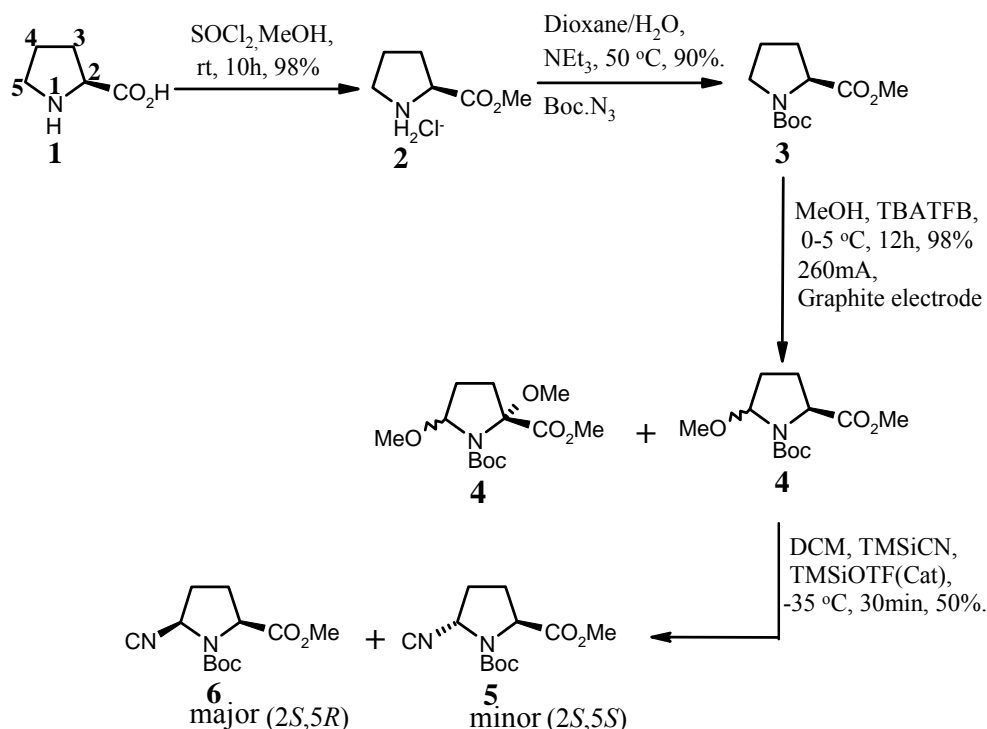


**Figure 5** Chemical structure of PNA and *amp*-PNA

## 2.4 Synthesis of amp-PNA monomers

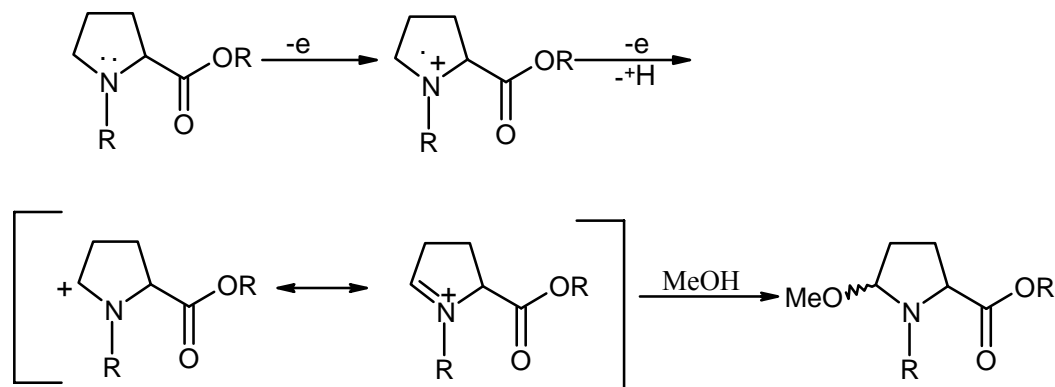
### Synthesis of (2*S*,5*S*) and (2*S*,5*R*)-N1-(*tert*-Butoxycarbonyl)-5-[(*N*Fluorenyl-methoxycarbonyl) aminomethyl]-Proline (9 and 10)

The synthesis of target *amp* PNA monomers **9** and **10** (Figure 4 and Scheme 1) was achieved starting from L-proline **1**, which on treatment with thionyl chloride in methanol afforded the 2-carboxymethyl ester **2** as its hydrochloride salt. The ring nitrogen (**N1**) of the ester **2** was protected as *tert*-butoxycarbonyl by treatment with *tert*-butyl carbazide and triethyl amine in dioxane/water to provide the N-(*tert*-butoxycarbonyl) proline carboxymethyl ester **3**. This was then subjected to electrochemical oxidation employing Ross-Eberson- Nyberg reaction.<sup>17</sup> Earlier reports<sup>17</sup> on use of this reaction on substituted pyrrolidine have revealed that the methoxylation occurs at the least substituted site adjacent to the nitrogen atom.



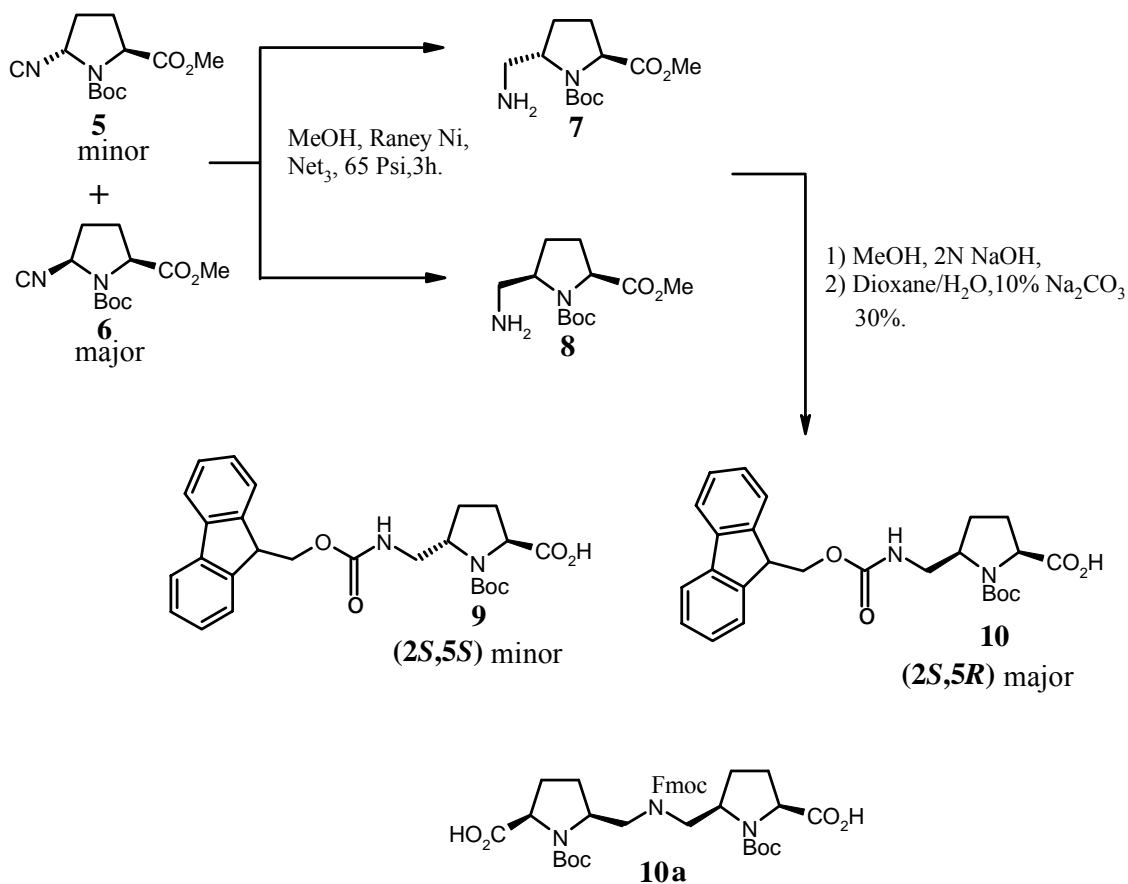
**Scheme 1:** Synthesis of (2*S*,5*R*) and (2*S*,5*S*) nitriles

The anodic oxidation involved the treatment of ester **3** with methanol as a solvent-reagent and tetrabutylammonium-tetrafluoroborate as a supporting electrolyte and passing a constant current of  $0.06\text{F}/\text{cm}^2$  (260 mA) using graphite electrodes. The reaction mixture was cooled to ice temperature before passing the current and the temperature of the reaction was maintained between 0-10 °C for about 12 h. The efficiency of the reaction depends on controlling the temperature and current optimally to avoid the formation of C-2 and C-5 dimethoxylated products. Compound **4** formed in 95% yield, as a non-separable diastereomeric mixture. The formation of **C5**-methoxylated compound was confirmed by the observance of multiple peaks for **C5**-methoxy ( $\text{OCH}_3$ ) at  $\delta$  3.30-3.45 in  $^1\text{H}$  NMR and appearance of peaks for ( $\text{OCH}_3$ ) at  $\delta$  51.64 in  $^{13}\text{C}$  NMR. The mechanism of methoxylation (Scheme 2) involves electrochemical removal of one electron from the lone pair on nitrogen in the initial step when inert supporting electrolytes (an electrolyte added to the solution for the sole purpose to increase the solution conductivity, while the electrolyte does not take part in any reactions) are used.<sup>18</sup> This reaction was explored in the synthesis of C-5 methoxyproline, which is the key intermediate in the synthesis of *amp* submonomers.



**Scheme 2:** Mechanism of electrochemical oxidation

The diastereomeric mixture of compound **4** was treated with TMSCN in DCM employing catalytic amount of TMSTF at  $-35\text{ }^{\circ}\text{C}$  for about 30 min, the reaction was quenched at  $-35\text{ }^{\circ}\text{C}$  using dry methanol resulting the formation of C5-nitriles<sup>19</sup> **5** and **6** in 50% yield. The product obtained as diastereomeric mixture was separable by chromatography on neutral alumina. The formation of compounds **5** and **6** confirmed by appearance of new peaks in the IR spectrum at  $2260\text{ cm}^{-1}$ , and appearance of a signal at  $\delta$  118 (C5-nitrile group) in the  $^{13}\text{C}$  NMR.



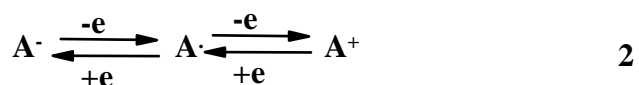
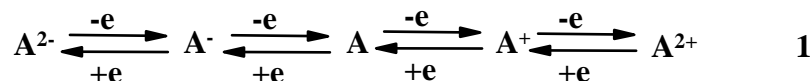
**Scheme 3:** Synthesis of (2*S*,5*S*) and (2*S*,5*R*) *amp*-PNA monomers

The diastereomers **5** and **6** showed different sign and magnitude of optical rotation of **5** ( $[\alpha]_D = -93.7$ ) and **6** ( $[\alpha]_D = +41.8$ ). These were individually subjected to hydrogenation at 65 psi, in MeOH employing Raney Ni as catalyst to afford the 5-methylaminopropine methyl esters **7** and **8**. The identity of compounds **7** and **8** was confirmed by the appearance of peaks at 3100 and 3200  $\text{cm}^{-1}$  in the IR spectrum due to the 5-methyl amino group. These amino compounds upon hydrolysis in 2N NaOH in MeOH yielded the sodium salt of the acid, which on treatment with fluorenyl chloroformate afforded the required *amp* monomers **9** and **10** in 30% yield, along with the by-product **10a** (Scheme3). Compound **10a** was characterized by NMR and Mass spectral data. When the reduction reaction was carried out in the presence of Pd(OH)<sub>2</sub>

formation of compound **10a** was observed in high percentage compared to that of the required monomers **9** and **10** (Scheme 3). The formation of compounds **9** and **10** was supported by observance of characteristic signals for Fmoc aromatic protons at  $\delta$  7.26-7.78 in  $^1\text{H}$  NMR and appearance of peaks for (Fmoc-CO) at  $\delta$  141.2 in  $^{13}\text{C}$  NMR. The observed mass for compound **9** is 491.50 (M+Na) and for compound **10** is 491.15 (M+Na) was in agreement with calculated mass 466.

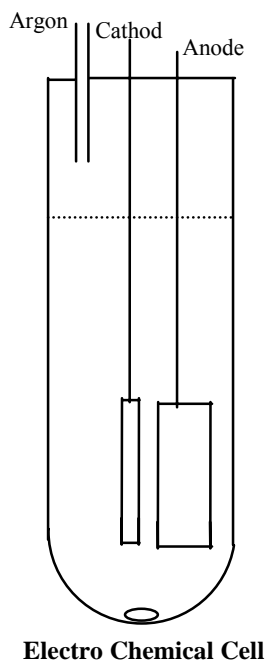
### Electro-oxidation

Electroorganic chemistry can be classified into two categories, that is, direct and indirect reactions. In both categories, the reaction is initiated by transfer of electron between electrode and a substrate A, and as shown in eqn (1), the substrate A is transformed to an anion radical or a cation radical depending on the transfer of electron. When the starting substrate A is radical or ionic species, the pattern of transformation of A is such as shown in eqn 2, where -e means the removal of one electron, and -2e means removal of two electrons; +[e] means addition of electrons in appropriate numbers.



*Electro-organic chemistry is to investigate the chemical behavior of activated species of A in solution.* The generation of the similar activated species may be possible by using common organic reactions. The chemical behavior of the same activated species is, however, often different between electro-organic chemistry and common organic chemistry. One of the major causes of this difference is that in an electro-organic

reaction, the activated species is not formed uniformly in homogeneous solution, but is generated only on the surface of electrode, whereas in common organic reactions, the active species is uniformly distributed in the solution. This difference in location of generation of activated species and in distribution of activated species brings about great difference in the reaction of the activated species.

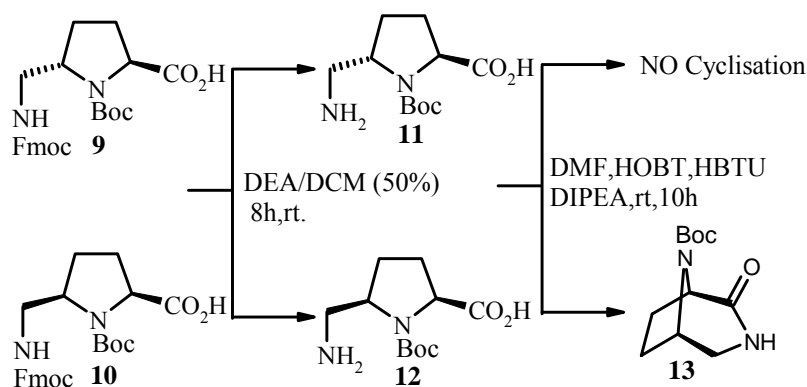


Viewed from the standpoint of organic synthesis, electroorganic chemistry has remarkable characteristics. In common organic reactions the reaction generally takes place between nucleophilic reagents (Nu) and electrophilic reagents (E), while reaction between reagents of the same polarity is not possible. Therefore, the inversion of polarity of one of the reagents is essential for carrying out the reaction between Nu and Nu or E and E. The inversion of polarity of reagents (Umpolung) is, however, not facile in common organic reactions, whereas in electroorganic reaction, the process of formation of the activated species is the Umpolung itself as shown in eqns (1) and (2). Thus, one of

the major characteristics of electro organic chemistry is the facility of Umpolung, which makes a variety of organic syntheses possible.

## 2.5 Assignment of absolute stereochemistry at C<sub>5</sub> position of *amp* PNA monomers (9 and 10).

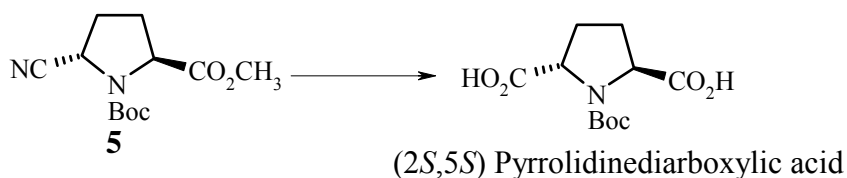
An important aspect remaining in the characterization of (2*S*,5*S*) and (2*S*,5*R*) *amp* PNA is the assignment of the configuration at C<sub>5</sub> position where a new chiral center was generated upon anodic oxidation. This was achieved as described in Scheme-4.



**Scheme 4** Configuration assignment of compound **9** and **10** *amp* monomers

Compounds **9** and **10** were individually treated with 50% DCM/DEA at rt for about 8 h to furnish the amino acids **11** and **12**. Compound **12** when treated with HOBT/HBTU, in DMF, amino acid **12** furnished the compound **13**. The formation of compound **13** was confirmed by appearance of peaks in IR spectrum at 1690 cm<sup>-1</sup> and observance of carbonyl (CONH) peaks at δ 172 in <sup>13</sup>C spectrum. The observed mass for compound **13** is 227.11 (M+1) was in agreement with the calculated mass 226. In case of amino acid **11**, no cyclisation product was observed. In compound **12** and hence in **10** the C<sub>5</sub> and C<sub>2</sub> substituents must be *cis* to each other to obtain the cyclized product. Since the configuration at C<sub>2</sub> is known in acid **10**, which is same as in starting material L-

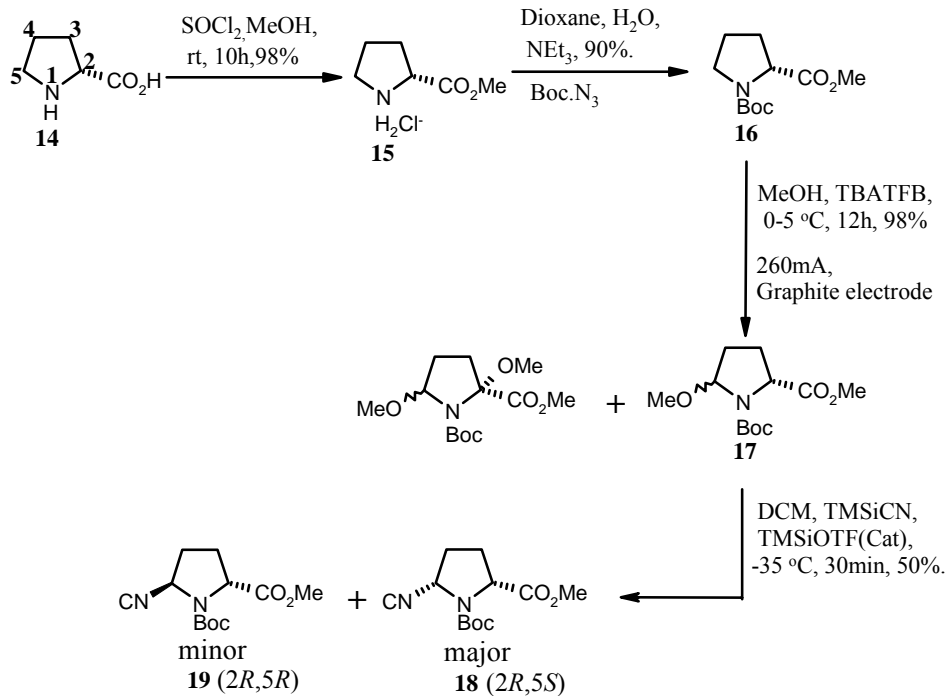
proline, the absolute configuration at C5 in the compound **10** that is *cis* to C2, would be R (*2S,5R*). The absolute configuration of acid **9** is therefore (*2S,5S*). In another approach the configuration at C5 was assigned by preparing (*2S,5S*) pyrrolidine dicarboxylic acid a marine natural product from the nitrile ester **5**, which is discussed in chapter 4.<sup>19a</sup>



**Scheme 4a**

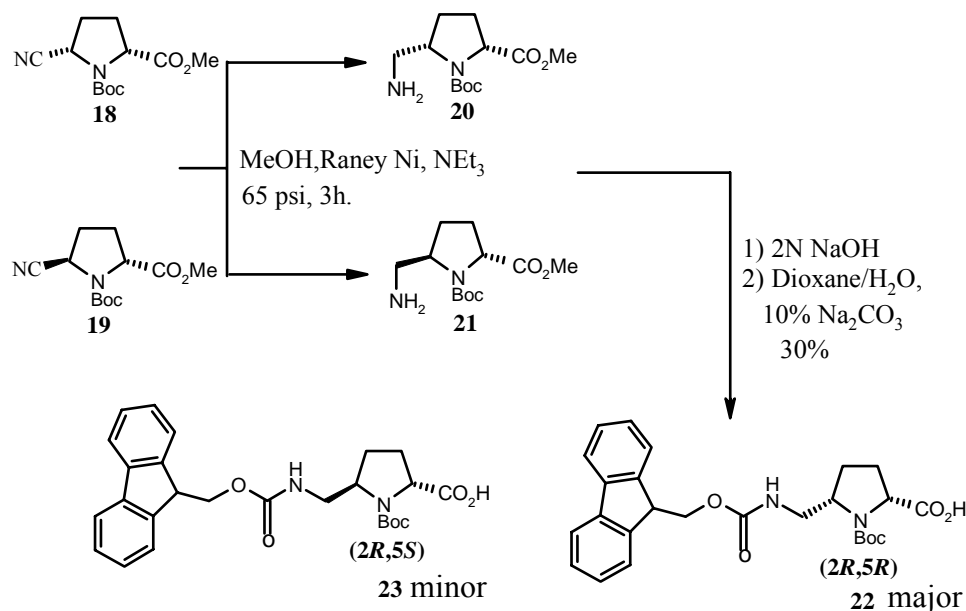
## 2.6 Synthesis of (*2R,5S*) and (*2R,5R*)-N1-(*tert*-Butoxycarbonyl)-5-[(N-Fluorenyl methoxycarbonyl) aminomethyle]-proline (**22** and **23**).

The synthesis of (*2R*)-5-[(N-fluorenylmethoxycarbonyl) aminomethyl-N1-(*tert*butoxycarbonyl) proline **22** and **23** were similarly achieved starting from D-proline **14** (Scheme 6). The steps involved esterification of D-proline, protection of the ring nitrogen, C5-functionalization by anodic oxidation and conversion of the 5-methoxy-N1-(*tert*butoxycarbonyl) proline methyl ester **17** to the separable C5-nitrile diastereomers **18** and **19**.



**Scheme 5:** Synthesis of (2*R*,5*R*) and (2*R*,5*S*) nitriles

The two nitrile compounds were subjected to reduction to get the amino- methyl ester **20** and **21**, which were hydrolysed using 2*N* NaOH, followed by protection of the amino group employing Fmoc-Cl to furnish the required *amp* PNA monomers **22** and **23**. The integrity of these monomers were confirmed by the appearance of peaks for (Fmoc protons) at  $\delta$  7.74-7.28 in  $^1\text{H}$  NMR and observance of peaks for (Fmoc aromatic carbons) at  $\delta$  127.57-125.21 in  $^{13}\text{C}$  NMR. The observed mass for compound **22** is 467.16 (M+1) and for compound **23** is 467.48 (M+Na) both in agreement with the calculated mass 466.

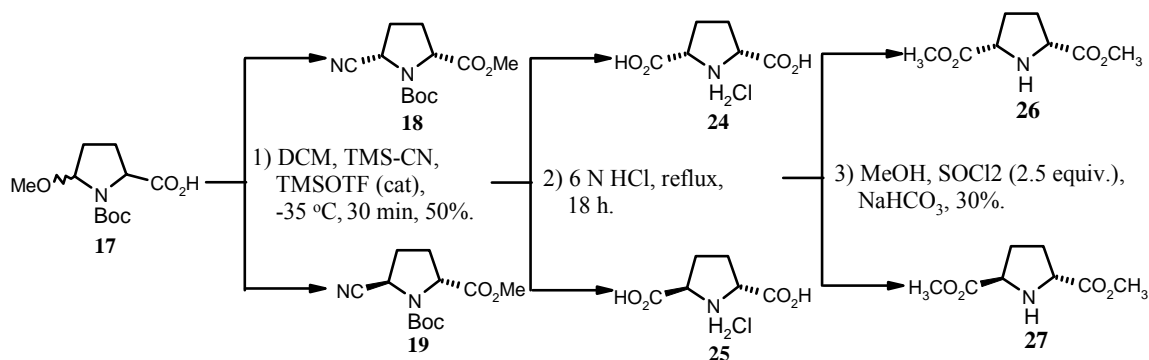


**Scheme 6:** Synthesis of (2*R*,5*R*) and (2*R*,5*S*)-amp monomers.

## 2.7 Assignment of absolute stereochemistry at C5 position of compound 18 and 19

(amp monomers).

The absolute stereochemistry at C5 of the compounds **18** and **19** was assigned as described in Scheme-7. The two 5-cyano proline esters **18** and **19** were individually subjected to hydrolysis in 6 N HCl for about 14 h to afford the hydrochloride salt of the



**Scheme 7** Configuration assignment of esters **18** and **19**

pyrrolidine 2,5-dicarboxylic acids **24** and **25**. These diacids were subjected to esterification employing SOCl<sub>2</sub> in MeOH followed by neutralization to furnish the diester **26** and **27** in 30% yield. The magnitude of the optical rotation of compound **26** is  $[\alpha]_D = 0$  since the

*configuration at C2 in ester **18** is known as R, the stereochemistry at C5 of diester **26** is cis to C2 (meso) with R configuration, and hence the configuration of ester **18** is (2R,5S). The stereochemistry of compounds amp **22** and **23** are therefore (2R,5S) and (2R,5R) respectively.*

## 2.8 4-Hydroxy *amp* monomer:

### Rational behind the design

The *amp* monomers (**9**, **10**) and (**22**, **23**) enable the study of the constrain and steric effects on the hybridization properties of incorporated PNA oligomers with complementary DNA. It will not provide any information about conformational effect of the proline ring. Proline is a cyclic imino acid and the bridging of the  $\alpha$ -carbon atom to the main chain amide nitrogen atom by 3 methylene bridge imposes further constrain on the main chain torsion angles  $\phi$  and  $\psi$  (Figure-5A).

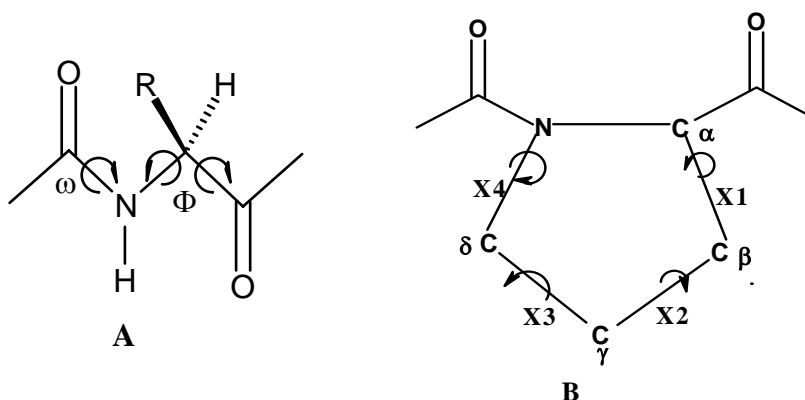


**Figure-5:** Main chain torsion angles of amino acid residues in polypeptides **A**;  
Endocyclic torsion angles in amino acid proline **B**.

Proline and substituted-proline rings exhibit two types of ring-pucker, and in analogy to ribo and deoxyribo sugars, they are named as *N* ( $\gamma$ -exo) and *S* ( $\gamma$ -endo) puckers. These ring-puckers are also expressed in terms of *endocyclic* torsion angles (Figure 5B). In proline the two puckers are almost equally preferred and the energy barrier to inter-conversion is very low.<sup>20</sup> However, in 4-substituted prolines, depending on the steric and electronic effects exerted by the 4-substituent, pyrrolidine ring may prefer any one of the ring-pucker, as found in both its crystal structures and in solution.<sup>20</sup>

This pucker preference has been attributed to the phenomenon of hydroxyl-amide *gauche* effect.<sup>21,22</sup>

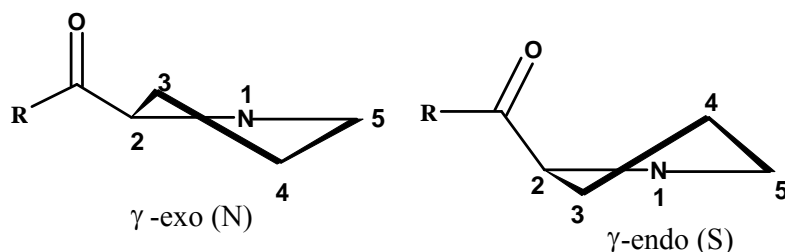


**Figure 6:** Ring-puckers of the pyrrolidine ring in proline and substituted proline

### Gauche effect on the ring-pucker preferences

Gauche effect may be described as “the preference of two electronegative atoms X and Y in vicinally substituted ethanes to remain gauche with respect each other rather than *anti*”.<sup>12</sup> This effect surprisingly arises from a combination of dipole repulsion and steric effects among the electronegative atoms on the vicinal substituents that are expected to remain *anti* to each other. Many molecules containing N, O, P, S, F or Cl show a preference for gauche conformation. The origin of the gauche effect is not very clear and *ab initio* quantum chemical calculations underestimate the *gauche* effect.  $\sigma$ -Hyper-conjugation<sup>22</sup> and bent- bonds<sup>23</sup> have been proposed to explain the phenomenon of the gauche effect. In 4-substituted prolines, the steric repulsion between the amide-ring nitrogen and the 4-substituent should result in a pseudo-equatorial positioning of the 4-substituent i.e., *anti* with respect to the ring amide-nitrogen. For example, 4*R*-hydroxyproline and 4*R*-fluoroproline may be expected to exhibit *γ-endo* ring-pucker (Figure-7). However analysis of X-ray crystal structure,  $^1\text{H}$ - $^1\text{H}$  and  $^{19}\text{F}$ - $^1\text{H}$  coupling constant analyses confirm the pseudo-axial positioning of fluorine and the resulting *γ-exo* ring-pucker<sup>24</sup>. This suggests that the *gauche* effect may be a dominating factor in determining the ring-pucker preference for proline with 4-electronegative substituent.

Similarly, in 4-*S*-fluoroproline with an opposite stereochemistry at C-4 the gauche effect leads to  $\gamma$ -*endo* ring-pucker (Figure 7B).<sup>25</sup>

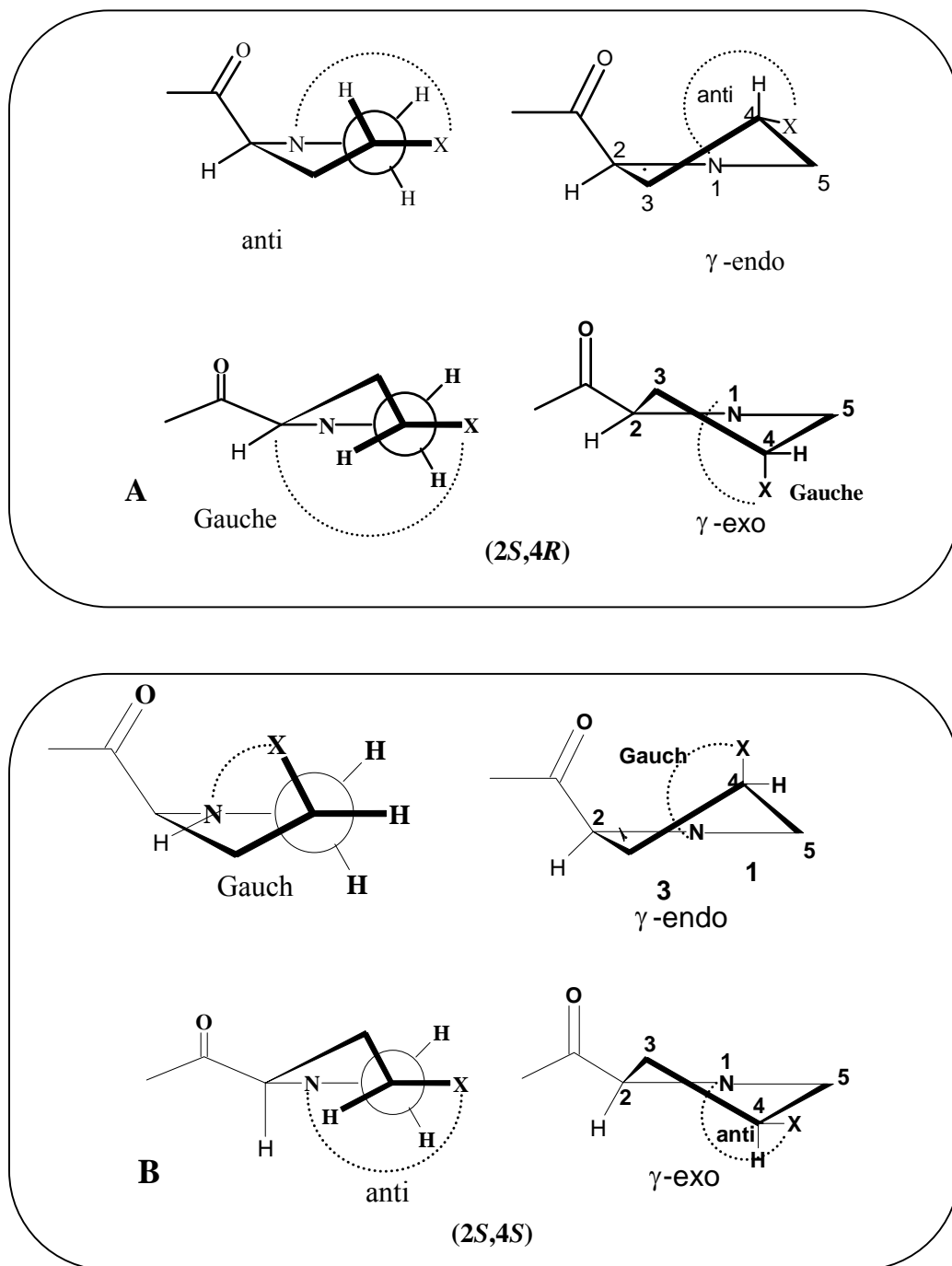
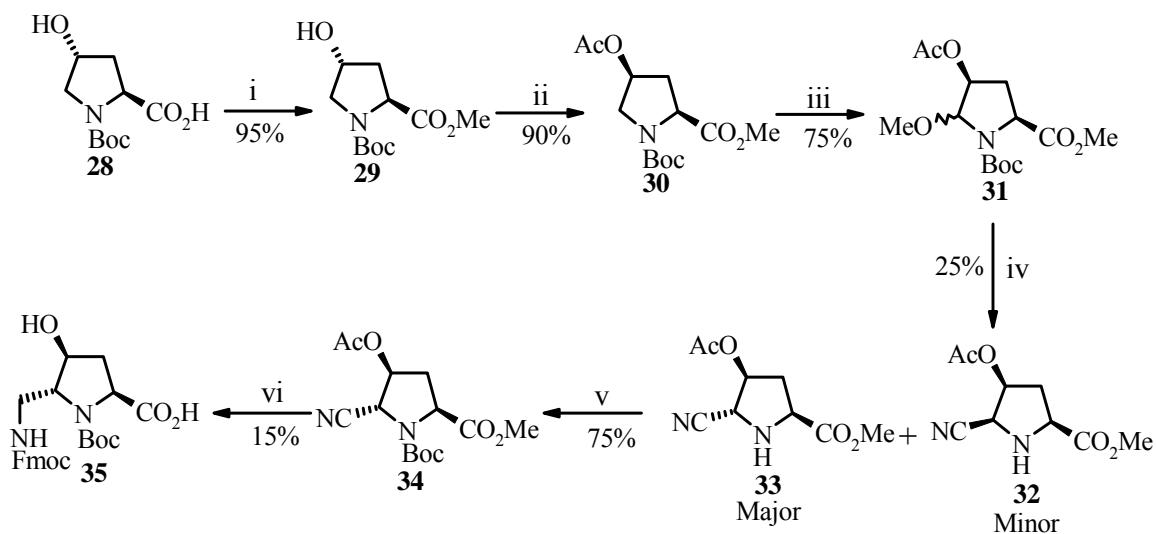


**Figure 7:** Newman and saw-horse projections depicting the gauche effect and the resulting pucker preferences in the prolines with electronegative A *4R*-substituent; B *4S*-substituent

In view of such 4-substituent effects on pyrrolidine ring conformation and hence consequently on the backbone, 4-substituted aminomethyl prolyl PNA monomers were synthesized.

## 2.9 Synthesis of 4-hydroxy aminomethyl prolyl (*amp*) monomer (35)

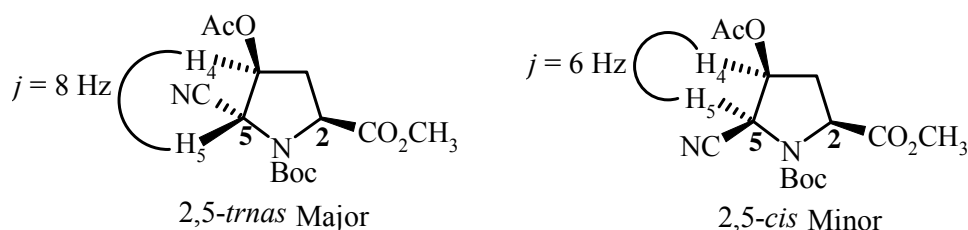
The synthesis of 4-hydroxy *amp*PNA monomer was achieved (Scheme 8a) starting from N-Boc hydroxyproline **28**, which on treatment with DMS/K<sub>2</sub>CO<sub>3</sub> in acetone afforded the methyl ester of hydroxyproline **29**. This under Mitsunobu conditions using acetic acid yielded the acetate **30**, which on electrochemical anodic oxidation afforded the methoxy compound **31** as a nonseparable distereomeric mixture. Treatment of **31** with TMSiCN in presence of BF<sub>3</sub>.Et<sub>2</sub>O in DCM, furnished the cyano derivatives **32** (minor) and **33** (major). Treatment of **33** with (Boc)<sub>2</sub>O, DMAP (Catalytic), rt, 12 h; (vi) (a) MeOH, RaneyNi, NEt<sub>3</sub> (3 equiv.), 60 Psi, rt, 4 h, (b) MeOH, 2 N NaOH, (c) Dioxane/H<sub>2</sub>O, Na<sub>2</sub>CO<sub>3</sub> (2 equiv.), Fmoc-Cl (1.2 equiv.) afforded the final product **35**.



**Scheme 8a** Synthesis of 4-hydroxy-*amp* monomer **35**

**Reagents and conditions:** (i) Acetone, K<sub>2</sub>CO<sub>3</sub> (3 equiv.), DMS (2 equiv.), Reflux 5 h; (ii) THF, DEAD (1.2 equiv.), (Ph)<sub>3</sub>P (1.1 equiv.), CH<sub>3</sub>CO<sub>2</sub>H (1.1 equiv.), rt, 8 h; (iii) MeOH, TBATFB, 260 mA, 0-5 °C, 6 h; (iv) DCM, BF<sub>3</sub>.Et<sub>2</sub>O (2.2 equiv.), TMSiCN (3.5 equiv.), 0 °C-rt, 3 h; (v) DCM, (Boc)<sub>2</sub>O, DMAP (Catalytic), rt, 12 h; (vi) (a) MeOH, RaneyNi, NEt<sub>3</sub> (3 equiv.), 60 Psi, rt, 4 h, (b) MeOH, 2 N NaOH, (c) Dioxane/H<sub>2</sub>O, Na<sub>2</sub>CO<sub>3</sub> (2 equiv.), Fmoc-Cl (1.2 equiv.).

The ring nitrogen in cyano derivative **33** was protected as Boc by treating with Boc anhydride in DCM employing catalytic amount of DMAP to provide nitrile compound **34**. The formation of compound **34** was confirmed by the observance of peaks for (C5-CN) in IR at  $2260\text{ cm}^{-1}$  and the appearance of the peak for (C5-CN) at  $\delta$  118 in  $^{13}\text{C}$  NMR. The observed mass for the compound **34** is 313 (M+1) was in agreement with calculated mass 312. The configuration at C-5 was assigned from the small coupling constant of H-4 and H-5 as reported in literature<sup>26</sup> (Scheme 8b). This was subjected to hydrogenation at 60 psi in the presence of Raney/Ni, followed by hydrolysis using 2N NaOH in MeOH to afford the sodium salt of 4-hydroxy aminomethyl proline (not isolated). This on treatment with Fmoc-Cl in presence of 10%  $\text{Na}_2\text{CO}_3$  in dioxane furnished the 4-hydroxy *amp* monomer **35**.



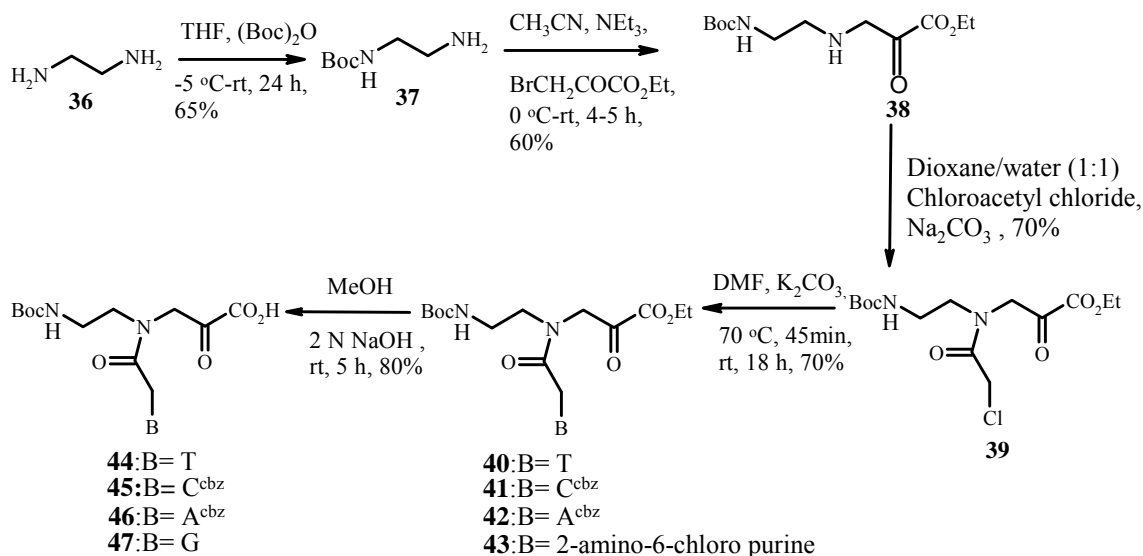
**Scheme 8b** Assigning the configuration at C5 of compound **34**<sup>26a</sup>

The integrity of 4-hydroxy *amp* monomer **35** was confirmed by the observance of characteristic peaks for (Fmoc protons) at  $\delta$  7.71-7.20 in  $^1\text{H}$  NMR and appearance of peaks for (Fmoc aromatic carbons) at  $\delta$  127.57-125.21 in  $^{13}\text{C}$  NMR. The observed mass for compound **35** is 505.13 (M + Na) which was in agreement with the calculated mass 482. Employing  $\text{BF}_3 \cdot \text{Et}_2\text{O}$  during the cyanation reaction afforded the ester compound **33** as the major isomer, with the diastereomeric ratio being 80:20.

## 2.10 Synthesis of Aminoethylglycyl (*aeg*) PNA monomers.

To study the influence of modified monomers on hybridization properties of PNA oligomers, *amp* PNA monomers were site specifically incorporated in *aeg* PNA oligomers along with the unmodified *aeg* PNA monomers, which were synthesized as described in Scheme 9.

The synthesis was carried out as reported in literature<sup>27-28</sup> starting from the readily available 1,2-diaminoethane (Scheme 9). The monoprotected derivative of **36** was prepared by treating a large excess of 1,2-diaminoethane with di-*t*-butyloxycarbonyl anhydride in THF under high dilution conditions to minimize the formation of di-*Boc* derivative. The di-*Boc* compound being insoluble was removed by filtration. The *N1-t-Boc*-1,2-diaminoethane was then subjected to *N*-alkylation using ethylbromoacetate and NEt<sub>3</sub> as base in acetonitrile to give compound **38**. The aminoethyl glycine ester **38** was not stable



Scheme 9 Synthesis of *aeg* PNA monomers

for longer time at room temperature and was treated with chloroacetyl chloride in aqueous dioxane with Na<sub>2</sub>CO<sub>3</sub> as a base to yield the chloro compound **39**. The ethyl *N*-(*t*-Bocaminoethyl)-*N*-(chloroacetyl)-glycinate **39** was used as a common intermediate for the preparation of all the four PNA monomers.

Alkylation of the ethyl *N*-(*t*-Boc-aminoethyl)-*N*-(chloroacetyl)-glycinate is regiospecific to *N*1 of thymine. Thymine was reacted with ethyl *N*-(*t*-Boc-aminoethyl)-*N*-(chloroacetyl)-glycinate using K<sub>2</sub>CO<sub>3</sub> as a base to obtain *N*-(*t*-Boc-aminoethylglycyl)-thymine ethyl ester **40** in high yield. In case of cytosine, the exocyclic-amine *N*4 was protected as Cbz (Scheme 10b) to obtain **52**,<sup>28</sup> which was used for alkylation employing K<sub>2</sub>CO<sub>3</sub> as the base to provide the *N*1-substituted product **41**. Adenine was treated with K<sub>2</sub>CO<sub>3</sub> in DMF to give potassium adenylate, which was then reacted with ethyl *N*-(*t*-Boc-aminoethyl)-*N*-(chloroacetyl)-glycinate to obtain *N*-(*t*-Bocaminoethylglycyl)-adenine ethyl ester **42** in moderate yield. The alkylation of 2-amino-6-chloro purine with ethyl *N*-(*t*-Boc-aminoethyl)-*N*-(chloroacetyl)-glycinate was facile with K<sub>2</sub>CO<sub>3</sub> as the base and yielded the corresponding *N*-(*t*-Boc-aminoethylglycyl)-(2-amino-6-chloro purine) ethyl ester **43** in excellent yield. All the compounds exhibited <sup>1</sup>H and <sup>13</sup>C NMR spectra were consistent with the reported data.<sup>27-29</sup> The ethyl esters except that of cytosine monomer were hydrolyzed in the presence of 2N NaOH to give the corresponding acids **44**, **45**, **47**, which were used for solid phase synthesis.

In case of 2-amino-6-chloropurine monomer ester hydrolysis, the chloro group is oxidized to keto group to give guanine monomer **47**. Cytosine monomer is more susceptible to Cbz deprotection in strong basic conditions and so in this case mild base LiOH was used for hydrolysis to afford the monomer acid **46**.

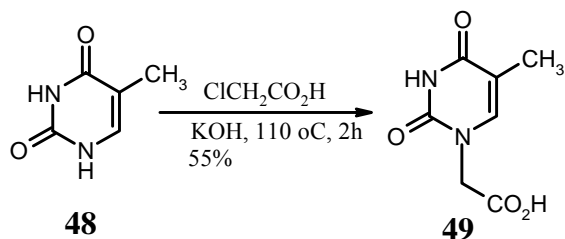
The need for the exocyclic amino group protection for adenine and guanine was eliminated, as they were found to be unreactive under the conditions used for peptide coupling.

## 2.11 Alkylation of Nucleobases:

*amp* PNA oligomers were synthesized by employing the submonomer<sup>30a</sup> strategy, in which the nucleobases were coupled to the ring nitrogen of *amp* monomer on solid support by converting to their N1-acetic acids, coupling was performed using HOBT/HBTU to obtain the *amp* PNA oligomers.

### 2.11.1 Synthesis of N<sup>1</sup>-Thyminy Acetic Acid (49)

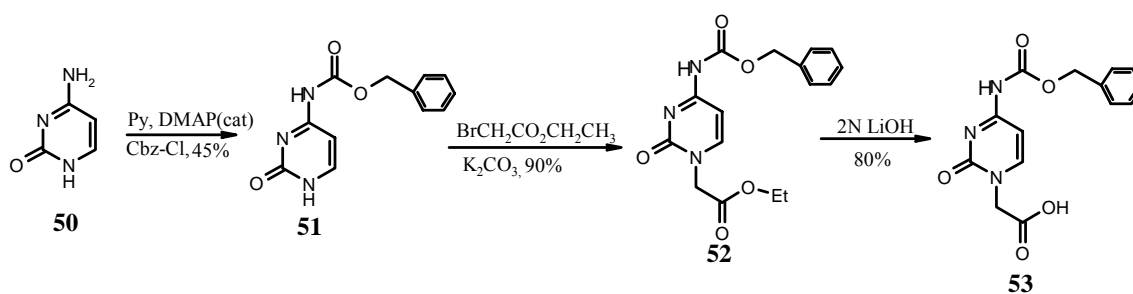
Thymine **48** was alkylated<sup>20</sup> as described in (Scheme 10a) using chloroacetic acid in aq KOH solution under reflux conditions for about 2h, maintaining the pH of the reaction by controlled addition of chloroacetic acid to the reaction mixture which is a key factor to obtain the acid **49** in good yields.



Scheme 10a: Synthesis of N<sup>1</sup>-Thyminy Aceticacid

### 2.11.1 Synthesis of N<sup>4</sup>-Benzyloxycarbonyl N<sup>1</sup>-cytosinyl Acetic Acid (53)

For the synthesis of ester **52**, protection of the exocyclic amino group of cytosine **50** is required in order to prevent the chain extension from this position during the peptide synthesis. The protection was done via its benzyloxycarbonyl derivative,<sup>29</sup> using benzyl chloroformate in anhydrous pyridine which afforded the protected derivative N4-benzyloxycarbonyl cytosine C<sup>Cbz</sup> **51** (Scheme 10b).

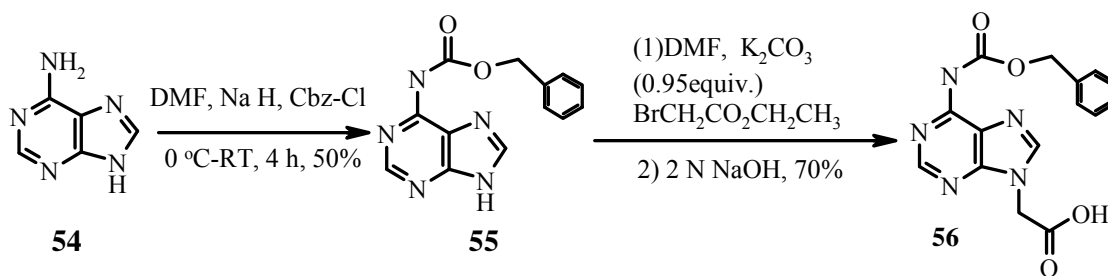


**Scheme 10b:** Synthesis of N<sup>4</sup>-Benzyloxycarbonyl N<sup>1</sup>-cytosinyl Acetic Acid

The N1-alkylation of C<sup>Cbz</sup> **51** was carried out using ethylbromoacetate and potassium carbonate in dry DMF to furnish the ester **52**. This on hydrolysis using 2N LiOH provided the required N4-(benzyloxycarbonyl) cytosin-1-yl acetic acid **53**.

### 2.11.2 Synthesis of (N<sup>6</sup>-Benzyloxycarbonyl) N<sup>9</sup>- Adenyl Acetic Acid (**56**)

The exocyclic amine of adenine **54** was protected as benzyloxycarbonyl using benzyl chloroformate as in Scheme 10c in anhydrous DMF employing NaH as base to obtain the N<sup>6</sup>-benzyloxy derivative **55**. This was subjected to alkylation with ethylbromoacetate in DMF using K<sub>2</sub>CO<sub>3</sub> as base and the resultant ester was hydrolyzed in 2N NaOH to afford the acid **56**.



**Scheme 10c:** Synthesis of (N<sup>6</sup>-Benzyloxy carbonyl) N<sup>9</sup>- Adenyl Acetic Acid

## 2.12 Solid Phase peptide Synthesis:

The solid phase peptide synthesis was devised by R. B. Merrifield in 1959. In this method the peptide is bound to an insoluble support in contrast to the solution phase method, and offers great advantages. The C-terminal amino acid is linked to an insoluble matrix such as polystyrene beads having reactive functional groups, which also acts as a permanent protection for the carboxylic acid (Figure 8). The N $\alpha$ -protected amino acid is coupled to the resin bound amino acid either by using an active pentafluorophenyl (pfp) or 3-hydroxy-2, 3-dihydro-4-oxo-benzotriazole (Dhbt) ester or by *in situ* activation with carbodiimide reagents. The excess amino acid is washed out and the deprotection and coupling reactions are repeated until the desired peptide is achieved.

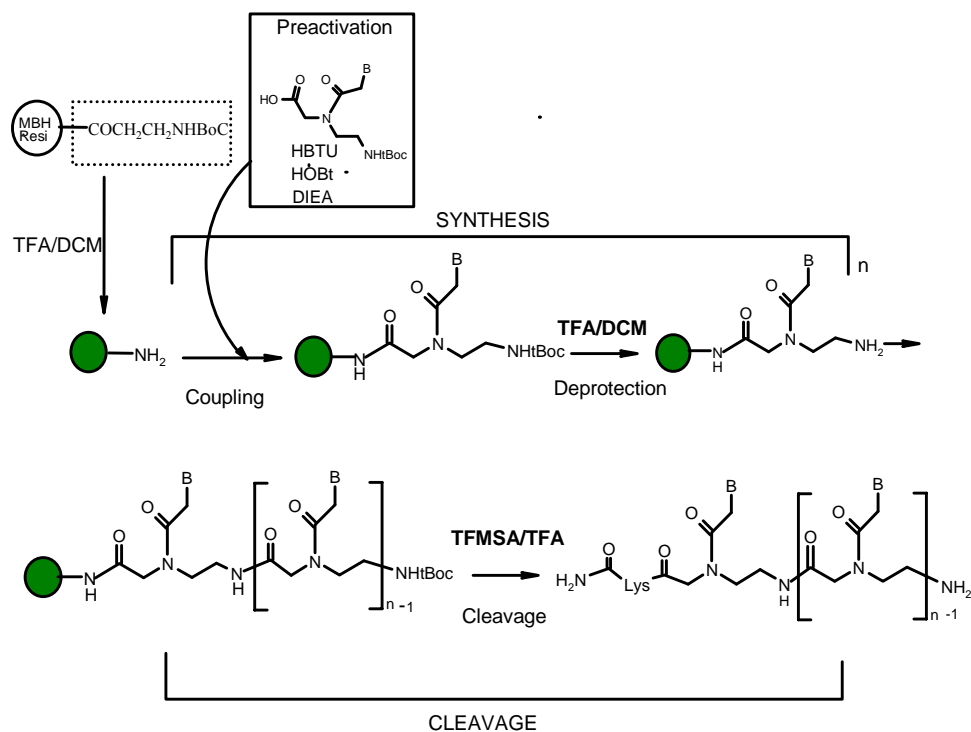


**Figure 8** Schematic representation of solid phase peptide synthesis



*The readily available MBHA resin was chosen as the polymer matrix on which the aeg PNA oligomers as well as the amp PNA oligomers were assembled. This resin yields the peptides with C-terminal amides upon cleavage at the end of the synthesis. The first amino acid is attached via amide linkage that can be cleaved easily at the end of the synthesis either by acidolysis to get the free peptide acid or by aminolysis to get the carboxyamide.*

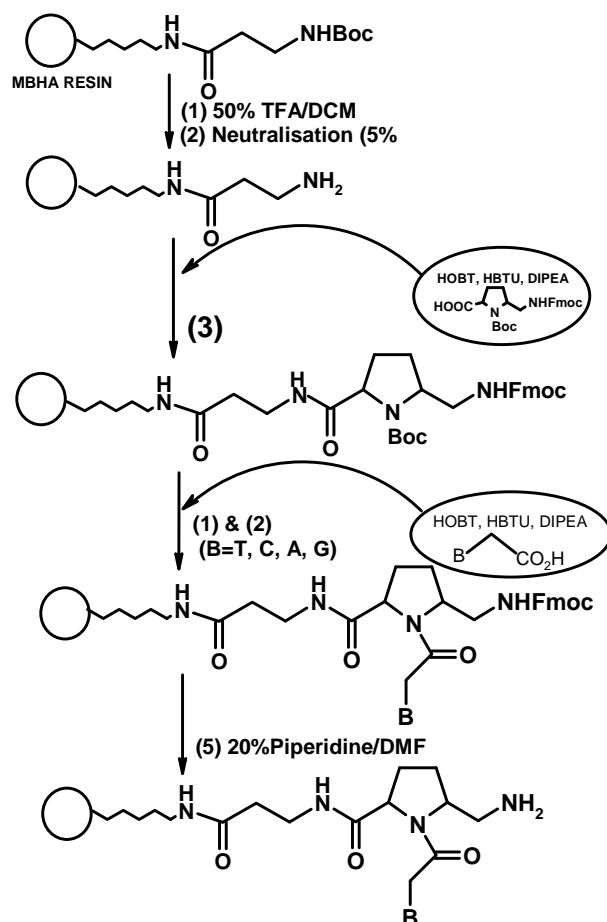
In the present work the orthogonal strategy was employed to construct the *amp* PNA oligomers followed by subsequent attachment of the nucleobases (sub monomer) strategy (Scheme 9). The *aeg* PNA monomers used have the amino function protected as the *tert*-butoxycarbonyl group and the modified bifunctional *amp* monomers (**9**, **10**, **22**, **23** and **35**) have the primary amino function protected as the Fmoc group and the ring nitrogen as *tert*-butoxycarbonyl group.

In both the cases, HOBt/HBTU activation coupling strategy was employed.<sup>31</sup> The use of Fmoc protection has drawback in PNA synthesis, as small amount of acyl migration is observed under basic conditions from the tertiary amide to the free amine liberated during the piperidine deprotection step.<sup>32</sup> However, Fmoc protection employed in case of the *amp* PNA monomers was found to be convenient for extending the oligomers. In the present study all the oligomers were built on MBHA resin using  $\beta$ -alanine as the C-terminal spacer- amino acid linker. Being achiral, its interference in spectral properties and hydrophobicity of the resulting PNA oligomers were negligible. The amine content on the resin was determined by the picrate assay and found to be 2 mmol/g and loading value was suitably lowered to approximately 0.250 mmol/g by

partial acetylation of total amine content using calculated amount of acetic anhydride.<sup>33,34</sup>

Free -NH<sub>2</sub> on the resin available for coupling was again estimated before starting synthesis. The PNA oligomers were synthesized using repetitive cycles (Scheme 11), each comprising of the following steps:

- a) Deprotection of the N1-*tert*-butoxycarbonyl function using 50% TFA in DCM
- b) Neutralization of the TFA salt to get the free amine using 5% DIPEA in DCM
- c) Deprotection of Fmoc group using 20% piperidine in DMF.
- d) Coupling of the amine on resin with 3 to 4 equivalents of free carboxylic function of the incoming amino acid using HOBt(1-hydroxybenzotriazole)/HBTU in DMF as solvent.
- e) Capping of the unreacted amino groups using Ac<sub>2</sub>O / Pyridine in CH<sub>2</sub>Cl<sub>2</sub> in case coupling does not go to completion. Scheme 11 represents a typical Solid phase peptide synthesis cycle. The deprotection of the *N-t*-Boc protecting group and the coupling reactions were monitored by Kaiser's test.<sup>34</sup> Alternatively, chloranil<sup>35</sup> and De Clercq<sup>36</sup> tests are useful to detect the secondary amine. The *t-Boc*-deprotection step leads to a positive Kaiser's test, where in the resin beads as well as the solution are blue in color (Rheumann's purple). On the other hand, upon completion of the coupling reaction, the Kaiser's test is negative, the resin beads remain colorless.



**Scheme 11:** Schematic representation of solid phase peptide synthesis using *orthogonal* and *submonomer* strategy

## 2.13 Synthesis of *amp* PNA oligomers

### Homopyrimidine Oligomers

The various PNA oligomers synthesized in the present study are shown in Table 1. The unmodified PNA oligomers T<sub>8</sub> and T<sub>10</sub> were synthesized using the Boc protected *aeg* PNA monomers (**57** and **58**). These were used as the control sequences for comparing the properties of the *amp* PNA oligomers. The synthesis of the oligomers (**59** to **87**) was achieved by incorporating the chiral, conformationally constrained modified *amp* PNA monomers at specific positions in the *aeg*-PNA oligomeric sequences. The

synthesis was done on solid support in a similar way, but using Fmoc chemistry for the *amp* monomer coupling and Boc chemistry for the *aeg* PNA monomer coupling to extend the oligomers. Since the *amp* monomers do not carry the nucleobases, these were introduced at desired positions by sub monomer coupling. After this, the *amp* amino acid that has acid stable Fmoc group at amino methyl terminus was treated with TFA to deprotect the ring nitrogen. The thyminylic acetic acid was then reacted with the resin using HOBt/HBTU as coupling agent to attach the nucleobases to the ring nitrogen. This was followed by treatment with 20% piperidine to remove base labile Fmoc group from aminomethyl terminus for initiating the next cycle (Scheme 11). This method involving orthogonal coupling proceeded with good efficiency leading to high purity products. It also circumvented the problem of pre-synthesis of *amp* monomers for each of the bases. *amp* PNA homo oligomers **65**, **71**, **77** and **83** were synthesized using sub monomer strategy,<sup>30a</sup> each oligomer requiring 16 steps for completion of the sequence.

### 2.13.1 Purine-Pyrimidine mix sequence

The polypyrimidine sequences discussed in the previous section are known to form triplexes with the complementary DNA in 2:1 (PNA<sub>2</sub>:DNA) stoichiometry. With the aim of studying the duplex forming potential of the present modification, *amp* monomers were also incorporated into a mixed decamer sequences **64**, **70**, **76**, **82** and **87** containing both the purines and pyrimidines using the Boc and Fmoc chemistry. The corresponding unmodified control *aeg* PNA sequence is **58**.

#### **2.14 Cleavage of the PNA Oligomers from the Solid Support:**

The oligomers were cleaved from the solid support, using trifluoromethanesulfonic acid (TFMSA) in the presence of trifluoroacetic acid (TFA) ('Low, High TFMSA-TFA method')<sup>37</sup> which yields peptide oligomers blocked as amides at their C-terminus. The synthesized PNA oligomers were cleaved from the resin (oligomer attached to  $\beta$ -alanine derivatized MBHA resin) using this procedure to obtain sequences bearing  $\beta$ -alanine-amide at their C-termini. A cleavage time of 60-90 min at room temperature was found to be optimum. The side chain protecting groups were also cleaved during this cleavage process. After cleavage reaction, the oligomer was precipitated from methanol with dry diethyl ether.

#### **2.15 Purification and characterization of PNA oligomers**

All the cleaved oligomers were subjected to initial gel filtration to remove small molecule impurities. These were subsequently purified by reverse phase HPLC (high pressure liquid chromatography) on a semi-preparative C8 RP column by gradient elution using an acetonitrile in water or by isocratic elution in 10% acetonitrile-water on a semi-preparative HPLC RP C4 column.

The purity of the oligomers was then checked by reverse phase HPLC on a C18 RP column and confirmed by MALDI-TOF mass spectroscopic analysis.<sup>38</sup>  $\alpha$ -cyano-4-hydroxycinnamic acid (CHCA) was used as the matrix and dry droplet method was employed in MALDI-TOF mass spectroscopic analysis. Some representative HPLC profiles and mass spectra are shown in appendix of this chapter. The purified PNA **57-87** sequences obtained are listed in Table 1

**Table 1** PNA Oligomers synthesized for the present study

Entry	Sequence code	PNA Sequence
1	<i>aeg</i> PNA <b>57</b>	H-T-T-T-T-T-T-T-(CH <sub>2</sub> ) <sub>2</sub> -CO <sub>2</sub> NH <sub>2</sub>
2	<i>aeg</i> PNA <b>58</b>	H-G-T-A-G-A-T-C-A-C-T-(CH <sub>2</sub> ) <sub>2</sub> -CO <sub>2</sub> NH <sub>2</sub>
3	<i>amp</i> PNA <b>59</b>	H-(t <sub>SR</sub> )-T-T-T-T-T-T-(CH <sub>2</sub> ) <sub>2</sub> -CO <sub>2</sub> NH <sub>2</sub>
4	<i>amp</i> PNA <b>60</b>	H-T-T-T-(t <sub>SR</sub> )-T-T-T-T-(CH <sub>2</sub> ) <sub>2</sub> -CO <sub>2</sub> NH <sub>2</sub>
5	<i>amp</i> PNA <b>61</b>	H-T-T-T-T-T-T-(t <sub>SR</sub> )-(CH <sub>2</sub> ) <sub>2</sub> -CO <sub>2</sub> NH <sub>2</sub>
6	<i>amp</i> PNA <b>62</b>	H-T-T-T-(t <sub>SR</sub> )-T-T-T-(t <sub>SR</sub> )-(CH <sub>2</sub> ) <sub>2</sub> -CO <sub>2</sub> NH <sub>2</sub>
7	<i>amp</i> PNA <b>63</b>	H-T-T-T-(t <sub>SR</sub> )-T-T-T-(t <sub>SS</sub> )-(CH <sub>2</sub> ) <sub>2</sub> -CO <sub>2</sub> NH <sub>2</sub>
8	<i>amp</i> PNA <b>64</b>	H-G-(t <sub>SR</sub> )-A-G-A-(t <sub>SR</sub> )-C-A-C-(t <sub>SR</sub> )-(CH <sub>2</sub> ) <sub>2</sub> -CO <sub>2</sub> NH <sub>2</sub>
9	<i>amp</i> PNA <b>65</b>	H-(t <sub>SR</sub> ) <sub>8</sub> -(CH <sub>2</sub> ) <sub>2</sub> -CO <sub>2</sub> NH <sub>2</sub>
10	<i>amp</i> PNA <b>66</b>	H-(t <sub>SS</sub> )-T-T-T-T-T-T-(CH <sub>2</sub> ) <sub>2</sub> -CO <sub>2</sub> NH <sub>2</sub>
11	<i>amp</i> PNA <b>67</b>	H-T-T-T-(t <sub>SS</sub> )-T-T-T-T-(CH <sub>2</sub> ) <sub>2</sub> -CO <sub>2</sub> NH <sub>2</sub>
12	<i>amp</i> PNA <b>68</b>	H-T-T-T-T-T-T-(t <sub>SS</sub> )-(CH <sub>2</sub> ) <sub>2</sub> -CO <sub>2</sub> NH <sub>2</sub>
13	<i>amp</i> PNA <b>69</b>	H-T-T-T-(t <sub>SS</sub> )-T-T-T-(t <sub>SS</sub> )-(CH <sub>2</sub> ) <sub>2</sub> -CO <sub>2</sub> NH <sub>2</sub>
14	<i>amp</i> PNA <b>70</b>	H-G-(t <sub>SS</sub> )-A-G-A-(t <sub>SS</sub> )-C-A-C-(t <sub>SS</sub> )-(CH <sub>2</sub> ) <sub>2</sub> -CO <sub>2</sub> NH <sub>2</sub>
15	<i>amp</i> PNA <b>71</b>	H-(t <sub>SS</sub> ) <sub>8</sub> -(CH <sub>2</sub> ) <sub>2</sub> -CO <sub>2</sub> NH <sub>2</sub>
16	<i>amp</i> PNA <b>72</b>	H-(t <sub>RS</sub> )-T-T-T-T-T-T-(CH <sub>2</sub> ) <sub>2</sub> -CO <sub>2</sub> NH <sub>2</sub>
17	<i>amp</i> PNA <b>73</b>	H-T-T-T-(t <sub>RS</sub> )-T-T-T-T-(CH <sub>2</sub> ) <sub>2</sub> -CO <sub>2</sub> NH <sub>2</sub>
18	<i>amp</i> PNA <b>74</b>	H-T-T-T-T-T-T-(t <sub>RS</sub> )-(CH <sub>2</sub> ) <sub>2</sub> -CO <sub>2</sub> NH <sub>2</sub>
19	<i>amp</i> PNA <b>75</b>	H-T-T-T-(t <sub>RS</sub> )-T-T-T-(t <sub>RS</sub> )-(CH <sub>2</sub> ) <sub>2</sub> -CO <sub>2</sub> NH <sub>2</sub>
20	<i>amp</i> PNA <b>76</b>	H-G-(t <sub>RS</sub> )-A-G-A-(t <sub>RS</sub> )-C-A-C-(t <sub>RS</sub> )-(CH <sub>2</sub> ) <sub>2</sub> -CO <sub>2</sub> NH <sub>2</sub>
21	<i>amp</i> PNA <b>77</b>	H-(t <sub>RS</sub> ) <sub>8</sub> -(CH <sub>2</sub> ) <sub>2</sub> -CO <sub>2</sub> NH <sub>2</sub>
22	<i>amp</i> PNA <b>78</b>	H-(t <sub>RR</sub> )-T-T-T-T-T-T-(CH <sub>2</sub> ) <sub>2</sub> -CO <sub>2</sub> NH <sub>2</sub>
23	<i>amp</i> PNA <b>79</b>	H-T-T-T-(t <sub>RR</sub> )-T-T-T-T-(CH <sub>2</sub> ) <sub>2</sub> -CO <sub>2</sub> NH <sub>2</sub>
24	<i>amp</i> PNA <b>80</b>	H-T-T-T-T-T-T-(t <sub>RR</sub> )-(CH <sub>2</sub> ) <sub>2</sub> -CO <sub>2</sub> NH <sub>2</sub>
25	<i>amp</i> PNA <b>81</b>	H-T-T-T-(t <sub>RR</sub> )-T-T-T-(t <sub>RR</sub> )-(CH <sub>2</sub> ) <sub>2</sub> -CO <sub>2</sub> NH <sub>2</sub>
26	<i>amp</i> PNA <b>82</b>	H-G-(t <sub>RR</sub> )-A-G-A-(t <sub>RR</sub> )-C-A-C-(t <sub>RR</sub> )-(CH <sub>2</sub> ) <sub>2</sub> -CO <sub>2</sub> NH <sub>2</sub>
27	<i>amp</i> PNA <b>83</b>	H-(t <sub>RR</sub> ) <sub>8</sub> -(CH <sub>2</sub> ) <sub>2</sub> -CO <sub>2</sub> NH <sub>2</sub>
28	<i>amp</i> PNA <b>84</b>	H-(t <sub>SSR</sub> )-T-T-T-T-T-T-(CH <sub>2</sub> ) <sub>2</sub> -CO <sub>2</sub> NH <sub>2</sub>
29	<i>amp</i> PNA <b>85</b>	H-T-T-T-(t <sub>SSR</sub> )-T-T-T-T-(CH <sub>2</sub> ) <sub>2</sub> -CO <sub>2</sub> NH <sub>2</sub>
30	<i>amp</i> PNA <b>86</b>	H-T-T-T-T-T-T-(t <sub>SSR</sub> )-(CH <sub>2</sub> ) <sub>2</sub> -CO <sub>2</sub> NH <sub>2</sub>
31	<i>amp</i> PNA <b>87</b>	H-G-T-A-G-A-(t <sub>SSR</sub> )-C-A-C-T-(CH <sub>2</sub> ) <sub>2</sub> -CO <sub>2</sub> NH <sub>2</sub>

A/G/C/T = *aeg* PNA Adenine/Guanine/Cytosine/Thymine monomers, t<sub>SR</sub> = (2*S*,5*R*)-*amp*-PNA Thymine monomer, t<sub>SS</sub> = (2*S*,5*S*)-*amp* PNA Thymine monomer, t<sub>RS</sub> = (2*R*,5*S*)-*amp*-PNA Thymine monomer, t<sub>RR</sub> = (2*R*,5*R*)-*amp* PNA Thymine monomer, t<sub>SSR</sub> = (2*S*,4*S*,5*R*)-*amp* PNA Thymine monomer

## 2.16 Synthesis of Complementary Oligonucleotides

The oligodeoxynucleotides **88-91** (Table 2) were synthesized on a Pharmacia Gene Assembler Plus DNA synthesizer using the standard  $\beta$ -cyanoethyl phosphoramidite chemistry. The oligomers were synthesized in the 3'-5' direction on a CPG solid support, followed by ammonia treatment. The oligonucleotides were de-salted by gel filtration, their purity as ascertained by RP HPLC on a C18 column was found to be more than 98% and were used without further purification in the biophysical studies of PNA. The RNA oligonucleotides **92-94** (Table 2) which are complementary to PNA oligomers **57-87** were obtained commercially from Genomech, Gainesville, FL, along with the HPLC purity and mass spectral data.

**Table 2** DNA/RNA Oligonucleotides

Entry	Sequence Code	Sequence	Type
		<b>DNA</b> sequence 5' to 3'	Corresponding to PNA
1	DNA <b>88</b>	C G C A A A A A A A A C G C	Match
2	DNA <b>89</b>	C G C A A A A C A A A C G C	Mismatch
3	DNA <b>90</b>	A G T G A T C T A C	Antiparallel
4	DNA <b>91</b>	C A T C T A G T G A	Parallel
		<b>RNA</b> sequences 5' to 3'	
5	RNA <b>92</b>	C G C A A A A A A A A C G C	Match
6	RNA <b>93</b>	A G U G A U C U A C	Antiparallel
7	RNA <b>94</b>	C A U C U A G U G A	Parallel

## 2.17 CONCLUSIONS

This chapter describes the synthesis of *amp* and *aeg* PNA monomers and sitespecific incorporation of *amp* monomers into *aeg* PNA oligomers. The monomers were synthesized starting from L/D proline, with additional methoxy functionality at C5 being introduced by electrochemical anodic oxidation. These were then transformed to the aminomethyl group to form part of the chiral PNA backbone. The modified PNA

monomers were introduced at desired places into the PNA oligomers by solid phase synthesis using submonomer strategy. This has the advantage for introduction of any of the bases during the solid phase synthesis, without making all pre-formed monomers. The oligomers was cleaved from the resin, purified by HPLC and charecterised by MALDI-TOF.

Next chapter describes the hybridization studies of above synthesized *amp/aeg*-PNA oligomers with DNA and RNA.

## **2.18 Experimental**

All reagents were obtained from commercial sources and used without further purification. NaH was obtained from Aldrich as 60% suspension in paraffin oil and the paraffin coating was washed off with pet-ether before use to remove the oil. The supporting electrolyte tetrabutyl ammonium tetrafluoroborate was obtained from Aldrich and used as such without further purification. All the solvents were dried according to literature procedures. IR spectra were recorded on a Perkin Elmer 599B instrument. <sup>1</sup>H NMR (200MHz), <sup>13</sup>C NMR (50 MHz) spectra were recorded on Bruker ACF200 spectrometer fitted with an Aspect 3000 computer. All chemical shifts are with reference to TMS as an internal standard and are expressed in d scale (ppm). The values given are directly from the computer printout and rounded to the decimal place. TLCs were carried out on (E.Merck 5554) precoated silicagel 60 F254 plates. TLCs were visualized with UV light and/or ninhydrin spray, followed by heating after exposing the HCl for the deprotection of the tert-butoxycarbonyl group. Optical rotations were measured on JASCODIP-181 polarimeter. All TLCs were run in pet-ether containing appropriate amount of ethyl acetate or dichloromethane containing appropriate amount of methanol

to get the *rf* value 0.5. All the compounds were purified by column chromatography using 100-200 silica gel obtained from Sisco Research Laboratory. In NMR spectra that show splitting of peaks due to the presence of rotameric mixtures, arising from the tertiary amide linkage, the major rotamer is designated as *maj.* and the minor rotamer as *min.* The ratio of major: minor is 80:20 unless otherwise mentioned. In cases, where minor isomer is <10% only the peaks of major rotamer are reported. Melting points of the compounds reported are uncorrected.

### **Methyl (2S) N1-(*tert*-Butoxycarbonyl) Proline carboxylate 3**

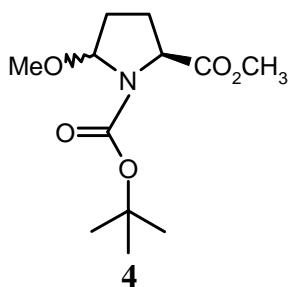
L-Proline **1** (10 g, 87 mmol) was suspended in methanol (100 mL) and cooled to 0 °C with stirring. To this was added thionyl chloride (7 mL, 95.7 mmol, 1.1 eq.) dropwise over a period of 10 min. Stirring was continued at 0 °C for 4 h. and then at ambient temperature until the completion of the reaction (12 h). Removal of methanol under vacuum gave an oily ester hydrochloride salt **2** (14.1 g, 97.9%). This hydrochloride salt was used for the next step without further purification.

Ester hydrochloride **2** (10 g, 60.4 mmol) was dissolved in dioxane/water (1:1v/v, 100 mL). To this were added triethylamine (23 mL, 166 mmol, 2.75 eq.) and BocN<sub>3</sub> (11.2 g, 78.5 mmol, 1.3 eq.) and the mixture was stirred at 50 °C for 24 h, under argon atmosphere. After the completion of the reaction, the mixture was concentrated to a paste by rotary evaporation, the mixture was diluted with H<sub>2</sub>O (75 mL), and extracted with ether (3 x 50 mL). Combined ether layer was washed with H<sub>2</sub>O (2 x 25 mL), followed by brine and dried over sodium sulphate. Evaporation of the solvent and purification by column chromatography using 60-120 silica gel and 10% ethyl acetate-

petroleum ether as eluent afforded 12.1 g of **3** as a yellow oily liquid. Yield 12.1 g, 82.9%.

#### **Methyl (2S)-N1-(*tert*-Butoxycarbonyl)-5-methoxy proline carboxylate **4****

N-(*tert*-Butoxycarbonyl)-L-proline methyl ester **3** (8 g, 34.9 mmol) was dissolved in a 0.5 M solution of tetrabutylammonium tetrafluoroborate in methanol (100 mL). The reaction flask was cooled to 5 °C in an ice bath. The stirred solution was oxidized at a carbon anode and cathode using a constant current (270 mA). After the completion of reaction (12h.) solvent was evaporated under reduced pressure and the residue was treated with ether (3 x 75 mL) leaving the supporting electrolyte as a crystalline solid. The combined ether layers were concentrated under vacuum to get the crude product as an oil which was purified by flash chromatography on 60-120 silica gel by isocratic elution using 10% ethyl acetate/petroleum ether as eluant to get the methoxylated product **4** (7.8 g, 86%).



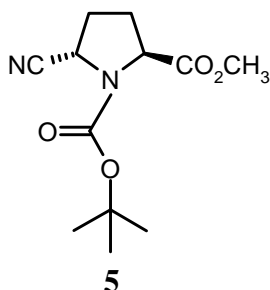
<sup>1</sup>H NMR (CDCl<sub>3</sub>, 200 MHz) δ 5.35-5.10 (m, 1H, H2), 4.45-4.15 (m, 1H, H5), 3.80-3.70 (m, 3H, -OCH<sub>3</sub> of ester), 3.45-3.30 (m, 3H, -OCH<sub>3</sub>), 2.50-1.65 (m, 4H, H3 & H4), 1.55-1.35 (d, 9H, Boc); 153.9 (methyl); <sup>13</sup>C NMR (CDCl<sub>3</sub>, 200 MHz) δ 173.0, 172.8 (-C=O ester); 89.7, 88.4 (C5); 80.3 (tertiary carbon); 59.1, 58.7 (C2); 55.9, 55.6, 54.9; 51.6 (-OCH<sub>3</sub>); 32.3, 30.9, 30.0, (C3); 28.0 (Boc methyl); 26.9 (C4).

#### **Methyl (2S)-N1-(*tert*-butoxycarbonyl)-5-cyano proline carboxylate **5** and **6****

To a solution of **4** (2.46.0 g, 9.5 mmol) in anhydrous dichloromethane (25 mL) was added TMSTf (0.25 mL,) at -35 °C, followed by slow addition of TMSCN (1.46 mL, 10.9 mmol, 1.15 eq.). After the completion of the reaction (30 minutes) methanol was added to the reaction mixture and the solvents were evaporated under reduced pressure.

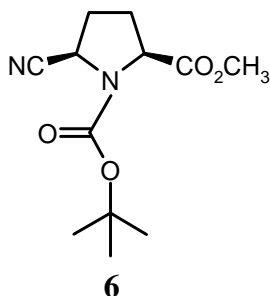
The residue was purified by column chromatography using neutral alumina (Al<sub>2</sub>O<sub>3</sub>) with 10% ethylacetate/ petether as eluant to get the diastereomeric nitriles **5** (minor isomer, upper spot on tlc R<sub>f</sub> 0.30 in 10% ethylacteate-petroleum ehter) 0.69 g & **6** (major isomer, top spot on tlc R<sub>f</sub> 0.3 in 10% ethylacetate-petroleum ether) 1.43 g. The diastereomeric ratio is (35: 70).

Minor isomer 5



<sup>1</sup>H NMR (CDCl<sub>3</sub>, 200 MHz) δ 4.77-4.64 (dd, *J* = 2.5 Hz, 1H, H2), 4.46-4.33 (dd, *J* = 3.75, 1H, H5), 3.74 (s, 3H, OCH<sub>3</sub>), 2.55-2.2 (m, 4H, H3 & H4), 1.51-1.42 (d, 9H, 3 x CH<sub>3</sub>); <sup>13</sup>C NMR (CDCl<sub>3</sub>, 400 MHz): δ 171.90 & 171.71 (ester.CO), 152.4 (Boc.CO), 18.2 (cayano), 82.3, 81.8 (C-(CH<sub>3</sub>)<sub>3</sub>), 59.4, 59.0 (C2), 52.3 (C5), 47.5, 47.2 (COOCH<sub>3</sub>), 30.3, 29.8 (C3), 28.1 (C4), 28.0 (CH<sub>3</sub>)<sub>3</sub>; **Ms** (m/z): (M+1) = 255 (5 %), 188.04 (85 %), 155.06 (100 %). [α]<sub>D</sub><sup>25</sup> = - 93.7 (C = 0.365, CHCl<sub>3</sub>).

Major isomer



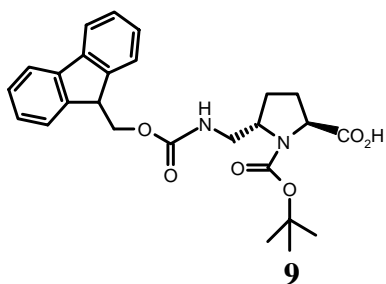
<sup>1</sup>H NMR (CDCl<sub>3</sub>, 200 MHz): δ 4.70-4.55 (m, 1H, H2), 4.52-4.26 (m, 1H, H5), 3.75 (s, 3H, ester -OCH<sub>3</sub>), 2.45-2.19 (m, 4H, H3 & H4), 1.52-1.43 (d, 9H, (CH<sub>3</sub>)<sub>3</sub>); <sup>13</sup>C NMR (CDCl<sub>3</sub>, 400 MHz): δ 172.4, 172.2 (ester.CO), 152.7, 152.6 (Boc.CO), 118. 8, 118.7 (cayano), 82.4, 81.9 (C-(CH<sub>3</sub>)<sub>3</sub>), 58. 9, 58.5 (C2), 51.9 (C5), 47.7, 47.6 (COOCH<sub>3</sub>), 30.0, 29.5(C3), 29.2(C4), 28.2 (CH<sub>3</sub>)<sub>3</sub>. **Ms** (m/z): (M+1) = 254.41 (5%), 277.41 (100 %), 221 (10 %), 144.60 (13 %), 95 (100 %); **IR** cm<sup>-1</sup> (neat): 2246, 1755, 1747, 1713. [α]<sub>D</sub><sup>25</sup> = +41.8 (C = 0.665, CHCl<sub>3</sub>).

**(2*S*, 5*R*) -N1-(*tert*-butoxycarbonyl)-[5-(flourenylemthoxycarbonyl)aminomethyl]**

### **Proline 9**

To a solution of **5** (0.4 g, 1.55 mmol) in methanol (2 mL) was added NEt<sub>3</sub> (0.5 mL) followed by raney Ni (400 mg). The mixture was subjected to hydrogenation at 65 psi , after completion of the reaction (4h) , reaction mixture was filtered through celite pad and the solvent was evaporated under reduce pressure to get amino ester **7** (not

isolated) as a oily liquid. This was subjected to hydrolysis using 2N aq. NaOH (2mL) and methanol (2 mL). After 30 minutes excess of sodium hydroxide was neutralized using potassium bisulfate and the pH was adjusted to 7.0. Methanol was removed by rotary evaporation and the residue was redissolved in 10% Na<sub>2</sub>CO<sub>3</sub> (2 mL) the reaction mixture was cooled to 0 °C in an ice-bath. To this was added of dioxane (2 mL) (peroxide free) followed by the slow addition of Fmoc-Cl (0.44 g, 1.7 mmol, 1.1 eq.) in dioxane at 0 °C. Stirring was continued at 0 °C for 4 h. followed by room temperature stirring for 18 h. The reaction was monitored by TLC, after the completion of the reaction contents were poured in ice- water and extracted with ether (2 x 20 mL) to remove the unreacted chloroformate. The aqueous phase was chilled in ice and acidified by the addition of saturated KHSO<sub>4</sub> solution. The pH of the solution was brought to 2.0 at which the compound started getting separated as foam. This was then extracted with ethyl acetate (3 x 10 mL) and dried over MgSO<sub>4</sub> and the solvent was removed under vacuum to get the crude product as a solid. This was purified by flash column chromatography on 60-120 silica gel using ethyleacetate/petether (0.3 R<sub>f</sub>) as eluant to get 0.27 g, 37 % of the desired product **9**.

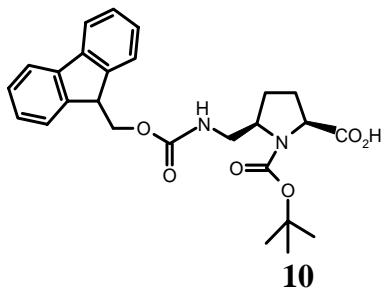


**<sup>1</sup>H NMR** (CDCl<sub>3</sub>, 400 MHz)  $\delta$  7.78-7.345 (m, 8H), 5.95-5.90(s,1H), 4.50-4.14(m,5H), 3.36-3.30(m,2H), 2.26-1.75(m,4H), 1.44(s,9H). **<sup>13</sup>C NMR** (CDCl<sub>3</sub>, 400 MHz):  $\delta$  177.4, 175.5 (acid CO),156.8 (Boc.CO), 154.9 (Fmoc.CO), 143.7, 143.6, 127.4, 126.8, 124.9, 124.6, 119.7 (Fmoc.carbons), 80.9 (C-(CH<sub>3</sub>)<sub>3</sub>), 65.6, 66.2, 59.8, 57.5, 52.5, 46.9, 45.0, 44.0, 28.3, 28.0 (Boc.(CH<sub>3</sub>)<sub>3</sub>), 26.6; Ms (m/z) : 491.50 (M+Na), (10%), 475 (100%),  $[\alpha]_D^{25} = +40.5$  (C = 0.2, CHCl<sub>3</sub>)

**(2*S*,5*S*) -N1-(*tert*-butoxycarbonyl)-[5-(flourenylemthoxycarbonyl)aminomethyl]**

***Proline 10***

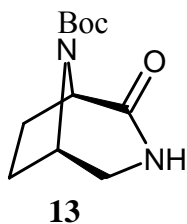
To a solution of **6** (0.4 g, 1.55 mmol) in methanol (2 mL) was added NEt<sub>3</sub> (0.5 mL) followed by raney Ni (400mg). The mixture was subjected to hydrogenation at 65 psi, after completion of the reaction (4h) , reaction mixture was filtered through celite pad and the solvent was evaporated under reduce pressure to get amino ester **7** (not isolated) as a oily liquid. This was subjected to hydrolysis using 2N aq. NaOH (2mL) and methanol (2 mL). After 30 minutes excess of sodium hydroxide was neutralized using potassium bisulfate and the pH was adjusted to 7.0. Methanol was removed by rotary evaporation and the residue was redissolved in 10% Na<sub>2</sub>CO<sub>3</sub> (2 mL). The reaction mixture was cooled to 0 °C in an ice-bath. To this was added of dioxane (2 mL) (peroxide free) followed by the slow addition of Fmoc-Cl (0.44 g, 1.7 mmol, 1.1 eq.) in dioxane at 0 °C. Stirring was continued at 0 °C for 4 h. followed by room temperature stirring for 18 h. The reaction as monitored by TLC, after the completion of the reaction contents were poured in ice- water and extracted with ether (2 x 20 mL) to remove the unreacted chloformate. The aqueous phase was chilled in ice and acidified by the addition of saturated KHSO<sub>4</sub> solution. The pH of the solution was brought to 2.0 at which the compound started getting separated as foam. This was then extracted with ethyl acetate (3 x 10 mL) and dried over MgSO<sub>4</sub> and the solvent was removed under vacuum to get the crude product as a solid. This was purified by flash column chromatography on 60-120 silica gel using ethyleacetate/petether (0.3 R<sub>f</sub>) as eluant to get 0.27 g, 37 % of the desired product **10** along with undesirable **10a** as the major product 0.48 g, 45 %.



**<sup>1</sup>H NMR** (CDCl<sub>3</sub>, 400 MHz)  $\delta$  7.74-7.72 (d,  $J$  = 2.5, 2H), 7.60-7.58 (d,  $J$  = 2.5, 2H), 7.38-7.27 (m, 4H) 6.21-6.15 (bs, 1H), 4.44-4.40 (m, 5H,) 3.52-3.43 (m, 2H, H2), 2.24-1.83 (m, 4H), 1.43 (s, 9H); **<sup>13</sup>C NMR** (CDCl<sub>3</sub>, 400, MHz):  $\delta$  177.6, 177.1 (acid.CO), 157.0 (Boc.CO), 154.8, 154.4, 144.2, 143.8, 144.2, 143.8, (Fmoc.CO), 127.6, 126.7, 125.2, 119.8, (Fmoc.aromatic carbons), 81.2 (C-(CH<sub>3</sub>)<sub>3</sub>), 67.0, 66.9, 58.3, 57.5, 47.0, 44.3, 43.5, 28.6, 28.2, 28.1 (Boc.(CH<sub>3</sub>)<sub>3</sub>); Ms (m/z): 491.15 (20%) (M+1+Na), 265.04 (100%), [ $\alpha$ ]<sub>D</sub><sup>25</sup> = -35.5 (C = 0.4, CHCl<sub>3</sub>)

### Synthesis of compound 13

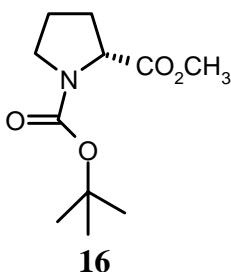
To a solution of **12** (50 mg, 0.204 mmol) in DCM (2 mL) was added diethyl amine (1 mL) at room temperature the mixture was stirred for 4h, after completion of the reaction solvent was evaporated under reduced pressure to get the **12** (not isolated). To a solution of **12** in DMF, HOBT(43.48mg, 0.321 mmol) and HBTU (121.75 mg, 0.321 mmol) were added at room temperature and stirred at for about 8h, DMF was evaporated and the mixture was dilute with H<sub>2</sub>O (5 mL) and extracted with ethyleacetate (2 x 10 mL). Drying of the combined organic phases (Na<sub>2</sub>SO<sub>4</sub>), evaporation of the solvent, and purification by column chromatography afforded 10 mg of **13** (46.1%) as a white solid.



**<sup>1</sup>H NMR** (CDCl<sub>3</sub>, 200 MHz)  $\delta$  6.5-6.25 (t, 1H, amide), 4.43-4.36 (m, 2H, H2 & H5), 3.71-3.64 (dd,  $J$  = 10, 4 Hz, 1H), 3.03-2.96 (dd,  $J$  = 7, 14 Hz, 1H), 2.20-2.05 (m, 3H), 1.80-1.74 (m, 1H). 1.43 (s, 9H, 3 x CH<sub>3</sub>); **<sup>13</sup>C NMR** (CDCl<sub>3</sub>, 400 MHz):  $\delta$  172.4, 153.6, 80.7, 59, 50.6, 47.5, 30.1, 28.2, 27.9; IR  $\gamma$  3240 (br), 1690, cm<sup>-1</sup>; Ms (m/z): (M+1) = 227.11 (25%), , (2 M<sup>+</sup>) 453 (85%), (2M+Na) 475 (100%).

### Methyl (2R)-N1-(*tert*-Butoxycarbonyl) proline carboxylate **17**

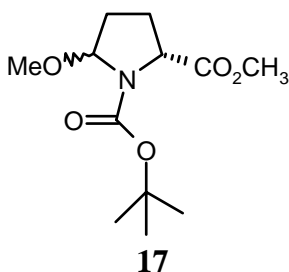
To a solution of **14** (6 g, 52.2 mmol) in methanol (50 mL) was added thionyl chloride (4.2 mL, 57.4 mmol, 1.1) as discussed in the case of compound **1**. Removal of methanol gave the ester **15** as a hydrochloride salt (8.30 g, 96 %). This was used as such for the next step without further purification. The ester **15** (5 g, 30.2 mmol) was dissolved in 1:1 dioxane/water, treated with triethylamine (10.5 mL, 75.5 mmol,) and BocN<sub>3</sub> (5.2 mL, 36.2 mmol) under argon atmosphere at 50 °C. Usual work up and purification as mentioned for the L-isomer gave the *tert*butoxycarbonyl derivative **16**. Yield: 6.1 g, 88 %.



<sup>1</sup>H NMR (CDCl<sub>3</sub>, 200 MHz): δ 4.35-4.10 (m, 1H, H2), 3.72 (s, 3H, CH 3), 3.60-3.25 (m, 2H, H5A & H5B), 2.30-1.70 (m, 4H, H3 & H4), 1.38 (d, 9H, 3 x (CH<sub>3</sub>)<sub>3</sub>); <sup>13</sup>C NMR (CDCl<sub>3</sub>, 200 MHz): δ 173.3 (ester CO), 153.4 (Boc.CO), 79.2 (C(CH<sub>3</sub>)<sub>3</sub>), 58.8 & 58.5 (C2), 51.5 (-OCH<sub>3</sub>), 46.1 (C5), 30.6 & 29.6 (C3), 27.9 ((CH<sub>3</sub>)<sub>3</sub>), 23.4 (C4); [α]<sub>D</sub><sup>25</sup> = + 61.30 (C = 1.135, CHCl<sub>3</sub>). IR cm<sup>-1</sup> (neat): 2977, 1747, 1699;

### Methyl (2R)-N1-(*tert*-Butoxycarbonyl)-5-methoxy proline carboxylate **17**

The ester **16** (4.5 g, 19.7 mmol) was oxidized electrochemically to get the 5-methoxy product **17** as a diastereomeric mixture after the work up and purification as mentioned for the L-isomer **3**. Yield 4.4 g, 88%.

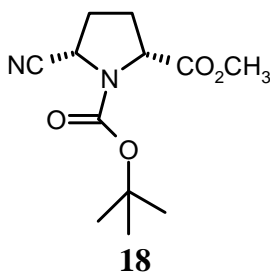


<sup>1</sup>H NMR (CDCl<sub>3</sub>, 200 MHz): δ 5.35-5.05 (m, 1H, H2), 4.40-4.15 (m, 1H, H5), 3.80-3.60 (m, 3H, ester methyl), 3.50-3.25 (m, 3H, methoxy), 2.50-1.70 (m, 4H, H3 & H4), 1.60-1.30 (d, 9H, 3 x CH<sub>3</sub>); <sup>13</sup>C NMR (CDCl<sub>3</sub>, 200 MHz): δ 159.5 (Boc.CO), 153.5 (ester.CO), 88.7, 88.0, 87.9, 80.1, 79.9, 59.1, 58.7, & 58.3, 55.5, 55.3 & 54.7, 51.7 & 51.4, 47.7, 32.4, 31.7, 30.6, 29.6, 27.6, 26.5.

## Methyl (2*R*)-N1-(*tert*-Butoxycarbonyl)- 5-cyano proline carboxylate **18** & **19**

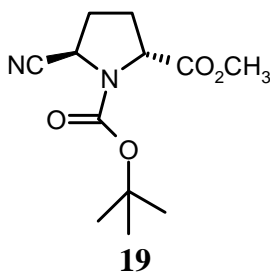
To a solution of **17** (2.46.0 g, 9.5 mmol) in anhydrous DCM (25 mL) were added TMSCN and TMSTf (1 %) at -35 °C to get the product **18** and **19** as separable diastereomeric mixture after the work up and purification as mentioned for the L-isomer. Major isomer **18** and minor isomer **19** in 68:32 ratio.

### Major isomer **18**



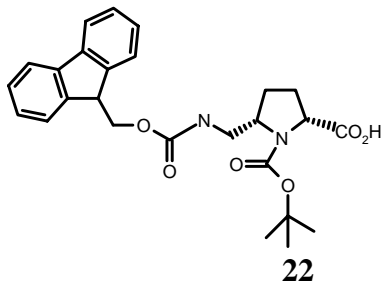
<sup>1</sup>H NMR (CDCl<sub>3</sub>, 400 MHz): δ 4.78-4.65 (dd, 1H), 4.46-4.38 (dd, 1H), 3.74 (s, 3H), 2.60-2.13 (m, 4H), 1.52-1.43 (d, 9H). <sup>13</sup>C NMR (CDCl<sub>3</sub>, 400 MHz): δ 172.0, 171.8 (ester CO), 152.5 (Boc.CO), 118.0 (cyano), 82.4, 82.0 (C-(CH<sub>3</sub>)<sub>3</sub>), 59.5, 59.1 (C2), 52.4 (C5), 47.6 (COOCH<sub>3</sub>), 30.4 (C3), 29.9, 29.6 (C4), 28.6, 28.1 (Boc.(CH<sub>3</sub>)<sub>3</sub>); **Lc-Ms** (EI) m/z (M+1) = 254, (M + Na) = 277.54 (100%), 158.68 (20%) [α]<sub>25</sub><sup>D</sup> = -39.8° (C = 0.4, CHCl<sub>3</sub>); **IR** cm<sup>-1</sup> (neat): 2934, 2243, 1747, 1715;

### Minor isomer **19**



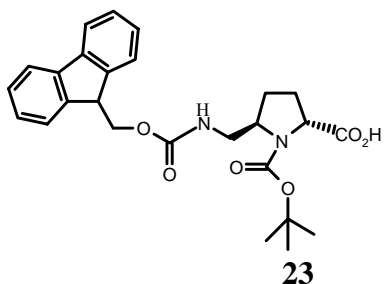
<sup>1</sup>H NMR (CDCl<sub>3</sub>, 400 MHz): δ 4.78-4.67 (dd, *J* = 2 Hz, 1H), 4.46-4.38 (dd, *J* = 2 Hz, 1H), 3.74 (s, 3H), 2.60-2.13 (m, 4H), 1.60-1.25 (d, 9H); <sup>13</sup>C, NMR (CDCl<sub>3</sub>, 400 MHz): δ 172.2, 172.0, (ester.CO), 152.5 (Boc.CO), 118.6, 118.8 (cyano), 82.2, 81.7 (C-(CH<sub>3</sub>)<sub>3</sub>), 58.7, 58.4 (COOCH<sub>3</sub>), 52.3, 52.2 (C2), 48.1 (C5), 47.6, 29.7 (C3), 28.4 (C4), 28.0 (Boc.(CH<sub>3</sub>)<sub>3</sub>); **Lc-Ms** (EI) m/z (M<sup>+</sup>) = 254, (M+Na) = 277 (5%), 128.66 (100%); [α]<sub>25</sub><sup>D</sup> + 101.5° (C = 0.476, CHCl<sub>3</sub>); **IR** cm<sup>-1</sup> (neat): 2243, 1747, 1716.

**(2R,5S)-N1-(tert-butoxycarbonyl)-[5-(flourenylmethoxycarbonyl)aminomethyl]  
Proline 22.**



$^1\text{H NMR}$  ( $\text{CDCl}_3$ , 400 MHz):  $\delta$  7.74-7.22 (d,  $J = 2$  Hz, 2H), 7.60-7.59 (d,  $J = 1$  Hz, 2H), 7.45-7.15 (m, 4H, aromatic), 6.20-5.95 (s, 1H, -NH), 4.43-4.04 (m, 5H, -CH, -CH<sub>2</sub>, CH<sub>2</sub>), 3.60-3.25 (m, 2H), 2.45-1.65 (m, 4H, H<sub>3</sub> & H<sub>4</sub>), 1.43 (s, 9H, 3 x CH<sub>3</sub>);  $^{13}\text{C NMR}$  ( $\text{CDCl}_3$ , 400 MHz):  $\delta$  177.3 (acid.CO), 157.4, 157.0 (Boc.CO), 154.9, 154.4, 144.0, 143.7, 141.2 (Fmoc.CO), 127.6, 126.7, 125.21, 119.9, 119.8 (Fmoc.aromatic.carbons), 81.2 (C-(CH<sub>3</sub>)<sub>3</sub>), 67.0, 60.5, 59.8, 58.4, 58.0, 47.1, 44.4, 43.5, 29.0, 28.2, 27, 28.2, (Boc.(CH<sub>3</sub>)<sub>3</sub>) 28.0 [ $\alpha$ ] $^{25}_D = -35^\circ$  (C = 0.26, CHCl<sub>3</sub>) **Lc-Ms** (EI)  $m/z$  (M + 1) = 467.16 (5%), 45.11 (100%) .

**(2R,5R)-N1-(tert-butoxycarbonyl)-[5-(flourenylmethoxycarbonyl)aminomethyl]  
Proline 23.**

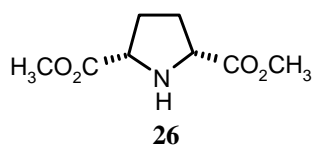


$^1\text{H NMR}$  ( $\text{CDCl}_3$ , 400 MHz)  $\delta$  7.74-7.72 (d,  $J = 2$  Hz, 2H, aromatic), 7.58-7.65 (m, 2H, aromatic), 7.37-7.28 (m, 4H, aromatic), 6.00 (bs, 1H, -NH), 4.45-4.00 (m, 5H, -CH, -CH<sub>2</sub>, -CH<sub>2</sub>NH), 3.77-3.69 (m, 1H), 3.31-3.05 (m, 2H), 2.28-1.73 (m, 4H, H<sub>3</sub> & H<sub>4</sub>), 1.42 (s, 9H, 3 x CH<sub>3</sub>);  $^{13}\text{C NMR}$  ( $\text{CDCl}_3$ , 400 MHz):  $\delta$  177.4 (acid CO), 158.9, (Boc.CO), 155.2, 154.8, (Fmoc.CO), 143.9, 141.4, 141.3, 127.6, 127.0, 125.1, 124.8, 119.9, 119.9, 81.2, 80.8, 67.0 (C-(CH<sub>3</sub>)<sub>3</sub>), 66.8, 57.7, 47.2, 45.5, 47.3, 45.5, 28.6, 28.4, 28.2 (Boc.(CH<sub>3</sub>)<sub>3</sub>), 27.0; **Lc-Ms** (EI)  $m/z$  (M+1) = 467.48 (5%) 245.15 (100%). [ $\alpha$ ] $^{25}_D = +38^\circ$  (C = 0.027, CHCl<sub>3</sub>).

**(2R,5S)-Pyrrolidine-2,5-dimethyldicarboxylate 26**

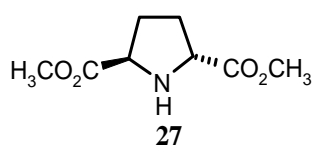
To a solution of **18** (0.4 g, 1.57 mmol) 6 N HCl (10 mL) was added refluxed for 24 h, and reaction mixture was concentrated under vacuo to obtain the hydrochloride salt of dicarboxylic acid **24**, yield 0.28 g (92%). The resultant salt was dissolved in methanol and cooled to 0 °C and SOCl<sub>2</sub> (0.25 mL) was added in a drop wise fashion. The reaction mixture was further stirred at room temperature for 12 h and concentrated under vacuo. The residue was treated with saturated aqueous NaHCO<sub>3</sub> solution and the aqueous layer

was extracted with ethyl acetate (3 x 10 mL), dried over Na<sub>2</sub>SO<sub>4</sub>, concentrated in vacuo to afforded 200 mg of **26**, yield (75%). R<sub>f</sub> = 0.25 (Ethylacetate/Petether = 1:0).



<sup>1</sup>H NMR (CDCl<sub>3</sub>, 500 MHz): δ 3.81-3.83 (t, *J* = 10 Hz, 2H, H<sub>2</sub>,H<sub>5</sub>), 3.73 (s, 6H, CO<sub>2</sub>CH<sub>3</sub>), 2.95 (bs, 1H, -NH), 2.14 (m, 2H), 1.80 (m, 2H); <sup>13</sup>C NMR (CDCl<sub>3</sub>, 125 MHz) 174.1 (COCH<sub>3</sub>), 59.9 (C2 & C5), 51.8 (OCH<sub>3</sub>), 29.4 (C3 & C4). [α]<sub>D</sub><sup>25</sup> = 0 (0.01, CHCl<sub>3</sub>)

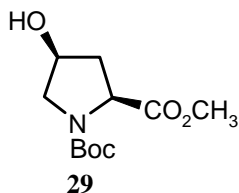
### (2*R*,5*R*)-Pyrrolidine-2,5-dimethyldicarboxylate **27**



<sup>1</sup>H NMR (CDCl<sub>3</sub>, 500 MHz): δ 4.0-3.98 (t, *J* = 10 Hz, 2H, H<sub>2</sub>,H<sub>5</sub>), 3.73 (s, 6H, CO<sub>2</sub>CH<sub>3</sub>), 2.18 (m, 2H), 1.96 (m, 2H); <sup>13</sup>C NMR (CDCl<sub>3</sub>, 125 MHz) 174.8 (COCH<sub>3</sub>), 59.4 (C2 & C5), 51.8 (OCH<sub>3</sub>), 29.4 (C3 & C4); [α]<sub>D</sub><sup>25</sup> = +32° (0.01, CHCl<sub>3</sub>)

### Compound **29**

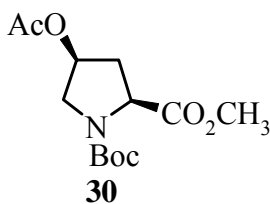
To a solution of **28** ( 10 gm, 43.29 mmol ) in acetone ( 500 mL ) K<sub>2</sub>CO<sub>3</sub> ( 23.37 gm, 129 mmol ) was added followed by slow addition of dimethyl sulphate (5.76 gm, 4.42 mL) and refluxed for 5h, after completion of the reaction concentrated the reaction mixture and dilute with H<sub>2</sub>O ( 35 mL ), followed by extraction with ethyl acetate ( 3 x 50 mL ). Drying of the combined organic phases (Na<sub>2</sub>SO<sub>4</sub>), evaporation of the solvent and purification by column chromatography afforded 9.5 gm of **29** (89.6%) as white solid.



<sup>1</sup>H NMR (CDCl<sub>3</sub>, 200 MHz): δ 4.44-4.3 (m, 2H, H<sub>3</sub>, H<sub>2</sub>), 3.70 (s, 3H, -CO<sub>2</sub>CH<sub>3</sub>), 3.57-3.26 (m, 2H, H<sub>5</sub>), 2.35-2.15 (m, 1H, H<sub>3</sub>), 2.10-1.90 (1H, H<sub>3</sub>), 1.42-1.37 (d, 9H, *J* = 10 Hz -3 x CH<sub>3</sub>); <sup>13</sup>C NMR (CDCl<sub>3</sub>, 200 MHz): δ 173.4, 173.2 (ester CO), 154.3, 153.7 (Boc CO), 80.0, 60.2, 68.5, (C<sub>4</sub>), 57.6, 57.2 (C<sub>2</sub>), 54.3 (C<sub>5</sub>), 51.7 (OCH<sub>3</sub>), 38.6, 37.9 (C<sub>3</sub>), 27.8 (Boc CO); IR γ 3018, 1745, 1720 cm<sup>-1</sup>.

### Compound 30

To a solution of **29** (4 gm, 16.32 mmol) in THF (60 mL), was added triphenylphosphine (4.7 gm, 17.95 mmol) as THF solution (15 mL) and reaction mixture was cooled to ice temperature, to this acetic acid (1.18 gm, 17.95 mmol) followed by DEAD (3.41 gm, 16.32 mmol) were added drop wise fashion and the reaction mixture was stirred at ambient temperature for 10h, after completion of the reaction solvent was removed and diluted with H<sub>2</sub>O (25 mL) followed by extraction with ethyl acetate (3 x 40 mL). Drying of the combined organic phases (Na<sub>2</sub>SO<sub>4</sub>), evaporation of the solvent and purification by column chromatography by 100-200 silica-gel afforded 4.3 gm (93.4%) of **30** as a oily liquid.

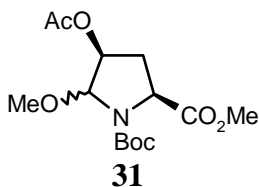


<sup>1</sup>H NMR (CDCl<sub>3</sub>, 200 MHz): δ 5.26-5.22 (m, 1H, H3), 4.52-4.34 (dd, *J* = 2 Hz, 1H, H1), 3.75 (s, 3H, -CO<sub>2</sub>CH<sub>3</sub>), 3.73-3.49 (m, 2H, H4), 2.60-2.20 (m, 2H, H2), 2.01 (s, 3H, -OCOCH<sub>3</sub>), 1.48-1.43 (d, *J* = 10 Hz, 9H, -CO<sub>2</sub>C(CH<sub>3</sub>)<sub>3</sub>); <sup>13</sup>C NMR (CDCl<sub>3</sub>, 200 MHz): δ 172.1, 171.8 (-COCH<sub>3</sub>), 169.8 (OCOCH<sub>3</sub>), 153.7, 153.2 (COOC(CH<sub>3</sub>)<sub>3</sub>), 179.9 (*t*Bu-C), 72.9, 71.8 (C4), 57.9, 57.5 (C2), 52.4, 52.4 (CO-OCH<sub>3</sub>), 52.2, 51.9 (C5), 36.4, 35.5 (C3), 28.5, 28.4, (Boc-C(CH<sub>3</sub>)<sub>3</sub>), 21.0 (OCO-CH<sub>3</sub>); IR γ 3020, 1737, 1693 cm<sup>-1</sup>; Ms: *m/z* = 288 [M+1] (6%), 277 (10%), 228 (93%), 188 (100%), 128 (96%); [α]<sub>D</sub><sup>25</sup> = -25.33 (C = 0.073, DCM).

### Compound 31

To a solution of **30** (6 gm, 20.90 mmol) in methanol was added tetrabutylammonium tetrafluoroborate (8 gm). The reaction flask was cooled to 5 °C in an ice bath. The stirred solution was oxidized at a carbon anode and cathode using a constant current (270 mA). After the completion of reaction 8h, solvent was evaporated under reduced pressure and the residue was treated with ether (3 x 75 mL) leaving the supporting electrolyte as a crystalline solid. The combined ether layers were concentrated under

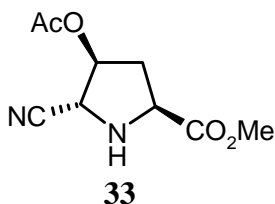
vacuum to get the crude product as an oil which was purified by column chromatography on 100-200 silica gel by isocratic elution using 10% ethyl acetate/petroleum ether as eluant to get the methoxylated product **31** (3.5 gm, 66%).



**<sup>1</sup>H NMR** (CDCl<sub>3</sub>, 200 MHz)  $\delta$  5.36-5.26 (m, 1H, H4), 4.95-4.73 (m, 1H, H2), 4.50-4.17 (m, 1H, -H5), 3.72-3.70 (3H, -OCH<sub>3</sub>), 3.47-3.43 (3H, OCH<sub>3</sub>), 2.64-2.50 (m, 1H, H3), 2.18-1.99 (4H, H3, COOCH<sub>3</sub>), 1.48-1.41 (m, 9H, Boc methyl); **<sup>13</sup>C NMR** (CDCl<sub>3</sub> 200 MHz)  $\delta$  172.6, 171.5 (COOCH<sub>3</sub>), 170.2, 189.9 (OCOCH<sub>3</sub>), 153.7 (COOC(CH<sub>3</sub>)<sub>3</sub>), 80.9, 84.7, 81.4, 80.8, (OCH<sub>3</sub>), 75.9, 74.7, 71.4, 70.8, (C4), 58.4, 57.8 (C2), 55.6, 54.7 (CO<sub>2</sub>CH<sub>3</sub>), 33.4, 32.4, 31.0, 30.2, (C3), 28.2, 28.0, (COOC(CH<sub>3</sub>)<sub>3</sub>), 20.7, (OCOCH<sub>3</sub>); **Ms:**  $m/z$  [M+1] = 260 (33%), 277 (55%), 128 (100%); **IR**  $\gamma$  3020, 2401, 1737.74, 1706.88 cm<sup>-1</sup>

### Compound 33

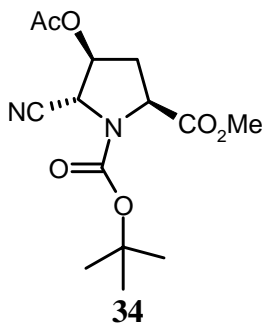
To a solution of **31** (1 gm, 3.15 mmol) in DCM was added TMSICN (0.812mL, 6.3 mmol) and reaction mixture was cooled to ice temperature, to this BF<sub>3</sub>-O(Et)<sub>2</sub> (0.997 mL, 7.875 mmol) was added drop wise fashion and stirred at ambient temperature for 14h, after completion of the reaction Na<sub>2</sub>CO<sub>3</sub> (160 mg, 0.5 mmol) was added and stirred for 2h to quench the excess Lewis acid present in the reaction. Evaporation of the solvent, and purification by column chromatography using neutral alumina afforded 150 mg of **33** (23%) as an oily liquid.



**<sup>1</sup>H NMR** (CDCl<sub>3</sub> 200 MHz)  $\delta$  5.31-5.28 (d,  $J$  = 6 Hz, 1H, H4), 4.23 (s, 1H, H2), 4.06-3.99 (dd,  $J$  = 4 Hz, H5), 3.77 (s, 3H), ( 2.72-2.57 (m, 1H, H2), 2.33-2.26 (m, 1H, H2), 2.03 (s, 3H, OCOCH<sub>3</sub>); **<sup>13</sup>C NMR** (CDCl<sub>3</sub> 200 MHz)  $\delta$  173.4 (CO<sub>2</sub>CH<sub>3</sub>), 169.5 (OCOCH<sub>3</sub>), 118.0 (CN), 76.0 (CO-OCH<sub>3</sub>), 58.0 (C5), 53.7 (C4), 52.3 (C2), 34.5 (C<sub>3</sub>), 20.4 (OCO-CH<sub>3</sub>); **IR**  $\gamma$  cm<sup>-1</sup> 3022., 2954, 1741

### Compound 34

To a solution of **33** (150 mg, 0.678) in DCM was added di tertiarybutyloxy carbonate (591.8 mg, 2.712 mmol) followed by catalytic amount of DMAP (16.56 mg, 0.135 mmol) at ice temperature and stirred at ambient for 8h. evaporation of the solvent and purification by flash chromatography afforded 220 mg of **34** (97%) as a oily liquid.

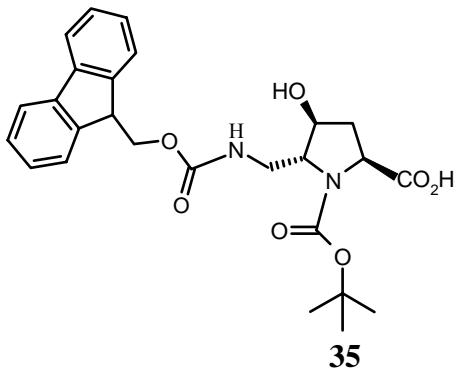


<sup>1</sup>H NMR (CDCl<sub>3</sub> 200 MHz)  $\delta$  1.54-1.45 (d,  $J$  = 18 Hz, COOC(CH<sub>3</sub>)<sub>3</sub>); 2.05-2.04 (d,  $J$  = 2 Hz, -OCO-CH<sub>3</sub>), 2.47-2.40 (d,  $J$  = 16 Hz, H3), 2.81-2.64 (m, 1H, H3), 3.76 (s, 3H), 4.61-4.47 (m, 1H) 4.68-4.64 (d,  $J$  = 8 Hz m, 1H), 5.38-5.36 (d,  $J$  = 4 Hz, 1H, H4), <sup>13</sup>C NMR (CDCl<sub>3</sub> 200 MHz)  $\delta$  171.0, 170.6 (CO<sub>2</sub>CH<sub>3</sub>), 169.4, 169.0 (OCO-CH<sub>3</sub>), 152.5, 152.21 (COOC(CH<sub>3</sub>)<sub>3</sub>), 115.7, 115.6 (CN), 82.8, 82.1, (COOC(CH<sub>3</sub>)<sub>3</sub>), 76 (OCH<sub>3</sub>), 58.0, 57.7 (C2), 53.6, 53.5 (C2), 53.6, 53.5 (C5), 52.5, 52.3 (C4), 35.2, 34.1 (C3), 20.5 (OCO-CH<sub>3</sub>); **Ms**:  $m/z$  = 333 [M+Na] (3%), 235.21(20%), 102.11 (100%).

### Compound 35

To a solution of **34** (220 mg, 0.709 mmol) in methanol (2 mL) was added NEt<sub>3</sub> (0.29 mL, 2.127 mmol) followed by raney Ni (250 mg). The mixture was subjected to hydrogenation at 65 psi, after completion of the reaction (4h), reaction mixture was filtered through celite pad and the solvent was evaporated under reduce pressure to get amino ester **7** (not isolated) as a oily liquid. This was subjected to hydrolysis using 2N aq. NaOH (1mL) and methanol (2 mL). After 30 minutes excess of sodium hydroxide was neutralized using potassium bisulfate and the pH was adjusted to 7.0. Methanol was removed by rotary evaporation and the residue was redissolved in 10% Na<sub>2</sub>CO<sub>3</sub> (1 mL) the reaction mixture was cooled to 0 °C in an ice-bath. To this was added of dioxane (2 mL) (peroxide free) followed by the slow addition of Fmoc-Cl (201 mg, 0.719) mmol, 1.1 eq.) in dioxane at 0 °C. Stirring was continued at 0 °C for 4 h. followed by room temperature stirring for 18 h. The reaction as monitored by TLC, after the completion of

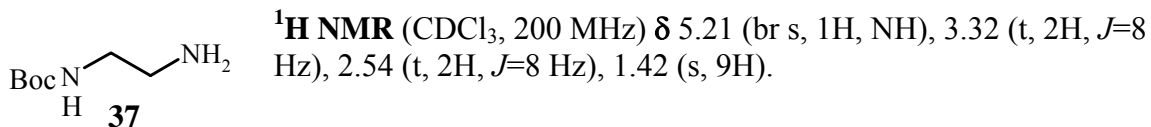
the reaction contents were poured in ice-water and extracted with ether (2 x 15 mL) to remove the unreacted chloroformate. The aqueous phase was chilled in ice and acidified by the addition of saturated KHSO<sub>4</sub> solution. The pH of the solution was brought to 2.0 at which the compound started getting separated as foam. This was then extracted with ethyl acetate (3 x 10 mL) and dried over MgSO<sub>4</sub> and the solvent was removed under vacuum to get the crude product as a solid. This was purified by flash column chromatography on 60-120 silica gel using ethylacetate/petether (0.3 Rf) as eluant to get 135 mg, (39 %) of the desired product **35** as a cream color solid.



<sup>1</sup>H NMR (CDCl<sub>3</sub>, 200 MHz) δ 7.69-7.65 (d, *J* = 8 Hz, 2H), 7.53-7.49 (d, *J* = 8 Hz, 2H), 7.31-7.17 (m, 4H), 5.94 (bs, 1H, -NH), 4.40-3.91 (m, 6H), 3.40-3.26 (m, 1H), 3.21-3.07 (m, 1H), 2.29-1.94 (m, 2H, H<sub>3</sub>); <sup>13</sup>C NMR (CDCl<sub>3</sub>, 400 MHz) δ 176.0, 159.0, 154.4, 143.8, 143.26, 127.7, 127.0, 125.2, 124.9, 119.9, 81.3, 73.2, 67.3, 52.6, 47.23, 43.4, 36.4, 28.2; Ms: *m/z* = 505.13 [M+Na] (3%), 277 (20%), 199 (75%), 155 (100%)

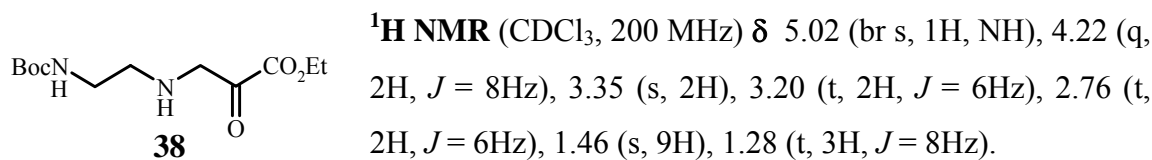
### ***N*1-(*t*-Boc)-1,2-diaminoethane (**37**)**

1,2-diaminoethane (20 g, 0.33 mol) was taken in THF (500 ml) and cooled in an ice-bath. Boc-anhydride (5 g, 35 mmol) in THF (150 ml) was slowly added with stirring. The mixture was stirred for at ambient temperature for 16 h and the resulting solution was concentrated to 100 ml. The *N*1, *N*2-di-Boc derivative not being soluble in water, precipitated, and it was removed by filtration. The corresponding *N*1-mono-Boc derivative was obtained by repeated extraction from the filtrate in ethyl acetate. Removal of solvents yielded the mono-Boc-diaminoethane **37** (3.45 g, 63%, Rf = 0.25, DCM: MeOH; 9:1).



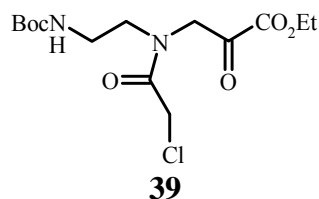
### Ethyl *N*-(2-Boc-aminoethyl)-glycinate (**38**)

The *N*1-(Boc)-1,2-diaminoethane **37** (3.2 g, 20 mmol) was treated with ethyl bromoacetate (2.25 ml, 20 mmol) in acetonitrile (100 ml) in the presence of N(Et)<sub>3</sub> (6.05 gm, 60 mmol) at 0 °C, the mixture was stirred at ambient temperature for 12 h. The reaction mixture was concentrated to paste and diluted with H<sub>2</sub>O (20 ml), and extracted with ethyl acetate (5 x 20 mL). Drying of the combined organic phases (Na<sub>2</sub>SO<sub>4</sub>) and evaporation of the solvent afforded 4.3 gm (83%) of **38** as oily liquid.



### Ethyl *N*-(Boc-aminoethyl)-*N*-(chloroacetyl)-glycinate (**39**)

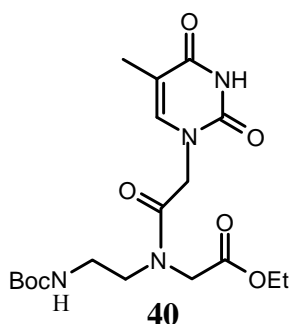
The ethyl *N*-(2-Boc-aminoethyl)-glycinate **38** (4.0 g, 14 mmol) was taken in 10% aqueous Na<sub>2</sub>CO<sub>3</sub> (75 ml) and dioxane (60 ml). Chloroacetyl chloride (6.5 ml, 0.75 mmol) was added in two portions with vigorous stirring. The reaction was completed within 5 min. The reaction mixture was brought to pH 8.0 by addition of 10% aqueous Na<sub>2</sub>CO<sub>3</sub> and concentrated to remove the dioxane. The product was extracted from the aqueous layer with dichloromethane and was purified by column chromatography to obtain the ethyl *N*-(Boc-aminoethyl)-*N*-(chloroacetyl)-glycinate **39** as a colorless oil in good yield (4.2 g, Yield, 80%; *R*<sub>f</sub> = 0.3, ethylacetate:petroleum ether; 2:8).



**<sup>1</sup>H NMR** (CDCl<sub>3</sub>, 200 MHz)  $\delta$  5.45 (br s, 1H), 4.1- 4.9 (S, 2H), 4.00 (s, 2H), 3.53 (t, 2H), 3.28 (q, 2H), 1.46 (s, 9H), 1.23 (t, 3H,  $J=8\text{Hz}$ ).

#### *N*-(Boc-aminoethylglycyl)-thymine ethyl ester (**40**)

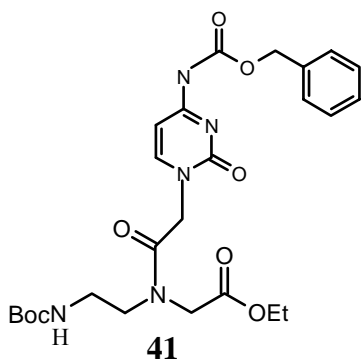
Ethyl *N*-(Boc-aminoethyl)-*N*-(chloroacetyl)-glycinate **39** (1.0 g, 3.1mmol) was stirred with anhydrous K<sub>2</sub>CO<sub>3</sub> (0.47 g, 3.4 mmol) in DMF with thymine (0.41 g, 3.25 mmol) to obtain the desired compound **40** in good yield. DMF was removed under reduced pressure and the oil obtained was purified by column chromatography to afford **40**. (1 g, Yield 83%; R<sub>f</sub> = 0.2, MeOH:DCM; 5:95).



**<sup>1</sup>H NMR** (CDCl<sub>3</sub>, 200 MHz):  $\delta$  9.00 (br s, 1H, T-NH), 7.05 (min) & 6.98 (maj) (s, 1H, T-H6), 5.65 (maj) & 5.05 (min) (br s, 1H, NH), 4.58 (maj) & 4.44 (min) (s, 1H, T-CH<sub>2</sub>), 4.25 (m, 2H, OCH<sub>2</sub>), 3.55 (m, 2H), 3.36 (m, 2H), 1.95 (s, 3H, T-CH<sub>3</sub>), 1.48 (s, 9H), 1.28 (m, 3H); **<sup>13</sup>C NMR** (CDCl<sub>3</sub>)  $\delta$ : 170.8, 169.3, 167.4, 164.3, 156.2, 151.2, 141.1, 110.2, 79.3, 61.8, 61.2, 48.5, 48.1, 47.7, 38.4, 28.1, 13.8, 12.2.

#### *N*-(Boc-aminoethylglycyl)-(N4-benzyloxycarbonyl cytosine)ethyl ester (**41**)

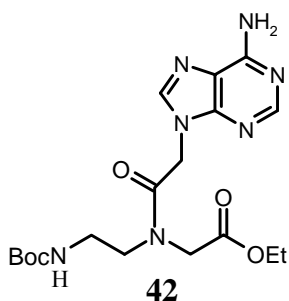
A mixture of NaH (0.25 g, 6.2 mmol) and N4-benzyloxycarbonyl cytosine **17** (1.24 g, 6.2 mmol) was taken in DMF and stirred at 75 °C till the effervescence ceased. The mixture was cooled and ethyl *N*-(Boc-aminoethyl)-*N*-(chloroacetyl)-glycinate **39** (2.0 g, 6.2 mmol) was added. Stirring was then continued at 75 °C to obtain the cytosine monomer, *N*-(Boc-aminoethylglycyl)-(N4-benzyloxycarbonyl cytosine)ethyl ester **41**, in moderate yield (1.75 g, 69%; ).



**<sup>1</sup>H NMR** (CDCl<sub>3</sub>, 200 MHz):  $\delta$  7.65 (d, 1H, C-H6,  $J$  = 8Hz), 7.35 (s, 5H, Ar), 7.25 (d, 1H, C-H5,  $J$  = 8Hz), 5.70 (br s, 1H, NH), 5.20 (s, 2H, Ar-CH<sub>2</sub>), 4.71 (maj) & 4.22 (min) (br s, 2H), 4.15 (q, 2H), 4.05 (s, 2H), 3.56 (m, 2H), 3.32 (m, 2H), 1.48 (s, 9H), 1.25 (t, 3H).

### ***N*-(Boc-aminoethylglycyl)-adenine ethyl ester (42)**

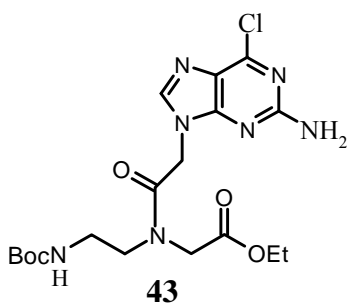
NaH (0.25 g, 6.1 mmol) was taken in DMF (15 ml) and adenine (0.8 g, 6.1 mmol) was added. The mixture was stirred at 75 °C till the effervescence ceased and the mixture was cooled before adding ethyl *N*-Boc-aminoethyl)-*N*-(chloroacetyl)-glycinate **39** (2.0 g, 6.1mmol). The reaction mixture was heated once again to 75 °C for 1 h, when TLC analysis indicated the disappearance of the starting ethyl *N*-(Boc-aminoethyl)-*N*-(chloroacetyl)-glycinate. The DMF was removed under vacuum and the resulting thick oil was taken in water and the product, extracted in ethyl acetate. The organic layer was then concentrated to obtain the crude product, which was purified by column chromatography to obtain the pure *N*-(Boc-aminoethylglycyl)-adenine ethyl ester **42**. (Yield 75%;  $R_f$  = 0.2, MeOH:DCM; 5:95).



**<sup>1</sup>H NMR** (CDCl<sub>3</sub>, 200 MHz):  $\delta$  8.32 (s, 1H), 7.95 (min) & 7.90 (maj) (s, 1H), 5.93 (maj) & 5.80 (min) (br, 2H), 5.13 (maj) & 4.95 (min), 4.22 (min) & 4.05 (maj) (s, 2H), 4.20 (m, 2H), 3.65 (maj) & 3.55 (min) (m, 2H), 3.40 (maj) & 3.50 (min) (m, 2H), 1.42 (s, 9H), 1.25 (m, 3H).

### ***N*-(Boc-aminoethylglycyl)-2-amino-6-chloropurine ethyl ester (43)**

A mixture of 2-amino-6-chloropurine (1.14 g, 6.8 mmol), K<sub>2</sub>CO<sub>3</sub> (0.93 g, 7.0 mmol) and ethyl *N*-(Boc-aminoethyl)-*N*-(chloroacetyl)-glycinate **39** (2.4 g, 7.0 mmol) were taken in dry DMF (20 ml) and stirred at room temperature for 4 h. K<sub>2</sub>CO<sub>3</sub> was removed by filtration, and the DMF, by evaporation under reduced pressure. The resulting residue was purified by column chromatography to obtain the *N*-(Boc-aminoethylglycyl)-2-amino-6-chloropurine ethyl ester (**43**) in excellent yield (2.55 g, 90%; R<sub>f</sub> = 0.25, MeOH:DCM; 5:95).



<sup>1</sup>H NMR (CDCl<sub>3</sub>, 200 MHz): δ 7.89 (min) & 7.85 (maj) (s, 1H), 7.30 (s, 1H), 5.80 (br s, 1H, NH), 5.18 (br, 2H), 5.02 (maj) & 4.85 (min) (s, 2H), 4.18 (min) & 4.05 (maj) (s, 2H), 3.65 (maj) & 3.16 (min) (m, 2H), 3.42 (maj) and 3.28 (min) (m, 2H), 1.50 (s, 9H), 1.26 (m, 3H).

### **Hydrolysis of the ethyl ester functions of PNA monomers (General method):**

The ethyl esters were hydrolyzed using 2N aqueous NaOH (5ml) in methanol (5ml) and the resulting acid was neutralized with activated Dowex-H<sup>+</sup> till the pH of the solution was 7.0. The resin was removed by filtration and the filtrate was concentrated to obtain the resulting Boc-protected acids (21-24) in excellent yield (>85%). In case of cytosine monomer ethyl ester, mild base 0.5 M LiOH was used to avoid deprotection of the exocyclic amine-protecting group by strong bases.

### **Thymine N1-acetic acid 49**

To thymine **48** (5 g, 39.7 mmol) and potassium hydroxide (3.8 g, 79.4 mmol) in H<sub>2</sub>O (30 mL) was added chloroacetic acid slowly (3.1 g, 39.7 mmol) in water (12 mL).

The pH of the solution was adjusted and kept at 10 by drop wise addition of aq. KOH solution. After refluxing for 2h, the solution was cooled and acidified to pH 2 with conc. HCl. The resulting precipitate was filtered, washed with cold water and dried to obtain the crude product, recrystallized from water to get pure **49** (4.9 g, 66%) as a white solid. mp 258 °C (260-261 °C).

#### **N4-Benzyloxycarbonyl cytosine 4**

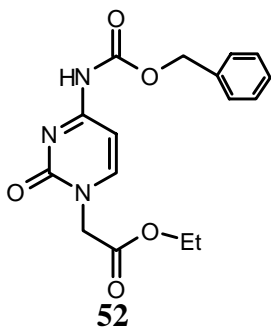
Cytosine **50** (1 g, 9 mmol) was suspended in dry pyridine (15 mL) and cooled to 0°C. To this was added benzyloxycarbonyl chloroformate (3.0 mL, 18 mmol. ) drop wise over a period of 15 min. under nitrogen atmosphere. The reaction mixture was stirred overnight. The pyridine suspension was evaporated to dryness in vacuo. To this were added water (10 mL) and 4N hydrochloric acid to bring the pH to 1. The resulting white precipitate was filtered off, washed with water and partially dried. The wet precipitate was boiled in absolute ethanol (25 mL) for 10 min. cooled to 0°C, filtered, washed thoroughly with ether, and dried, in vacuo to get **52** as a white solid.

<sup>1</sup>H NMR (DMSO D<sub>6</sub>):  $\delta$  7.85-7.70 (d, 1H, H6), 7.45-7.20 (m, 5H, aromatic), 7.00-6.80 (d, 1H, H5), 5.15 (s, 2H, benzyl CH<sub>2</sub>). Mass (m/e) 245 (M<sup>+</sup>).

#### **Ethyl (N4-Benzyloxycarbonyl- N1cytosinyl) acetate 52**

A suspension of N4-Benzyloxycarbonyl cytosine **51** (0.5 g, 2 mmol) and K<sub>2</sub>CO<sub>3</sub> (0.28 g, 2 mmol) in dry DMF was cooled to 0°C and ethyl bromoacetate (0.133 mL, 1.2 mmol, 0.6 eq.) was added drop wise and the mixture was stirred vigorously overnight, filtered and evaporated to dryness. Water (7 mL) and 4 N HCl (0.2 mL) were added and the mixture was stirred for 15 minutes at 0° C, filtered, and washed with water (2 x 10

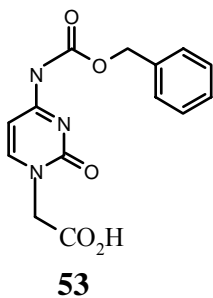
mL). The isolated precipitate was purified by column chromatography on silica gel using ethylacetate/petether as an eluent to get the pure ester **52** as a white solid. Yield 0.48g, 71%.



<sup>1</sup>H NMR (CDCl<sub>3</sub>, 200 MHz): δ 7.75 (bs, NH), 7.60-7.45 (d, 1H, H6), 7.45-7.30 (m, 5H, aromatic), 7.30-7.20 (d, 1H, H5), 5.20 (s, 2H, benzyl CH<sub>2</sub>), 4.60 (s, 2H, N-CH<sub>2</sub>), 4.35-4.15 (q, 2H, -CH<sub>2</sub>), 1.35-1.20 (t, 3H, CH<sub>3</sub>). Mass (m/e) 331 (M+1).

#### N4-Benzyloxycarbonyl cytosine-N1-acetic acid **53**

Ester **52** (0.25 g, 0.74 mmol) in water (1.5 mL) was treated with 2N NaOH (1.5 mL) for 15 min. filtered, cooled to 0°C and neutralized with 4N HCl (0.5 mL). The product acid was isolated by filtration and the precipitate was washed thoroughly with water to get the free acid **53** as a white solid. Yield 0.195 g, 92 %.



<sup>1</sup>H NMR (DMSO D<sub>6</sub>): δ 10.2 (bs, 1H), 8.10-7.90 (d, 2H, H6), 7.60-7.25 (m, 5H), δ7.05-6.90 (d, 1H, H5), 5.2 (s, 2H, benzyl CH<sub>2</sub>), 4.5 (s, 2H, N-CH<sub>2</sub>).

#### 2.19 Functionalization of MBHA resin

The commercially available MBHA resin has loading value of (2meq/g) which is not suitable for oligomer synthesis. Hence it is required to minimize the loading value to

0.17-0.27 meq/g to avoid the syntheses problems due to aggregation of developing oligomer. Dry resin (2 gm) was taken in solid phase funnel and swelled in DCM (20 mL) for 1 h. The solvent was drained off and the resin was treated with calculated amount of acetic anhydride in 5% DIPEA /DCM solution for about 15 min then the solvent was drained off, resin was washed with DCM and DMF thoroughly to remove the traces of acetic anhydride and dried in vacuum desiccator. The dried resin was taken in to solid phase funnel and swelled in DCM for about 1h and functionalized with Boc protected  $\beta$ -allanine.

### **2.19.1 Picric acid assay for the estimation of the amino acid loading**

The functionalized dry resin (5 mg) was taken in a sintered funnel and swelled in  $\text{CH}_2\text{Cl}_2$  for 1 h. The solvent was drained off and the resin was treated with 50% TFA/DCM for 15 min (1 mL x 2) each time. The resin was thoroughly washed with  $\text{CH}_2\text{Cl}_2$  and the TFA salt was neutralized with 5% diisopropyl ethylamine for 2 min (1 mL x 3). The free amine was treated with picric acid 0.1 M in DCM (2 mL x 3) 3 min for each time. The resin was thoroughly washed with  $\text{CH}_2\text{Cl}_2$  to remove the unbound picric acid. The picrate bound to amino groups was eluted with 5% diisopropyl ethylamine in  $\text{CH}_2\text{Cl}_2$ , followed by washing with  $\text{CH}_2\text{Cl}_2$ . The eluant was collected into a 10 ml volumetric flask and made up to 10 ml using  $\text{CH}_2\text{Cl}_2$ . An aliquot (0.2 ml) of picrate eluant was diluted to 2 ml with ethanol and the optical density was measured at 358 nm, and the loading value of the resin (0.27 meq/g) was calculated using the molar extinction coefficient of picric acid as  $\epsilon_{358}=14,500 \text{ cm}^{-1} \text{ M}^{-1}$  at 358 nm.

### **2.20 Reference:**

1. Nielsen, P. E.; Egholm, M.; Berg, R. H.; Buchardt, O. Sequence-selective recognition of DNA by strand displacement with a thymine-substituted polyamide. *Science* **1991**, *254*, 1497.
2. Egholm, M.; Buchardt, O.; Christensen, L.; Behrens, C.; Freier, S. M.; Driver, D. A.; Berg, R.H.; Kim, S. K.; Nordon, B.; Nielsen, P. E. PNA hybridizes to complementary oligonucleotide obeying the Watson-Crick hydrogen-bonding rules. *Nature* **1993**, *365*, 566.
3. Jensen, K. K.; Qrum, H.; Nielsen, P. E.; Norden, B. Hybridization kinetics of peptide nucleic acids (PNA) with DNA and RNA studied with BIA core Technique. *Biochemistry* **1997**, *36*, 5072.

4. Demidov, V. V.; Potaman, V. N.; Frank-Kamenetskii, M. D.; Egholm, M.; Buchardt, O.; Sonnichsen, S. H.; Nielsen, P. E. Stability of peptide nucleic acids in human serum and cellular extracts. *Biochem. Pharmacol.* **1994**, *48*, 1310.
5. (a) Good, L.; Nielsen, P. E. Progress in developing PNA as gene targeted drugs. *Antisense Nucleic Acid Drug Dev.* **1997**, *7*, 431. (b) De Mesmaeker, A. et al: *Curr. Opin. Struct. Biol.* **1995**, *5*, 343. (c) Uhlmann, E.; Peyman, A.; Breipohl, G.; Will, D. W: PNA: Synthetic polyamide Nucleic Acids with Unusual Binding Properties. *Angew. Chem. Int. Ed.* **1998**, *37*, 2796.
6. Ganesh, K. N.; Nielsen, P. E. *Curr. Org. Chem.* **2000**, *4*, 931 and the references sited there in.
7. Kumar, V.A.; Ganesh, K. N. Conformationally Constrained PNA Analogues. *Acc. chem. research.* **2005**, *38*, 404.
8. Shirude, P. S.; Kumar, V. A.; Ganesh, K. N. Chimeric peptide nucleic acids incorporating (2S,5R)-aminoethyl pipercolyl units: synthesis and binding studies. *Tetrahedron Lett.* **2004**, *45*, 3085.
9. Lonkar, P. S.; Kumar, V. A. Design and synthesis of conformationally frozen peptide nucleic acid backbone: chiral piperidine PNA as a hexitol nucleic acid surrogate. *Bioorg. Med. Chem. Lett.* **2004**, *14*, 2147.
10. (a) M. D. Costa, V. A. Kumar, K. N. Ganesh. *Org. Lett.* **1999**, *1*, 1513. (b) M. D. Costa, V. A. Kumar, K. N. Ganesh, *Org. Lett.* **2001**, *3*, 1281.
11. Sharma, N.; Ganesh, K. N. Expanding the repertoire of pyrrolidyl PNA analogues for DNA/RNA hybridization selectivity: aminoethylpyrrolidinone PNA (aepone-PNA). *Chem. Commun.* **2003**, 2484.
12. (a)Gangamani, B. P.; Kumar, V. A.; Ganesh, K. N. Synthesis of NR (purinyl/pyrimidinyl acetyl)-4-aminoproline diastereomers with potential use in PNA synthesis. *Tetrahedron* **1996**, *52*, 15017. (b) Conformationally restrained chiral PNA conjugates: Synthesis and DNA complementation studies. *Nucleosides Nucleotides* **1999**, *18*, 1409-1011. (c) Gangamani, B. P.; Kumar, V. A.; Ganesh, K. Chiral analogues of peptide nucleic acids: Synthesis of 4-aminoprolyl nucleic acids and complementation studies using UV/CD spectroscopy. *Tetrahedron* **1999**, *55*,

177. (d) Meena; Kumar V. A. Pyrrolidine carbamate nucleic acids: Synthesis and DNA binding studies. *Bioorg. Med. Chem.* **2003**, *16*, 3393.
13. (a) Hickman, D. T.; King, P. M.; Cooper, M. A.; Slater, J. M.; Mickelfield, J. Unusual RNA and DNA binding properties of a novel pyrrolidine-amide oligonucleotide mimic (POM). *Chem. Commun.* **2000**, 2251. (b) Kumar, V. A.; Pallan, P. S.; Meena.; Ganesh, K. N. Pyrrolidine nucleic acids: DNA/PNA oligomers with 2-hydroxy/aminomethyl-4-(thymine-1-yl)pyrrolidine-N-acetic acid. *Org. Lett.* **2001**, *3*, 1269. (c) Kumar, V. A.; Meena Pyrrolidine PNA-DNA chimeric ligonucleotides with extended backbone. *Nucleosides Nucleotides Nucleic acids* **2003**, *22*, 1101. (d) D'Costa, M.; Kumar, V. A.; Ganesh, K. N. Synthesis of 4(S)-(NBoc-amino)-2(S/R)-(thymine-1-yl)-pyrrolidine-N-1-acetic acid: a novel cyclic PNA with constrained flexibility. *Tetrahedron. Lett.* **2002**, *43*, 883.
14. (a) Govindaraju, T.; Kumar, V. A.; Ganesh, K. N. (1S,2R/1R,2S)-ciscyclopentylPNA (cpPNA) as constrained PNA analogues: Synthesis and evaluation of *aeg-cp* PNA chimera and stereopreferences in hybridization with DNA/RNA. *J. Org. Chem.* **2004**, *69*, 5725. (b) Govindaraju, T.; Kumar, V. A.; Ganesh, K. N. cis-Cyclopentyl PNA (*cp*-PNA) as constrained chiral PNA analogues: stereochemical dependence of DNA/RNA hybridization. *Chem. Commun.* **2004**, 860. (c) Myers, M. C.; Witschi, M. A.; Larinova, N. V.; Franck, J. M.; Haynes, R. D.; Hara, T.; Grakowski A.; Appella, D. H. A cyclopentane conformational restraint for a peptide nucleic acid: Design, synthesis and improved binding affinity to DNA and RNA. *Org. Lett.* **2003**, *5*, 2695.
15. (a) Lagriffoule, P.; Wittung, P.; Eriksson, M.; Jensen, K. K.; Norden, B.; Buchardt, O.; Nielsen, P. E. Peptide nucleic acids (PNAs) with conformationally constrained, Chiral cyclohexyl derived backbone. *Chem. Eur. J.* **1997**, *3*, 912. (b) govindaraju, T.; Gonnade, R.; Badbhade, M.; Kumar V. A.; Ganesh, K. N. (1S,2R/1R,2S)-aminocyclohexyl glycylyl thymine PNA: Synthesis, monomer crystal structures and DNA/RNA hybridization studies. *Org. Lett.* **2003**, *5*, 3013. (c) Govindaraju, T.; Kumar, V. A.; Ganesh, K. N. Synthesis and evaluation of (1S,2R/1R,2S) aminocyclohexylglycylyl PNAs as conformationally preorganized PNA analogues for DNA/RNA recognition. *J. Org. Chem.* **2004**, *69*, 1858.

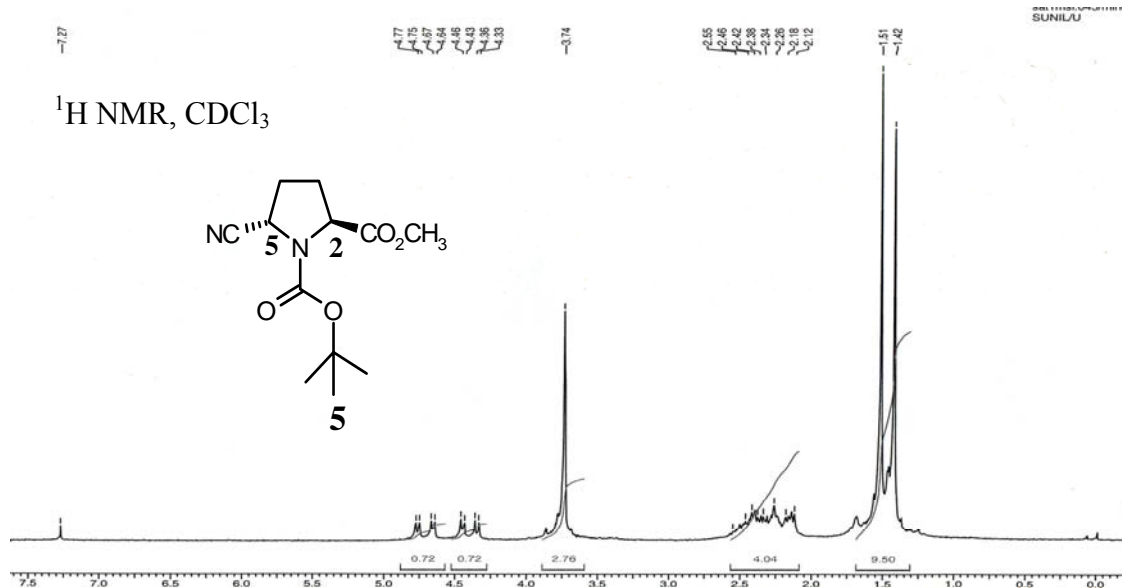
16. P. S. Lonkar, V. A. Kumar, K. N. Ganesh, *Nucleosides, Nucleotides Nucleic Acids* **2001**, *20*, 1197.
17. Shono, T. Electroorganic chemistry in organic synthesis. *Tetrahedron* **1984**, *40*, 811.
18. Shono, T.; Hamaguchi, H.; Matsumura. Electroorganic chemistry. XX. Anodic oxidation of carbamates. *J. Am. Chem. Soc.* **1975**, *97*, 4264.
19. (a) Arndt, H. A.; Polborn, K.; Koert, U. Stereoselective synthesis of a terpyrrolidine unit, a potential building block for anion recognition *Tetrahedron Lett.* **1997**, *38*, 3879. (b) Sunil, K. G.; Nagamani, D.; Argade, N. P.; Ganesh, K. N. Synthesis of Marine Natural Product (2*S*,5*S*)-Pyrrolidine-2,5-dicarboxylic Acid. *Synthesis* **2003**, *15*, 2304.
20. Haasnoot, C. A. G.; De leeuw, A. A. M.; De leeuw, H. P. M.; Altona, C. *Biopolymers* **1981**, *20*, 1211.
21. Eberhardt, E. S.; panasik, N. jr.; Raines, R. T. Inductive Effects on the Energetics of Prolyl Peptide Bond Isomerization: Implications for Collagen Folding and Stability *J. Am. chem. Soc.* **1996**, *118*, 12261.
22. Bretscher, L. E.; Jenkins, C. L.; Taylor, K. M.; DeRider, M. L.; Raines, R.T. Conformational Stability of Collagen Relies on a Stereoelectronic Effect *J. Am. Chem. Soc.* **2001**, *123*, 777.
23. (a) Wolfe, S. *Acc. Chem. Res.* **1972**, *5*, 102. (b) Brunck, T. K.; Weinhold, F. *J. Am. Chem. Soc.* **1979**, *101*, 1700.
24. Parker, D.; Senanayake, K.; Vepsäläinen, J.; Williams, S.; Batsanov A. S.; Howard, A. K. *J. Chem. Soc. Perkin Trans. 2*, 1997, *8*, 1445.
25. Wiberg, K. B. Bent Bonds in Organic Compounds *Acc. Chem. Res.* **1996**, *29*, 229.
26. Barrett, A. G. M.; Pilipaukas, D. *J. Org. Chem.* **1991**, *55*, 5194. (a) Thaning, M.; Wistrand, L. G. *Helv. chim. Acta* **1986**, *69*, 1711.
27. Egholm, M.; Buchardt, O.; Nielsen, P. E. Peptide nucleic acids (PNA). Oligonucleotide analogs with an achiral peptide backbone. *J. Am. Chem. Soc.* **1992**, *114*, 1895.
28. Egholm, M.; Nielsen, P. E.; Buchardt, O. Berg, R. H. Recognition of guanine and adenine in DNA by cytosine and thymine containing peptide nucleic acids (PNA). *Am. Chem. Soc.* **1992**, *114*, 9677.

29. Dueholm, K. L.; Egholm, M.; Behrens, C.; Christensen, L.; Hansen, H. F.; Vulpius, T.; Petersen, K. H.; Berg, R. H.; Nielsen, P. E.; Buchardt, O. Synthesis of Peptide Nucleic Acid Monomers Containing the Four Natural Nucleobases: Thymine, Cytosine, Adenine, and Guanine and Their Oligomerization. *J. Org. Chem.* **1994**, *59*, 5767.
30. (a) Richter, L. S.; Zuckermann, R. N. *Bioorg. Med. Chem. Lett.* **1995**, *5*, 1159.  
(b) Merrifield, B. Solid Phase Peptide Synthesis. I. The Synthesis of a Tetrapeptide *J. Am. Chem. Soc.* **1963**, *85*, 2149.
31. Christensen, L.; Fitzpatrick, R.; Gildea, B.; Petersen, K.; Hansen, H. F.; Koch, C.; Egholm, M.; Buchardt, O.; Nielsen, P. E.; Coull, J.; Berg, R. H. *J. Peptide Sci.* **1995**, *3*, 175.
32. Erickson, B. W.; Merrifield, R. B. *Solid Phase Peptide Synthesis In The Proteins* Vol. II, 3<sup>rd</sup> Ed. H. Neurath and R. L. Hill, eds. Academic Press, New York, **1976**, pp 255.
33. Merrifield, R. B.; Stewart, J. M.; Jernberg, N. *Anal. Chem.* **1966**, *38*, 1905.
34. (a) Kaiser, E.; Colescott, R. L.; Bossinger, C. D.; Cook, P. I. *Anal. Biochem.* **1970**, *34*, 595. (b) Kaiser, E.; Bossinger, C. D.; Colescott, R. L.; Olsen, D. B. *Anal. Chim. Acta.* **1980**, *118*, 149. (c) Sarin, V. K.; Kent, S. B. H.; Tam, J. P.; Merrifield, R. B. *Anal. Biochem.* **1981**, *117*, 147.
35. Christensen, T. *Acta, chem. Scand.* **1979**, *34*, 594.
36. Madder, A.; Farcy, N.; Hosten, N. G. C.; De Muynck, H.; De Clereq, P.; Barry, J.; Davis, A.P. A Novel Sensitive Colorimetric Assay for Visual Detection of Solid-Phase Bound Amines *Eur. J. Org. Chem.* **1999**, *11*, 2787.
37. Christensen, L.; Fitzpatrick, R.; Gildea, B.; Petersen, K. H.; Hansen, H. F.; Koch, T.; Egholm, M.; Buchardt, O.; Nielsen, P. E.; Coull, J.; Berg, R. H. *J. Peptide Sci.* **1995**, *3*, 175.
38. (a) Butler, J. M.; Jiang-Baucom, P.; Huang, M.; Belgrader, P.; Girard, J. Peptidenucleic Acid Characterization by MALDI-TOF Mass Spectrometry. *Analytical Chemistry* **1996**, *68*: 3283. (b) Ross, P. L.; Lee, K.; Belgrader, P. Discrimination of Single-Nucleotide Polymorphisms in Human DNA using Peptide Nucleic Acid Probes detected by MALDI-TOF mass spectrometry. *Analytical Chemistry* **1997**, *69*, 4197. Jiang-Baucom P, Girard JE: DNA typing of Human

Leukocyte Antigen sequence Polymorphisms by Peptide Nucleic Acid Probes and MALDI-TOF mass Spectrometry. *Analytical Chemistry* **1997**, *69*: 4894.

## 2.21 Appendix

<b>Entry</b>	<b>Details</b>	<b>Page Number</b>
<b>1</b>	Compound <b>5</b> ; $^1\text{H}$ NMR and Mass spectra	<b>135</b>
<b>2</b>	Compound <b>5</b> ; $^{13}\text{C}$ and DEPT spectra	<b>136</b>
<b>3</b>	Compound <b>6</b> ; $^1\text{H}$ NMR and Mass spectra	<b>137</b>
<b>4</b>	Compound <b>6</b> ; $^{13}\text{C}$ and DEPT spectra	<b>138</b>
<b>5</b>	Compound <b>9</b> ; $^1\text{H}$ NMR and Mass spectra	<b>139</b>
<b>6</b>	Compound <b>9</b> ; $^{13}\text{C}$ and DEPT spectra	<b>140</b>
<b>7</b>	Compound <b>10</b> ; $^1\text{H}$ NMR and Mass spectra	<b>141</b>
<b>8</b>	Compound <b>10</b> ; $^{13}\text{C}$ and DEPT spectra	<b>142</b>
<b>9</b>	Compound <b>13</b> ; $^1\text{H}$ NMR and Mass spectra	<b>143</b>
<b>10</b>	Compound <b>13</b> ; $^{13}\text{C}$ and DEPT spectra of	<b>144</b>
<b>11</b>	Compound <b>18</b> ; $^1\text{H}$ NMR and Mass spectra	<b>145</b>
<b>12</b>	Compound <b>18</b> ; $^1\text{H}$ NMR and Mass spectra	<b>146</b>
<b>13</b>	Compound <b>19</b> ; $^1\text{H}$ NMR and Mass spectra	<b>147</b>
<b>14</b>	Compound <b>19</b> ; $^{13}\text{C}$ and DEPT spectra	<b>148</b>
<b>15</b>	Compound <b>22</b> ; $^1\text{H}$ NMR and Mass spectra	<b>149</b>
<b>16</b>	Compound <b>22</b> ; $^{13}\text{C}$ and DEPT spectra	<b>150</b>
<b>17</b>	Compound <b>23</b> ; $^1\text{H}$ NMR and Mass spectra	<b>151</b>
<b>18</b>	Compound <b>23</b> ; $^{13}\text{C}$ and DEPT spectra	<b>152</b>
<b>19</b>	Compound <b>26</b> ; $^1\text{H}$ NMR and Mass spectra	<b>153</b>
<b>20</b>	Compound <b>26</b> ; $^{13}\text{C}$ and DEPT spectra	<b>154</b>
<b>21</b>	Compound <b>27</b> ; $^1\text{H}$ NMR and Mass spectra	<b>155</b>
<b>22</b>	Compound <b>27</b> ; $^{13}\text{C}$ and DEPT spectra	<b>156</b>
<b>23</b>	Compound <b>34</b> ; $^1\text{H}$ NMR and Mass spectra	<b>157</b>
<b>24</b>	Compound <b>34</b> ; $^{13}\text{C}$ NMR and DEPT spectra	<b>158</b>
<b>25</b>	Compound <b>35</b> ; $^1\text{H}$ NMR and Mass spectra	<b>159</b>
<b>26</b>	Compound <b>35</b> ; $^{13}\text{C}$ and DEPT spectra	<b>160</b>
<b>27</b>	Compound <b>49</b> and <b>53</b> ; $^1\text{H}$ NMR and spectra	<b>161</b>
<b>28</b>	HPLC-Profiles of <i>amp</i> -PNAs	<b>163-167</b>
<b>29</b>	MALDI-TOF spectra of <i>amp/aeg</i> PNA oligomers	<b>168-172</b>



QSTAR MultiView 1.5.0  
 Thursday, September 29, 2005 4:40 PM  
 page 1 of 1  
 Cyano upper (No Title)  
 Period 1, Expt. 1; Mass range: 50.0 to 650.0 by 0.0 amu; Dwell: 1.0 ms; Pause: 5.0 ms  
 Acq. Time: Thu, Sep 29, 2005 at 10:37:14 AM

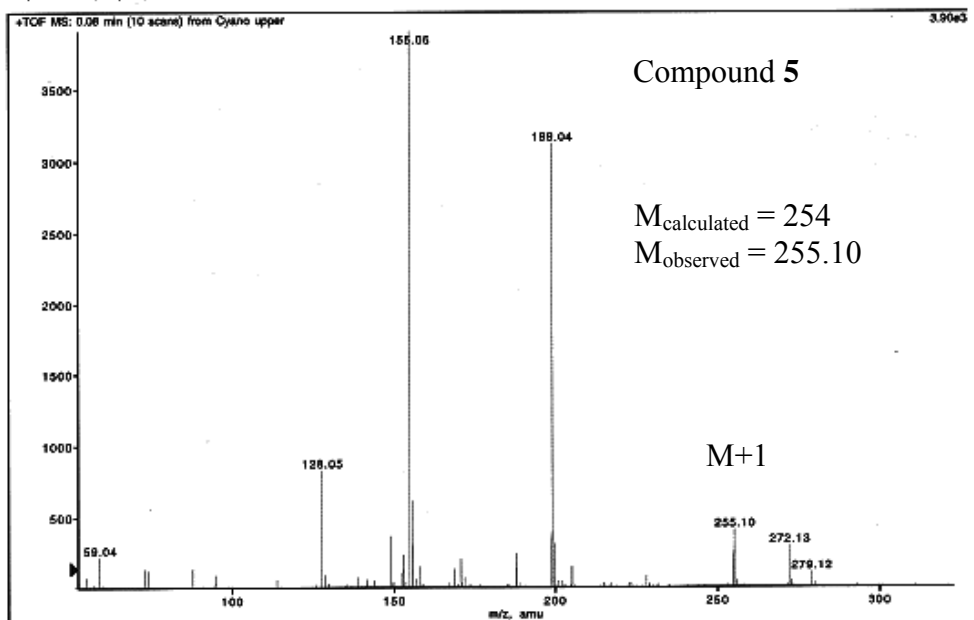
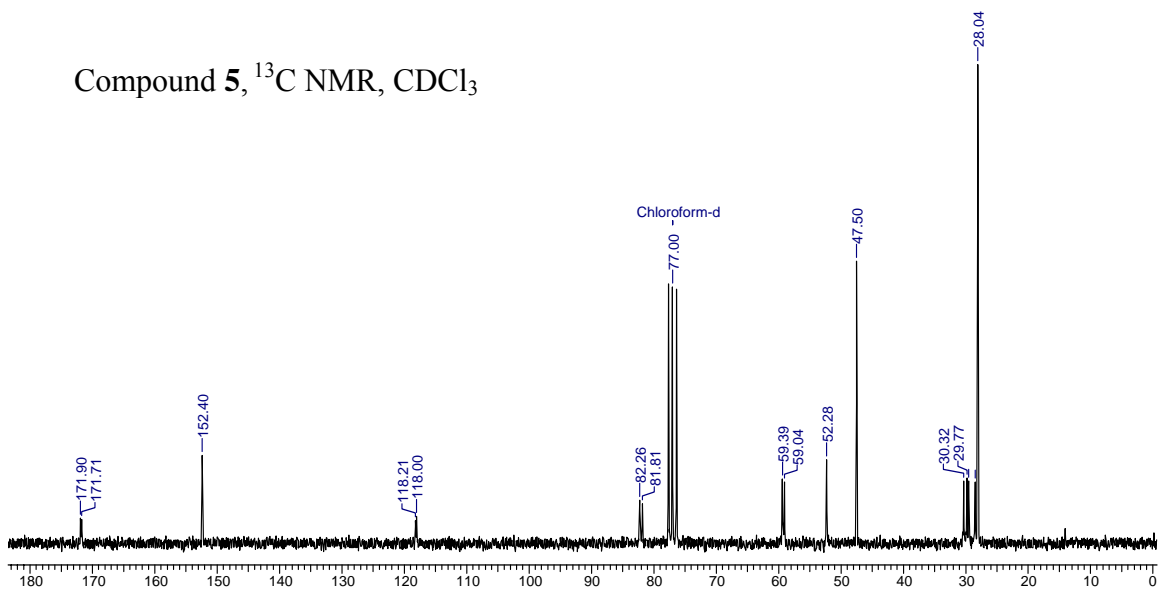
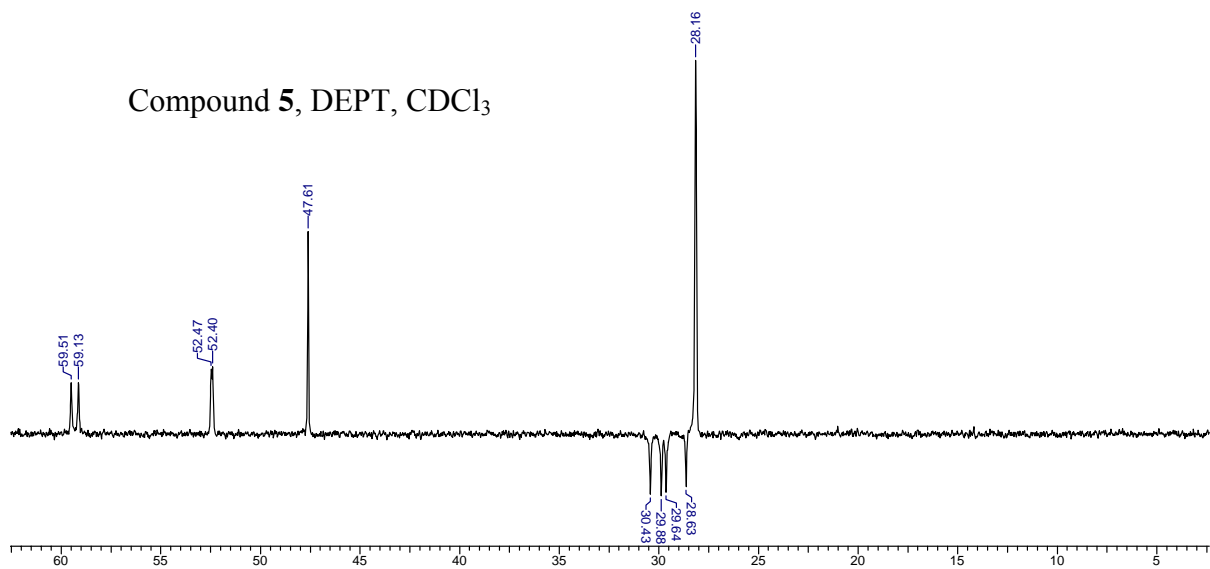


Figure 10 <sup>1</sup>H NMR and Mass spectra of compound 5

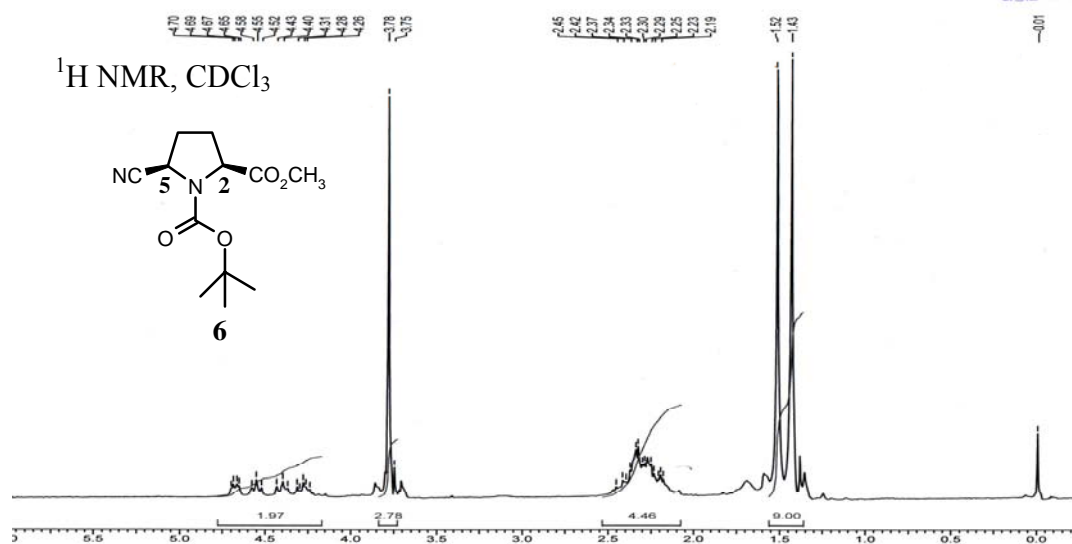
Compound **5**,  $^{13}\text{C}$  NMR,  $\text{CDCl}_3$



Compound **5**, DEPT,  $\text{CDCl}_3$



**Figure 11**  $^{13}\text{C}$  and DEPT spectra of compound **5**



QSTARMultiView 1.5.0  
 L-CYNO-CIS (No Title)  
 Thursday, March 16, 2006 10:27 AM  
 Period 1, Expt. 1; Mass range: 100.0 to 600.0 by 0.0 amu; Dwell: 1.0 ms; Pause: 5.0 ms  
 Acq. Time: Tue, Mar 14, 2006 at 12:08:07 PM

page 1 of 1

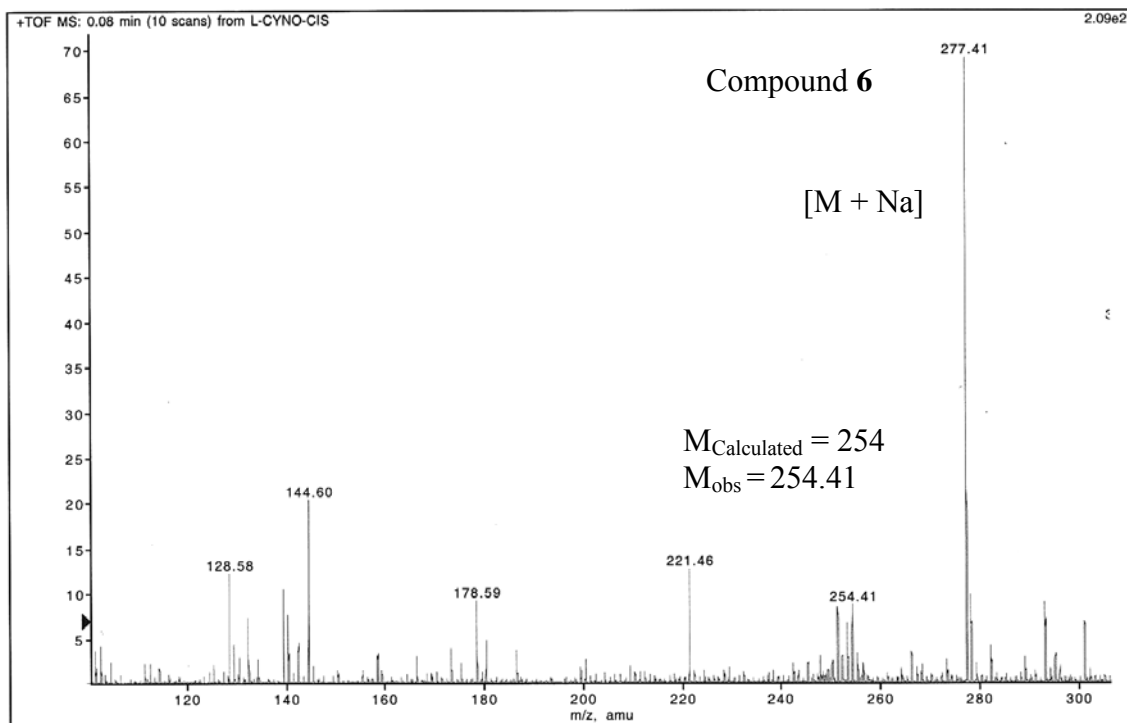
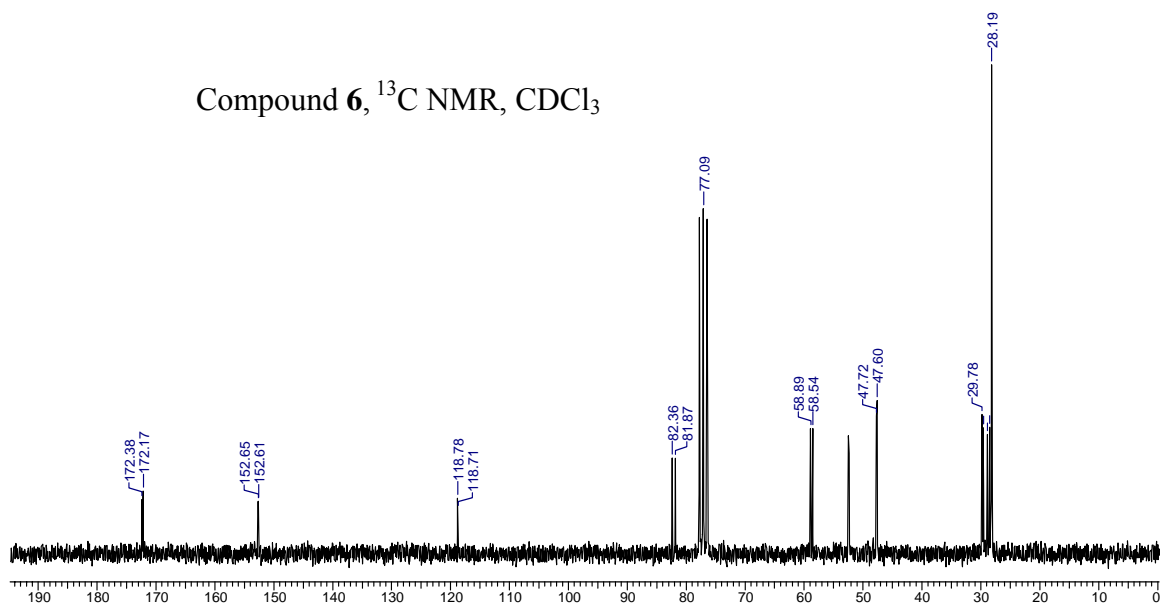


**Figure 12** <sup>1</sup>H NMR and Mass spectra of compound 6

Compound **6**,  $^{13}\text{C}$  NMR,  $\text{CDCl}_3$



Compound **6**, DEPT,  $\text{CDCl}_3$

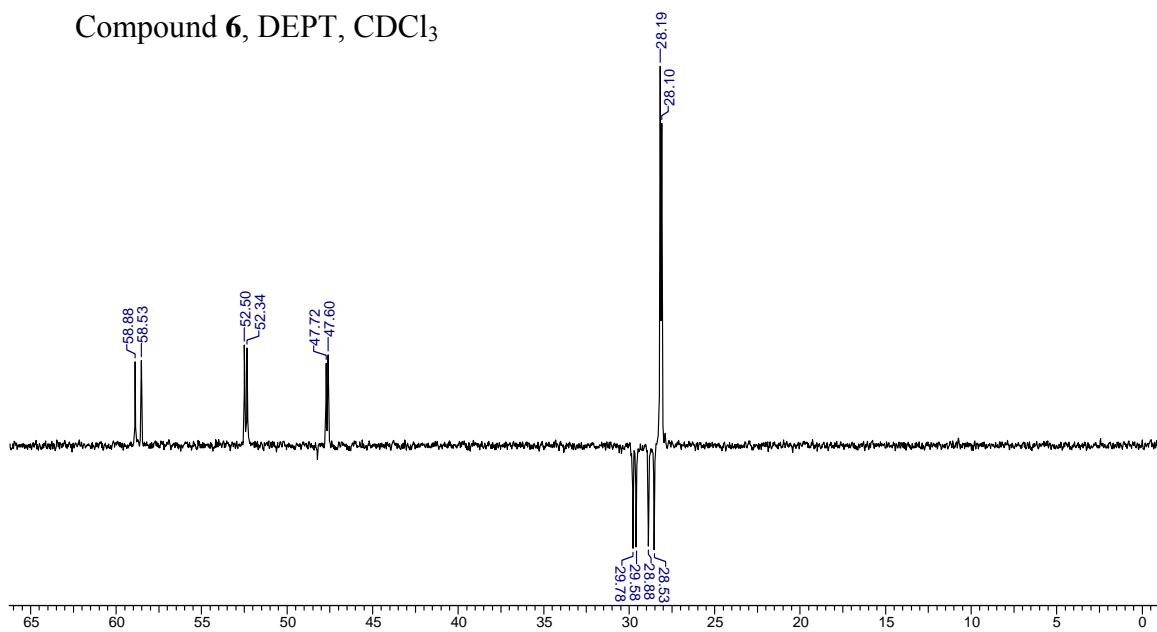
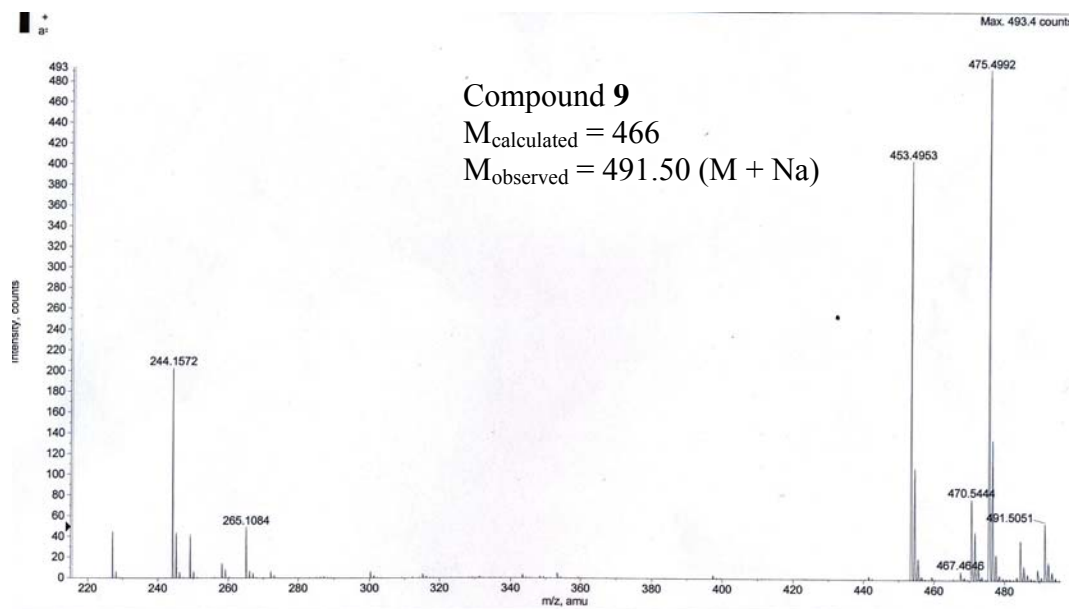
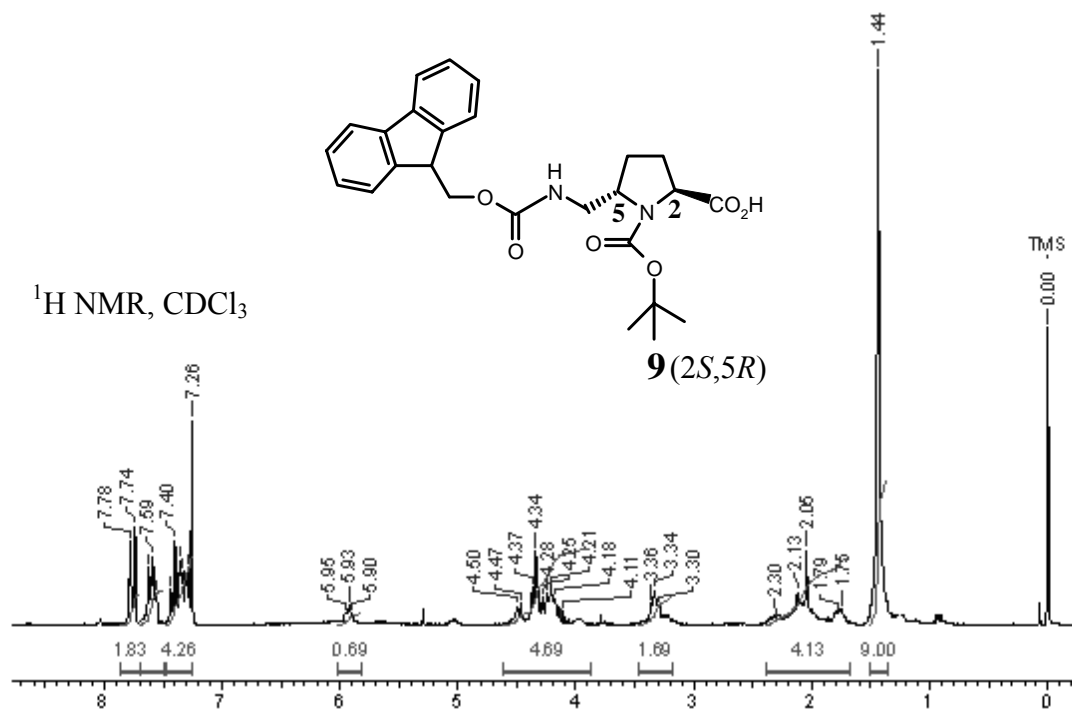
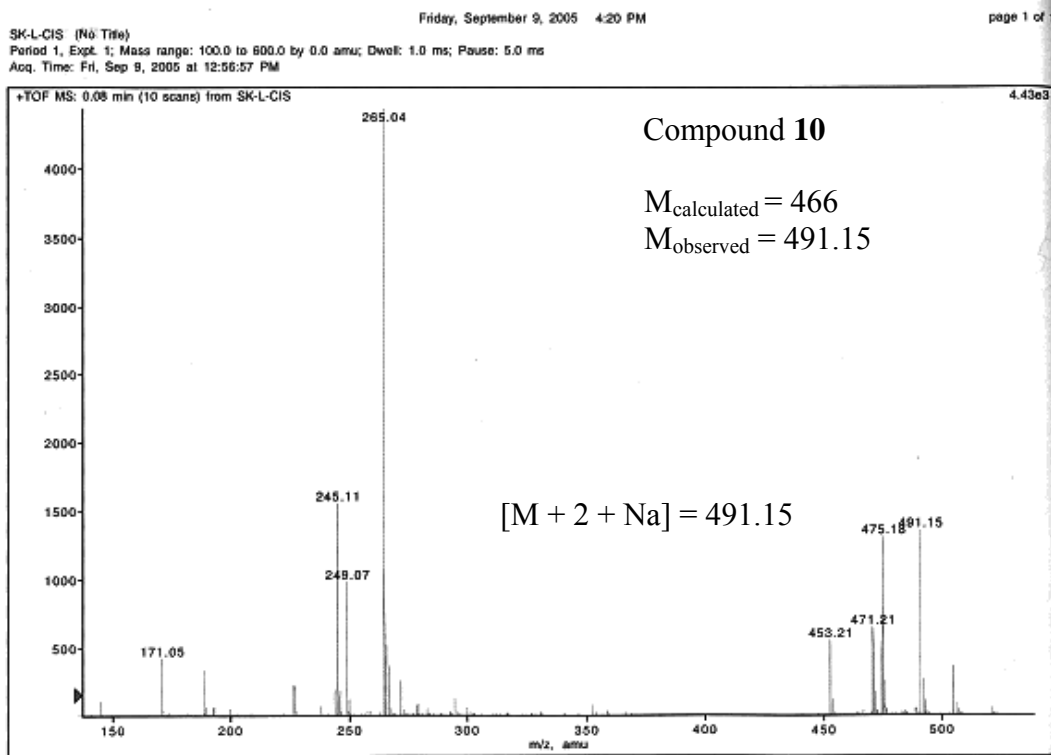
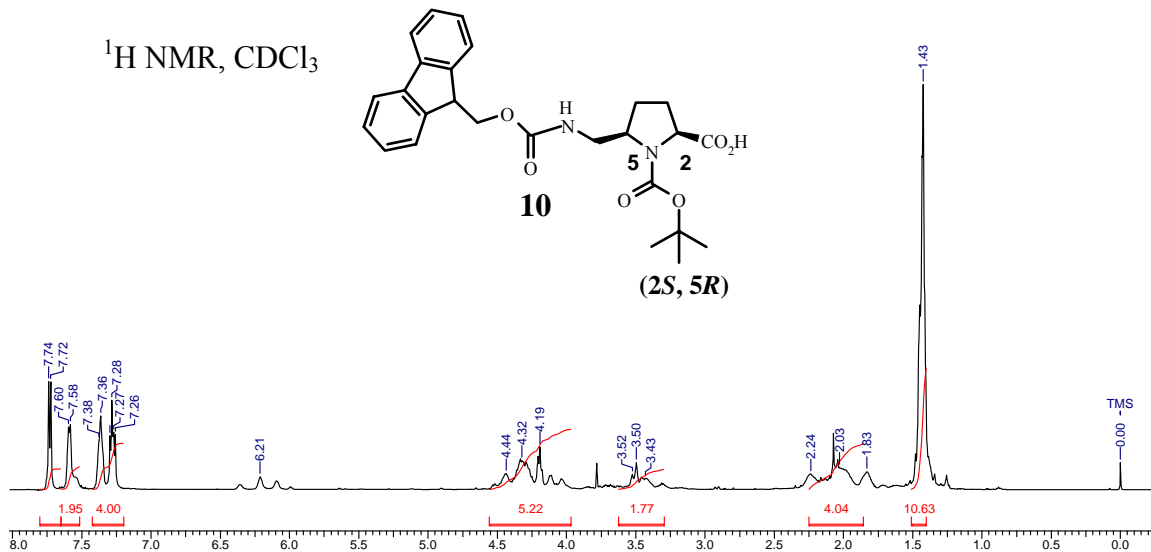


Figure 13  $^{13}\text{C}$  and DEPT spectra of compound **6**



**Figure 14** <sup>1</sup>H NMR and Mass spectra of compound **9**





**Figure 16** <sup>1</sup>H NMR and Mass spectra of compound **10**

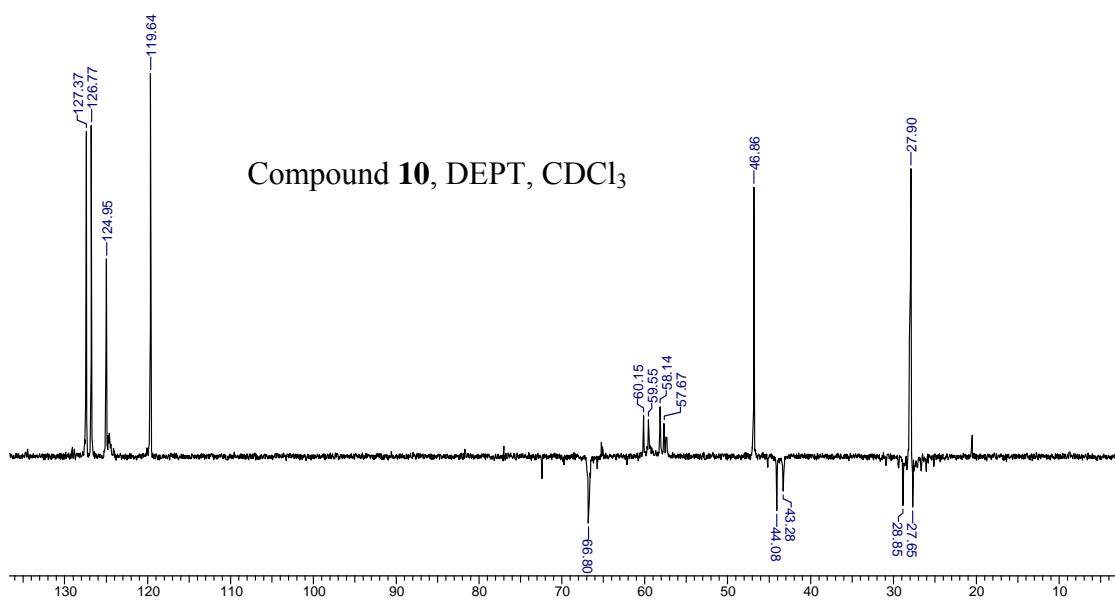
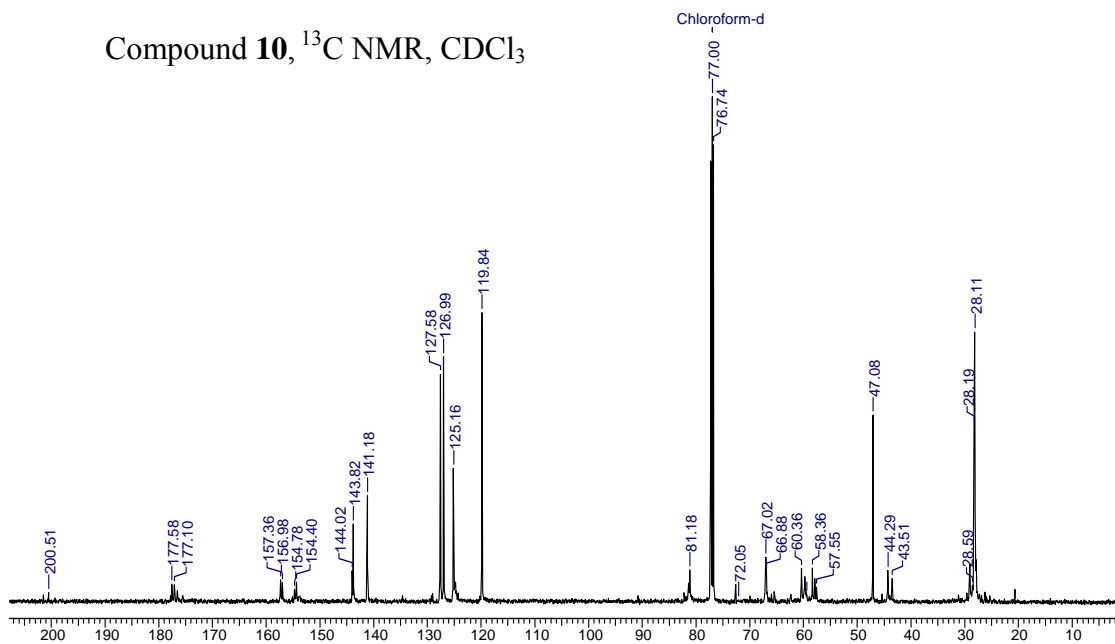
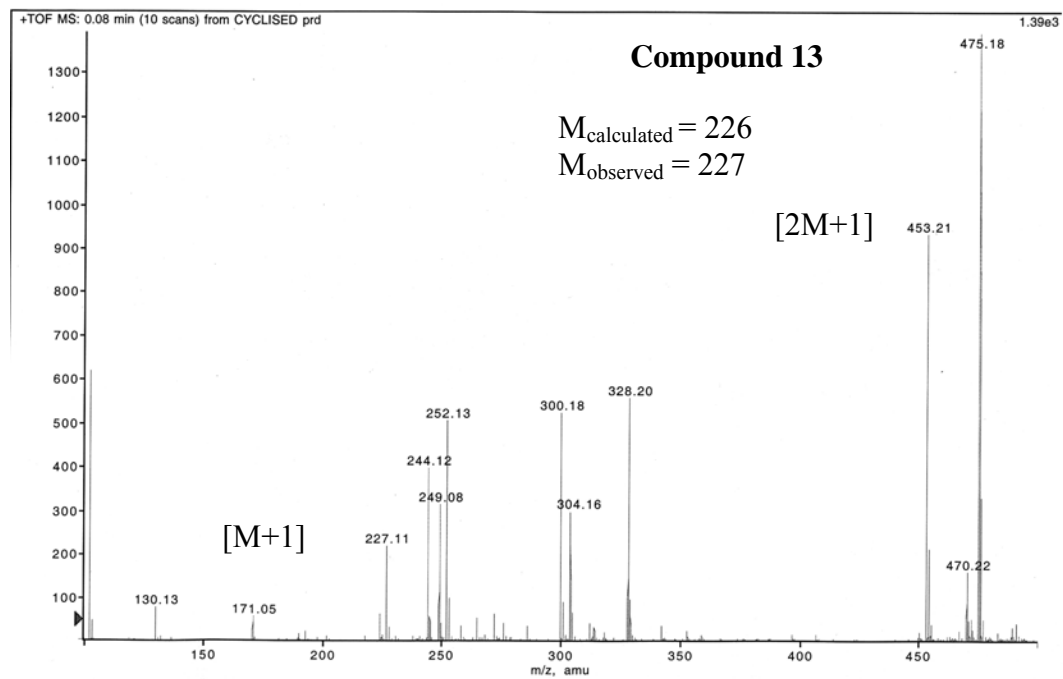
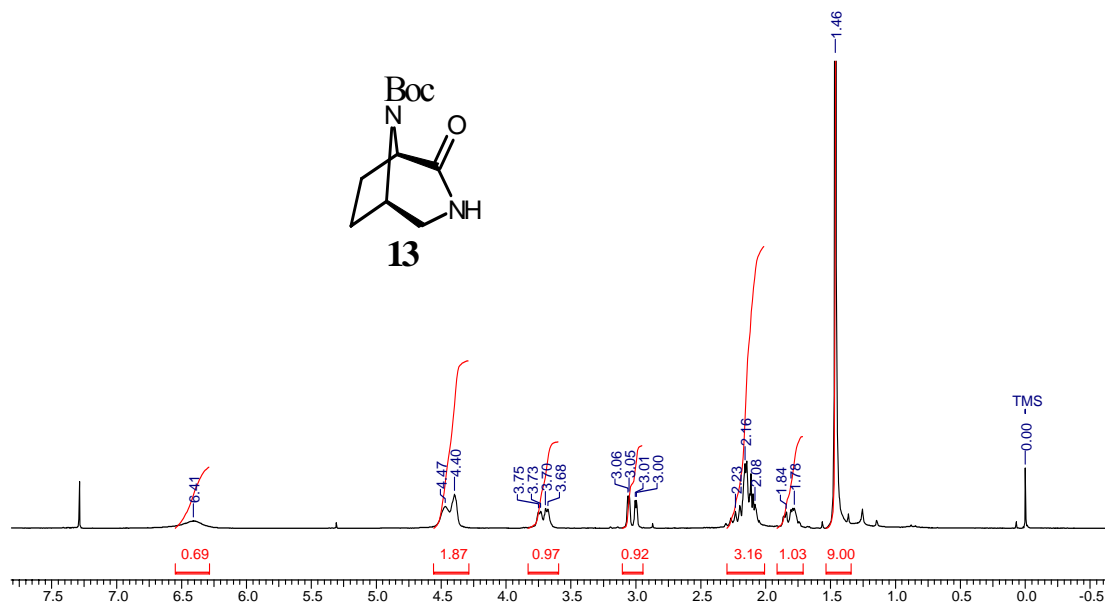
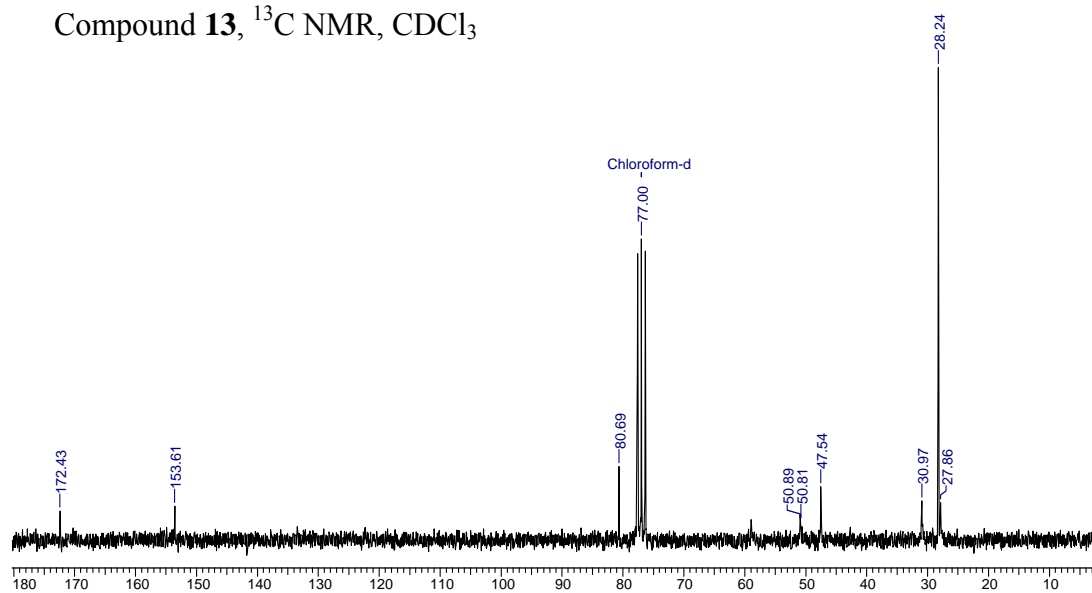


Figure 17  $^{13}\text{C}$  and DEPT spectra of compound **10**



**Figure 18**  $^1\text{H}$  NMR and Mass spectra of compound **13**

Compound **13**,  $^{13}\text{C}$  NMR,  $\text{CDCl}_3$



Compound **13**, DEPT,  $\text{CDCl}_3$

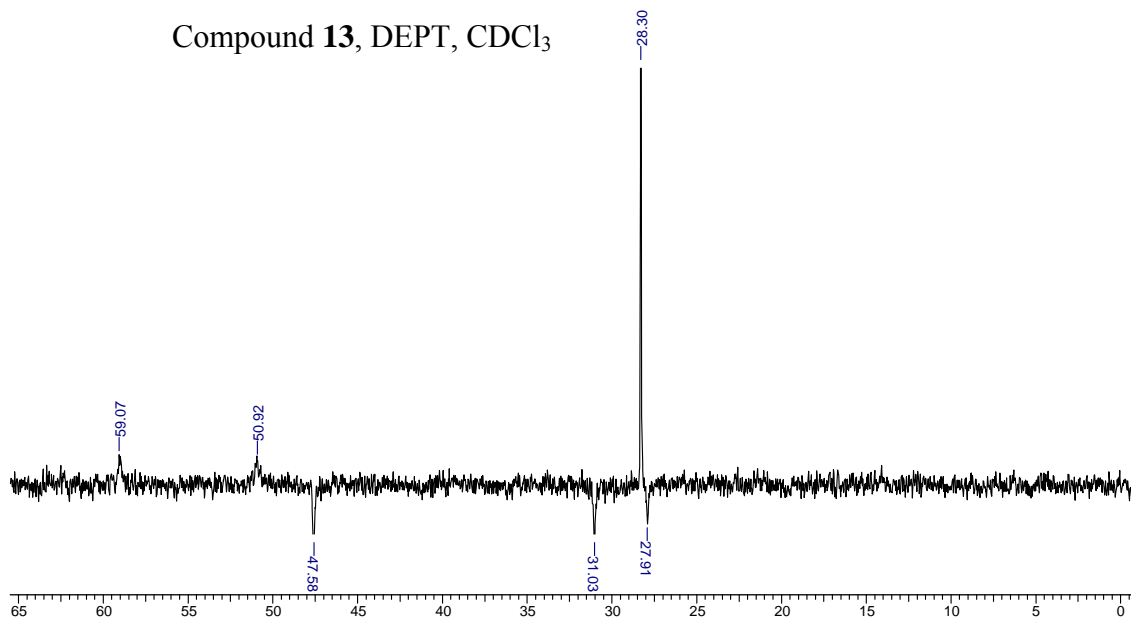
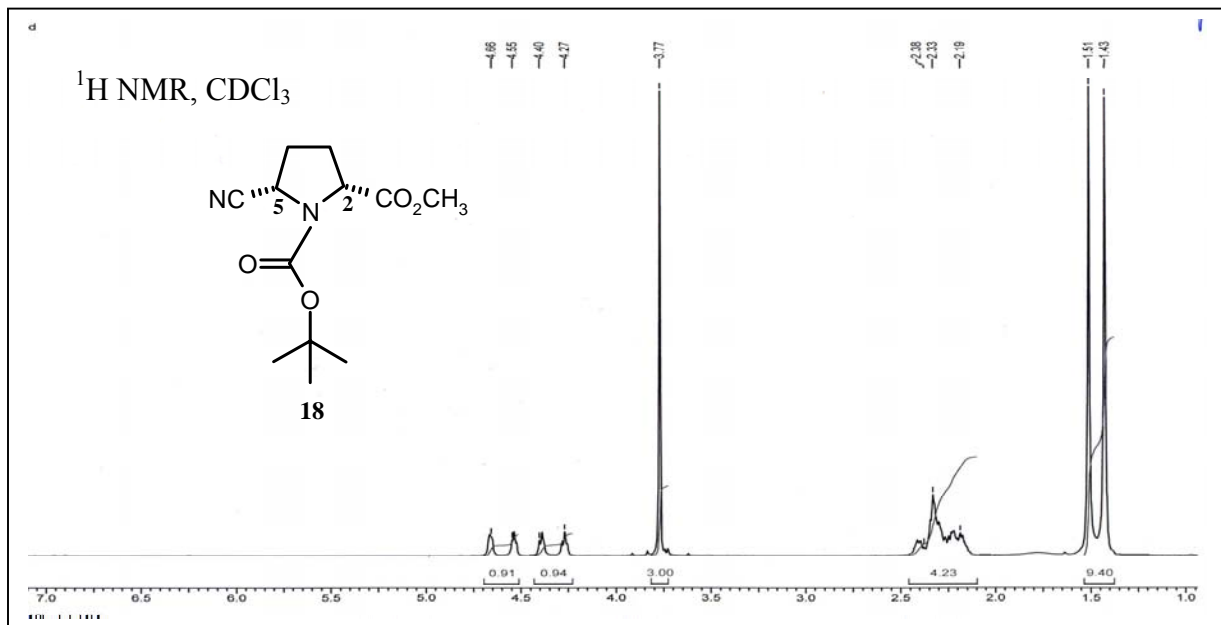


**Figure 19**  $^{13}\text{C}$  and DEPT spectra of compound **13**



QSTARMultiView 1.5.0  
 D-CYNO-CIS (No Title)  
 Period 1, Expt. 1; Mass range: 100.0 to 600.0 by 0.0 amu; Dwell: 1.0 ms; Pause: 5.0 ms  
 Acq. Time: Tue, Mar 14, 2006 at 12:18:17 PM

Thursday, March 16, 2006 10:30 AM

page 1 of 1

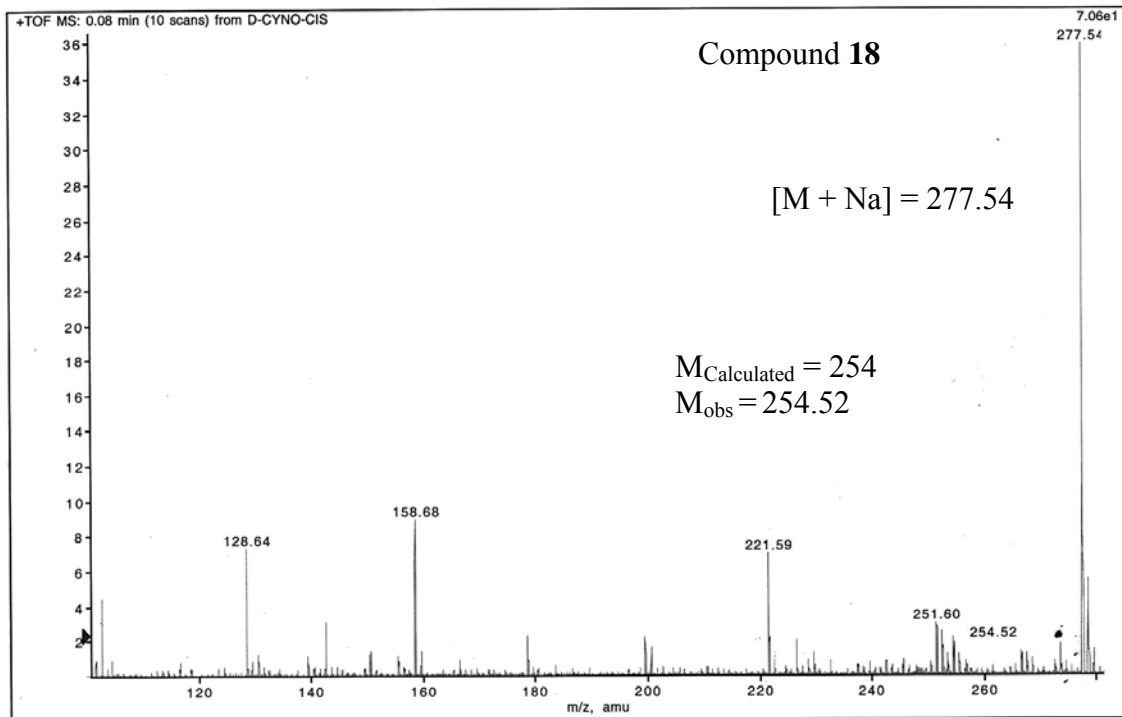


**Figure 20** <sup>1</sup>H NMR and Mass spectra of compound **18**

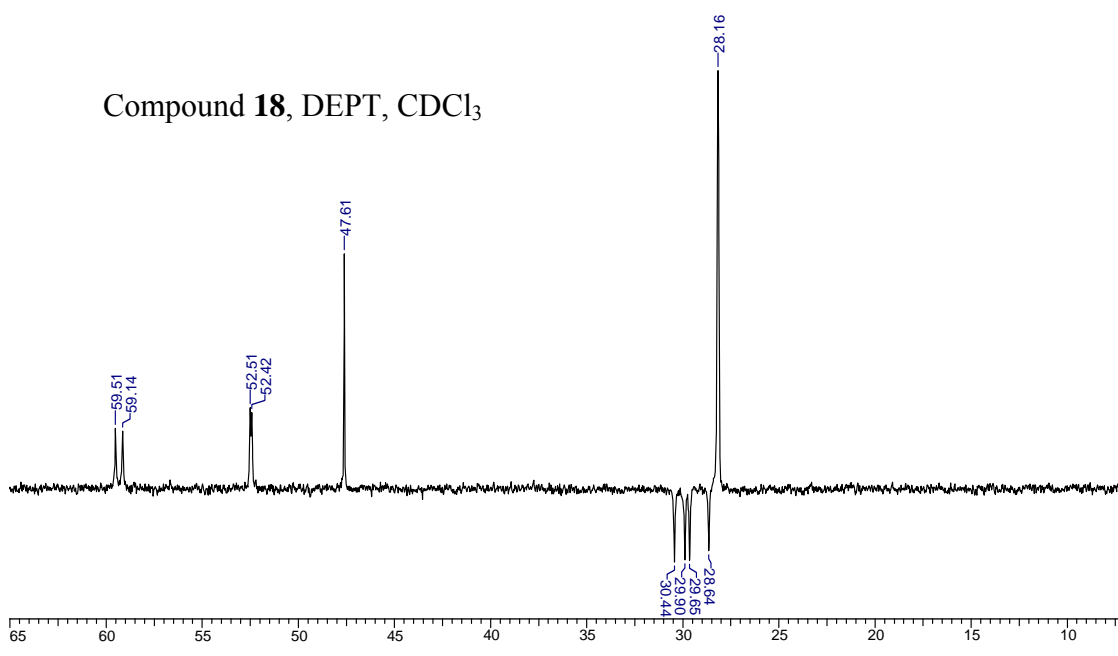
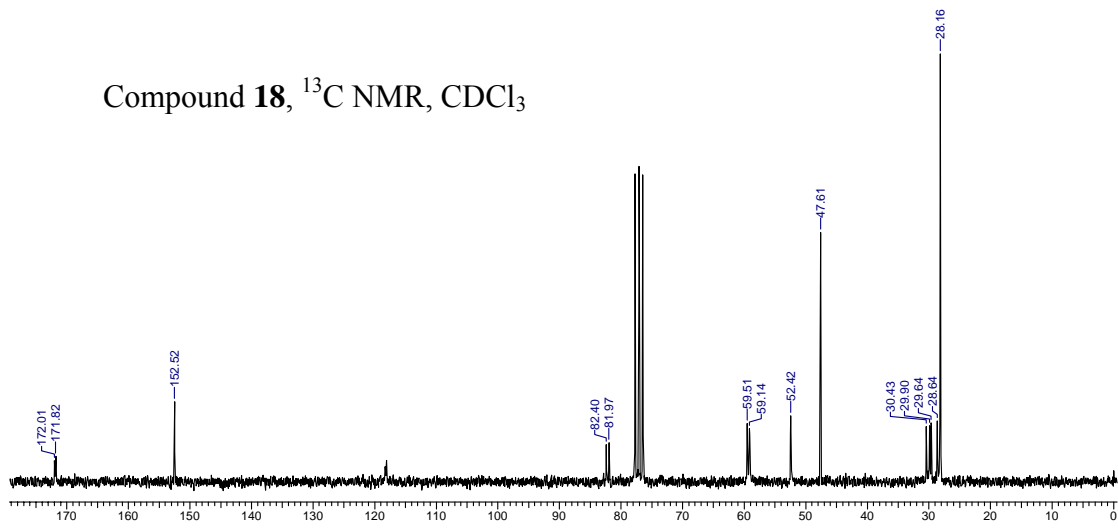
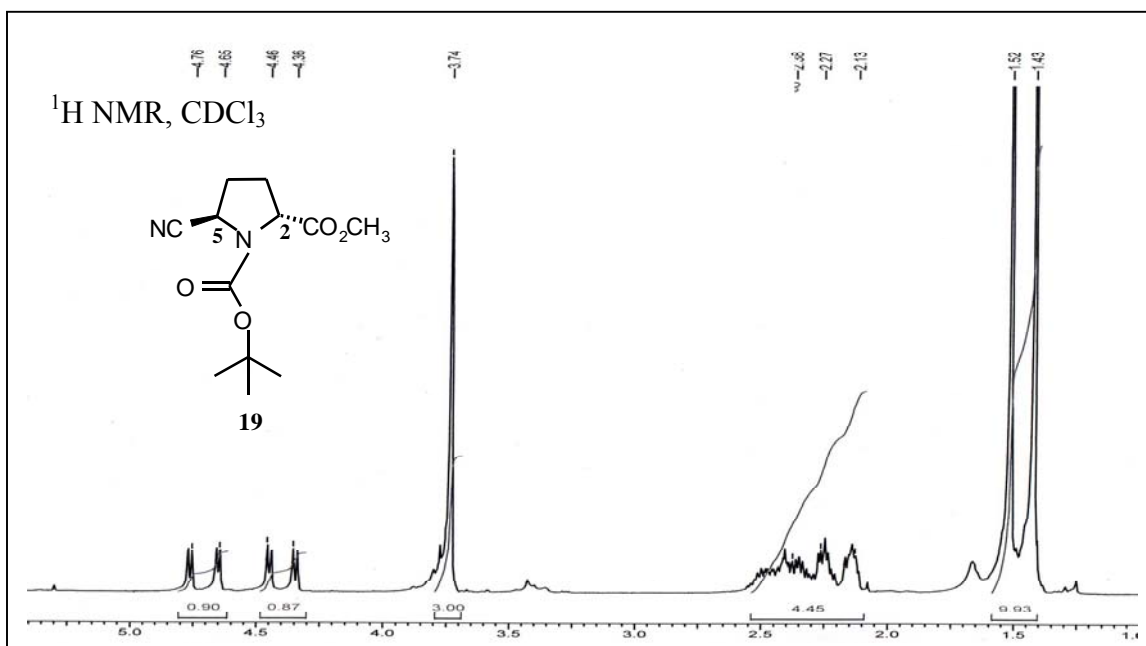
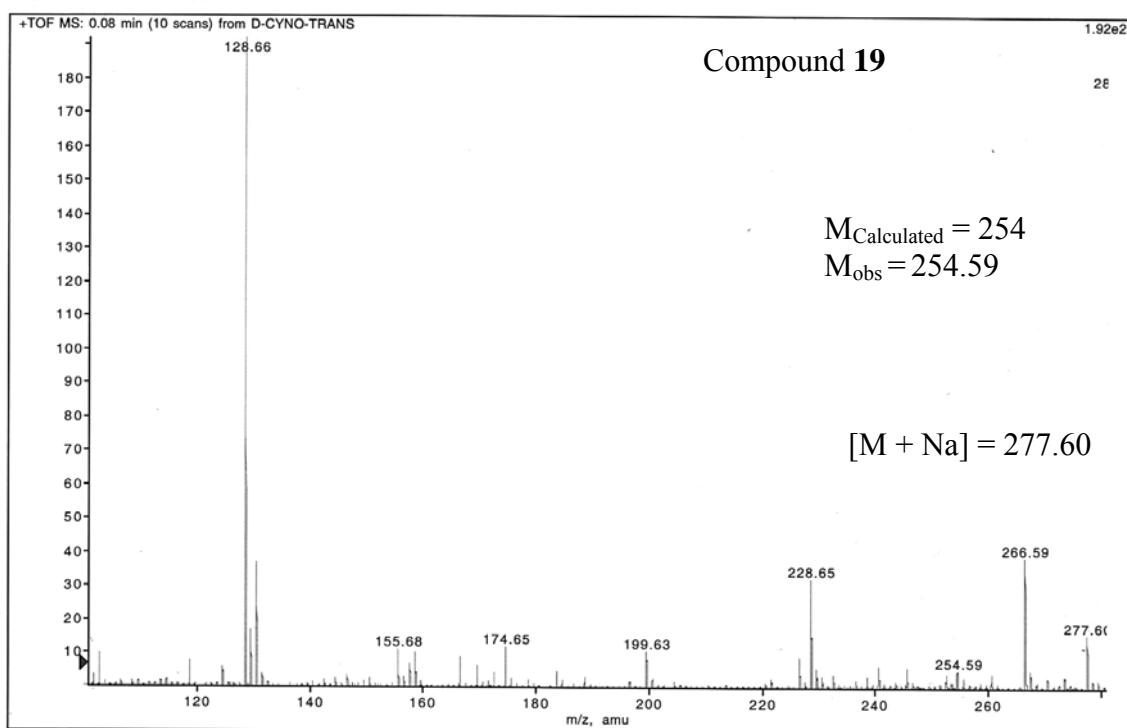


Figure 21  $^{13}\text{C}$  and DEPT spectra of compound **18**

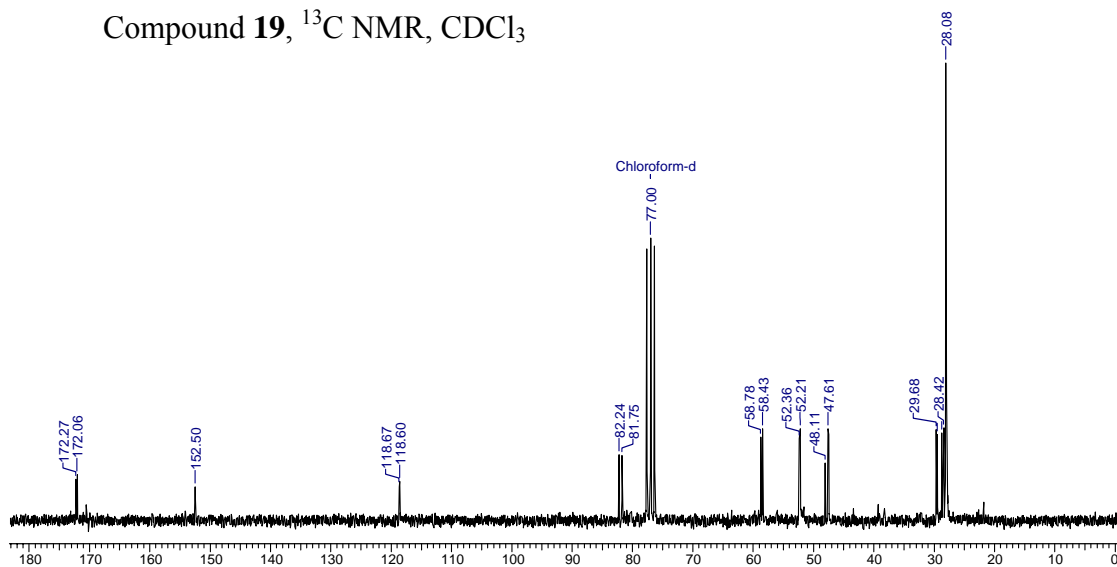


page 1 of 1



**Figure 22** <sup>1</sup>H NMR and Mass spectra of compound **19**

Compound **19**,  $^{13}\text{C}$  NMR,  $\text{CDCl}_3$



Compound **19**, DEPT,  $\text{CDCl}_3$

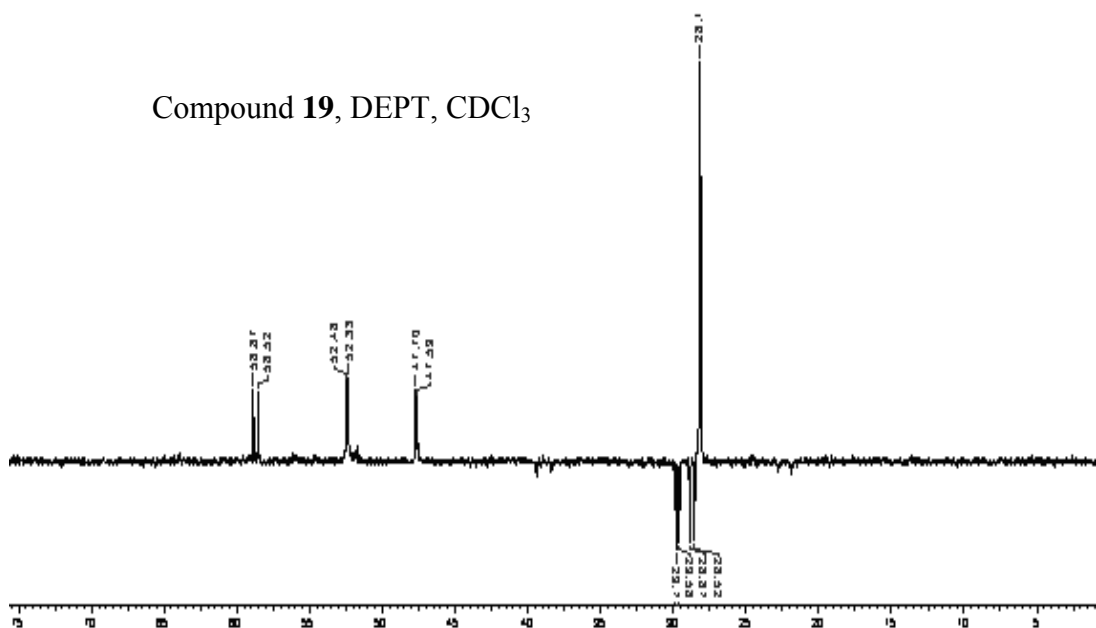
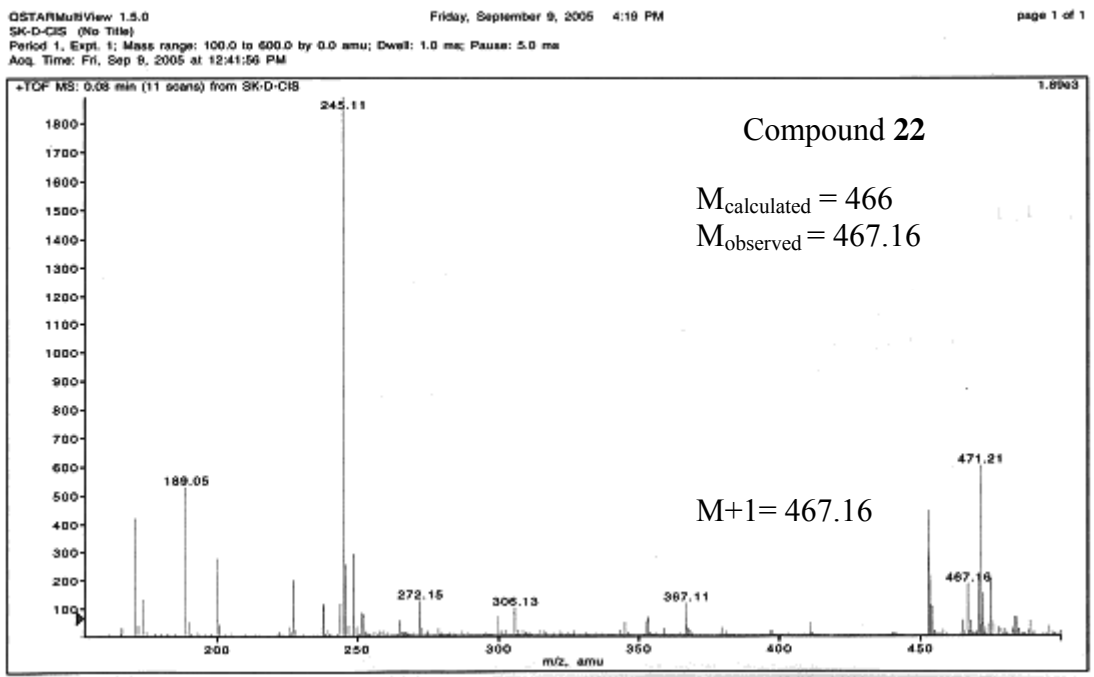
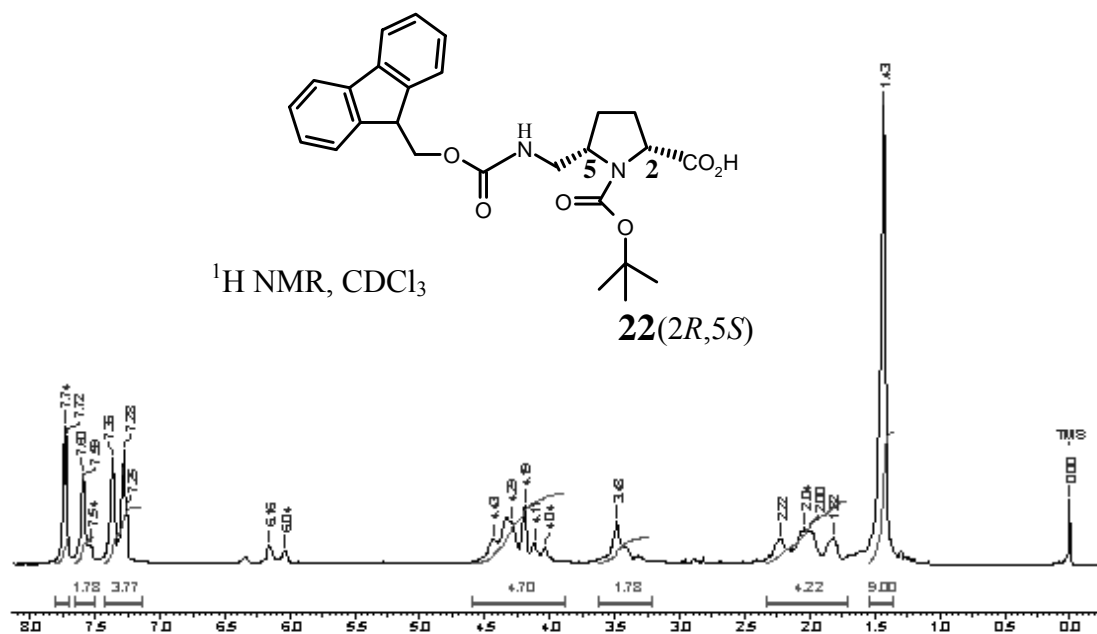
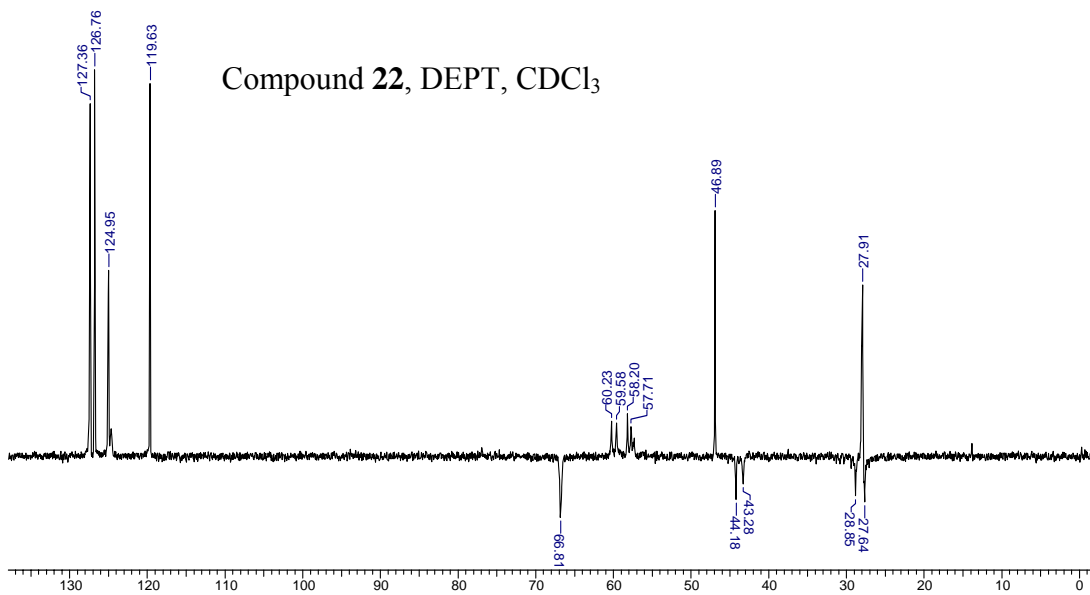
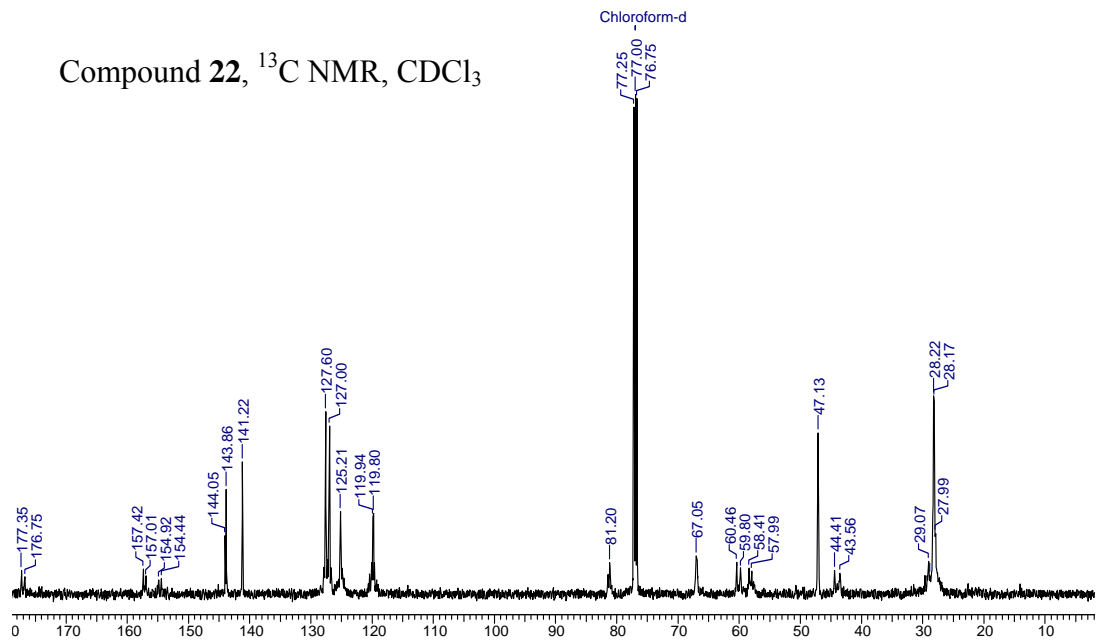


Figure 23  $^{13}\text{C}$  and DEPT spectra of compound **19**



**Figure 24** <sup>1</sup>H NMR and Mass spectra of compound **22**



**Figure 25**  $^{13}\text{C}$  and DEPT spectra of compound **22**

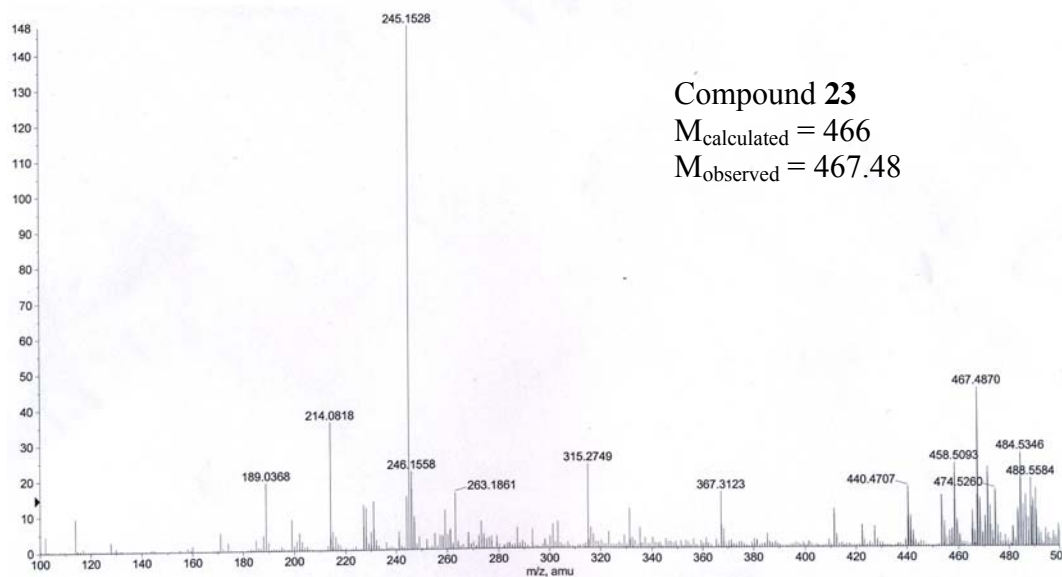
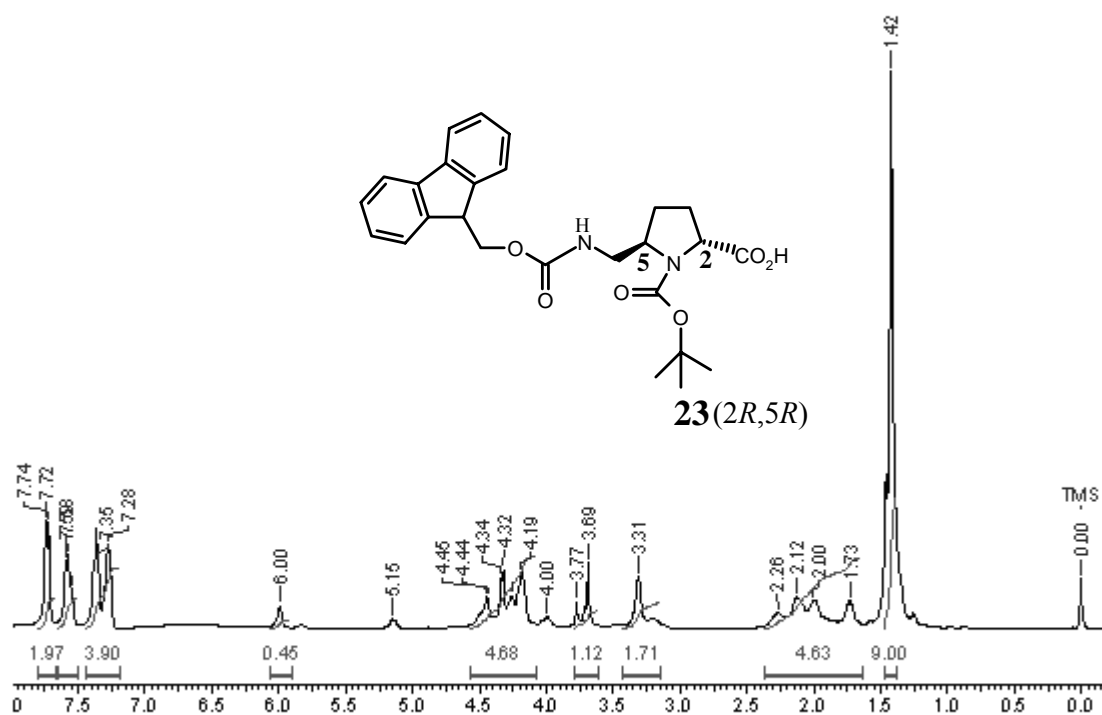


**Figure 26** <sup>1</sup>H NMR and Mass spectra of compound **23**

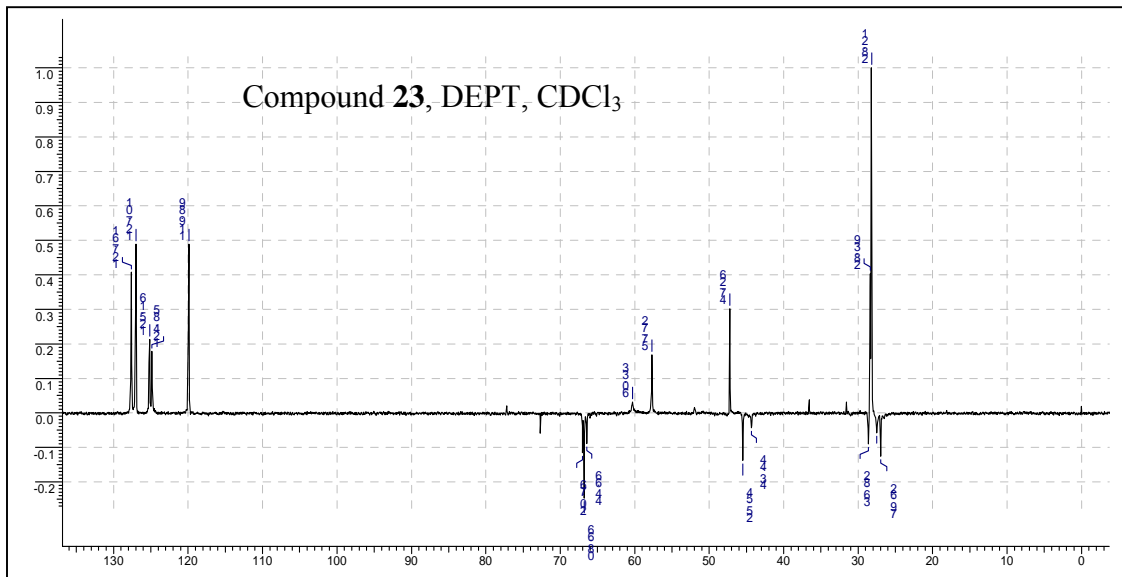
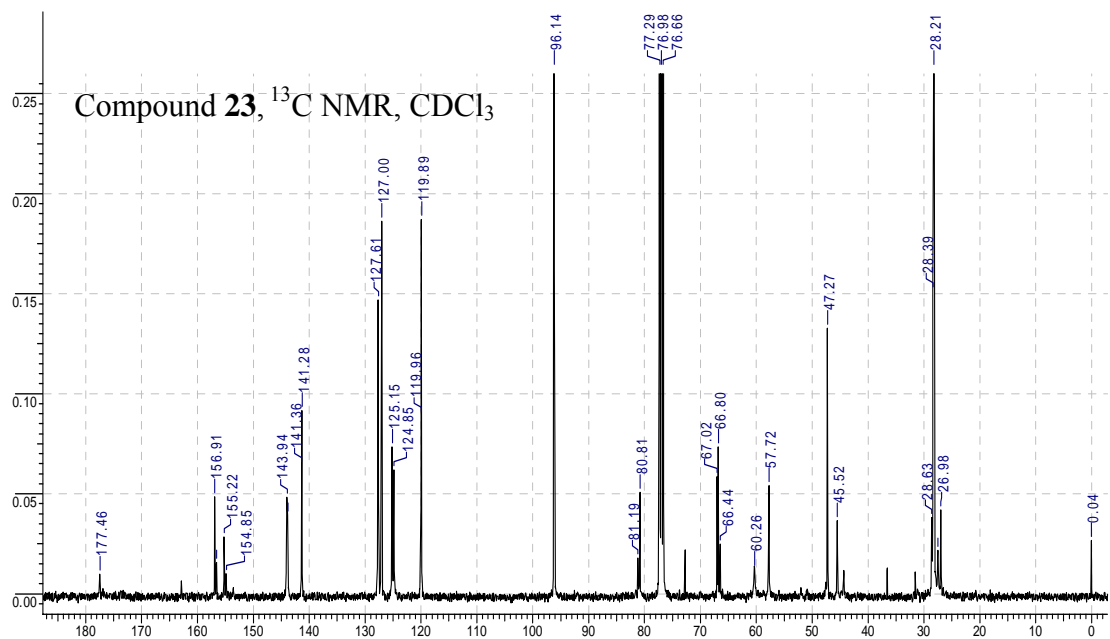
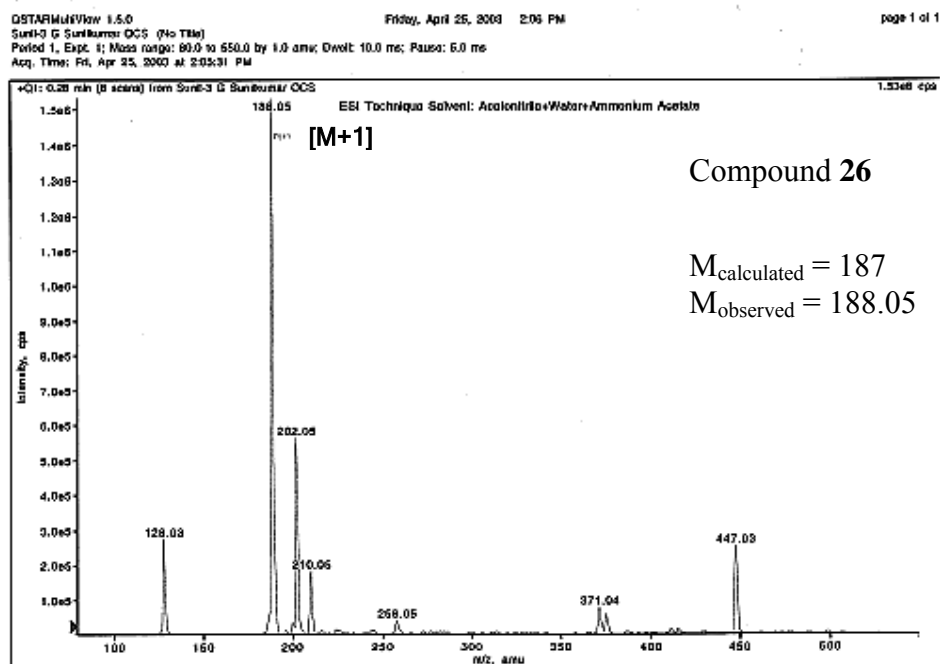
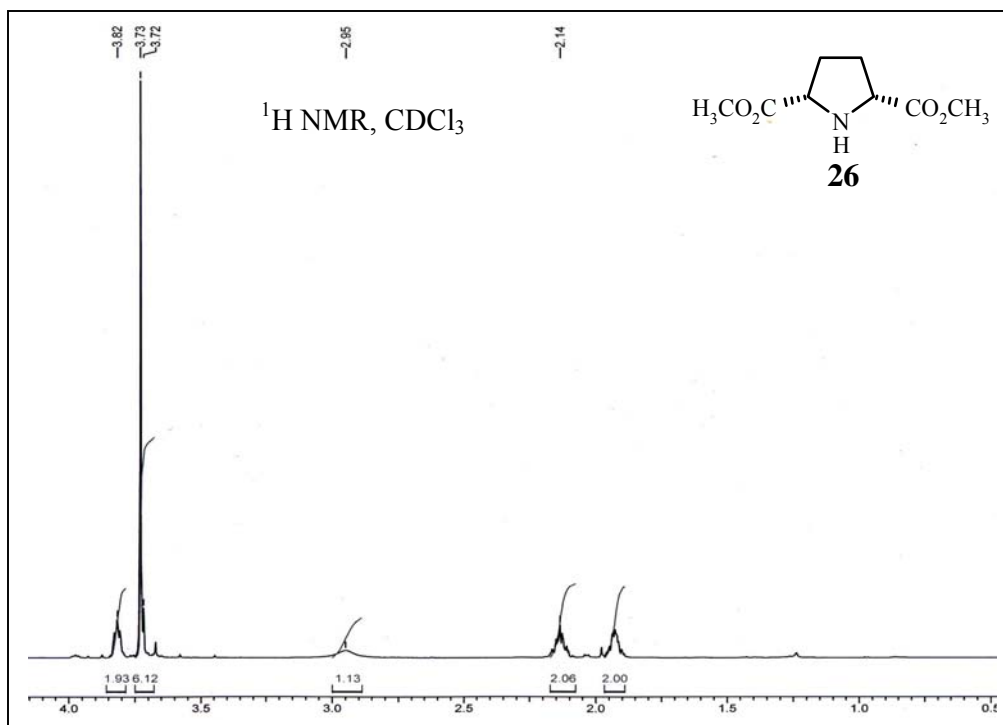
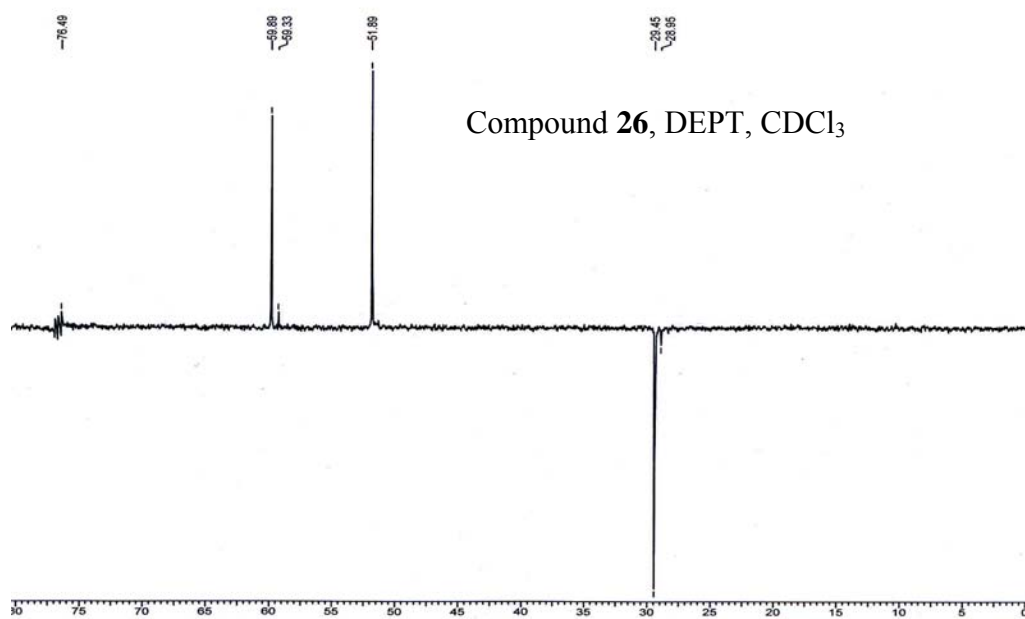
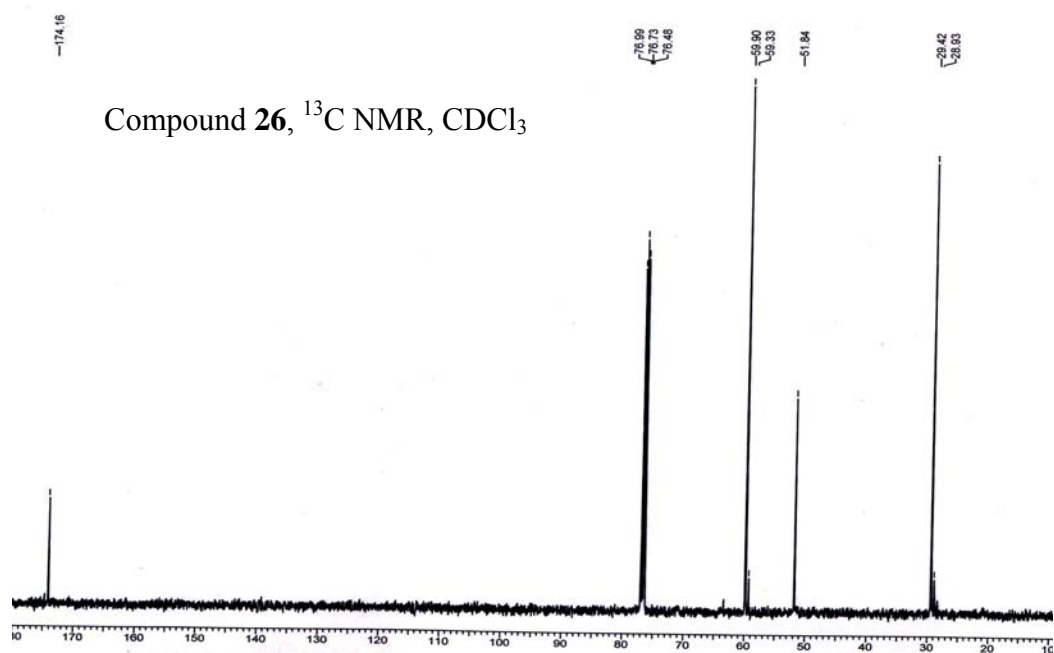


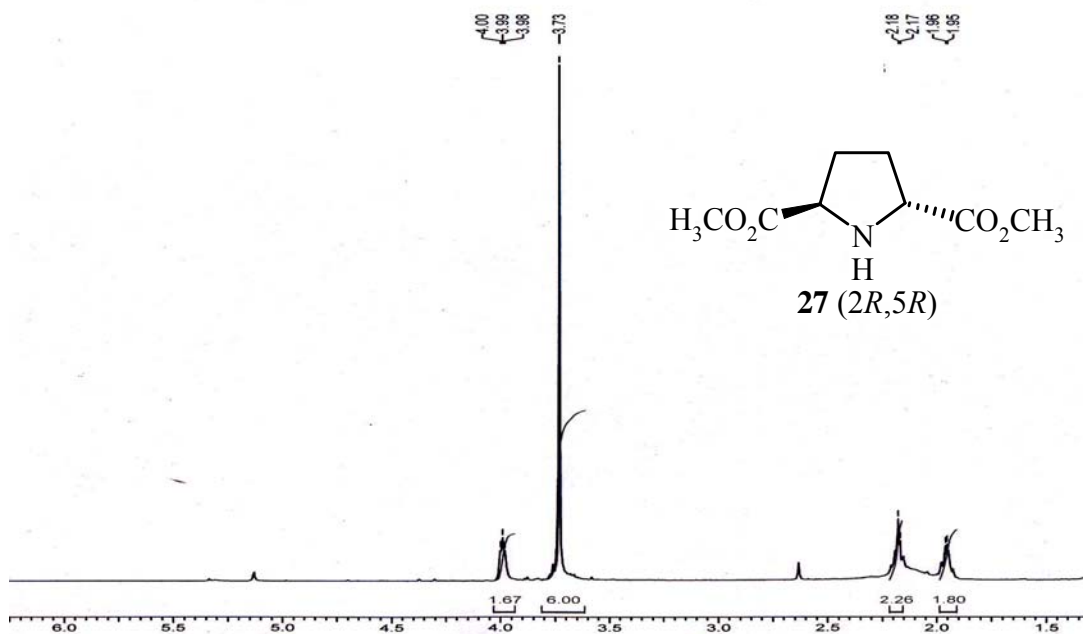
Figure 27  $^{13}\text{C}$  and DEPT spectra of compound **23**



**Figure 28** <sup>1</sup>H NMR and Mass spectra of compound **26**



**Figure 29**  $^{13}\text{C}$  and DEPT spectra of compound **26**



QSTARMultiView 1.5.0 Friday, April 25, 2003 2:19 PM page 1 of 1  
 Suni-7 G Sunikumar OCS (No Title)  
 Period 1, Expt. 1; Mass range: 80.0 to 350.0 by 1.0 amu; Dwell: 10.0 ms; Pause: 5.0 ms  
 Acq. Time: Fri, Apr 25, 2003 at 2:18:28 PM

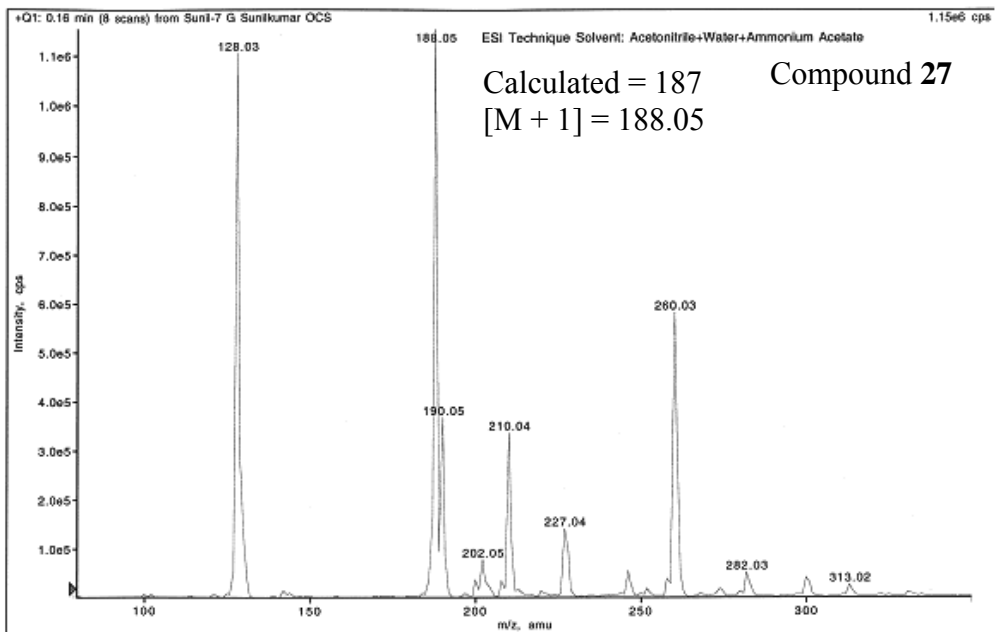


**Figure 30**  $^1\text{H}$  NMR and Mass spectra of compound **27**

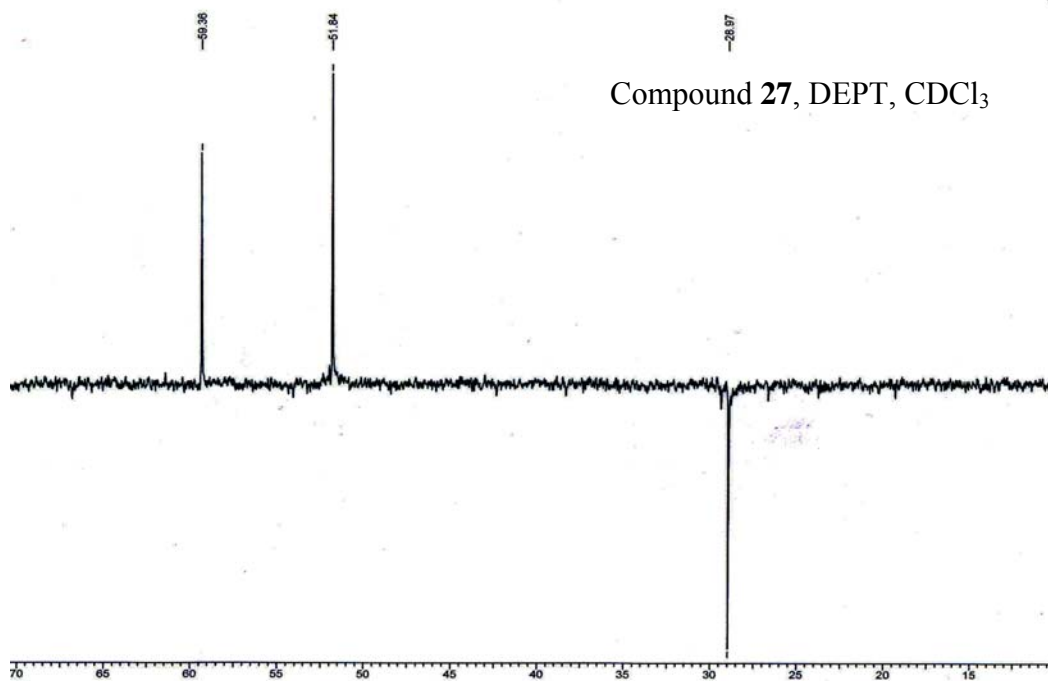
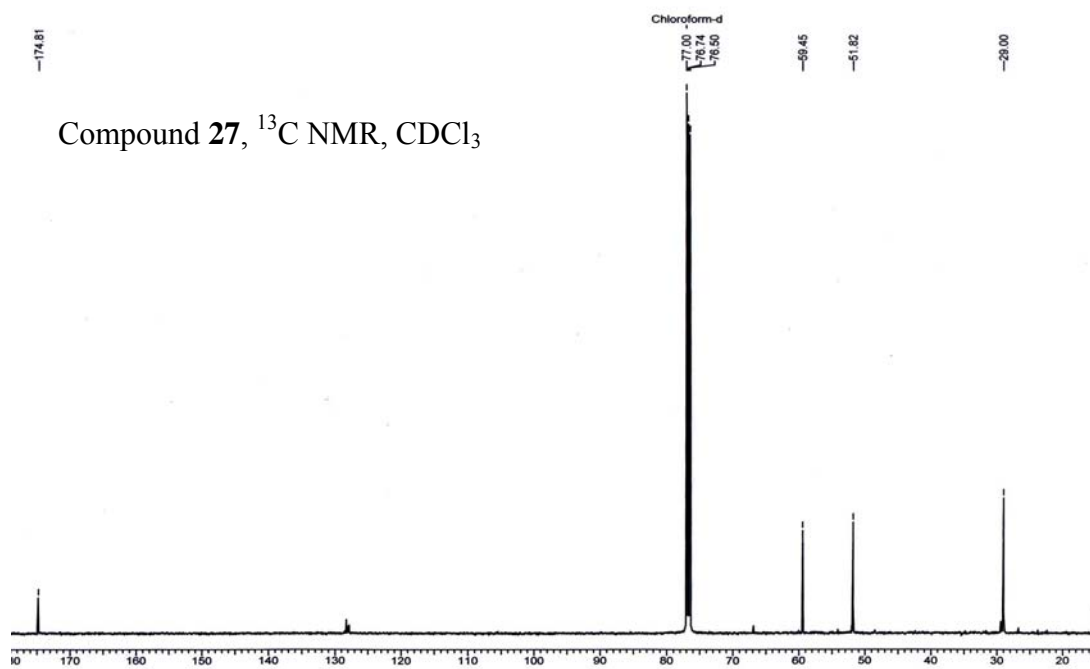
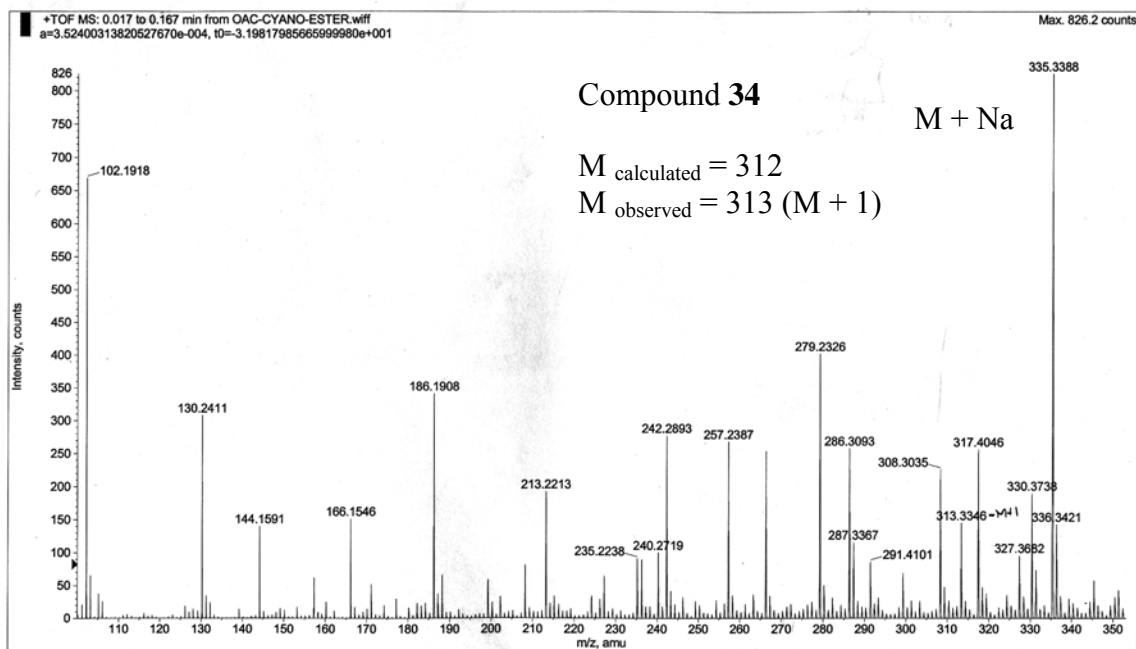
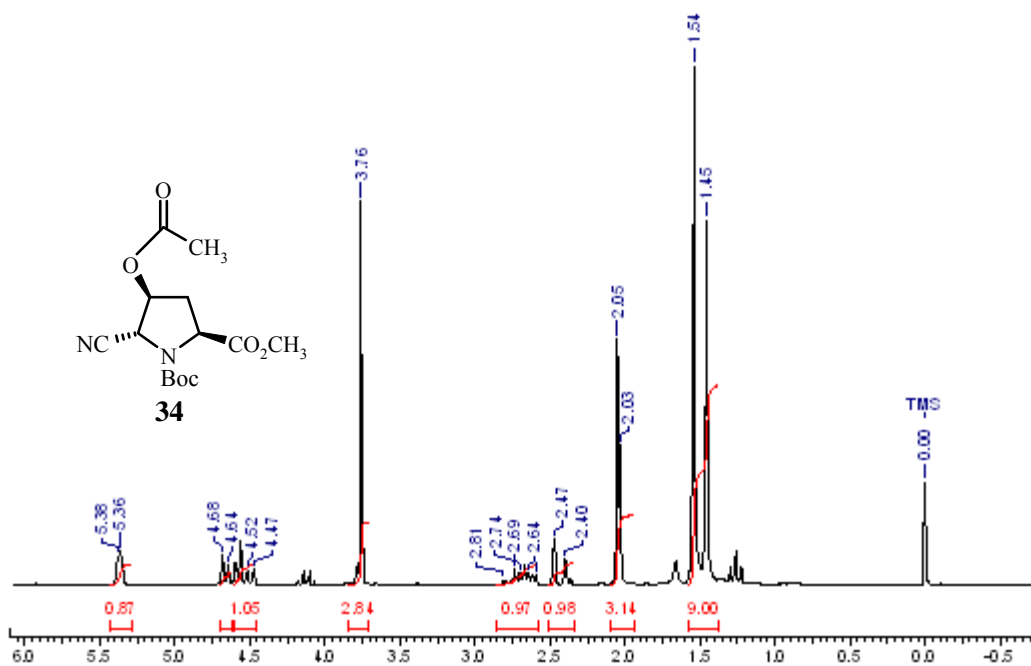
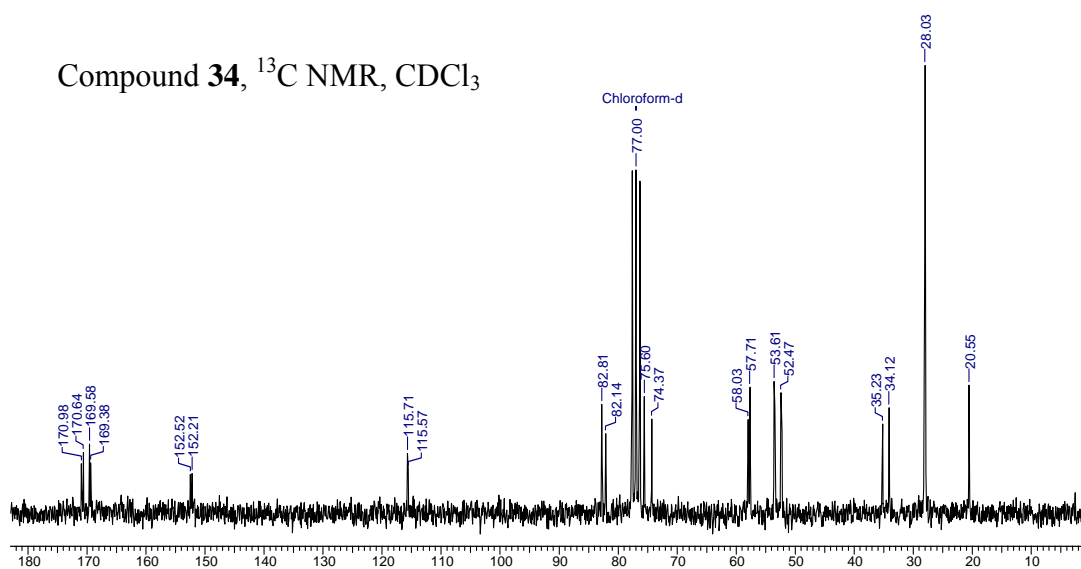


Figure 31  $^{13}\text{C}$  and DEPT spectra of compound 27

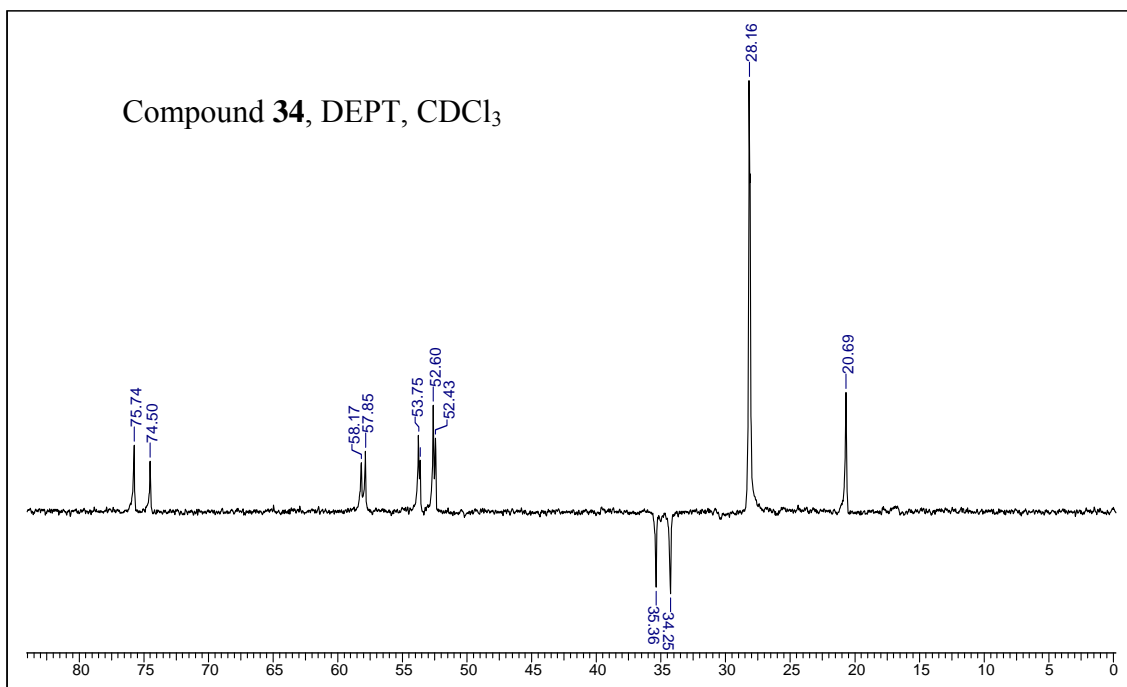


**Figure 32** <sup>1</sup>H NMR and Mass spectra of compound **34**

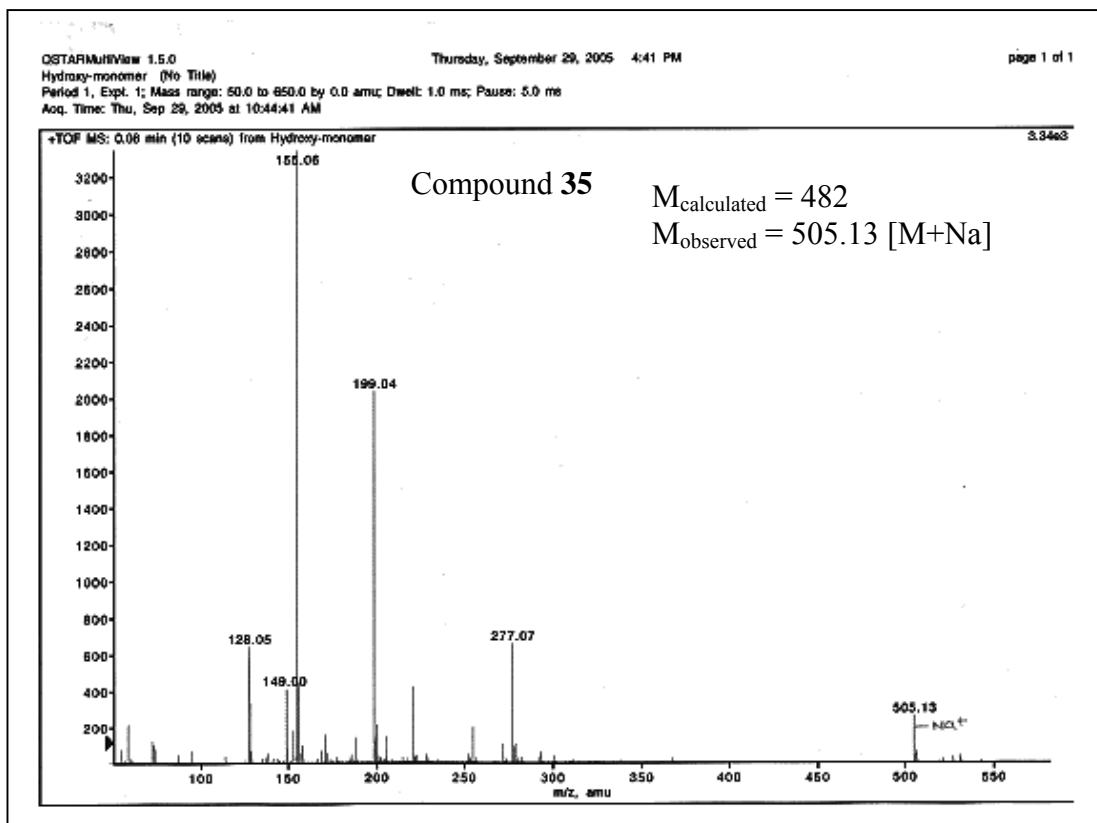
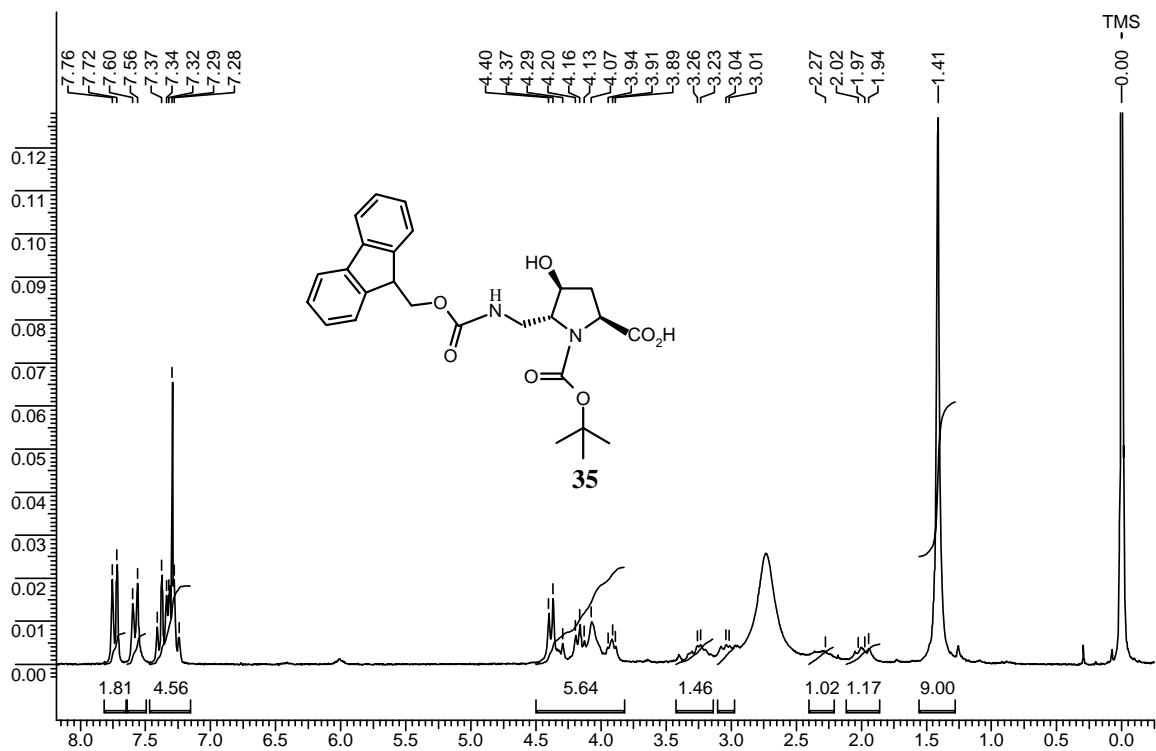
Compound **34**,  $^{13}\text{C}$  NMR,  $\text{CDCl}_3$



Compound **34**, DEPT,  $\text{CDCl}_3$



**Figure 33**  $^{13}\text{C}$  NMR and DEPT spectra of compound **34**



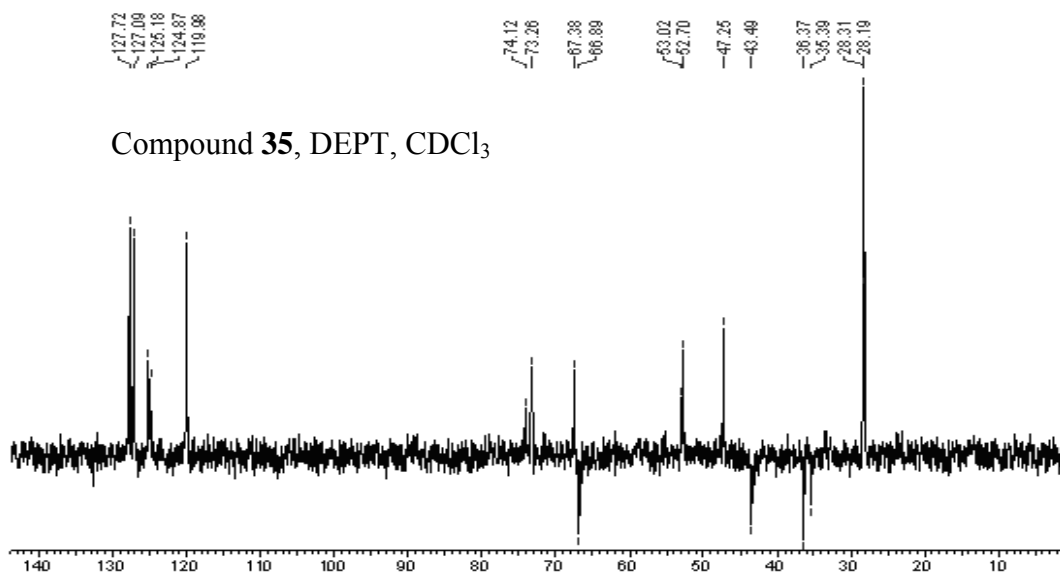
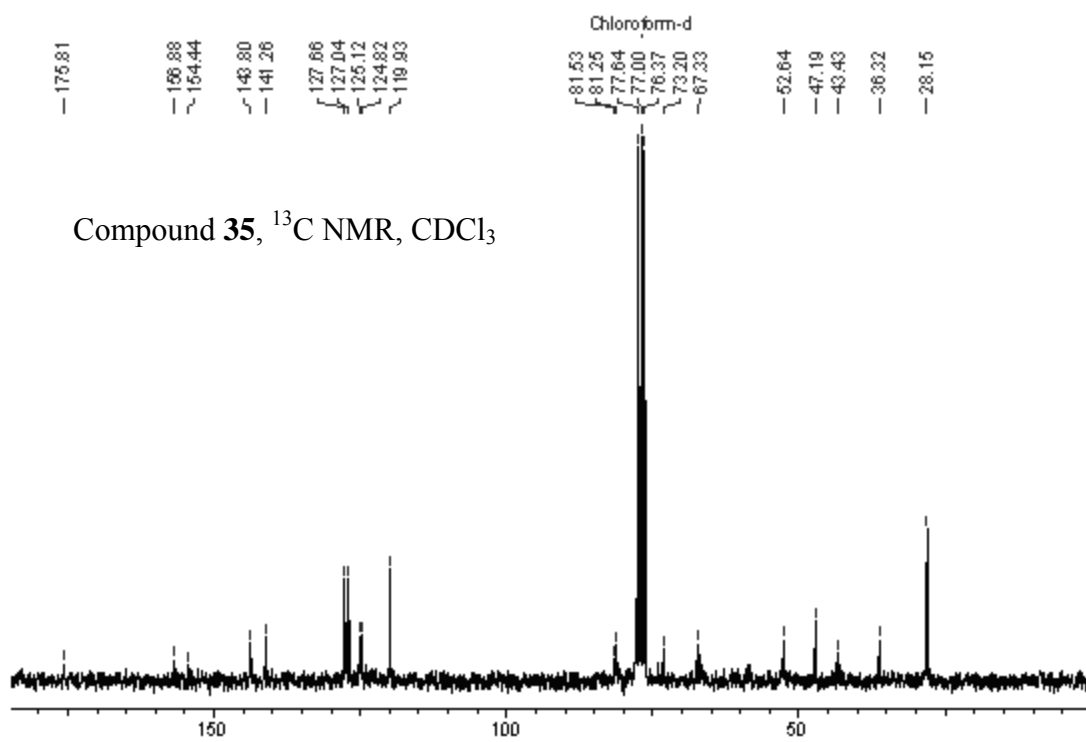


**Figure 35**  $^{13}\text{C}$  and DEPT spectra of compound **35**

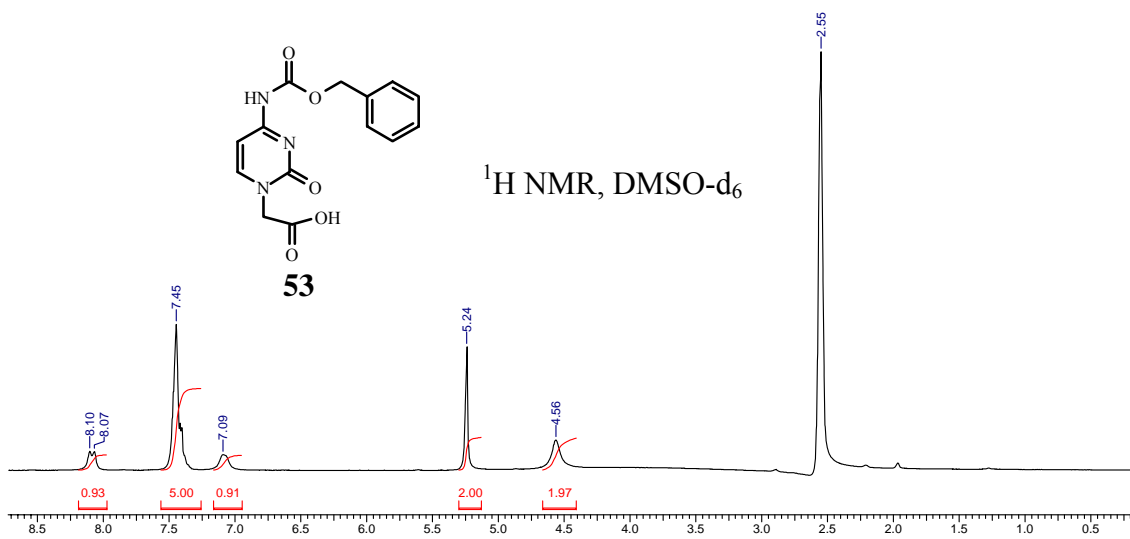
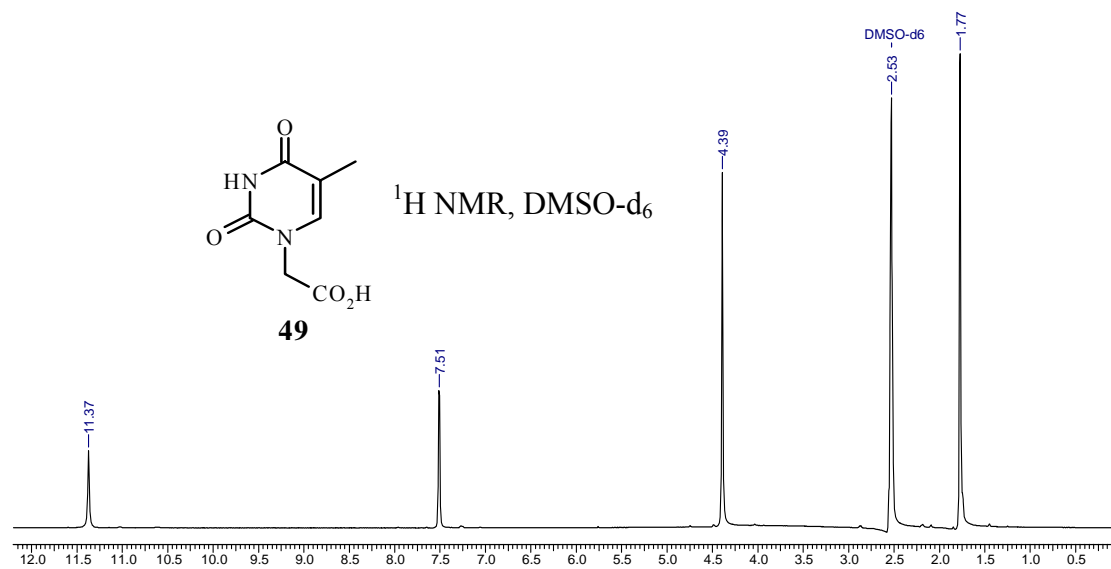


**Figure 36** <sup>1</sup>H NMR and spectra of compound **49** and **53**

**Table 3 HPLC and MALDI-TOF mass spectral analysis of modified *amp*-PNAs**

Entry	PNA	Retention Time (min)	Calculated Mass	Observed Mass
1	<i>aeg</i> PNA <b>57</b>	7.696	2215	2218.58 [M + 3H]
2	<i>aeg</i> PNA <b>58</b>	11.330	2793	2832.28 [M + K]
3	SR- <i>amp</i> PNA <b>59</b>	8.174	2241	2240.28
3	SR- <i>amp</i> PNA <b>60</b>	7.730	2241	2240.83
5	SR- <i>amp</i> PNA <b>61</b>	8.14	2241	2241.37
6	SR- <i>amp</i> PNA <b>62</b>	8.168	2267	2265.86 [M -1H]
7	SR/SS- <i>amp</i> PNA <b>63</b>	8.970	2267	2268.47 [M + 1H]
8	SR- <i>amp</i> PNA <b>64</b>	11.075	2871	2876.31 [M+5]
9	SR- <i>amp</i> PNA <b>65</b>	9.719	2423	2423.34
10	SS- <i>amp</i> PNA <b>66</b>	8.177	2241	2243.51 [M + 2H]
11	SS- <i>amp</i> PNA <b>67</b>	7.834	2241	2239.97
12	SS- <i>amp</i> PNA <b>68</b>	8.101	2241	2244.7 [M + 3H]
13	SS- <i>amp</i> PNA <b>69</b>	8.30	2267	2266.19[M -1H]
14	SS- <i>amp</i> PNA <b>70</b>	11.059	2871	2874.73 [M+3H]
15	SS- <i>amp</i> PNA <b>71</b>	11.066	2423	2423.80
16	RS- <i>amp</i> PNA <b>72</b>	8.165	2241	2244.09 [M + 3H]
17	RS- <i>amp</i> PNA <b>73</b>	8.132	2241	2263.28 [M + Na]
18	RS- <i>amp</i> PNA <b>74</b>	8.143	2241	2242.00 [M + 1H]
19	RS- <i>amp</i> PNA <b>75</b>	8.306	2267	2267.08
20	RS- <i>amp</i> PNA <b>76</b>	11.119	2871	2894.37 [M+ Na]
21	RS- <i>amp</i> PNA <b>77</b>	11.547	2423	2425.48[M + 2H]
22	RR- <i>amp</i> PNA <b>78</b>	7.944	2241	2240.88[M + 1H]
23	RR- <i>amp</i> PNA <b>79</b>	7.845	2241	2263.28[M + Na]
24	RR- <i>amp</i> PNA <b>80</b>	8.236	2241	2242.85[M + 2H]
25	RR- <i>amp</i> PNA <b>81</b>	8.855	2267	2268.47[M + 1H]
26	RR- <i>amp</i> PNA <b>82</b>	11.512	2871	2878.74 [M+ 7H]
27	RR- <i>amp</i> PNA <b>83</b>	10.286	2423	2425.09[ M + 2H]
28	SRR- <i>amp</i> PNA <b>84</b>	8.617	2257	2261.60 [M +9]
29	SRR- <i>amp</i> PNA <b>85</b>	8.891	2257	2259.70 [M + 3H]
30	SRR- <i>amp</i> PNA <b>86</b>	8.379	2257	2252.83 [M – 4H]
31	SRR- <i>amp</i> PNA <b>87</b>	9.247	2835	2836.47 [M + 1H]

**Figure 37** Reverse phase HPLC- Profiles of *amp/aeg* PNAs

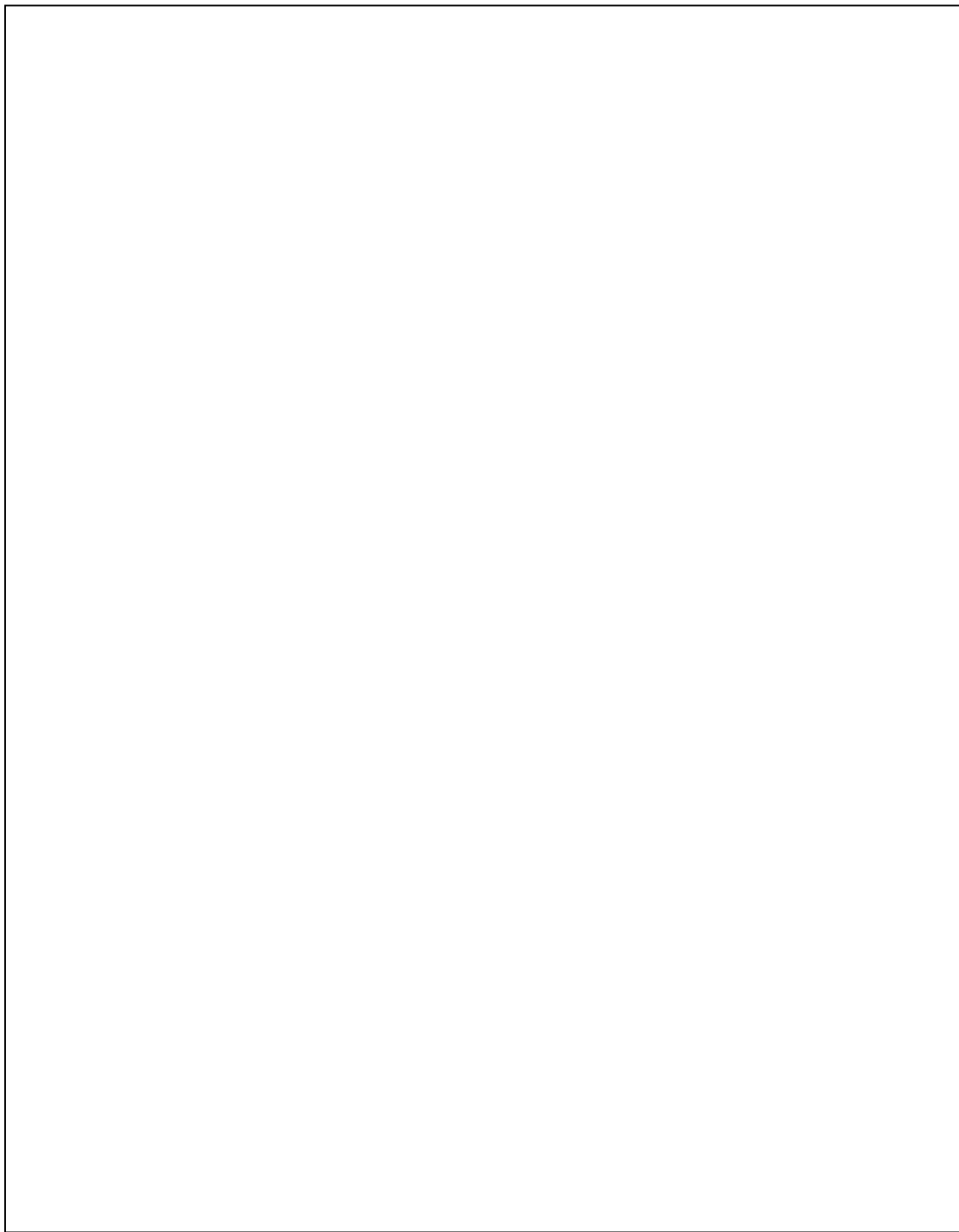


**Figure 37a** HPLC- Profiles of *amp/aeg* PNAs **57-63**

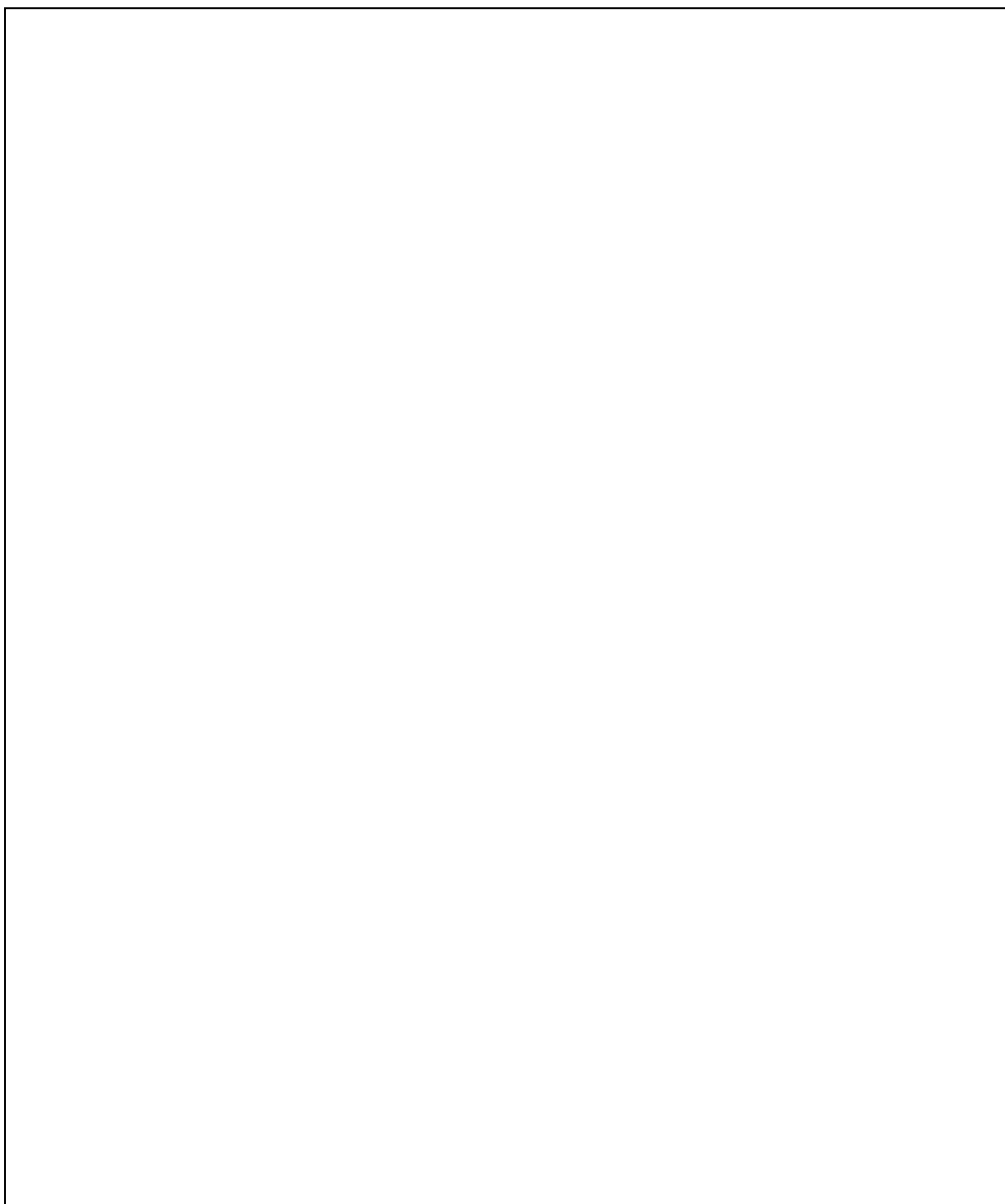


**Figure 37b** HPLC-Profiles of *amp*-PNAs **64-69**

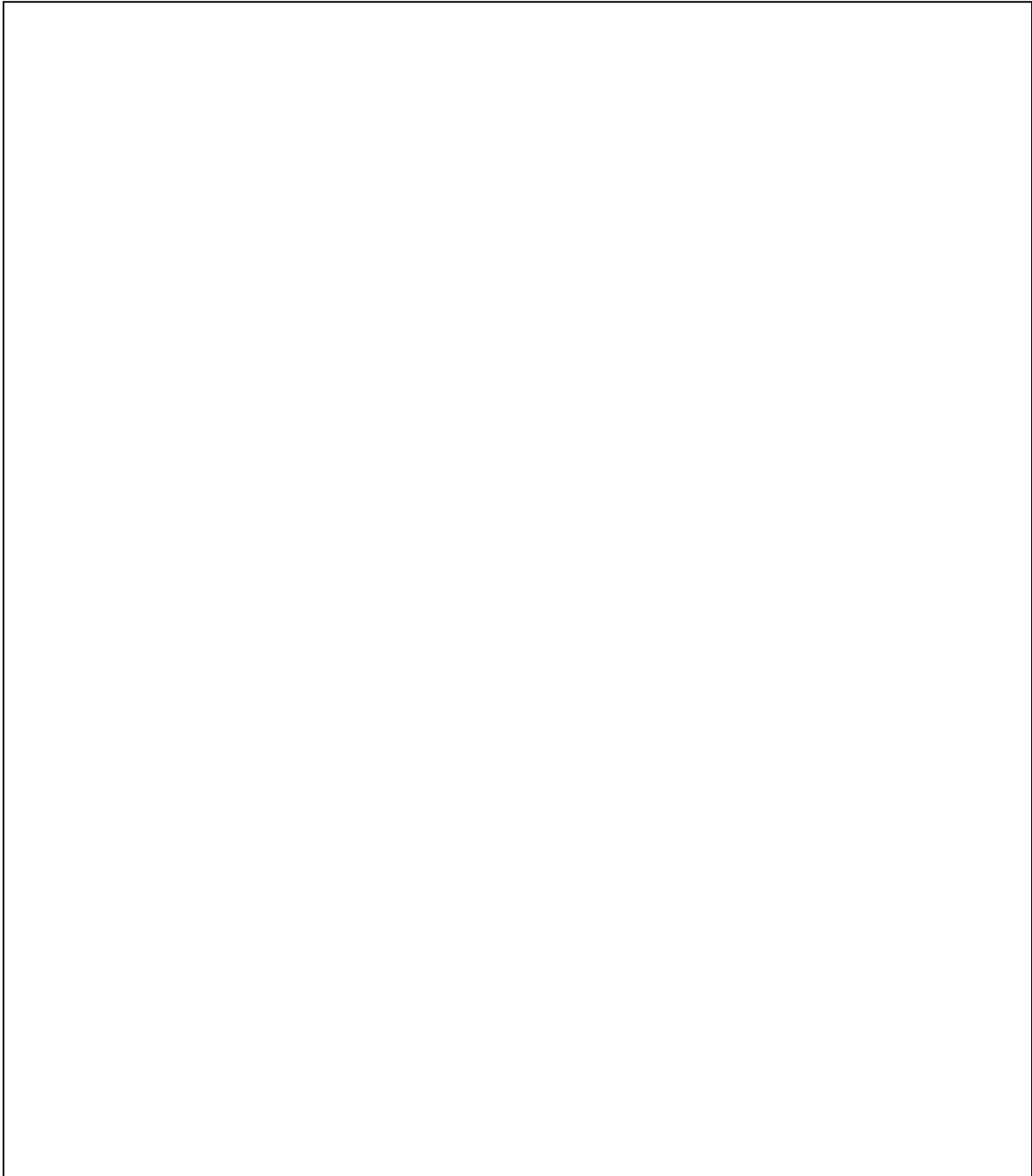


**Figure 37c** HPLC-profiles of *amp*-PNAs **70-75**

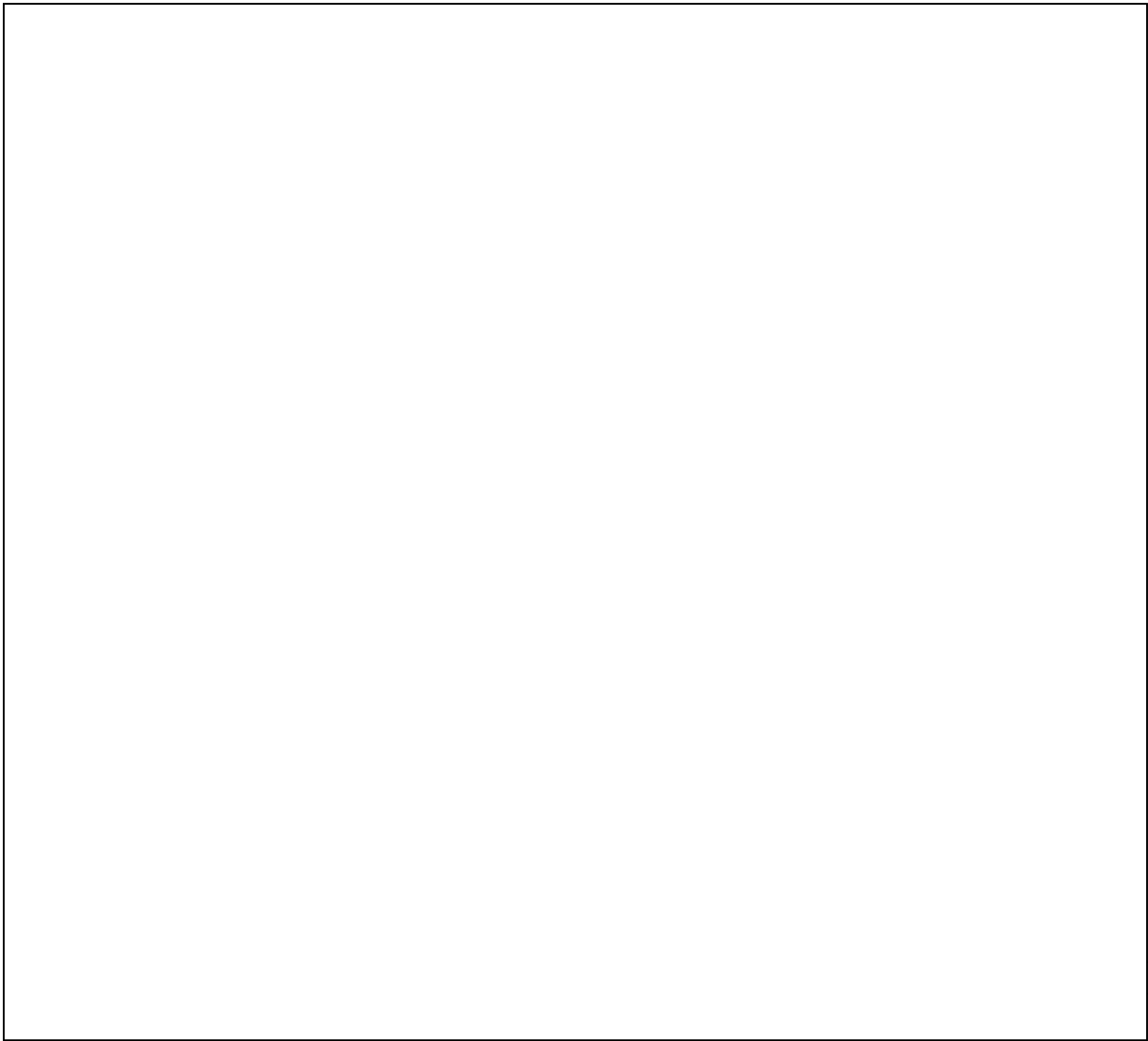


**Figure 37d** HPLC-Profiles of *amp*-PNAs **76-81**

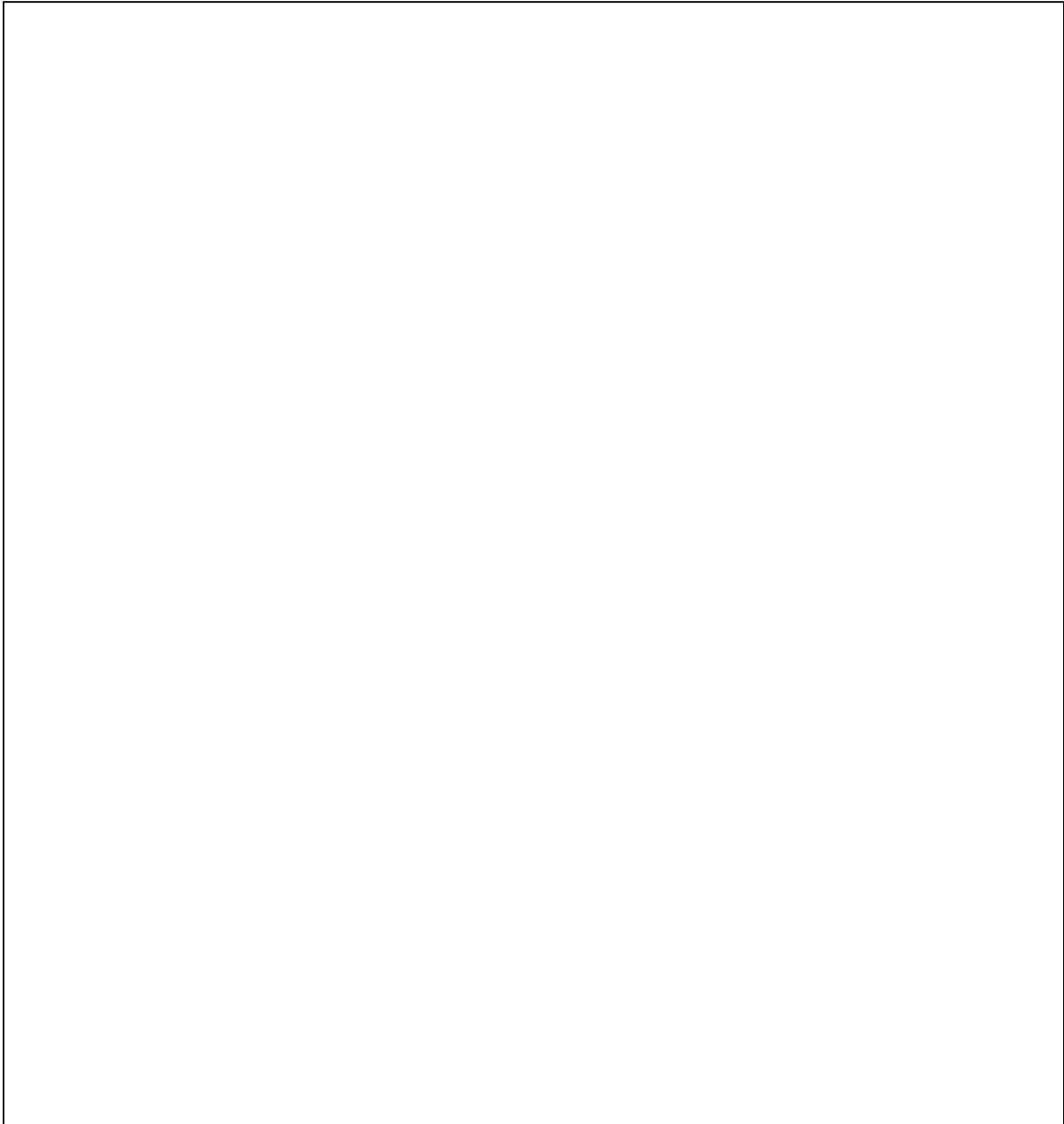


**Figure 37e** HPLC-Profiles of *amp*-PNAs **82-87**

Figure 38 MALDI-TOF spectra of *amp/ae*g PNA oligomers

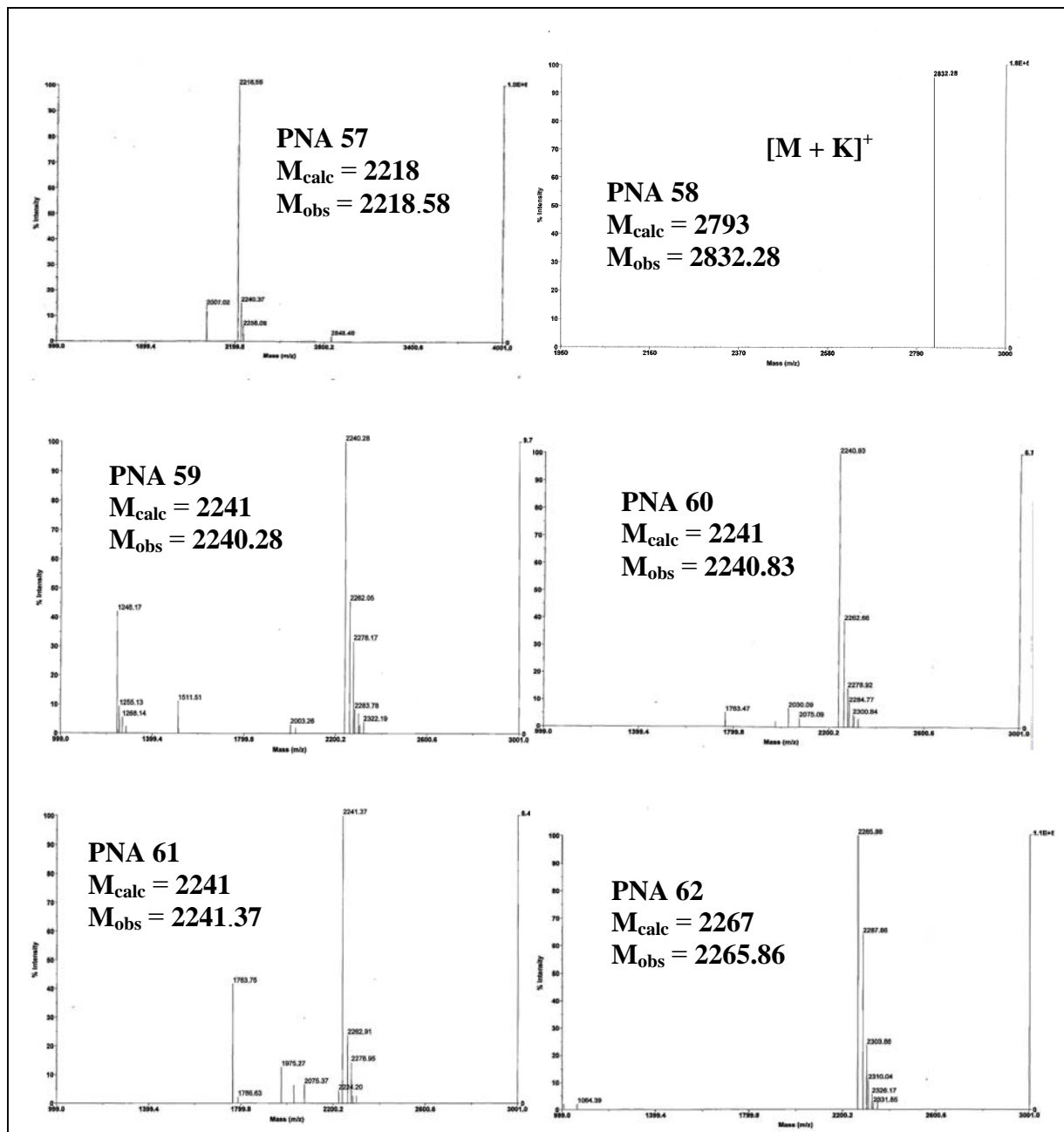


Figure 38a MALDI-TOF spectra of *amp*-PNAs 57-62

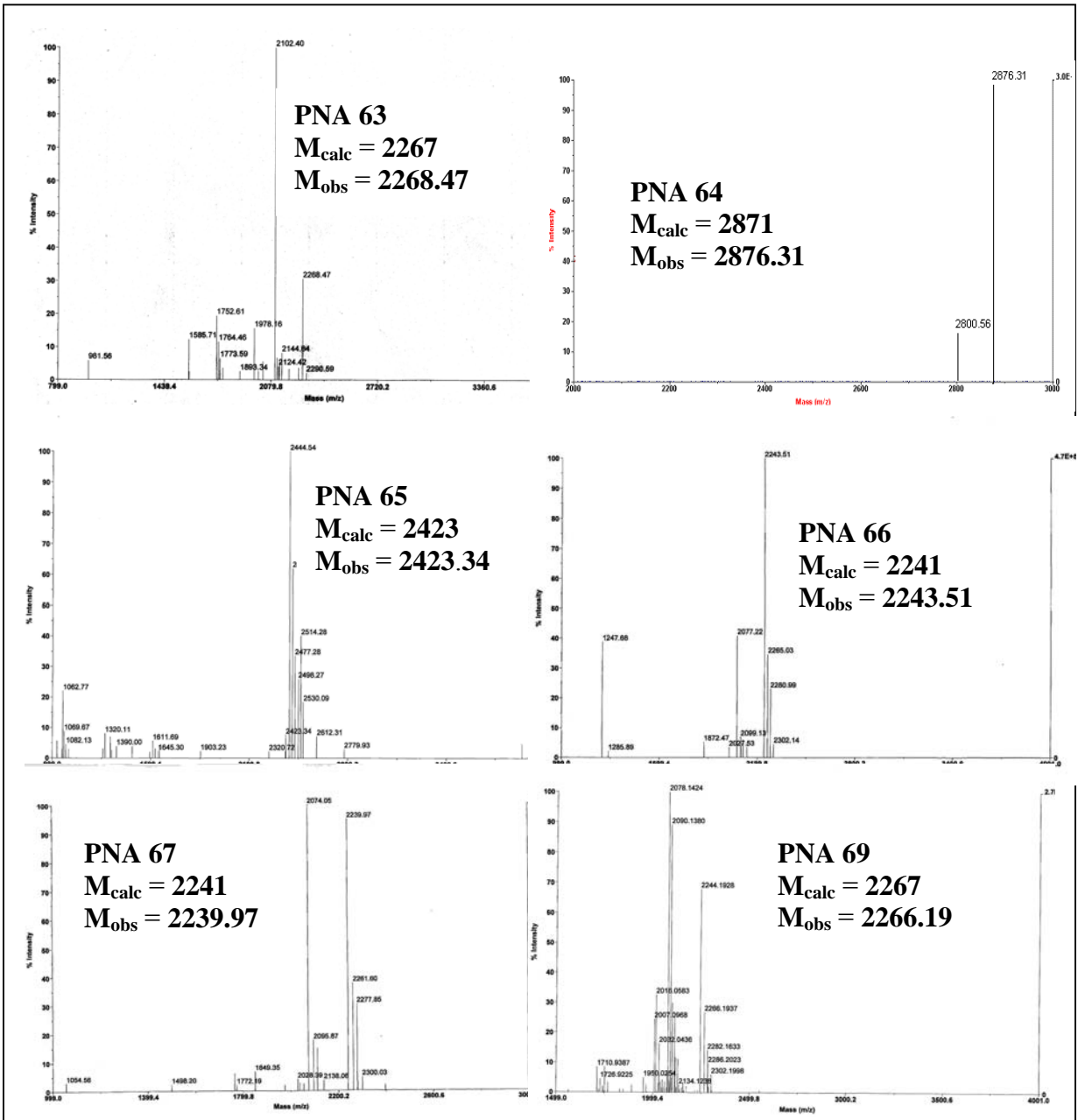
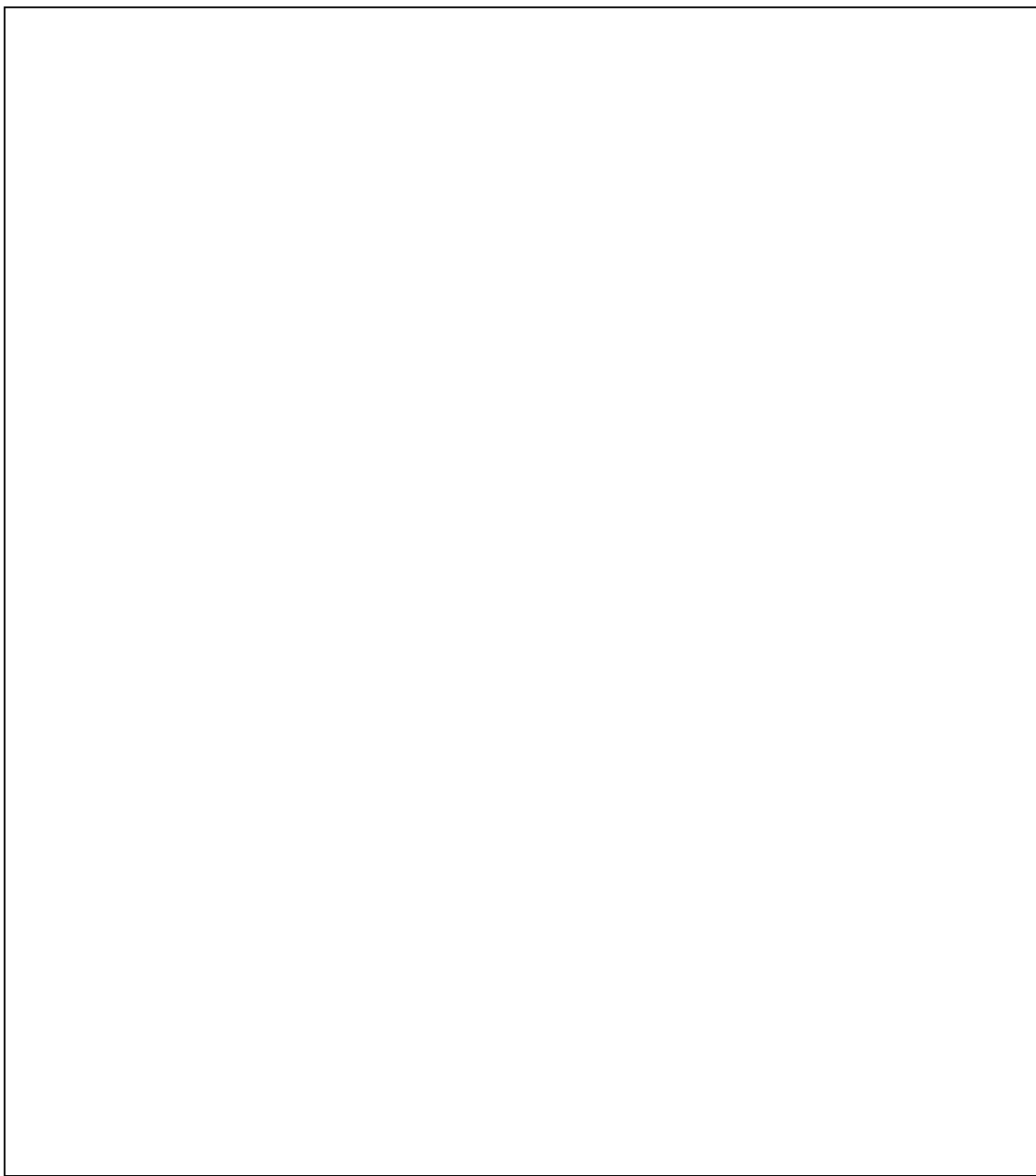
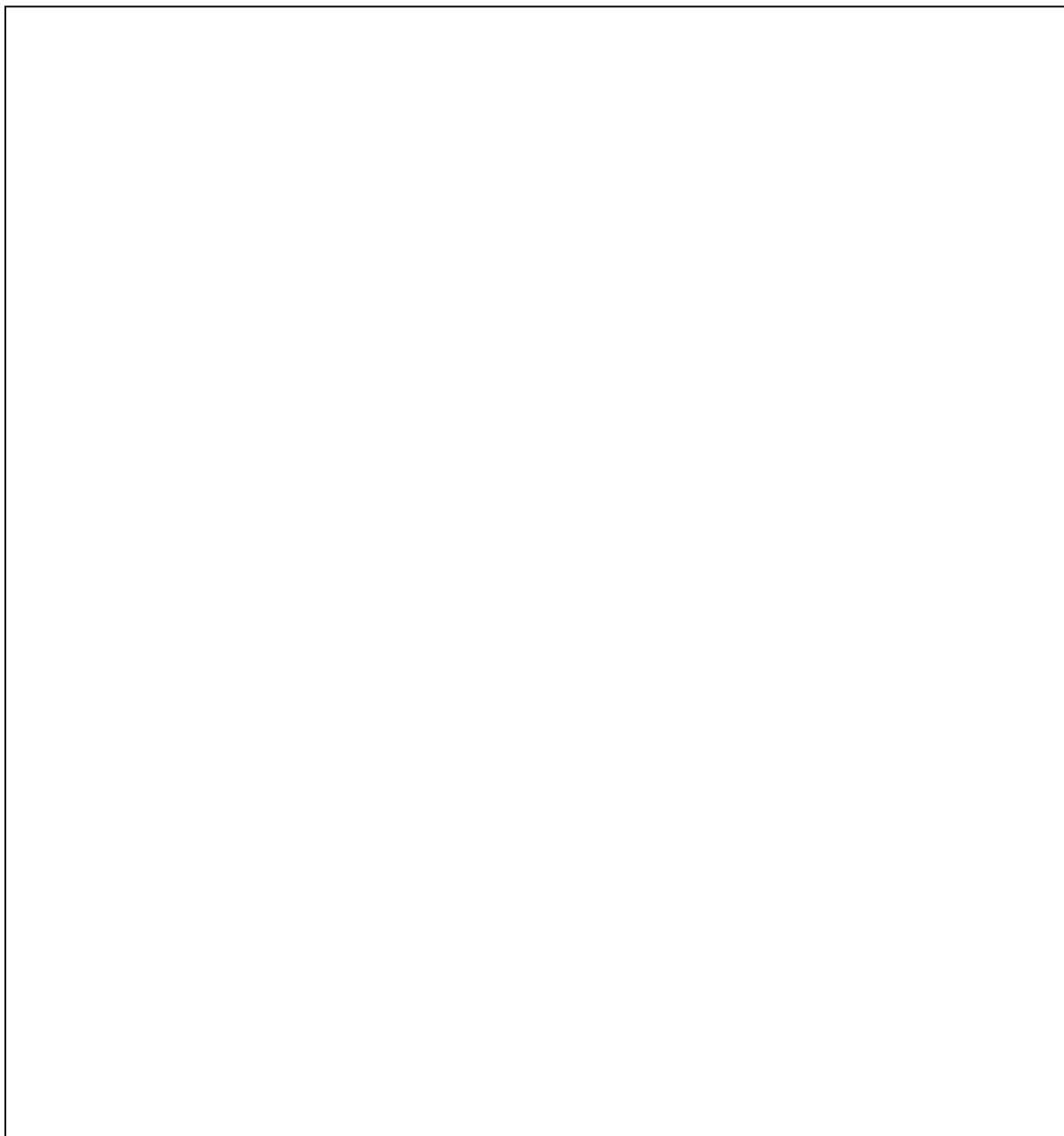


Figure 38b MALDI-TOF spectra of *amp*-PNAs 63-69



**Figure 38c** MALDI-TOF spectra of *amp*-PNAs **70-75**



**Figure 38d** MALDI-TOF spectra of *amp*-PNAs **76-81**

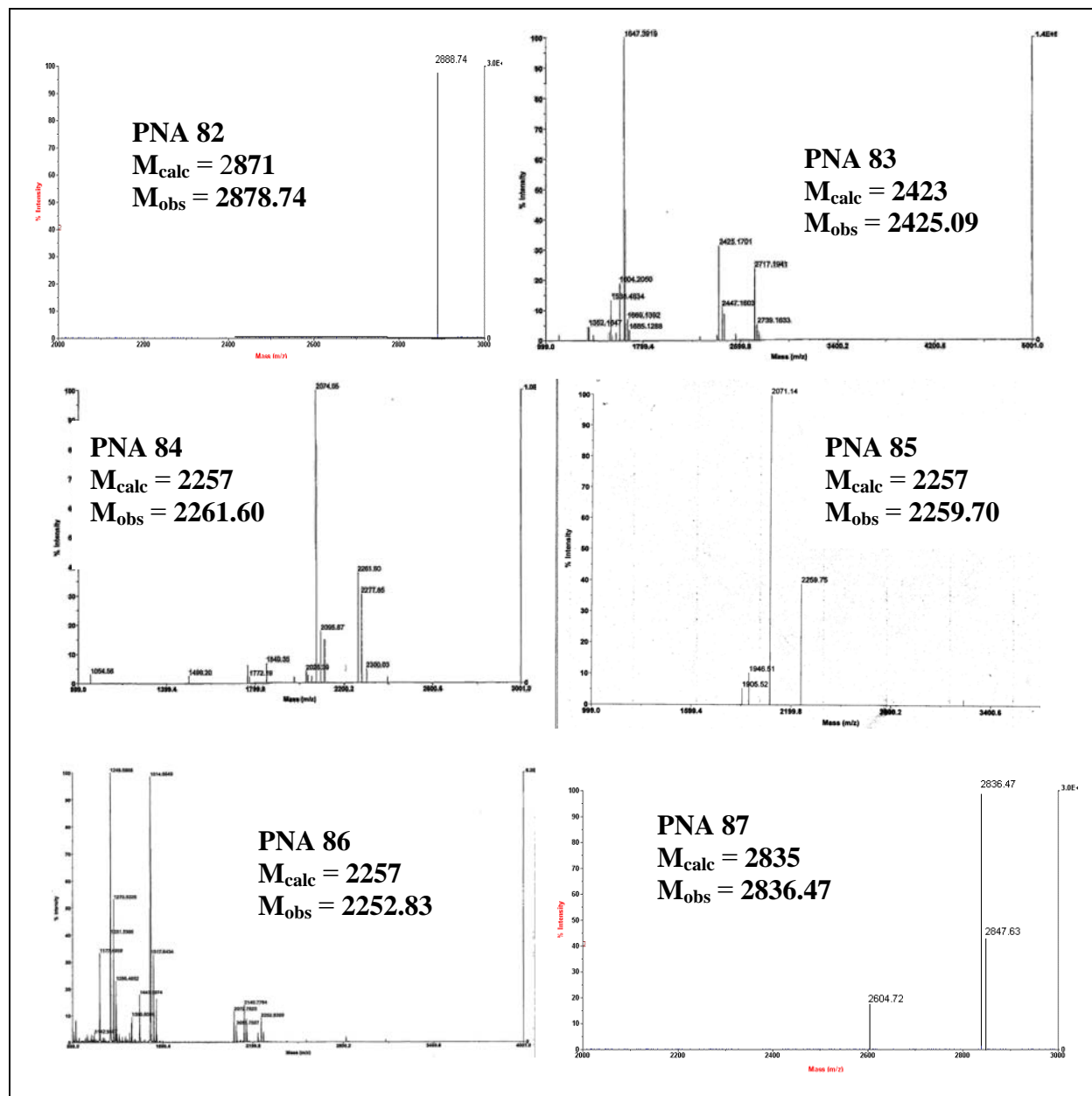


Figure 38e MALDI-TOF spectra of *amp*-PNAs 82-87

---

## **CHAPTER 3**

### Biophysical studies

---

### **3 Introduction**

Biophysics is an interdisciplinary field in which the techniques from the physical sciences are applied to understand the biological structure and function. Some of the biophysical techniques useful in studying structures of nucleic acid and analogues are as follows.

#### **3.1 Biophysical techniques**

**3.1.1 Transmission electron microscopy (TEM):** TEM is a very direct way of determining macromolecular structure, which has reached near-atomic resolution for protein structures in the 1990s. In the 1930s, Ruska<sup>1a</sup> built the first EM, using electromagnetic lenses to focus the electron beam. The TEM is used heavily in both [material science/metallurgy](#) and the [biological sciences](#). In both cases, the specimens must be very thin and able to withstand the high vacuum present inside the instrument.

#### **3.1.2 EPR spectroscopy:**

EPR can be used to identify biological molecules that contain free radicals or transition metal ions in their structure. Even more usefully EPR is a quantitative technique i.e. we can determine the concentration of unpaired electrons present in a sample even if we do not know the exact nature of the free radical being observed. EPR spectroscopy has been shown to be useful in understanding the pathophysiology and underlying chemical mechanism of a wide range of diseases. Examples studied include Parkinson's disease, birth asphyxia, stroke, septic shock, kidney damage and coronary heart disease.

### **3.1.3 Neutron scattering:**

Neutrons are most aptly applied to the determination of hydration patterns and the structure of macromolecules, their complexes, interaction and dynamic activity. Neutron scattering is not a mainstream technique in biomedical research. The interaction of neutrons with nuclei is very weak and consequently the longer times are needed to collect a large amount of high resolution data using them (for example, weeks of measuring time for neutron crystallography). Alternatively, it is often found that the amount of sample required is very large, or that the amount of information (e.g. spatial resolution) provided is very small.

### **3. 1. 4 X-ray Crystallography:**

*It is the principal method by which the detailed 3-dimensional structures of molecules - especially those present in living systems have been discovered.*

### **3. 1. 5 Circular Dichroism Spectroscopy CD:**

CD spectroscopy belongs to a class absorption spectroscopy that can provide information on the structures of many types of biological macromolecules. Circular dichroism is the difference between the absorption of left and right handed circularly-polarised light and is measured as a function of wavelength. The absence of regular structure results in zero CD intensity, while an ordered structure results in a spectrum which contains both positive and negative signals.

Circular dichroism spectroscopy is particularly effective for determining whether a protein is folded, and if so characterizing its secondary structure, tertiary structure, and

the structural family to which it belongs. It is possible to compare the structures of a protein obtained from different sources (e.g. species or expression systems) or comparing structures for different mutants of the same protein demonstrating difference in solution conformation after changes in manufacturing processes or formulation studying the conformational stability of a protein under stress (thermal stability, pH stability, and stability to denaturants) and how this stability is altered by buffer composition or addition of stabilizers and excipients. CD is excellent for finding solvent conditions that increase the melting temperature and/or the reversibility of thermal unfolding, conditions which generally enhance shelf life.

Determining whether protein-protein interactions alter the conformation of protein is possible from observing changes in the sub function spectrum of the complex from the sum of the individual components. CD spectroscopy is usually used to study proteins (Table 1) in solution, and thus it complements X-ray methods that study the solid-state. There is also a limitation, in which many proteins are embedded in membranes in their native state, and solutions containing membrane structures are often strongly scattering. CD is also sometimes measured in thin films.

### CD of soluble proteins

**Table 1** Characteristic CD-signatures of different peptides

$\alpha$ -helix	positive	$\pi \rightarrow \pi^*$	190-195 nm	60,000 to 80,000 deg cm <sup>2</sup> dmol <sup>-1</sup>
	negative	$\pi \rightarrow \pi^*$	208	-36,000 $\pm$ 3,000
	negative	$n \rightarrow \pi^*$	222	-36,000 $\pm$ 3,000
$\beta$ -sheet	positive	$\pi \rightarrow \pi^*$	195 - 200	30,000 to 50,000
	negative	$n \rightarrow \pi^*$	215 - 220	-10,000 to -20,000
random	negative	$\pi \rightarrow \pi^*$	ca. 200	-20,000
	positive	$n \rightarrow \pi^*$	220	small

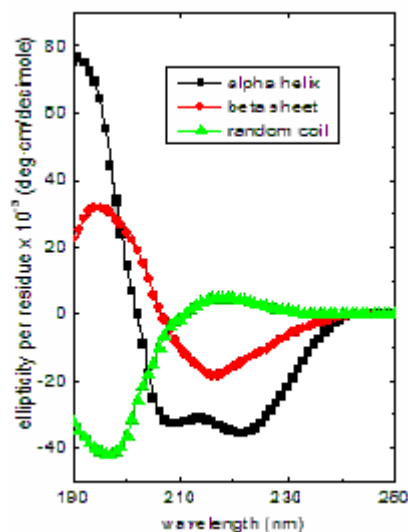


**Figure 1a:** Typical CD spectra of poly-L-lysine peptides

### 3. 2 CD spectroscopy of PNA:

CD spectroscopy is also useful for monitoring the structural changes of nucleic acids in solutions and for diagnosing whether new or unusual structures are formed by particular polynucleotide sequences. PNA is non-chiral and hence CD silent. Chirality can be induced in the achiral PNA strand by linking chiral moieties like amino acids,<sup>1</sup> peptides,<sup>2</sup> or oligonucleotides<sup>3</sup> to the PNA termini. PNA can also be rendered chiral by the incorporation of chiral amino acids in its backbone.<sup>4-11</sup> The CD is predominantly an effect of coupling between the transition moments of the nucleobases as a result of their helical stacking. The reliance on CD spectroscopy to study nucleic acid conformations has stemmed from the sensitivity and ease of CD measurements, the non-destructive nature of measurements and the fact that conformations can be studied in solution.

Although detailed structural information, such as X-ray crystallography or NMR spectroscopy is not available from CD spectra, but it can provide a reliable determination

of its overall conformational state when compared with the CD spectra of reference samples. In case of nucleic acids, the sugar units of the backbone provide chirality and the bases attached to sugars are chromophores. In the CD spectrum of polynucleotide with stacked bases, the magnitude of CD signals is larger in the 260-280 nm region where the nucleobases absorb and significantly higher at 200 nm. The PNA backbone is inherently achiral and does not exhibit CD signals. The complex formed as a consequence of the binding of achiral PNA and chiral DNA leads to the formation of a chiral complex and thus CD assumes importance in the characterization of such complexes.

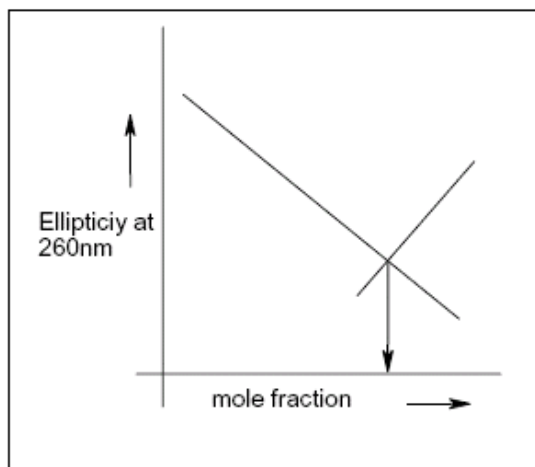


**Figure 1b** CD mixing showing PNA:DNA binding stoichiometry

Job's plot<sup>12</sup> (CD mixing) involving CD spectroscopy, is used to find out the binding stoichiometry of PNA:DNA complexes<sup>13</sup> in which the evolution of ellipticity at specific wavelength is followed as a function of the mole fraction of added PNA/DNA (Figure 1b).

### 3.3 UV-Spectroscopy

Monitoring the UV absorption at 260 nm as a function of temperature has been extensively used to study the thermal stability of nucleic acid system and consequently, PNA:DNA/RNA hybrids as well. Increasing temperature perturbs this system, inducing a structural transition by causing disruption of hydrogen bonds between the base pairs, diminished stacking between adjacent nucleobases and larger torsional motions in the backbone leading to a loss of secondary and tertiary structure. This is evidenced by an increase in the UV absorption at 260 nm, termed as hyperchromicity. The DNA melting is readily monitored by measuring its absorbance at a wavelength of 260 nm. A plot of absorbance *versus* temperature gives a sigmoidal curve in case of duplexes/triplexes and mid point of transition gives the  $T_m$  (Figure 2A). In case of triplexes, the first transition corresponding to triplex melting to the duplex (Watson–Crick duplex) and the third strand (Hoogsteen strand). This is followed by second transition due to the duplex dissociation at higher temperature into two single strands. The DNA triplex thus shows a characteristic double sigmoidal transition with separate melting temperatures for each transition.

A non-sigmoidal (e.g., linear) transition with low hyperchromicity is a consequence of non-duplexation (non-complementation). In many cases, the transitions are broad and the exact  $T_m$ s are obtained from the peak in the first derivative plots. This technique has provided valuable information regarding complementary interactions in nucleic acid hybrids involving DNA, RNA and PNA.

The UV mixing experiments are carried out by mixing the appropriate oligomers in different molar ratios keeping the total concentration constant. The stoichiometry of paired strands may be obtained from the mixing curves, in which the optical property at

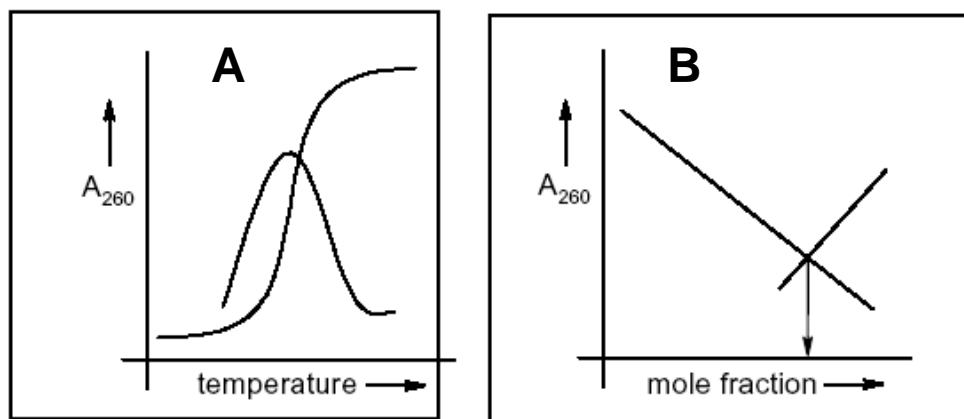


**Figure 2** Schematic representation of A.UV-melting (thermal stability), B.UV-mixing

a given wavelength is plotted against the mole fraction of each strand, known as Job's plot. Two triplex forming oligomers are mixed in various proportions, which can form 1:1, 1:2 or 2:1 complex, depending on the conditions in the medium and binding ability of the two interacting oligomers. By varying the oligomer proportions, one gets a UV mixing curve. The hypochromic change in absorbance upon formation of double and triple stranded complexes results in inflection points at either 0.5, 0.33 or 0.67 mole fraction of one strand (Figure 2B). These points correspond to the complete involvement of strands in complexes.

The fidelity of base-pairing in the PNA:DNA complexes can be examined by challenging the PNA oligomer with a DNA strand bearing a mismatch at a desired site, preferably opposite the site of modification. The base mismatch leads to the absence or incorrect hydrogen bonding between the bases and causes a drop in the measured melting temperature. A modification of the PNA structure is considered good if it gives a much

lower  $T_m$  with DNA sequences containing mismatches as compared to that with unmodified PNA. It is to be pointed out that in all biophysical experiments described herein, the modified PNAs are always evaluated against the unmodified control PNA.

### **3. 4 Gel electrophoresis**

Electrophoresis is a technique used to separate, purify and characterize the macromolecules - especially proteins and nucleic acids - that differ in size, charge or conformation. As such, it is one of the most widely used techniques in biochemistry and molecular biology. This technique is based on the observation that protein:DNA complexes migrate more slowly than free DNA molecules when subjected to non-denaturing polyacrylamide or agarose gel electrophoresis. Because the rate of DNA migration is shifted or retarded upon protein binding, the assay is referred as a gel shift or gel retardation assay.

Gel mobility-shift assay is based on the fact that the electrophoretic mobility of a DNA-fragment in a native polyacrylamide gel typically is reduced by the presence of a PNA strand displacement complex. The shift in gel mobility is apparently not due to the increase in mass but rather reflects structural changes. In addition, the gel-shift assay is fast and technically simple and therefore often used to determine the degree of binding. Frequently, binding of PNA results in not only one but two or more shifted bands. These distinct bands presumably reflect structural isomers or alternative stoichiometry.

### **PRESENT WORK:**

#### **3. 5 CD Studies: Effect of Chiral PNAs**

The achiral PNA backbone does not show any significant CD spectrum. However, single-stranded (*ss*) PNAs with modified chiral backbone when complexed with

complementary DNA sequences are capable of exhibiting characteristic CD signals. A preferred handedness in the complex may be induced by introducing chiral centers within the PNA strand. The process is described as a “seeding of chirality, beginning from the terminal base pair and migrating through the stack of the bases”.<sup>14</sup> The presence of chiral monomers reorganizes the single stranded PNAs and also enhance the helical preferences of the PNA:DNA complexes.

### 3. 5. 1 CD studies (2*S*,5*S*), (2*S*,5*R*), (2*R*,5*S*) and (2*R*,5*R*) of *amp* monomers

The CD-spectra of methanolic solutions of *amp* monomers **22** (2*R*,5*S*), **10** (2*S*,5*R*), **23** (2*R*,5*R*) and **9** (2*S*,5*S*) are shown in Figure 3A. A positive ellipticity was observed for the monomer **22** (2*R*,5*S*) and a negative ellipticity was observed for the monomer **10** (2*S*,5*R*). Trans monomers **9** (2*S*,5*S*) and **23** (2*R*,5*R*) showed positive ellipticity (Figure 3B).

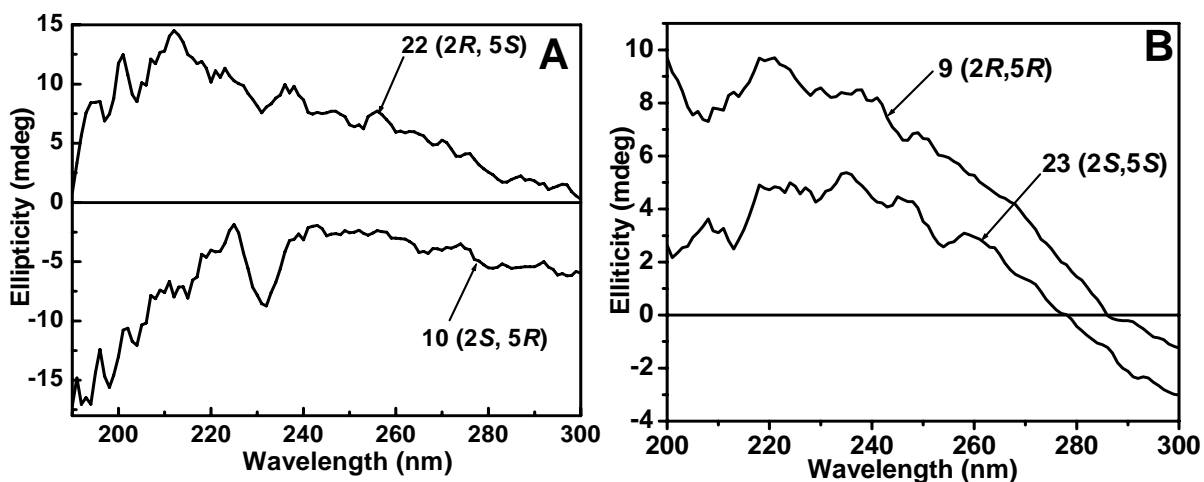


**Figure 3:** CD spectra of enantiomeric *amp* monomers (A) **22** (2*R*,5*S*) and **10** (2*S*,5*R*), (B) **23** (2*R*,5*R*) and **9** (2*S*,5*S*). Buffer: 10 mM sodium phosphate, 10 mM NaCl, pH 7.3.

### 3. 5. 2 CD studies of single strand *amp* PNA oligomers:

As part of the chimeric backbone in *amp-aeg*-PNA oligomers, the chirality of *amp*-PNA oligomers was thought to direct the preferred structure of ssPNAs. These monomers were therefore incorporated into triplex forming homopyrimidine PNA T<sub>8</sub> sequences at N-terminus (PNA **59**, **66**, **72**, **78** and **84**), C-terminus (PNA **61**, **68**, **74**, **80** and **86**), with in the sequence (**60**, **67**, **73**, **79** and **85**) and simultaneously at two positions i.e. at C terminus and second *amp* unit at the fifth (**62**, **63**, **69**, **75** and **81**). In PNA **63** (*2S*, *5R*) *amp*-PNA monomer was incorporated at C-terminus and (*2S,5S*) *amp*-PNA monomer was incorporated at fifth positions respectively to study the additivity of any structural pre-organization due to preferential base stacking. Although the CD spectra of the *amp*-PNA-T<sub>8</sub> single strands differed depending on the stereochemistry and the number of *amp*PNA units. These *amp*-PNA single strand oligomers exhibited CD signals with maxima at 230-260 nm and minima at 210 nm (except *amp*-PNA **62** and **75**) irrespective

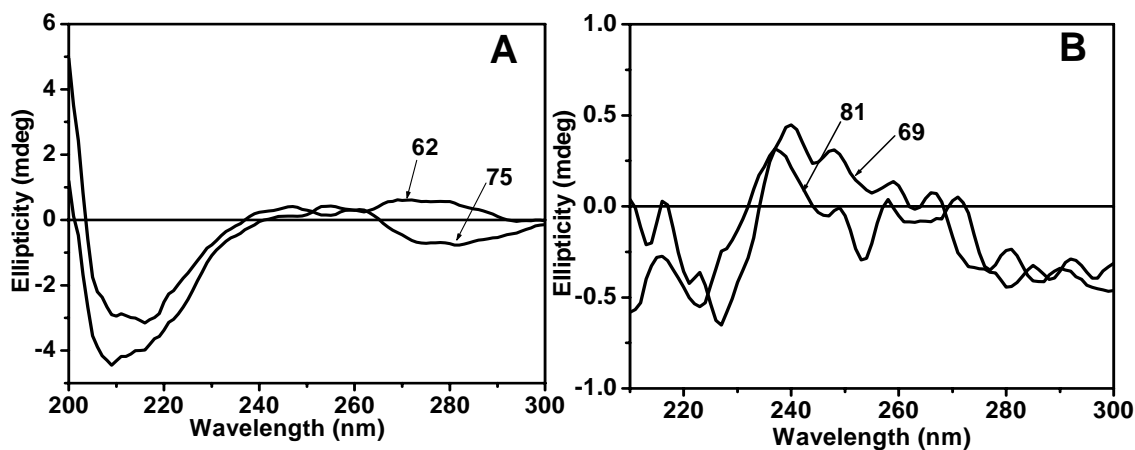


**Figure 4** (A) CD Spectra of ss *amp*-PNA **63**, and PNA**75** (B) *ss amp*-PNA **81** and **69**. Buffer: 10 mM sodium phosphate, 10 mM NaCl, pH 7.3

of the stereochemistry of the pyrrolidine unit. The effect of substitution of the enantiomeric single pyrrolidine *cis* monomers (*2S,5R* and *2R,5S*) and trans monomers (*2S,5S* and *2R,5R*) in the central position of the oligomers **60**, **67**, **73**, **79** and **85** did not reflect in CD. When two units of pyrrolidine enantiomers were present in the PNA oligomers **62**, **63**, **69**, **75** and **81** a close mirror image relationship emerged in their CD profiles (Figure 4). CD spectral data on single strand chiral PNAs thus suggested that propagation of chiral induction.

### 3. 5. 3 CD studies of *amp*-PNA<sub>2</sub>:DNA/RNA triplexes:

Upon complex formation with the complementary DNA, the CD exhibited by the *amp*-PNA:DNA complex (triplexes) was similar to that of the *aeg*-PNA:DNA control triplex in which DNA makes a major contribution to the CD of the complex (Figure 5). However, PNA, a polyamide, can be expected to form helices via intramolecular hydrogen bonding leading to a racemic mixture of right-hand and left-handed helices, with no observable net CD. Upon complexation with DNA/RNA, which are chiral

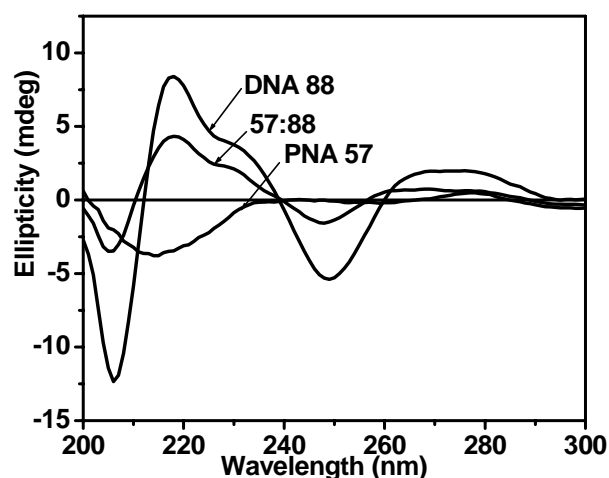


**Figure 5** CD Spectra of *ss*DNA **88**, *ssaeg*-PNA **57** and complex of (*aeg*-PNA **57**)<sub>2</sub>:DNA **88**. Buffer: 10 mM sodium phosphate, 10 mM NaCl, pH 7.3.

molecules, PNA:DNA/RNA triplexes/duplexes exhibit strong CD signals. It is known that formation of PNA triplexes is accompanied by appearance of positive CD bands at 258 nm and 285 nm that are not present in PNA complexes and exhibit characteristic CD signatures due to chirality induced by DNA/RNA (Figures 6, 7 and 8).

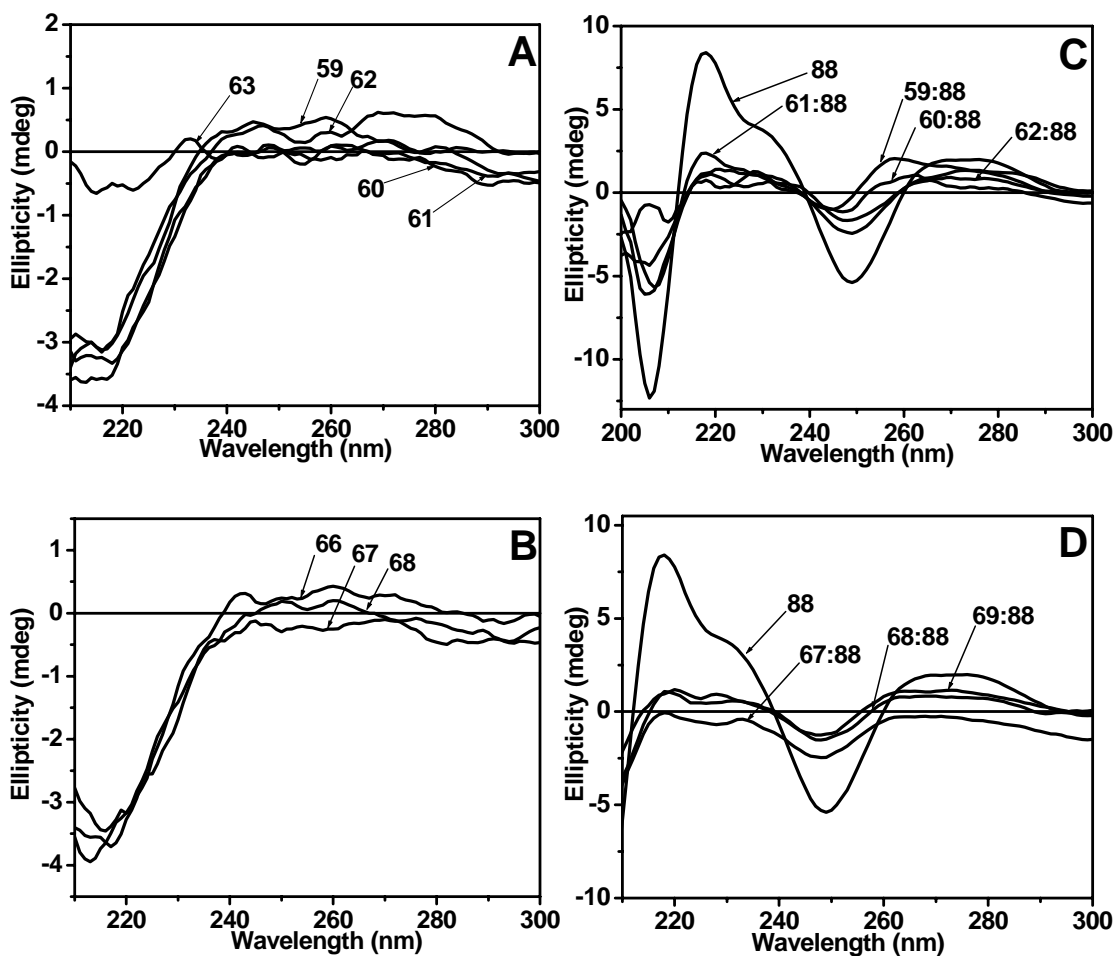


**Figure 6 (A-B)** Representative CD spectra of *ss*(2*S*,5*R*), (2*S*,5*S*) and *ss*(2*R*,5*S*)-*amp*-PNA oligomers. **(C-D)** CD spectra of triplex complexes of *amp*-PNAs with DNA **88**. (Buffer: 10 mM sodium phosphate, 10 mM NaCl, pH = 7.3). DNA **88** = 5'(CGC-AAAAAAAAA-CGC)3'

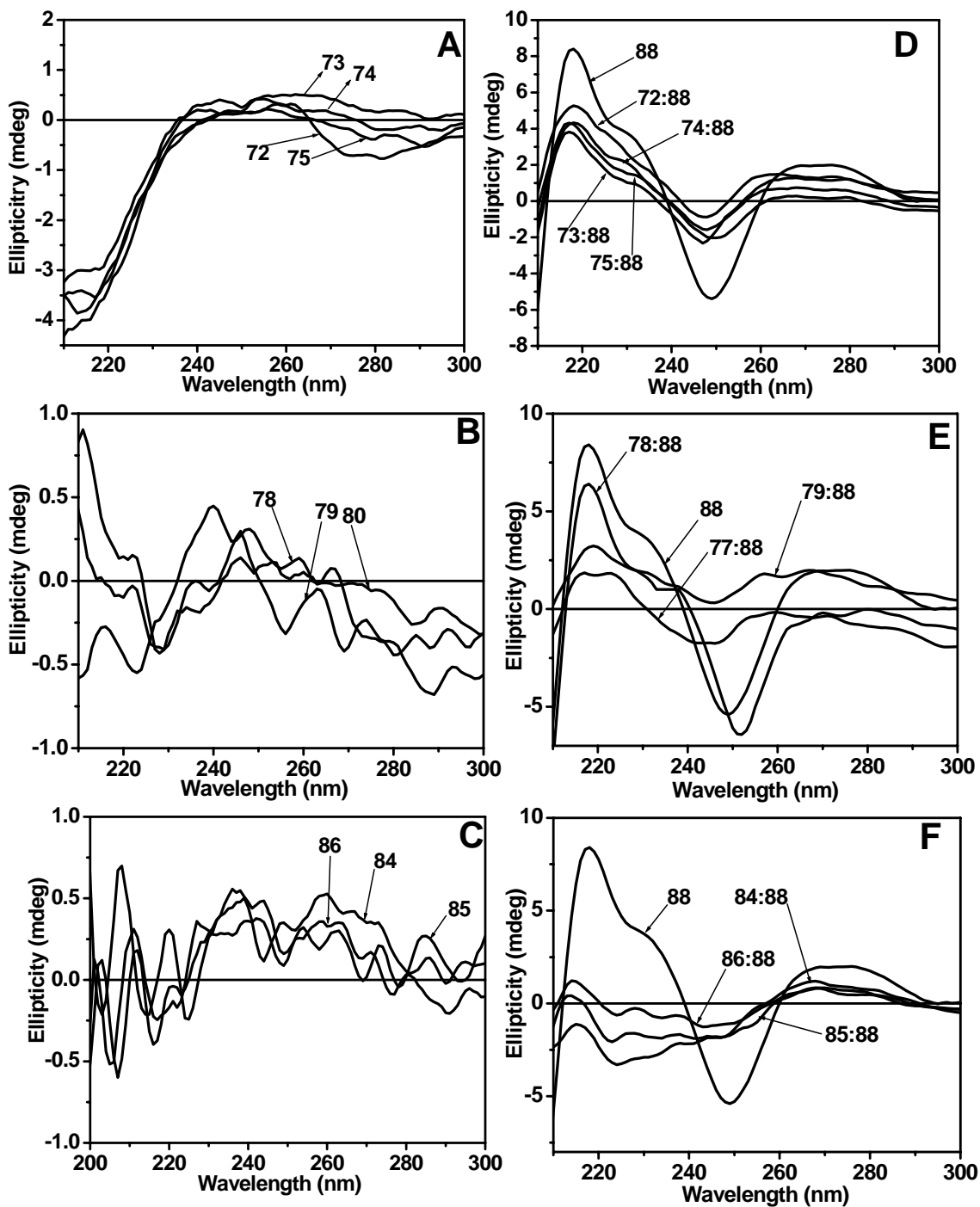


**Figure 7** (A-C) Representative CD spectra of *ss*(2*R*,5*S*), *ss*(2*R*,5*R*) and *ss*(2*S*,4*S*,5*R*)-*amp*-PNA oligomers. (D-F) CD spectra of triplex complexes of *ss*(2*R*,5*S*), (2*R*,5*R*) and *ss*(2*S*,4*S*,5*R*) *amp*-PNAs with DNA **88**. (Buffer, 10 mM sodium phosphate, 10 mM NaCl, pH = 7.3). DNA **88** = 5'(CGC-AAAAAAAAA-CGC)3'

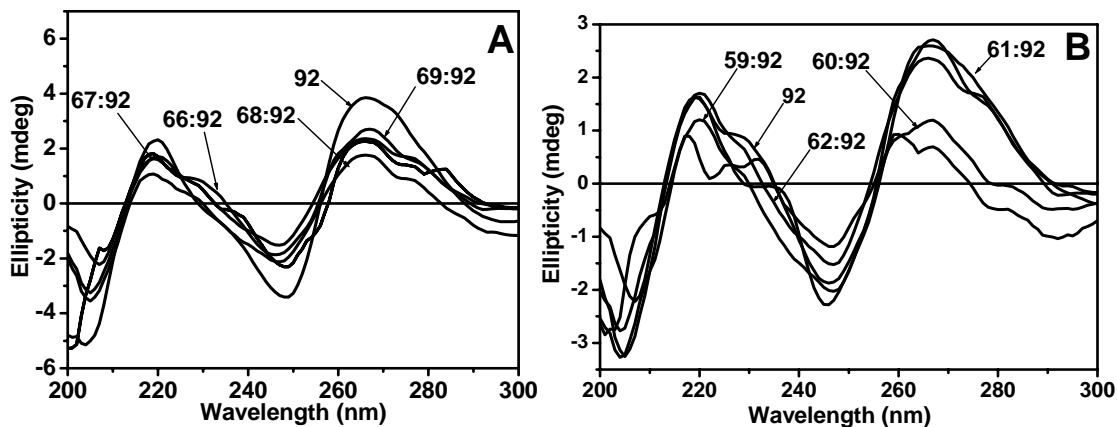


**Figure 8** Representative spectra of *amp*-PNA<sub>2</sub>:RNA triplexes. **A)** CD profiles of (2*S*,5*R*)-*amp*-PNA<sub>2</sub>:RNA triplexes. **B)** CD-Spectra of (2*S*,5*S*) *amp*-PNA<sub>2</sub>:RNA triplexes.

### 3. 5. 4 CD studies of Homooligomers

Homooligomeric octamers, each bearing eight modified units of (2*S*,5*R*)-*amp*-PNA**65**, (2*S*,5*S*)-*amp*-PNA**71**, (2*R*,5*S*)-*amp*-PNA**77**, and (2*R*,5*R*)-*amp*-PNA**83** *amp* PNA were also synthesized to study the effect of only modified backbone. Homooligomer (2*S*,5*R*)-PNA**65** exhibited negative ellipticity with CD signal maxima at 240 nm and minima at 210 nm, whereas (2*R*,5*S*)-PNA**77** exhibited CD signal with maxima at 210 nm and minima at 240 nm. Thus a mirror image relationship has emerged in the CD profiles of the enantiomeric homooligomers (2*R*,5*S*)-*amp*-PNA **65** and (2*R*,5*S*)-*amp***77** (Figure 9A). The CD profile of homooligomers PNA (2*S*,5*S*)-*amp*-PNA**71** and (2*R*,5*R*)-*amp*-PNA **83** also exhibit a mirror image relationship (Figure 9B). Upon complex formation with complementary DNA, CD positive maxima at 220-230 nm and 260-280 nm, negative minima at 246 nm with crossover points at 240-250 nm were observed. The positive bands in the region of 260-280 nm seen in the CD spectra of complexes, are characteristic of PNA<sub>2</sub>:DNA triplex. (Figure 8).

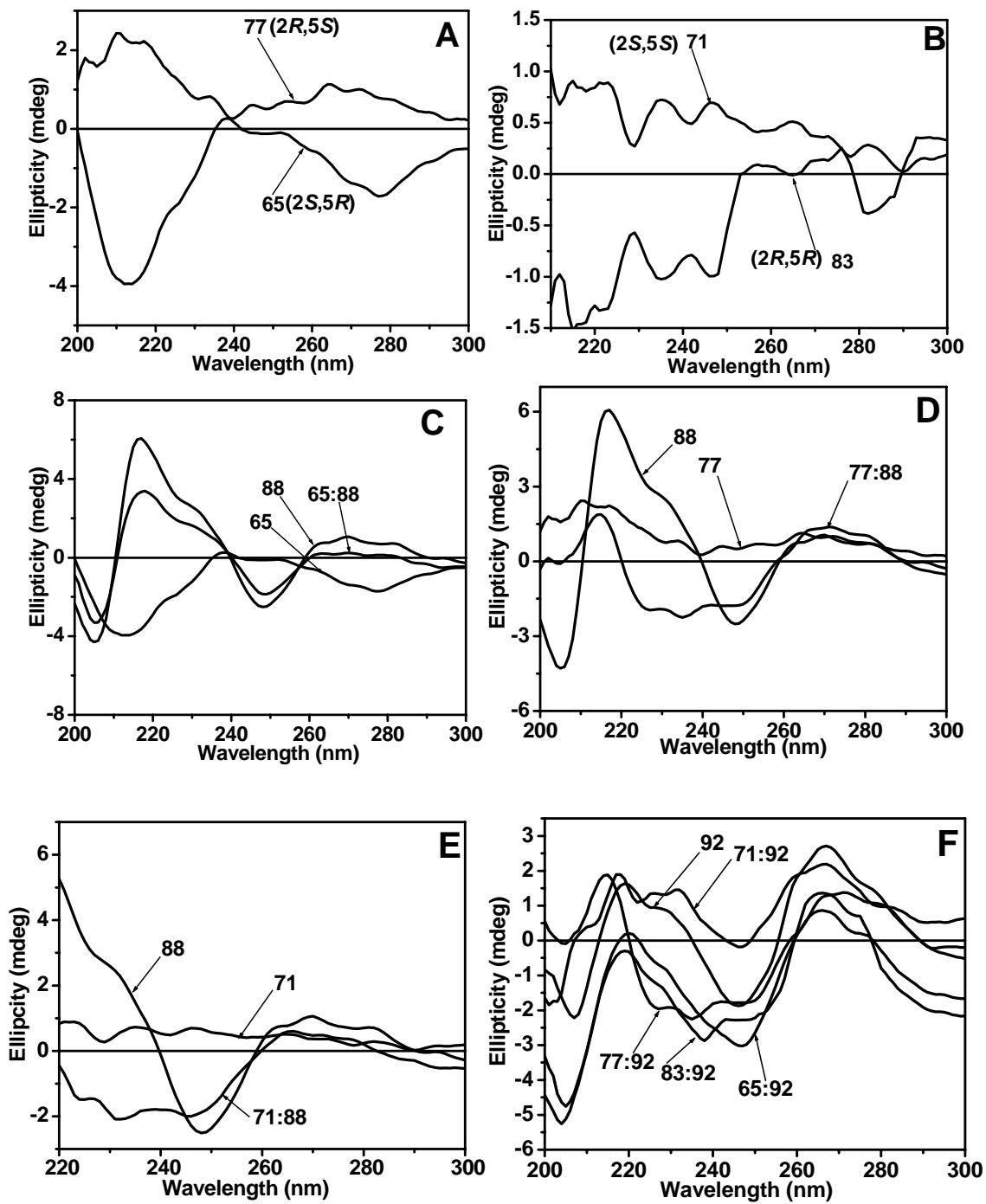


**Figure 9** (A-B) CD spectra of (2S,5R), (2S,5S), (2R,5S) and (2R,5R)-amp-PNA-T8 homooligomers (C,D and E) Homooligomer triplex with DNA **88** 5'(CGC-AAAAAAAA-CGC)3'. **F**) Homooligomer triplexes with RNA **92**. (Buffer, 10 mM sodium phosphate, 10 mM NaCl, pH = 7.3).

### 3. 6 Binding Stoichiometry: CD and UV-mixing Curves

Ultraviolet (UV) absorption and circular dichroism (CD) measurements are extremely useful to determine the stoichiometry and stability of duplexes and triplexes. The stoichiometry of the paired strands may be obtained from the mixing curves, in which the optical property at a given wavelength is plotted as a function of the mole fraction of each strand from isodichroic and isoabsorptive point (Job's plot).<sup>15</sup> The combination of absorption and CD spectra provides unambiguous determination of the complex formation and strand stoichiometry than is provided by absorption spectra alone.

Various stoichiometric mixtures of *amp*-PNA65 and DNA88 were made with relative molar ratios of (*amp*-PNA65:DNA88) strands of 0:100, 20:80, 40:60, 50:50, 60:40, 80:20, 100:0, keeping all the same total strand concentration 2  $\mu$ M in sodiumphosphate buffer, 100 mM NaCl (10 mM, pH 7.3). The samples with the individual

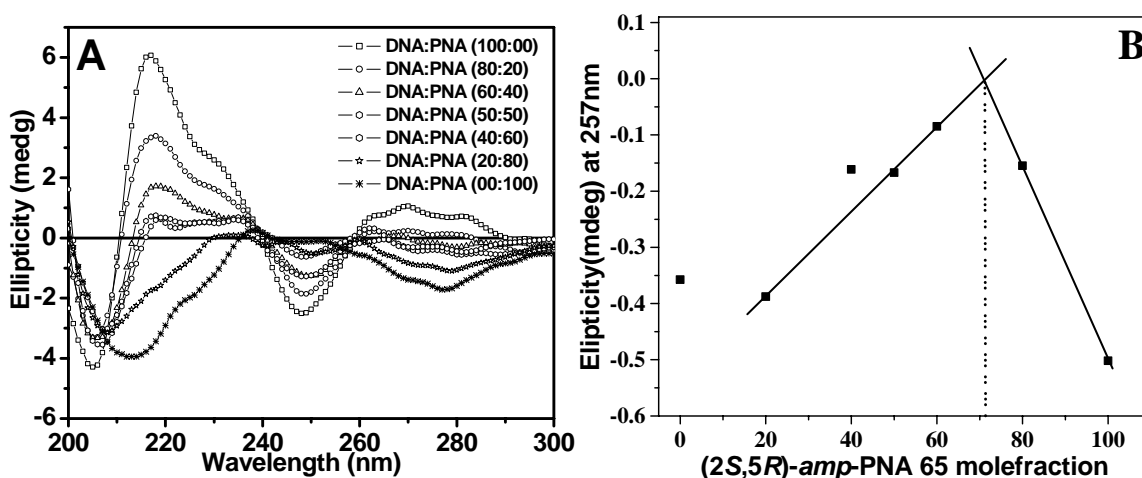


**Figure 10** A) CD-curves for mixture of *amp*-PNA 65 and the complementary DNA 88 =5' (CGC-AAAAAAAAA-CGC) 3' mixtures in the molar ratios of 0:100, 10:90, 20:80, 40:60, 50:50, 60:40, 80:20, 100:0 (Buffer, 10 mM Sodium phosphate pH 7.3, 10 mM NaCl), B) UV-job plot corresponding to 248 nm.

strand combinations were annealed and the CD spectra were recorded (Figure 10A). The CD spectra at different molar ratios show a isodichroic point (wavelength of equal CD magnitude) around 265 nm. This systematic change in the CD spectral features upon variable stoichiometric mixing of PNA and DNA components can be used to generate Job's plot which indicated a binding ratio of 2:1 for the *amp*-PNA<sub>2</sub>:DNA complexes, expected for triplex formation. UV- absorbance spectra were recorded for the mixtures of *amp*-PNA **65**:DNA **88** in different proportions as mentioned above. A mixing curve was plotted, using absorbance at fixed wavelength ( $\lambda_{\max}$  260 nm) against mole fractions of *amp*-PNA **65**. Figure 10B shows the change in  $\lambda_{\max}$  observed for the mixtures of different molar fractions. There is a drastic shift in the  $\lambda_{\max}$  value when the concentration of *amp*-PNA **65** in the mixtures increased to 70%, which further increases behind that proportion. These results supports the formation of (*amp*-PNA **65**)<sub>2</sub>:DNA **88** triplexes. Same results were observed with (2*R*,5*S*)-*amp*-PNA **77** (Figure 11B).

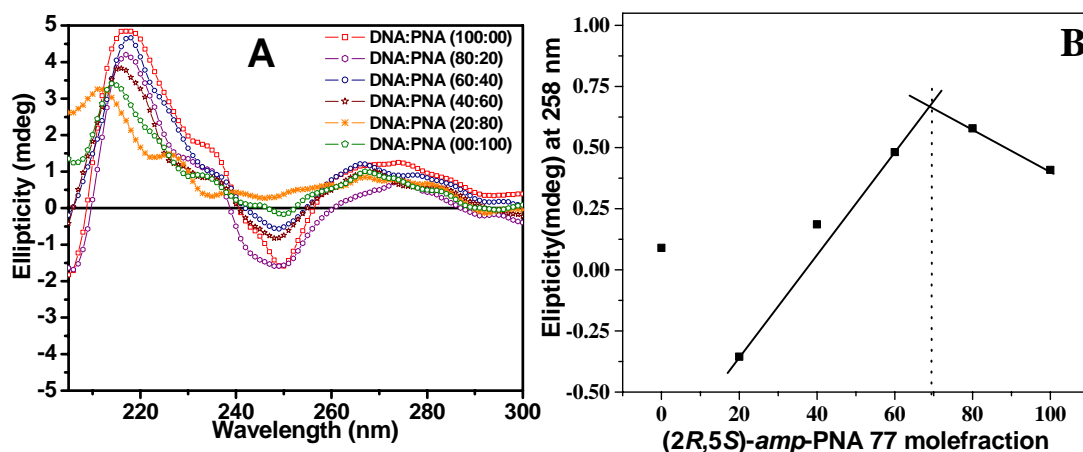


**Figure 11** A) CD-curves for mixtures of (2*R*,5*S*)-*amp*-PNA **77** and the complementary DNA **88** 5'(CGC-AAAAAAAA-CGC)3' in the molar ratios of 0:100, 10:90, 20:80, 40:60, 50:50, 60:40, 80:20, 100:0 (Buffer, 10 mM Sodium phosphate pH 7.3, 10 mM NaCl), B) CD-job plot corresponding to 248 nm .

The UV-titration (Figure 12 and 13) experiments involving the stoichiometric addition of *amp*-PNAs **69**, **81** and **86** to DNA **88** led to a decrease in UV absorbance with *amp* PNAs. The absorbance showed a similar saturation minima around 2:1 stoichiometry suggesting the formation of a PNA<sub>2</sub>:DNA triplex.

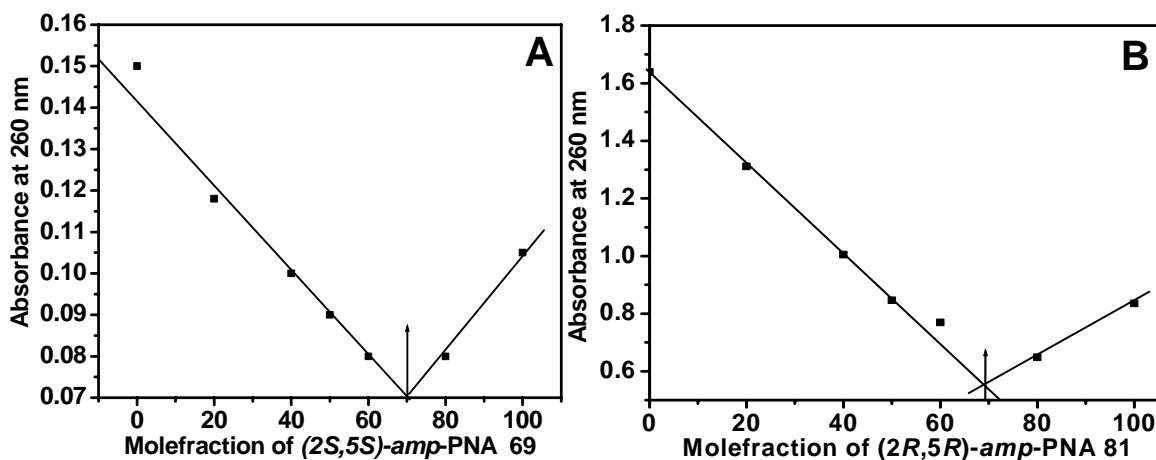


**Figure 12** A) UV-titration of (2S,5S)-*amp*-PNA **69**:DNA **88** complexes. B) UV-titration of (2R,5R)-*amp*-PNA **81**:DNA **88** complexes. Buffer 10 mM Sodium phosphate pH 7.3, 10 mM NaCl. DNA **88** = 5'(CGC-AAAAAAAA-CGC)3'

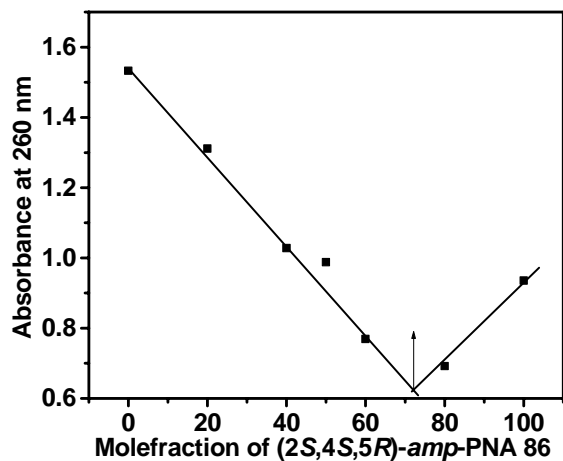


**Figure 13** UV-titration of (2R,4S,5R)-*amp*-PNA **86**:DNA **88** complexes. Buffer, 10 mM Sodium phosphate pH 7.3, 10 mM NaCl. DNA **88** = 5'(CGC-AAAAAAAA-CGC)3'

### 3. 7 CD Spectra of duplexes:

The *amp*-PNA:DNA duplexes (Figure 14) show CD profiles similar to that of *aeg*-PNA:DNA duplex, with a positive band at 277 nm and a low intensity negative band at 250 nm. The single stranded *amp*PNAs containing chiral (2*S*,5*R*)- and (2*R*,5*S*)-aminomethyl prolyl units have strong and distinct CD spectra PNA **64** and **76** (Figure 14A and 14B). The single strand *amp*PNAs having chiral (2*S*,5*S*), (2*R*,5*R*) and (2*S*,4*S*,5*R*) units exhibited weak CD signature PNAs **70**, **82** and **87**. The dominant CD contributions from DNA, strands in the complexes, differences are due to *SR/RS* and *SS/RR* are not apparent.

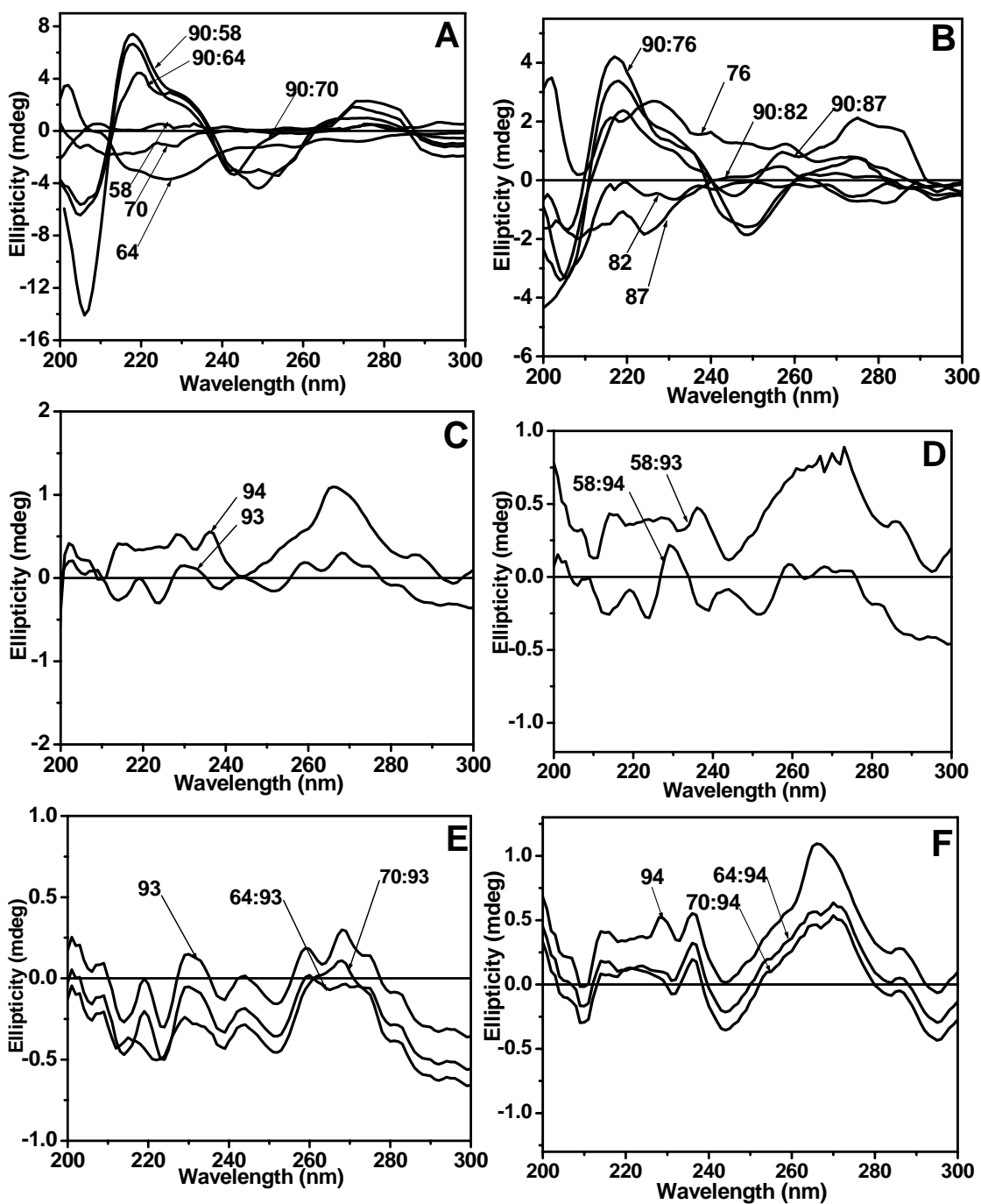


**Figure 14** (A-B) CD profiles of *amp*-PNA:DNA duplexes. C) CD-Spectra of ssRNA-**93** and **94**. D) CD spectra of *aeg*-PNA **58** duplexes with RNA-**93** and **94**. (E-F) Duplex of (*2S,5R*)-*amp*-PNA-**64** and (*2S,5S*)-*amp*-PNA-**70** with corresponding *antiparallel* and *parallel* sequences **93** and **94**. (Buffer, 10 mM Sodium phosphate pH 7.3, 10 mM NaCl). DNA-**90** = 5'AGTGATCTAC3' (*antiparallel*); DNA-**91** = 5'CATCTAGTGA; RNA-**93**=5'AGUGAUCUAC3'; RNA- **94** = 5'CAUCUAGUGA3'.

### 3. 8 UV-Melting studies of (2*S*,5*R*) and (2*S*, 5*S*) *amp*-PNA<sub>2</sub>-DNA triplexes

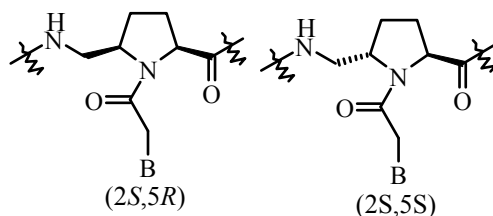


**Figure 15** (2*S*,5*R*) and (2*S*,5*S*) *amp*-PNAs

Hybridization studies of modified PNAs (Figure 15) with complementary DNA **88** sequences were done by temperature dependent UV-absorbance experiments. The stoichiometry for homopyrimidine PNA<sub>2</sub>:DNA complexation as established by UV absorbance mixing data at 260 nm (Job's plot),<sup>15</sup> was 2:1 ratio (Figure 10A). The thermal stabilities ( $T_m$ ) of PNA<sub>2</sub>:DNA triplexes were obtained for different PNA modifications with complementary DNA **88** (Figure 16) given in Table 2.

Table 2 shows the  $T_m$  values for PNA<sub>2</sub>:DNA complexes derived from various *aeg*-PNA and *amp*-PNA sequences of different stereochemistry and degree of modification. The first derivative plots of temperature-percent hyperchromicity for PNA<sub>2</sub>:DNA triplexes indicated a single transition (Figure 16 A to C), characteristic of both PNA strands dissociating simultaneously from DNA in a single step. The  $T_m$  values (Table 2, entry 2 and 8) indicate that the *amp*-PNA oligomers **59** and **66** having single modification at N-terminus exhibited stabilization compared to the unmodified PNA T<sub>8</sub> homooligomer **57**. One (2*S*,5*R*)-*amp* unit at the N-terminus has a better stability of its complex with the complementary DNA **88** as compared to (2*S*,5*S*). The situation was reversed for the corresponding modification at C-terminus; the (2*S*,5*S*)-*amp*-PNA **68** (Table 2, entry 4) forming a much more stable hybrid compared to that of the (2*S*,5*R*)-*amp*-PNA **61** oligomer (Table 2, entry 10). The *amp*-PNA oligomer **60** (Table 2) having

modification in the center of the sequence destabilized the complexes with DNA **88** (Table 2, entry 3), while *amp*-PNA oligomer **67** (entry 9) having the same modification with (2*S*,5*S*) stereo-chemistry stabilized the complex with DNA **88** in comparison to the control PNA **57** (entry 1).

**Table 2** UV-Melting temperatures ( $T_m$  values in °C) of *amp*PNA<sub>2</sub>:DNA**88** triplexes.

Entry	PNA	$T_m$ °C	$\Delta T_m$ °C
1	<i>aeg</i> PNA <b>57</b> H-T-T-T-T-T-T-T-T-(CH <sub>2</sub> ) <sub>2</sub> -CONH <sub>2</sub>	43	
2	<i>amp</i> PNA <b>59</b> H- <b>t</b> <sub>SR</sub> -T-T-T-T-T-T-T-CH <sub>2</sub> ) <sub>2</sub> -CONH <sub>2</sub>	53	+10
3	<i>amp</i> PNA <b>60</b> H-T-T-T- <b>t</b> <sub>SR</sub> -T-T-T-T-(CH <sub>2</sub> ) <sub>2</sub> -CONH <sub>2</sub>	35	-8
4	<i>amp</i> PNA <b>61</b> H-T-T-T-T-T-T-T- <b>t</b> <sub>SR</sub> -(CH <sub>2</sub> ) <sub>2</sub> -CONH <sub>2</sub>	46	3
5	<i>amp</i> PNA <b>62</b> H- <b>t</b> <sub>SR</sub> -T-T-T- <b>t</b> <sub>SR</sub> -T-T-T (CH <sub>2</sub> ) <sub>2</sub> -CONH <sub>2</sub>	39	-4
6	<i>amp</i> PNA <b>63</b> H- <b>t</b> <sub>SR</sub> -T-T-T- <b>t</b> <sub>SS</sub> -T-T-T (CH <sub>2</sub> ) <sub>2</sub> -CONH <sub>2</sub>	45	+2
7	<i>amp</i> PNA <b>65</b> H-( <b>t t t t t t t t</b> ) <sub>SR</sub> -(CH <sub>2</sub> ) <sub>2</sub> -CONH <sub>2</sub>	77	+34
8	<i>amp</i> PNA <b>66</b> H- <b>t</b> <sub>SS</sub> -T-T-T-T-T-T-T-CH <sub>2</sub> ) <sub>2</sub> -CONH <sub>2</sub>	47	+4
9	<i>amp</i> PNA <b>67</b> H-T-T-T- <b>t</b> <sub>SS</sub> -T-T-T-T-(CH <sub>2</sub> ) <sub>2</sub> -CONH <sub>2</sub>	43	-
10	<i>amp</i> PNA <b>68</b> H-T-T-T-T-T-T-T- <b>t</b> <sub>SS</sub> -(CH <sub>2</sub> ) <sub>2</sub> -CONH <sub>2</sub>	50	+7
11	<i>amp</i> PNA <b>69</b> H- <b>t</b> <sub>SS</sub> -T-T-T- <b>t</b> <sub>SS</sub> -T-T-T (CH <sub>2</sub> ) <sub>2</sub> -CONH <sub>2</sub>	44	+1
12	<i>amp</i> PNA <b>71</b> H-( <b>t t t t t t t t</b> ) <sub>SS</sub> -(CH <sub>2</sub> ) <sub>2</sub> -CONH <sub>2</sub>	43	-1

Buffer: 10 mM sodium phosphate, 10 mM NaCl, pH 7.3.  $T_m$  values are accurate to ( $\pm$ ) 0.5°C. Experiments were repeated at least thrice and the  $T_m$  values were obtained from the peaks in the first derivative plots.  $\Delta T_m$  indicates the difference in  $T_m$  with the control experiment *aeg*-PNA **57**. T and **t** indicating *aeg* and *amp*-PNA respectively. DNA **88** = 5'(CGC-AAAAAAAAA-CGC) 3'

In case of *amp*-PNA oligomers **62**, **63** and **69** (Table 2, entry 5, 6 and 11) having two modified units, one at N-terminal and another at center, a decrease in  $T_m$  was observed in case of (2*S*,5*R*)-*amp*-PNA **62**, whereas (2*S*,5*S*)-*amp*-PNA **69** stabilized the complex with DNA **88** in comparison to control PNA **57**. PNA **63** contains two diastereomeric *amp* units, (2*S*,5*R*)-*amp* at N-terminus and (2*S*,5*R*)-*amp* unit at the center of the sequence and stabilized the triplex with DNA **88** better than PNA **62** and **69** having the two identical modifications (*SS* or *RR*). Thus a synergetic effect was observed when

two diastereomeric *amp* units were site specifically incorporated in to PNA oligomer (entry 6).

Octamers bearing eight modified units as in homooligomers of (2*S*,5*R*)-*amp* PNA **65**, (2*S*,5*S*)-*amp*-PNA **71**, were synthesized to study the effect of stereochemistry on completely modified backbone. Significantly, in contrast to singly and doubly modified analogues, the all-modified homooligomeric, homochiral *amp*-PNA-(2*S*,5*R*)-**65** exhibited high thermal stabilities ( $\Delta T_m = +34$  °C) compared to the unmodified PNA **57**. Homooligomeric, homochiral (2*S*,5*S*)-*amp*-PNA **71** ( $\Delta T_m = -1$  °C, entry 12 ) marginally destabilized the complex with DNA **88**.

The *amp*-PNA sequence with single modification in the center with (2*S*,5*R*)-*amp*-PNA **60**, largely destabilized the complex with DNA **88**. This could be a result of introduction of unfavorable conformational discontinuity at the modification site. However, in the fully modified oligomer **65** with the same stereochemistry, the stability is regained perhaps due to the uniform conformational change over the entire backbone, without any sharp discontinuities.

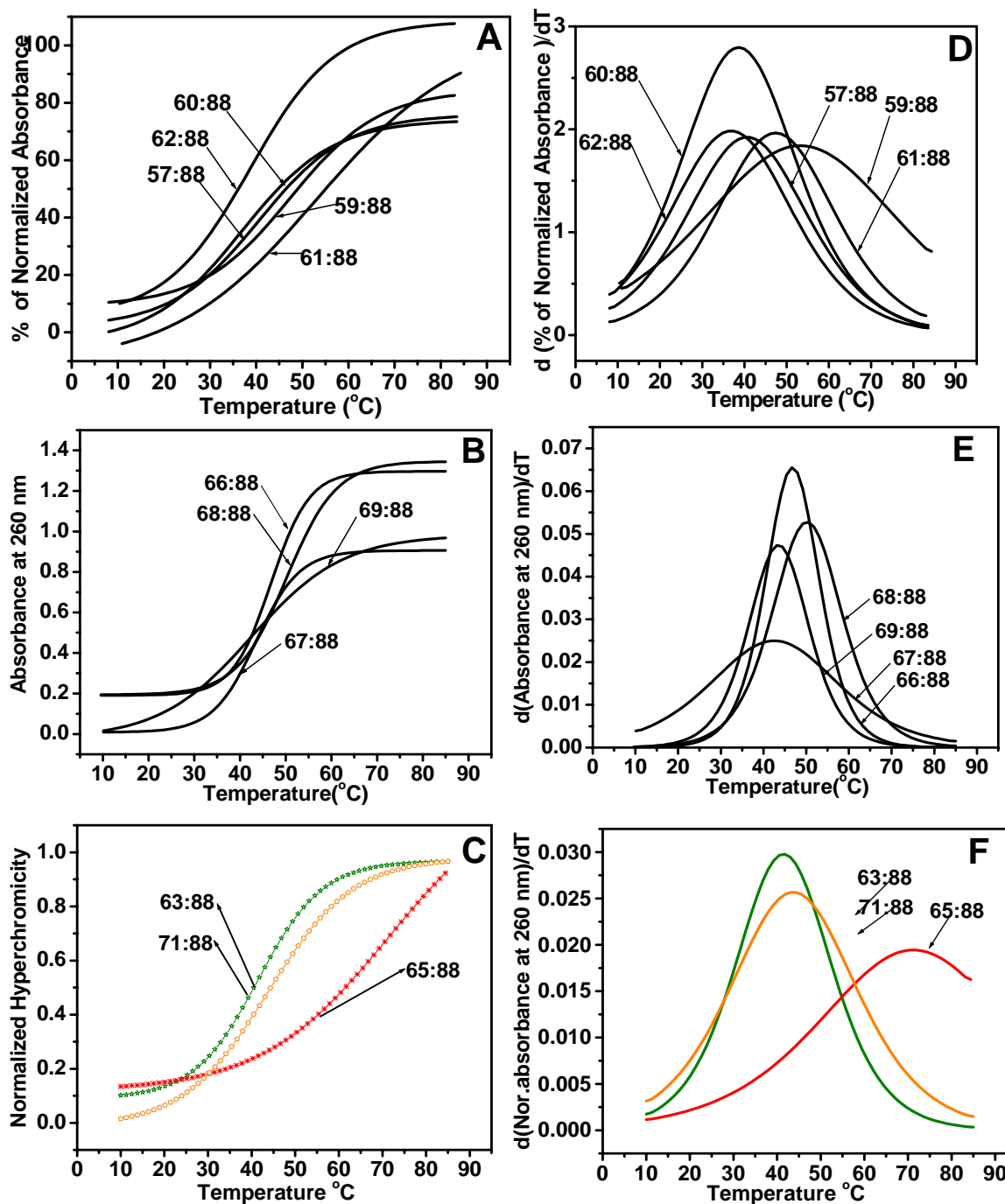


**Figure 16** (A, B and C) UV-Melting profiles of  $(2S,5R)$ -amp-PNA<sub>2</sub>:DNA **88** and  $((2S,5S)$ -amp-PNA)<sub>2</sub>:DNA **88** complexes. (D, E and F) UV-Melting first derivative curves of  $(2S,5R)$  and  $(2S,5S)$ -amp-PNA triplexes. (Buffer, 10 mM Sodium phosphate pH = 7.3, 10 mM NaCl), DNA **88** = 5'(CGC-AAAAAAAA-CGC)3'

### 3. 8. 1 UV- $T_m$ Studies of Duplexes

The oligothymine sequences described above were found to form triplexes in which the relative binding orientation (*parallel-antiparallel*) of the two PNA strands involved in complex formation does not matter. In order to study the *parallel* and *antiparallel* orientational preferences of PNA:DNA binding, mixed purine pyrimidine sequences that form duplexes were synthesized.

The mixed 10-mer PNA sequences PNA **58**, has been demonstrated to form duplexes with the complementary DNAs **90** (*antiparallel*) and **91** (*parallel*) and hence useful to examine the orientational selectivity in binding to DNA. Hence,  $T_m$  studies of PNA:DNA duplexes derived from PNA oligomers (PNA **64** and PNA **70**) containing (*2S,5R*) and (*2S,5S*)-*amp*-PNA units were carried out. The duplexes were constituted by individually mixing equimolar amounts of complementary achiral *aeg*-PNA **58** and chiral *amp*-PNAs **64** and **70** with DNA oligomers **90** and **91** in phosphate buffer. The UV- $T_m$  profiles of complexes PNAs **58**, **64** and **70** with DNA sequences **90** and **91** designed to bind in *antiparallel* and *parallel* orientations respectively is shown in Figure 17 and the values given in Table 3. In both PNAs, the *antiparallel* duplex was more stable than the *parallel* duplex.

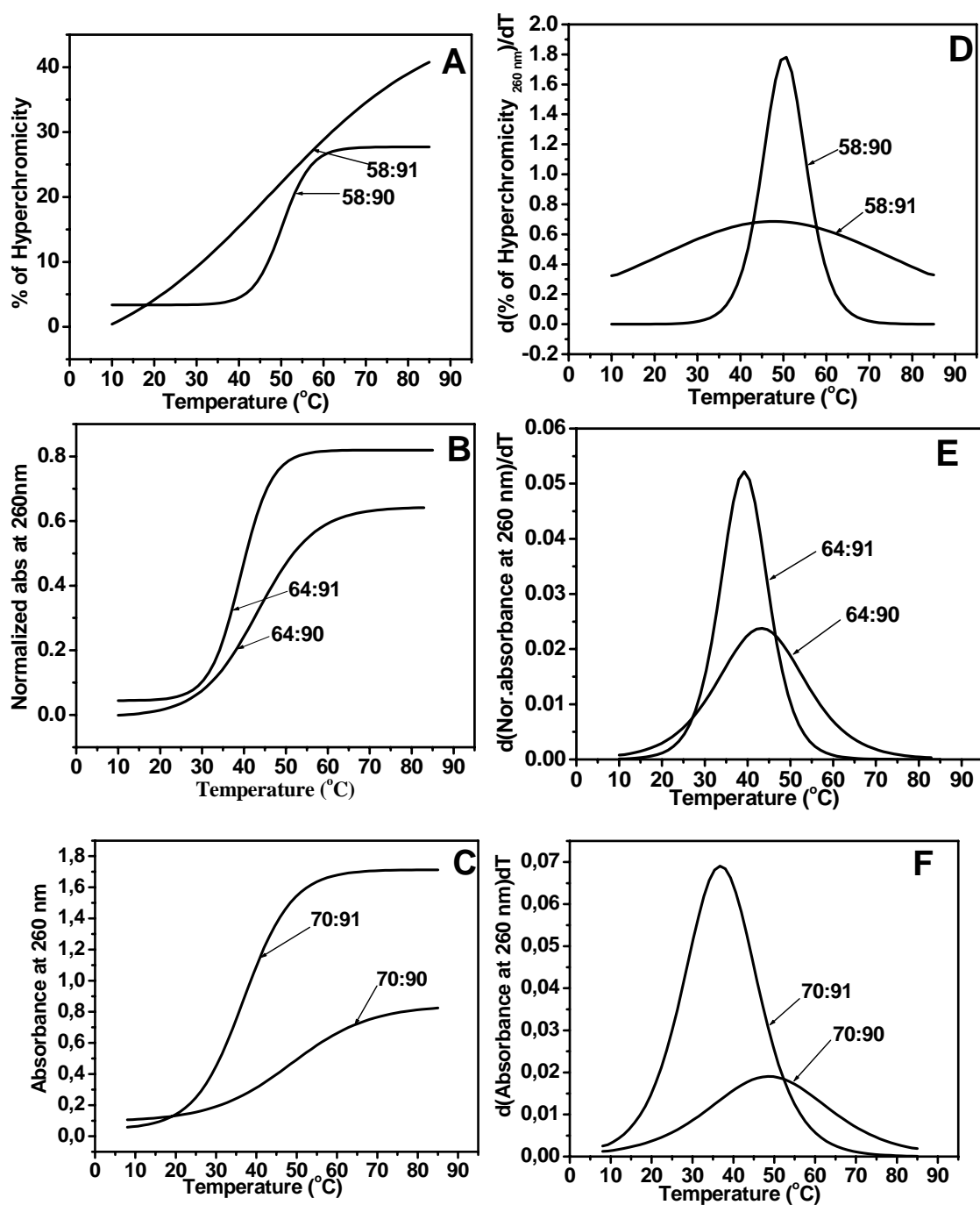


**Figure 17** (A, B and C) UV-Melting profiles of duplexes of *aeg*-PNA58, (2*S*,5*R*)-*amp*-PNA64 and (2*S*,5*S*)-*amp*-PNA70 with DNA 90 (*antiparallel*) and DNA 91 (*parallel*) D, E and F) UV-Melting first derivative curves of *aeg*-PNA, (2*S*,5*R*) and (2*S*,5*S*)-*amp*-PNA (Buffer, 10 mM Sodium phosphate, 10 mM NaCl, pH = 7.3). DNA 90 = 5' AGTGATCTAC 3' (*antiparallel*); DNA 91 = 5' CATCTAGTGA 3' (*parallel*).

The unmodified PNA **58** with achiral  $\beta$ -alanine at C-terminus formed duplex with complementary DNA in both *parallel* and *antiparallel* orientations, with *parallel* mode slightly destabilizing than the *antiparallel* duplex. (Table 3, Figure 17 A and D). However, the modified (2*S*,5*R*)-*amp*-PNA **64** destabilized both the *antiparallel* and *parallel* duplexes, while the (2*S*,5*S*)-*amp*-PNA **70** marginally stabilized the *antiparallel* duplex and destabilized the *parallel* duplex by 13 °C in comparison to control PNA-**58**.  $T_m$  values are listed in Table-3. The results indicate that the (2*S*,5*R*) and (2*S*,5*S*)-amino methyl-*aeg*PNA oligomers bind preferentially in *ap*-mode with complementary DNA. The difference in the  $T_m$  of *antiparallel* and *parallel* duplex complexes of *amp*-PNA oligomers reflects the selectivity in orientational binding towards DNA **90** and **91**.

It is seen that the (2*S*,5*S*)-*amp*-PNA **70** discriminates between *parallel* and *antiparallel* binding much better than the (2*S*,5*R*)-*amp*-PNA **64**

**Table 3** UV-Melting temperatures (in °C) of (2*R*,5*S*) and (2*R*,5*R*)-*amp*-PNA:DNA *ap/p* duplexes

Entry	PNA	$T_m$	$^*\Delta T_m$	$\#\Delta T_m$
1	<i>amp</i> PNA <b>58</b> H-G-T-A-G-A-T-C-A-C-T-(CH <sub>2</sub> ) <sub>2</sub> CONH <sub>2</sub>	50 ( <i>ap</i> )	-	2
2	<i>amp</i> PNA <b>58</b> H-G-T-A-G-A-T-C-A-C-T-(CH <sub>2</sub> ) <sub>2</sub> CONH <sub>2</sub>	48 ( <i>p</i> )	-	-
3	<i>amp</i> PNA <b>64</b> H-G- <b>t</b> <sub>SR</sub> -A-G-A- <b>t</b> <sub>SR</sub> -C-A-C- <b>t</b> <sub>SR</sub> -(CH <sub>2</sub> ) <sub>2</sub> CONH <sub>2</sub>	43 ( <i>ap</i> )	-7	4
4	<i>amp</i> PNA <b>64</b> H-G- <b>t</b> <sub>SR</sub> -A-G-A- <b>t</b> <sub>SR</sub> -C-A-C- <b>t</b> <sub>SR</sub> -(CH <sub>2</sub> ) <sub>2</sub> CONH <sub>2</sub>	39.2 ( <i>p</i> )	-9	-
5	<i>amp</i> PNA <b>70</b> H-G- <b>t</b> <sub>SS</sub> -A-G-A- <b>t</b> <sub>SS</sub> -C-A-C- <b>t</b> <sub>SS</sub> -(CH <sub>2</sub> ) <sub>2</sub> CONH <sub>2</sub>	51 ( <i>ap</i> )	1	14
6	<i>amp</i> PNA <b>70</b> H-G- <b>t</b> <sub>SS</sub> -A-G-A- <b>t</b> <sub>SS</sub> -C-A-C- <b>t</b> <sub>SS</sub> -(CH <sub>2</sub> ) <sub>2</sub> CONH <sub>2</sub>	36.41( <i>p</i> )	11.6	-

A/G/C/T = *aeg*-PNA Adenine /Guanine /Cytosine /Thymine monomers, **t**<sub>SR</sub> = (2*S*,5*R*)-*amp*-PNA Thymine monomer, **t**<sub>SS</sub> = (2*S*,5*S*)-*amp*PNA Thymine monomer.  $^*\Delta T_m$  Indicate the difference in  $T_m$  with the control experiment *aeg*-PNA **58**.  $\#\Delta T_m$  Indicate difference in the  $T_m$  of *antiparallel* and *parallel* binding modes. The values reported here are the average of 3 independent experiments and are accurate to  $\pm 0.5^\circ\text{C}$ .  $T_m$  = melting temperature (measured in the buffer 10 mM sodium phosphate, 10 mM NaCl, pH = 7.3). DNA **90** = 5'AGTGATCTAC3'; DNA **91** = 5' CATCTAGTGA3'.



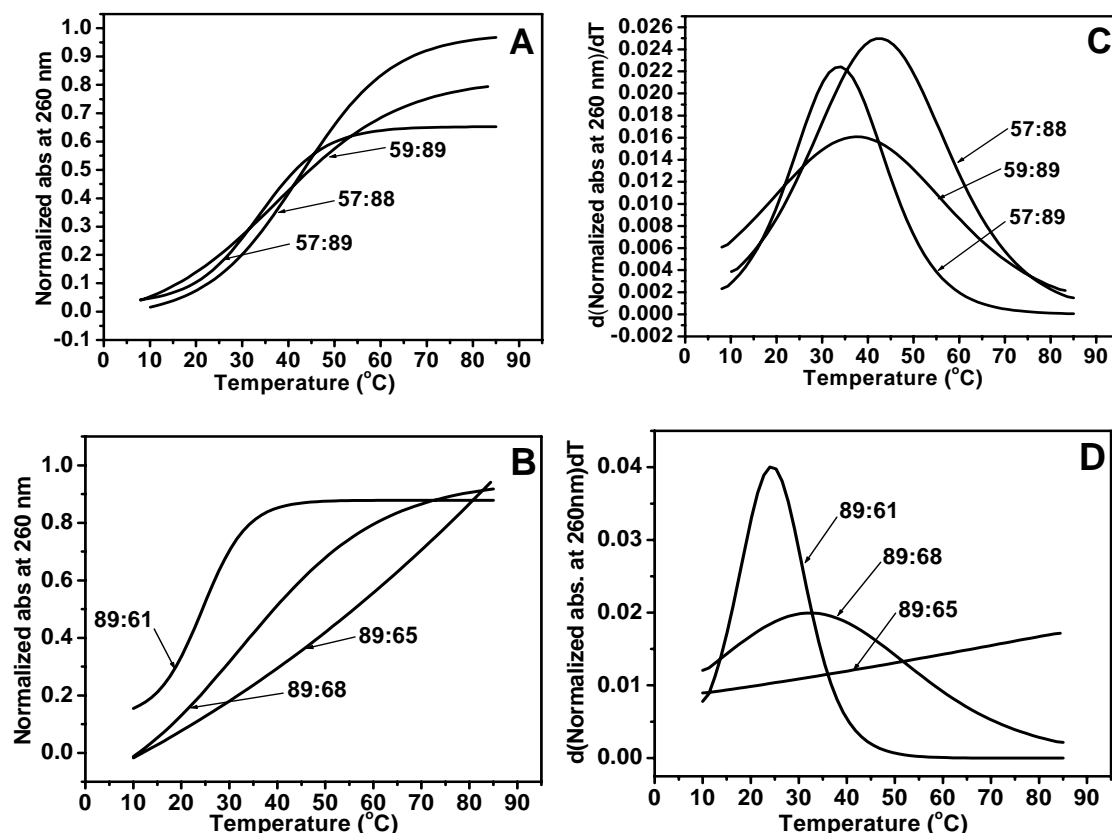


**Figure 19** (A) UV-Melting profiles of *amp*-PNA **59** and *aeg*-PNA**57** with DNA **89**, (B) UV-Melting profiles *amp*-PNAs **61**, **65**, and **68** with DNA **89**. (C,D) UV-Melting first derivative curves of mismatched *aeg*-PNA<sub>2</sub>:DNA **89** and *amp*-PNA<sub>2</sub>:DNA **89** mismatched complexes. (Buffer, 10 mM Sodium phosphate pH = 7.3, 10 mM NaCl). DNA **88** = 5'CGCA<sub>8</sub>CGC3'; DNA **89** = 5'CGCA<sub>4</sub>CA<sub>3</sub>CGC3'

**Table 4** UV- $T_m$  (°C) of PNA<sub>2</sub>:DNA mismatched triplexes.

Entry	PNA	$T_m$ (°C)	$\Delta T_m$
1	<i>aeg</i> PNA <b>57</b> H-T-T-T-T-T-T-T-(CH <sub>2</sub> ) <sub>2</sub> -CONH <sub>2</sub>	33.6	9.4
2	<i>amp</i> PNA <b>59</b> H- t <sub>SR</sub> -T-T-T-T-T-T-T-(CH <sub>2</sub> ) <sub>2</sub> -CONH <sub>2</sub>	37	16
3	<i>amp</i> PNA <b>61</b> H-T-T-T-T-T-T-t <sub>SR</sub> -(CH <sub>2</sub> ) <sub>2</sub> -CONH <sub>2</sub>	24	22
4	<i>amp</i> PNA <b>68</b> H-T-T-T-T-T-T-t <sub>SS</sub> -(CH <sub>2</sub> ) <sub>2</sub> -CONH <sub>2</sub>	33	17
5	<i>amp</i> PNA <b>65</b> H-(t t t t t t t t) <sub>SR</sub> -(CH <sub>2</sub> ) <sub>2</sub> -CONH <sub>2</sub>	ND	-

$T_m$  values are accurate to ( $\pm$ ) 0.5°C. Experiments were repeated at least thrice and the  $T_m$  values were obtained from the peaks in the first derivative plots. ND not detected,  $\Delta T_m$  indicates the difference in  $T_m$  of the corresponding sequence with the DNA **88**. DNA **89** = 5'CGCA<sub>4</sub>CA<sub>3</sub>CGC 3' Buffer, 10 mM Sodium phosphate pH = 7.3, 10 mM NaCl.

### 3.9 UV- $T_m$ studies of (2*R*,5*S*) and (2*R*,5*R*) *amp*PNA<sub>2</sub>:DNA triplexes:

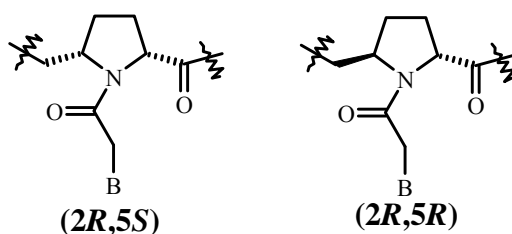


**Figure 20** (2*R*,5*S*) and (2*R*,5*R*)-*amp*-PNAs

The UV-temperature studies on (2*R*,5*S*) and (2*S*,5*R*)-*amp*-PNA<sub>2</sub>:DNA triplexes to understand the effect on thermal stability in terms of these different chiral modifications were undertaken. The normalized absorbance or % hyperchromicity *versus* temperature plots derived from the UV melting data indicated a single transition indicative of the simultaneous dissociation of the two PNA strands from the DNA in the PNA<sub>2</sub>:DNA complex (Figure 21). Table 8 and Figure 21 summarize the  $T_m$  data obtained for UV melting experiments of various PNA<sub>2</sub>:DNA hybrids. The  $T_m$  values (Table 5) indicated that single modifications at C-terminus (2*R*,5*S*)-*amp*-PNA **74** and (2*R*,5*R*)-*amp*-PNA **80** (Table 5, entry 4 and 9) and N-terminus modified *amp*-PNAs **72** and **78** (Table 5, entry 2 and 7) exhibited a good stabilization in comparison to the control *aeg*-PNA **57**. When a single (2*R*,5*S*) and (2*R*,5*R*) *amp* unit was present at the center of the sequence (Table 5, entry 3 and 8) destabilization of the derived *amp*-PNA<sub>2</sub>:DNA was observed (Figure 21 A, PNA **73**: DNA **88** and B, PNA **79**: DNA **88**). In case of doubly modified *amp*-PNAs **75** and **81** marginal tolerance was observed (Figure 21, A, 75:88 and B, 81:88), with  $T_m$  similar to that of *aeg*-PNA complex.

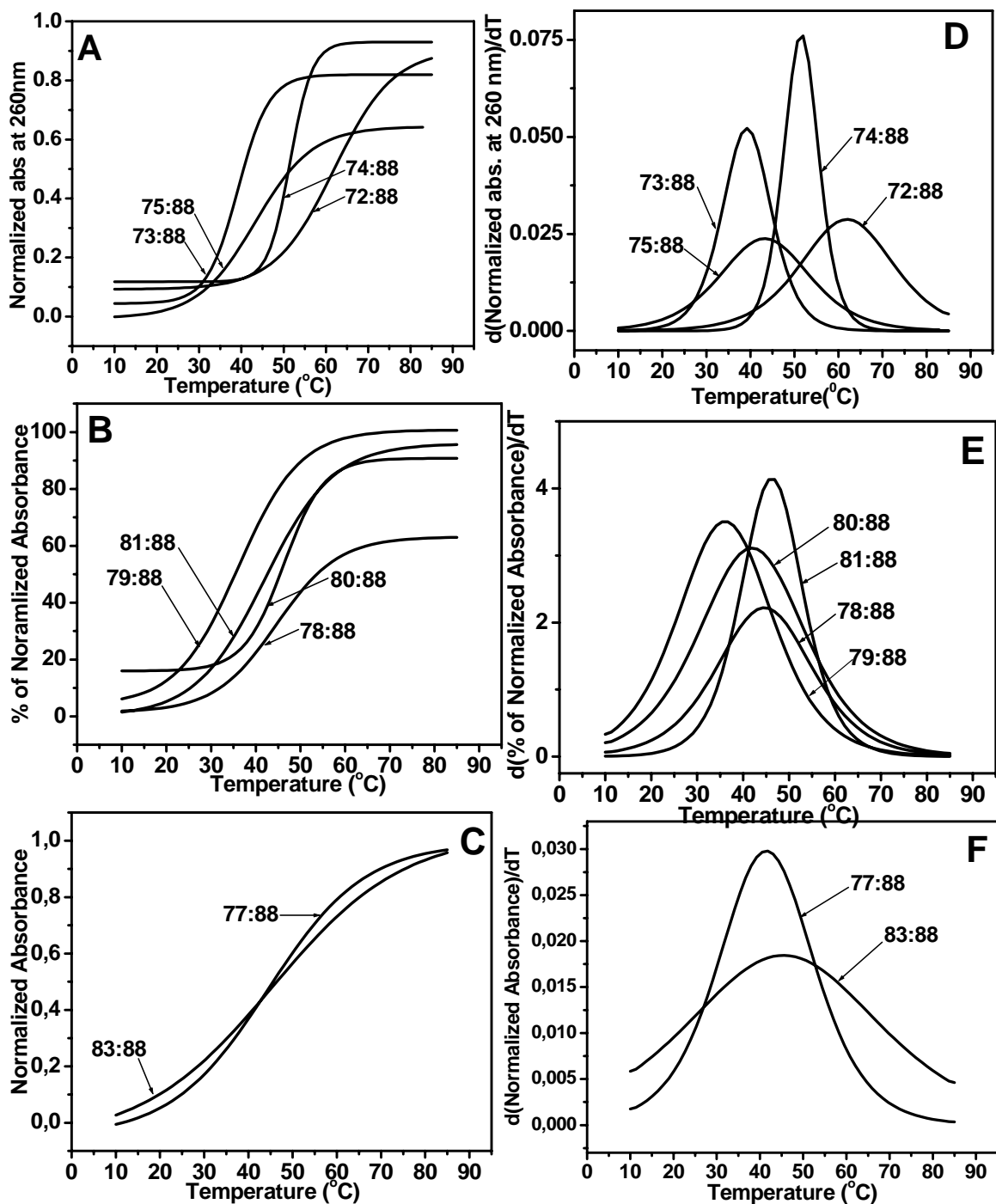


**Figure 21.** (A, B and C) UV-Melting profiles for *(2R,5S)* and *(2R,5R)*-amp-PNA:DNA 88 triplexes (D, E and F) UV-Melting first derivative curves of corresponding-amp-PNAs. DNA 88 = 5' (CGC-AAAAAAAAA-CGC)3' Buffer: 10 mM sodium phosphate, 10 mM NaCl, pH 7.3.

**Table 5** UV-Melting temperatures of (2*R*,5*S*) and (2*S*,5*R*) *amp*PNA<sub>2</sub>:DNA **88** triplexes.

Entry	<i>PNA</i>	<i>T<sub>m</sub></i> (°C)	Δ <i>T<sub>m</sub></i>
1	<i>aeg</i> PNA <b>57</b> H-T-T-T-T-T-T-T-T-(CH <sub>2</sub> ) <sub>2</sub> -CONH <sub>2</sub>	43	
2	<i>amp</i> PNA <b>72</b> H- <b>t</b> <sub>RS</sub> -T-T-T-T-T-T-T-CH <sub>2</sub> ) <sub>2</sub> -CONH <sub>2</sub>	62	19
3	<i>amp</i> PNA <b>73</b> H-T-T-T- <b>t</b> <sub>RS</sub> -T-T-T-T-(CH <sub>2</sub> ) <sub>2</sub> -CONH <sub>2</sub>	39	-4
4	<i>amp</i> PNA <b>74</b> H-T-T-T-T-T-T-T- <b>t</b> <sub>RS</sub> -(CH <sub>2</sub> ) <sub>2</sub> -CONH <sub>2</sub>	52	+9
5	<i>amp</i> PNA <b>75</b> H- <b>t</b> <sub>RS</sub> -T-T-T- <b>t</b> <sub>RS</sub> -T-T-T (CH <sub>2</sub> ) <sub>2</sub> -CONH <sub>2</sub>	43	-
6	<i>amp</i> PNA <b>77</b> H-( <b>t t t t t t t t</b> ) <sub>RS</sub> -(CH <sub>2</sub> ) <sub>2</sub> -CONH <sub>2</sub>	46	+3
7	<i>amp</i> PNA <b>78</b> H- <b>t</b> <sub>RR</sub> -T-T-T-T-T-T-T-CH <sub>2</sub> ) <sub>2</sub> -CONH <sub>2</sub>	44	+1
8	<i>amp</i> PNA <b>79</b> H-T-T-T- <b>t</b> <sub>RR</sub> -T-T-T-T-(CH <sub>2</sub> ) <sub>2</sub> -CONH <sub>2</sub>	36	-7
9	<i>amp</i> PNA <b>80</b> H-T-T-T-T-T-T-T- <b>t</b> <sub>RR</sub> -(CH <sub>2</sub> ) <sub>2</sub> -CONH <sub>2</sub>	46	+3
10	<i>amp</i> PNA <b>81</b> H- <b>t</b> <sub>RR</sub> -T-T-T- <b>t</b> <sub>RR</sub> -T-T-T (CH <sub>2</sub> ) <sub>2</sub> -CONH <sub>2</sub>	43	-
11	<i>amp</i> PNA <b>83</b> H-( <b>t t t t t t t t</b> ) <sub>RR</sub> -(CH <sub>2</sub> ) <sub>2</sub> -CONH <sub>2</sub>	44	+1

*T<sub>m</sub>* values are accurate to (±) 0.5°C. Experiments were repeated at least thrice and the *T<sub>m</sub>* values were obtained from the peaks in the first derivative plots. Δ *T<sub>m</sub>* indicates the difference in *T<sub>m</sub>* with the control experiment *aeg*-PNA **57**. T and t indicating *aeg* and *amp*-PNA respectively. Buffer: 10mM sodium phosphate, 10 mM NaCl, pH 7.3 DNA **88** = 5'(CGC-AAAAAAAAA-CGC)3'

The all-modified homooligomeric, homochiral *amp*-PNAs (2*R*,5*S*)-**77** and (2*R*,5*R*) **83** exhibited minimal stabilities (Figure 21, Δ*T<sub>m</sub>* = +3 °C and +1 °C) compared to the unmodified *aeg*-PNA **57**.

These results indicate that *amp* (2*R*,5*S*) and (2*R*,5*R*) units at N/C terminus seem to assist *aeg*-PNA in binding to complementary DNA in triplex mode. In comparison, both (2*R*,5*S*) and (2*R*,5*R*) *amp*-PNA units in the middle of the sequence of the oligomer were detrimental to the PNA<sub>2</sub>:DNA complex stability. In all modifications (2*R*,5*S*)-*amp* unit exhibited better stabilization properties over (2*R*,5*R*)-*amp* unit. However, in the fully modified oligomers **77** and **83**, the stability is as good as that with unmodified PNA.

### 3. 9. 1 UV- $T_m$ studies of (2*R*,5*S*) and (2*R*,5*R*)-*amp*-PNA:DNA Duplexes

The introduction of chiral *amp*-PNA monomers into *aeg*-PNA oligomer was envisaged to impart specific directionality in DNA/PNA binding and hence differentiate between *parallel* and *antiparallel* modes of binding. The establishment of correct duplexes were indicated by sigmoidal transitions and confirmed by peaks in the first derivative plots (Figure 21a). The (2*R*,5*S*)-*amp*-PNA **76** and (2*R*,5*R*)-*amp*-PNA **82** were synthesized by replacing the *aeg*-PNA thymine by *amp*-thymine monomers in *aeg*-PNA **58**.

The UV- $T_m$  results in Table 6 indicate that (2*R*,5*S*)-*amp*-PNA **76** stabilized the complexes with DNA **90** and **91** (Figure 21a B and D ) and showing a 4 °C selectivity in binding towards *antiparallel* orientation (DNA **90**), in comparison to *aeg*-PNA-**58**. In case of (2*R*,5*R*)-*amp*-PNA **82**, destabilization was observed in *antiparallel* mode. Duplexes comprising the (2*R*,5*R*)-*amp*-PNA **82** and DNA **91** gave linear, non-sigmoidal plot and failed to show any peak in the first derivative plots. As a consequence, no melting temperature was detected for the complex (2*R*,5*R*)-*amp*-PNA **82**:**91**. Table 6 summarizes the  $T_m$  data obtained for UV melting experiments of (2*R*,5*S*) and (2*R*,5*R*)-*amp*-PNA:DNA duplex hybrids.

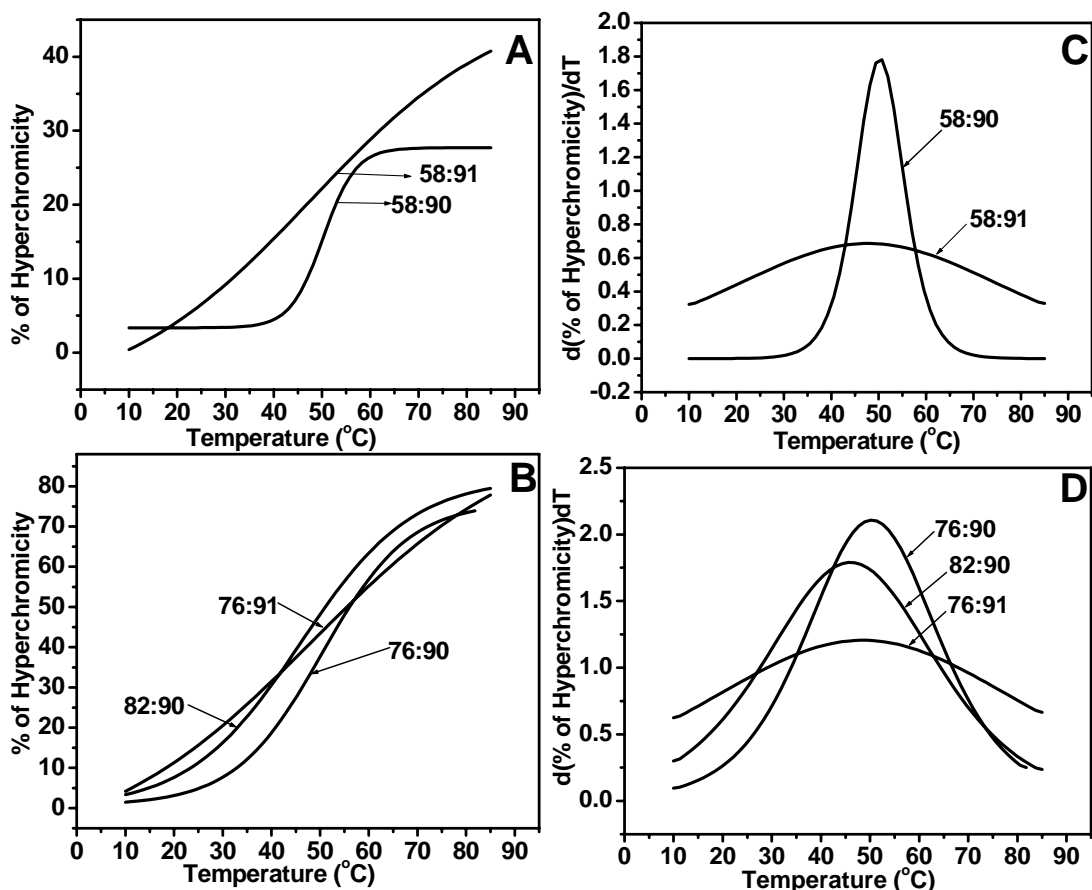


**Figure 21a** A and B) UV-Melting profiles of (2*R*,5*S*) and (2*R*,5*R*) *amp*PNA:DNA duplexes C and D) first derivative curves corresponding complexes (Buffer, 10 mM Sodium phosphate, 10 mM NaCl, pH 7.3) DNA **90** = 5'AGTGATCTAC3'(antiparallel); DNA **91** = 5'CATCTAGTGA3'(parallel).

**Table 6** UV- $T_m$  of (2*R*,5*S*) and (2*R*,5*R*)-*amp*-PNA:DNA Duplexes

Entry	PNA	$T_m$ °C	* $\Delta T_m$ °C	# $\Delta T_m$ °C
1	<i>amp</i> PNA <b>58</b> H-G-T-A-G-A-T-C-A-C-T-(CH <sub>2</sub> ) <sub>2</sub> CONH <sub>2</sub>	50( <i>ap</i> )	-	2
2	<i>amp</i> PNA <b>58</b> H-G-T-A-G-A-T-C-A-C-T-(CH <sub>2</sub> ) <sub>2</sub> CONH <sub>2</sub>	48( <i>p</i> )	-	-
3	<i>amp</i> PNA <b>76</b> H-G- <b>t<sub>RS</sub></b> -A-G-A- <b>t<sub>RS</sub></b> -C-A-C- <b>t<sub>RS</sub></b> -(CH <sub>2</sub> ) <sub>2</sub> CONH <sub>2</sub>	52( <i>ap</i> )	+2	4
4	<i>amp</i> PNA <b>76</b> H-G- <b>t<sub>RS</sub></b> -A-G-A- <b>t<sub>RS</sub></b> -C-A-C- <b>t<sub>RS</sub></b> -(CH <sub>2</sub> ) <sub>2</sub> CONH <sub>2</sub>	48( <i>p</i> )	0	-
5	<i>amp</i> PNA <b>82</b> H-G- <b>t<sub>RR</sub></b> -A-G-A- <b>t<sub>RR</sub></b> -C-A-C- <b>t<sub>RR</sub></b> -(CH <sub>2</sub> ) <sub>2</sub> CONH <sub>2</sub>	46( <i>ap</i> )	-4	-
6	<i>amp</i> PNA <b>82</b> H-G- <b>t<sub>RR</sub></b> -A-G-A- <b>t<sub>RR</sub></b> -C-A-C- <b>t<sub>RR</sub></b> -(CH <sub>2</sub> ) <sub>2</sub> CONH <sub>2</sub>	NB( <i>p</i> )	-	-

A/G/C/T = *aeg*-PNA Adenine/Guanine/Cytosine/Thymine monomers, **t<sub>RS</sub>** = (2*R*,5*S*)-*amp*PNA Thymine monomer, **t<sub>RR</sub>** = (2*R*,5*R*)-*amp*PNA Thymine monomer. \* $\Delta T_m$  Indicate the difference in  $T_m$  with the control experiment *aeg*-PNA **58**. # $\Delta T_m$  = difference in the  $T_m$  of *ap* and *parallel* binding modes. The values reported here are the average of 3 independent experiments and are

accurate to  $\pm 0.5^\circ\text{C}$ .  $T_m$  = melting temperature (measured in the buffer 10 mM sodium phosphate, 10 mM NaCl, pH = 7.3). T and t indicating *aeg* and *amp*-PNA respectively. DNA **90** = 5'AGTGATCTAC 3'; DNA **91** = 5'CATCTAGTGA3'.

In conclusion,  $(2R,5S)$ -*amp*-PNA oligomers exhibit better hybridization properties with complementary DNA sequences to form duplexes in comparison to  $(2R,5R)$ -*amp*-PNA oligomers. The high affinity-binding property of  $(2R,5S)$ -*amp*-PNA oligomers impart a balanced and optimum conformation in to the *aeg* backbone for better binding with DNA. The fully modified backbone in  $(2R,5S)$ -*amp*-PNA **77** and  $(2R,5R)$ -*amp*-PNA **83** bind to DNA but with reduced strength compared with the single or double modified oligomers. The  $(2R,5S)$  *amp*-PNA units marginally stabilize the duplex complexes in comparison to triplexes, perhaps due to of over preorganization caused by 3 *amp*-PNA units present in the single strand.

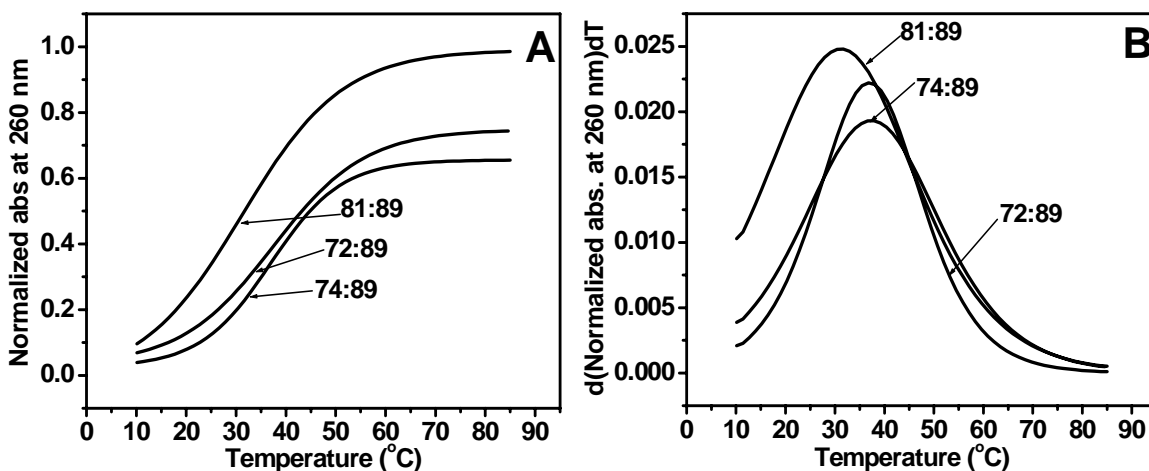


**Figure 22** (A) UV-Melting profiles of triplex of  $(2R,5S)$ -*amp*-PNA **72**, **74** and  $(2R,5R)$ -*amp*-PNA **81** with DNA **89**, (B) UV-Melting first derivative curves of mismatched *amp*PNA<sub>2</sub>:DNA **89** mismatched complexes. (Buffer, 10 mM Sodium phosphate pH = 7.3, 10 mM NaCl). DNA **89** = 5'(CGC-AAACAAAA-CGC)3'

### 3. 9. 2 Mismatch studies of $(2R,5S)$ and $(2R,5R)$ *amp*-PNA triplex with DNA.

The triplex of *amp*-PNAs **72**, **74** and **81** were constituted with DNA **89** containing one mismatch base and the melting profiles are given in Figure 22. The  $T_m$  values (Table 7) indicated that these triplexes were destabilized to a larger extent ( $\Delta T_m = 25$ , 15 and 12

°C) respectively. The PNA<sub>2</sub>:DNA complex comprising the (2*R*,5*S*)-*amp*-PNA **72** and **74** with DNA **89** exhibited a destabilization of ( $\Delta T_m = 25$  and  $15$  °C), while triplex comprising (2*R*,5*R*)-*amp*-PNA **81** and DNA **89** having a single mismatch exhibited a destabilization of ( $\Delta T_m = 9$  °C). The  $T_m$  of unmodified *aeg*-PNA **57** with DNA **89** having one mismatch decreases by  $9.4$  °C.

**Table 7** UV- $T_m$  (°C) of PNA<sub>2</sub>:DNA mismatched complexes

Entry	PNA	$T_m$ (°C)	$\Delta T_m$
1	<i>aeg</i> PNA <b>57</b> H-T-T-T-T-T-T-T-T-(CH <sub>2</sub> ) <sub>2</sub> -CONH <sub>2</sub>	33.6	9.4
2	<i>amp</i> PNA <b>72</b> H- <b>t</b> <sub>SR</sub> -T-T-T-T-T-T-T-T-(CH <sub>2</sub> ) <sub>2</sub> -CONH <sub>2</sub>	37	25
3	<i>amp</i> PNA <b>74</b> H-T-T-T-T-T-T-T- <b>t</b> <sub>SR</sub> -(CH <sub>2</sub> ) <sub>2</sub> -CONH <sub>2</sub>	37	15
4	<i>amp</i> PNA <b>81</b> H-T-T-T-T-T-T-T- <b>t</b> <sub>SS</sub> -(CH <sub>2</sub> ) <sub>2</sub> -CONH <sub>2</sub>	31	10

$T_m$  values are accurate to ( $\pm$ )  $0.5$ °C. Experiments were repeated at least thrice and the  $T_m$  values were obtained from the peaks in the first derivative plots.  $\Delta T_m$  indicates the difference in  $T_m$  of the corresponding sequence with the DNA **88**. T and **t** indicating *aeg* and *amp*-PNA respectively. Buffer: 10mM sodium phosphate, 10 mM NaCl, pH 7.3. DNA **88** = 5'(CGC-AAACAAAA-CGC)3'

Thus (2*R*,5*S*)-*amp*-PNA modifications induce higher destabilization of triplexes having mismatches compared to (2*R*,5*R*)-*amp*-PNA and unmodified PNA **57**, whereas (2*R*,5*S*)-*amp*-PNA exhibited equal mismatch destabilization in comparison to unmodified (PNA **57**)<sub>2</sub>: DNA triplexes. This suggests a greater discrimination of DNA mismatches by (2*R*,5*S*)-*amp*-PNAs.

### 3. 10 UV- $T_m$ Studies of 4-hydroxy-*amp*-PNA<sub>2</sub>:DNA triplexes

The *amp* monomers enable the study of the constrain and steric effects on the hybridization properties of PNA oligomers with complementary DNA. It will not provide any information about the conformational effects of the proline ring on hybridization properties of PNA oligomers. In proline, the two puckers are almost equally preferred and the energy barrier to inter-conversion is very low.<sup>16</sup> However, in 4-substituted prolines, depending on the steric and electronic effects exerted by the 4-substituent, pyrrolidine ring may prefer any one of the ring-pucker, as found in both its crystal structures and in solution.<sup>16</sup> In order to carryout these studies, the oligomers *amp*-PNA **84-86** ( Figure 23, Table 8) were synthesized and their thermal stability evaluated through UV- $T_m$  experiments (Figure 24).

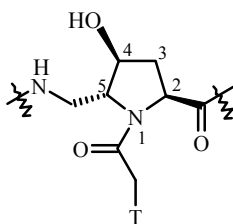


**Figure 23** (2*S*,4*S*,5*R*)-*amp*-PNAs

The  $T_m$  values (Table 8) indicate that the single modifications at C-terminus (2*S*,4*S*,5*R*) *amp*-PNA **86**, N-terminus *amp*-PNAs **84** or at the center of the sequence *amp*-PNA **86** (Table 8, entry 3) stabilized the *amp*-PNA<sub>2</sub>:DNA triplexes by 2 and 7 °C respectively in comparison to the control sequence PNA **57** . The increased thermal stability of these complexes compared to unsubstituted *amp*-PNA and *aeg*-PNA is due to the induction of favorable pre-organization in to the *aeg* backbone by the incorporation of chiral (2*S*,4*S*,5*R*) *amp*-PNA units.

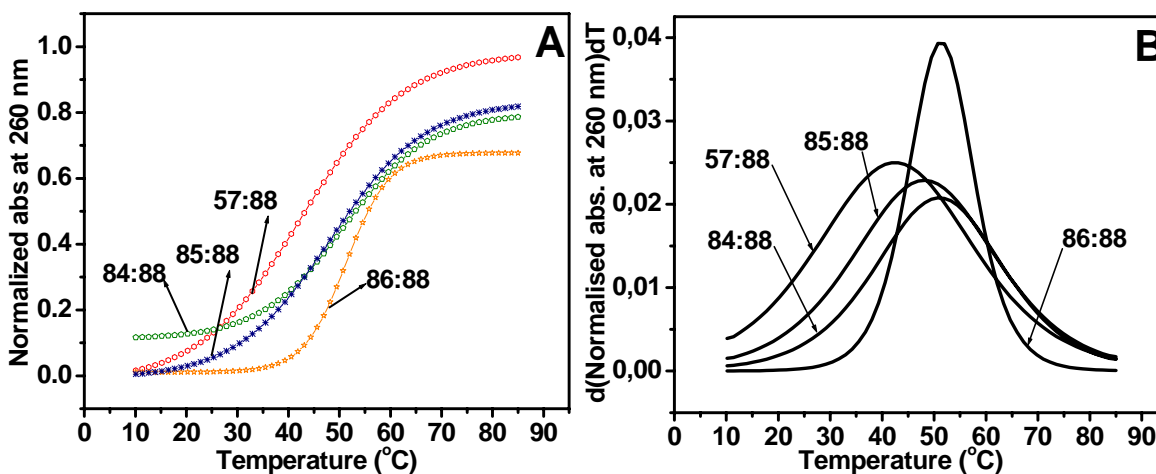


**Figure 24** A) UV-Melting profiles and B) UV-Melting first derivative curves of PNA<sub>2</sub>:DNA triplexes of (2*S*,4*S*,5*R*) *amp*-PNA **84**, **85** and **86** with DNA **88**. (Buffer, 10 mM Sodium phosphate, 10 mM NaCl, pH = 7.3.) DNA **88** = 5'(CGC-AAAAAAAA-CGC)3'

**Table 8** UV- $T_m$  (°C) of (2*S*,4*S*,5*R*) *amp* PNA<sub>2</sub>:DNA triplexes

Entry	PNA	$T_m$ (°C)	$\Delta T_m$
1	<i>aeg</i> PNA <b>57</b> H-T-T-T-T-T-T-T-T-(CH <sub>2</sub> ) <sub>2</sub> -CONH <sub>2</sub>	43	
2	<i>amp</i> PNA <b>84</b> H-t <sub>SSR</sub> -T-T-T-T-T-T-T-T-T-(CH <sub>2</sub> ) <sub>2</sub> -CONH <sub>2</sub>	48.50	+6
3	<i>amp</i> PNA <b>85</b> H-T-T-T-t <sub>SSR</sub> -T-T-T-T-(CH <sub>2</sub> ) <sub>2</sub> -CONH <sub>2</sub>	45	+2
4	<i>amp</i> PNA <b>86</b> H-T-T-T-T-T-T-T-t <sub>SSR</sub> -(CH <sub>2</sub> ) <sub>2</sub> -CONH <sub>2</sub>	49.50	+7

$T_m$  values are accurate to ( $\pm$ ) 0.5°C. Experiments were repeated at least thrice and the  $T_m$  values were obtained from the peaks in the first derivative plots.  $\Delta T_m$  indicates the difference in  $T_m$  with the control experiment *aeg*-PNA **57**. T and t indicating *aeg* and *amp*-PNA respectively. Buffer: 10 mM sodium phosphate, 10 mM NaCl, pH 7.3. DNA **88** = 5'(CGC-AAAAAAAA-CGC)3'

### 3. 10. 1 UV- $T_m$ studies of 4-hydroxy-*amp*-PNA:DNA duplexes

The oligothymine sequences described above were found to form triplexes in which the relative binding orientation (*parallel-antiparallel*) of the two PNA strands involved in complex formation is immaterial. In order to study the orientational preferences, *parallel* and *antiparallel* PNA:DNA duplexes having mixed purine and pyrimidine sequences were synthesized (Table 9) by incorporating a (2*S*,4*S*,5*R*) *amp* thymine unit in the center of the *aeg*-PNA **58**.

Results in Table 9 indicates that *amp*-PNA **87** exhibits good thermal stability with both *parallel* and *antiparallel* DNA sequences in comparison to the control sequence PNA **58** (Figure 25, Table 9, entry 3 and 4). The difference in the  $T_m$  of *parallel* and *antiparallel* ( $\Delta T_m, ap/p = 0$ ) indicates the short of selectivity between the *parallel* and *antiparallel* modes of binding .

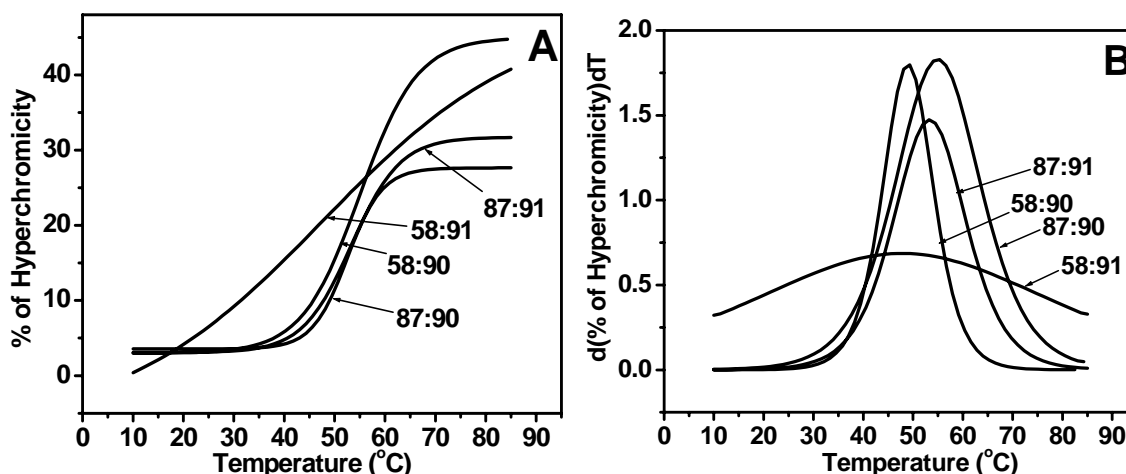


**Figure 25.** (A) UV-Melting profiles and (B) UV-Melting first derivative curves of PNA:DNA duplex of (2*S*,4*S*,5*R*) *amp*-PNA **87** and *aeg*-PNA **58** with DNA **90** and **91**. (Buffer 10 mM sodium phosphate, 10 mM NaCl, pH = 7.3). DNA **90** = 5'AGTGATCTAC3' (*antiparallel*); DNA **91** = 5'CATCTAGTGA3' (*parallel*).

**Table 9** UV- $T_m$  (°C) of (2*S*,4*S*,5*R*)-*amp*-PNA:DNA duplexes.

Entry	PNA	$T_m$ (°C)	* $\Delta T_m$	# $\Delta T_m$
1	<i>aeg</i> -PNA <b>58</b> H-G-T-A-G-A-T-C-A-C-T-(CH <sub>2</sub> ) <sub>2</sub> CONH <sub>2</sub>	50 ( <i>ap</i> ),	-	2
2	<i>aeg</i> -PNA <b>58</b> H-G-T-A-G-A-T-C-A-C-T-(CH <sub>2</sub> ) <sub>2</sub> CONH <sub>2</sub>	48 ( <i>p</i> )	-	-
3	<i>amp</i> -PNA <b>87</b> H-G-T-A-G-A-t <sub>SSR</sub> -C-A-C-T-(CH <sub>2</sub> ) <sub>2</sub> CONH <sub>2</sub>	55 ( <i>ap</i> ),	5	0
4	<i>amp</i> -PNA <b>87</b> H-G-T-A-G-A-t <sub>SSR</sub> -C-A-C-T-(CH <sub>2</sub> ) <sub>2</sub> CONH <sub>2</sub>	53 ( <i>p</i> )	5	-

A/G/C/T = *aeg*-PNA Adenine /Guanine /Cytosine /Thymine monomers, t<sub>SSR</sub> = (2*S*,4*S*,5*R*)-*amp*-PNA Thymine monomer.  $T_m$  values are accurate to ( $\pm$ ) 0.5°C. Experiments were repeated at least thrice and the  $T_m$  values were obtained from the peaks in the first derivative plots. T and t indicating *aeg* and *amp*-PNA respectively. \* $\Delta T_m$  Indicate the difference in  $T_m$  with the control experiment *aeg*-PNA **58**. # $\Delta T_m$  = difference in the  $T_m$  of *antiparallel* and *parallel* binding modes. (measured in the buffer 10 mM sodium phosphate, 10 mM NaCl, pH = 7.3). DNA **90** = 5'AGTGATCTAC3'; DNA **91** = 5'CATCTAGTGA3'.

### 3. 10. 2 Mismatch studies of (2*S*,4*S*,5*R*)-*amp*-PNA triplexes with DNA **89**

The triplexes of PNAs were constituted with DNA containing a mismatch base (Figure 26). The PNA<sub>2</sub>:DNA complexes comprising the *aeg*-PNA **57** and *amp*-PNA **85** with DNA **89** having a single mismatch were subjected for UV-melting. The  $T_m$  of the mismatched triplexes (2*S*,4*S*,5*R*)-*amp*-PNA **85**:DNA **89** indicated that the triplex was destabilized to a larger extent ( $\Delta T_m = 20$  °C). While the  $T_m$  of unmodified *aeg*-PNA **57** with DNA **89** having one mismatch decreases by 10 °C. Thus (2*S*,4*S*,5*R*)-*amp*-PNA modifications induce 10 °C higher destabilization of mismatch triplexes in comparison to unmodified *aeg*-PNA **57** with DNA **89** this suggests a greater discrimination of DNA mismatches by (2*S*,4*S*,5*R*)-*amp*-PNAs (Figure 26, Table 10).

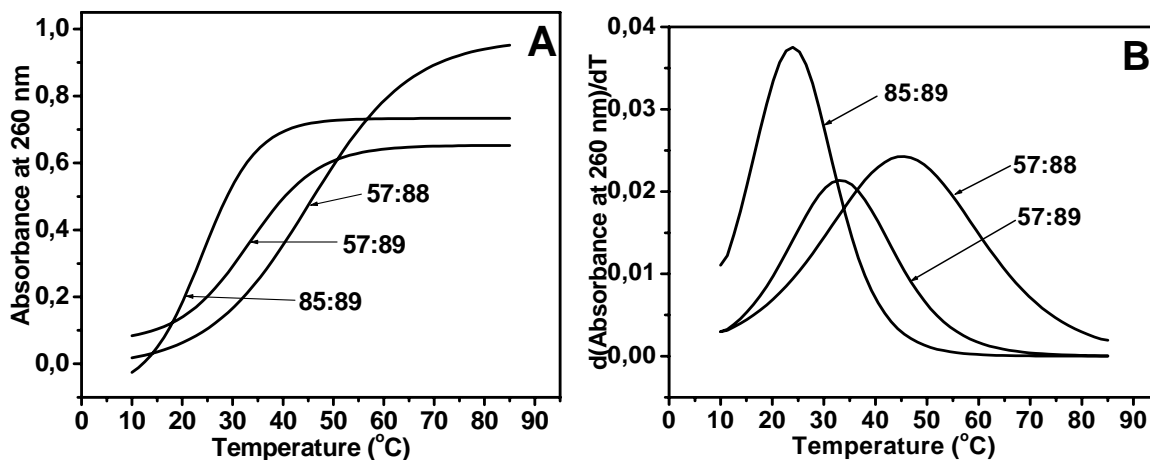


**Figure 26** (A) UV-Melting profiles of *amp*-PNA **85** and *aeg*-PNA **57** with DNA **89**, (B) UV-Melting first derivative curves of mismatch triplexes *aeg*-PNA<sub>2</sub>:DNA **89** and *amp*-PNA<sub>2</sub>:DNA **89** mismatched triplexes. (Buffer, 10 mM Sodium phosphate pH = 7.3, 10 mM NaCl). DNA **88** = 5'CGCA<sub>8</sub>CGC3'; DNA **89** = 5'CGCA<sub>4</sub>CA<sub>3</sub>CGC3'

**Table 10** UV- $T_m$  ( $^{\circ}\text{C}$ ) of PNA<sub>2</sub>:DNA **89** mismatched triplexes

Entry	PNA	$T_m$ ( $^{\circ}\text{C}$ )	$\Delta T_m$
1	<i>aeg</i> -PNA <b>57</b> H-T-T-T-T-T-T-T-T-(CH <sub>2</sub> ) <sub>2</sub> -CONH <sub>2</sub>	33.6	9.4
2	<i>amp</i> -PNA <b>85</b> H-T-T-T-t <sub>SSR</sub> -T-T-T-T-(CH <sub>2</sub> ) <sub>2</sub> -CONH <sub>2</sub>	24	20

$T_m$  values are accurate to ( $\pm$ ) 0.5 $^{\circ}\text{C}$ . Experiments were repeated at least thrice and the  $T_m$  values were obtained from the peaks in the first derivative plots.  $\Delta T_m$  indicates the difference in  $T_m$  with the control experiment *aeg*-PNA **57** with DNA **89** = 5'CGCA<sub>4</sub>CA<sub>3</sub>CGC 3'. T and t indicating *aeg* and *amp*-PNA respectively. Buffer, 10 mM Sodium phosphate pH = 7.3, 10 mM NaCl.

### 3. 11 UV- $T_m$ studies of (2*S*,5*R*) and (2*S*,5*S*) *amp*PNA<sub>2</sub>:RNA Triplexes

The melting profiles of triplexes derived from *amp*-PNA and RNA and their derivative curves are given in Figure 27. Single modification of (2*S*,5*R*)-*amp*-PNA at N-terminus stabilized the *amp*-PNA **59**:RNA triplex by +2  $^{\circ}\text{C}$  (Table 11, entry 2), whereas (2*S*,5*S*) *amp*PNA destabilized the triplex by -12  $^{\circ}\text{C}$  (Table 11, entry 7). A single modification at C-terminus in PNA caused a destabilization of triplex (PNA **62**)<sub>2</sub>:RNA **92** in comparison to (PNA **57**)<sub>2</sub>:RNA **92** by -1 $^{\circ}\text{C}$  (Table 11, entry 4). The same kind of modification in case of (2*S*,5*S*)-*amp*-PNA **68** stabilized the triplex by +1  $^{\circ}\text{C}$  (Table 11, entry 9). Single modification of (2*S*,5*R*) and (2*S*,5*S*)-*amp*-PNA in the middle of the sequence induced destabilization of (PNA **61** and **67**)<sub>2</sub>:RNA **92** complex over the control triplex (PNA **57**)<sub>2</sub>:RNA **92** by -14 and -2  $^{\circ}\text{C}$  respectively (Table 11, entry 3 and 8). Bi-modified *amp*-PNA **63** and **69** gave linear, non-sigmoidal plots and failed to show any peak in the first derivative plots. As a consequence, no melting temperature was detected for these complexes (Table 11, entry 5 and 10). The triplex of the homooligomer of (2*S*,5*R*)-*amp*-PNA-T<sub>8</sub> (PNA **65**)<sub>2</sub>:RNA **92** indicated destabilization of over control triplexes (PNA **57**)<sub>2</sub>: RNA **92** by -10  $^{\circ}\text{C}$  (Table 11, entry ). The PNA<sub>2</sub>:DNA complexes comprising the homooligomer *amp*-PNA **71** stabilized the triplex complex with RNA **92** by +2  $^{\circ}\text{C}$  (Table 11, entry 11) over control experiment.

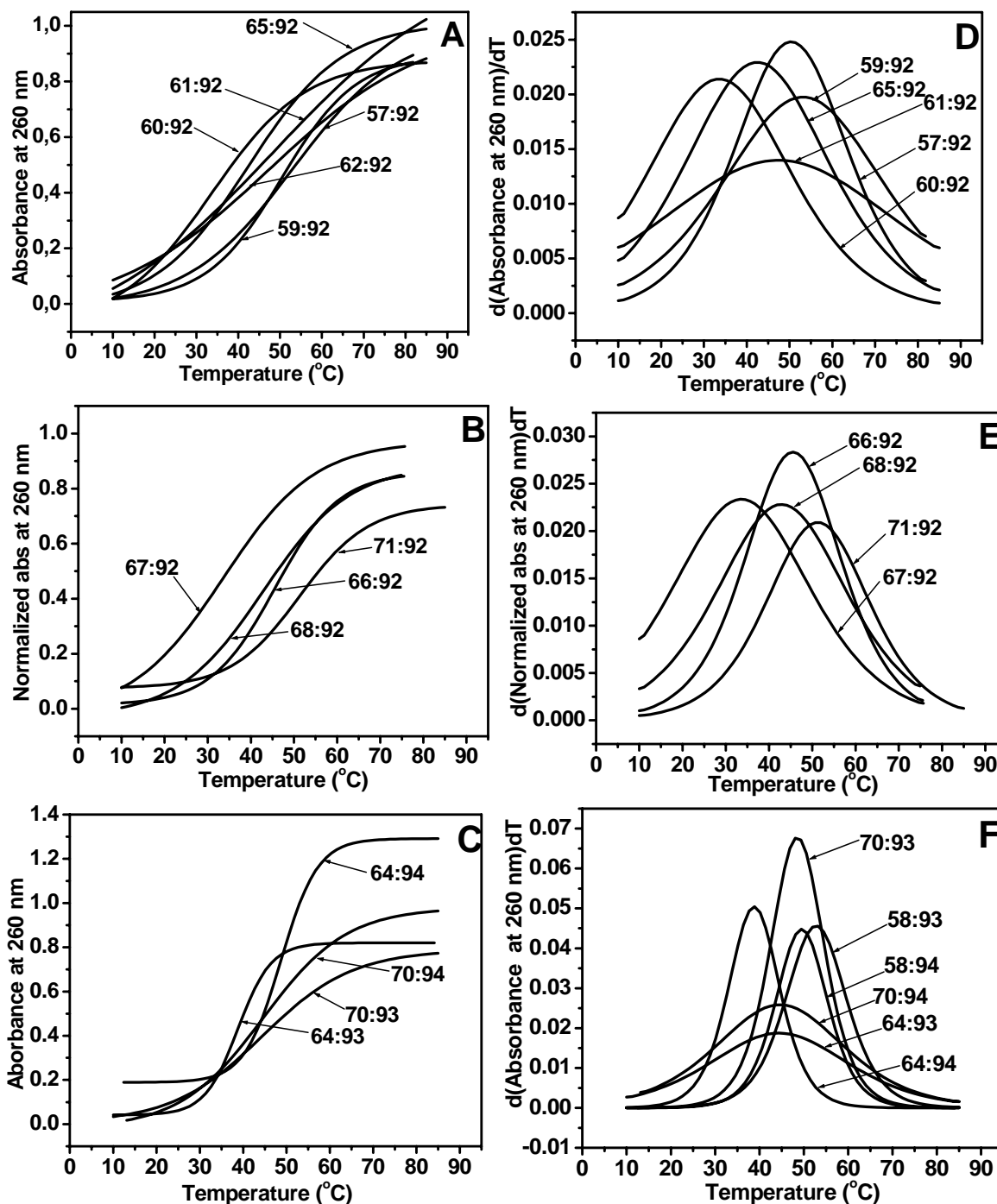


**Figure 27** A-B) UV-Melting profiles, D-E) UV-Melting first derivative curves of (2*S*,5*R*) and (2*S*,5*S*) *amp*-PNA<sub>2</sub>:RNA 92 triplexes C-F) UV-Melting profiles of *aeg*-PNA 58 and (2*S*,5*R*) (2*S*,5*S*) *amp*-PNA:RNA 93 and 94 duplexes and its first derivative curves. Buffer 10 mM sodium phosphate, 10 mM NaCl, pH = 7.3. RNA 92 = 5' (CGC-AAAAAAAA-CGC)3' RNA 93 = 5'AGUGAUCUAC 3'; RNA 94 = 5'CAUCUAGUGA3'.

**Table 11** UV-Melting temperatures of (2*S*,5*R*) and (2*S*,5*S*) *amp*-PNA<sub>2</sub>:RNA triplexes

Entry	PNA Sequence	$T_m$ (°C)	$\Delta T_m$ °C
1	<i>aeg</i> PNA <b>57</b> - H-T-T-T-T-T-T-T-T-(CH <sub>2</sub> ) <sub>2</sub> -CONH <sub>2</sub>	50	-
2	<i>amp</i> PNA <b>59</b> -H-t <sub>SR</sub> -T-T-T-T-T-T-T-CH <sub>2</sub> ) <sub>2</sub> -CONH <sub>2</sub>	52	2
3	<i>amp</i> PNA <b>61</b> -H-T-T-T-t <sub>SR</sub> -T-T-T-T-(CH <sub>2</sub> ) <sub>2</sub> -CONH <sub>2</sub>	33.26	-17.7
4	<i>amp</i> PNA <b>62</b> -H-T.T-T-T-T-T-T-t <sub>SR</sub> -(CH <sub>2</sub> ) <sub>2</sub> -CONH <sub>2</sub>	49	-1
5	<i>amp</i> PNA <b>63</b> -H-t <sub>SR</sub> -T-T-T-t <sub>SR</sub> -T-T-T-(CH <sub>2</sub> ) <sub>2</sub> -CONH <sub>2</sub>	ND	ND
6	<i>amp</i> PNA <b>65</b> -H-(t <sub>SR</sub> ) <sub>8</sub> -(CH <sub>2</sub> ) <sub>2</sub> -CONH <sub>2</sub>	40	-10
7	<i>amp</i> PNA <b>66</b> -H-t <sub>SS</sub> -T-T-T-T-T-T-T-CH <sub>2</sub> ) <sub>2</sub> -CONH <sub>2</sub>	38	-12
8	<i>amp</i> PNA <b>67</b> -T-T-T-t <sub>SS</sub> -T-T-T-T-(CH <sub>2</sub> ) <sub>2</sub> -CONH <sub>2</sub>	48	-2
9	<i>amp</i> PNA <b>68</b> -H- T.T-T-T-T-T-T-t <sub>SS</sub> -(CH <sub>2</sub> ) <sub>2</sub> -CONH <sub>2</sub>	51	1
10	<i>amp</i> PNA <b>69</b> -H- t <sub>SS</sub> -T-T-T-T-t <sub>SS</sub> -T-T-T-(CH <sub>2</sub> ) <sub>2</sub> -CONH <sub>2</sub>	ND	ND
11	<i>amp</i> PNA <b>71</b> -H-(t <sub>SS</sub> ) <sub>8</sub> -(CH <sub>2</sub> ) <sub>2</sub> -CONH <sub>2</sub>	52	2

$\Delta T_m$  Indicate the difference in  $T_m$  with the control experiment *aeg*-PNA **57**. The values reported here are the average of 3 independent experiments and are accurate to  $\pm 0.5^\circ\text{C}$ .  $T_m$  = melting temperature (measured in the buffer 10 mM sodium phosphate, 10 mM NaCl, pH = 7.3). ND = Not detected. T and t indicating *aeg* and *amp*-PNA respectively. RNA **92** = 5'(CGC-AAAAAAAAA-CGC)3'

### 3. 11. 1 UV- $T_m$ studies of (2*S*,5*R*) and (2*S*,5*S*) *amp*-PNA:RNA duplexes:

The melting profiles of these complexes and their derivative curves are given in Figure 27 (C-F).  $T_m$  values derived from various *aeg*-PNA and (2*S*,5*R*) and (2*S*,5*S*)*amp*-PNA sequences with different degrees of modifications are in listed in Table 12 (entry 1-6). The results in Table 12 indicates that the (2*S*,5*R*)-*amp*-PNA oligomer exhibited the destabilization of the duplex with RNA **93** and **94** by  $-9^\circ\text{C}$  (Table 12, entry 3 and 4) in comparison to unmodified *aeg*-PNA **58**. The (2*S*,5*S*) *amp*-PNA**70** exhibited  $-3^\circ\text{C}$  of destabilization in (*ap*)-mode of binding with RNA **93**, where as  $-7^\circ\text{C}$  destabilization with RNA **94** was observed (Table 12, entry 5 and 6) in comparison to PNA **58**.

**Table 12** UV-Melting temperatures of (2*S*,5*R*) and (2*S*,5*S*) *amp*-PNA:RNA duplexes

Entry	Mixed Sequence	$T_m$ (°C)	* $\Delta T_m$	# $\Delta T_m$
1	<i>amp</i> PNA <b>58</b> -H-G-T-A-G-A-T-C-A-C-T-(CH <sub>2</sub> ) <sub>2</sub> -CONH <sub>2</sub>	53( <i>ap</i> )	-	-
2	<i>amp</i> PNA <b>58</b> -H-G-T-A-G-A-T-C-A-C-T-(CH <sub>2</sub> ) <sub>2</sub> -CONH <sub>2</sub>	49( <i>p</i> )	-	-
3	<i>amp</i> PNA <b>64</b> -H-G- <b>t</b> <sub>SR</sub> -A-G-A- <b>t</b> <sub>SR</sub> -C-A-C- <b>t</b> <sub>SR</sub> -(CH <sub>2</sub> ) <sub>2</sub> CONH <sub>2</sub>	44( <i>ap</i> )	-9	4
4	<i>amp</i> PNA <b>64</b> -H-G- <b>t</b> <sub>SR</sub> -A-G-A- <b>t</b> <sub>SR</sub> -C-A-C- <b>t</b> <sub>SR</sub> -(CH <sub>2</sub> ) <sub>2</sub> CONH	40( <i>p</i> )	-9	-
5	<i>amp</i> PNA <b>70</b> -H-G- <b>t</b> <sub>SS</sub> -A-G-A- <b>t</b> <sub>SS</sub> -C-A-C- <b>t</b> <sub>SS</sub> -(CH <sub>2</sub> ) <sub>2</sub> CONH <sub>2</sub>	50( <i>ap</i> )	-3	8
6	<i>amp</i> PNA <b>70</b> -H-G- <b>t</b> <sub>SS</sub> -A-G-A- <b>t</b> <sub>SS</sub> -C-A-C- <b>t</b> <sub>SS</sub> -(CH <sub>2</sub> ) <sub>2</sub> CONH <sub>2</sub>	42( <i>p</i> )	-7	-

$T_m$  values are accurate to ( $\pm$ ) 0.5°C. Experiments were repeated at least thrice and the  $T_m$  values were obtained from the peaks in the first derivative plots \* $\Delta T_m$ . Indicate the difference in  $T_m$  with the control experiment *aeg*-PNA **58**. # $\Delta T_m$  = difference in the  $T_m$  of *antiparallel* and *parallel* binding modes. T and **t** indicating *aeg* and *amp*-PNA respectively. RNA **93** = 5' AGUGAUCUAC 3'; RNA **94** = 5' CAUCUAGUGA 3'.

### 3. 12 UV- $T_m$ studies of (2*R*,5*S*) and (2*R*,5*R*)-*amp*-PNA<sub>2</sub>:RNA Triplexes

To see if there is any binding selectivity for *amp*-PNA between DNA and RNA, *amp*-(PNA **72-83**)<sub>2</sub>:RNA **92** complexes were constituted from *aeg*-PNA-T<sub>8</sub> **57**, and homooligomers of *D-cis*-(2*R*,5*S*)-*amp*-PNA**77** and (2*R*,5*R*) *D-trans* *amp*-PNA **83** with RNA **92**. The UV-melting profiles of these complexes and their derivative curves are given in Figure 28.  $T_m$  values derived for various *aeg*-PNA<sub>2</sub>:RNA and *amp*-PNA<sub>2</sub>:RNA complexes with different degrees of modifications are in listed in Table 13. Single modification of (2*R*,5*S*)-*amp*-PNA at N-terminus or at C-terminus in PNA caused a stabilization of triplexes (PNA **72**)<sub>2</sub>: RNA **92** and (PNA **74**)<sub>2</sub>:RNA **92** over the control (PNA **57**)<sub>2</sub>:RNA **92** by +6 and +2 °C (Table 13, entry 2 and 4) whereas (2*R*,5*R*) *amp* unit at the same positions destabilized the complex by -1 and -5 °C (Table 13, entry **7** and **9**). Single modification of (2*R*,5*S*) and (2*R*,5*R*)-*amp*PNA in the middle of the sequence induced destabilization of (*amp*-PNA **73** and **79**)<sub>2</sub>:RNA **92** complex over the control triplex (PNA **57**)<sub>2</sub>:RNA **92** by -4 and -7 °C (Table 13, entry 3 and 8) respectively. Doubly modified (2*R*,5*S*)-*amp*-PNA **75** (Table 13, entry 5) exhibited the minimal

stabilization over the control PNA **57**, whereas (2*S*,5*S*)-*amp*-PNA **81** destabilized the PNA<sub>2</sub>:RNA complex by -6 °C (Table 13, entry 10). The triplex of the homooligomer of ((2*R*,5*S*)-*amp*-PNA **77**)<sub>2</sub>:RNA **92** indicated minimal destabilization of over control triplexes (PNA **57**)<sub>2</sub>: RNA **92** by  $\Delta T_m = -1$  °C (Table 13, entry 6). The PNA<sub>2</sub>:RNA complexes comprising the homooligomer *amp*-PNA **83** and RNA **92** gave linear, non-sigmoidal plots and failed to show any peak in the first derivative plots. As a consequence, no melting temperature was detected for these complexes.

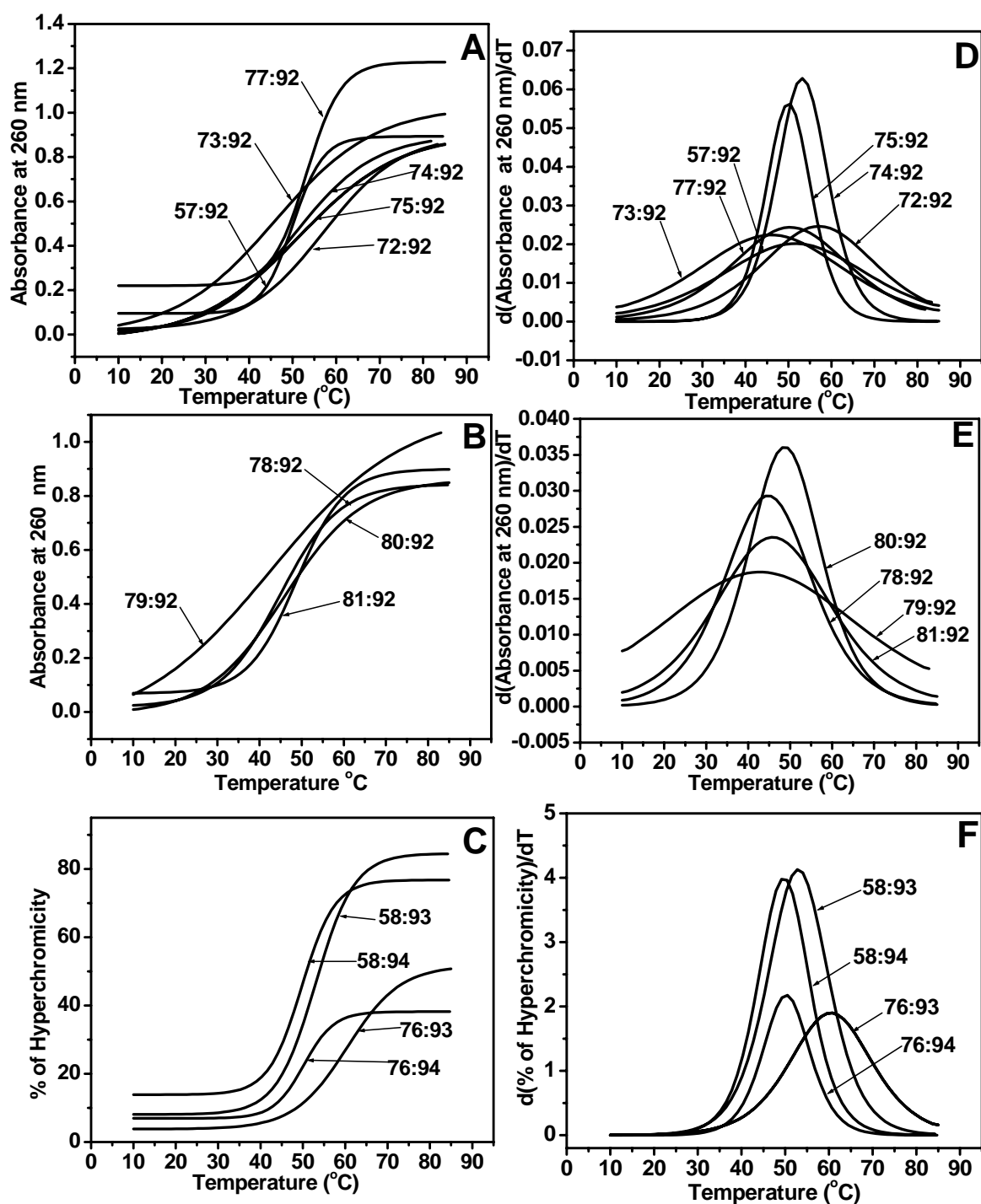


**Figure 28 (A-B)** UV-Melting profiles, **(D-E)** UV-Melting first derivative curves of  $(2R,5S)$  and  $(2R,5R)$  *amp*-PNA<sub>2</sub>:RNA **92** triplexes **(C-F)** UV-Melting profiles of  $(2R,5S)$  and  $(2R,5R)$ -*amp*-PNA:RNA **93** and **94** duplexes and its first derivative curves. Buffer 10 mM sodium phosphate, 10 mM NaCl, pH = 7.3. RNA **92** = 5'CGC-AAAAAAAA-CGC3' RNA **93** = 5'AGUGAUCUAC3'; RNA **94** = 5'CAUCUAGUGA3'.

**Table 13** UV-Melting temperatures of (2*R*,5*S*) and (2*R*,5*R*)-*amp*-PNA<sub>2</sub>:RNA triplexes

Entry	PNA	$T_m$ °C	$\Delta T_m$ °C
1	<i>aeg</i> PNA <b>57</b> H-T-T-T-T-T-T-T-(CH <sub>2</sub> ) <sub>2</sub> -CONH <sub>2</sub>	50	-
2	<i>amp</i> PNA <b>72</b> H-t <sub>RS</sub> -T-T-T-T-T-T-T-(CH <sub>2</sub> ) <sub>2</sub> -CONH <sub>2</sub>	56	6
3	<i>amp</i> PNA <b>73</b> H-T-T-T-t <sub>RS</sub> -T-T-T-T-(CH <sub>2</sub> ) <sub>2</sub> -CONH <sub>2</sub>	46	-4
4	<i>amp</i> PNA <b>74</b> H-T-T-T-T-T-T-T-t <sub>RS</sub> -(CH <sub>2</sub> ) <sub>2</sub> -CONH <sub>2</sub>	52	2
5	<i>amp</i> PNA <b>75</b> H-t <sub>RS</sub> -T-T-T-t <sub>RS</sub> -T-T-T (CH <sub>2</sub> ) <sub>2</sub> -CONH <sub>2</sub>	50	-
6	<i>amp</i> PNA <b>77</b> H-(t t t t t t t t) <sub>RS</sub> -(CH <sub>2</sub> ) <sub>2</sub> -CONH <sub>2</sub>	50	-
7	<i>amp</i> PNA <b>78</b> H-t <sub>RR</sub> -T-T-T-T-T-T-T-(CH <sub>2</sub> ) <sub>2</sub> -CONH <sub>2</sub>	49	-1
8	<i>amp</i> PNA <b>79</b> H-T-T-T-t <sub>RR</sub> -T-T-T-T-(CH <sub>2</sub> ) <sub>2</sub> -CONH <sub>2</sub>	43	-7
9	<i>amp</i> PNA <b>80</b> H-T-T-T-T-T-T-T-t <sub>RR</sub> -(CH <sub>2</sub> ) <sub>2</sub> -CONH <sub>2</sub>	45	-5
10	<i>amp</i> PNA <b>81</b> H-t <sub>RR</sub> -T-T-T-t <sub>RR</sub> -T-T-T (CH <sub>2</sub> ) <sub>2</sub> -CONH <sub>2</sub>	44	-6
11	<i>amp</i> PNA <b>83</b> H-(t t t t t t t t) <sub>RR</sub> -(CH <sub>2</sub> ) <sub>2</sub> -CONH <sub>2</sub>	ND	-

$T_m$  values are accurate to ( $\pm$ ) 0.5°C. Experiments were repeated at least thrice and the  $T_m$  values were obtained from the peaks in the first derivative plots.  $\Delta T_m$  indicates the difference in  $T_m$  with the control experiment *aeg*-PNA **57**. ND = Not detected. T and t indicating *aeg* and *amp*-PNA respectively. RNA **92** = 5'CGC-AAAAAAAA-CGC 3'

### 3. 12. 1 UV- $T_m$ studies of (2*R*,5*S*) and (2*R*,5*R*)-*amp*-PNA:RNA duplexes:

(2*R*,5*S*)-*amp*-PNA **76** and (2*R*,5*R*)-*amp*-PNA **82** were targeted to bind complementary *antiparallel* RNA **93** and *parallel* RNA **94** to constitute both types duplexes. For comparison, unmodified PNA **58** was used. (Table 14). The melting profiles of these complexes and their derivative curves are given in Figure 28 (C-F).  $T_m$  values derived from various *aeg*-PNA and *amp*-PNA sequences with different degrees of modifications are in listed in Table 14. The results in Table 14 indicate that the (2*R*,5*S*)-*amp*-PNA oligomer bind preferentially in *ap*-mode with complementary RNA-**93**. The difference in the  $T_m$  of *antiparallel* and *parallel* duplex complexes of above *amp*-PNA oligomers reflects the selectivity in orientational binding between RNA **93** and **94**. The (2*R*,5*S*)-*amp*-PNA **76** exhibited the stabilization of the duplex with RNA **93** and **94** by +6 and +2 °C respectively in comparison to unmodified PNA **58** and a selectivity of +8 °C between *antiparallel* and *parallel* mode of binding. The PNA:RNA duplex complexes

comprising the (2*R*,5*R*)-*amp*-PNA **82** with three modifications gave linear, non-sigmoidal plots and failed to show any peak in the first derivative plots. As a consequence, no melting temperature was detected for these complexes.

**Table 14** UV-Melting temperatures of (2*R*,5*S*) and (2*R*,5*R*) *amp*-PNA:RNA duplexes

Entry	PNA	$T_m$ (°C)	* $\Delta T_m$ °C	# $\Delta T_m$ °C
1	<i>amp</i> PNA <b>58</b> H-G-T-A-G-A-T-C-A-C-T-(CH <sub>2</sub> ) <sub>2</sub> CONH <sub>2</sub>	53( <i>ap</i> ),	-	4
2	<i>amp</i> PNA <b>58</b> H-G-T-A-G-A-T-C-A-C-T-(CH <sub>2</sub> ) <sub>2</sub> CONH <sub>2</sub>	49( <i>p</i> )	-	-
3	<i>amp</i> PNA <b>76</b> H-G- <b>t</b> <sub>RS</sub> -A-G-A- <b>t</b> <sub>RS</sub> -C-A-C- <b>t</b> <sub>RS</sub> -(CH <sub>2</sub> ) <sub>2</sub> CONH <sub>2</sub>	59( <i>ap</i> ),	6	8
4	<i>amp</i> PNA <b>76</b> H-G- <b>t</b> <sub>RS</sub> -A-G-A- <b>t</b> <sub>RS</sub> -C-A-C- <b>t</b> <sub>RS</sub> -(CH <sub>2</sub> ) <sub>2</sub> CONH <sub>2</sub>	51( <i>p</i> )	2	-
5	<i>amp</i> PNA <b>82</b> H-G- <b>t</b> <sub>RR</sub> -A-G-A- <b>t</b> <sub>RR</sub> -C-A-C- <b>t</b> <sub>RR</sub> -(CH <sub>2</sub> ) <sub>2</sub> CONH <sub>2</sub>	ND	-	-
6	<i>amp</i> PNA <b>82</b> H-G- <b>t</b> <sub>RR</sub> -A-G-A- <b>t</b> <sub>RR</sub> -C-A-C- <b>t</b> <sub>RR</sub> -(CH <sub>2</sub> ) <sub>2</sub> CONH <sub>2</sub>	ND	-	-

$T_m$  values are accurate to ( $\pm$ ) 0.5°C. Experiments were repeated at least thrice and the  $T_m$  values were obtained from the peaks in the first derivative plots.  $\Delta T_m$  indicates the difference in  $T_m$  with the control experiment *aeg*-PNA **57**. T and t indicating *aeg* and *amp*-PNA respectively \* $\Delta T_m$  Indicate the difference in  $T_m$  with the control experiment *aeg*-PNA **58**. # $\Delta T_m$  = difference in the  $T_m$  of *antiparallel* and *parallel* binding modes. ND = Not determine. RNA **92** = 5' (CGC-AAAAAAAA-CGC)3' RNA **93** = 5' AGUGAUCUAC 3'; RNA **94** = 5' CAUCUAGUGA 3'.

### 3. 13 UV- $T_m$ studies of (2*S*,4*S*,5*R*)-*amp*-PNA<sub>2</sub>:RNA Triplexes

In order to study the conformational and hydroxyl effect on *amp*-PNA units, complexes of ((2*S*,4*S*,5*R*)-*amp*-PNA)<sub>2</sub>:RNA **92** were constituted from *aeg*-PNA-T<sub>8</sub> **57**.  $T_m$  values derived from various *aeg*-PNA and *amp*-PNA sequences with different degrees of modifications are listed in Table 15. Single modification of (2*S*,4*S*,5*R*)-*amp*-PNA at N-terminus stabilized the (2*S*,4*S*,5*R*)-*amp*-PNA **84**:RNA **92** triplex by +2 °C (Table 15, entry 2). Whereas a single modification at C-terminus in *aeg*-PNA **57** caused marginal destabilization of triplex (2*S*,4*S*,5*R*)-*amp*-PNA **86**:RNA **92** in comparison to *aeg*-PNA**57**.

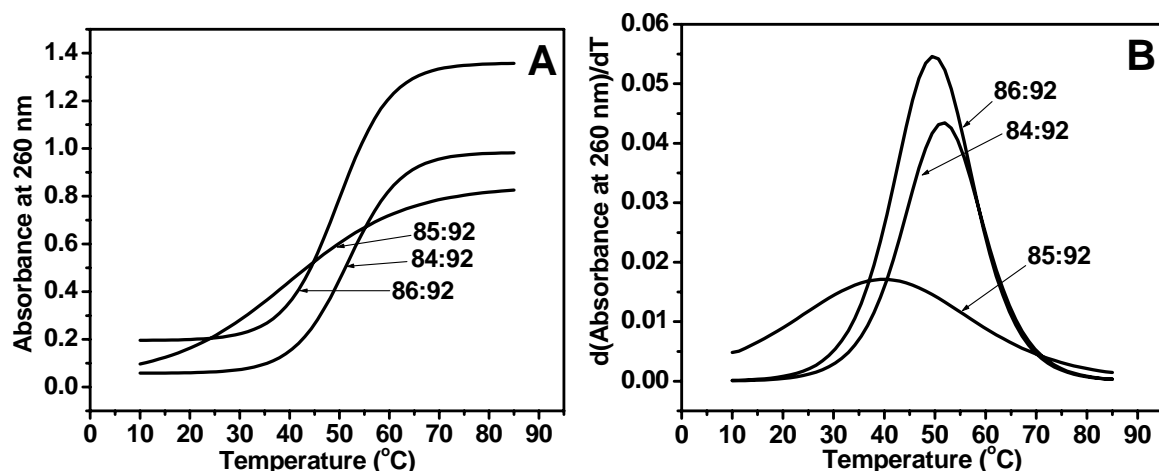


**Figure 29** (A) UV-Melting profiles, (B) UV-Melting first derivative curves of (2*S*,4*S*,5*R*)-*amp*-PNA:RNA **92** Buffer 10 mM sodium phosphate, 10 mM NaCl, pH = 7.3. RNA **92** 5'CGC-AAAAAAAAA-CGC3'

**Table 15** UV-Melting temperatures of (2*S*,4*S*,5*R*)-*amp*-PNA<sub>2</sub>:RNA duplexes

Entry	PNA	$T_m$ (°C)	$\Delta T_m$
1	<i>aeg</i> PNA <b>57</b> H-T-T-T-T-T-T-T-T-(CH <sub>2</sub> ) <sub>2</sub> -CONH <sub>2</sub>	50	-
2	<i>amp</i> PNA <b>84</b> H-t <sub>SSR</sub> -T-T-T-T-T-T-T-CH <sub>2</sub> ) <sub>2</sub> -CONH <sub>2</sub>	52	2
3	<i>amp</i> PNA <b>85</b> H-T-T-T-t <sub>SSR</sub> -T-T-T-T-(CH <sub>2</sub> ) <sub>2</sub> -CONH <sub>2</sub>	40	-10
4	<i>amp</i> PNA <b>86</b> H-T-T-T-T-T-T-t <sub>SSR</sub> -(CH <sub>2</sub> ) <sub>2</sub> -CONH <sub>2</sub>	49	-1

$T_m$  values are accurate to ( $\pm$ ) 0.5°C. Experiments were repeated at least thrice and the  $T_m$  values were obtained from the peaks in the first derivative plots.  $\Delta T_m$  Indicate the difference in  $T_m$  with the control experiment *aeg*-PNA**57**. T and t indicating *aeg* and *amp*-PNA respectively. Buffer: 10mM sodium phosphate, 10 mM NaCl, pH 7.3 RNA **92** = 5'CGC-AAAAAAAAA-CGC3'

### 3. 13. 1 UV- $T_m$ studies of (2*S*,4*S*,5*R*)-*amp*-PNA:RNA duplexes

The melting profiles of these complexes and their derivative curves are given in Figure 30. The results in Table 16 indicate that the (2*S*,4*S*,5*R*)-*amp*-PNA oligomer exhibited the destabilization of the duplex with RNA **93** and **94** by -3 °C and -2 °C respectively. (Table 16, entry 3 and 4) in comparison to unmodified *aeg*-PNA **58**.

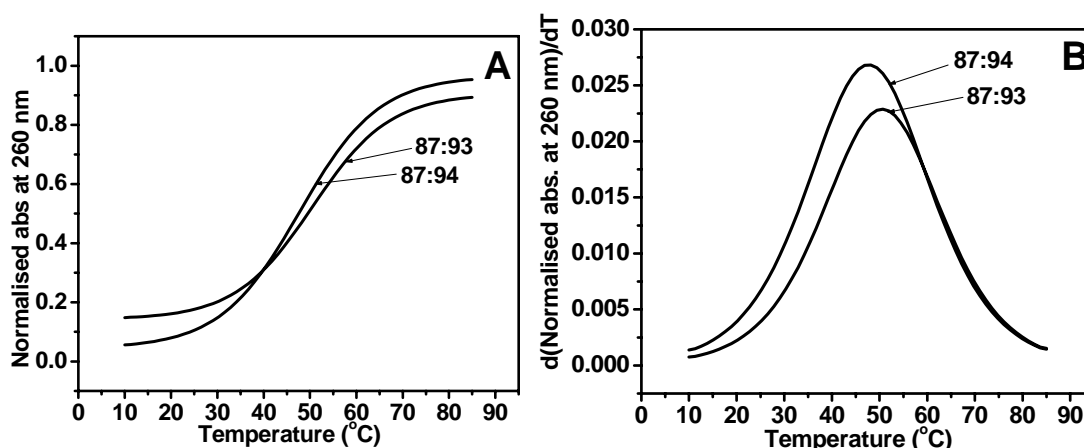


**Figure 30** A) UV-Melting profiles, B) UV-Melting first derivative curves of (2*S*,4*S*,5*R*)-*amp*-PNA:RNA **92** and **93** Buffer 10 mM sodium phosphate, 10 mM NaCl, pH = 7.3. RNA **92** = 5'-CGC-AAAAAAAA-CGC3' RNA **93** = 5'-AGUGAUCUAC3'; RNA **94** = 5'-CAUCUAGUGA3'.

**Table 16** UV-Melting temperatures of (2*S*,4*S*,5*R*)-*amp*-PNA:RNA duplexes

Entry	PNA	$T_m$ (°C)	* $\Delta T_m$	# $\Delta T_m$
1	<i>aeg</i> -PNA <b>58</b> H-G-T-A-G-A-T-C-A-C-T-(CH <sub>2</sub> ) <sub>2</sub> CONH <sub>2</sub>	53 ( <i>ap</i> )	-	2
2	<i>aeg</i> -PNA <b>58</b> H-G-T-A-G-A-T-C-A-C-T-(CH <sub>2</sub> ) <sub>2</sub> CONH <sub>2</sub>	49 ( <i>p</i> )	-	-
3	<i>amp</i> -PNA <b>87</b> H-G-T-A-G-A-t <sub>SSR</sub> -C-A-C-T-(CH <sub>2</sub> ) <sub>2</sub> CONH <sub>2</sub>	50( <i>ap</i> )	-3	1
4	<i>amp</i> -PNA <b>87</b> H-G-T-A-G-A-t <sub>SSR</sub> -C-A-C-T-(CH <sub>2</sub> ) <sub>2</sub> CONH <sub>2</sub>	47 ( <i>p</i> )	-2	-

$T_m$  values are accurate to ( $\pm$ ) 0.5°C. Experiments were repeated at least thrice and the  $T_m$  values were obtained from the peaks in the first derivative plots.  $\Delta T_m$  indicates the difference in  $T_m$  with the control experiment *aeg*-PNA **57**. T and t indicating *aeg* and *amp*-PNA respectively \* $\Delta T_m$  Indicate the difference in  $T_m$  with the control experiment *aeg*-PNA **58**. # $\Delta T_m$  = difference in the  $T_m$  of *antiparallel* and *parallel* binding modes. Buffer: 10 mM sodium phosphate, 10 mM NaCl, pH 7.3. RNA **93** = 5'-AGUGAUCUAC3'; RNA **94** = 5'-CAUCUAGUGA3'

### 3. 14 Comparison studies of *amp*-PNA hybrids with complementary DNA

New conformationally restricted aminomethyl prolyl (*amp*)-monomers have been synthesized. These monomers were introduced in the *aeg*-PNA backbone using solid phase peptide synthesis protocol. The % hyperchromicity *versus* temperature plots derived from the UV melting data indicated a single transition characteristic of PNA<sub>2</sub>:DNA melting, wherein both PNA strands dissociate from the DNA strands simultaneously, in a single step. A single modification of the *amp* monomer unit at center of the sequence destabilized the corresponding DNA triplex except in the case of (2*S*,5*S*) *amp* monomer (Table 17, entry 4). In case of doubly modified *amp*-PNAs (2*S*,5*S*) and (2*S*,5*R*) derived *amp* units exhibited destabilization whereas (2*R*,5*S*) derived *amp* units marginally stabilized the corresponding DNA hybrids (Table 17, entry 6). The triplexes of the *amp*-PNA homooligomers stabilized the corresponding DNA hybrids in comparison to *aeg*-PNA **57**. Homooligomer derived of (2*S*,5*R*) *amp* monomer unit showed strong stabilization (+34 °C) and a minimal destabilization was observed in case of (2*S*,5*S*) *amp* monomer (Table 17, entry 7).

The (2*S*,5*S*) and (2*S*,5*R*) derived *amp*-PNA:DNA duplex complexes exhibited large destabilization, whereas (2*R*,5*S*) derived *amp*-PNA:DNA exhibited marginal stabilization in comparison to *aeg*-PNA **58**.

The (2*S*,4*S*,5*R*)-*amp* derived PNAs showed better stabilization compared to the other *amp*-PNAs, the duplexes complexes expressed the good orientational selectivity between the *antiparallel* and *parallel* orientation.

**Table 17** UV- $T_m$  ( $^{\circ}\text{C}$ ) of *amp*-PNA<sub>2</sub>:DNA and *amp*-PNA:DNA complexes

Entry	PNA	$T_m$								
1	H-T-T-T-T-T-T-T-(CH <sub>2</sub> ) <sub>2</sub> -CONH <sub>2</sub>	43								
2	H-GTAGATCACT-(CH <sub>2</sub> ) <sub>2</sub> CONH <sub>2</sub> ( <i>ap</i> )	50								
	H-GTAGATCACT-(CH <sub>2</sub> ) <sub>2</sub> CONH <sub>2</sub> ( <i>p</i> )	48								
			<i>S/R</i>	$\Delta T_m$	<i>S/S</i>	$\Delta T_m$	<i>R/S</i>	$\Delta T_m$	<i>R/R</i>	$\Delta T_m$
3	H- <b>t</b> -T-T-T-T-T-T-T-CH <sub>2</sub> ) <sub>2</sub> -CONH <sub>2</sub>	53	10	47	4	62	18	44	1	
4	H-T-T-T- <b>t</b> -T-T-T-T-(CH <sub>2</sub> ) <sub>2</sub> -CONH <sub>2</sub>	35	-8	43	-2	39	-4	36	-5	
5	H-T-T-T-T-T-T-T- <b>t</b> -(CH <sub>2</sub> ) <sub>2</sub> -CONH <sub>2</sub>	46	3	50	7	52	9	46	3	
6	H- <b>t</b> -T-T-T- <b>t</b> -T-T-T-(CH <sub>2</sub> ) <sub>2</sub> -CONH <sub>2</sub>	39	-4	40	-3	44	1	43	-0	
7	H-( <b>t t t t t t t t</b> )-(CH <sub>2</sub> ) <sub>2</sub> -CONH <sub>2</sub>	77	34	43	0	46	3	44	1	
8	H-G- <b>t</b> -AGA- <b>t</b> -CAC- <b>t</b> -(CH <sub>2</sub> ) <sub>2</sub> CONH <sub>2</sub> ( <i>ap</i> )	43	-7	50	0	52	2	46	-4	
	H-G- <b>t</b> -AGA- <b>t</b> -CAC- <b>t</b> -(CH <sub>2</sub> ) <sub>2</sub> CONH <sub>2</sub> ( <i>p</i> )	39	-9	37	-11	48	0	-	-	

A/G/C/T = *aeg*-PNA Adenine /Guanine /Cytosine /Thymine monomers, **t**<sub>SR</sub> = (2*S*,5*R*)- **t**<sub>SS</sub> = (2*S*,5*S*), **t**<sub>RS</sub> = (2*R*,5*S*), **t**<sub>SS</sub> = (2*S*,5*S*)-*amp*-PNA Thymine monomer.  $T_m$  values are accurate to ( $\pm$ ) 0.5 $^{\circ}\text{C}$ . Experiments were repeated at least thrice and the  $T_m$  values were obtained from the peaks in the first derivative plots.  $\Delta T_m$  indicates the difference in  $T_m$  with the control experiment *aeg*-PNA **57** and PNA **58** (mixed sequence). T and **t** indicating *aeg* and *amp*-PNA respectively. (measured in the buffer 10 mM sodium phosphate, 10mM NaCl, pH = 7.3), PNA<sub>2</sub>-DNA complexes. DNA **88**= 5'CGC-AAAAAAAA-CGC3' DNA **90** = 5'AGTGATCTAC3' (*antiparallel*); DNA **91** = 5'CATCTAGTGA3'(*parallel*).

### 3. 15 Comparison studies of *amp*-PNA hybrids with the complementary RNA

Unmodified *aeg*-PNA binds to DNA and RNA equally well without appreciable selectivity among these nucleic acids. To see if there is any binding selectivity for *amp*-PNA between DNA and RNA, *amp*-PNA<sub>2</sub>:RNA **92** complexes were constituted from *aeg*-PNA-T<sub>8</sub> **57**, and homooligomers.  $T_m$  values derived from various *aeg*-PNA and *amp*-PNA sequences with different degrees of modifications are in listed in Table 18. The  $T_m$  values indicate that, a single modification of *amp* (2*S*,5*S* and 2*R*,5*R*) unit at N-terminus caused destabilization in *amp*-PNA:RNA **92** triplexes, where as corresponding *cis-amp* units stabilized the triplexes (Table 18 entry 1). A single modification at C-terminus caused stabilization or minimal destabilization (S/R and R/R, Table 18 entry 5) in *amp*-PNA:RNA hybrids. A single modification at center of the sequence exhibited

destabilization of triplexes with irrespective of stereochemistry of the *amp* unit incorporated (Table 18, entry 4). Homooligomeric (*2S,5S* and *2S,5R*) *amp* PNAs exhibited stabilization, where as (*2S,5R*)-*amp*-PNA caused destabilization of corresponding RNA triplexes. In case of purine, pyrimidine mix sequence, (*2R,5S*)-*amp*-PNA oligomers exhibited good stabilization as well as orientational selectivity, where as (*2S,5S*) *amp*-PNA oligomers showed stabilization in antiparallel orientation and destabilized parallel PNA:RNA triplexes (Table 18, entry 8).

### 18 UV- $T_m$ (°C) of *amp*-PNA<sub>2</sub>:DNA and *amp*-PNA:RNA complexes

Entry	PNA	$T_m$								
1	H-T-T-T-T-T-T-T-(CH <sub>2</sub> ) <sub>2</sub> -CONH <sub>2</sub>	50								
2	H-GTAGATCACT-(CH <sub>2</sub> ) <sub>2</sub> CONH <sub>2</sub> ( <i>ap</i> )	53								
	H-GTAGATCACT-(CH <sub>2</sub> ) <sub>2</sub> CONH <sub>2</sub> ( <i>p</i> )	49								
			<i>S/R</i>	$\Delta T_m$	<i>S/S</i>	$\Delta T_m$	<i>R/S</i>	$\Delta T_m$	<i>R/R</i>	$\Delta T_m$
3	H-t-T-T-T-T-T-T-T-CH <sub>2</sub> ) <sub>2</sub> -CONH <sub>2</sub>	52	2	38	-12	56	6	49	-4	
4	H-T-T-T-t-T-T-T-T-(CH <sub>2</sub> ) <sub>2</sub> -CONH <sub>2</sub>	33	-18	48	-2	46	-4	43	-7	
5	H-T-T-T-T-T-T-T-t-(CH <sub>2</sub> ) <sub>2</sub> -CONH <sub>2</sub>	49	-1	51	1	52	2	45	-5	
6	H-t-T-T-T-t-T-T-T (CH <sub>2</sub> ) <sub>2</sub> -CONH <sub>2</sub>	ND		ND	-	50	-	44	-6	
7	H-(t t t t t t t t)-(CH <sub>2</sub> ) <sub>2</sub> -CONH <sub>2</sub>	40	-10	52	2	49	-1	ND	-	
8	H-G-t-AGA-t-CAC-t-(CH <sub>2</sub> ) <sub>2</sub> CONH <sub>2</sub> ( <i>ap</i> )	44	-9	50	-3	59	6	ND	-	
	H-G-t-AGA-t-CAC-t-(CH <sub>2</sub> ) <sub>2</sub> CONH <sub>2</sub> ( <i>p</i> )	40	-9	42	-7	51	2	-	-	

$\Delta T_m$  Indicate the difference in  $T_m$  with the control experiment *aeg*-PNA **57** and PNA **58** (mixed sequence). (measured in the buffer 10 mM sodium phosphate, 10 mM NaCl, pH = 7.3), PNA<sub>2</sub>-DNA complexes. A/G/C/T = *aeg*PNA Adenine /Guanine /Cytosine /Thymine monomers,  $t_{SR}$  = (*2S,5R*)-  $t_{SS}$  = (*2S,5S*),  $t_{RS}$  = (*2R,5S*),  $t_{SS}$  = (*2S,5S*)-*amp*PNA Thymine monomer The values reported here are the average of 3 independent experiments and are accurate to  $\pm 0.5^\circ\text{C}$ . T and t indicating *aeg* and *amp*-PNA respectively. ND = Not determine. RNA **92** = 5'CGCA<sub>8</sub>CGC3'; RNA **93** = 5'AGUGAUCUAC 3'; RNA **94** = 5'CAUCUAGUGA3'.

### 3. 16 Comparison studies of *amp*-PNA:DNA and *amp*-PNA:RNA hybrids

#### 3. 16. 1 Studies of triplex hybrids of *amp*-PNAs

In order to introduce PNA binding selectivity between DNA and RNA and higher affinity, optically pure (*2S,5R*), (*2S,5S*), (*2S,5S*) and (*2R,5R*)-*amp*-PNA oligomers were

synthesized. UV melting temperatures of these *amp*-PNAs with complementary DNA and RNA indicated that middle modified *amp*-PNAs (*amp*-PNAs **60**, **67**, **73**, and **79**) exhibited either destabilization or marginal stabilization with complementary DNA **88** and RNA **92**. N and C-terminal modified *amp*-PNAs exhibited stabilization with complementary DNA **88** and RNA **92**, whereas *(2R,5R)*-*amp*-PNAs with RNA-**92** shown destabilisation. Doubly modified *amp*-PNAs (**62**, **69**, **75**, and **81**) exhibited either destabilization or marginal stabilization with complementary DNA **88** and RNA **92**. In case of *(2R,5S)* doubly modified *amp*-PNA stabilization was observed. Homooligomers (*amp*-PNAs **65**, **71**) expressed good affinity and stability with the complementary DNA/RNA. *(2S,5S)* *amp*-PNA **65** stabilized the triplex with DNA by 34 °C but destabilized the triplex with RNA **92** by –10 °C, whereas *(2S,5S)*-*amp*-PNA **71** marginally destabilized the DNA **88** triplex but exhibited 6 °C of stabilization with RNA **92**. These results are presented in Figure 31.

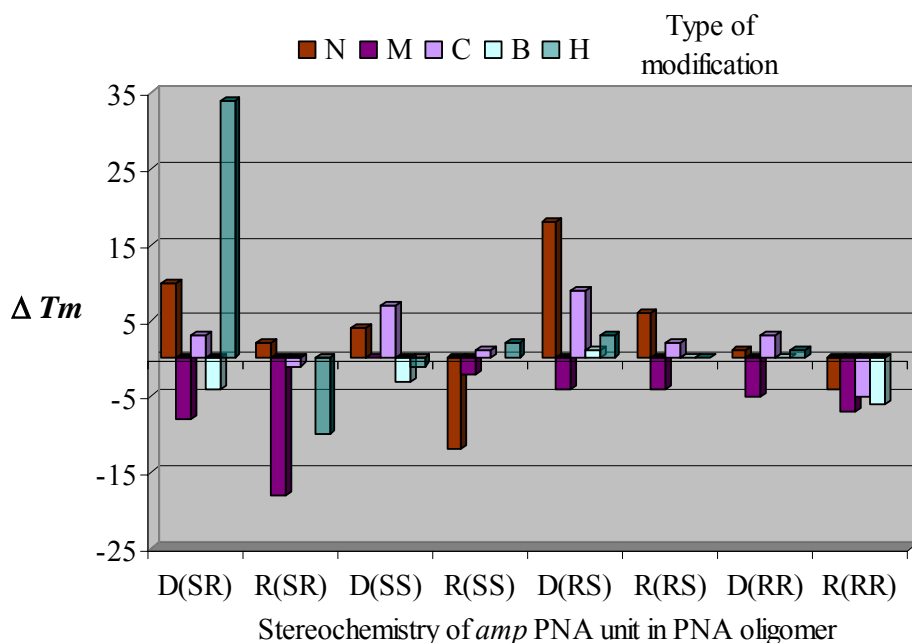
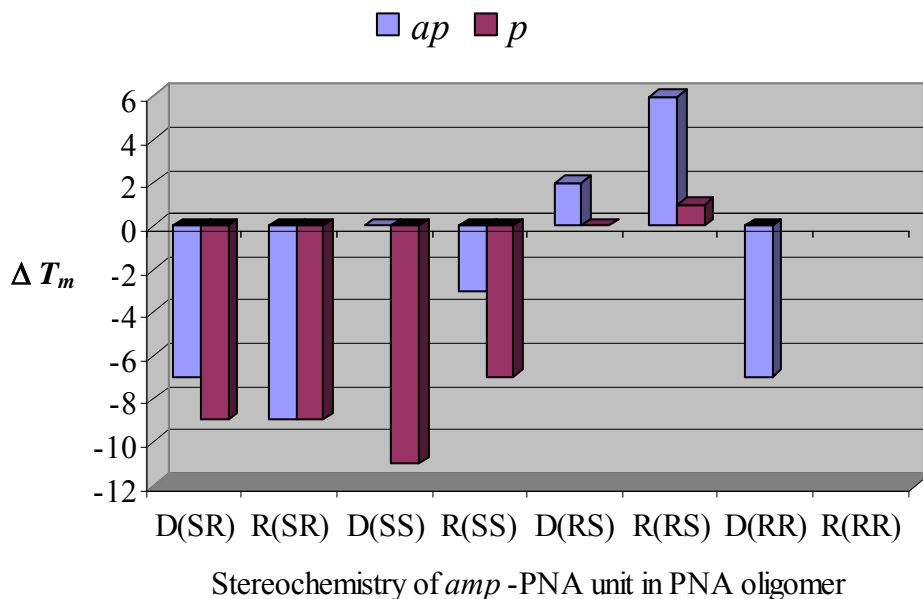


**Figure 31** Comparative  $\Delta T_m$  (°C) values of  $(amp-PNA)_2:DNA$  **88** and  $(amp-PNA)_2:RNA$  **92** complexes. The lower case letters on X-axis refer to the stereochemistry of *amp*-PNA. (D = DNA, R = RNA, N = N terminal modification, M = middle modification, C = C-Terminal modification, B = Bi-modification, H = Modified homooligomer). DNA **88** = CGCA<sub>8</sub>CGC.

### 3. 16. 2 Comparison studies of duplex hybrids of *amp*-PNAs

In order to study the *parallel* and *antiparallel* orientational preferences of PNA:DNA and PNA:RNA binding, mixed purine pyrimidine sequences (*amp*-PNAs **64**, **70**, **76** and **82**) that form duplexes were synthesized. All mixed purine pyrimidine



sequences except (2*R*,5*S*) stereochemistry exhibited strong destabilization towards complimentary DNA and RNA strands. The (2*R*,5*S*)-*amp*-PNA **76** exhibited good affinity and selectivity towards RNA in comparison to the unmodified *aeg*-PNA-**58**. Whereas (2*S*,5*S*)-*amp*-PNA **70** expressed a large destabilization and discrimination between *parallel* and *antiparallel* binding modes with both DNA and RNA. Above results are summarized in Figure 32.

**Figure 32** Comparative  $\Delta T_m$  ( $^{\circ}\text{C}$ ) values of (*amp*-PNA):DNA and (*amp*-PNA):RNA complexes with DNA **90**(*ap*) / **91**(*p*) and RNA **93**(*ap*) / **94**(*p*).  $\Delta T_m$  Indicate the difference in  $T_m$  with the control experiment *aeg*-PNA**58**. The lower case letters on X-axis refer to the stereochemistry of *amp*-PNA. (D = DNA, R = RNA, N = N terminal modification, M = middle modification, C = C-Terminal modification, B = Bi-modification, H = Modified homooligomer). DNA **90** = 5'AGTGATCTAC3' (*antiparallel*); DNA **91** = 5'CATCTAGTGA3'(*parallel*). RNA **93** = 5'AGUGAUCUAC3'; RNA **94** = 5'CAUCUAGUGA 3'.

### 3. 16. 3 Studies of triplex and duplex hybrids of *amp*-PNAs: DNA Vs RNA

The *amp*-PNA oligomers demonstrated a good binding affinity towards DNA triplex hybrids than the RNA triplexes. The *amp*-PNA:DNA and *amp*-PNA:RNA duplexes exhibited strong destabilization in comparison to *aeg*-PNA **58**. Homooligomers containing (2*S*,5*R*) *amp*-units exhibited selectivity between DNA and RNA, while (2*R*,5*S*)-*amp*-PNAs stabilized the DNA and RNA duplexes by inclining towards the *antiparallel* mode of binding.

### 3.16. 4 Studies of (2*S*,4*S*,5*R*)-*amp*-PNA:DNA and (2*S*,4*S*,5*R*)-*amp*-PNA:RNA hybrids

#### Studies of triplex hybrids of (2*S*,4*S*,5*R*)-*amp*-PNAs

In order to study the PNA binding selectivity and affinity between DNA and RNA, optically pure (2*S*,4*S*,5*R*)-*amp*-PNAs **84**, **85** and **86** oligomers were synthesized. UV melting temperatures of these *amp*-PNAs with complementary DNA and RNA

indicated that N-terminal modification stabilized both  $(2S,4S,5R)$ -*amp*-PNA:DNA and  $(2S,4S,5R)$ -*amp*-PNA:RNA triplexes by 6 °C and 2 °C respectively in comparison to *aeg*-PNA **57**. Middle modification of  $(2S,4S,5R)$ -*amp*-PNA exhibited the 2 °C of stabilization with DNA but a large destabilization was observed in case of RNA. C-terminal modification of  $(2S,4S,5R)$ -*amp*-PNA stabilized the  $(2S,4S,5R)$ -*amp*-PNA<sub>2</sub>:DNA **88** complex by 7 °C whereas same modification exhibited large destabilization with RNA triplexes. Thus  $(2S,4S,5R)$ -*amp*-PNA:DNA triplexes demonstrated more stability for DNA than RNA triplexes. These results are summarized in Figure 33.

### 3. 16. 5 Studies of duplex hybrids of $(2S,4S,5R)$ -*amp*-PNAs

To see the *parallel* and *antiparallel* orientational preferences of PNA:DNA and PNA:RNA binding, mixed purine pyrimidine sequence  $(2S,4S,5R)$ -*amp*-PNA **87** was synthesized. The duplex complexes of  $(2S,4S,5R)$ -*amp*-PNA **87** with DNA **90** and **91** stabilized by 5 °C in comparison to un modified *aeg*-PNA **58**. No selectivity was observed between *antiparallel* and *parallel* mode of binding orientation. In case of RNA, destabilization was observed in both orientations by -3 °C (*ap*) and -1 °C (*p*) in comparison to *aeg*-PNA **58**. These results suggest that  $(2S,4S,5R)$ -*amp*-PNAs having more affinity towards DNA than the RNA. The above results are presented in Figure 33.

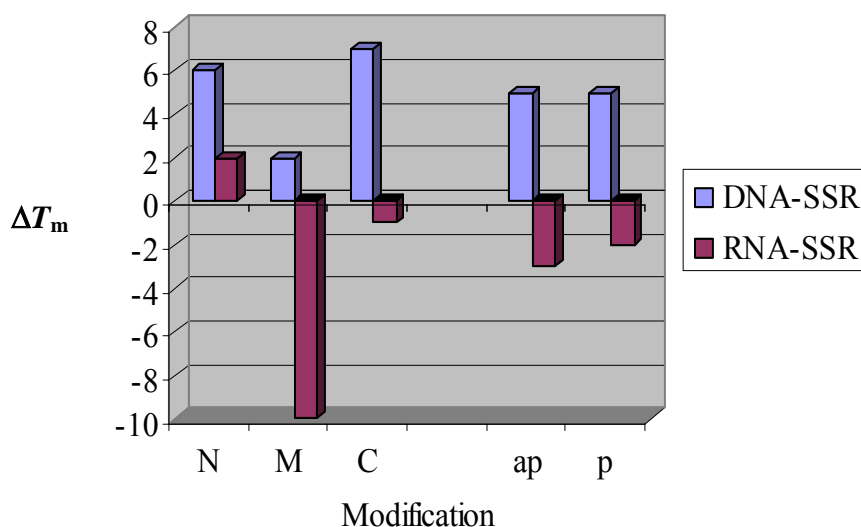


**Figure 33** Comparative  $\Delta T_m$  ( $^{\circ}\text{C}$ ) values of  $(2S,4S,5R)\text{-amp-PNA}_2\text{:DNA}$  **88**,  $(\text{amp-PNA})_2\text{:RNA}$  **92**,  $(2S,4S,5R)\text{-amp-PNA}\text{:DNA}$  and  $(\text{amp-PNA})\text{:RNA}$  complexes with DNA **90**(*ap*) / **91**(*p*) and RNA **93**(*ap*) / **94**(*p*) complexes.  $\Delta T_m$  Indicate the difference in  $T_m$  with the control experiment *aeg*-PNA**58** (tiplexes) and *aeg*-PNA **58** (duplexes). The lower case letters on X-axis refer to the modification of *amp*-PNA. (N = N terminal modification, M = middle modification, C = C-Terminal modification). DNA **90** = 5' AGTGATCTAC3' (*antiparallel*); DNA **91** = 5'CATCTAGTGA3'(*parallel*). RNA **93** = 5'AGUGAUCUAC3'; RNA **94** = 5' CAUCUAGUGA3', DNA **88** = 5'(CGC-AAAAAAAA-CGC)3'

### 3. 17 Aminomethyl thiazolidine (*amt*) PNA

In 2001 Ge'rrard Chassaing et al<sup>17</sup> were synthesized *anti* and *syn*-aminomethyl)-thiazolidine (*amt*) PNA monomers and incorporated in to central position of *aeg*-PNA(10 mer) to study the binding and selectivity towards DNA and RNA.

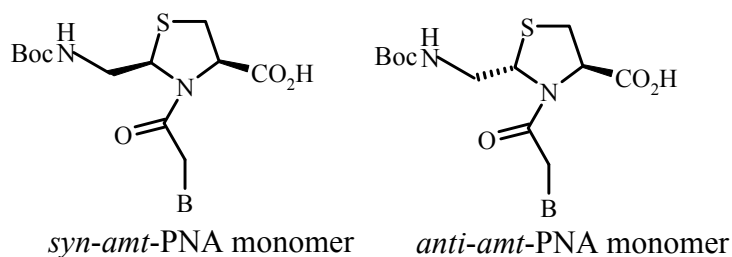


**Figure 34** *amt*-PNA monomers

The *anti* and *syn- amt*-PNAs demonstrated strong destabilization of (–17 and –22 °C) respectively in comparison to control experiment.  $T_m$  value of poly (rA) revealed a destabilization of –20 °C by both *anti* and *syn –amt*-PNAs.

### 3.18 Conclusion

In order to introduce PNA binding selectivity between DNA and RNA and higher affinity, we have synthesized *amp*-PNAs by incorporating optically pure (2*S*,5*R*), (2*S*,5*S*), (2*R*,5*S*) and (2*R*,5*R*) aminomethyl prolyl(*amp*) monomers in to *aeg* backbone. The UV- $T_m$ s in Table 17 and 18 indicates that, the single middle modification showed destabilization irrespective of the stereochemistry of the *amp* units. This could be a result of introduction of unfavored conformational discontinuity at the modification site. PNAs containing a *amp* unit at C or N terminus exhibited strong affinity towards DNA than RNA. The preorganisation imparted by *amp* units (C or N terminus) in to *aeg* backbone resulted in a favorable conformation for DNA and the same favorable conformation behaved as antagonist to RNA. The doubly modified (2*R*,5*S*)-*amp*-PNAs showed stabilization with both DNA and RNA and the same modification with other *amp* units destabilized the DNA and RNA complexes. This could be a result of the induction of moderately favorable preorganization into *aeg* backbone. The degree of selectivity expressed by *amp* units between DNA and RNA is not clear in case of singly and doubly modified *amp*-PNAs. The (2*S*,5*R*) homooligomer exhibited strong DNA affinity, the same modification destabilized the RNA triplex, in case of (2*S*,5*S*) *amp* unit reverse trend was seen. Thus a high degree of selectivity is seen in case of homooligomers between DNA and RNA. The stability and selectivity of homooligomer is the result of the uniform conformational change over the entire backbone, without any sharp

discontinuities and the selectivity is due to chiral nature of the back bone which was ultimately induced by the stereochemistry of the *amp* unit. In the case of homooligomers these results suggesting that the effect of stereochemistry of *amp* unit is the dominant factor in deciding the native conformation of peptide, which in turn effect the binding affinity *amp*-PNA oligomers towards complementary sequence.

The stability and the selectivity between (*ap/p*) exhibited by 4-hydroxy *amp* units is the result of positive preorganization and the chirality (3-chiral centers) induced by the 4-substituted *amp* in tothe *aeg* backbone. The selectivity of *amp*-PNA **87** is due to the flexible ring puckering nature of 4-substituted *amp* unit allows better torsional adjustments to attain hybridization competent conformation which is absent in the *amp* unit.

The  $T_m$  of the *amp*-PNA duplexes reflects the weak affinity of *amp*-PNA oligomers towards DNA and RNA. Only (*2R,5S*)-*amp*-PNAs exhibited strong affinity towards DNA and RNA. This could be a result of introduction of unfavored conformational discontinuity at the three consecutive places into *aeg* backbone at modification sites. The differences in the stabilization of duplex versus triplex modes with *amp* units could arise from the difference in their structural features that fine tune the internucleobase geometries. The divergence observed in the  $T_m$ s of modified *amp*-PNAs is the result of degree of favorable preorganizaton induced by the stereochemistry and the site of the *amp* units in to *aeg* backbone.

These results lead us to believe that a biased pre-organized conformation capable of maintaining the correct internucleobase-distance could be particularly important in order to preserve specific base pairing. Structural differences in PNA:DNA,

PNA:RNA and PNA<sub>2</sub>:DNA reflected in the control of *aeg*-PNA complex formation with DNA/RNA sequences through elegant use of stereo chemistry pattern of 5-substituted proline derivatives. Further studies on sequence dependent and RNA/DNA discriminatory effects of *amp*-PNA in mixed base *amp*-PNA sequences having all modified *amp*-PNA (A/G/C/T) monomers and their thermodynamic studies to delineate entropic and enthalpic contributions are need to be carried out and also molecular modeling or NMR Solution structure and X-ray crystal structure analysis of the corresponding triplexes and duplexes are necessary to understand the structure-activity relationships (SAR) and the observed results.

### 3. 19 Reference:

1. (a) Knoll, M.; Ruska, E. Z. (munich) **1932**, *8*, 318. (b) Magarino, J.; Tuchendler, J.; Beauvillain, P.; Laursen, I. Epr experiments in LiTbF<sub>4</sub>, LiHoF<sub>4</sub> and LiErF<sub>4</sub> at submillimeter frequencies *Physical review B*. **1980**, *21*, 18. (c) Wollan, E. O.; Shull, C. G.; Marney, M. C. Laue Photography of Neutron Diffraction *Phys. Rev.* **1948**, *73*, 527. Egholm, M.; Buchardt, O.; Christensen, L.; Behrens, C.; Freier, S. M.; Driver, D. A.; Berg, R. H.; Kim, S. K.; Nordén, B.; Nielsen, P. E. PNA hybridizes to complementary oligonucleotides obeying the Watson-Crick hydrogen-bonding rules. *Nature*, **1993**, 566.
2. Koch, T.; Naesby, M.; Wittung, P.; Jorgensen, M.; Larsson, C.; Buchardt, O.; Stanley, C. J.; Nordén, B.; Nielsen, P. E.; Qrum, H. PNA-Peptide Chimerae. *Tetrahedron Lett.* **1995**, *36*, 6933.

3. Bergmann, F.; Bannwarth, W.; Tam, S. Solid phase synthesis of directly linked PNA-DNA-hybrids. *Tetrahedron Lett.* **1995**, *36*, 6823.
4. Kosynkina, L.; Wang, W.; Liang, T. C. A convenient synthesis of chiral peptide nucleic acid (PNA) monomers. *Tetrahedron Lett.* **1994**, *35*, 5173.
5. Dueholm, K. L.; Petersen, K. H.; Jensen, D. K.; Nielsen, P. E.; Egholm, M.; Buchardt, O. Peptide nucleic acid (PNA) with a chiral backbone based on alanine. *Bioorg. Med. Chem. Lett.* **1994**, *4*, 1077.
6. Lowe, G.; Vilaivan, T. Solid-phase synthesis of novel peptide nucleic acids. *J. Chem. Soc. Perkin Trans I*, **1997**, 555.
7. Gangamani, B. P.; Kumar, V. A.; Ganesh, K. N. Chiral analogues of peptide nucleic acids: Synthesis of 4-aminopropyl nucleic acids and DNA complementation studies using UV/CD spectroscopy. *Tetrahedron*, **1999**, *55*, 177.
8. Howarth, N. M.; Wakelin, L. P. G.  $\alpha$ -PNA: A novel peptide nucleic acid analogue of DNA. *J. Org. Chem.* **1997**, *62*, 5441.
9. Altmann, K-H.; Chiesi, C. S.; Garcíá- Echeverría, C. Polyamide based nucleic acid analogs - synthesis of  $\delta$ -amino acids with nucleic acid bases bearing side chains. *Bioorg. Med. Chem. Lett.* **1997**, *7*, 1119.
10. Zhang, L.; Min, J.; Zhang, L. Studies on the synthesis and properties of new PNAanalogs consisting of L- and D-lysine backbones. *Bioorg. Med. Chem. Lett.* **1999**, *9*, 2903.
11. Van der Laan, A. C.; van Amsterdam, I.; Tesser, G. I.; van Boom, J. H.; Kuyll-Yeheskiely, E. Synthesis of chirally pure ornithine based PNA analogues. *Nucleosides & Nucleotides*, **1998**, *17*, 219.
12. Kim, S. K.; Nielsen, P. E.; Egholm, M.; Buchardt, O.; Berg, R. H.; Nord, B. Right-handed triplex formed between peptide nucleic acid PNA-Ts and Poly(dA) shown by linear and Circular dichroism spectroscopy. *J. Am. Chem. Soc.* **1993**, *115*, 6477.
13. Peptide Nucleic Acids Protocols and Applications, Edited by Nielsen, P. E.; Egholm, M. Horizon scientific Press, 1999.

14. Sforza, S.; Haaima, G.; Marchelli, R.; Nielsen, P. E. Chiral peptide nucleic acids (PNAs): helix handedness and DNA recognition. *Eur. J. Org. Chem.* **1999**, 197-204.
15. Job, P. *Ann. Chim.* **1928**, 9, 113. (b) Cantor, C. R.; Schimmel, P. R. *Biophys. Chem. Part III* **1980**, 624.
16. Haasnoot, C. A. G.; De leeuw, A. A. M.; De leeuw, H. P. M.; Altona, C. *Biopolymers* **1981**, 20, 1211.
17. Sarah, B.; Fabienne, B.; Jacqueline, V.; Ge' rard, C. Synthesis and Hybridization Properties of Thiazolidine PNAs. *Eur. J. Org. Chem.* **2001**, 3285.

---

## **CHAPTER-4**

### **SECTION-I**

Introduction of 2,5-disubstituted pyrrolidines

---

## Introduction

### 4.1 2,5-Disubstituted pyrrolidines

Pyrrolidines, the 5-membered aza-heterocycles substituted at 2<sup>nd</sup> and 5<sup>th</sup> positions, are often encountered in the living organisms. The first pyrrolidine alkaloids were found in the *solenopsis* ant's venom. These compounds have been extracted from plants, animals and microorganisms, but only in very micro quantities. Because of scarcity of these naturally occurring products, only few studies on their biological activity and mechanism of action have been performed.

2,5-Dialkylated pyrrolidines extracted from venomous ants and frogs<sup>1</sup> have shown insecticide<sup>2,3</sup> hemolytic and antiendinergetic<sup>4</sup> activities. Polyhydroxy pyrrolidines isolated from several plants of the *companulaceae* and *fabaceae* families have shown very potent activity as enzyme inhibitors (e.g. codonosine).<sup>5</sup> Apart from the medicinal uses, these compounds possessing a C<sub>2</sub> symmetry axis, may be used as very powerful catalyst in numerous asymmetric reactions.<sup>6</sup> All these reasons make these compounds interesting targets for synthetic chemist.

This section briefly presents the stereoselective synthesis of 2,5-disubstituted pyrrolidines and will be subdivided in two main sections : (1) where the 5-membered ring is formed by stereospecific methods and (2) where the already formed ring is functionalized at the 2<sup>nd</sup> and 5<sup>th</sup> positions.

#### 4.1.1 Synthesis with formation of the pyrrolidine ring:

##### 4.1.1.a Radical cyclization:

Several methods have been reported in the literature for the synthesis of 2,5-substituted pyrrolidines by means of intramolecular cyclization of  $\delta$ -alkenyl amines via

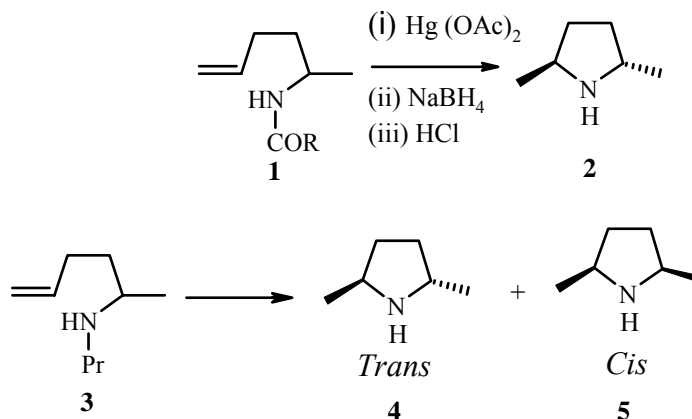


**Figure 1.** Amido and amino mercuration

the aminyl radical as an intermediate. Photolysis,<sup>7</sup> thermolysis, of *N*-chloroamines<sup>8</sup> and anodic oxidation of lithium amides and hydroxylamines<sup>9,10</sup> are the most encountered methods. Anodic oxidation of  $\gamma,\delta$ -unsubstituted lithium amides furnish the exclusively *cis*-2,5-substituted pyrrolidines, where as *N*-chloroalkenylamine in the presence of tributyltin hydride and azoisobutyronitrile ( $n\text{-Bu}_3\text{SnH-AIBN}$ ) giving rise almost to *trans* 2,5-substituted pyrrolidines.

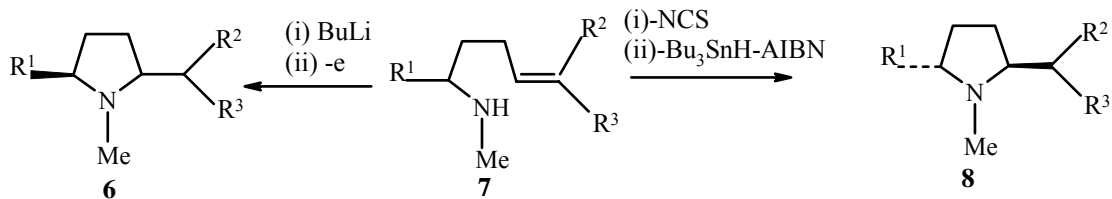


**Figure 2.** Radical cyclization of bis homoallylic amines

### 4.1.1.b Electrophilic cyclisation

This is subdivided in to intramolecular cyclization and intermolecular cyclization.

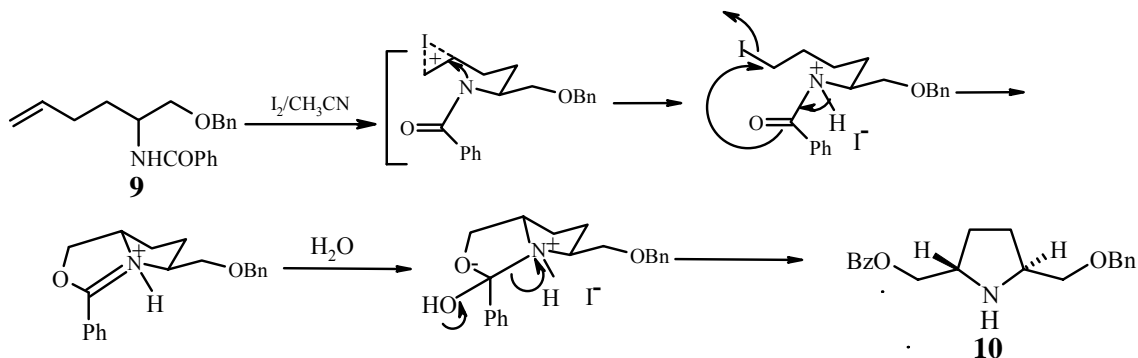
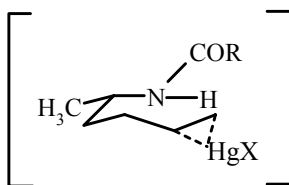


**Figure 3.** Iodocyclisation

#### A. Intramolecular cyclization:

Iodocyclization<sup>11</sup> and amino and amido mercuration<sup>12</sup> are the two prominent methods employed in the synthesis of 2,5-substituted pyrrolidines. Iodocyclization  $\delta$ -alkenylamines in presence of  $I_2$  and aqueous  $CH_3CN$  preferentially furnish the *trans* 2,5-substituted pyrrolidines.



Amino and amido mercuration of  $\delta$ -alkenylamines have been studied by Perie in 1972. Treatment of  $\delta$ -alkenylamines with  $Hg(OAc)_2$  leads to the formation of both *cis*-*trans* products, in case of amido mercuration, exclusively *trans* product was observed. The stereochemistry of the cyclization may be explained by the preferred chair transition state with the equatorial methyl group.

## B. Intermolecular cyclization.

### Intermolecular cyclization of chiral silanes:

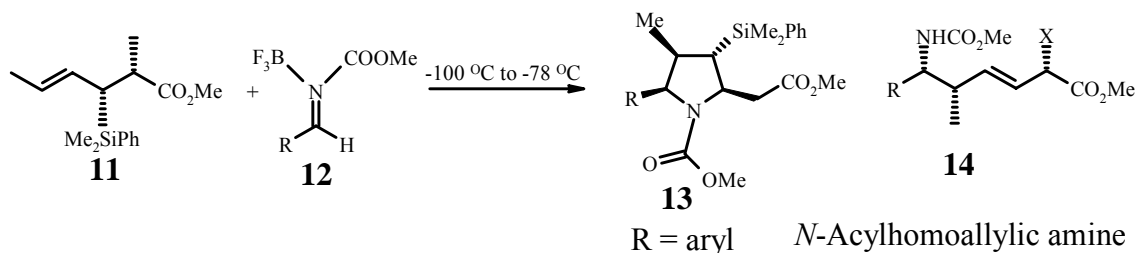
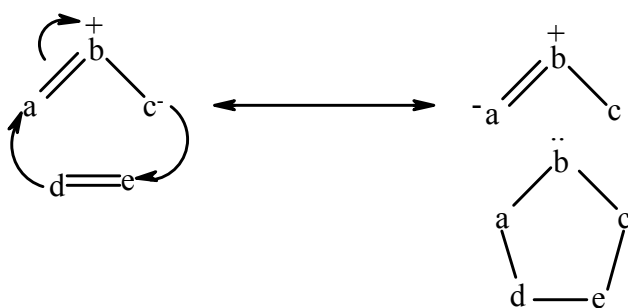


**Figure 4.** Cyclization of chiral allylsilanes

This method was discovered by Panek and Naresh<sup>13</sup> in which chiral allylsilanes were treated with *N*-Acyylimines, generated in situ at temp  $-100\text{ }^{\circ}\text{C}$  to  $-78\text{ }^{\circ}\text{C}$  formation of *N*-acyl pyrrolidines was observed, when the temperature raised to  $-78\text{ }^{\circ}\text{C}$  to  $-20\text{ }^{\circ}\text{C}$  *N*-acylhomoallylic amines were formed.

#### 4.1.2 1,3-Dipolar cycloadditions:

The 1,3-dipolar cycloadditions are among the efficient methods for the synthesis of pyrrolidines<sup>14</sup> and pyrrolines. These reactions are concerted and exhibit high stereo- and regioselectivity.



Compounds with  $4\pi$ -electrons named as 1,3-dipolar, which is formed by 3 atoms a-b-c, of which a has a sextet of electrons in outer shell and c has octet with at least one

unshared pair and it can be drawn as zwitterions, where the +ve charge localizes at central atom, negative charge distributes at terminal atoms. Compound with  $2\pi$ -electrons is known as alkene and named as dipolarophile. Azomethine ylides and nitrones are two allylic dipoles used for the synthesis of polysubstituted pyrrolidines.

#### 4.1.2.a Azomethine ylides:

Imines of  $\alpha$ -amino esters react with electron deficient alkenes in the presence of Lewis acids to give polysubstituted pyrrolidines. Reaction proceeds via the formation of metallodipole, which is formed by co-ordination of metal with nitrogen atom and carbonyl of the imine, followed by deprotection. Use of a tertiary amine favors the formation of metallodipole.

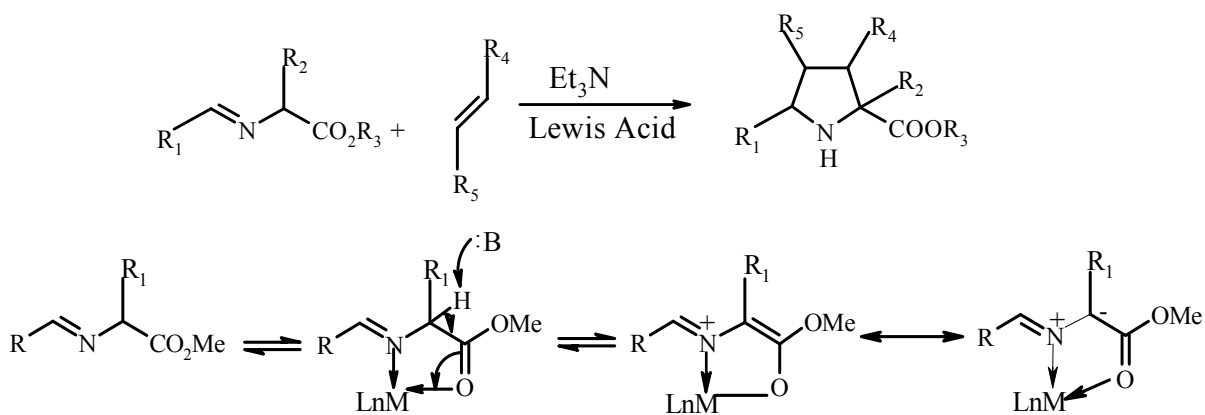


**Figure 5.** Formation of metallodipole

Asymmetric 1,3-dipolar cycloadditions of azomethine ylides<sup>15</sup> were performed by using (i) chiral dipolarophiles<sup>16</sup> (ii) chiral azomethine ylides<sup>17</sup> and (iii) chiral catalyst.<sup>18</sup>

#### 4.1.2.b 1,3-Dipolar cycloadditions of nitrones:

Tufariello and Puglis<sup>19</sup> noted in 1986 that cyclo adducts **16**, obtained by addition of 1-oxyde-1-pyrrolidine **15** on mono substituted alkene in the presence of a carboxylic peracid, allowed the regiospecific access to nitronone **17**. A second cycloaddition will stereoselectively lead to trans 2,5-dialkyl pyrrolidines generally with good de.

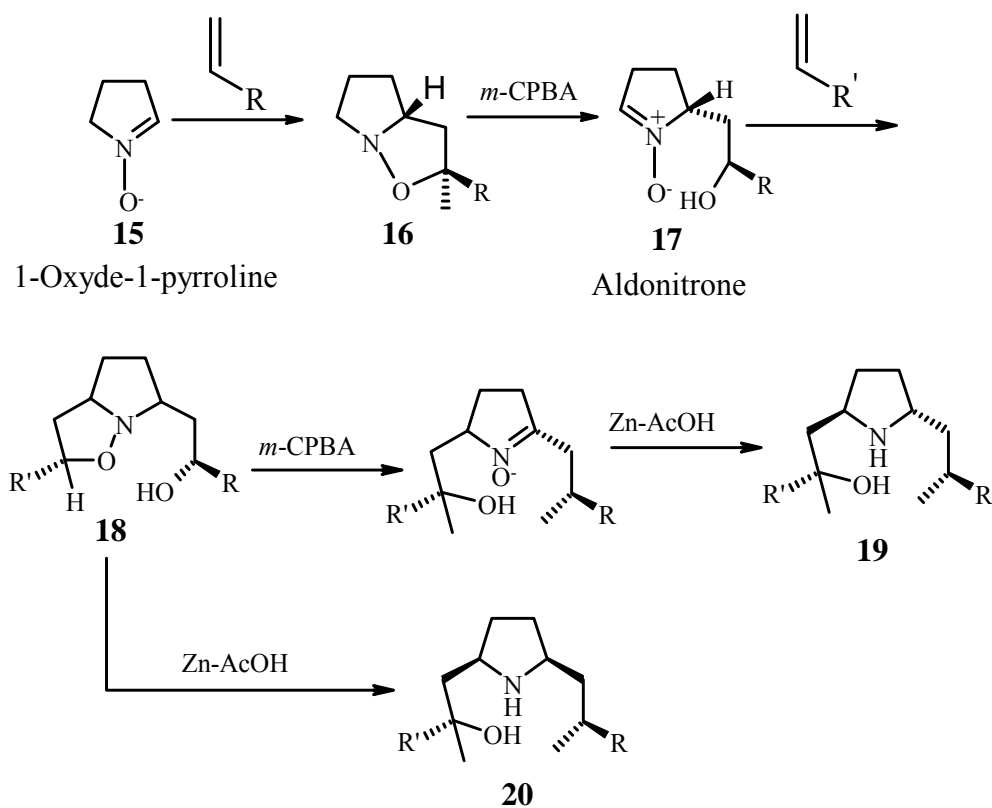


Figure 6

#### 4.1.2.c Cycloaddition of azapentadienyl anions:

In 1994<sup>20</sup> Pearson and Jacobs reported the synthesis of 2-alkenyl pyrrolidines **24**, by anionic cyclization of 2-azapentadienyl anion **23** with electron rich alkenes. This reaction is contrary to the cycloaddition of azomethine ylides in which electron deficient

alkene takes part for the formation of pyrrolidine rings depending on the nature of the electrophiles and alkenes yields are ranging from 43-93%.

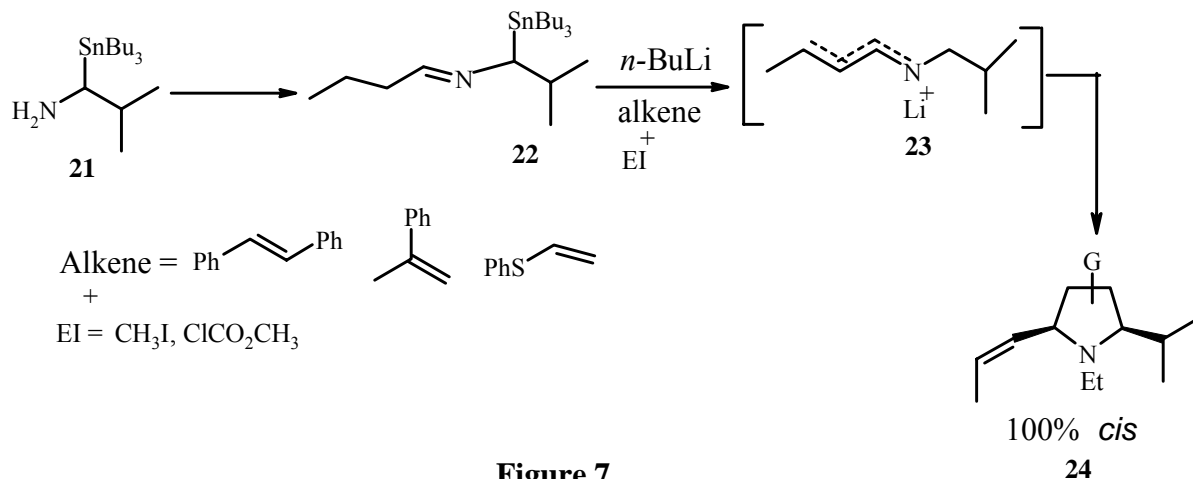


Figure 7

#### 4.1.3.1 Reduction-cyclization of $\gamma$ -aza-derivative ketones:

This section briefly describes the reductive amination of  $\gamma$ -azaderivative ketones in the presence of hydrogen and a metal such as Pt or Pd.

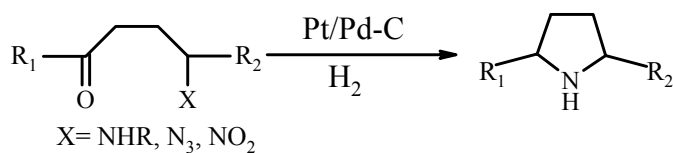
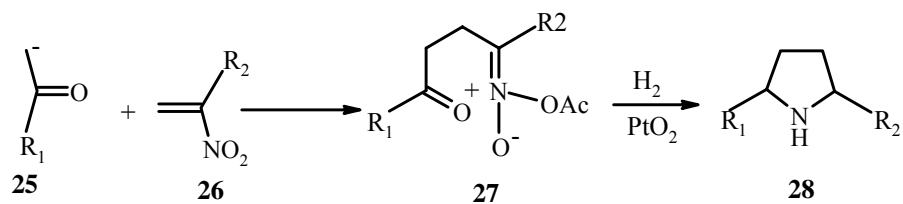


Figure 8

##### 4.1.3.1a Hydrogenation of nitrones:

In 1990 Yoshikoshi et al.<sup>21</sup> reported the synthesis of 2,5 dialkyl pyrrolidines from hydrogenation of acetylnitronates **27**, prepared from nitroalkanes & enolates, low diastereoselectivity was observed in this procedure. Oppolzer<sup>22</sup> used chiral cyclic nitrones for the synthesis of 2,5-dialkyl pyrrolidines.



**Figure 9**

#### 4.1.3.1b Hydrogenation of nitroketones:

Hydrogenation of nitroketones is very often used method for the synthesis of aza-heterocycles Kloetzel<sup>23</sup> in 1947 described first synthesis of polysubstituted pyrrolidine through this method. Stenens and Lee<sup>24</sup> in 1982 synthesized compound 30 from  $\gamma$ -nitroketones.

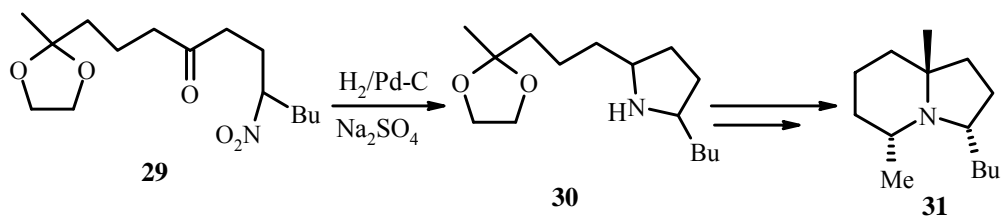


**Figure 10**

#### 4.1.3.1c Reductive amination of azidoketones:

Paulsen et al.<sup>25</sup> first used this method for the synthesis of 2,3,4,5-tetrasubstituted pyrrolidine from chiral  $\alpha$ -azidoaldehydes and dihydroxyacetonephosphate as shown in Figure 11.

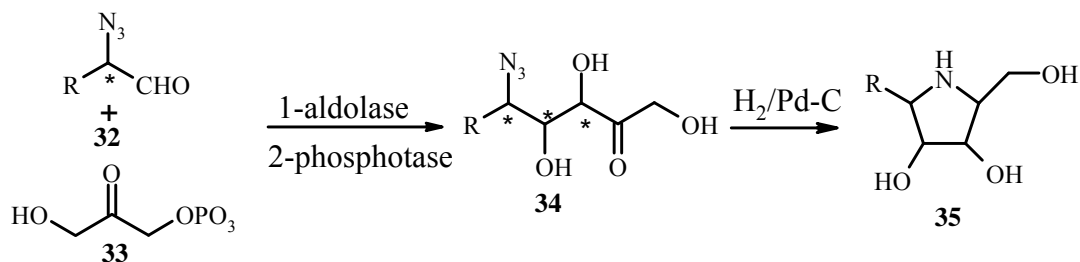


**Figure 11**

Chiral  $\alpha$ -azidoaldehydes **32** were first condensed with DHAP (dihydroxyacetone phosphate) **33**, through an aldolase catalyzed reaction. Then the azidoketone **34**, after removal of the phosphate group, is hydrogenated on palladium to give the expected azasugars **35**.

#### 4.1.3.2 Reductive amination of 1,4-diketones:

The reductive amination of 1,4-diketones is one of the oldest method for the preparation of 2,5-disubstituted pyrrolidines Figure 12.

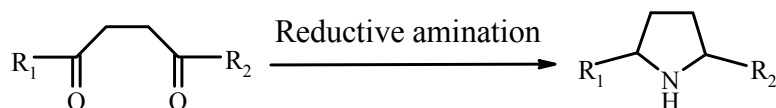


**Figure-12**

This method is not stereoselective, Jones and Blum<sup>26</sup> optimized this method and showed that a treatment of 1,4-diketones **36** by an excess of ammonium carbonate allows the formation of the non isolated pyrrole intermediates **37** which are hydrogenated to give the *trans* isomers as the major compounds (d.e. = 85:15). Alkaloids **38a-c** were synthesized through this methodology and the *trans* isomer was always the major one (Figure 13).

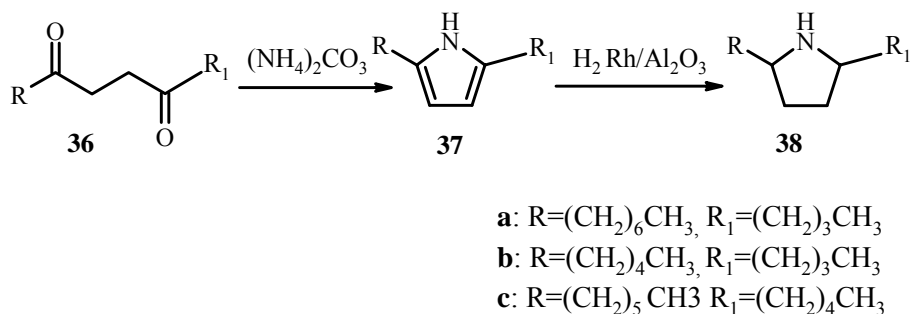


**Figure 13**

#### 4.1.4 Cyclization by S<sub>N</sub>2 reactions

##### 4.1.4.1 Intramolecular cyclization

Synthesis of functionalized pyrrolidines **40** were prepared by intermolecular S<sub>N</sub>2 substitution from aminoalcohol derivatives such as **39** are described in literature. The cyclization is usually stereospecific and a very little epimerisation occurs during the process (Figure 14).

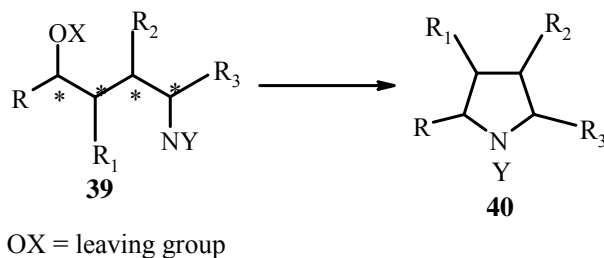


**Figure 14**

##### 4.1.4.1a Aminoalcohol derivatives:

Wightman et.al.<sup>27</sup> achieved the synthesis of **43** via the non isolable aminoalcohol derivative, which was obtained through a diastereoselective addition of ammonia to  $\alpha,\beta$ -unsaturated esters **41** (Figure 15).

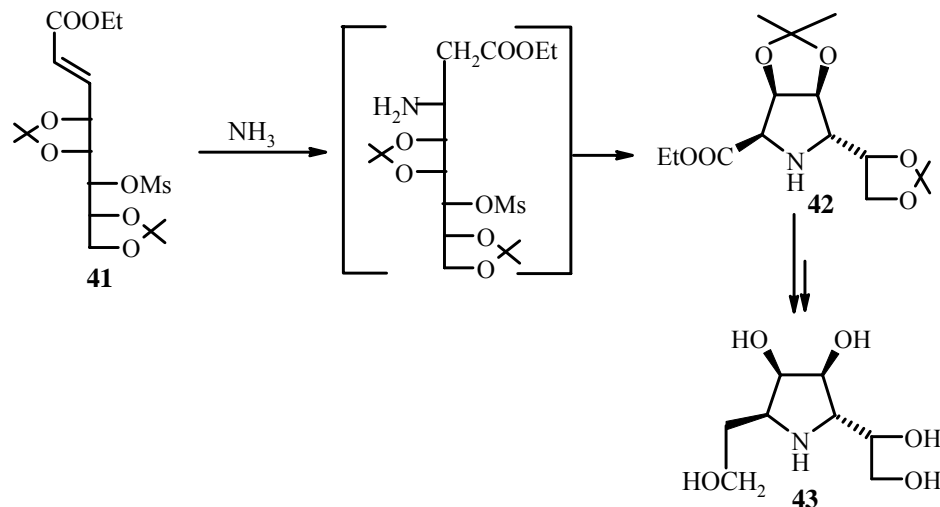


**Figure 15**

MacGavrey et.al<sup>28</sup> reported that addition of ammonia was dependent both on the stereochemical relationship of the alkene and the bulkyness of the acetal.<sup>29</sup> The major isomer formed was the *trans* pyrrolidine.

#### 4.1.4.1b Nucleophilic opening of aziridines:

Depezay et.al<sup>30</sup> described the nucleophilic opening of bis-aziridines **44** by phenylthiolates ions or azides, followed by cyclization into pyrrolidines. A mixture of polysubstituted pyrrolidines **46b** and piperidines **46a** was thus obtained (Figure 16). Usually, pyrrolidines **46b** are the major compounds so formed (along with 7 % of piperidines **46a**) with chemical yields ranging from 51 to 84 %.

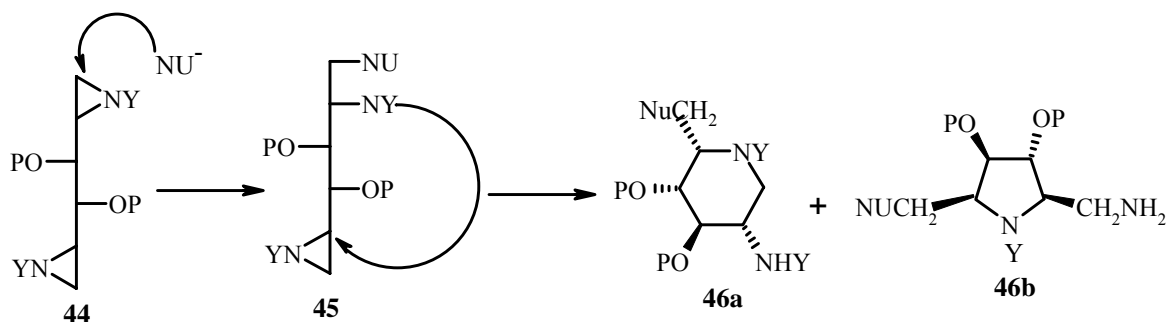


**Figure 16**

#### 4.1.4.1c Aminoepoxides:

Intramolecular cyclization of  $\gamma$ -aminoepoxides is a very attractive method for the preparation of 2,5-disubstituted pyrrolidines. Langlois et. al.<sup>31</sup> in 1986 used this strategy for the synthesis of neothramycines (Figure 17).

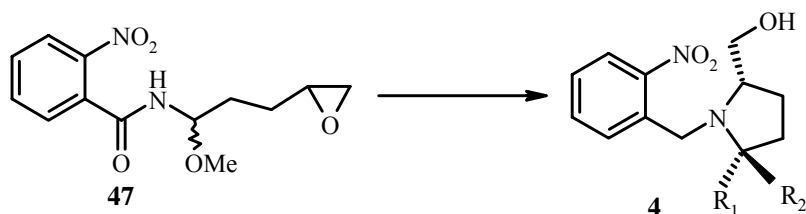


Figure 17

Biellmann et.al.<sup>32</sup> in 1992 synthesized the compound **52** and **53** as shown in figure 18. The dianion of propynylamine **49** (Figure 18) is obtained by treatment with LDA, and reacted with the bromide **50** leading to an unseparable mixture (30:70) of amino carbamate epoxides **51** with 60% chemical yield. The mixture of **51** is then either treated by silica gel at 65 °C (2 giving a mixture of products **53** (*cis:trans* 11:9), or by trifluoroacetic acid at 0 °C leading to pyrrolidines **52** with a 15:85/*cis:trans* ratio.

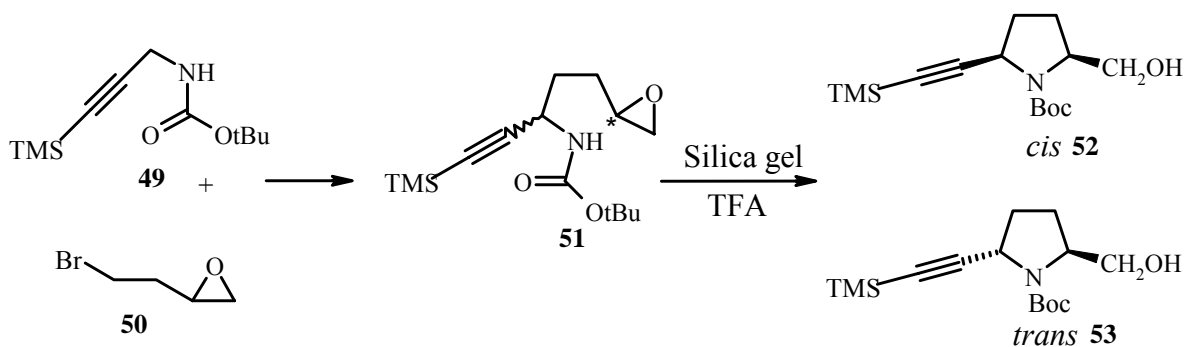
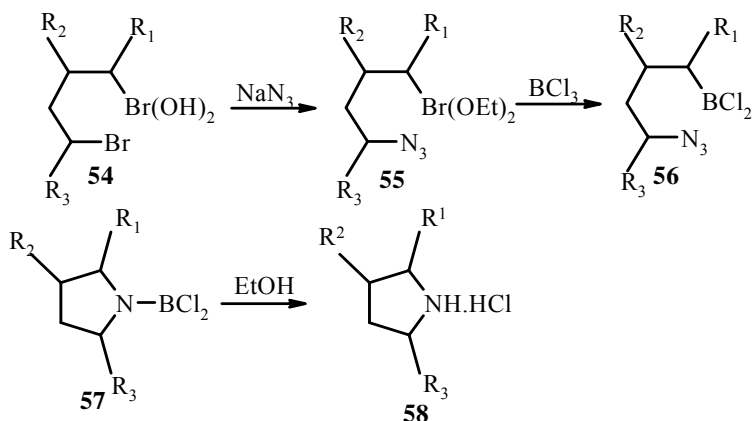


Figure 18

#### 4.1.4.1d Intramolecular cyclization of $\omega$ -azidoalkyl boronic esters:

Carboni et. al.<sup>33</sup> showed in 1989 that  $\omega$ -azidoalkyl boronic esters **55**, after reduction, cyclized in situ to give the corresponding heterocycles **57** (Figure 19). From diastereoisomerically and enantiomerically pure boronic esters (prepared by asymmetric



**Figure 19**

hydroboration), the corresponding pyrrolidines **58** are obtained with a total control of the configurations and with excellent yields (80 to 89 %, depending on the nature of  $R^1$ ,  $R^2$  and  $R^3$ ).

#### **4.1.4.2 Intermolecular cyclizations:**

##### **4.1.4.2a Aminocyclization of 2,5-dibromoadipic acid esters:**

In 1960, Gignarella et al.<sup>34</sup> described the synthesis of pyrrolidine-2,5-dimethyldicarboxylate starting from dibromo adipic acid ester and benzylamine (Figure-20). In 1992, Yamamoto<sup>35</sup> replaced benzylamine by (-)-(S)-phenylethylamine and obtained enantiomerically pure compounds.

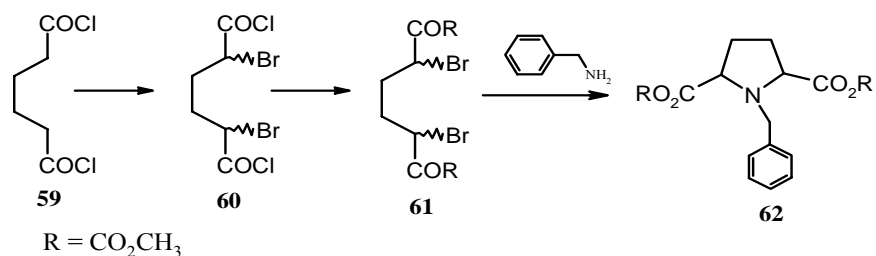


**Figure 20**

#### 4.1.4.2b *Trans amination of 1,4-dihydroxy derivatives:*

Nucleophilic attack followed by cyclization of 1,4-dihydroxy derivatives by primary amine to form trans 2,5-disubstituted pyrrolidines is a well known reaction directly derived from the studies on the aminocyclizations of 2,5-dibromoadipic acid esters (Figure 21).

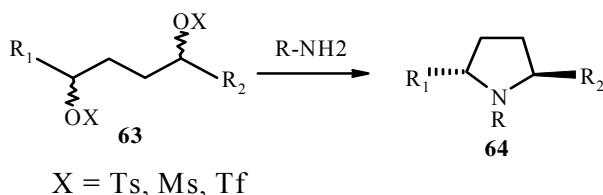


**Figure 21**

Numerous amines were used: e.g. ammonia, benzylamine, hydrazine, hydroxylamine, allylamine. Several leaving groups were also employed such as tosylates, triflates and mesylates. Usually the stereoselectivity, and the stereospecificity are excellent. In the non racemic cases, the chirality may be introduced by: (i) the diols may be enantiomerically pure and because the cyclization occurs through a S<sub>N</sub>2 type reaction, inversions of both stereogenic centres are observed; (ii) a chiral auxiliary such as the

amine allows the stereoselective formation of enantiomerically pure pyrrolidines from a racemic mixture of 1,4-dihydroxy derivatives.<sup>36</sup>

## 4.2 Synthesis from aza-heterocycles:

### 4.2.1 Synthesis from proline:

Shono<sup>37,38</sup> prepared the  $\alpha$ -methoxylated methyl ester of proline with 87% yield but without diastereomeric excess.

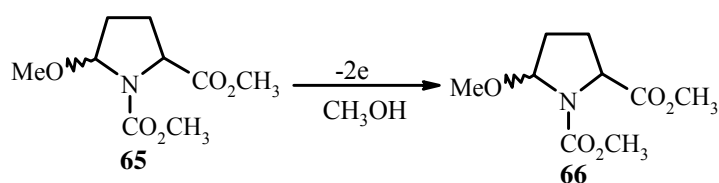


Figure 22

Thaning and Wistrand<sup>39</sup> studied the influence of the hydroxyl group at (4-hydroxyproline). He observed the formation of a mixture of compounds in a 58:26:16

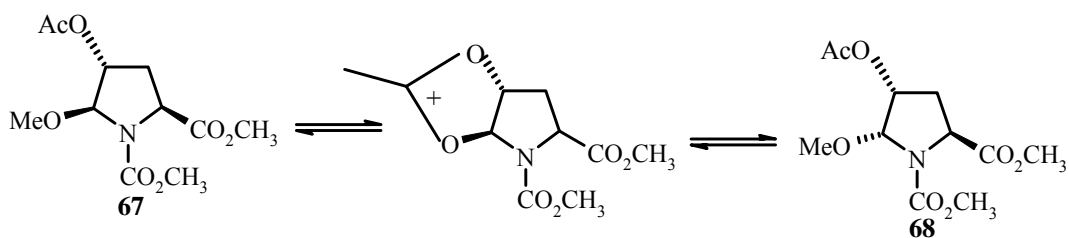


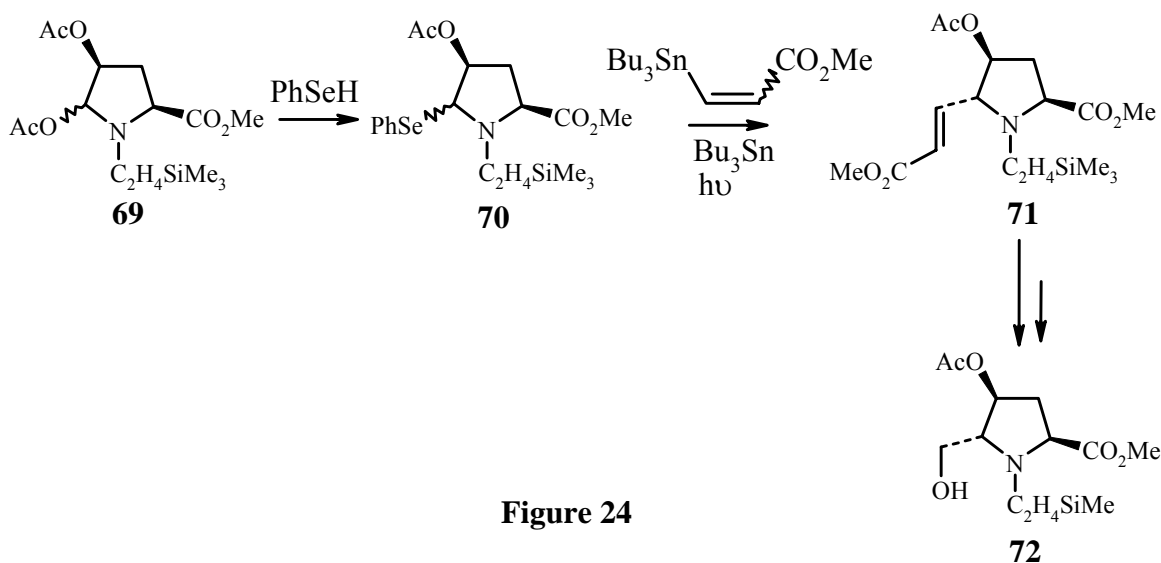
Figure 23

C-4 ratio (cis:trans  $\alpha,\alpha'$ -disubstituted products) and found that the cis isomer can be epimerized into the trans product by treatment with  $\text{BF}_3 \cdot \text{Et}_2\text{O}$  as depicted on Figure 23. These 2-methoxy-5-carboxy-proline derivatives are the good substrates to perform nucleophilic substitutions at the pseudo-anomeric positions. Barrett and Pilipauskas<sup>40</sup>

synthesized bacterial metabolite bulgecinine by employing above strategy, anodic oxidation followed by radical reaction as shown in Figure 24.

#### 4.2.2 Synthesis from glutamic acid

Glutamic acid, possesses three advantages which make this natural (*R*-amino acid a very versatile starting material: (i) it is a very inexpensive compound, (ii) commercially available as its *-R*) or *-S*) form, (iii) which can be quantitatively and stereospecifically



converted into pyroglutamic acid, a cyclic analogue with a pyrrolidinone ring possessing a stereogenic center. Syntheses using pyroglutamic acid as starting material can be divided into 4 sections: (i) reductions of the lactam followed by a nucleophilic substitution of the acyliminium ions, (ii) syntheses through a  $\beta$ -enaminoester intermediate, (iii) or from a thiolactam, (iv) and reactions through an acyclic intermediate obtained by nucleophilic substitution.

##### 4.2.2.1a Partial reduction:

The pyroglutamic acid obtained by pyrolysis of the corresponding glutamic acid is partially reduced into the hemiaminal. Then, functionalization of the free hydroxyl

followed by nucleophilic substitution allows the access to 2,5-disubstituted pyrrolidines (Figure 25). The partial reduction can be performed under several reaction conditions (DIBAL-H,<sup>41,42</sup> NaBH<sub>4</sub><sup>43</sup>, and LiEt<sub>3</sub>BH<sup>44</sup>) in high yields.

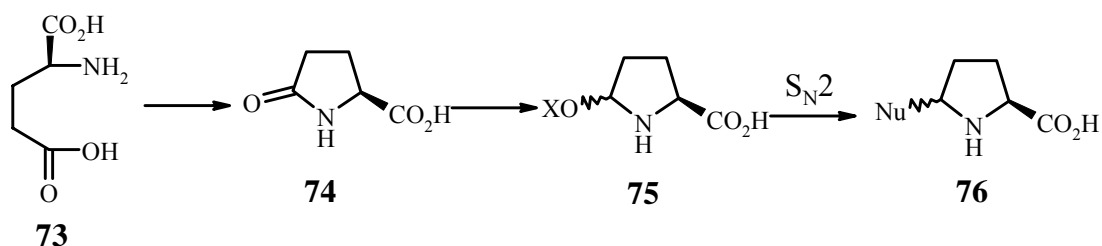


**Figure 25**

#### 4.2.2.1b Complete reduction:

Related hemiaminals can be obtained in a two steps sequence by a first reduction leading to the  $\gamma$ -hydroxylamine which after an oxidation step gives the desired

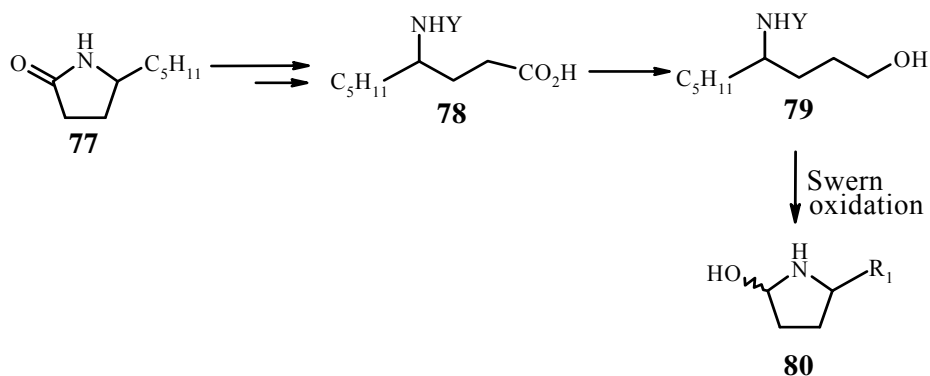


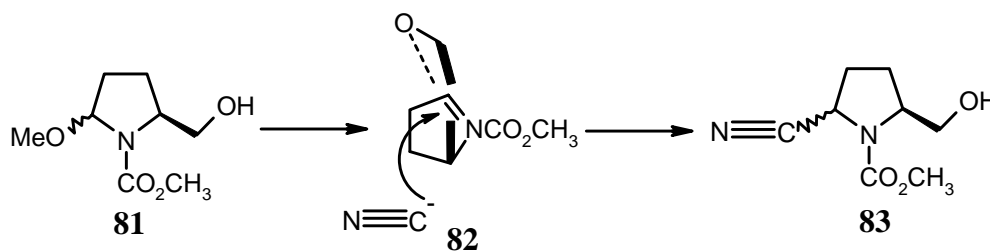
**Figure 26**

hemiaminal. For instance, Holmes et.al<sup>45</sup> in 1991 used a Swern oxidation for the last step (Figure 26).

#### 4.2.2.1c Nucleophilic substitution of *N*-acyliminium ions obtained from L-proline or glutamic acid:

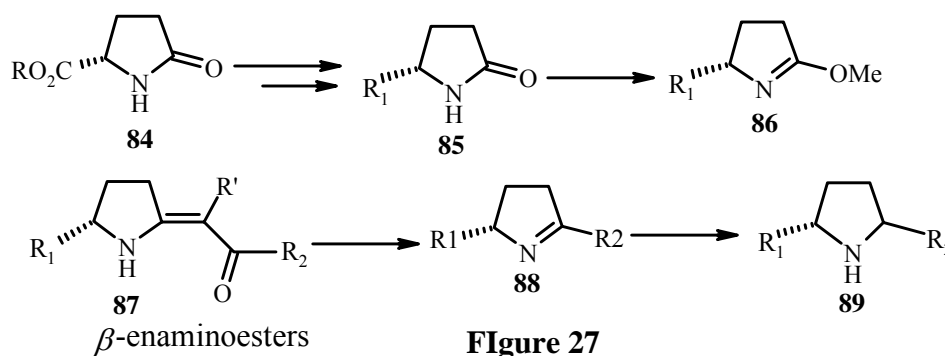
Nucleophilic substitution of *N*-acyliminium ions obtained from L-proline or L-glutamic acid *N*-acyliminium ions obtained from the 2-OAc or -OMe pyrrolidinic precursors are very convenient intermediates for

nucleophilic additions. The influences on the stereoselectivity of the reaction of several factors have been studied: e.g. Lewis acid used, nature of the nucleophile and the nature of the protection groups used.



#### 4.2.2.2a Syntheses via the $\beta$ -enaminoesters:

The  $\beta$ -enaminoesters **87** are obtained by reaction of the corresponding lactams **84** with dimethylsulfate followed by condensation with either the Meldrum acid<sup>46,47,48</sup> or with 2-acetylbutyrolactone<sup>47</sup> (Figure 27). The  $\beta$ -enaminoesters **87** are decarboxylated ( $\text{H}_3\text{BO}_3/\Delta$  or  $\text{HCl}$ , 3N) leading to the corresponding 2,5-disubstituted.



pyrrolines **88** with chemical yields from 37 to 90% depending on the nature of  $\text{R}_1$  and  $\text{R}_2$ . Then, Lhommet<sup>49</sup> studied the reduction of the pyrrolines **88** with various reducing agents ( $\text{AlLiH}_4\text{-Me}_3\text{Al}$ ,  $\text{AlLiH}_4\text{-Ni(acac)}_2$ , DIBAL-H,  $\text{NaBH}_3\text{CN}$ ,  $\text{NaBH}_4$ ,<sup>49</sup>  $\text{H}_2$ ,  $\text{Pd/C}$ ,  $\text{HCl}$  10%,  $\text{H}_2$ - $\text{Pd/BaSO}_4$ <sup>47</sup>) to obtain the pyrrolidines **89**.

#### 4.2.2.2b Syntheses via the thiolactams

In 1985, Shiosaki and Rapoport<sup>50</sup> achieved the diastereo- and enantioselective synthesis of *trans* and *cis* 5-butyl-2-beptylpyrrolidines from either D or L-glutamic acid via a thiolactam as intermediate. The importance of their strategy is that either *trans* product is obtained or *cis* product is obtained with ee 94% from the same intermediate via an Eschenmoser reaction (Figure 28).

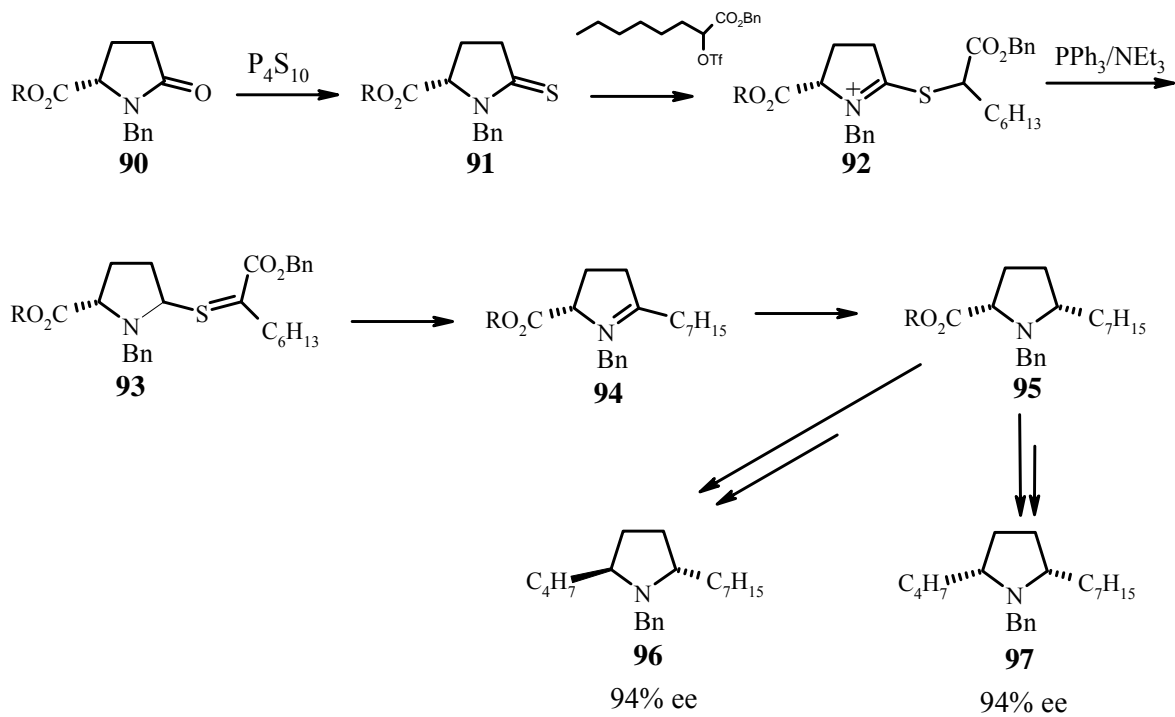


**Figure 28**

Brossi et al.<sup>51</sup> in 1987 synthesized some (+)-*trans*-2,5-dialkylpyrrolidines via a thiolactam which was obtained from the *Lukes-Sorm* dilactams **98** (Figure 29).

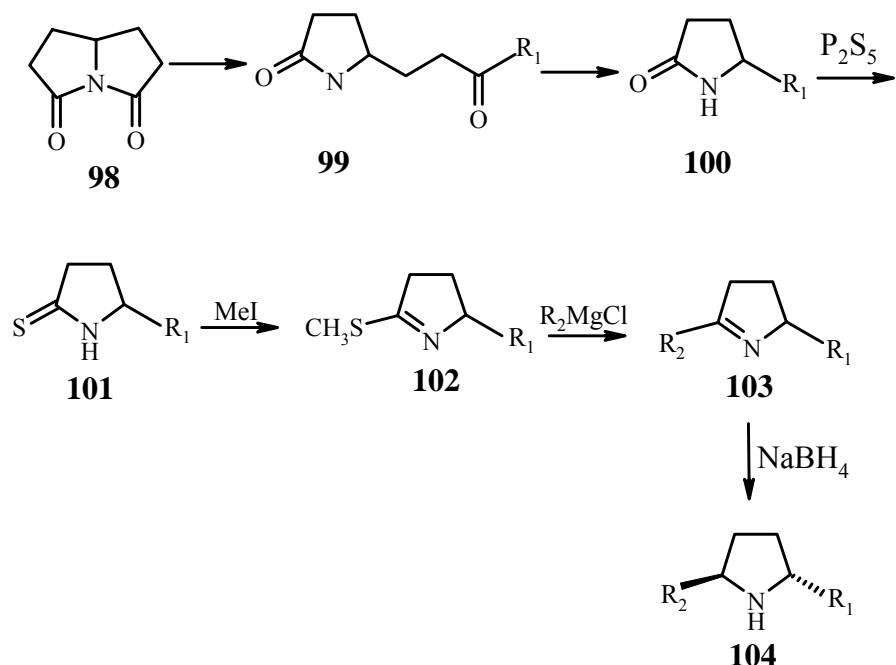


**Figure 29**

#### 4.2.2.2c Synthesis via nucleophilic opening of the pyroglutamic ring:

Ezquerro in 1993<sup>52</sup> synthesized the *cis* and *trans*-2,5-dicarboxylic acid pyrrolidines, through the acyclic compound **106** (Figure 30) which was obtained by the opening of *N*-Boc ethyl pyroglutamate with methyl *p*-tosylsulfinyl lithium anion.

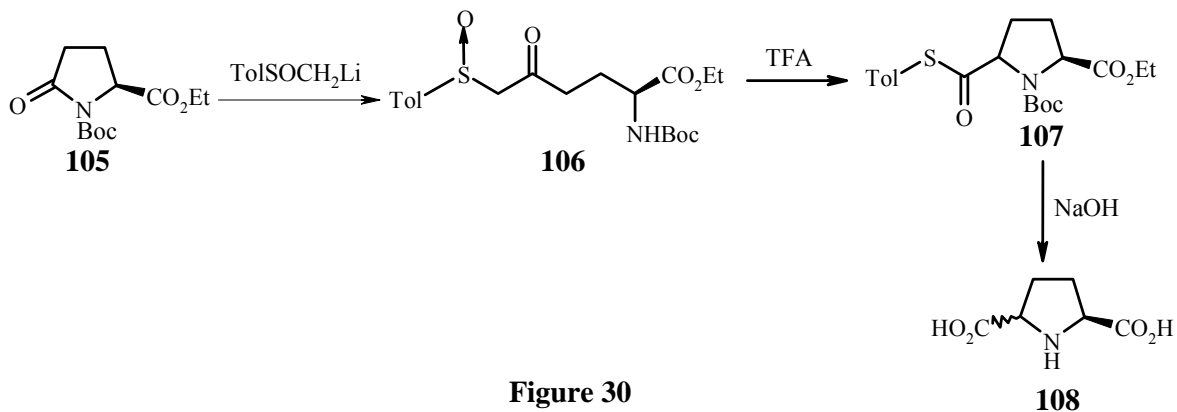


**Figure 30**

### 4.3. Syntheses from commercially available pyrrolidines and pyrrolines:

**3.1.a Electrophilic substitutions:** In 1976, Fraser and Passannanti<sup>53</sup> synthesized 2,5-dialkylated pyrrolidines **110** via alkylation of metallated nitrosamines (Figure 30) compound **111** is alkylated twice at the  $\alpha$  and  $\alpha'$  positions with an excellent regioselectivity and a good

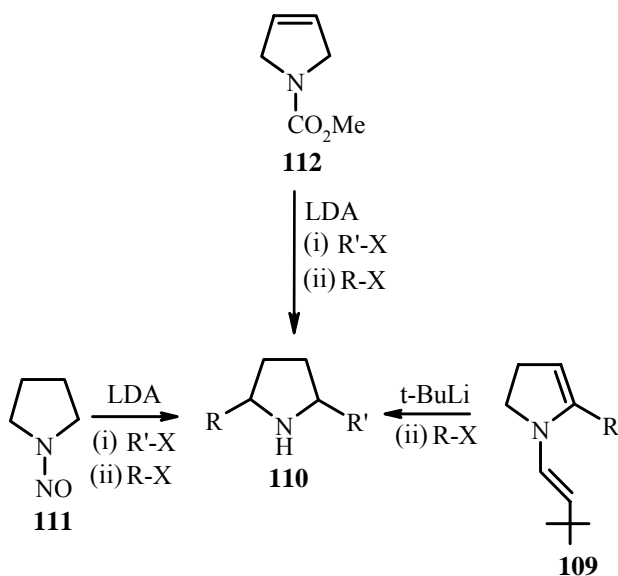


**Figure 31**

stereoselectivity hence the *cis:trans* ratios are in favor of the *trans* compounds (de 85:15 to 62:38), depending on the nature of both the lithium amide and the alkylating reagent. Mac Donald<sup>54</sup> described the same type of reaction but starting with a pyrroline derivative and found that the regio- (>97% at  $\alpha$ ,  $\alpha'$ -positions) and diastereoselectivity were excellent (*trans* >95%) (Figure 31). Meyers et al. in 1985, studied the electrophilic substitutions of derivatives of formamidine anions for the preparation of 2,5-dialkylated pyrrolidines [e.g. from enamidine **109**, obtained par lithiation-selenation-elimination of *N-tert*-butylforamidine (TBF) heptylpyrrolidine<sup>55</sup>] (Figure 31). Unfortunately, no selectivity was observed and a 50:50 mixture of *cis* and *trans* isomers was obtained.

### 4.3.1.b Nucleophilic substitution:

Moore *et al.*<sup>66</sup> described the synthesis of acid **83** (Figure 32) starting from nitron **113**, which on treatment with KCN afforded N-hydroxynitriles in high yields.

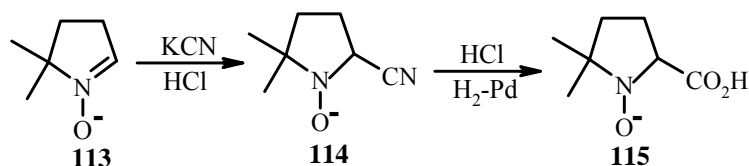


**Figure 32**

Magnus<sup>57</sup> in 1994 described the synthesis of 2,5-diazides pyrrolidines **86** by treatment of *N*-acylated pyrrolidines **116** with the mixture of PhIO/TMSN<sub>3</sub> at -25°C (Figure 33). Magnus found that pyrrolidines are more reactive than piperidines, and that  $\alpha$ -azidation increases with the electron donating power of X. The  $\alpha$  and  $\alpha'$  disubstitution is favored with the *N*-Boc and *N*-C<sub>6</sub>H<sub>2</sub>(-3,4,5-OMe) derivatives leading to the major *trans* compounds.

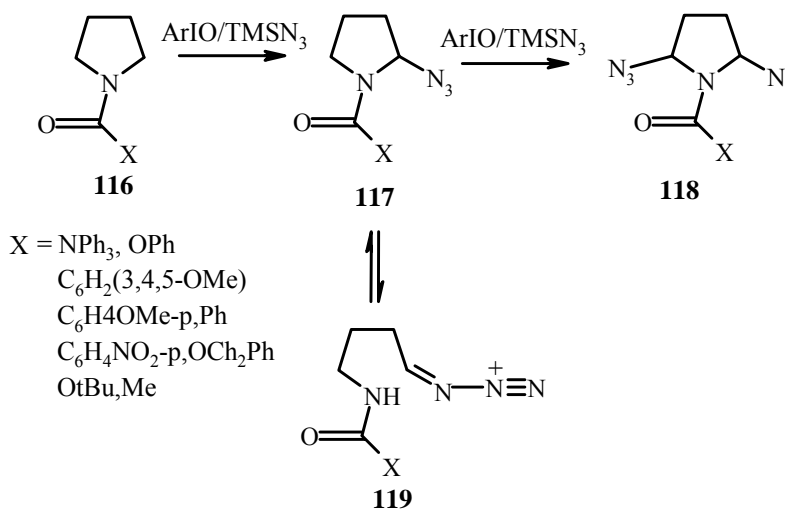


**Figure 33**

### 4.3.2 Synthesis from pyrrole derivatives:

Casiraghi and Rassu<sup>58</sup> developed the use of N-Boc-2-tert-butylidimethylsilyloxy-pyrrole **120** for the synthesis of natural products. He has shown that N-Boc-2-tertbutyldimethylsilyloxy-pyrrole (TBSOP) **87** adds regio- and stereoselectively on several synthons **121** (Figure 34) leading to  $\alpha,\beta$ -unsaturated- $\gamma$ -lactams **122**, which can be further reduced and substituted as L-proline or glutamic derivatives **123**. This strategy has been used for the synthesis of azasugars e.g. N-Boc-4'-azauridine.<sup>59</sup>

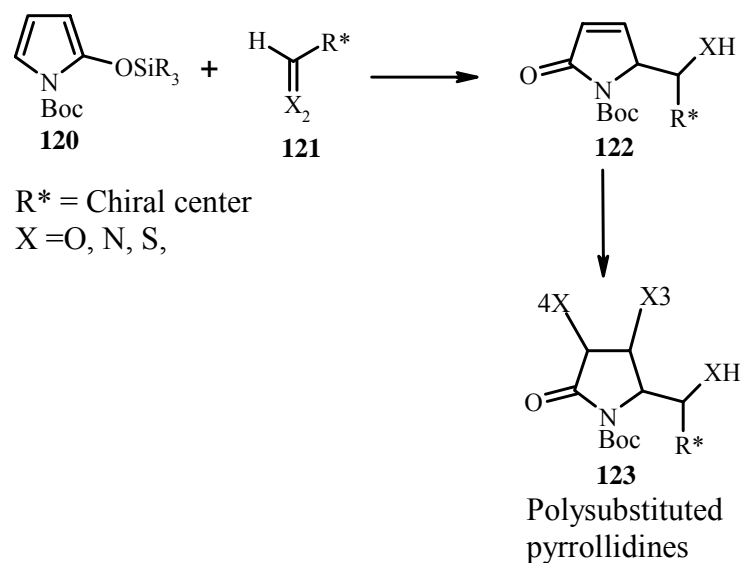
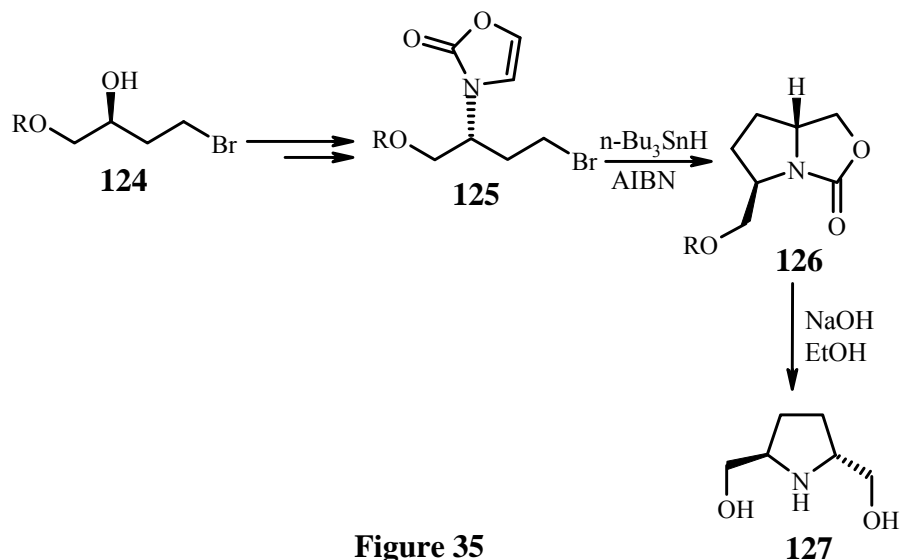


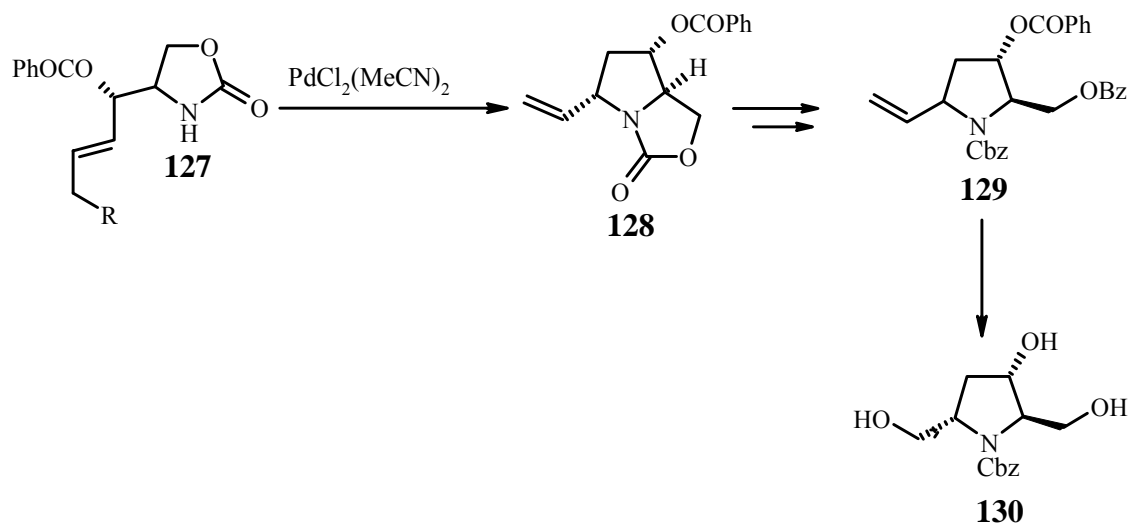
Figure 34

### 4.3.3 Syntheses from bicyclic amino derivatives:

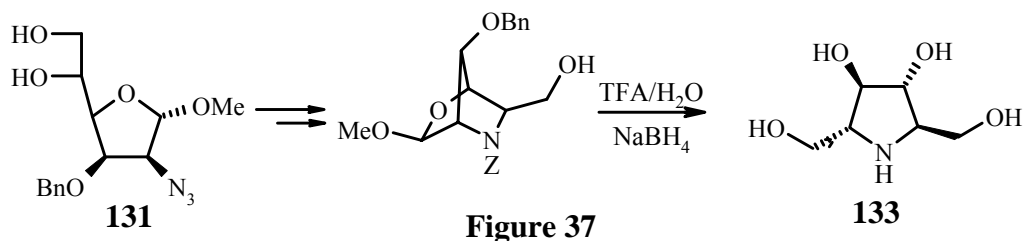
Shibuya et.al<sup>60</sup> in 1994 proposed the synthesis of 2,5-disubstituted pyrrolidines via stereospecific radical cyclization of  $\Delta^{4,5}$  oxazolidin-one **92** (Figure 35). The same year, Shibuya synthesized (+) bulgecinine using the identical strategy.



Momose synthesized Bulgecinine through the intermediate **128** (Figure 36) obtained by palladium catalyzed  $N \rightarrow \pi$  cyclization of  $\gamma$ -unsaturated oxazolidin-2-one **127**.

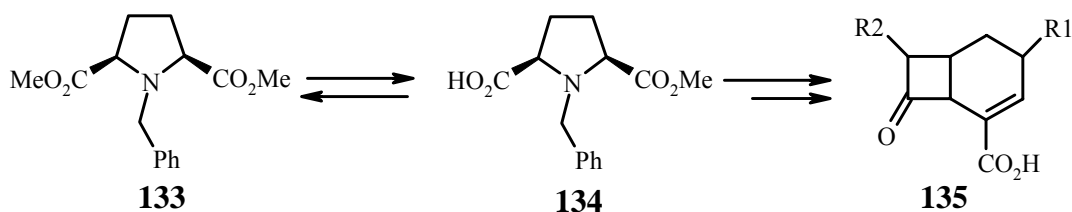


In 1987, Fleet and Smith<sup>61</sup> reported the synthesis of 2,5-dideoxy-2,5-imino-D-mannitol **133** (Figure 37) via the bicyclic [2.2.1] amine intermediate **132** obtained by hydrogenation of azide **131**.



#### 4.3.4 Resolution of racemic mixtures of pyrrolidines:

Resolution of racemic mixtures of pyrrolidines is still a very efficient method for the preparation of enantiomerically pure compounds. In 1985, Ohno et.al<sup>62</sup> used the enzymatic desymmetrization of meso pyrrolidines for the preparation of carbapenem antibiotics (Figure 38).



Achiwa<sup>63</sup> reported that the Pig Liver Esterase (PLE) gave different e.e. and chemical yields depending on the substituent on the nitrogen atom (for *N*-benzylpyrrolidines yield 54%, ee. 23% for *SS*-isomer and for NH compounds, yield 71%, ee. 10% for the *RR* isomer). Boutelje<sup>64</sup> studied the influence of the co-solvent on the enantiomeric purity of the *cis N*-benzyl monoester obtained in this reaction without dimethylsulfoxide ee. is 17%, whereas in the presence of 25% of DMSO the ee. is 100%. Sibi<sup>65</sup> in 1994 converted the racemic *trans* 2,5-dihydroxymethyl-*N*-benzylpyrrolidine into the corresponding enantiomerically pure mono or diacetate compound by treatment with the PS enzyme (Figure 39).

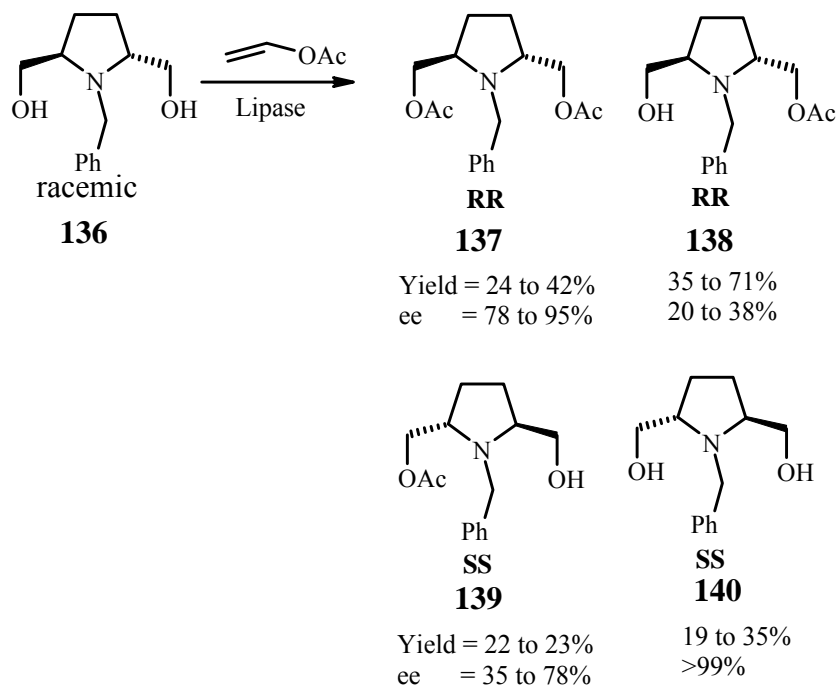


**Figure 39**

#### 4.4 Conclusion

2,5-Disubstituted pyrrolidines have attracted many synthetic chemists, because of the challenge in synthesizing in an enantiospecific way such products, and because of the biological potential of these bioactive compounds. Furthermore, 2,5-disubstituted pyrrolidines possessing a C<sub>2</sub> symmetry axis are very interesting chiral auxiliaries for numerous asymmetric reactions<sup>6</sup>. The discovery in the next future of new natural 2,5-disubstituted pyrrolidines is probably to come, and efficient syntheses of these products will be still needed for their access in large quantities for biological studies.

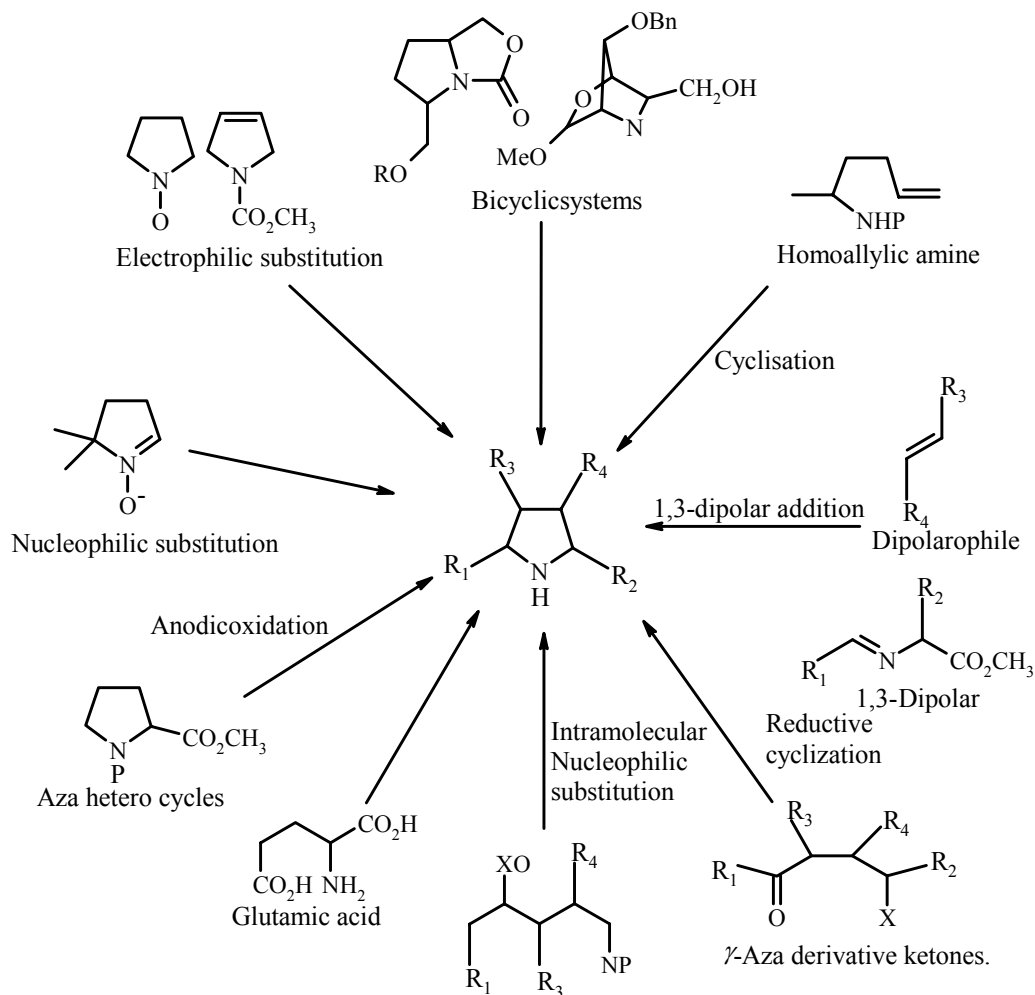


**Figure 40** Various pathways for the synthesis of substituted pyrrolidines

## 4.5 Reference

1. Creighton, W.S. *Bull. Mus. Comp. Zool.* **1950**, *1*, 104.
2. Bacos, D.; Basselier, J. J.; Celerier, J. P.; Lange, C.; Marx, E.; Lhomme, G.; Escoubas, P.; Lemaire, M.; Clement, J. P. *Tetrahedron Lett.* **1988**, *29*, 3061.
3. Clement, J. L.; Lemaire, M.; Lange, C.; Lhomme, G.; Celerier, J. P.; Basselier, J. J.; Cassier, P. *Fr. Appl.* *84*, 6980.
4. Ronzani, N.; Lajat, M. *Bioorg. Med. Chem. Lett.* **1995**, *5*, 1131.
5. Massiot, G.; Delaude, C.; "The Alkaloids", Brossi, A.; Ed., Academic Press, New-York, **1986**, *27*, 269.
6. (a) Whitesell, J. *Chem. Rev.* **1989**, *89*, 1581. (b) Kawanami, Y.; Ito, Y.; Kitagawa, T.; Taniguchi, Y.; Katsuki, T.; Yamaguchi, M. *Tetrahedron Lett.* **1984**, *25*, 857. (c) Uchikawa, M.; Hanamoto, T.; Katsuki, T.; Yamaguchi, M. *Tetrahedron Lett.* **1986**, *27*, 4577. (d) Katsuki, T.; Yamaguchi, M. *Tetrahedron Lett.* **1987**, *28*, 651. (e) Kawanami, Y.; Katsuki, T.; Yamaguchi, M. *Bull. Chem. Soc. Jpn.* **1987**, *60*, 4190. (f) Takano, S.; Moriya, M.; Iwabuchi, Y.; Ogasawara, K. *Tetrahedron Lett.* **1989**, *30*, 3805. (g) Ghosez, L.; Chen, L.Y. *Tetrahedron Lett.* **1990**, *31*, 4467. (h) Yamamoto, Y.; Ohmori, H.; Sawada, S. *Synlett* **1991**, 319.
7. Karady, S.; Corley, E.G.; Abramson, N.L.; Weinstock, L.M. *Tetrahedron Lett.* **1989**, *30*, 2191.
8. Stella, L. *Angew. Chem. Int. Ed. Engl.* **1983**, *22*, 337.
9. Tokuda, M.; Miyamoto, T.; Fujita, H.; Suginome, H. *Tetrahedron* **1991**, *47*, 747.
10. Tokuda, M.; Fujita, H.; Suginome, H. *J. Chem. Soc., Perkin. Trans. 1* 1994, 777.
11. Takano, S.; Moriya, M.; Iwabuchi, Y.; Ogasawara, K. *Tetrahedron Lett.* 1989, *30*, 3805.
12. Perie, J. J.; Laval, J. P.; Roussel, J.; Lattes, A. *Tetrahedron* **1972**, *28*, 675.
13. Paneck, J. S.; Nareshkumar, F. J. *J. Org. Chem.* **1994**, *59*, 2674.
14. Carruthers, W.; *Cycloaddition Reactions in Organic Synthesis*, Tetrahedron Organic Chemistry Series, vol. 8, Pergamon Press, 1990, pp. 269.
15. Grigg, R. *Tetrahedron Asymmetry* **1995**, *6*, 2475.
16. Kanemasa, S.; Hayashi, T.; Tanaka, J.; Yamamoto, H.; Sakurai, T. *J. Org. Chem.* **1991**, *56*, 4473.

17. Williams, R. M.; Zhai, W.; Aldous, D. J. *J. Org. Chem.* **1992**, *57*, 6527.
18. Allway, P.; Gdgg, R. *Tetrahedron Lett.* **1991**, *32*, 5817.
19. Tufariello, J. J.; Puglis, J. M. *Tetrahedron Lett.* **1986**, *27*, 1489.
20. Pearson, W. H.; Jacobs, V.A. *Tetrahedron Lett.* **1994**, *35*, 7001.
21. Miyashita, M.; Awen, B. Z. E.; Yoshikoshi, A. *Chem. Leg.* **1990**, 239.
22. Oppolzer, W.; Bochet, C. G.; Medfield, E. *Tetrahedron Lett.* **1994**, *35*, 7015.
23. Kloetzel, M. C. *J. Am. Chem. Soc.* **1947**, *69*, 2271.
24. Stevens, R. V.; Lee, A. W. M. *J. Chem. Soc. Chem Commun.* **1982**, 102.
25. Paulsen, M.; Sangster, I.; Heyns, K. *Chem. Ber.* **1967**, *100*, 802.
26. Blum, M. S.; Jones, T. H. *Naturwissenschaften.* **1980**, *67*, 144.
27. Robina, I.; Gearing, R. P.; Buchanan J. G.; Wightman, R. H. *J. Chem. Soc., Perkin Trans.1* **1990**, 2622.
28. Me Garvey, G. M.; Kimura, M.; Oh, T.; Williams, J. M. *J. Carbohydr. Chem.* **1984**, *3*, 125.
29. Matsunga, H.; Sakamaki, T.; Nagoka, H.; Yamada, Y. *Tetrahedron Lett.* **1983**, *24*, 3009.
30. Fitremann, J.; Durault, A.; Depezay, J. C. *Tetrahedron Lett.* **1994**, *35*, 1201.
31. Langlois, N.; Bourrel, P.; Andriamialisoa, Z. Z. *Heterocycles* **1986**, *24*, 777.
32. Manfr, F.; Kern, J.-M.; Biellman, J. F. *J. Org. Chem.* **1992**, *57*, 2060.
33. Jogo, J.-M.; Carboni, B.; Vaultier, M.; Carrie, R. *J. Chem. Soc., Chem. Commun.* **1989**, 142.
34. Cignarella, G.; Nathansohn, G. *J. Org. Chem.* **1961**, *26*, 1500.
35. Yamamoto, Y.; Hoshina, J.; Fujimoto, Y.; Ohmoto, J.; Sawada, S. *Synthesis* **1992**, 298.
36. Zwaagstra, M. E.; Meetsma, A.; Feringa, B. L. *Tetrahedron Asymmetry* **1993**, *4*, 2163.
37. Shono, T.; Matsumura, Y.; Tsubata, K.; Uchida, K. *J. Org. Chem.* **1986**, *51*, 2590.
38. Shono, T.; Matsumura, Y.; Tsubata, K.; Sugihara, Y.; Yamane, S-I.; Kanazawa, T.; Aoki, T. *J. Am. Chem. Soc.* **1982**, *104*, 6697.
39. Thaning, M.; Wistrand, L. G. *Helv. Chim. Acta* **1986**, *69*, 1711.
40. Barrett, A.G. M.; Pilipauskas, D. *J. Org. Chem.* **1991**, *56*, 2787.

41. Ahman, J.; Somfai, P. *Tetrahedron*. **1992**, *48*, 9537.
42. Katoh, T.; Nagata, Y.; Kobayashi, Y.; Arai, K.; Minami, J.; Terashima, S. *Tetrahedron Lett.* **1993**, *34*, 5743.
43. Altmann, K. H. *Tetrahedron Lett.* **1993**, *34*, 7721.
44. Pedregal, C.; Ezquerra, J.; Escribano, A.; Carreno, M. C.; Ruano, J. L. G. *Tetrahedron Lett.* **1994**, *35*, 2053.
45. Holmes, A. B.; Smith, A. L.; Williams, S. F.; Hughes, L. R.; Lidert, Z.; Swithenbank, C. *J. Org. Chem.* **1991**, *56*, 1393.
46. Bacos, D.; Celerier, J. P.; Marx, E.; Rosset, S.; Lhommet, G. *J. Heterocyclic Chem.* **1990**, *27*, 1387.
47. Provot, O.; Celeder, J. P.; Petit, H.; Lhommet, G. *J. Org. Chem.* **1992**, *57*, 2163.
48. Fleurant, A.; Grandjean, C.; Provot, O.; Rosset, S.; Celerier, J. P.; Lhommet G. *Heterocycles*. **1993**, *36*, 929.
49. Bacos, D.; Celeder, J.-P.; Marx, E.; Saliou, C.; Lhommet, G. *Tetrahedron Lett.* **1989**, *30*, 1081.
- 50 Shiosaki, K.; Rapoport, H.; *J. Org. Chem*, **1985**, *50*, 1229.
- 51 Gessner, W.; Takahashi, K.; Brossi, A. *Helv. Chem Acta* **1987**, *70*, 2003.
- 52 Ezquerra, J.; Rubio, A.; Pedregal, C.; Sanz, G.; Rodriguez, J. H.; Ruano, J. L. G. *Tetrahedron Lett.* **1993**, *34*, 4989.
- 53 Fraser, R. R.; Passannanti, S. *Synthesis* **1976**, 540.
- 54 Mac Donald, T. L. *J. Org. Chem.* **1980**, *45*, 193.
- 55 Meyers, A. I.; Edwards, P. D.; Bailey, T. R.; Jagdmann, G. E. *J. Org. Chem.* **1985**, *50*, 1019.
- 56 Magaard, V. W.; Sanchez, R. M.; Bean, J. W.; Moore, M. L. *Tetrahedron Lett.* **1993**, *34*, 381.
- 57 Magnus, P.; Hulme, C.; Weber, W. *J. Am. Chem. Soc.* **1994**, *116*, 4501.
- 58 Casiraghi, G.; Rassu, G. *Synthesis* **1995**, 607.
- 59 Rassu, G.; Pinna, L.; Spanu, P.; Ulgheri, F.; Casiraghi, G. *Tetrahedron Lett.* **1994**, *35*, 4019.
- 60 Yuasa, Y.; Ando, J.; Shibuya, S. *J. Chem. Soc., Chem. Commun.* **1994**, 455.
- 61 Fleet, G. W. J.; Smith, P. W. *Tetrahedron* **1987**, *43*, 971.

- 62 Kurihara, M.A.; Kamiyama, K.; Kobayashi, S.; Ohno, M. *Tetrahedron Lett.* **1985**, 26, 5831.
- 63 Morimoto, Y.; Terao, Y.; Achiwa, K. *Chem. Pharm. Bull.* **1987**, 35, 2266.
- 64 Bjorkling, F.; Boutelje, J.; Hjalmarsson, M.; Hult, K.; Norin, T. *J. Chem. Soc., Chem. Commun.* **1987**, 1041.
- 65 Sibi, M. P.; Lu, J. L. *Tetrahedron Lett.* **1994**, 35, 4915.

---

## SECTION II

Studies towards the synthesis of (2*S*, 5*S*)-Pyrrolidine-2,5-dicarboxylic acid and (2*S*, 4*S*, 5*R*)- Bulgecinine

---

#### 4.6 (2*S*,5*S*)-Pyrrolidine-2,5-dicarboxylic acid:

The (2*S*,5*S*)-pyrrolidine-2,5-dicarboxylic acid (**1**) has been isolated<sup>1</sup> as marine natural product from the red alga *Schizmenia dubyi* and it has been used as a potential chiral building block in  $\beta$ -lactams synthesis,<sup>2</sup> also as an elegant chiral auxiliary in asymmetric synthesis<sup>3</sup> and synthesis of peptides and proteins with unusual conformational properties of therapeutic utility.<sup>4</sup>

##### 4.6.1 Earlier Synthesis of (2*S*,5*S*)-pyrrolidine-2,5-dicarboxylic acid:

Till date eight synthesis of **1** starting from enantiomerically pure (*S*)-pyroglutamate derivatives,<sup>4-7</sup> (*S*)-*O*-benzyl-glycidol,<sup>8</sup> pyrrolidine derivatives<sup>9,10</sup> and *meso* dimethyl 2,5-dibromoadipate<sup>11</sup> using variety of elegant synthetic strategies are known in the literature.

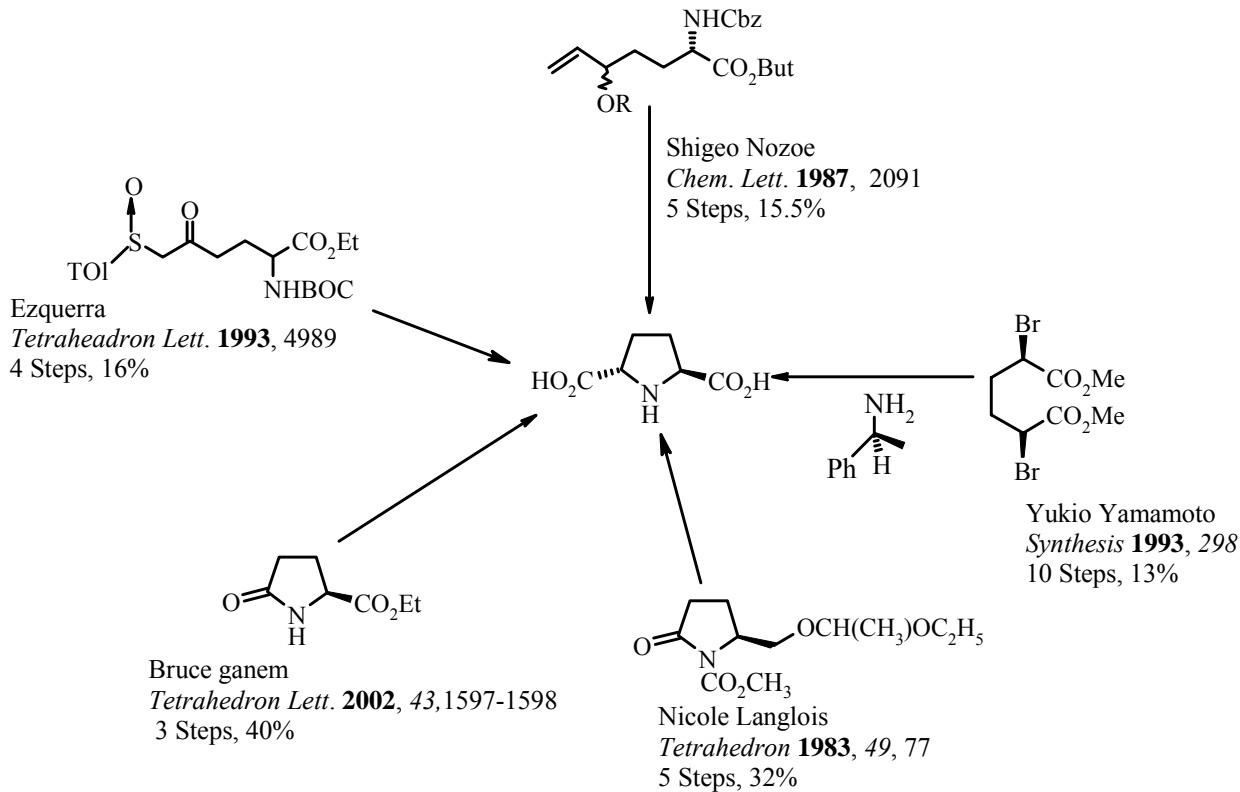


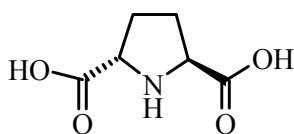
**Figure 1** Earlier synthesis of (2*S*,5*S*)-pyrrolidine-2,5-dicarboxylic acid

First synthesis was reported by Shigeo nozoe et al in 1987. The synthesis involves chain elongation reaction of *N*-carbamoyl pyrroglutamates at C<sub>5</sub> and a pyrrolidine ring formation.

Yukio Yamamoto achieved the synthesis by employing (-)-1-phenylethylamine as a chiral auxillary, three diastereomeric isomers of 2,5-bis(methoxycarbonyl)pyrrolidine derivatives are prepared from dimethyl *rac*-2,5-dibromoadipate and separated by crystallization and chromatographic fraction involving stereoselective hydrolysis.

B. Ganem et al reported the synthesis in 2002, by using Cp<sub>2</sub>ZrHCl (Schwartz's reagent) for the reduction of pyrrolidone to Pyrroline, which was isolated and cyanated this on hydrolysis resulted the target molecule.

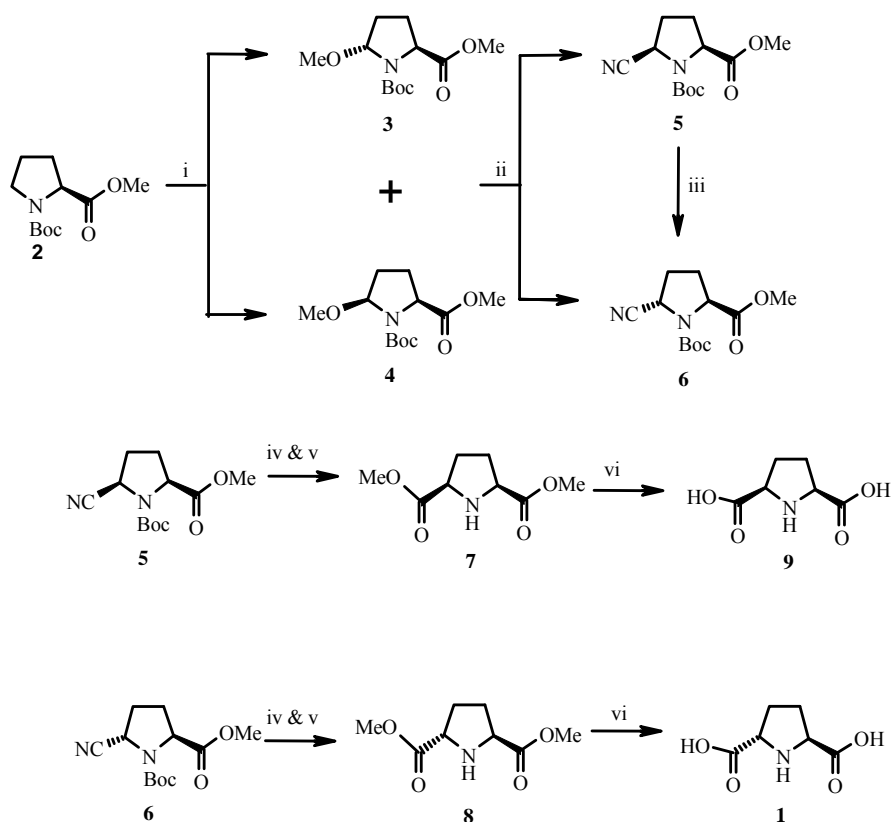
The (2*S*,5*S*)-pyrrolidine dicarboxylic acid **1** has been isolated from the red alga *Schiznmenia duby*. It has been used as a potential chiral building block in  $\beta$ -lactam synthesis, and as an elegant chiral auxiliary in asymmetric synthesis of peptides and proteins with unusual conformational properties.



(2*S*,5*S*) Pyrrolidine dicarboxylic acid (**1**)

#### 4.6.2 Present work:

We envisaged the stereoselective synthesis of **1** starting from readily available (*S*)-proline derivative **2** via an electrochemical oxidation route<sup>12</sup> (Scheme 1).



### Scheme 1

*Reagents and conditions* (i) Electrochemical oxidation (Carbon electrode, 230 mA/28 cm<sup>2</sup>), MeOH, TBATFB (0.5 M solution), 0–15 °C, 10 h (95%, **3:4** = 7:3); (ii) TMSOTf (0.1 equiv), TMSiCN (1.1 equiv), DCM, –35 °C, 30 min (70%, **5:6** = 3:7); (iii) *t*-BuOK (1 equiv), THF, rt, 6 h (80%, racemic mixture); (iv) 6 N HCl, reflux, 24 h (92%); (v) SOCl<sub>2</sub>, MeOH, rt, 12 h (75%); (vi) H<sub>2</sub>O, reflux, 24 h (92%).

The methyl ester of BOC-protected (*S*)-proline **2** on stereoselective electrochemical oxidation at 230 mA current in methanol using tetrabutylammonium tetrafluoroborate (TBATFB) as an electrolyte furnished mixture of 5-methoxylated proline derivatives **3** and **4** in 7:3 ratio (by <sup>1</sup>H NMR) with 95% yield. The mixture of diastereomers **3** and **4** was not separable using column chromatography. The mixture of compounds **3** plus **4** on treatment with trimethylsilyl cyanide (1.1 equiv) in CH<sub>2</sub>Cl<sub>2</sub> at –30 °C gave the mixture of cyano compounds **5** and **6** with complete inversion of

configuration at C<sub>5</sub>-chiral centre in 7:3 ratio (by <sup>1</sup>H NMR) with 70% yield. We could very easily separate the mixture of cyano compounds **5** and **6** using neutral alumina column. The major *cis*-isomer **5** in the mixture of **5** plus **6** or as pure **5** on treatment with potassium *tert*-butoxide (1 equiv) in THF at room temperature under went very smooth isomerization to furnish the thermodynamically more stable *trans*-isomer **6** in 80% yield, but with complete racemization. We search for conditions to obtain the desired *trans*-isomer **6**, without loss of optical purity. The *trans*-cyanoester **6** in refluxing 6 N hydrochloric acid yielded the hydrochloride salt of the natural product **1** in 92% yield and the conversion of hydrochloride salt to **1** using propylene oxide treatment with 87% yield is known.<sup>5</sup> The hydrochloride of **1** on reaction with methanol-thionyl chloride followed by base induced neutralization of formed hydrochloride yielded the *trans* dimethyl ester **8** in 75% yield, which on refluxing in water for 24 hours furnished the natural product (2*S*,5*S*)-pyrrolidine-2,5-dicarboxylic acid (**1**) in 92% yield. The analytical and spectral data obtained for **1** and **8** were in complete agreement with the reported data.<sup>4-11,13</sup> The enantiomerically pure *cis*-isomer **5** on repetition of similar reaction sequence gave the *meso* diester **7** and diacid **9**.

## 4.7 Experimental Procedure

*Methyl (2S)-N-(tert-butoxycarbonyl)-5(R/S)-methoxyprolinecarboxylate(3 + 4)*

*Methyl ester of N-(tert-butoxycarbonyl)-L-proline (2, 8.0 g, 34.9 mmol) was dissolved in a 0.5 M solution of tetrabutylammonium tetrafluoroborate in methanol (100 mL). The reaction mixture was cooled to 5 °C in an ice bath and the stirred solution was oxidized at carbon anode and cathode using a constant current (230 mA/28 cm<sup>2</sup>) for 10 h. The reaction mixture was concentrated under vacuo and the*

*residue was treated with diethyl ether (3 x 75 mL) leaving the supporting electrolyte as a crystalline solid. The combined ether layer was concentrated in vacuo to get the crude product as an oil which was purified by chromatography on 230-400 silica gel by isocratic elution using 10% ethyl acetate/petroleum ether as eluent to obtain the mixture of diastereomers 3 + 4; yield 8.32 g (95%). Thick oil (mixture of diastereomers).*

#### **Methyl (2*S*)-*N*-(*tert*-butoxycarbonyl)-5(*R/S*)-cyanoprolinecarboxylate (5 and 6)**

The mixture of **3** & **4** (2.46 g, 9.5 mmol) was dissolved in anhydrous dichloromethane (25 mL) and cooled to  $-35\text{ }^{\circ}\text{C}$  by a cryostat. To this was added 1% of TMSOTf (0.25 mL) and TMSCN (1.46 mL, 10.9 mmol) in a drop wise fashion at  $-35\text{ }^{\circ}\text{C}$  with stirring. The reaction mixture was further stirred for 30 min and diluted with methanol (1 mL). The reaction mixture was concentrated under vacuo and the residue was purified by neutral alumina column using 12% ethyl acetate/petroleum ether to obtain the diastereomeric nitriles, yield: major isomer **5**, 1.4 g (70%); minor isomer **6**, 0.69 g (30%).

Major isomer **5** (more polar), thick oil.

$[\alpha]_{\text{D}}^{25} = +41.8$  ( $c = 0.665$ ,  $\text{CHCl}_3$ ).

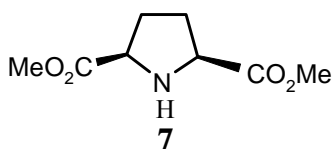
#### **(2*S*,5*R*)-Pyrrolidine-2,5-dimethyldicarboxylate (7)**

Solution of isomer **5** (0.4 g, 1.57 mmol) in 6 N HCl (10 mL) was refluxed for 24 h, and reaction mixture was concentrated under vacuo to obtain the hydrochloride salt of dicarboxylic acid, yield 0.28 g (92%). The resultant salt was dissolved in methanol and cooled to  $0\text{ }^{\circ}\text{C}$  and  $\text{SOCl}_2$  (0.25 mL) was added in a dropwise fashion. The reaction mixture was further stirred at room temperature for 12 h and concentrated under vacuo.

The residue was treated with saturated aqueous NaHCO<sub>3</sub> solution and the aqueous layer was extracted with ethyl acetate (3 x 10 mL), dried over Na<sub>2</sub>SO<sub>4</sub>, concentrated in vacuo to

**<sup>1</sup>H NMR** (CDCl<sub>3</sub>, 300 Hz): δ = 1.80-2.05 (m, 2H), 2.05-2.25 (m, 2H), 2.90 (bs, 1H), 3.70 (s, 6H), 3.90- 4.05 (m, 2H). **<sup>13</sup>C NMR** (CDCl<sub>3</sub>, 125 MHz): δ = 28.8, 51.8, 59.2, 174.7. Ms: *m/z* = 187 (21%), 128 (69%). IR (CHCl<sub>3</sub>): 3005, 1741 cm<sup>-1</sup>. [α]<sub>D</sub><sup>25</sup> = - 38.0 (c = 0.001, CHCl<sub>3</sub>).

obtain **7**, yield 0.2 g (75%). Thick oil.



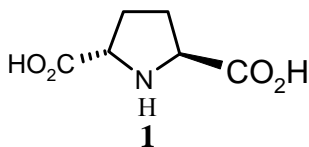
**<sup>1</sup>H NMR** (CDCl<sub>3</sub>, 300 MHz): δ = 1.85-2.00 (m, 2H), 2.05-2.20 (m, 2H), 2.77 (bs, 1H), 3.73 (s, 6H), 3.75-3.85 (m, 2H). **<sup>13</sup>C NMR** (CDCl<sub>3</sub>, 125 MHz): δ = 29.4, 51.8, 59.8, 174.2. Ms: *m/z* = 187 (25%), 128 (60%). IR (CHCl<sub>3</sub>): 3000, 1740 cm<sup>-1</sup>.

#### (2*S*,5*S*)-Pyrrolidine-2,5-dimethyldicarboxylate (**8**)

Repetition of the above procedure with **5** furnished **7**; yield: 75%; thick oil.

#### (2*S*, 5*S*)-Pyrrolidine-2,5-dicarboxylic acid (**1**)

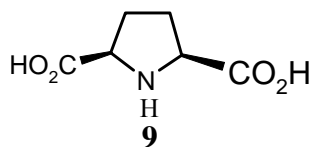
The solution of diester **8** (200 mg, 1.08 mmol) in water (10 mL) was refluxed for 24 h, concentrated in vacuo and dried to obtain **1** as a free flowing solid, yield 0.16 g (92%).



**<sup>1</sup>H NMR** (D<sub>2</sub>O, 500 MHz): δ = 2.05-2.15 (m, 2H), 2.30-2.40 (m, 2H), 4.28- 4.35 (m, 2H). **<sup>13</sup>C NMR** (D<sub>2</sub>O, 125 MHz) δ = 28.2, 60.9, 172.6. [α]<sub>D</sub><sup>25</sup> = - 105 (c = 0.001, H<sub>2</sub>O), (lit.<sup>12</sup> [α]<sub>D</sub><sup>25</sup> = - 108). IR (Nujol): 3170, 1710 cm<sup>-1</sup>, Mp 278 °C (lit.<sup>12</sup> 272-277 °C).

#### (2*S*, 5*R*)-Pyrrolidine-2,5-dicarboxylic acid (**9**)

The repetition of same procedure with **7** furnished **9**, 92% yield.



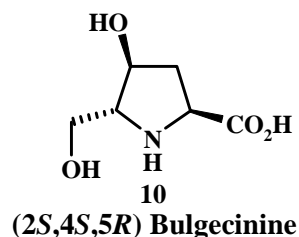
<sup>1</sup>H NMR (D<sub>2</sub>O, 500 MHz): δ = 1.95-2.15 (m, 2H), 2.20-2.40 (m, 2H), 4.15- 4.30 (m, 2H).

<sup>13</sup>C NMR (D<sub>2</sub>O, 125 MHz): δ = 28.4, 61.0, 172.5.

Ms: *m/z* = 159 (5%).

IR (Nujol): 3170, 1709 cm<sup>-1</sup>. **Mp** 268 °C.

#### 4.8 Chemical studies towards the synthesis of Bulgecinine:



Bulgecins are glycopeptide bacterial metabolites isolated from the cultures of *Pseudomonas acidophila* and *Pseudomonas mesoacidophila*.<sup>14</sup> These compounds do not show any antibacterial activity on their own but when used with the β-lactam antibiotics, show synergetic effects. Bulgecinine 10 is a constituent amino acid of the Bulgecins. Till date 30 syntheses of 10 are known in the literature<sup>15</sup> starting from D-glucose<sup>16</sup>, 2-amino pentanoic acid<sup>17</sup>, D-glucuronolactone<sup>18</sup>, D-Serine<sup>19</sup>, *N*-carbamoyl-L-pyroglutamate<sup>20</sup> using variety of elegant synthetic strategies are known in the literature.

##### 4.8.1 Earlier synthesis

First synthesis of bulgecinine was reported by Tetsuo Shiba and co workers in 1985, employing the D-glucose as a chiral precursor.

Chavan<sup>15</sup> et al. achieved the synthesis of Bulgecinine starting from the readily available nonchiral pool starting material *cis*-2-butene-1,4-diol in which a Claisen orthoester rearrangement and a Sharpless asymmetric dihydroxylation were used as the key steps with 43% overall yield.

Karen E. Holt<sup>21</sup> reported a scaleable route to both isomers of *Z*-2-*tert*-butoxycarbonylamino-6-hydroxyhex-4-enoic acid from 2-butyne-1,4-diol, utilizing L- and D-acylase enzymes. These intermediates were readily converted to multigram quantities of *N*-Boc-(2*S*,4*S*,5*R*)- and *N*-Boc-(2*R*,4*R*,5*S*)-Bulgecinine.

In 1997 Klaus Burger<sup>22</sup> reported the synthesis of bulgecinine starting from (*S*)-aspartic acid, [Rh(OAc)<sub>2</sub>]<sub>2</sub> catalyzed stereospecific transformation (de >98%) of the

hexafluoroacetone protected diazoketone into the 4-oxoproline derivative. is the key step of the synthesis.

In 2004 Apurba datta<sup>23</sup> achieved the synthesis of Bulgecinine in 13 steps, utilizing D-serine as a chiral template. Regio-stereoselective amido mercuration-oxidation protocol was the key step in the synthesis.

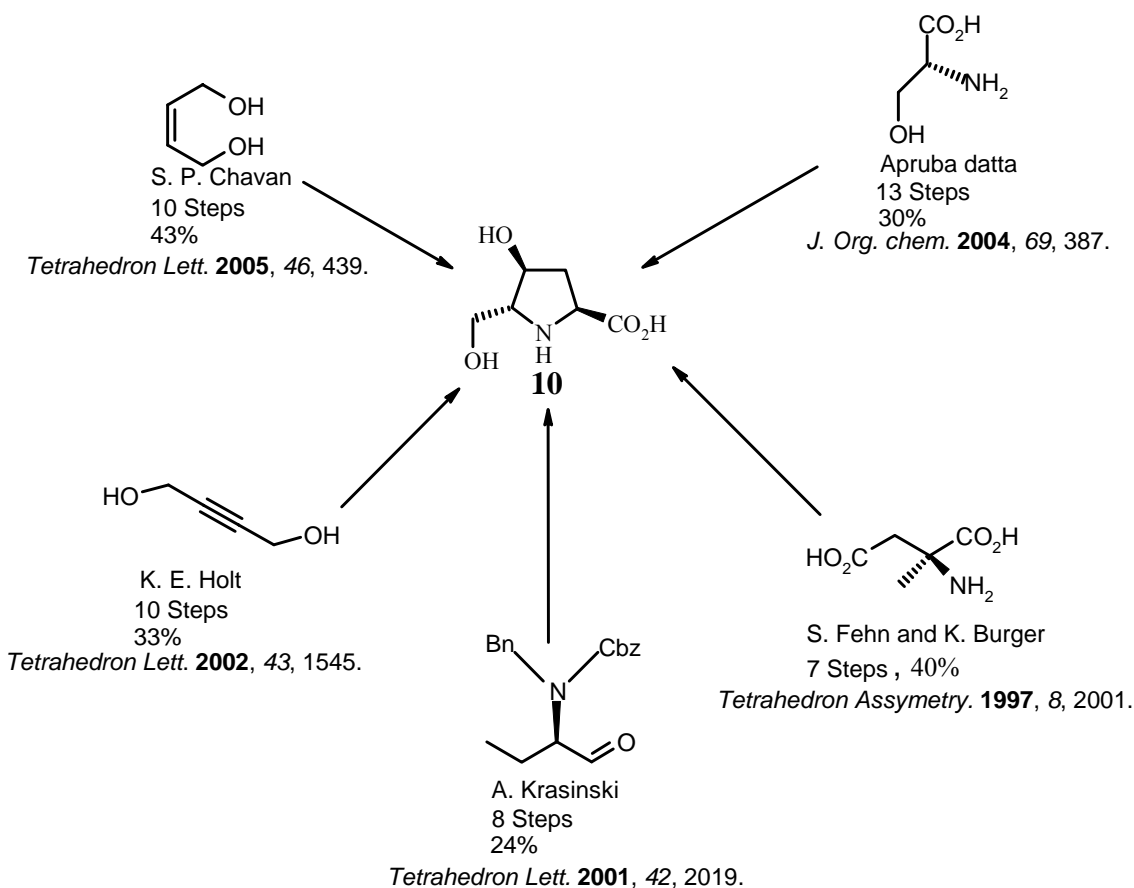
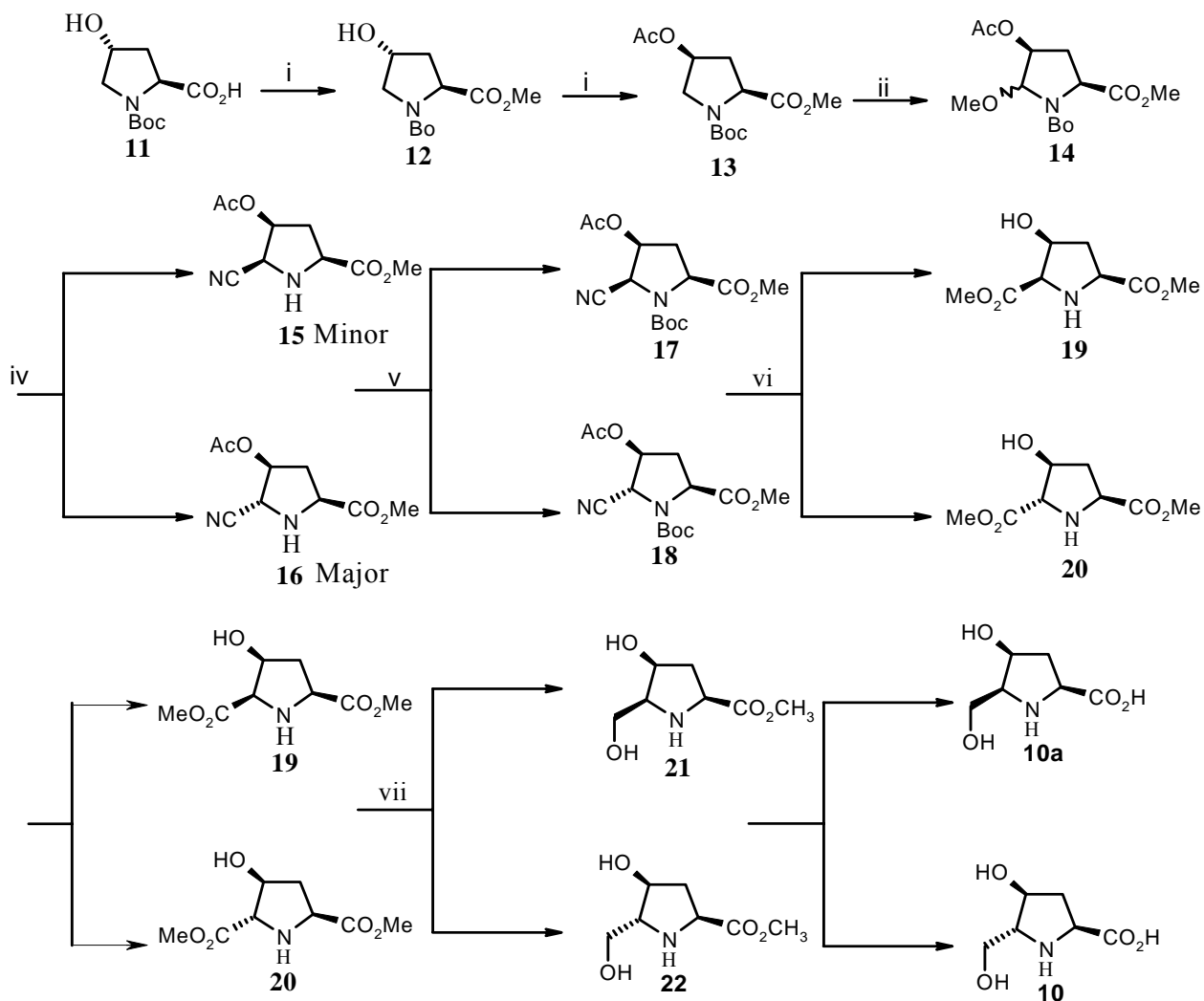


**Figure 2** Earlier synthesis of (2*S*,4*S*,5*R*) Bulgecinine

## 4.9 Present work

### 4.9.a Synthesis of bulgecinine by hydroxyl directed ester reduction approach



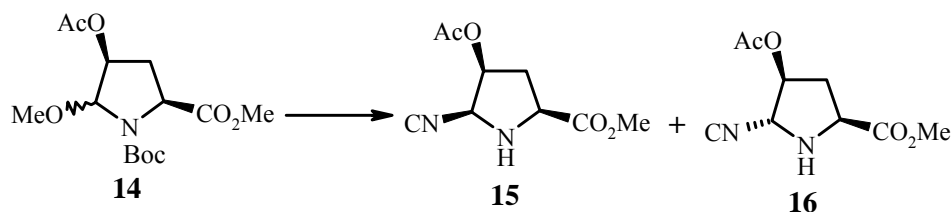
**Scheme 2**

*Reagents and conditions:* (i) Acetone,  $K_2CO_3$  (3 equiv.), DMS (2 equiv.), Reflux 5 h; (ii) THF, DEAD (1.2 equiv),  $(Ph)_3P$  (1.1 equiv.),  $CH_3CO_2H$  (1.1 equiv.), rt, 8 h; (iii) MeOH, TBATFB, 260mA, 0-5 °C, 6 h; (iv) DCM, TMSO-tf (3 equiv.), HMDS (2.5 equiv.), TMSiCN (3.5 equiv.); (v) DCM,  $(Boc)_2O$ , DMAP (cat), rt, 6h; (vi) (a) 6 N HCl, reflux, 12 h, (b)  $SOCl_2$ , MeOH, rt, 16 h; (vii) THF,  $BH_3$ -DMS,  $NaBH_4$  (cat), rt 50h.

Synthesis of (2*S*,4*S*,5*R*) Bulgecinine was carried out as in Scheme-2 by employing 4-hydroxy proline as a starting material. On treatment with DMS (dimethylsulphate), K<sub>2</sub>CO<sub>3</sub> in acetone furnished proline ester **12**, which under Mitsunobu conditions using acetic acid furnished proline ester **13**. Subjecting ester **13** to electrochemical oxidation 5-methoxyproline ester **14** was obtained as non-separable diastereomeric mixture. This on treatment with TMSCN/TMSOTf in DCM gave 5-nitrile proline ester as separable mixture. Nitriles **15** and **16** (major) were converted to diester compounds **19** and **20** by refluxing in 6 N HCl followed by esterification using SOCl<sub>2</sub> in MeOH. The configuration at C-5 was assigned from the small coupling constant of H-4 and H-5 of compounds **17** and **18** as reported in literature<sup>24</sup>. Diester **20** on treatment with BH<sub>3</sub>-DMS and NaBH<sub>4</sub> in THF gave 5-methyl hydroxyl ester **22**.<sup>25</sup> Conversion of **22** and **21** to desired **10** and **10a** are in progress.

#### 4.10 Attempts to increase the diastereoselectivity of the reaction (Scheme-3)

Various reaction conditions were tried (Table 1) to improve the diastereoselectivity and yield of the cyanation reaction (Scheme 3). When reactions were performed at -78 °C, only starting material was recovered irrespective of the Lewis acid used in the reaction. In the case of ytterbium triflate no conversion was observed in the



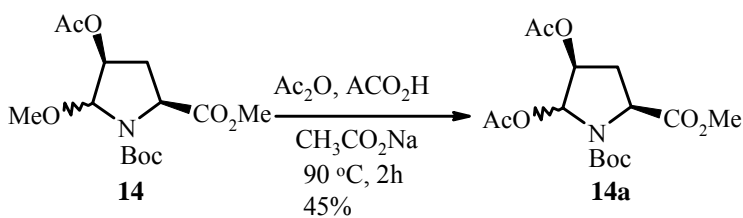
Scheme 3

reaction at -78 °C and at room temperature. Employing TMSOTf and BF<sub>3</sub>.Et<sub>2</sub>O yielded both isomers in the ratio of 1:1 (**a:b**) and 2:1 respectively (Entry 4 and 6).

**Table 1**

<i>Entry</i>	<i>Lewis Acid</i>	<i>Reaction conditions</i>	<i>Result</i>
1	TMSOTf (Cat)	DCM, -78 °C, 3h, TMSCN (1.2 eq)	No reaction
		DCM, -78 °C - RT, TMSCN (1.2 eq)	No reaction
2	TMSOTf (1.2 eq)	DCM, -78 °C - RT, TMSCN (1.2 eq)	No reaction
3	TMSOTf (1.2 eq)	DCM, -78 °C - RT, TMSCN (1.2 eq) Collidine, HMDS, 18h	No reaction
4	TMSOTf (3 eq)	DCM, 0 °C - RT, TMSCN (3 eq) HMDS, 18h	1:1
5	TiCl <sub>4</sub>	DCM, -78 °C - RT, TMSCN (1.2 eq)	2:1 (Poor Yields)
6	BF <sub>3</sub> -O-(Et) <sub>2</sub> (3.5)	DCM, 0 °C - RT, TMSCN (3 eq)	2:1
7	Ytterbium triflate	DCM, 0 °C - RT, TMSCN (3 eq)	No reaction

In another approach compound **14** was subjected to reflux in presence of acetic acid and acetic anhydride to afford compound **14a** (Scheme 4), where acyl group facilitates substitution by cyano group better than the methoxy at this position. Cyanation was performed on substrate **14a** to get better yields, neither diastereoselectivity nor yield was improved. Reaction conditions have been tabulated in Table 2.

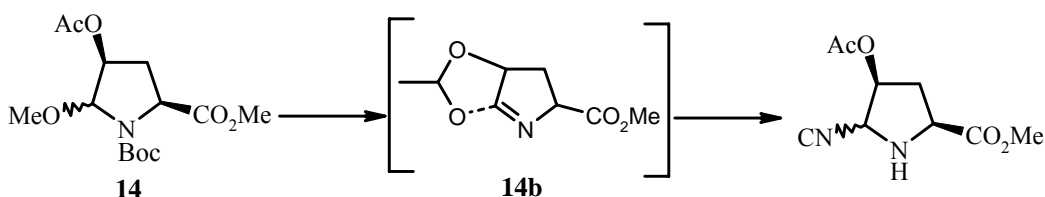


## Scheme-4

S. No	Lewis Acid	Reaction conditions	Result
1	TMSOTf	DCM, -78 °C, 6h, TMSCN, HMDS	No reaction
2	TMSOTf	DCM, 0 °C-RT, 18h, TMSCN, HMDS	1:1

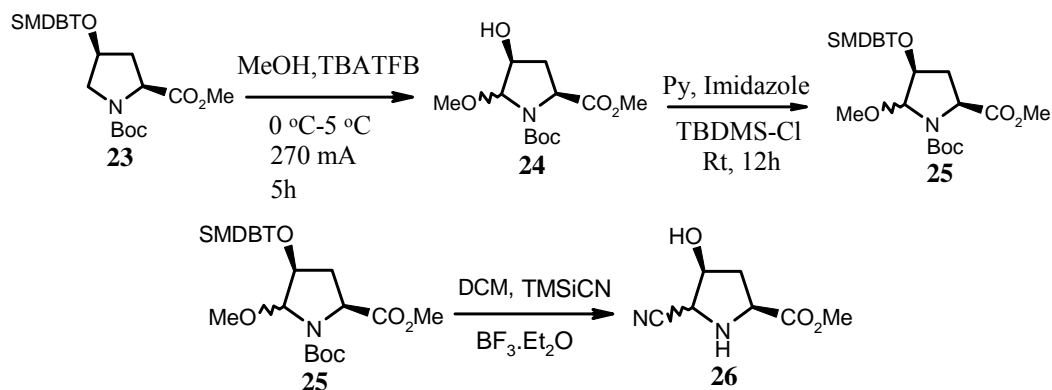
**Table 2**

In literature it is reported that cyanation reaction proceeds through intermediate **14b** (Scheme-5) in which carbonyl of the acetyl group intramolecularly coordinates with the



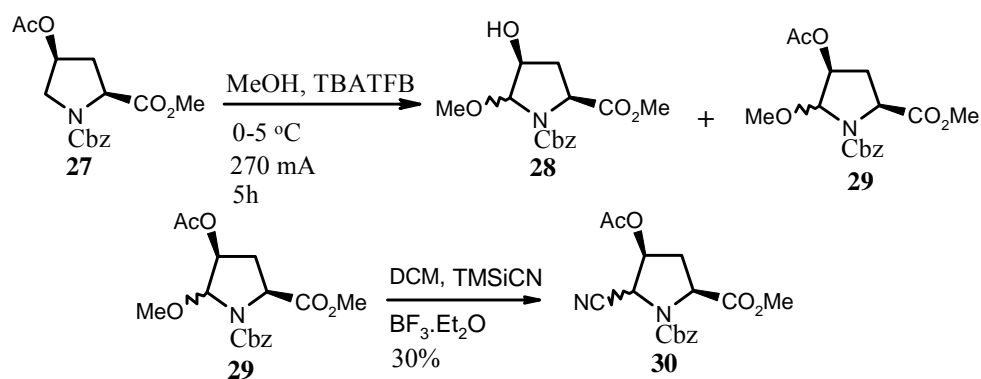
Imine function, we thought that the resultant intermediate may effect the course of the reaction in some or other way, to over come this hurdle compound **22** was synthesized as shown in Scheme 6.

The ester **23** (Scheme 6) was subjected to electrochemical oxidation to obtained 5-methoxyproline ester **24** as separable diastereomeric mixture, the free hydroxyl of the **24** was reprotected as TBDMS, using pyridine as a solvent to furnish ester **25** as a mixture of diastereoisomers. When ester was subjected to cyanation in presence of TMSiCN and TMSOTf, nitrile **26** was obtained with 30% yield. Due to the purification problems and low yield associated with nitrile **26**, this scheme was abandoned.



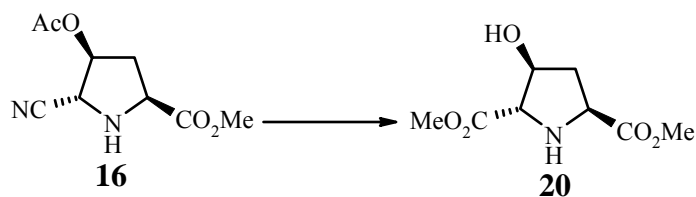
**Scheme 6**

Finally cyanation reaction was performed on compound **29** (Scheme 7) in presence of  $\text{BF}_3 \cdot \text{Et}_2\text{O}$  to get nitrile **30** (Scheme 7) with high diastereoselectivity, but very less conversion of starting material was observed in the reaction, hence reaction has to be repeated under suitable conditions.



T

he other low yielding reaction in the scheme is the conversion of nitriles **15**, **16** to **17** and **18** respectively (Scheme 2). Several reaction conditions were tried to get the better yield of **19** and **20**. Which have been tabulated in Table 3.

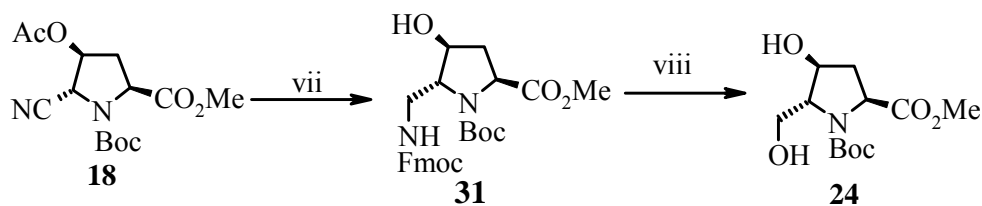


<i>Entry</i>	<i>Reaction conditions</i>	<i>Result</i>
1	TMS-Cl, MeOH, (1:1), rt-50 °C. <sup>26a</sup>	Amide
2	PTSA (3eq), MeOH, reflux, 4h.	Complex reaction mixture
3	PTSA (1eq), MeOH, reflux, 4h.	Amide
4	Acidic MeOH, 0 °C, 16h. <sup>26b</sup>	Amide
5	Acid (cat), MeOH, reflux, 16h. Base (cat), MeOH, reflux, 16h.	Amide
6	6N HCl, reflux, 16h. SOCl <sub>2</sub> , MeOH, rt, 18h.	Diester, 20%

**Table 3** Various conditions tried for alcoholysis of nitrile<sup>26</sup>

#### 4.11 Diazotisation approach:

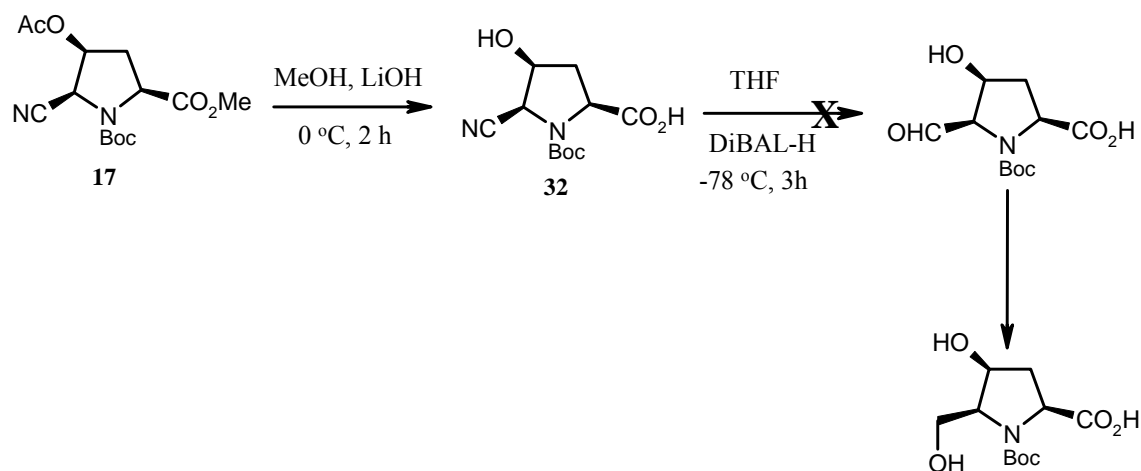
In the diazotization approach (Scheme 8) catalytic reduction of the cyano compound **18** yielded the 5-aminomethyl derivative (not isolated), which on treatment with Fmoc-Cl in the presence of dioxane 4-hydroxy ester **31** as a white solid. On treatment of ester **31** with 50% DCM/DEA provided the 5-aminomethyl 4-hydroxy proline ester (not isolated). This was subjected to diazotisation under basic conditions<sup>27</sup> in THF for the transformation of primary amine to hydroxyl group to obtain the target molecule **24**. Search for the suitable reaction conditions for the conversion of **31** to desired **24** is in progress.



#### Scheme

*Reagents, conditions:* (vii) (a) MeOH, NEt<sub>3</sub>, Raney Ni, 65 Psi, 4 h, (b) MeOH, 2 N NaOH, rt, 45 min, (c) Dioxane/H<sub>2</sub>O, 10% Na<sub>2</sub>CO<sub>3</sub>, Fmoc-Cl (1.5 equiv.); (viii) (a) DEA/DCM (50%), (b) Na<sub>2</sub>NOFe(CN)<sub>6</sub>, K<sub>2</sub>CO<sub>3</sub>, THF, rt, 16 h

In another approach (Scheme 9) nitrile **17** was hydrolyzed in LiOH solution to furnish acid **32** as solid compound, which was treated with DIBAL at -78 °C in THF for about 3h, to obtain aldehyde, this on reduction in presence of NaBH<sub>4</sub> gives the N-protected form of bulgecinine. Due to the solubility problem of the nitrile **32** DIBAL reaction did not proceed.



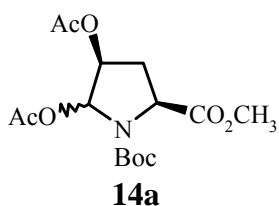
#### 4.12 Experimental

All reagents were obtained from commercial sources and used without further purification. NaH was obtained from Aldrich as 60% suspension in paraffin oil and the paraffin coating was washed off with pet-ether before use to remove the oil. The supporting electrolyte tetrabutyl ammonium tetrafluoroborate was obtained from Aldrich and used as such without further purification. All the solvents were dried according to literature procedures. IR spectra were recorded on a Perkin Elmer 599B instrument.  $^1\text{H}$  NMR (200MHz),  $^{13}\text{C}$  NMR (50 MHz) spectra were recorded on Bruker ACF200 spectrometer fitted with an Aspect 3000 computer. All chemical shifts are with reference to TMS as an internal standard and are expressed in  $\delta$  scale (ppm). The values given are directly from the computer printout. TLCs were carried out on (E.Merck 5554) precoated silicagel 60 F254 plates. TLCs were visualized with UV light and/or ninhydrin spray, followed by heating after exposing the HCl for the deprotection of the tert-butoxycarbonyl group. Optical rotations were measured on JASCODIP-181 polarimeter. All TLCs were run in pet-ether containing appropriate amount of ethyl acetate or

dichloromethane containing appropriate amount of methanol to get the *r<sub>f</sub>* value 0.5. All the compounds were purified by column chromatography using 100-200 silica gel obtained from Sisco Research Laboratory. In NMR spectra that show splitting of peaks due to the presence of rotameric mixtures, arising from the tertiary amide linkage, the major rotamer is designated as maj. and the minor rotamer as min. The ratio of major minor is 80:20 unless otherwise mentioned. In cases, where minor isomer is <10% only the peaks of major rotamer are reported.

## Compound 14a

To a solution of **14** (0.4 gm, 1.26 mmol) in CH<sub>3</sub>CO<sub>2</sub>H/AC<sub>2</sub>O (1:1, 8 mL) was added sodium acetate (0.51 gm, 6.3 mmol) and reaction mixture was heated to 100 °C for about 12 h, after completion of the reaction solvent was evaporated under vacuo and extracted with ethyl acetate (3 x 10 mL). Evaporation of the solvent, and purification by column chromatography afforded 217 mg of 14a (50%) as an oily liquid.

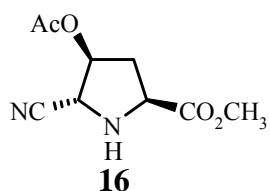


<sup>1</sup>H NMR (CDCl<sub>3</sub>, 200 Hz): δ = 1.46 (bs, 9H), 2.04-2.40 (m, 7H), 2.50-2.75 (m, 1H), 3.74-3.78 (d, *J* = 8 Hz, 3H), 4.10-4.60 (m, 1H), 5.00-5.25 (m, 1H), 4.44 (m, 1H), 6.47-6.70 (m, 1H); <sup>13</sup>C NMR (CDCl<sub>3</sub>, 50 MHz): δ = 20.3, 20.7, 27.8, 51.9, 52.1, 57.6, 58.0, 74.9, 76.0, 79.0, 81.3, 84.1, 85.0, 152.5, 188.5, 188.9, 169.3, 171.1; IR (CHCl<sub>3</sub>) γ = 1670, 1770, 1771 cm<sup>-1</sup>.

## Compound 15 and 16

To a solution of **14** (1 gm, 3.15 mmol) in DCM was added TMSICN (0.812 mL, 6.3 mmol) and reaction mixture was cooled to ice temperature, to this BF<sub>3</sub>.Et<sub>2</sub>O (0.997 gm, 7.8 mL) was added drop wise fashion and stirred at ambient temperature for 14 h, after completion of the reaction Na<sub>2</sub>CO<sub>3</sub> (160 mg, 0.5 mmol) was added and stirred for

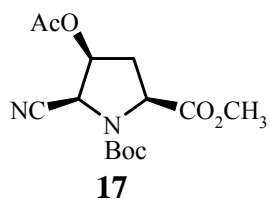
2h to quench the excess Lewis acid present in the reaction. Evaporation of the solvent, and purification by column chromatography using neutral alumina afforded 133 mg of **16** (19%) and 60 mg of **15** (8%) as an oily liquid.



**<sup>1</sup>H NMR** (CDCl<sub>3</sub>, 200 Hz): δ = 2.03 (s, 3H), 2.26-2.33 (d, *J* = 14 Hz, 1H), 2.57-2.72 (m, 1H), 3.77 (s, 1H), 3.99-4.06 (dd, *J* = 4 Hz, 1H), (4.25, s, 1H), 5.28-5.31 (m, 1H), **<sup>13</sup>C NMR** (CDCl<sub>3</sub>, 50 MHz): δ = 20.4, 28.0, 34.6, 52.3, 53.8, 58.2, 76.0, 114.2, 118, 169.6, 173.4

#### Compound 17

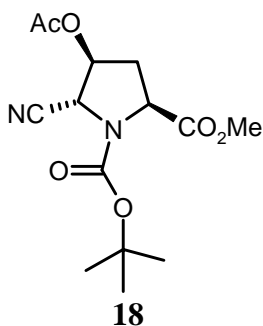
To a solution of **15** (60 mg, 0.312 mmol) in DCM was added di-tertiarybutyloxy carbonate (300 mg, 1.352 mmol) followed by catalytic amount of DMAP (8.23 mg, 0.73 mmol) at ice temperature and stirred at ambient temperature for 8h. evaporation of the solvent and purification by flash chromatography afforded 120 mg of **17** (70%) as a oily liquid.



**<sup>1</sup>H NMR** (CDCl<sub>3</sub>, 200 Hz): δ = 1.44-1.50 (d, 9H), 2.16 (s, 3H), 2.26-2.40 (m, 1H), 2.58-2.76 (m, 1H), 3.76 (m, 1H), 4.25-4.50 (m, 1H), 5.03-5.15 (dd, *J* = 6 Hz, 1H), 5.22-5.30 (m, 1H); **<sup>13</sup>C NMR** (CDCl<sub>3</sub>, 50 MHz): δ = 20.5, 28.0, 33.3, 33.9, 50.9, 51.6, 56.6, 82.4, 82.9, 114.2, 152.2, 169.8, 171.0 [ $\alpha$ ]<sub>25</sub><sup>D</sup> = -30 (0.006, DCM).

## Compound 18

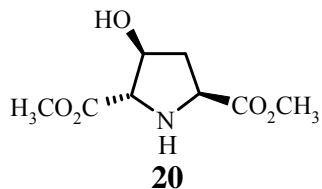
Following the above procedure synthesis of compound **18** was achieved.



<sup>1</sup>H NMR (CDCl<sub>3</sub> 200 MHz)  $\delta$  1.54-1.45 (d,  $J$  = 18 Hz, COOC(CH<sub>3</sub>)<sub>3</sub>); 2.05-2.04 (d,  $J$  = 2 Hz, -OCO-CH<sub>3</sub>), 2.47-2.40 (d,  $J$  = 16 Hz, H3), 2.81-2.64 (m, 1H, H3), 3.76 (s, 3H), 4.61-4.47 (m, 1H) 4.68-4.64 (d,  $J$  = 8 Hz m, 1H), 5.38-5.36 (d,  $J$  = 4 Hz, 1H, H4), <sup>13</sup>C NMR (CDCl<sub>3</sub> 200 MHz)  $\delta$  171.0, 170.6 (CO<sub>2</sub>CH<sub>3</sub>), 169.4, 169.0 (OCO-CH<sub>3</sub>), 152.5, 152.21 (COOC(CH<sub>3</sub>)<sub>3</sub>), 115.7, 115.6 (CN), 82.8, 82.1, (COOC(CH<sub>3</sub>)<sub>3</sub>), 76 (OCH<sub>3</sub>), 58.0, 57.7 (C2), 53.6, 53.5 (C2), 53.6, 53.5 (C5), 52.5, 52.3 (C4), 35.2, 34.1 (C3), 20.5 (OCO-CH<sub>3</sub>); **Ms**:  $m/z$  = 333 [M+Na] (3%), 235.21(20%), 102.11 (100%).

## Compound 20

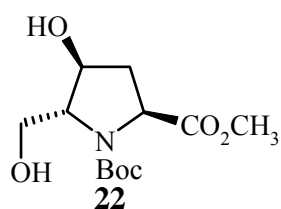
Solution of isomer **16** (0.2 g, 0.641 mmol) in 6 N HCl (10 mL) was refluxed for 24 h, and reaction mixture was concentrated under vacuo to obtain the hydrochloride salt of dicarboxylic acid, yield 0.122 g, (0.576 mmol, 90%). The resultant salt was dissolved in methanol and cooled to 0 °C and SOCl<sub>2</sub> (0.25 mL) was added in a drop wise fashion. The reaction mixture was further stirred at room temperature for 12 h and concentrated under vacuo. The residue was treated with saturated aqueous NaHCO<sub>3</sub> solution and the aqueous layer was extracted with ethyl acetate (3 x 10 mL), dried over Na<sub>2</sub>SO<sub>4</sub>, concentrated in vacuo to obtain **20**, yield 0.05 g (50%). Thick oil.



**<sup>1</sup>H NMR** (CDCl<sub>3</sub>, 200 Hz): δ = 2.01-2.08 (m, 1H), 2.24-2.38 (m, 1H), 3.39 (bs, 2H), 3.74 (s, 6H), 3.93 (s, 1H), 4.00-4.07 (dd, *J* = 4 Hz, 1H), 4.44 (m, 1H); **<sup>13</sup>C NMR** (CDCl<sub>3</sub>, 125 MHz): δ = 37.2, 52.4, 58.0, 68.2, 74.7, 173.1, 175.6 [ $\alpha$ ]<sub>25</sub><sup>o</sup> = +10 (C = 0.007, DCM).

## Compound 22

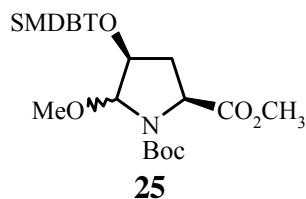
To a solution of **20** (6mg, 0.03 mmol) in dry THF was added borane-dimethyl sulphate (5.04 mg) as drop wise fashion and reaction stirred at 0 °C for about 2 h, to this solution added NaBH<sub>4</sub> (powder, catalytic amount) and stirred at ambient temperature for about 50 h. Evaporation of the solvent and purification by flash chromatography afforded 5 mg of **24** as a sticky solid.



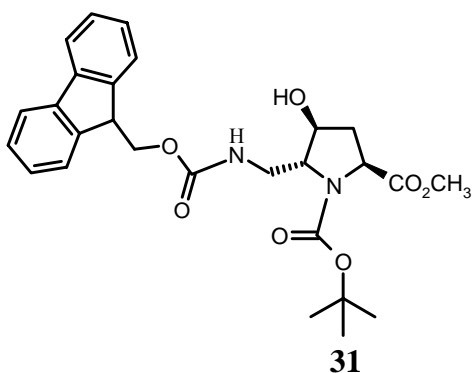
**<sup>1</sup>H NMR** δ = 4.5-4.4 (m, 1H), 4.25-4.1 (ddd, 1H, *j* = 8 Hz); 4.1-4.0 (dd, 1H, *j* = 8 Hz, 4 Hz); 3.92-3.87 (m, 1H); 3.74 (d 2H); 3.1-2.9 (bs, 2H); 2.35-2.22 (m, 1H); 2.09-2.00 (m, 1H).

## Compound 25

To a solution of **24** (0.4 gm, 1.45 mmol) in pyridine (10 mL) was added imidazole (0.147 gm, 2.17 mmol) and the reaction mixture was cooled to ice temperature, to this TBDMS-Cl (0.26 gm, 1.745 mmol) was added in portion wise and



**<sup>1</sup>H NMR** (CDCl<sub>3</sub>, 200 Hz): δ = 0.025-0.10 (6H), 0.80-0.90 (9H), 1.35-1.50 (9H), 2-2.45 (2H), 3.30-3.50 (3H), 3.67-3.80 (3H), 4.05-4.60 (2H), 4.80-5.0 (1H); **<sup>13</sup>C NMR** (CDCl<sub>3</sub>, 100 MHz): δ = 4.9, 4.8, 17.9, 18.2, 25.6, 28.1, 28.3, 33.9, 34.7, 36.0, 36.8, 52.0, 52.1, 52.1, 52.3, 54.6, 55.6, 55.2, 57.6, 57.7, 57.88, 58.6, 74.0, 74.7, 80.5, 80.7, 80.9, 93.8, 94.08, 173.2, 173.4.



**<sup>1</sup>H NMR** (CDCl<sub>3</sub>, 200 Hz): δ = 1.43 (bs, 9H), 1.90-2.10 (m, 1H), 2.25-2.26 (m, 1H), 3.15-3.4 (m, 2H), 3.65-3.85 (d, *J* = 2 Hz, 3H), 3.9-4.5 (m, 5H), 7.26-7.44 (m, 4H), 7.26-7.44 (m, 4H), 7.57-7.61 (d, *J* = 8 Hz, 2H), 7.74-7.78 (d, *J* = 8 Hz, 2H); Ms: *m/z* = *M*+1 = 497 (13%), 155 (100%), 199 (15%), 277 (16%).

the reaction mixture was stirred at ambient temperature for about 16 h, after completion of the reaction solvent was evaporated under vacuo and extracted with ethyl acetate (3 x 15 mL). Evaporation of the solvent, and purification by column chromatography afforded 537.25 mg of **25** (95%) as a oily liquid.

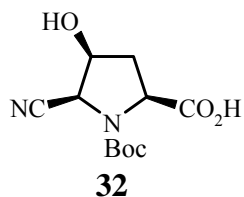
Compound 31

To a solution of **18** (120 mg, 0.384 mmol) in methanol (2 mL) were added NEt<sub>3</sub> (0.15 mL, 2.0 mmol) followed by raney Ni (250 mg). The mixture was subjected to hydrogenation at 65 psi, after completion of the reaction (4 h), reaction mixture was filtered through celite pad and the solvent was evaporated under reduce pressure to get amino ester (not isolated) as a oily liquid. This was redissolved in 10% Na<sub>2</sub>CO<sub>3</sub> (1 mL) and the reaction mixture was cooled to 0 °C in an ice-bath. To this was added dioxane (2 mL) (peroxide free) followed by the slow addition of Fmoc-Cl (201 mg, 0.719 mmol), in dioxane at 0 °C. Stirring was continued at 0 °C for 4 h, followed by room temperature stirring for 18 h. The reaction as monitored by TLC, after the completion of the reaction

solvent was evaporated under vacuo and extracted with ethyl acetate (3 x 10 mL). Evaporation of the solvent, and purification by column chromatography afforded 56 mg of **31** (30%) as a white solid.

Compound 32

To a solution of **17** (0.1 gm, 0.370 mmol) in methano (2 mL) was added 0.4 mL 1N aq. NaOH (15.67 mg, 0.391 mmol) and the reaction mixture was stirred for about 4 h, after completion of the reaction, solvent was neutralized with cationic exchange resin filtration followed by evaporation afforded 74 mg of **32** (75 %) as a hygroscopic solid.



**<sup>1</sup>H NMR** (CDCl<sub>3</sub>/CD<sub>3</sub>OD 200 Hz):  $\delta$  = 1.4-1.50 (d,  $J$  = 6 Hz, 9H), 1.95-2.10 (m, 1H), 2.12-2.25 (m, 1H), 3.95-4.25 (m, 1H), 4.25-4.5 (m, 1H), 4.60-4.80 (m, 2H); **<sup>13</sup>C NMR** (CDCl<sub>3</sub>/CD<sub>3</sub>OD 50 MHz):  $\delta$  = 26.6, 35.8, 36.1, 53.9, 54.8, 60.3, 69.5, 70.9, 80.6, 115.2, 153.6, 178.4.

4.13 Reference:

- (a) Impellizzeri, G.; Mangiafico, S.; Oriente, G.; Piattelli, M.; Sciuto, S.; Fattorusso, E.; Magno, S.; Santacroce, C.; Sica, D. *Phytochemistry* **1975**, *14*, 549.  
(b) Sato, M.; Sato, Y.; Tsuchiya, Y. *Nippon Suisan Gakkaishi* **1981**, *47*, 1605; *Chem. Abstr.* **1982**, *97*, 3787.

2. (a) Lowe, G.; Ridley, D. D. *J. Chem. Soc., Perkin Trans. 1* **1973**, 2024. (b) Kurihara, M.; Kamiyama, K.; Kobayashi, S.; Ohno, M. *Tetrahedron Lett.* **1985**, 26, 5831 and references cited therein 2a-b.
3. (a) Whitesell, J. *Chem. Rev.* **1989**, 89, 1581. (b) Kawanami, Y.; Ito, Y.; Kitagawa, T.; Taniguchi, Y.; Katsuki, T.; Yamaguchi, M. *Tetrahedron Lett.* **1984**, 25, 857. (c) Uchikawa, M.; Hanamoto, T.; Katsuki, T.; Yamaguchi, M. *Tetrahedron Lett.* **1986**, 27, 4577. (d) Katsuki, T.; Yamaguchi, M. *Tetrahedron Lett.* **1987**, 28, 651. (e) Kawanami, Y.; Katsuki, T.; Yamaguchi, M. *Bull. Chem. Soc. Jpn.* **1987**, 60, 4190. (f) Takano, S.; Moriya, M.; Iwabuchi, Y.; Ogasawara, K. *Tetrahedron Lett.* **1989**, 30, 3805. (g) Ghosez, L.; Chen, L. Y. *Tetrahedron Lett.* **1990**, 31, 4467. (h) Yamamoto, Y.; Ohmori, H.; Sawada, S. *Synlett* 1991, 319. (i) Katsuki, T.; Yamaguchi, M. *J. Syn. Org. Chem.* **1986**, 44, 532.
4. Xia, Q.; Ganem, B. *Tetrahedron Lett.* **2002**, 43, 1597.
5. Ohta, T.; Hosoi, A.; Kimura, T.; Nozoe, S. *Chem. Lett.* **1987**, 2091.
6. Langlois, N.; Rojas, A. *Tetrahedron* **1993**, 49, 77.
7. Ezquerra, J.; Rubio, A.; Pedregal, C.; Sanz, G.; Rodriguez, J. H.; GarcíaRuano, J. L. *Tetrahedron Lett.* **1993**, 34, 4989.
8. Takano, S.; Moriya, M.; Iwabuchi, Y.; Ogasawara, K. *Tetrahedron Lett.* **1989**, 30, 3805.
9. Thaning, M.; Wistrand, L. G. *Acta Chem. Scand.* **1992**, 46, 194.
10. Baldwin, J. E.; Hulme, C.; Schofield, C. J. *J. Chem. Res., Synop.* **1992**, 6, 173.
11. Yamamoto, Y.; Hoshino, J.; Fujimoto, Y.; Ohmoto, J.; Sawada, S. *Synthesis* **1993**, 298.
12. (a) Shono, T.; Matsumura, Y.; Tsubata K. *Org. Synth.* **1984**, 63, 206. (b) Barrett, A. G. M.; Pilipauskas, D. *J. Org. Chem.* **1991**, 56, 2787.
13. The stereochemical assignments are based on the optical rotation of the known compounds.
14. Shinagawa, S.; Maki, M.; Kintaka, K.; Imada, A.; Asai, M. *J. Antibiot.* **1985**, 38, 17.

15. Chavan, S. P.; Cherukupally, P.; Pallavi, S.; Kalkote, U. R. *Tetrahedron Lett.* **2005**, *46*, 439-441 and references cited there in.
16. Tateaki, W.; Keiko Y.; Masahiro, N.; Tetsuo, S. *Tetrahedron Lett.* **1985**, *26*, 4759.
17. Yasufumi, O.; Keiko, H.; Masahiro, S. *Tetrahedron Lett.* **1986**, *27*, 6079.
18. Bharat. P. B.; Hak-Fun C.; George W. J. F. *Tetrahedron* **1987**, *43*, 423.
19. Antoni, K.; Skia .; Janusz, J. *Tetrahedron Lett.* **2001**, *42*, 2019.
20. Tomihisa, O.; Akio, H.; Shigeo, N. *Tetrahedron Lett.* **1988**, *29*, 329.
21. Karen E. Holt.; Jonathan P. Swift.; Mark E. B. Smith.; Stephen J. C. Taylor and Raymond McCague. *Tetrahedron Lett.* **2002**, *43*, 1545.
22. Susanna, F.; Klaus, B. *Tetrahedron Asymmetry* 1997, *8*, 2001.
23. Kharaf, J.K.; Datta, A. *J. Org. Chem.* **2004**, *69*, 387.
24. Thaning, M.; Wistrand, L. G. *Helv.chim.Acta* **1986**, *69*, 1711.
25. Saitu, S.; Ishiiwa. T.; Kuroda, A.; Koga, K.; Moriwake. T. *Tetrahedron* **1992**, *48*, 4067.
26. (a) Tair Luo. F.; and Jeevanandam. A. *Tetrahedron Lett.* **1998**, *39*, 9455.  
(b) Cushman. M.; and Wong. W. C. *Tetrahedron Lett.* **1986**, *27*, 2103.
27. Altz. H.; Grant. M. A.; Navaroli. M. C. *J. Org. Chem.* **1976**, *36*, 363.

#### 4.14 Appendix

<b>Entry</b>	<b>Details</b>	<b>Page Numbers</b>
1	Compound <b>1</b> ; $^1\text{H}$ NMR and Mass spectra	292
2	Compound <b>1</b> ; $^{13}\text{C}$ and DEPT spectra	293
3	Compound <b>7</b> ; $^1\text{H}$ NMR and $^{13}\text{C}$ spectra	294
4	Compound <b>7</b> ; DEPT and Mass spectra	295
5	Compound <b>8</b> <sup>1</sup> ; $^1\text{H}$ NMR and $^{13}\text{C}$ spectra	296
6	Compound <b>8</b> <sup>1</sup> ; DEPT and Mass spectra	297
7	Compound <b>9</b> <sup>1</sup> ; $^1\text{H}$ NMR and $^{13}\text{C}$ spectra	298
8	Compound <b>9</b> ; DEPT spectrum	299
9	Compound <b>13</b> ; $^1\text{H}$ NMR and $^{13}\text{C}$ spectra	300
10	Compound <b>13</b> ; DEPT and Mass spectra	301
11	Compound <b>14</b> ; $^1\text{H}$ NMR and $^{13}\text{C}$ spectra	302
12	Compound <b>14</b> ; DEPT and Mass spectra	303
13	Compound <b>15</b> ; $^1\text{H}$ NMR and $^{13}\text{C}$ spectra	304
14	Compound <b>16</b> ; $^1\text{H}$ NMR and $^{13}\text{C}$ spectra	305
15	Compound <b>16</b> ; DEPT spectrum	306
16	Compound <b>17</b> ; $^1\text{H}$ NMR and $^{13}\text{C}$ spectra	307
17	Compound <b>17</b> ; DEPT spectrum of	308
18	Compound <b>20</b> ; $^1\text{H}$ NMR and $^{13}\text{C}$ spectra	309
19	Compound <b>20</b> ; DEPT spectrum	310
20	Compound <b>22</b> ; $^1\text{H}$ NMR spectrum	310
21	Compound <b>24</b> ; $^1\text{H}$ NMR spectrum	311
22	Compound <b>25</b> ; $^1\text{H}$ NMR and $^{13}\text{C}$ spectra	312
23	Compound <b>25</b> ; DEPT and Mass spectra	313
24	Compound <b>31</b> ; $^1\text{H}$ NMR and Mass spectra	314
25	Compound <b>35</b> ; $^1\text{H}$ NMR and $^{13}\text{C}$ spectra of	315

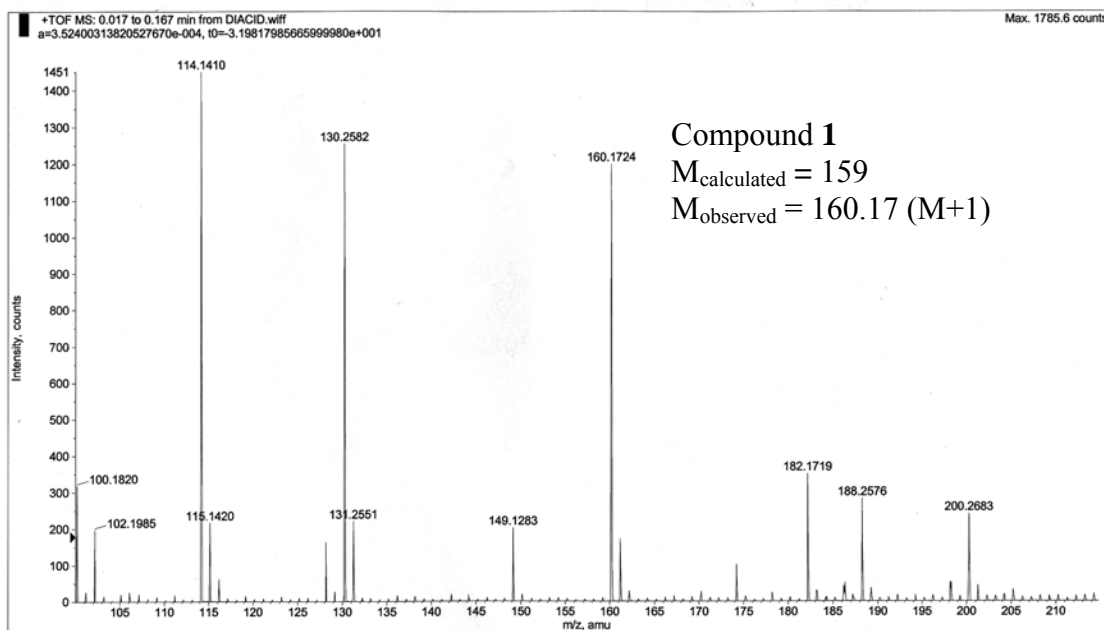
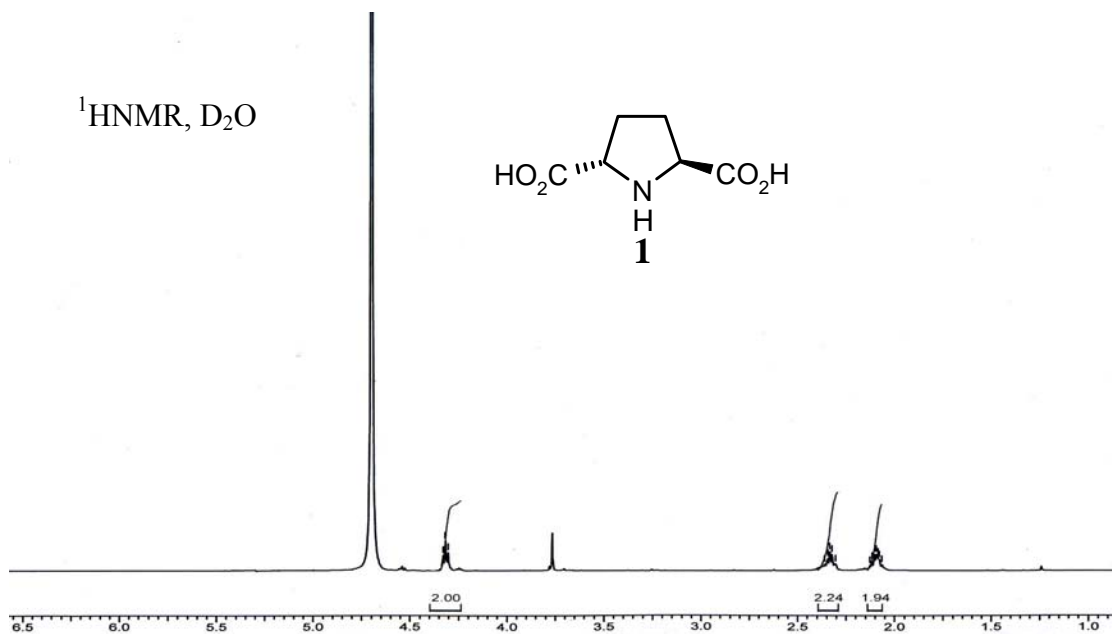


**Figure 3**  $^1\text{H}$  NMR and Mass spectra of compound 1

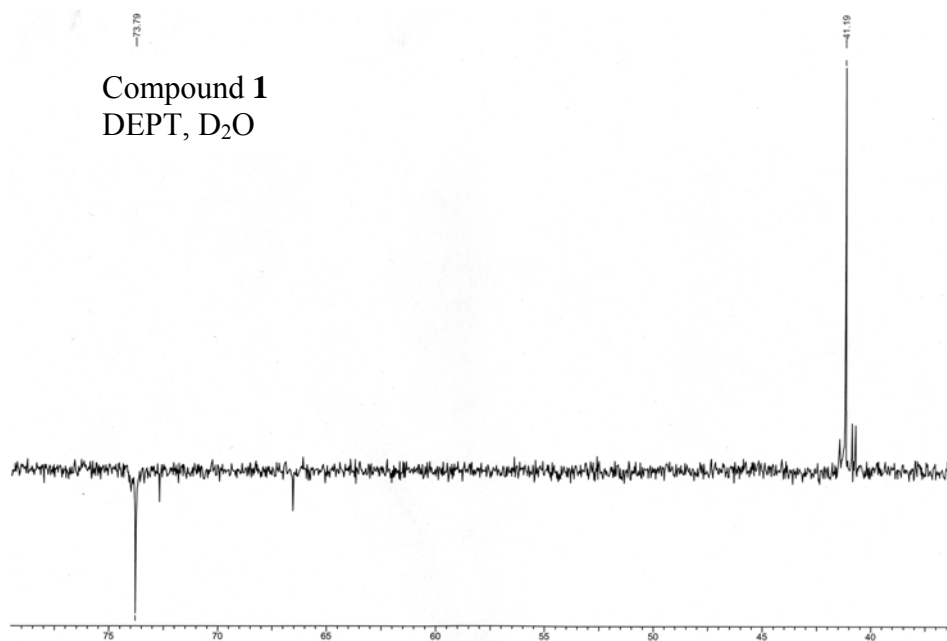
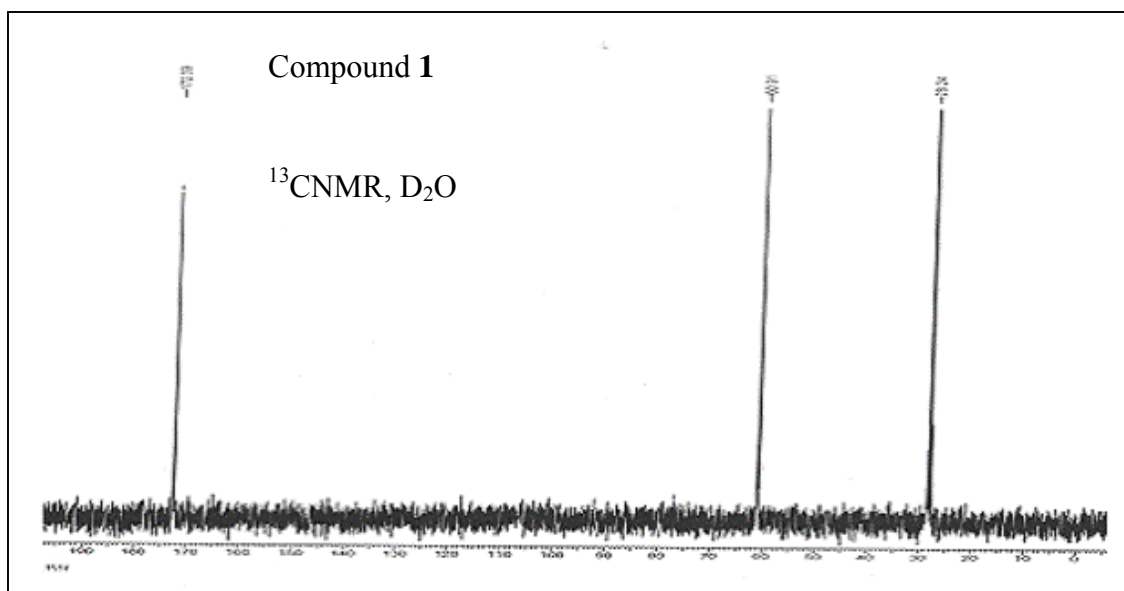


**Figure 4**  $^{13}\text{C}$  and DEPT spectra of compound 1

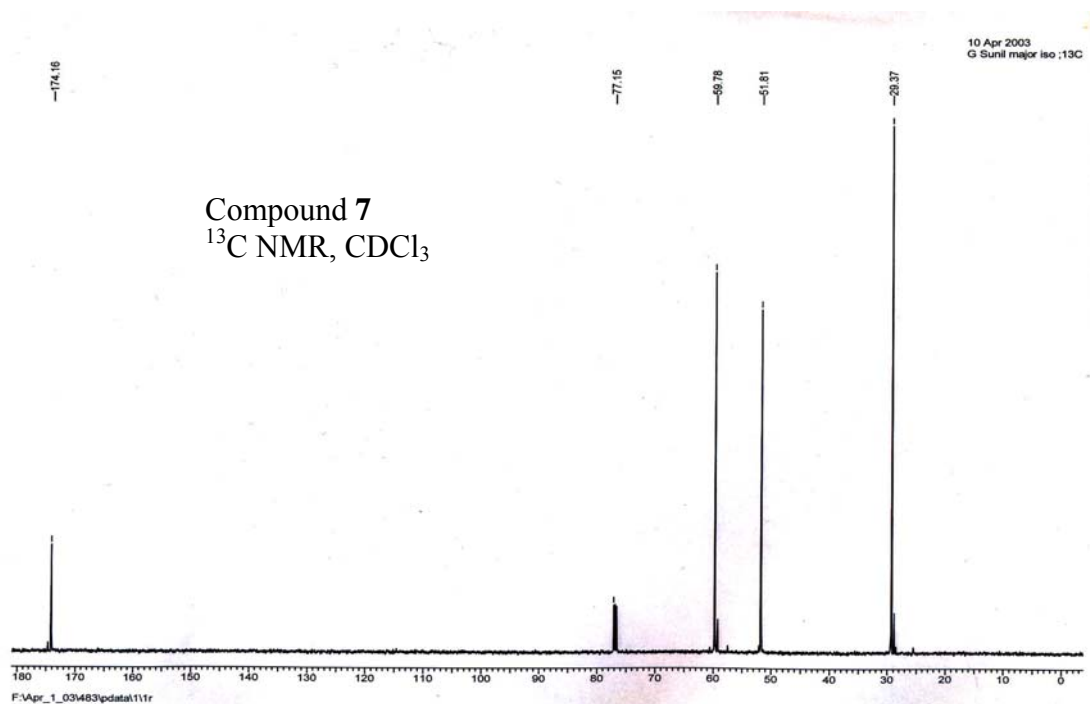
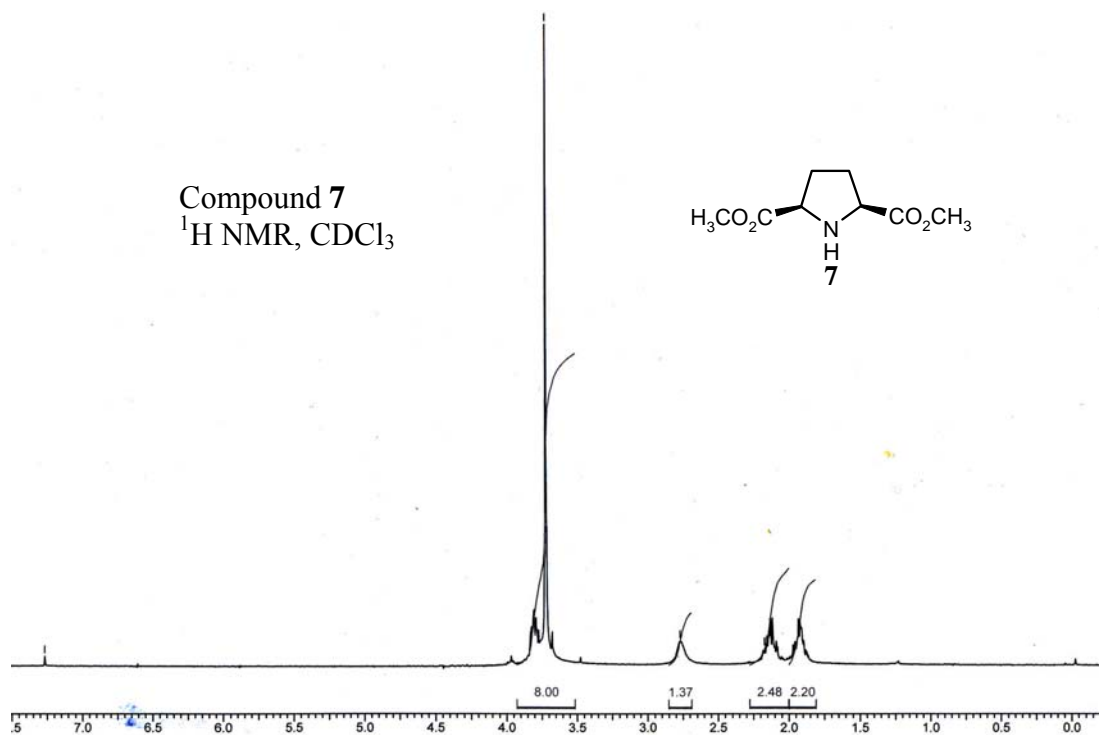
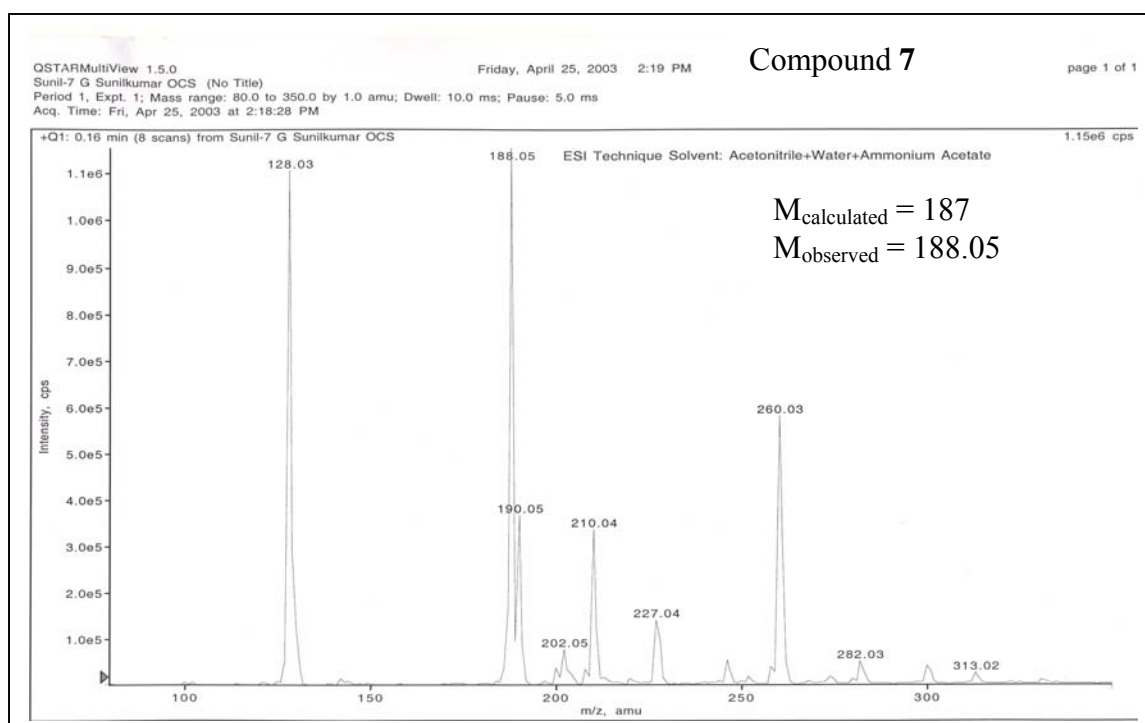
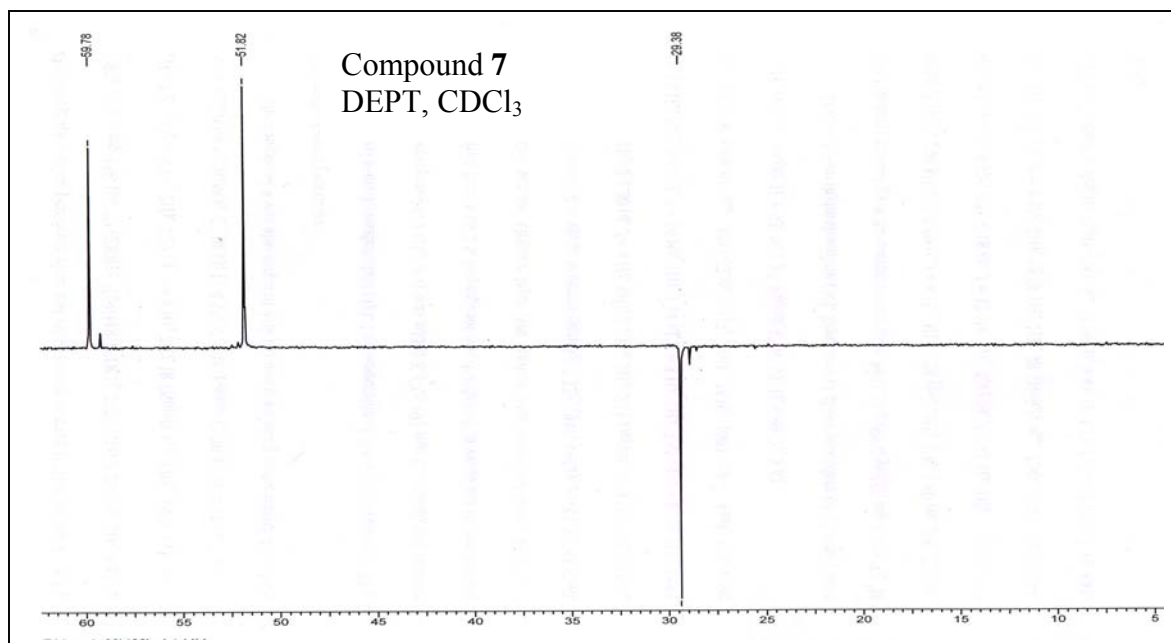
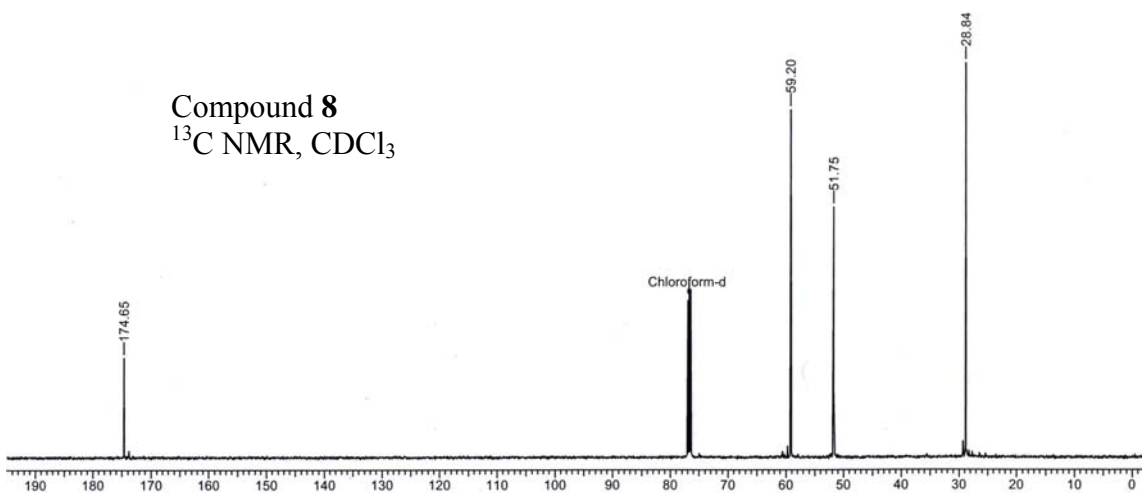
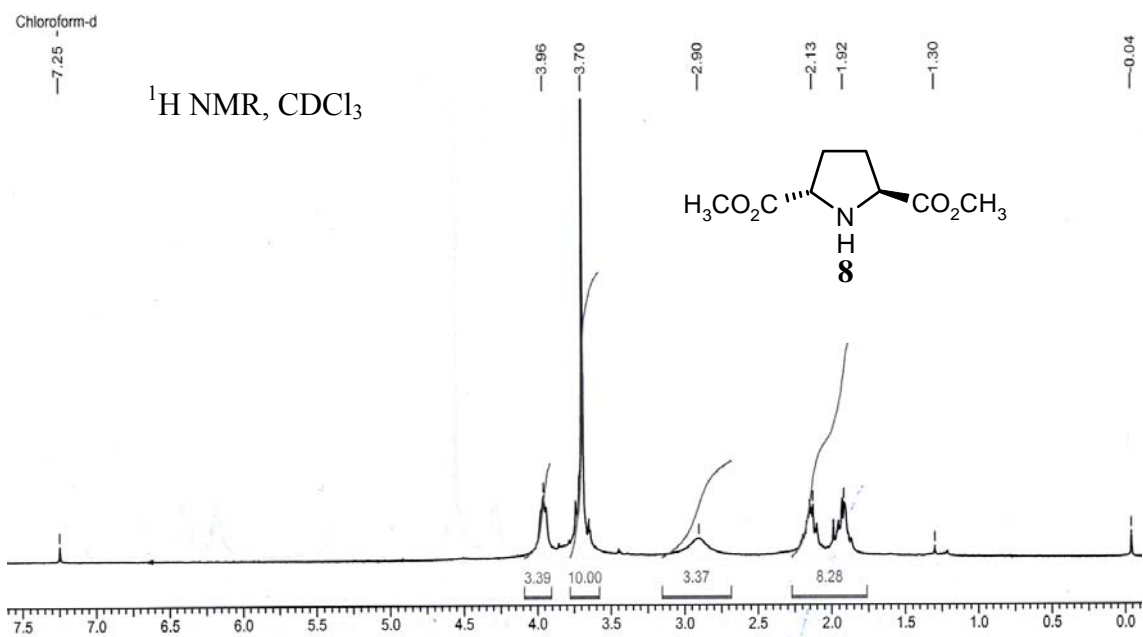


Figure 5  $^1\text{H}$  NMR and  $^{13}\text{C}$  spectra of compound 7



**Figure 6** DEPT and Mass spectra of compound 7



**Figure 7**  $^1\text{H NMR}$  and  $^{13}\text{C}$ spectra of compound **8**

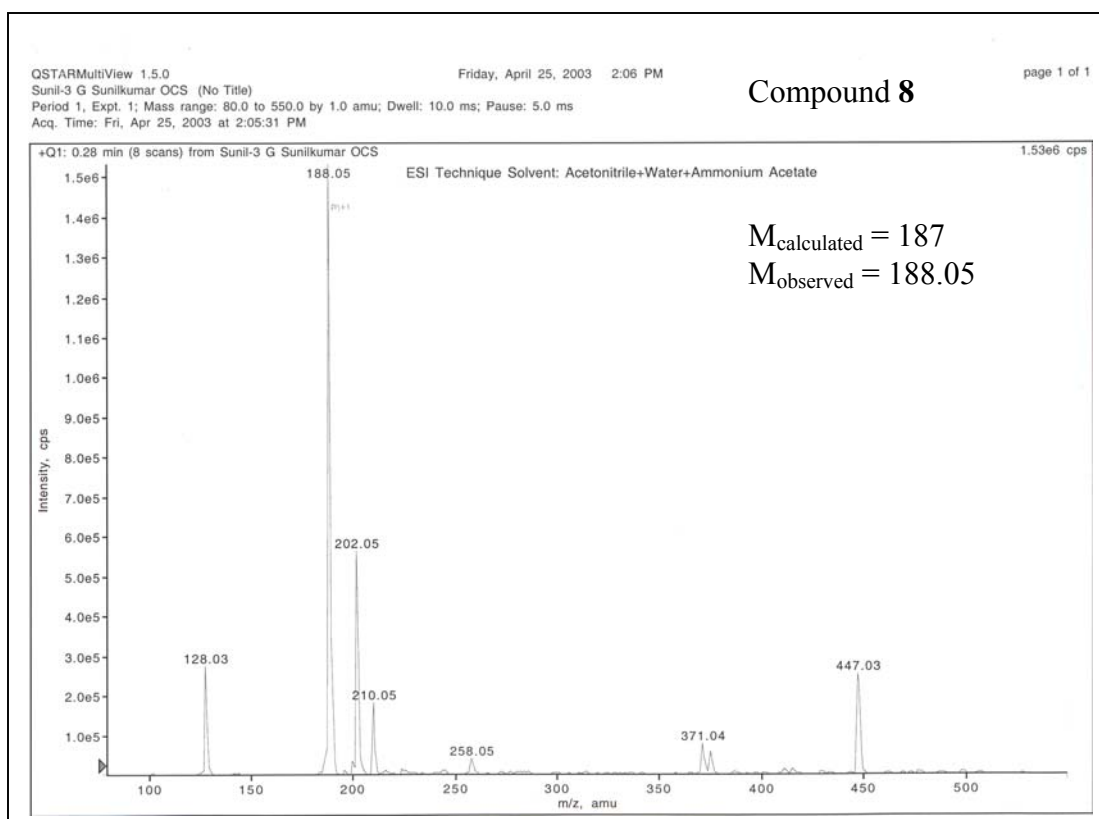
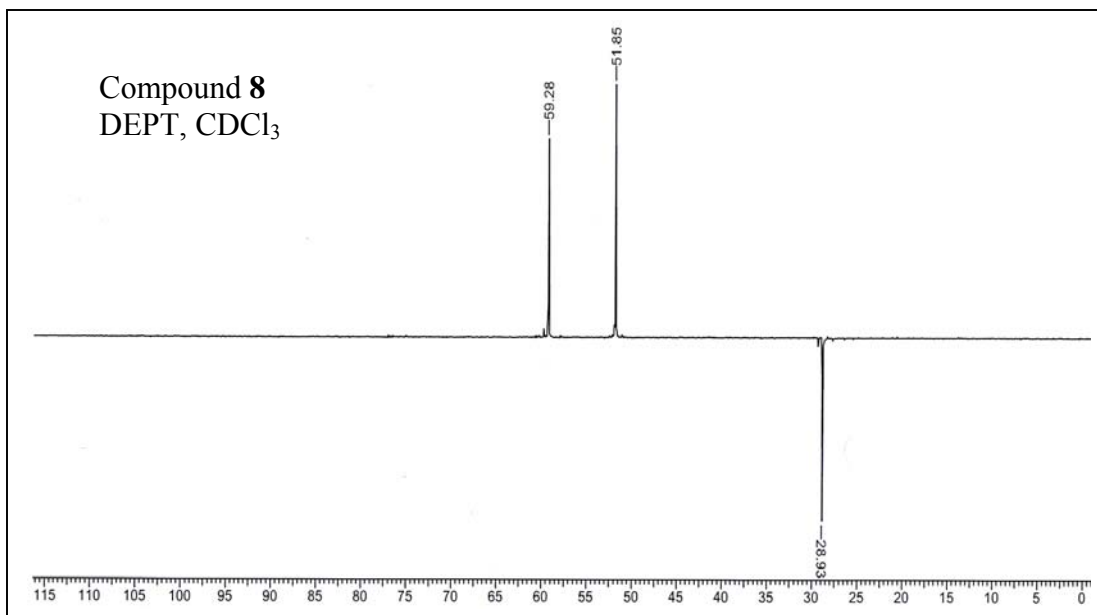


**Figure 8** DEPT and Mass spectra of compound **8**

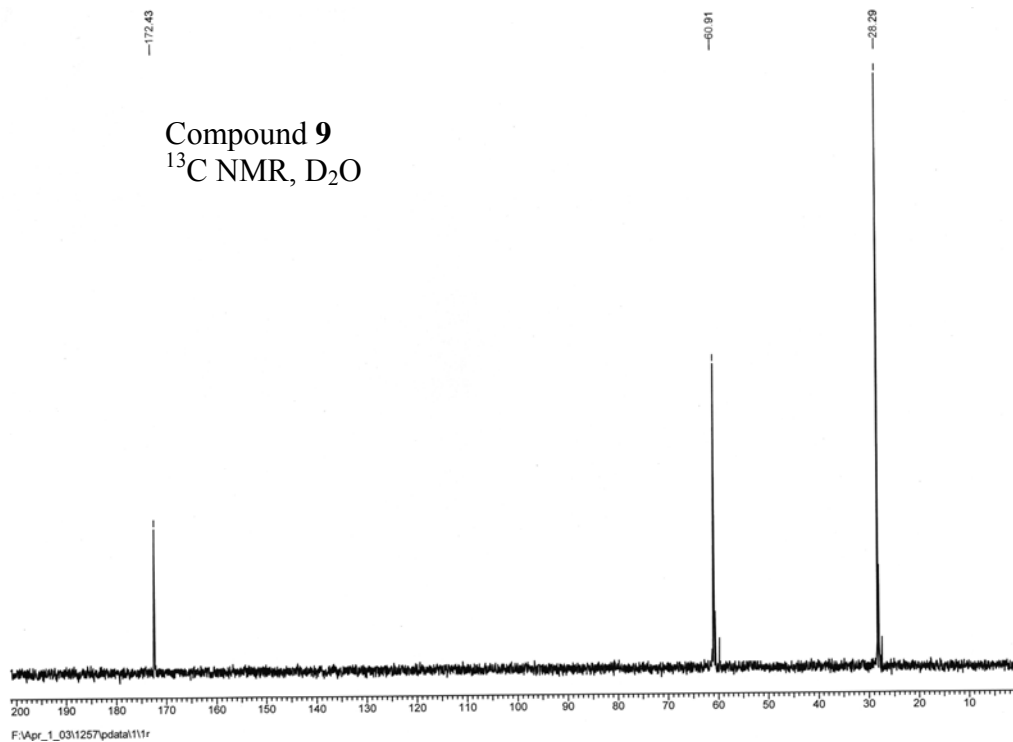
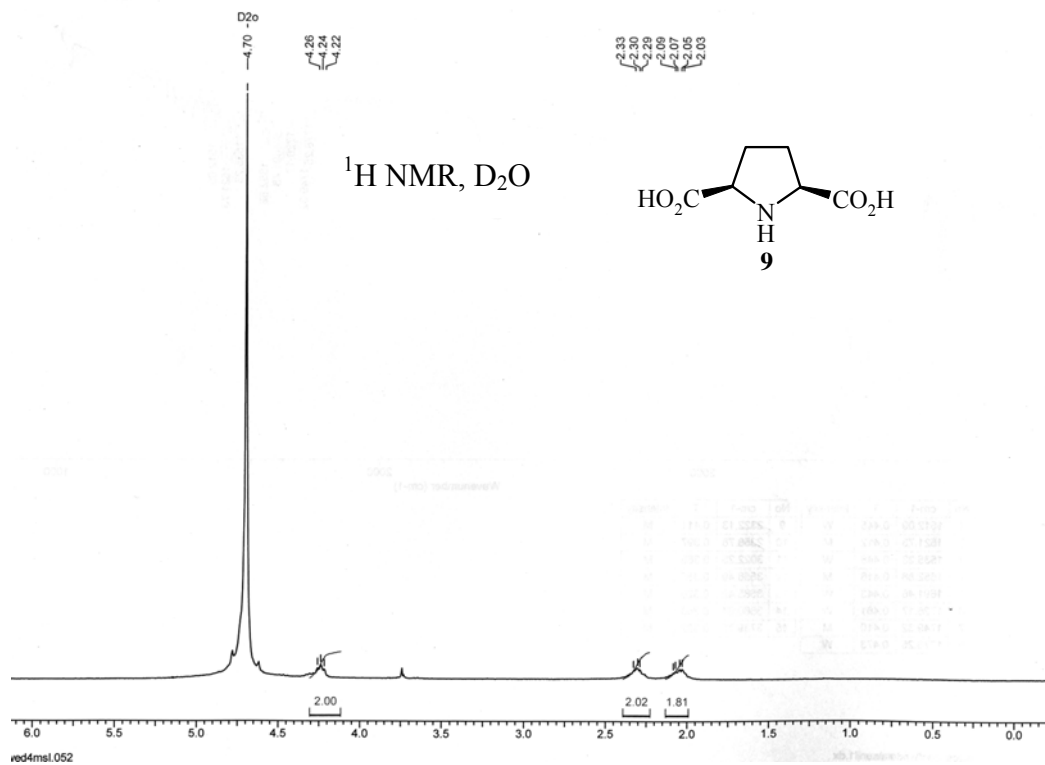


**Figure 9** <sup>1</sup>H NMR and <sup>13</sup>C spectra of compound **9**

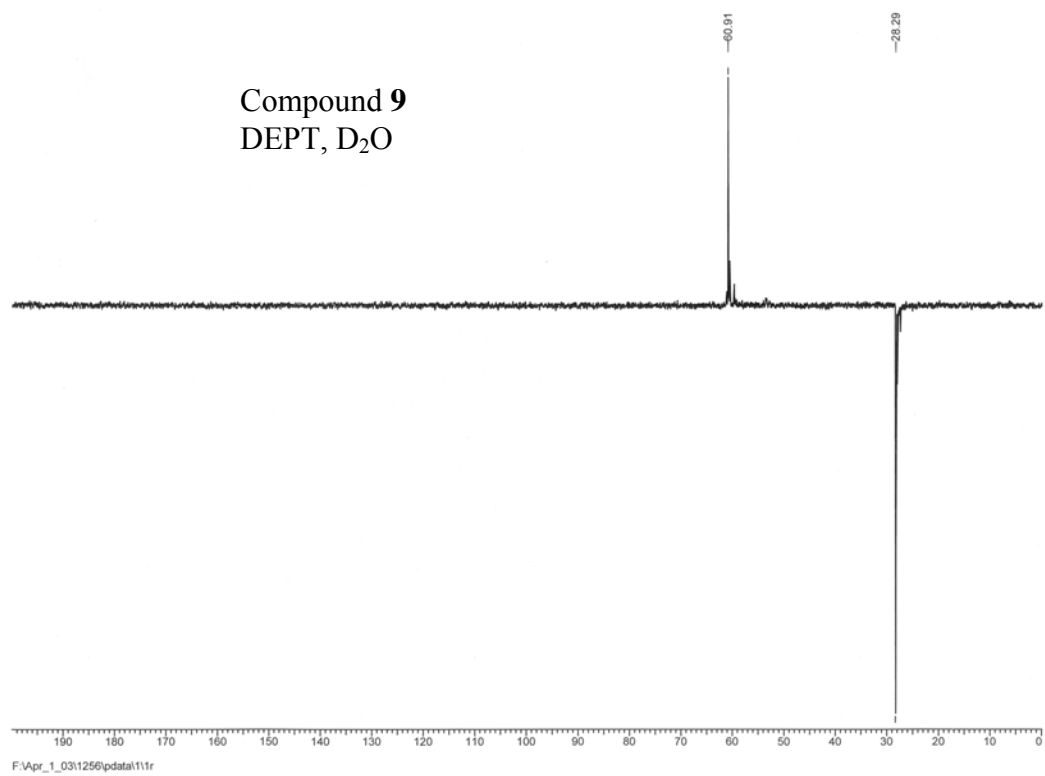


**Figure 10** DEPT spectrum of compound **9**

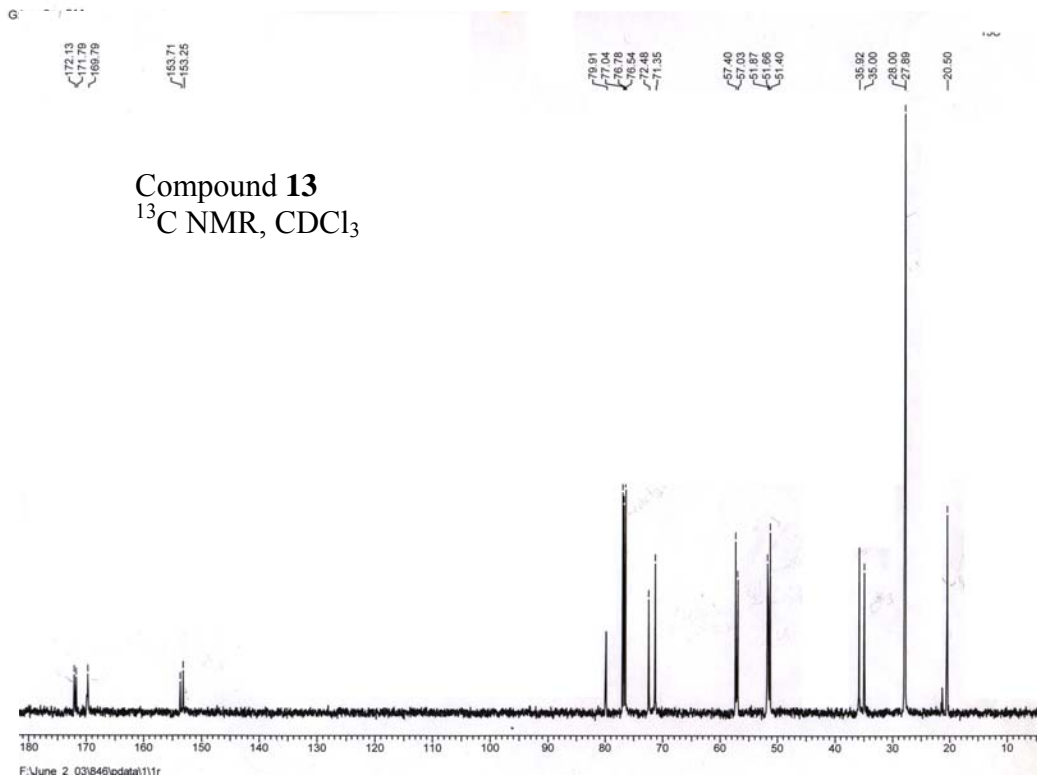
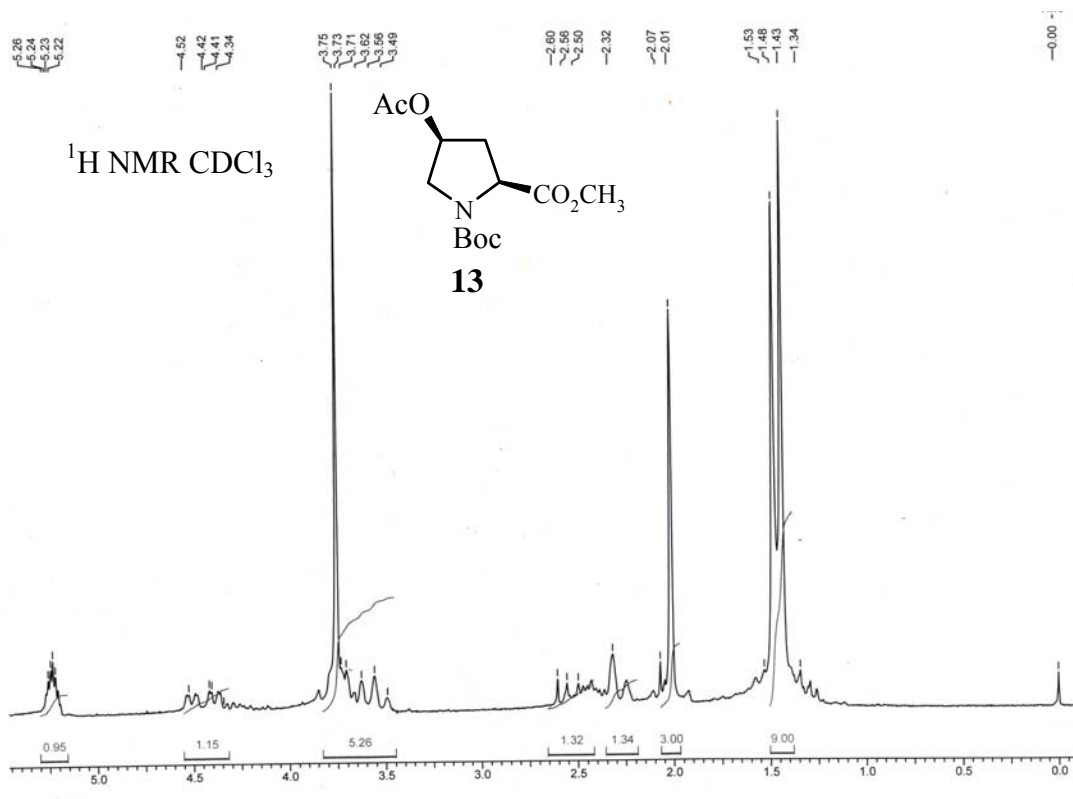


Figure 11 <sup>1</sup>H NMR and <sup>13</sup>C spectra of compound 13

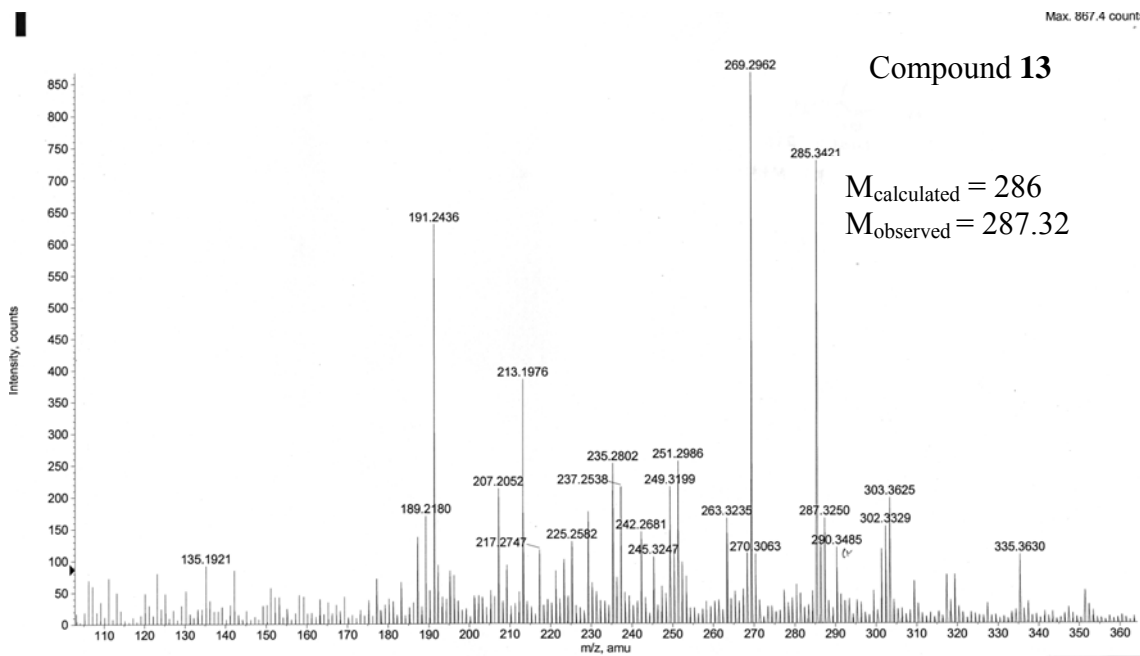
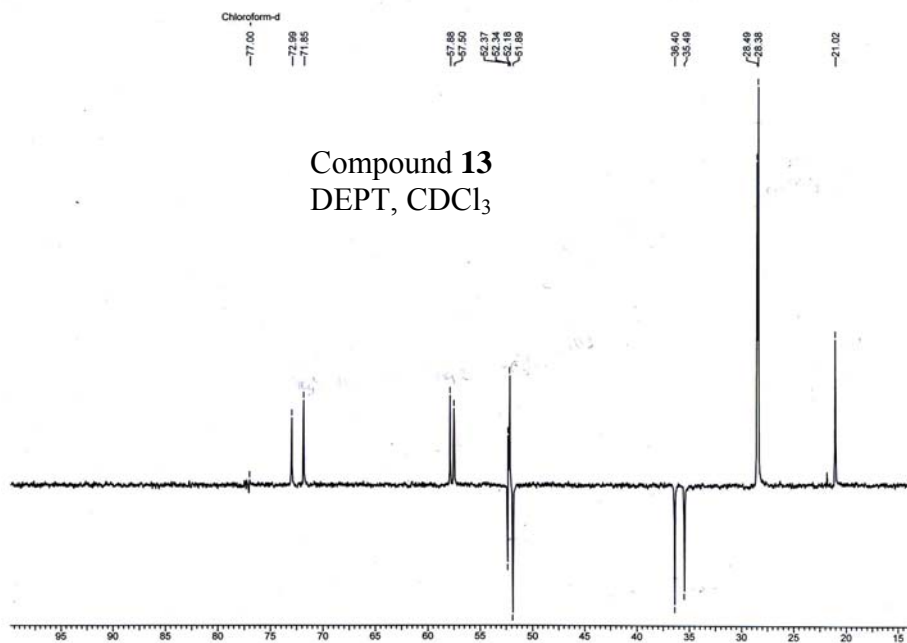
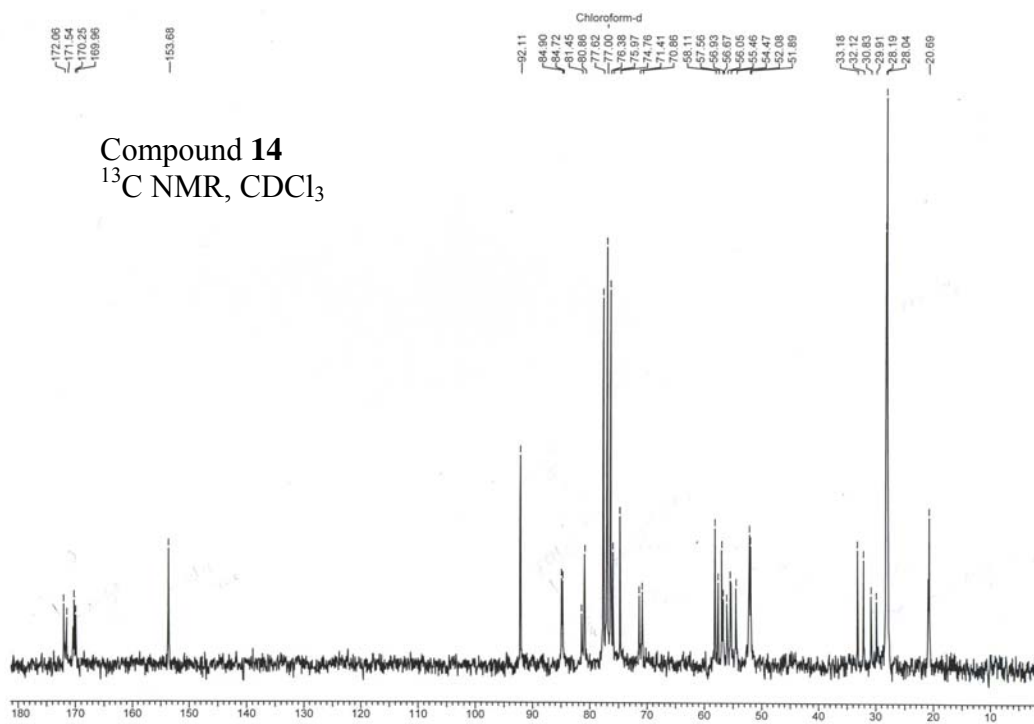
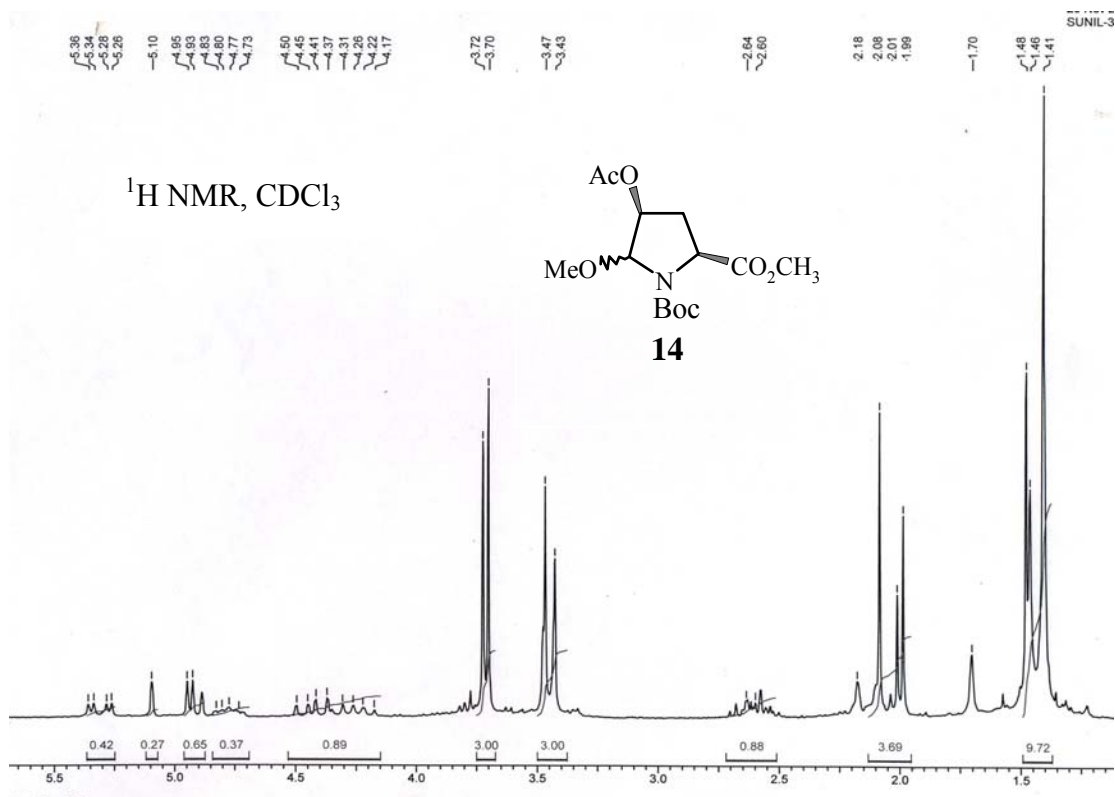
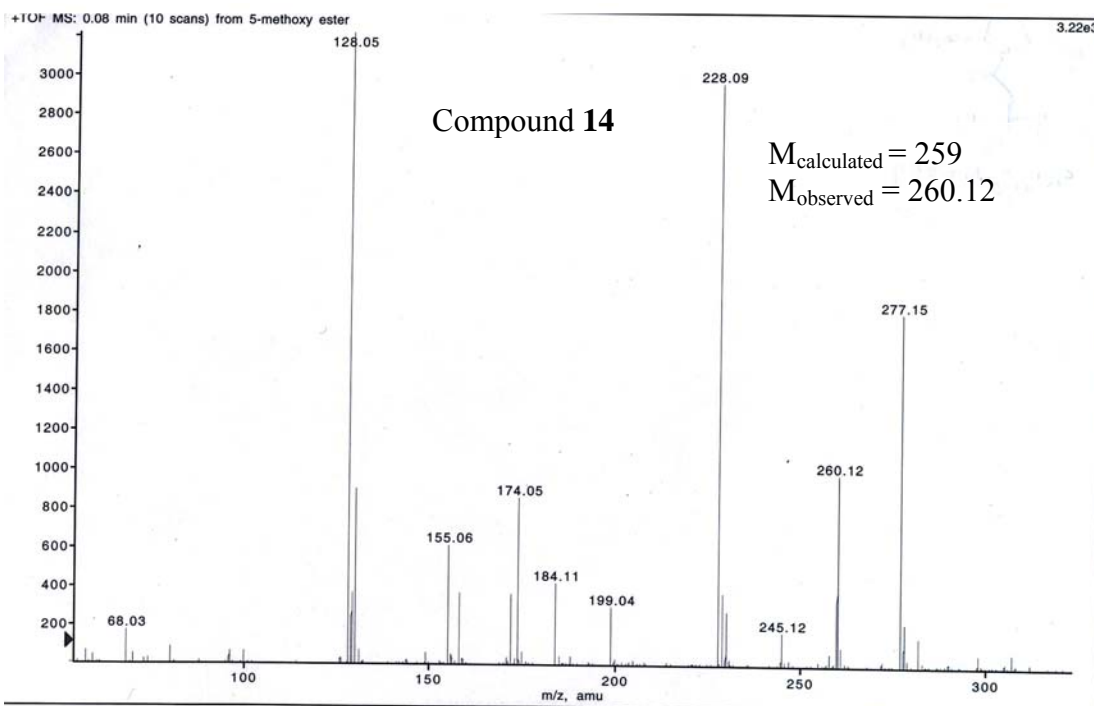
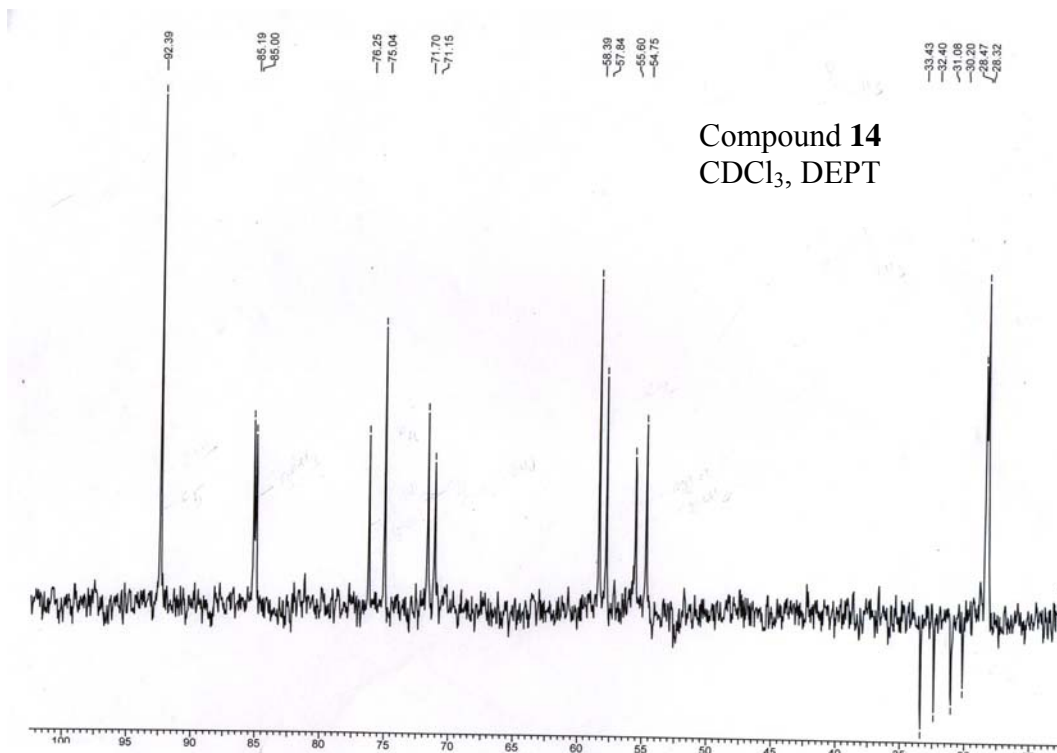


Figure 12 DEPT and Mass spectra of compound 13



**Figure 13** <sup>1</sup>H NMR and <sup>13</sup>C spectra of compound **14**



**Figure 14** DEPT and Mass spectra of compound **14**

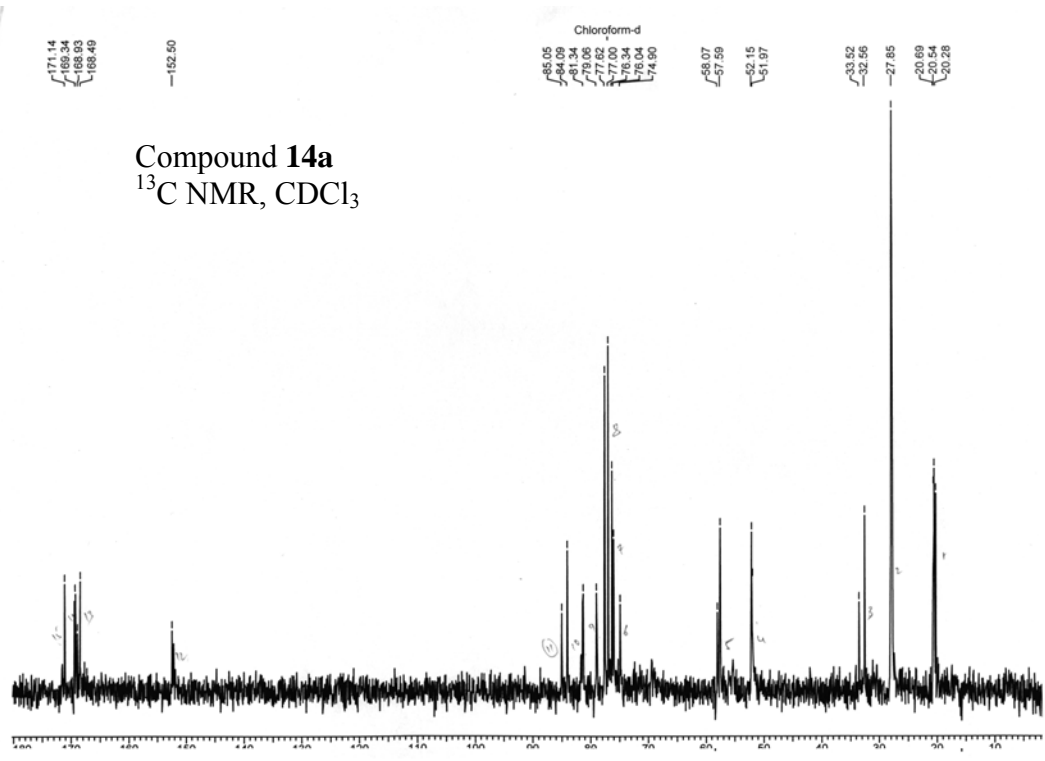
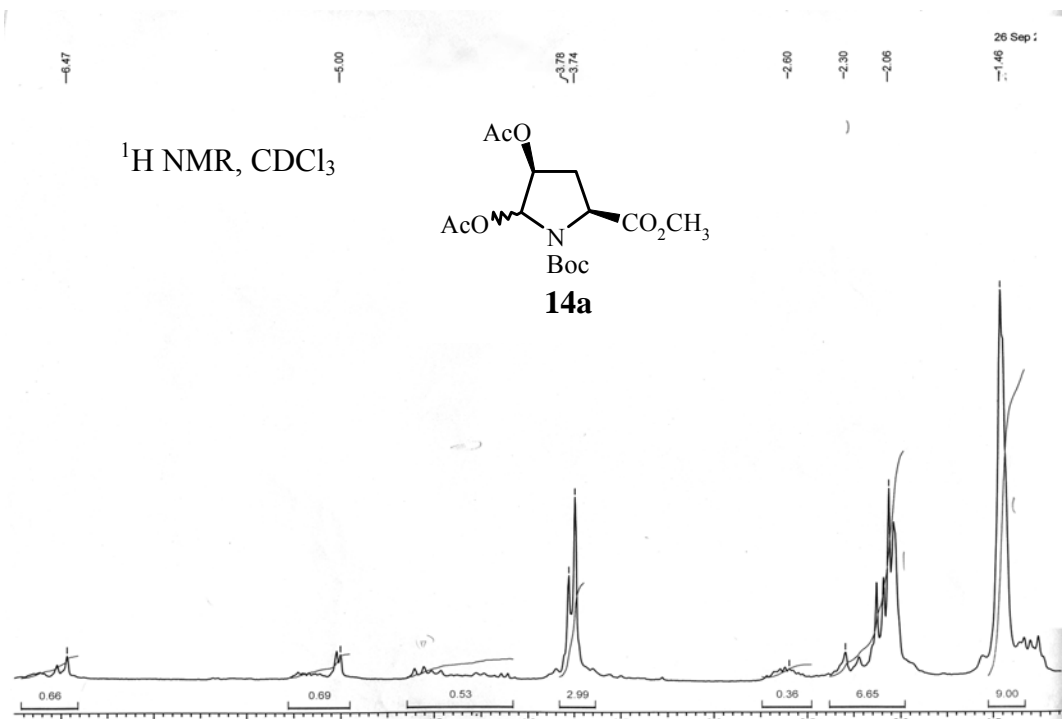
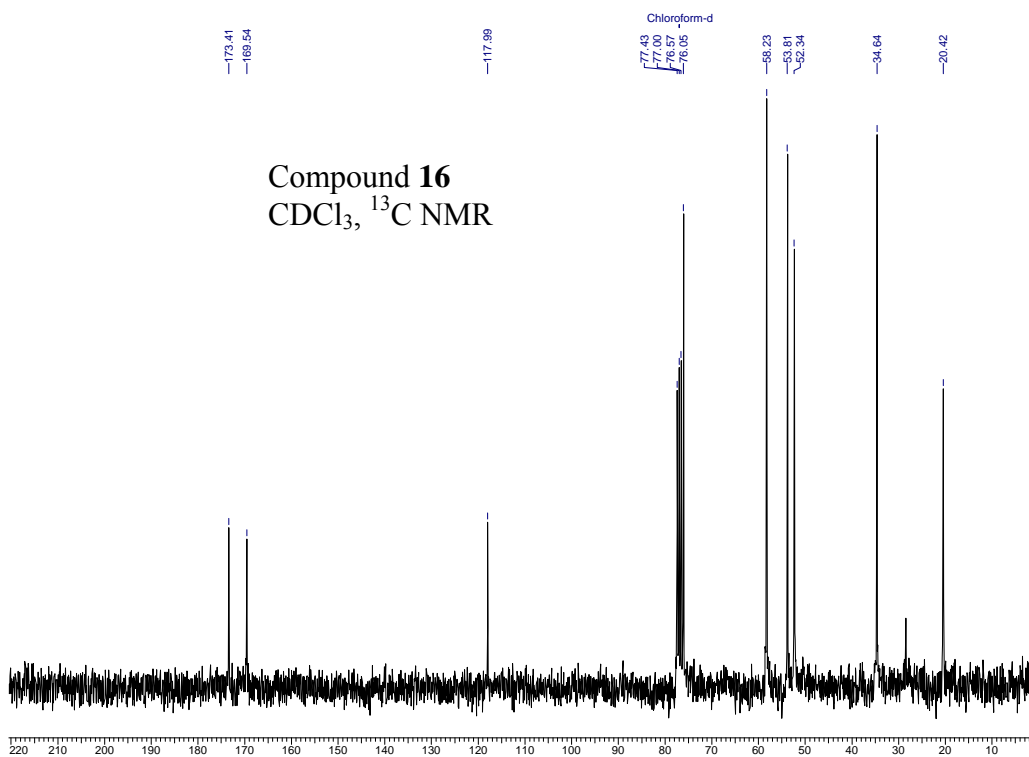
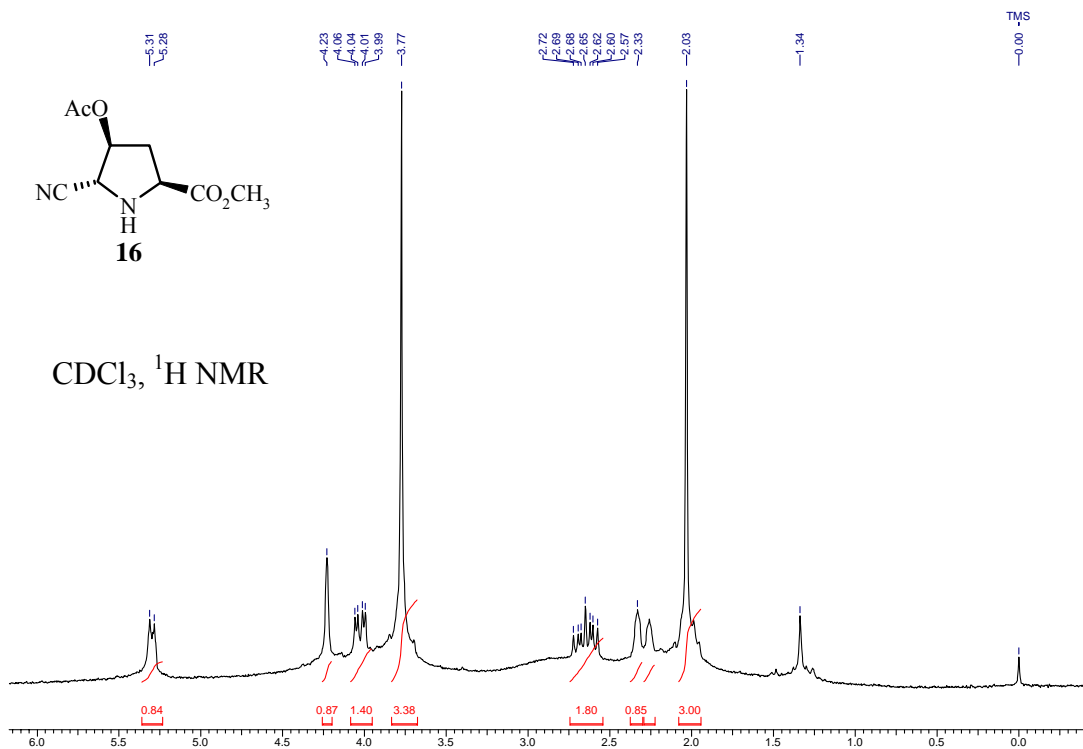
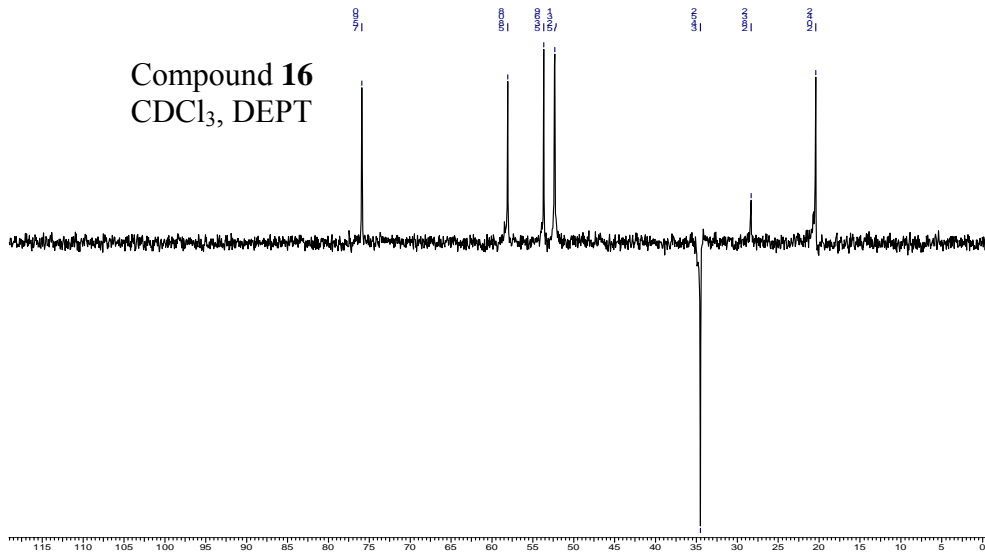


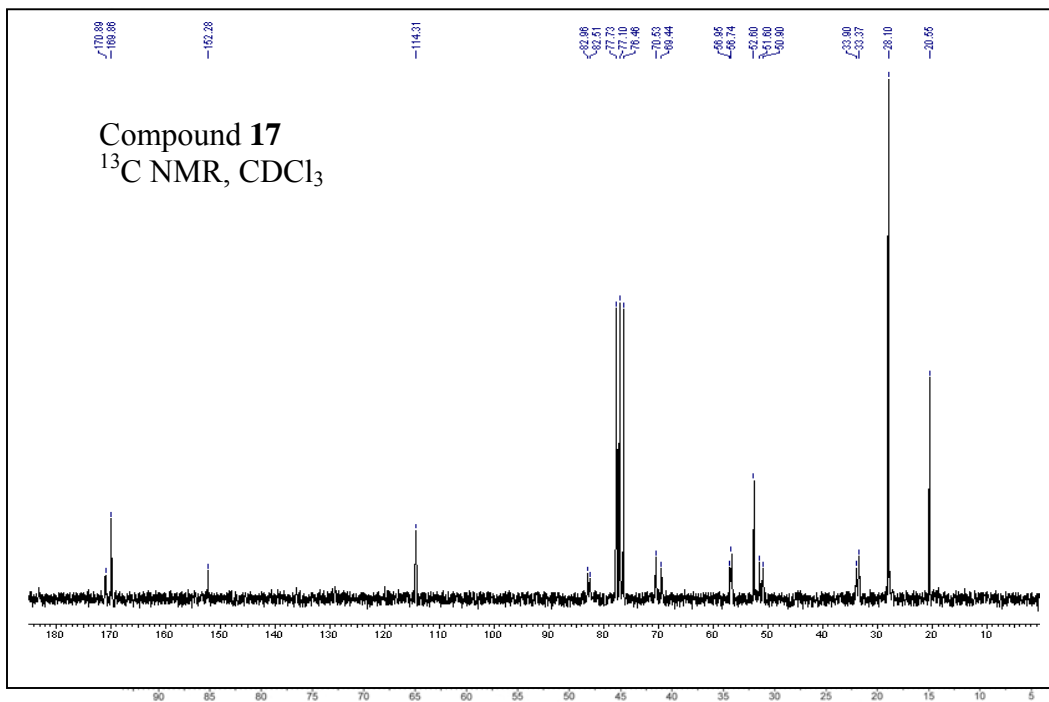
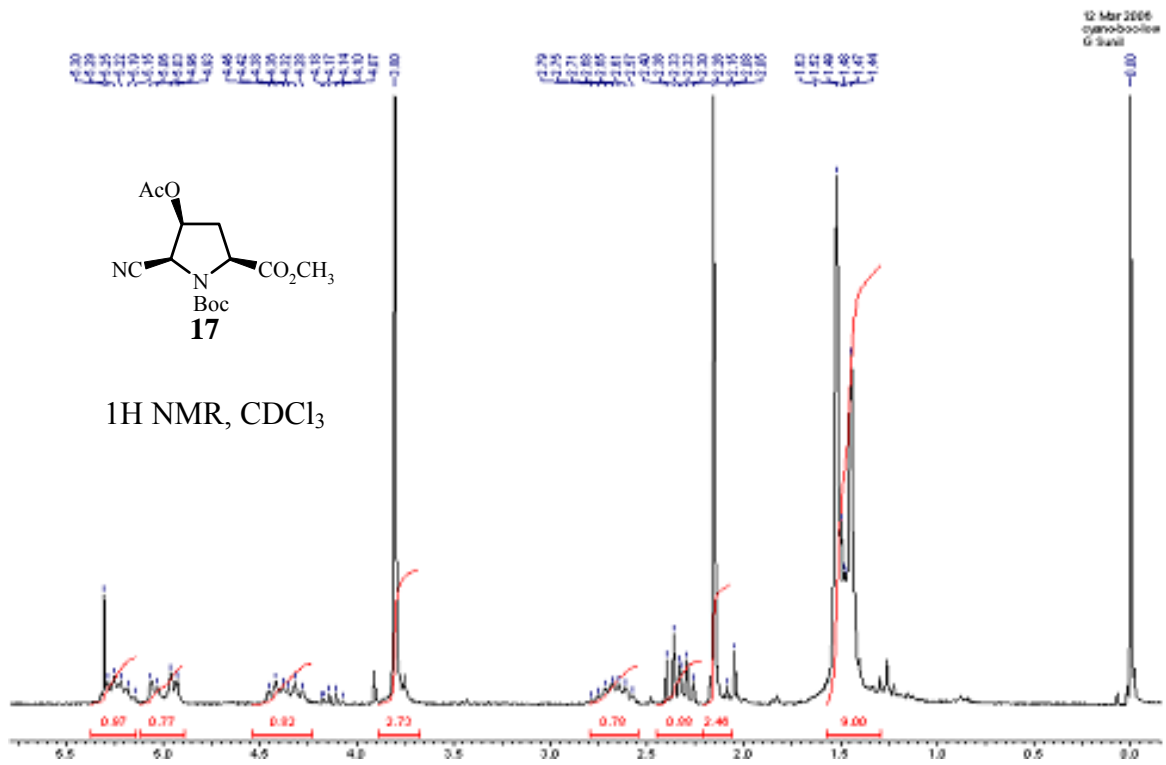
Figure 15 <sup>1</sup>H NMR and <sup>13</sup>C spectra of compound 15



**Figure 16**  $^1\text{H}$  NMR and  $^{13}\text{C}$  spectra of compound **16**

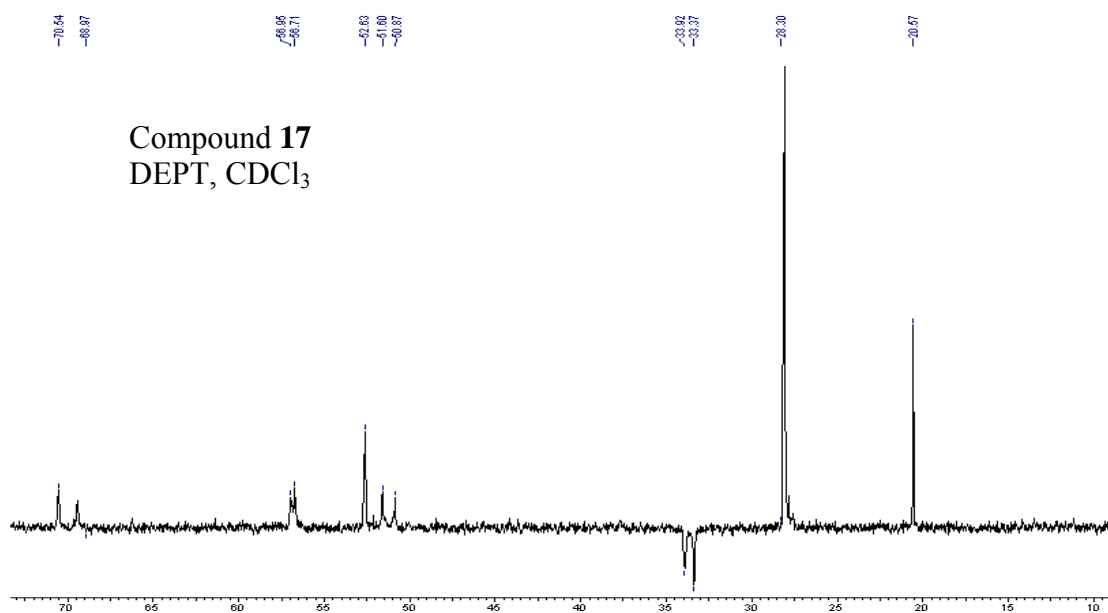


**Figure 17** DEPT spectrum of compound **16**



**Figure 18** <sup>1</sup>H NMR and <sup>13</sup>C spectra of compound **17**

Figure 19 DEPT spectrum of compound 17



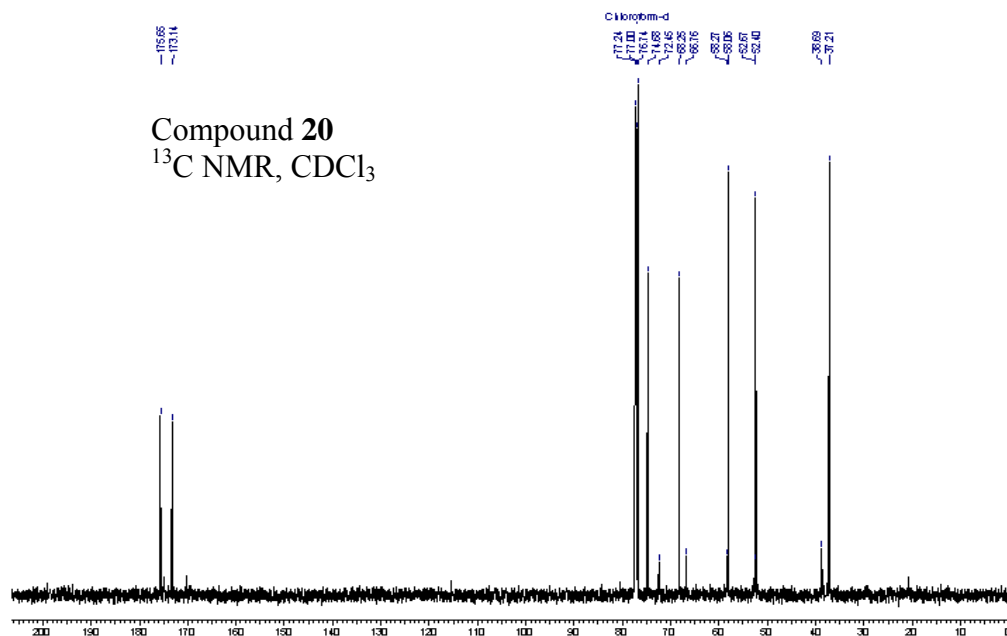
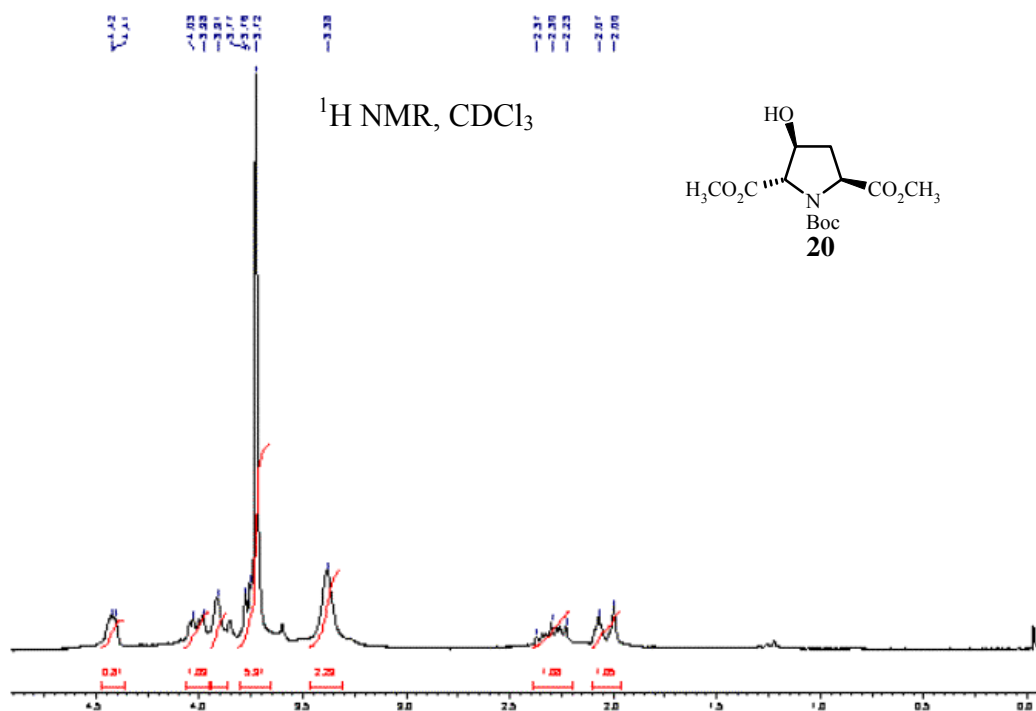


Figure 20 <sup>1</sup>H NMR and <sup>13</sup>C spectra of compound 20

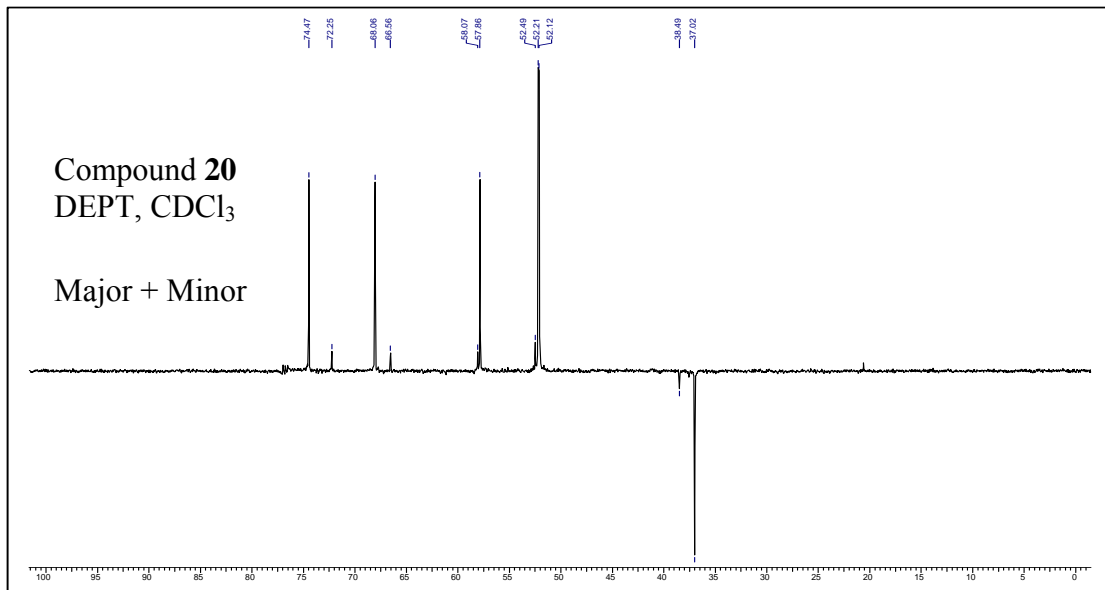


Figure 21 DEPT spectrum of compound **20**

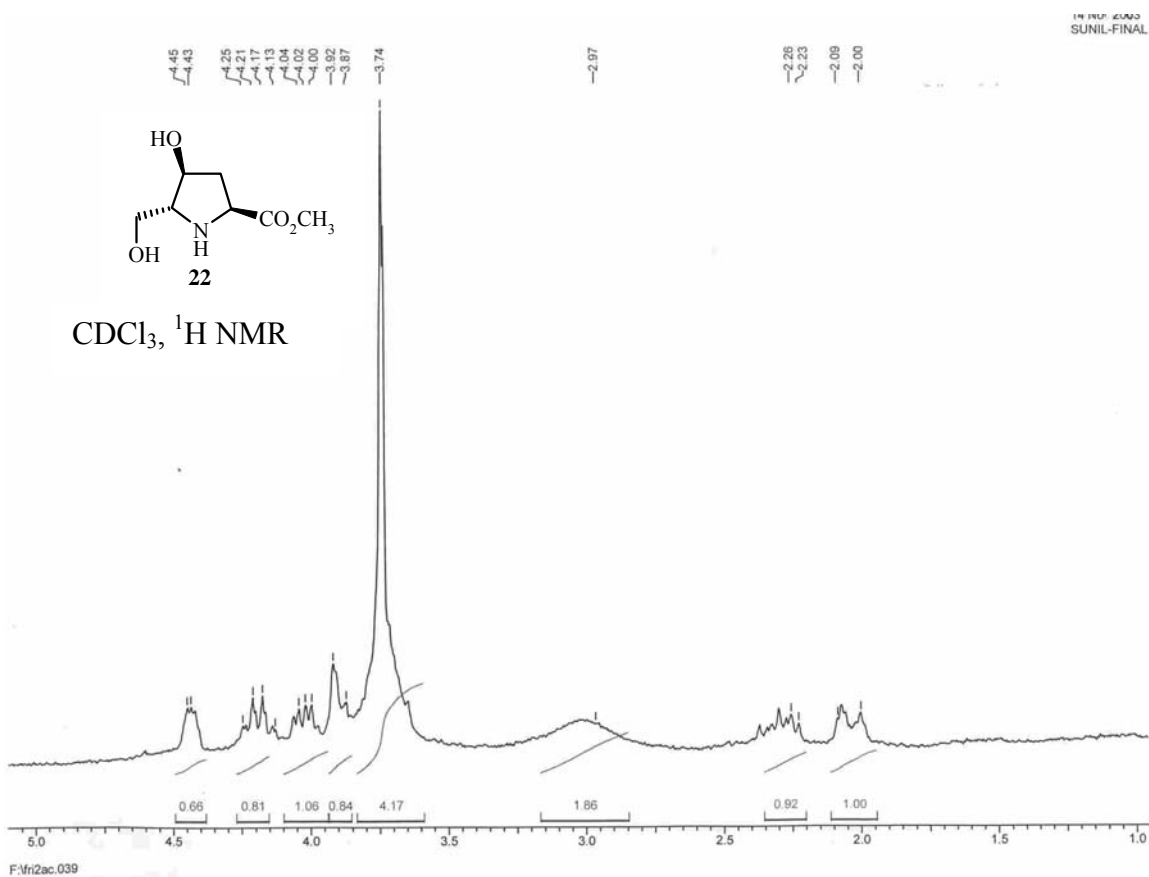
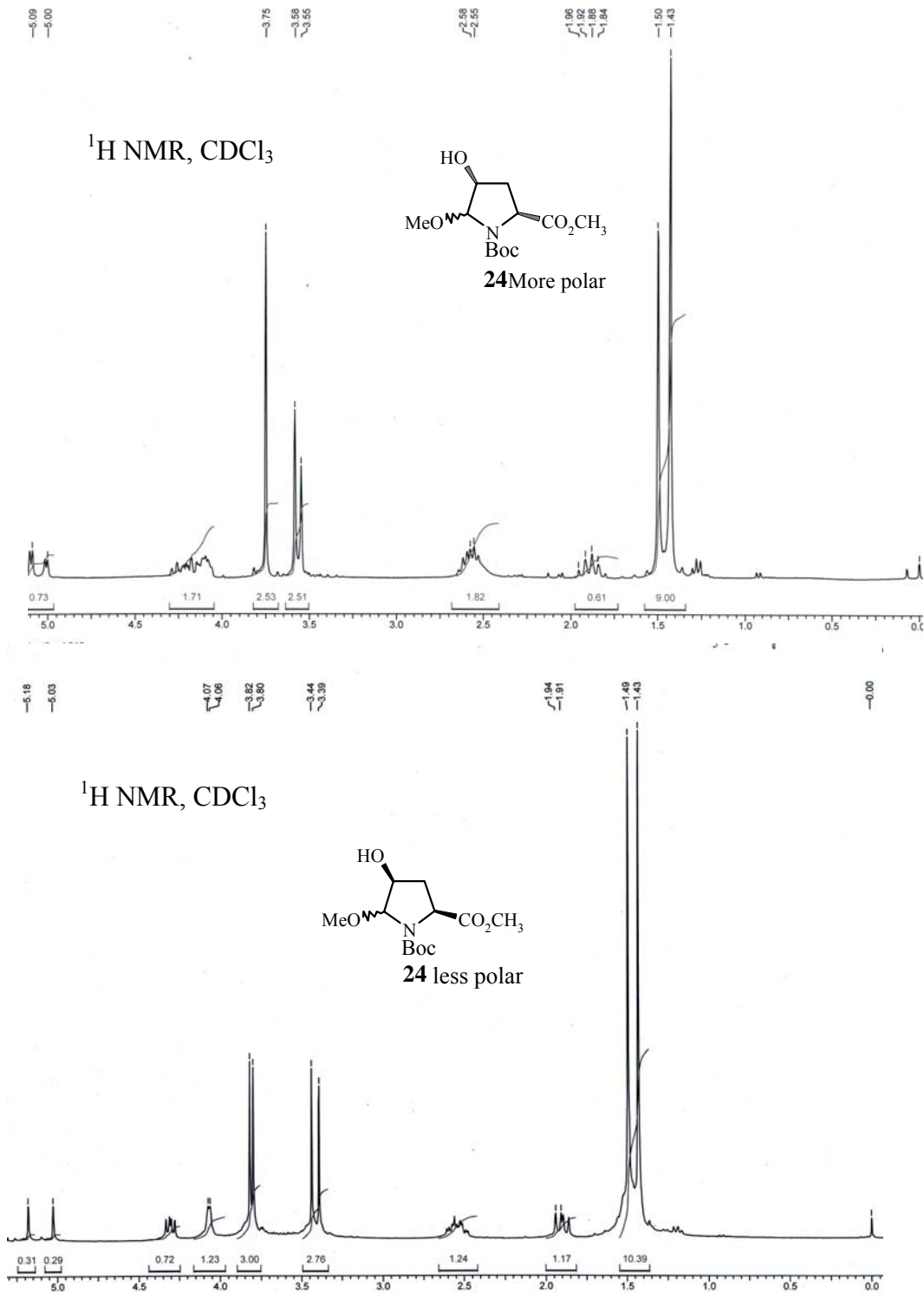
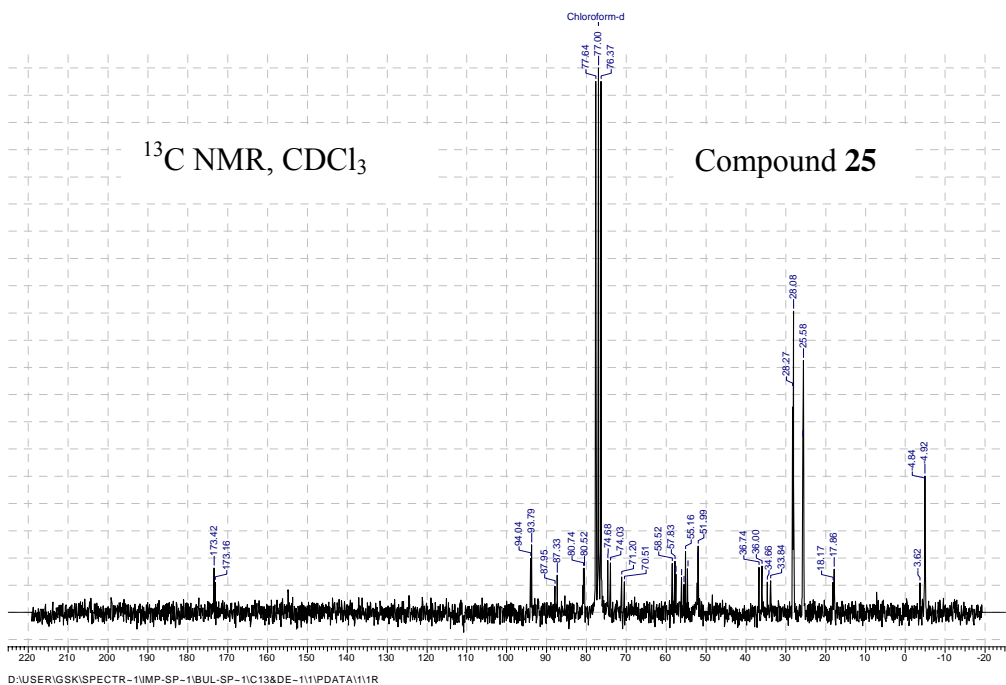
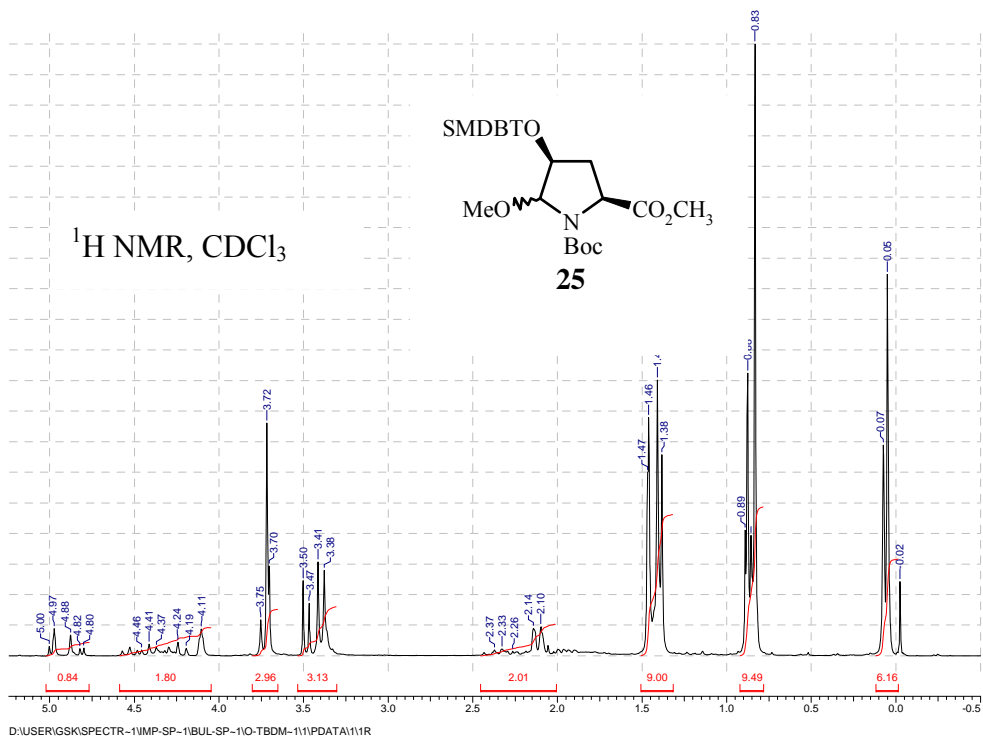


Figure 22 <sup>1</sup>H NMR spectrum of compound **22**



**Figure 23** <sup>1</sup>H NMR of compound **24**



**Figure 24** <sup>1</sup>H NMR and <sup>13</sup>C spectra of compound **25**



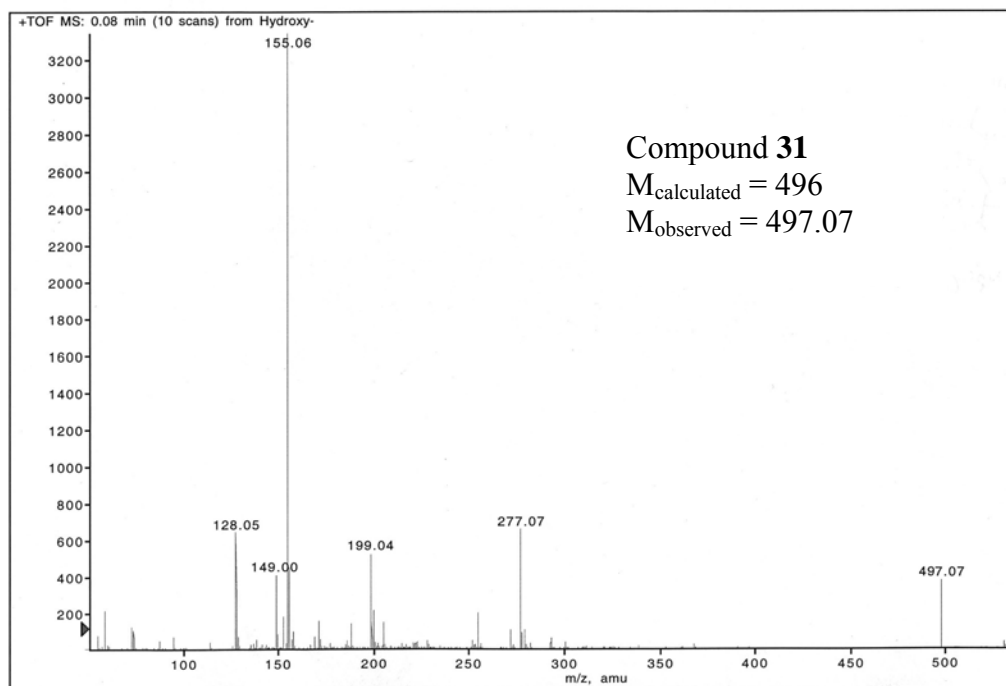
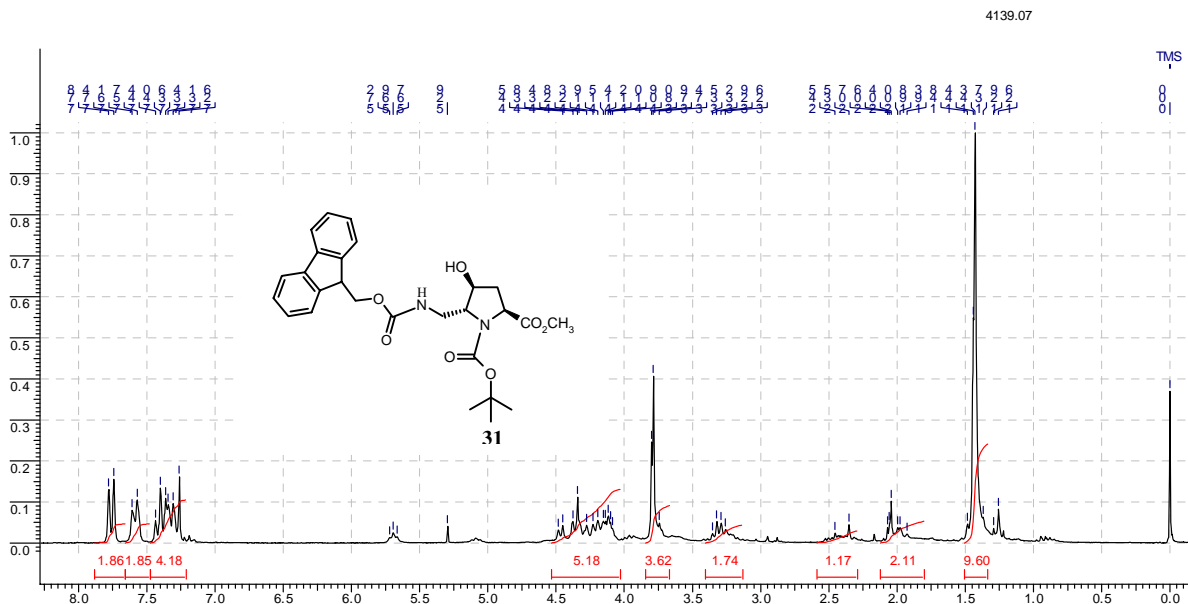


**Figure 26**  $^1\text{H}$  NMR and Mass Spectra of Compound **31**

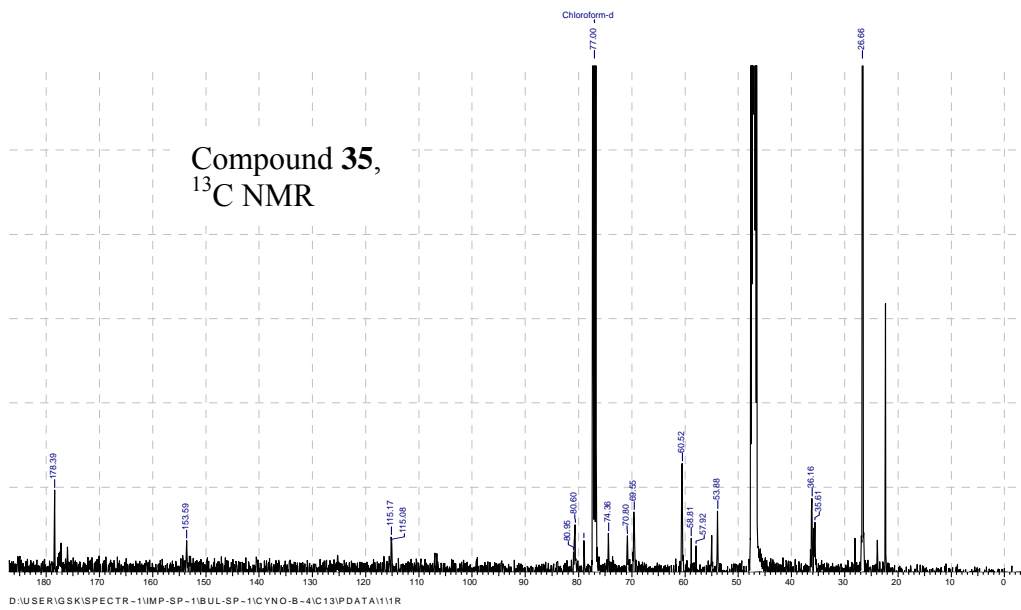
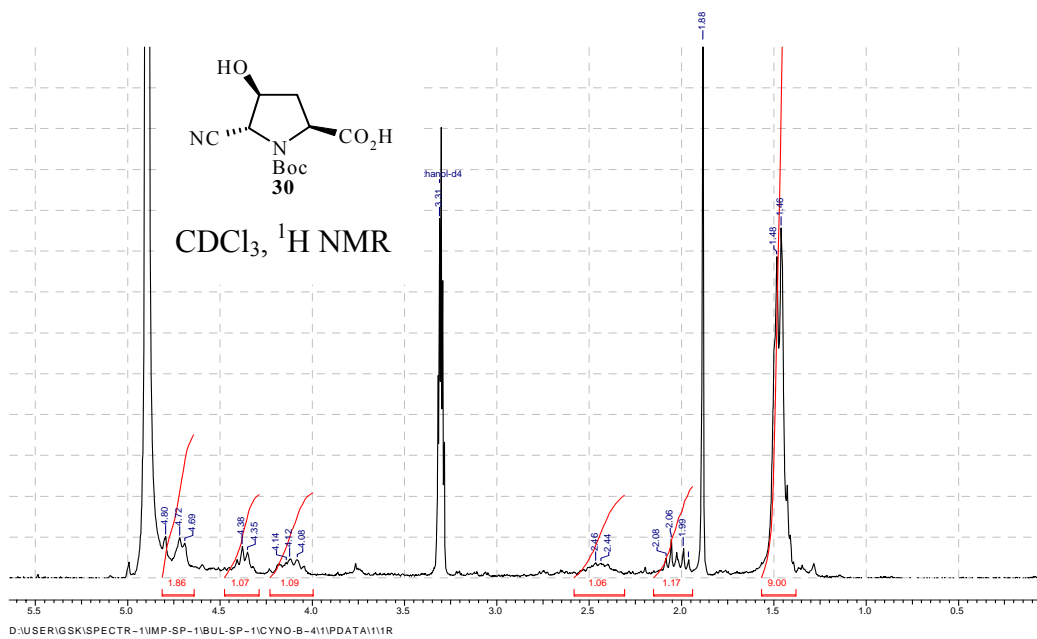


Figure 27  $^1\text{H NMR}$  and  $^{13}\text{C}$  spectra of compound 35